Managing concurrent evolution of resistance to fungicides

A thesis submitted for the degree of Doctor of Philosophy

School of Agriculture, Policy and Development, University of Reading

Net Zero and Resilient Farming, Rothamsted Research

Isabel Corkley

December 2024

Acknowledgements

Abstract

Evolution of resistance to fungicides threatens control of plant pathogens. Resistance management tactics such as application of fungicides with different modes of action (MoA) in mixture or alternation can slow selection for resistance, but it is unclear which strategies work against resistance evolving concurrently to two or more MoA. In this thesis, mathematical epidemiological models of polycyclic fungal foliar diseases were used to investigate potential resistance management tactics.

Use of integrated pest management (IPM) can reduce the fungicide intensity required for disease control, but resistance management benefits of cultural control methods are rarely quantified. I developed a model to estimate the resistance management benefits of a phytosanitary cultural control measure, the 'soybean-free period', used in Brazil to delay infection of soybean crops by *Phakopsora pachyrhizi* (Asian soybean rust). I considered interactions with use of fungicide mixtures and varying dose, application rates and timings.

Mixing two MoAs may require splitting the total dose of each MoA across more applications, increasing exposure time. Using a model of *Zymoseptoria tritici* (septoria tritici blotch), I showed that dose splitting of a solo MoA increases selection, but the effect varies with fungicide properties and the type and magnitude of resistance. I then compared alternation with 'splitting and mixing' as tactics against concurrent evolution of resistance to two MoA, modelling a sexually reproducing *Z. tritici* population. The best strategy varied with fungicide and resistant strain properties.

Incomplete cross-resistance between active substances with the same MoA could be utilised for resistance management. I used a novel modelling approach to investigate the resistance management benefits of within-MoA mixtures with incomplete cross-resistance. Resistance management benefits were greatest when the level of cross-resistance between active substances was low or negative; the rate of selection was also dependent on the variation in the fitness of pathogen strains against individual mixture components.

Declaration of original authorship

I confirm that this is my own work and the use of all material from other sources has been properly and fully acknowledged.

Isabel Corkley

Contribution to jointly authored papers

The thesis includes published papers, papers accepted for publication and papers prepared for submission for publication. These papers are jointly authored and are therefore written using plural first-person pronouns. I can confirm that I am the lead author of the research papers included in Chapters 3, 4, 5 and 6, and that I have made a substantial contribution to each of the papers included. A description of my contribution to each paper is given below, and an estimate of each author's contribution to the research and preparation of the manuscript is given in Table 1.

Chapter 2 is formed by the following published review paper: Corkley, I., Fraaije, B., & Hawkins, N. (2022). Fungicide resistance management: Maximizing the effective life of plant protection products. *Plant Pathology*, **71**(1):150-169. I wrote the original draft of the following sections: 4. Resistance management, 4.1 Dose rates, 4.2 Timing, 4.3 Mixtures or alternations and 6. Principle versus practice. I also prepared Figure 1, reviewed the original draft of other sections of the paper and contributed to subsequent revisions of all parts of the paper.

Chapter 3 consists of the following published paper: Corkley, I. Helps, J., van den Bosch, F., Paveley, N.D., Milne, A.E., Mikaberidze, A., Sierotzki, H. & Skirvin, D.J. (2025). Delaying Infection Through Phytosanitary Soybean-Free Periods Contributes to Fungicide Resistance Management in *Phakopsora pachyrhizi*: A Modelling Analysis. *Plant Pathology*, **74**(4):1078-1096.
I carried out the research described in collaboration with my co-authors and prepared the original draft and revisions of the manuscript.

Chapter 4 consists of the following published paper: Corkley, I. Mikaberidze, A., Paveley, N., van den Bosch, F., Shaw, M.W. & Milne, A.E (2025). Dose Splitting Increases Selection for Both Target-Site and Non-Target-Site Fungicide Resistance – A Modelling Analysis. *Plant Pathology*, **74**(4):1152-1167.
I carried out the research described, supervised by my co-authors, and prepared the original draft and revisions of the manuscript.

Chapter 5 consists of the following manuscript prepared for submission for publication: Corkley, I. Mikaberidze, A., van den Bosch, F., Paveley, N.D. & Milne, A.E (2024). Which resistance management strategies work against concurrent evolution of resistance to fungicides?

I carried out the research described, supervised by my co-authors, and prepared the original draft and revisions of the manuscript.

Chapter 6 consists of the following manuscript prepared for submission for publication: Corkley, I., Paveley, N.D., Fraaije, B.A., Helps, J., Shaw, M.W., Milne, A.E., Hawkins, N.J., van den Bosch, F. (2024). Azole mixtures: Modelling resistance management benefits of incomplete cross-resistance within a fungicide mode of action group.

A short paper published in "Modern Fungicides and Antifungal Compounds", Vol. X. (Proceedings of the Reinhardsbrunn Symposium) is included as an appendix: Corkley, I., van den Bosch, F., Fraaije, B.A., Shaw, M.W., Helps, J. Mikaberidze A., Milne, A.E., Paveley, N.D. (2023). Modelling resistance management benefits of diversity within a fungicidal mode of action with incomplete cross-resistance: the azoles example. In: Deising HB; Fraaije B; Mehl A; Oerke EC; Sierotzki H; Stammler G (Eds), "Modern Fungicides and Antifungal Compounds", Vol. X, pp. 291-296. © 2023. Deutsche Phytomedizinische Gesellschaft, Braunschweig, ISBN: 978-3-941261-17-4.

I carried out the research described in close collaboration with Frank van den Bosch, with supervisory input from Michael Shaw, Neil Paveley and other co-authors. The original manuscripts were prepared jointly by myself and Frank van den Bosch, as detailed in Table i. The research used data collected by Bart Fraaije and Nichola Hawkins that is reported as part of the paper.

Table i: Contribution of authors to each of the included papers.

Author	Percentage contribution		
	Conception, initiation and planning	Execution	Preparing the manuscript
Fungicide resistance management: Maximizing the effective life of plant protection products.			
Corkley, I.	**30**	**N/A**	**45**
Fraaije, B.A.	10	N/A	5
Hawkins, N.	60	N/A	50
Delaying infection through phytosanitary soybean-free periods contributes to fungicide resistance management in *Phakopsora pachyrhizi* – A modelling analysis			
Corkley, I.	**21**	**50**	**54**
Helps, J.	12	14	5
van den Bosch, F.	20	11	8
Paveley, N.D.	20	6	8
Milne, A.E.	2	1	10
Mikaberidze, A.	1	1	5
Sierotzki, H.	10	2	5
Skirvin, D.J.	14	15	5
Dose splitting increases selection for both target-site and non-target-site fungicide resistance – a modelling analysis			
Corkley, I.	**35**	**70**	**60**
Mikaberidze, A.	10	6	10
Paveley, N.D.	15	2	5
van den Bosch, F.	10	1	5
Shaw, M.W.	15	6	5
Milne, A.E.	15	15	15
Which resistance management strategies work against concurrent evolution of resistance to fungicides?			
Corkley, I.	**60**	**80**	**80**
Mikaberidze, A.	8	5	7
van den Bosch, F.	8	3	5
Paveley, N.D.	12	2	8
Milne, A.E.	12	10	10
Azole mixtures: Modelling resistance management benefits of incomplete cross-resistance within a fungicide mode of action group			
Corkley, I.	**25**	**50**	**50**
Paveley, N.D.	20	7	3
Fraaije, B.A.	3	3	3
Helps, J.	10	3	3
Shaw, M.W.	3	8	2
Milne, A.E.	1	1	8
Hawkins, N.J.	3	3	1
van den Bosch, F.	35	25	30

Contents

List of Figures

List of Tables

Chapter 1

Introduction

1.1 Why does resistance to fungicides matter?

The global human population surpassed 8 billion people in 2022, and is projected to reach nearly 10 billion people by 2050 (UN, 2024). This poses enormous challenges to safeguard food security whilst adapting food production to a changing climate and minimising loss of natural ecosystems to land-use for agricultural production (Searchinger et al., 2019). Fungal plant pathogens are associated with substantial yield losses in key food and cash crops globally. Average yield losses from fungal plant pathogens have been estimated as 10-23%, but vary between pathosystems, and are typically highest in areas in food-deficit with fast-growing populations. Yield losses are currently limited in many cases by the application of fungicides (Fisher et al., 2012; Oerke, 2006; Savary et al., 2019; Steinberg & Gurr, 2020). Climate change is likely to increase the rate of fungal infection and to drive emergence of new plant pathogens and shifts in the geographic ranges of existing pathogens (Chaloner et al., 2021; Fones et al., 2020). Maintaining control of fungal plant pathogens is therefore a vital component of food security.

'Integrated Pest Management' (IPM) approaches advocate combining multiple options for disease control, including use of crop cultivars with resistance to pathogens and cultural control methods, to reduce yield losses from disease. However, fungicides remain the cornerstone of disease control in many instances, and are an important part of the grower's IPM toolbox. In particular, fungicides play a vital role in maintaining disease control in years when disease pressure is high (te Beest et al., 2013), and for use in reducing selection for increased pathogen virulence against cultivar host resistance genes (Carolan et al., 2017; Taylor & Cunniffe, 2023a). However, the use of fungicides to control plant pathogens is threatened by the emergence of pathogen strains with resistance to fungicides (Corkley et al., 2022; Lucas et al., 2015).

The risk of evolution of resistance is particularly high in polycyclic foliar fungal pathogens which have large population sizes and many generations per year (Grimmer et al., 2015). These economically damaging pathogens include potato

late blight (*Phytophthora infestans*), Asian soybean rust (*Phakopsora pachyrhizi*), grey mould (*Botrytis cinerea*) in many crops, barley net blotch (*Pyrenophora teres*), apple scab (*Venturia inaequalis*), Cercospora leaf spot (Cercospora beticola) in sugar beet, and septoria tritici blotch (STB) (*Zymoseptoria tritici*) in wheat. Increasing levels of resistance to multiple fungicide modes of action (MoAs) have been reported in these pathogens, with a corresponding decline in the level of disease control provided by the affected fungicides (Abuley et al., 2023; Blake et al., 2018; Hellin et al., 2021; Ivanov et al., 2021; Jørgensen et al., 2022; Mair et al., 2020, 2023; Müller et al., 2021; Nasonov & Yakuba, 2024; Pütsepp et al., 2024; Rangel et al., 2020; Rosenzweig et al., 2020; Rupp et al., 2017; Sofianos et al., 2023). The pipeline for introduction of new MoAs to the market is limited due to rapid increases in the costs and time taken to develop and register new active substances. An increasing level of effort is required to find new compounds that combine the required level of field efficacy with an acceptable environmental and toxicity profile (Bryson, 2022). Fungicide resistance management strategies are therefore needed to reduce selection for resistance to fungicides and safeguard future yields.

1.2   How does resistance evolve?

Resistance may arise through mechanisms that are specific to an individual mode of action (MoA), usually involving mutations in the pathogen target-site (target-site resistance) or target-site overexpression. In contrast, generalist, non-target-site resistance mechanisms such as enhanced efflux and detoxification can affect multiple MoAs (Dorigan et al., 2023; Hawkins et al., 2019). Fungicides with a mode of action (MoA) affecting a single pathogen target site, such as quinone outside inhibitor (QoI), succinate dehydrogenase inhibitor (SDHI) and demethylation inhibitor (DMI) fungicides, are at a higher risk of resistance development than multi-site fungicides, as a single mutation is more likely to result in a moderate or high level of resistance to the fungicide (Hollomon & Brent, 2009).

The driving force for the spread of any resistance allele in a pathogen population is natural selection (Hollomon & Brent, 2009): pathogen strains with a heritable increase in resistance to the action of a fungicide have greater fitness in the presence of that fungicide than strains that are sensitive to the fungicide. Over time and with repeated applications of the fungicide, resistant strains outcompete sensitive strains and increase in proportion in the pathogen population, replacing the sensitive strains (Figure 1.1). As the frequency of resistant strains increases,

the overall sensitivity of the pathogen population to the fungicide decreases (van den Bosch et al., 2011).

Within a single season, the epidemic of many polycyclic fungal foliar pathogens increases primarily through asexual reproduction producing haploid pycnidiospores (Eriksen & Munk, 2003), with overlapping generations consistently reproducing the same allele combinations and resistance phenotype. To understand evolutionary processes within a season, it is therefore helpful to consider the epidemic in terms of the per capita rate of increase, or 'growth rate' (*r*) of each strain: a number which combines the repeating stages of lesion establishment, growth and sporulation into a single measure of the success of a strain at a given point in time. The rate of selection for a resistant strain is determined by the difference in growth rates between the resistant strain and the more sensitive strains in the population (van den Bosch et al., 2014a). The greater the difference in growth rates, the faster the rate of selection for the resistant strain.
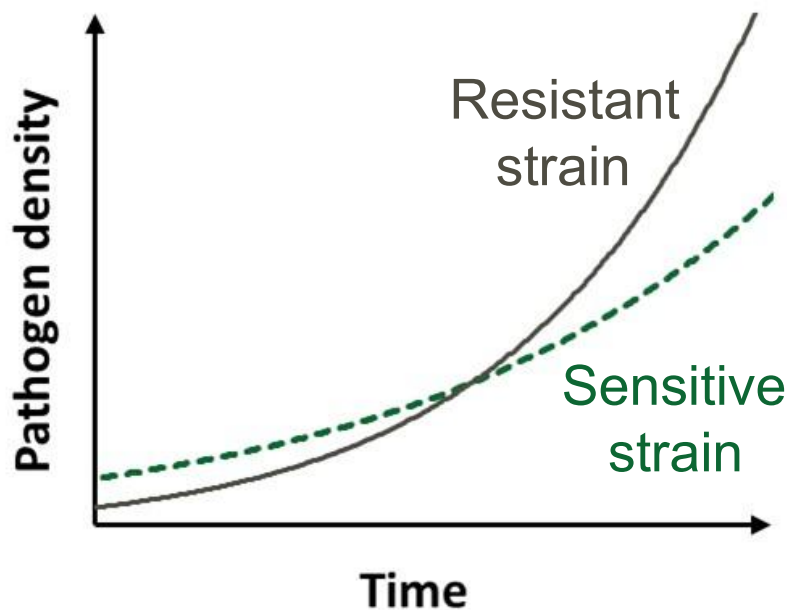
Figure 1.1: When fungicide is applied, resistant strains grow at a faster rate than sensitive strains, leading to an increase in the proportion of the pathogen population that is resistant.

Resistance mutations in a pathogen's genome may already be present at low levels as 'standing genetic variation', or new ('*de novo*') mutations may occur by chance (Hawkins et al., 2019). If no fungicide is applied, strains with these mutations do not have a fitness advantage, and the frequency of resistance genes is likely to remain low. Resistant lineages at low frequencies may die out due to

chance (a stochastic process known as 'genetic drift'). When a fungicide is applied, the strong fitness advantage conferred by resistance mutations means that these genes are likely to increase in frequency and become fixed in the population. The time taken for *de novo* mutations to become fixed in the population is known as the 'emergence phase' of resistance development. The emergence phase is followed by a 'selection phase' once a resistance gene becomes sufficiently common that it is unlikely to be lost from the population by genetic drift (van den Bosch et al., 2011; Hobbelen et al., 2014).

1.3   What is a resistance management strategy?

A successful resistance management strategy should delay the build-up of resistance to fungicides in pathogen populations for as long as possible, whilst maintaining adequate disease control (Corkley et al., 2022; van den Bosch et al., 2014a; van den Bosch & Gilligan, 2008). A tactic that only accomplishes one of these goals without the other is not a successful resistance management strategy. For example, stopping application of fungicides would delay the build-up of resistance to fungicides indefinitely, but disease control would be inadequate without fungicide in many years (Steinberg & Gurr, 2020), so this would not be an acceptable resistance management strategy. Conversely, increasing fungicide dose in order to compensate for a decline in fungicide efficacy is a short-term tactic to maintain adequate disease control (Shaw, 2006; van den Bosch et al., 2014a, 2018), but it is likely to accelerate selection for resistance to the fungicide, so this should not be viewed as a resistance management strategy (van den Bosch et al., 2011).

Previous modelling and experimental studies have considered a range of potential changes to fungicide programmes which could form part of a fungicide resistance management strategy, as reviewed by van den Bosch et al. (2014a) and Corkley et al. (2022). Depending on the change made, and variation in the biology of different pathogens, such changes could either increase or decrease selection for resistance (Birch & Shaw, 1997; Elderfield et al., 2018; Hobbelen et al., 2011b; Shaw, 2006; Taylor & Cunniffe, 2023b; van den Berg et al., 2013; van den Bosch et al., 2011, 2014b):

- Change the fungicide dose at each application
- Change the number of fungicide applications
- Change the timings of fungicide applications.

- Apply two or more different fungicidal modes of action in mosaic within a landscape.
- Apply two or more different fungicidal modes of action in mixture or alternation.

Van den Bosch et al. (2014a) consider each of these strategies in terms of 'governing principles of selection for resistant strains', building on work by Milgroom & Fry (1988). They conclude that the cumulative difference in growth rates of the resistant and sensitive strains, and therefore selection for resistance, can be reduced in three ways (or a combination of the three), as follows.

1. Reduce the growth rates of both the sensitive and resistant strains.

2. Reduce the growth rate of the resistant strain relative to that of the sensitive strain.

3. Reduce the time span over which selection takes place (exposure time).

Van den Bosch et al. (2014a) summarise these principles using the following equation:

$$sT = (r_R - r_S)T \qquad (1)$$

where s is the selection coefficient, r_R is the growth rate of the resistant strain, r_S is the growth rate of the sensitive strain, and T is the exposure time of the pathogen population to a fungicide. Reducing sT therefore reduces the rate of increase of resistant strains in the population. For example, increasing the number of applications of a fungicide increases exposure time, and has been shown to increase selection for resistance (Hobbelen et al., 2011a; van den Bosch et al., 2014a). Increasing the dose rate of a fungicide application is predicted to increase the cumulative difference in the growth rates of resistant and sensitive strains, and so increase selection for resistance (van den Bosch et al., 2011). Conversely, modelling and experimental evidence suggest that resistance development can be slowed by applying at-risk fungicides in mixture with a fungicide with a different MoA that the resistant strains are sensitive to (Hobbelen et al., 2011b; van den Bosch et al., 2014a, 2014b), as this reduces the difference in the growth rates of resistant and sensitive strains.

In practice, the effect of fungicide on strain growth rates varies over time as the foliar concentration of the fungicide decreases due to the effects of plant metabolism and the abiotic environment including solar radiation and rainfall (Fantke & Juraske, 2013; van den Bosch et al., 2014a). Pathogen growth rates

may also become limited by density dependence towards the end of the growing season, if there is limited healthy leaf area left for infection due to crop senescence and existing infection (van den Bosch & Gilligan, 2008). The growth rate of strain 'R' at time t can be denoted as $r_R(t)$. Equation (1) can then be adapted to represent total selection over time T with time-varying pathogen growth rates:

$$s(T) = \int_{t=0}^{T} (r_R(t) - r_S(t)) \, \mathrm{d}t \tag{2}$$

There is an important distinction between strategies aiming to prevent emergence of resistance alleles in the first place, and those aiming to slow the selection phase. As the selection phase may be rapid (Deising et al., 2008) even with the use of resistance management tactics, the greatest gains in the number of seasons for which fungicides are effective may be achieved by delaying emergence. Ideally, a resistance management strategy should balance both aims, but this is not straightforward. If the mutation rate is constant, then keeping pathogen populations small should reduce the chance of a mutation conferring resistance to fungicides occurring (Milgroom, 1990). Emergence of resistance can therefore be slowed by larger doses in limited circumstances if they reduce the pathogen population sufficiently to restrict mutational supply (Mikaberidze et al., 2017). However, this might occur only at dose rates in excess of the maximum label dose, and also conflicts with increased selection for resistance alleles affecting the same mode of action that are in the selection phase (Mikaberidze et al., 2017; van den Bosch et al., 2011, 2014a). Mikaberidze et al. (2017) concluded that larger doses would accelerate emergence in most biologically plausible scenarios: even following fungicide treatment, the population size (and corresponding number of cell divisions) and genetic diversity of fungal foliar pathogen populations can be so large that the rate of evolution of resistance is unlikely to be limited by mutational supply (McDonald et al., 2022; Mikaberidze et al., 2017).

Resistance management strategies should also make use of resistant cultivars and other IPM measures (Jørgensen et al., 2014; Taylor & Cunniffe, 2023a) to reduce the growth rate of the pathogen and therefore minimise differences in growth rates between sensitive and resistant strains. There is a risk of evolution of virulence to resistant cultivars; the risk is lower for host resistance that is due to a combination of many quantitative resistance genes, each with a small effect, than host resistance that relies on a few major genes (Brown, 2015). Cultural control measures are often aimed at reducing pathogen inoculum. For example, burning,

burial or covering of wheat stubble and potato discard piles can be effective strategies to reduce *Z. tritici* and *P. infestans* inoculum, and leaf shredding is a useful strategy for control of *V. inaequalis* (Cooke et al., 2011; McDonald & Mundt, 2016; Meitz-Hopkins et al., 2023; Vincent et al., 2004). Strategies also include elimination of weeds and volunteer crops that can act as 'green bridges' for pathogen survival after harvest, or that play an important role in the pathogen life cycle. For example, barberry (*Berberis* spp.) is an important host for the pathogen wheat stem rust (*Puccinia gramini* f. sp. *tritici*) for sexual reproduction to produce overwintering teliospores. Control of barberry can therefore be a very effective control strategy in areas with cold winter weather (Barnes et al., 2020; Peterson, 2018). A soybean-free period has been introduced in parts of Brazil with the aim of minimising green bridges and reducing *P. pachyrhizi* inoculum (Godoy et al., 2016; Yorinori, 2021). Use of cultivar mixtures to reduce disease pressure (Kristoffersen et al., 2020) and choice of tolerant cultivars which yield well even under high disease pressure (Jørgensen et al., 2014; van den Bosch et al., 2022) can also be useful as they enable a reduction in fungicide dose rates, reducing selection for resistance.

In general, stacking disease control measures reduces the potential fitness advantage for the pathogen of evolving resistance to any individual measure (Corkley et al., 2022); a diverse disease control strategy that relies most heavily on measures at lower risk of evolution of resistance will therefore be more resilient to evolution of resistance (Figure 1.2). **However, the fungicide resistance management benefits of many IPM measures are currently unquantified.**
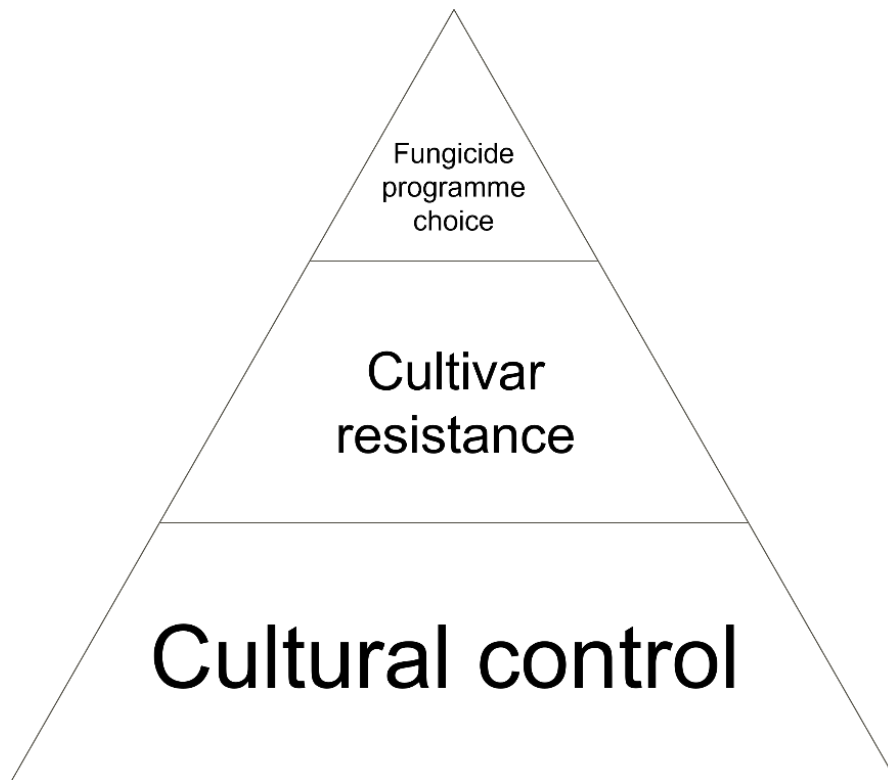
Figure 1.2: IPM pyramid for disease control and resistance management. Disease control should rely most heavily on measures at lower risk of resistance evolution, likely to include many cultural control measures and use of tolerant crop cultivars (bottom segment of the pyramid). Cultivar resistance can provide durable disease control, especially if many quantitative host resistance genes are stacked together, but there is a risk that pathogens might evolve virulence (middle segment of the pyramid). Although any application of fungicides will increase selection for fungicide resistance, choice of fungicide programme can be used to diminish the rate of selection for resistance (top segment of the pyramid).

1.4   Additional challenges for resistance management when resistance is evolving concurrently to two or more fungicides

Strains with multi-fungicide resistance have been observed in multiple fungal pathogens, including *B. cinerea*, *V. inaequalis*, *C. beticola, P. pachyrhizi* and *Z. tritici* (Chapman et al., 2011; Chatzidimopoulos et al., 2022; Garnault et al., 2019; Müller et al., 2021; Omrane et al., 2017; Rupp et al., 2017; Trkulja et al., 2017). Both generalist resistance mechanisms such as enhanced efflux and strains combining target-site mutations to multiple MoAs are of concern (Ballu et al., 2024). The availability of low-risk multisite fungicides is increasingly restricted

through regulation, and the rate of development of new MoAs has slowed, resulting in less flexibility for disease control and resistance management. It is not clear what the best strategies are for managing resistance evolving to two or more fungicidal modes of action (MoA) at the same time ('concurrent evolution of resistance'): this situation introduces complex trade-offs. The best strategy for one MoA might not represent the optimal strategy for a second MoA. For example, Dooley *et al.* (2016) showed that mixtures of a DMI fungicide and a SDHI fungicide reduced selection for resistance against the DMI fungicide, but that the selection for the SDHI fungicide was not reduced by mixture with the DMI fungicide.

The use of mixture introduces trade-offs if resistance is evolving concurrently to both MoA (Figure 1.3). In many years, multiple fungicide applications are required to keep *Z. tritici* below damaging levels of severity, so use of mixture would require splitting the total dose of a fungicide across two or more applications: 'splitting and mixing'. Dose-splitting reduces the dose of each MoA per application but increases the exposure time of the pathogen to the fungicide, with counteracting effects on selection. Modelling studies predict that the effect of additional exposure time on selection will generally outweigh the effect of reduced dose and this is supported by some experimental evidence (van den Bosch et al., 2014a). However, the effects of dose-splitting on selection for partial fungicide resistance mechanisms that are effective only at smaller fungicide concentrations have not been modelled. In addition, recent experimental evidence did not show an effect of dose splitting on selection (Young et al., 2021). **There is therefore a need to better understand how fungicide properties (efficacy and decay rate) and the type and magnitude of resistance determine the effect of dose splitting on selection**, to help identify cases where, overall, the use of dose-splitting to enable mixture would be beneficial.

There is also a need to understand how strategies such as alternation and 'splitting and mixing' of two MoA compare in terms of the rate of selection for double-resistant strains when resistance is evolving concurrently to both MoA. Many fungal foliar pathogens undergo sexual reproduction at some point in their life cycle. Sexual reproduction will produce new combinations of resistance alleles through reassortment and crossing over, maintaining high levels of genetic diversity and potentially producing new pathogen strains or boosting the frequency of rarer strains (Chen & McDonald, 1996; McDonald et al., 2022; Zhan et al., 2003), or potentially diluting double-resistant strains if there is population mixing with untreated, more sensitive populations (Helps et al., 2020). It is therefore important

to **investigate the effects of sexual reproduction on the concurrent evolution of resistance to two or more MoA** (Taylor & Cunniffe, 2023b).
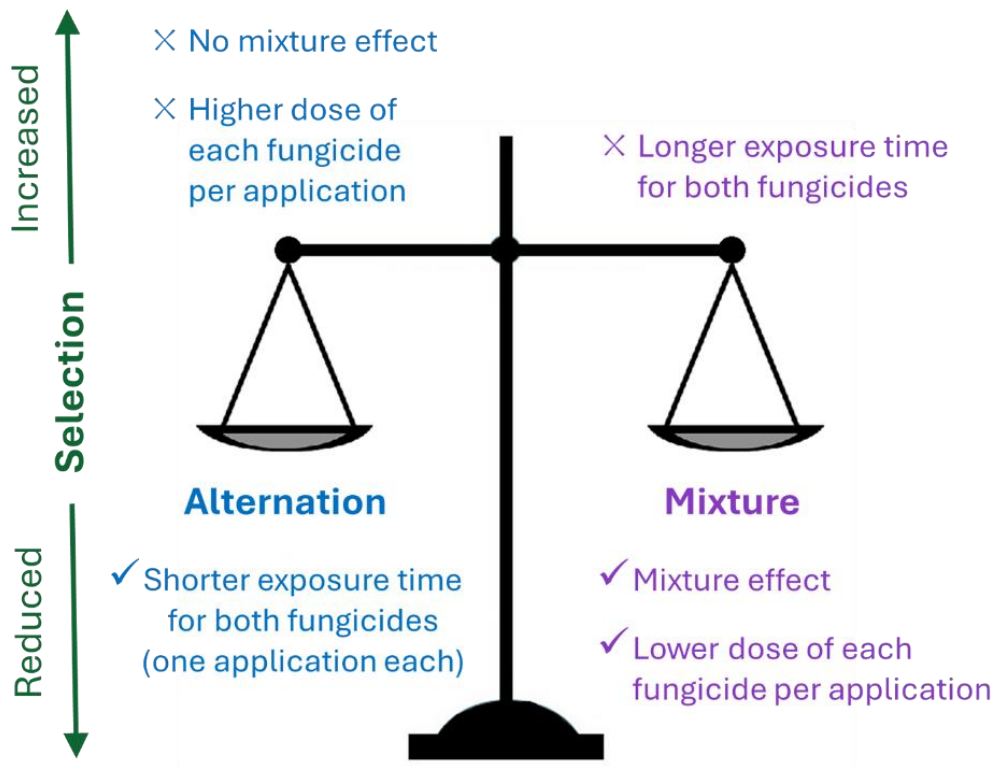
Figure 1.3: A balancing act: trade-offs of alternating or 'splitting & mixing' two at-risk fungicidal modes of action.

1.5   Models of the evolution of fungicide resistance

Models of plant disease epidemiology attempt to capture the fundamental processes in complex systems encompassing the effects and interactions of pathogen life cycles, crop development, the action of fungicides, and human and physical geography (Cunniffe et al., 2015). Model simulations that combine the governing principles of evolutionary biology with the specific effects of fungicide programmes, resistance genes, and pathogen biology can be used to predict the effects of different resistance management strategies (van den Bosch et al., 2014a). Field experiments can be costly to run, and repetition over multiple sites and years is usually required to understand biological processes that can be highly variable. Modelling enables exploration of many possible strategies and scenarios that it may be impractical, expensive or unethical to investigate using field trials.

As noted by the statistician George Box, "All models are wrong, but some models are useful" (Box, 1976). A balance between model realism and model parsimony

is required. One benefit of using models is the ability to simplify very complex systems, to better understand the effects of a subset of factors. Conversely, simplifying model assumptions excluding important processes might lead to different model results and conclusions. For example, the inclusion of density dependence and competition for limited host resources can have a substantial effect on model results (van den Bosch & Gilligan, 2008). The inclusion, or otherwise, of stochasticity (Shaw, 1994) and levels of spatial heterogeneity (Cunniffe et al., 2015; Parnell et al., 2006; Shaw, 2000) should also be considered. However, it must be recognised that model parameter values for aspects of the system that are currently poorly understood can be very uncertain (Cunniffe et al., 2015; Shaw, 1994), but could still have a large impact on model results. Wherever possible, models should be parameterised and validated against experimental data, including data from field trials, to enable greater confidence in the model results.

The representation of the action of fungicides against the pathogen has an important influence on the conclusions of modelling studies (van den Bosch & Gilligan, 2008). Some models represent the average effect of a fungicide on pathogen severity or growth rate (Shaw, 1989), which can be directly calculated from experimental data if one assumes that the effect of the fungicide is constant over the period between application and measurement of fungicide efficacy. Models that explicitly represent fungicide dose decay and the resultant variation in the effect of the fungicide on the pathogen over time are more suitable for modelling cases where there is time-dependent interaction between factors affecting selection for resistance (for example Hobbelen et al., 2011a; Milne et al., 2007; van den Berg et al., 2013). The effect of a fungicide on the pathogen growth rate is a result of the combined effects of the fungicide on various pathogen life cycle processes, such as germination rate, sporulation rate and the length of the latent phase, which protectant and systemic fungicides may affect differently; this is represented explicitly in some modelling studies (e.g. Hobbelen et al., 2011b; Milne et al., 2007; van den Berg et al., 2013). The representation of the effect of fungicides in mixtures also affects model conclusions: for example whether the effect of two fungicides is additive or multiplicative (Morse, 1978; Paveley et al., 2003), and whether there is any synergy or antagonism (Shaw, 1989) between the fungicides. **Joint action of fungicides with incomplete cross-resistance within a MoA is not adequately represented by either the additive or multiplicative**

models, but is relevant for some important MoA groups including DMIs and SDHIs.

1.6   Project aims

The aim of my research is to investigate which strategies are likely to provide both effective resistance management and robust disease control in cases where resistance is evolving to two or more fungicides at the same time, both for fungicides with different modes of action (MoA) and in cases where there is variable resistance to fungicides with the same MoA ('incomplete cross-resistance'). I aim to use model simulations of the evolution of resistance for a wide range of scenarios to improve understanding of the trade-offs involved in managing concurrent evolution of resistance and inform strategies for current and future MoA.

1.7   Modelling approach

In this thesis, I use models derived from the approach of Hobbelen et al. (2011a, 2011b) to investigate the effects of different resistance management strategies on the rate of selection for resistance. These models were parameterised and validated with data on disease epidemic progress from multiple sites and years, and have subsequently been applied or adapted in a number of modelling studies (Elderfield et al., 2018; Hobbelen et al., 2013; Taylor & Cunniffe, 2023; van den Berg et al., 2013, 2016). The modelling approach describes the fungicide dose response curve as a combination of the foliar fungicide decay rate, which is used to track the 'effective dose' remaining at any point in time $D(t)$, and the effect of that dose on pathogen life cycle parameters such as transmission rate and latent period, measured as a fractional reduction, $f(t)$. The impact of the fungicide on the pathogen life cycle is greatest at large effective doses, where the maximum effect is defined by an 'asymptote parameter', and the rate at which the effect decreases with reducing fungicide doses is defined by a 'curvature parameter'. The type and magnitude of fungicide resistance is defined by its effect on the dose response of pathogen strains to the fungicide, reducing the asymptote or curvature parameters (Figure 1.4). Complete resistance means that the fungicide does not have any effect on the growth rate of the pathogen at any legal dose rate. Partial resistance might take the form of a reduction in the maximum effect of the fungicide on the pathogen growth rate even at large effective doses, or a reduction in the effect of smaller effective doses. I refer to these cases as 'asymptote shifts' and 'curvature shifts' respectively, representing their impacts on the dose response curve.
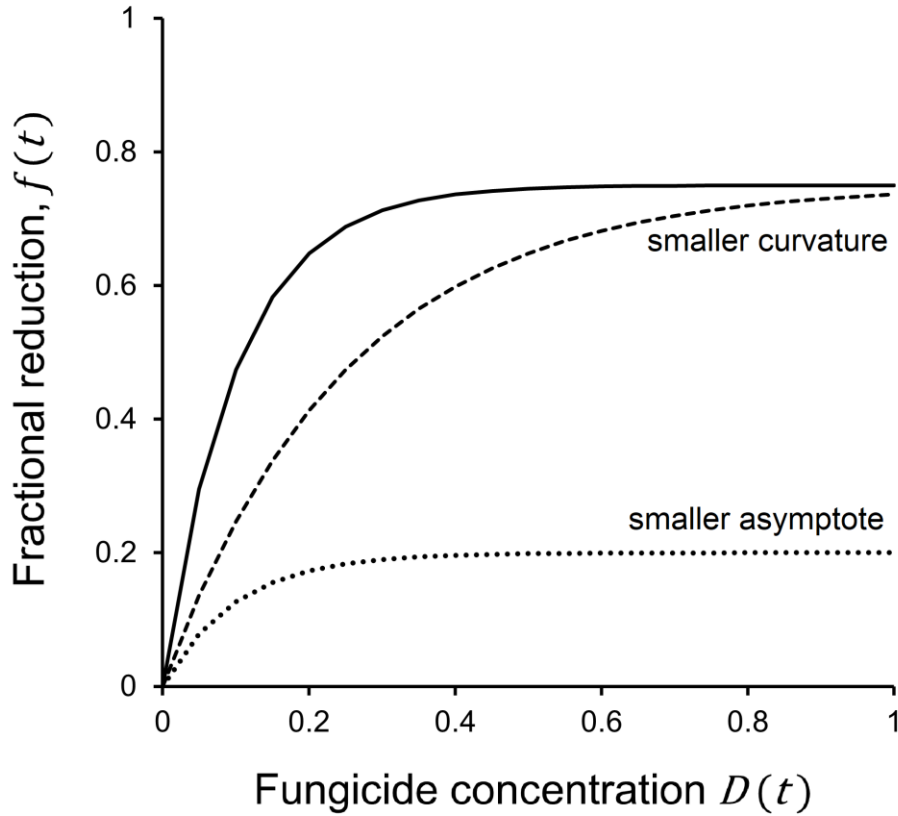
Figure 1.4: Fungicide dose response: effect of asymptote, curvature, and fungicide concentration, $D(t)$, on the fractional reduction $f(t)$ of pathogen life cycle parameters. $D(t)$ is expressed as a proportion of the maximum permitted individual dose (as defined on the product label).

I model two economically damaging foliar fungal pathogens in this thesis: *P. pachyrhizi* and *Z. tritici*. These pathogens are important case studies in their own right for management of fungicide resistance, but many of the evolutionary drivers I consider in my thesis are also generalisable to other fungal pathogens with similar life cycles. *Phakopsora pachyrhizi* is an obligate biotrophic foliar fungal pathogen of soybean crops, of concern in many soybean-producing regions including in Brazil (Godoy et al., 2016). It has a rapid population growth rate through asexual reproduction and can cause severe defoliation with yield losses of up to 80% when untreated, especially if infection occurs early in plant development (Dalla Lana et al., 2015; Hartman et al., 1991; Kumudini et al., 2008). Fungicides are a vital part of disease control in Brazil; due to the rapid development of epidemics, calendar-based application of two to five fungicide sprays per growing season is common (Beruski et al., 2020; Yorinori, 2021). However, this reliance on fungicides has led to rapid evolution of fungicide resistance (Dalla Lana et al., 2018; Godoy et al., 2016; Müller et al., 2021). *Zymoseptoria tritici* is one of the most common,

widespread and damaging pathogens affecting winter wheat crops in the UK, Ireland and Europe. When uncontrolled, it is associated with a reduction in crop quality and yield losses of 20-50% (Burke & Dunne, 2008; Fones & Gurr, 2015; Steinberg & Gurr, 2020), due to a reduction in the green leaf area of the crop available for photosynthesis. *Zymoseptoria tritici* infection of the upper leaf canopy proceeds mostly through asexual pycnidiospores, but it forms overwintering ascospores through sexual reproduction (Eriksen & Munk, 2003; Shaw & Royle, 1989). *Zymoseptoria tritici* is a highly adaptable pathogen (McDonald & Mundt, 2016) and has evolved varying levels of resistance to multiple MoAs, including QoI, DMI and SDHI fungicides, with impacts on disease control (Blake et al., 2018; Cools & Fraaije, 2013; Hellin et al., 2021; Jørgensen et al., 2022; Torriani et al., 2009; van den Bosch et al., 2020).

1.8   Key research questions

In this thesis, I address the following research questions:

1.a. What information does existing research provide to support choice of fungicide resistance management strategies, and what barriers prevent uptake of fungicide resistance management strategies?

These questions are addressed in a review paper (Chapter 2), summarising existing experimental and modelling evidence on the effect of fungicide dose rates, application timing, mixture and alternation strategies on selection for resistance. There is abundant evidence to support resistance management strategies against evolution of resistance to a single at-risk fungicide, but little evidence on which strategies are likely to work against concurrent evolution of resistance. Social, economic and information barriers preventing full uptake of fungicide resistance management strategies are reviewed in the section 'Principle versus practice'.

2. What is the value of phytosanitary cultural control for fungicide resistance management?

IPM measures have value for disease control and are typically at lower risk than fungicides from evolution of resistance or pathogen adaptation. IPM measures that directly suppress pathogen growth rates will minimise the difference between the growth rates of sensitive and resistant strains, directly reducing the fitness advantage of resistant strains and therefore contributing to fungicide resistance management. The fungicide resistance management value of phytosanitary cultural control methods that do not suppress pathogen growth rates after the onset of infection is less clear. However, delaying the onset of disease has the potential

to reduce the maximum severity of the epidemic and to reduce the level of chemical control required for adequate disease control. In Chapter 3, I explore the value of phytosanitary cultural control methods in the asexual pathogen *Phakopsora pachyrhizi* (Asian soybean rust) for resistance management of a strain with resistance to an SDHI fungicide, in combination with mixtures of different MoAs with varying dose rates, number and timing of applications. I describe the development and parameterisation of a compartment epidemiological model of *P. pachyrhizi*, including parameterisation and validation of fungicide dose response parameters from commercial field trial data.

3. How does the impact of dose splitting vary with fungicide properties and the type and magnitude of resistance?

Dose splitting is a key trade-off for management of concurrent evolution of resistance, as if multiple applications are needed to control disease, use of mixture would require splitting the total dose of a fungicide across two or more applications. The drivers of variation in the effects of dose splitting are not well understood. Previous modelling studies have predicted that dose splitting without a mixture partner will increase selection for strains with an asymptote shift, because increased exposure time increases selection more than halving the dose at each application timing reduces selection. However, variable effects of dose splitting on selection for resistance have been observed in field experiments, and the effect of dose splitting on selection for partially resistant strains with a curvature shift is not known. In Chapter 4, I use a compartmental epidemiological model of *Z. tritici* to investigate how the effect of dose splitting on selection for resistance to a single fungicide varies with fungicide properties and the type and magnitude of resistance.

4. Which is the better strategy against concurrent evolution of resistance: alternation or splitting and mixing?

To address this question, I use *Z. tritici* as a case study to investigate the rate of selection for double-resistant strains when two at-risk MoA are either mixed (with dose-splitting) or alternated (without dose-splitting). In Chapter 5, I extend the model developed in Chapter 4 to include the effects of sexual reproduction on the frequencies of sensitive, single-resistant and double-resistant strains. Since the results reported in Chapter 4 show that the effect of dose splitting on selection for resistance varies with fungicide properties and the type and magnitude of resistance, I model scenarios of concurrent evolution of resistance across a large

range of combinations of fungicide dose response parameters, asymptote and curvature shifts.

5. Can incomplete cross-resistance within a fungicidal mode of action be useful for resistance management?

The success of mixture between fungicides with different MoA relies on the general absence of cross-resistance between MoAs. Mixtures of fungicides with the same MoA and complete cross-resistance do not contribute to resistance management. Existing models of the joint action in mixture of two or more fungicides on pathogen growth rates typically use either an additive dose model (ADM) or a multiplicative survival model (MSM), assuming complete cross-resistance or the complete absence of cross-resistance respectively. However, in some cases cross-resistance is only partial within a MoA, for example azole fungicides in the demethylation inhibitor (DMI) group. In Chapter 6, I describe the development of a mathematical population genetic model to explore possible resistance management benefits of mixtures of fungicides with the same MoA with incomplete cross-resistance. I investigate how the resistance management benefits of mixture of fungicides with the same MoA but incomplete cross-resistance vary with the number of fungicides and the degree of cross-resistance between fungicides included in the mixture. I compare the performance of programmes utilising mixture, alternation or mosaic within a MoA with incomplete cross-resistance.

1.9   References

Abuley, I.K., Lynott, J.S., Hansen, J.G., Cooke, D.E.L., & Lees, A.K. (2023). The EU43 genotype of *Phytophthora infestans* displays resistance to mandipropamid. *Plant Pathology*, *72*(7), 1305–1313. https://doi.org/10.1111/ppa.13737

Ballu, A., Ugazio, C., Duplaix, C., Noly, A., Wullschleger, J., Torriani, S.F.F. et al. (2024). Preventing multiple resistance above all: New insights for managing fungal adaptation. *Environmental Microbiology*, *26*(4). https://doi.org/10.1111/1462-2920.16614

Barnes, G., Saunders, D.G.O., & Williamson, T. (2020). Banishing barberry: The history of *Berberis vulgaris* prevalence and wheat stem rust incidence across Britain. *Plant Pathology*, *69*(7), 1193–1202. https://doi.org/10.1111/ppa.13231

Beruski, G.C., Del Ponte, E.M., Pereira, A.B., Gleason, M.L., Câmara, G.M.S., Araújo Junior, I. P. et al. (2020). Performance and Profitability of Rain-Based

Thresholds for Timing Fungicide Applications in Soybean Rust Control. *Plant Disease*, *104*(10), 2704–2712. https://doi.org/10.1094/PDIS-01-20-0210-RE

Birch, C.P.D., & Shaw, M.W. (1997). When can Reduced Doses and Pesticide Mixtures Delay the Build-up of Pesticide Resistance? A Mathematical Model. *The Journal of Applied Ecology*, *34*(4), 1032. https://doi.org/10.2307/2405292

Blake, J.J., Gosling, P., Fraaije, B.A., Burnett, F.J., Knight, S.M., Kildea, S. et al. (2018). Changes in field dose–response curves for demethylation inhibitor (DMI) and quinone outside inhibitor (QoI) fungicides against *Zymoseptoria tritici*, related to laboratory sensitivity phenotyping and genotyping assays. *Pest Management Science*, *74*(2), 302–313. https://doi.org/10.1002/ps.4725

Box, G.E.P. (1976). Science and Statistics. *Journal of the American Statistical Association*, *71*(356), 791. https://doi.org/10.2307/2286841

Brown, J.K.M. (2015). Durable Resistance of Crops to Disease: A Darwinian Perspective. *Annual Review of Phytopathology*, *53*(1), 513–539. https://doi.org/10.1146/annurev-phyto-102313-045914

Bryson, R. (2022). Evaluating the contribution of synthetic fungicides to cereal plant health and CO_2 reduction targets against the backdrop of the increasingly complex regulatory environment in Europe. *Plant Pathology*, *71*(1), 170–186. https://doi.org/10.1111/ppa.13494

Burke, J.J., & Dunne, B. (2008). Field testing of six decision support systems for scheduling fungicide applications to control *Mycosphaerella graminicola* on winter wheat crops in Ireland. *The Journal of Agricultural Science*, *146*(4), 415–428. https://doi.org/10.1017/S0021859607007642

Carolan, K., Helps, J., van den Berg, F., Bain, R., Paveley, N., & van den Bosch, F. (2017). Extending the durability of cultivar resistance by limiting epidemic growth rates. *Proceedings of the Royal Society B: Biological Sciences*, *284*(1863), 20170828. https://doi.org/10.1098/rspb.2017.0828

Chaloner, T.M., Gurr, S.J., & Bebber, D.P. (2021). Plant pathogen infection risk tracks global crop yields under climate change. *Nature Climate Change*, *11*(8), 710–715. https://doi.org/10.1038/s41558-021-01104-8

Chapman, K.S., Sundin, G.W., & Beckerman, J.L. (2011). Identification of Resistance to Multiple Fungicides in Field Populations of *Venturia inaequalis*. *Plant Disease*, *95*(8), 921–926. https://doi.org/10.1094/PDIS-12-10-0899

Chatzidimopoulos, M., Zambounis, A., Lioliopoulou, F., & Vellios, E. (2022). Detection of Venturia inaequalis Isolates with Multiple Resistance in Greece. *Microorganisms*, *10*(12), 2354. https://doi.org/10.3390/microorganisms10122354

Chen, R.-S., & McDonald, B.A. (1996). Sexual Reproduction Plays a Major Role in the Genetic Structure of Populations of the Fungus *Mycosphaerella graminicola*. *Genetics*, *142*(4), 1119–1127. https://doi.org/10.1093/genetics/142.4.1119

Cooke, L.R., Schepers, H.T.A.M., Hermansen, A., Bain, R.A., Bradshaw, N.J., Ritchie, F. et al. (2011). Epidemiology and Integrated Control of Potato Late Blight in Europe. *Potato Research*, *54*(2), 183–222. https://doi.org/10.1007/s11540-011-9187-0

Cools, H.J., & Fraaije, B.A. (2013). Update on mechanisms of azole resistance in *Mycosphaerella graminicola* and implications for future control. *Pest Management Science*, *69*(2), 150–155. https://doi.org/10.1002/ps.3348

Corkley, I., Fraaije, B., & Hawkins, N. (2022). Fungicide resistance management: Maximizing the effective life of plant protection products. *Plant Pathology*, *71*(1). https://doi.org/10.1111/ppa.13467

Cunniffe, N.J., Koskella, B., Metcalf, C.J.E., Parnell, S., Gottwald, T. R., & Gilligan, C.A. (2015). Thirteen challenges in modelling plant diseases. *Epidemics*, *10*, 6–10. https://doi.org/10.1016/j.epidem.2014.06.002

Dalla Lana, F., Paul, P.A., Godoy, C.V., Utiamada, C.M., Da Silva, L.H.C.P., Siqueri, F.V. et al. (2018). Meta-analytic modeling of the decline in performance of fungicides for managing soybean rust after a decade of use in Brazil. *Plant Disease*, *102*(4), 807–817. https://doi.org/10.1094/PDIS-03-17-0408-RE

Dalla Lana, F., Ziegelmann, P.K., De Maia, A.H.N., Godoy, C.V., & Del Ponte, E.M. (2015). Meta-analysis of the relationship between crop yield and soybean rust severity. *Phytopathology*, *105*(3), 307–315. https://doi.org/10.1094/PHYTO-06-14-0157-R

Deising, H.B., Reimann, S., & Pascholati, S.F. (2008). Mechanisms and significance of fungicide resistance. *Brazilian Journal of Microbiology*, *39*, 286–295.

Dooley, H., Shaw, M.W., Spink, J., & Kildea, S. (2016). The effect of succinate dehydrogenase inhibitor/azole mixtures on selection of *Zymoseptoria tritici* isolates with reduced sensitivity. *Pest Management Science*, *72*(6), 1150–1159. https://doi.org/10.1002/ps.4093

Dorigan, A.F., Moreira, S.I., da Silva Costa Guimarães, S., Cruz-Magalhães, V., & Alves, E. (2023). Target and non-target site mechanisms of fungicide resistance and their implications for the management of crop pathogens. *Pest Management Science*, *79*(12), 4731–4753. https://doi.org/10.1002/ps.7726

Elderfield, J.A.D., Lopez-Ruiz, F.J., van den Bosch, F., & Cunniffe, N.J. (2018). Using Epidemiological Principles to Explain Fungicide Resistance Management Tactics: Why do Mixtures Outperform Alternations? *Phytopathology®*, *108*(7), 803–817. https://doi.org/10.1094/PHYTO-08-17-0277-R

Eriksen, L., & Munk, L. (2003). The Occurrence of *Mycosphaerella graminicola* and its Anamorph *Septoria tritici* in Winter Wheat during the Growing Season. *European Journal of Plant Pathology*, *109*(3), 253–259. https://doi.org/10.1023/A:1022851502770

Fantke, P., & Juraske, R. (2013). Variability of Pesticide Dissipation Half-Lives in Plants. *Environmental Science & Technology*, *47*(8), 3548–3562. https://doi.org/10.1021/es303525x

Fisher, M.C., Henk, D.A., Briggs, C.J., Brownstein, J.S., Madoff, L.C., McCraw, S.L. et al. (2012). Emerging fungal threats to animal, plant and ecosystem health. *Nature*, *484*(7393), 186–194. https://doi.org/10.1038/nature10947

Fones, H., & Gurr, S. (2015). The impact of Septoria tritici Blotch disease on wheat: An EU perspective. *Fungal Genetics and Biology*, *79*, 3–7. https://doi.org/10.1016/j.fgb.2015.04.004

Fones, H.N., Bebber, D.P., Chaloner, T.M., Kay, W.T., Steinberg, G., & Gurr, S.J. (2020). Threats to global food security from emerging fungal and oomycete crop pathogens. *Nature Food*, *1*(6), 332–342. https://doi.org/10.1038/s43016-020-0075-0

Garnault, M., Duplaix, C., Leroux, P., Couleaud, G., Carpentier, F., David, O. et al. (2019). Spatiotemporal dynamics of fungicide resistance in the wheat pathogen *Zymoseptoria tritici* in France. *Pest Management Science*, *75*(7), 1794–1807. https://doi.org/10.1002/ps.5360

Godoy, C.V., Seixas, C.D.S., Soares, R.M., Marcelino-Guimarães, F.C., Meyer, M.C., & Costamilan, L.M. (2016). Asian soybean rust in Brazil: past, present, and future. *Pesquisa Agropecuária Brasileira*, *51*(5), 407–421. https://doi.org/10.1590/S0100-204X2016000500002

Grimmer, M.K., van den Bosch, F., Powers, S.J., & Paveley, N.D. (2015). Fungicide resistance risk assessment based on traits associated with the rate of pathogen evolution. *Pest Management Science*, *71*(2), 207–215. https://doi.org/10.1002/ps.3781

Hartman, G.L., Wang, T.C., & Tschanz, A.T. (1991). Soybean Rust Development and the Quantitative Relationship Between Rust Severity and Soybean Yield. *Plant Disease*, *75*(6), 596. https://doi.org/10.1094/PD-75-0596

Hawkins, N.J., Bass, C., Dixon, A., & Neve, P. (2019). The evolutionary origins of pesticide resistance. *Biological Reviews*, *94*(1), 135–155. https://doi.org/10.1111/brv.12440

Hellin, P., Duvivier, M., Heick, T.M., Fraaije, B.A., Bataille, C., Clinckemaillie, A. et al. (2021). Spatio-temporal distribution of DMI and SDHI fungicide resistance of *Zymoseptoria tritici* throughout Europe based on frequencies of key target-site alterations. *Pest Management Science*, *77*(12), 5576–5588. https://doi.org/10.1002/ps.6601

Helps, J.C., Paveley, N.D., White, S., & van den Bosch, F. (2020). Determinants of optimal insecticide resistance management strategies. *Journal of Theoretical Biology*, *503*, 110383. https://doi.org/10.1016/j.jtbi.2020.110383

Hobbelen, P.H.F., Paveley, N.D., Fraaije, B.A., Lucas, J.A., & van den Bosch, F. (2011a). Derivation and testing of a model to predict selection for fungicide resistance. *Plant Pathology*, *60*(2), 304–313. https://doi.org/10.1111/j.1365-3059.2010.02380.x

Hobbelen, P.H.F., Paveley, N.D., & van den Bosch, F. (2011b). Delaying selection for fungicide insensitivity by mixing fungicides at a low and high risk of resistance development: A modeling analysis. *Phytopathology*, *101*(10), 1224–1233. https://doi.org/10.1094/PHYTO-10-10-0290

Hobbelen, P.H.F., Paveley, N.D., Oliver, R.P., & van den Bosch, F. (2013). The Usefulness of Fungicide Mixtures and Alternation for Delaying the Selection for Resistance in Populations of *Mycosphaerella graminicola* on Winter Wheat: A Modeling Analysis. *Phytopathology®*, *103*(7), 690–707. https://doi.org/10.1094/PHYTO-06-12-0142-R

Hobbelen, P. H. F., Paveley, N. D., & van den Bosch, F. (2014). The Emergence of Resistance to Fungicides. *PLoS ONE*, *9*(3), e91910. https://doi.org/10.1371/journal.pone.0091910

Hollomon, D.W., & Brent, K.J. (2009). Combating plant diseases—the Darwin connection. *Pest Management Science*, *65*(11), 1156–1163. https://doi.org/10.1002/ps.1845

Ivanov, A.A., Ukladov, E.O., & Golubeva, T.S. (2021). *Phytophthora infestans*: An Overview of Methods and Attempts to Combat Late Blight. *Journal of Fungi*, *7*(12), 1071. https://doi.org/10.3390/jof7121071

Jørgensen, L.N., Hovmøller, M.S., Hansen, J.G., Lassen, P., Clark, B., Bayles, R. et al. (2014). IPM Strategies and Their Dilemmas Including an Introduction to www.eurowheat.org. *Journal of Integrative Agriculture*, *13*(2), 265–281. https://doi.org/10.1016/S2095-3119(13)60646-2

Jørgensen, L.N., Matzen, N., Heick, T.M., O'Driscoll, A., Clark, B., Waite, K. et al. (2022). Shifting sensitivity of septoria tritici blotch compromises field performance and yield of main fungicides in Europe. *Frontiers in Plant Science*, *13*. https://doi.org/10.3389/fpls.2022.1060428

Kristoffersen, R., Heick, T.M., Müller, G.M., Eriksen, L.B., Nielsen, G.C., & Jørgensen, L.N. (2020). The potential of cultivar mixtures to reduce fungicide input and mitigate fungicide resistance development. *Agronomy for Sustainable Development*, *40*(5), 36. https://doi.org/10.1007/s13593-020-00639-y

Kumudini, S., Godoy, C.V., Board, J.E., Omielan, J., & Tollenaar, M. (2008). Mechanisms involved in soybean rust-induced yield reduction. *Crop Science*, *48*(6), 2334–2342. https://doi.org/10.2135/cropsci2008.01.0009

Lucas, J.A., Hawkins, N.J., & Fraaije, B.A. (2015). *The Evolution of Fungicide Resistance* (pp. 29–92). https://doi.org/10.1016/bs.aambs.2014.09.001

Mair, W.J., Thomas, G.J., Dodhia, K., Hills, A.L., Jayasena, K.W., Ellwood, S.R. et al. (2020). Parallel evolution of multiple mechanisms for demethylase inhibitor fungicide resistance in the barley pathogen *Pyrenophora teres* f. sp. *maculata*. *Fungal Genetics and Biology*, *145*, 103475. https://doi.org/10.1016/j.fgb.2020.103475

Mair, W.J., Wallwork, H., Garrard, T.A., Haywood, J., Sharma, N., Dodhia, K.N. et al. (2023). Emergence of resistance to succinate dehydrogenase inhibitor fungicides in *Pyrenophora teres* f. *teres and P. teres* f. *maculata* in Australia. *bioRxiv* 2023.04.23.537974. https://doi.org/10.1101/2023.04.23.537974

McDonald, B.A., & Mundt, C.C. (2016). How Knowledge of Pathogen Population Biology Informs Management of Septoria Tritici Blotch. *Phytopathology®*, *106*(9), 948–955. https://doi.org/10.1094/PHYTO-03-16-0131-RVW

McDonald, B.A., Suffert, F., Bernasconi, A., & Mikaberidze, A. (2022). How large and diverse are field populations of fungal plant pathogens? The case of *Zymoseptoria tritici*. *Evolutionary Applications*, *15*(9), 1360–1373. https://doi.org/10.1111/eva.13434

Meitz-Hopkins, J.C., von Diest, S.G., Koopman, T.A., Tobutt, K.R., Xu, X., & Lennox, C.L. (2023). Leaf shredding as an alternative strategy for managing apple scab resistance to demethylation inhibitor fungicides. *Frontiers in Horticulture*, *2*. https://doi.org/10.3389/fhort.2023.1175168

Mikaberidze, A., Paveley, N., Bonhoeffer, S., & van den Bosch, F. (2017). Emergence of Resistance to Fungicides: The Role of Fungicide Dose.

Phytopathology®, *107*(5), 545–560. https://doi.org/10.1094/PHYTO-08-16-0297-R

Milgroom, M.G. (1990). A Stochastic Model for the Initial Occurrence and Development of Fungicide Resistance in Plant Pathogen Populations. *Phytopathology*, *80*(4), 410. https://doi.org/10.1094/Phyto-80-410

Milgroom, M.G., & Fry, W.E. (1988). A Simulation Analysis of the Epidemiological Principles for Fungicide Resistance Management in Pathogen Populations. *Phytopathology*, *78*(5), 565. https://doi.org/10.1094/Phyto-78-565

Milne, A., Paveley, N., Audsley, E., & Parsons, D. (2007). A model of the effect of fungicides on disease-induced yield loss, for use in wheat disease management decision support systems. *Annals of Applied Biology*, *151*(1), 113–125. https://doi.org/10.1111/j.1744-7348.2007.00158.x

Morse, P.M. (1978). Some Comments on the Assessment of Joint Action in Herbicide Mixtures. *Weed Science*, *26*(1), 58–71. https://doi.org/10.1017/S0043174500032690

Müller, M.A., Stammler, G., & May De Mio, L.L. (2021). Multiple resistance to DMI, QoI and SDHI fungicides in field isolates of Phakopsora pachyrhizi. *Crop Protection*, *145*, 105618. https://doi.org/10.1016/j.cropro.2021.105618

Nasonov, A.I., & Yakuba, G.V. (2024). Apple Scab: Resistance to Chemical Fungicides. *Biology Bulletin Reviews*, *14*(S1), S17–S30. https://doi.org/10.1134/S2079086424600802

Oerke, E.-C. (2006). Crop losses to pests. *The Journal of Agricultural Science*, *144*(1), 31–43. https://doi.org/10.1017/S0021859605005708

Omrane, S., Audéon, C., Ignace, A., Duplaix, C., Aouini, L., Kema, G. et al. (2017). Plasticity of the *MFS1* Promoter Leads to Multidrug Resistance in the Wheat Pathogen *Zymoseptoria tritici*. *MSphere*, *2*(5). https://doi.org/10.1128/mSphere.00393-17

Parnell, S., van den Bosch, F., & Gilligan, C.A. (2006). Large-Scale Fungicide Spray Heterogeneity and the Regional Spread of Resistant Pathogen Strains. *Phytopathology®*, *96*(5), 549–555. https://doi.org/10.1094/PHYTO-96-0549

Paveley, N.D., Thomas, J.M., Vaughan, T.B., Havis, N.D., & Jones, D.R. (2003). Predicting effective doses for the joint action of two fungicide applications. *Plant Pathology*, *52*(5), 638–647. https://doi.org/10.1046/j.1365-3059.2003.00881.x

Peterson, P.D. (2018). The Barberry Eradication Program in Minnesota for Stem Rust Control: A Case Study. *Annual Review of Phytopathology*, *56*(1), 203–223. https://doi.org/10.1146/annurev-phyto-080417-050133

Pütsepp, R., Mäe, A., Põllumaa, L., Andresen, L., & Kiiker, R. (2024). Fungicide Sensitivity Profile of *Pyrenophora teres* f. *teres* in Field Population. *Journal of Fungi*, *10*(4), 260. https://doi.org/10.3390/jof10040260

Rangel, L.I., Spanner, R.E., Ebert, M.K., Pethybridge, S.J., Stukenbrock, E.H., de Jonge, R. et al. (2020). *Cercospora beticola* : The intoxicating lifestyle of the leaf spot pathogen of sugar beet. *Molecular Plant Pathology*, *21*(8), 1020–1041. https://doi.org/10.1111/mpp.12962

Rosenzweig, N., Hanson, L.E., Mambetova, S., Jiang, Q., Guza, C., Stewart, J. et al. (2020). Temporal population monitoring of fungicide sensitivity in *Cercospora beticola* from sugarbeet (*Beta vulgaris*) in the Upper Great Lakes. *Canadian Journal of Plant Pathology*, *42*(4), 469–479. https://doi.org/10.1080/07060661.2019.1705914

Rupp, S., Weber, R.W.S., Rieger, D., Detzel, P., & Hahn, M. (2017). Spread of *Botrytis cinerea* Strains with Multiple Fungicide Resistance in German Horticulture. *Frontiers in Microbiology*, *7*. https://doi.org/10.3389/fmicb.2016.02075

Savary, S., Willocquet, L., Pethybridge, S.J., Esker, P., McRoberts, N., & Nelson, A. (2019). The global burden of pathogens and pests on major food crops. *Nature Ecology & Evolution*, *3*(3), 430–439. https://doi.org/10.1038/s41559-018-0793-y

Searchinger, T., Waite, R., Hanson, C., Ranganathan, J., Dumas, P., Matthews E., et al. (2019). Creating a Sustainable Food Future: A Menu of Solutions to Feed Nearly 10 Billion People by 2050. World Resources Institute Report. Available at: https://research.wri.org/sites/default/files/2019-07/WRR_Food_Full_Report_0.pdf [Accessed 22 November 2024].

Shaw, M.W. (1989). Independent action of fungicides and its consequences for strategies to retard the evolution of fungicide resistance. *Crop Protection*, *8*(6), 405–411. https://doi.org/10.1016/0261-2194(89)90065-3

Shaw, M.W. (1994). Modeling stochastic processes in plant pathology. *Annual Review of Phytopathology*, *32*(1), 523–544. https://doi.org/10.1146/annurev.py.32.090194.002515

Shaw, M.W. (2000). Models of the Effects of Dose Heterogeneity and Escape on Selection Pressure for Pesticide Resistance. *Phytopathology®*, *90*(4), 333–339. https://doi.org/10.1094/PHYTO.2000.90.4.333

Shaw, M.W. (2006). Is there such a thing as a resistance management strategy? A modeller's perspective. *Annals of Applied Biology*, *78*, 95–103.

Shaw, M.W., & Royle, D.J. (1989). Airborne inoculum as a major source of *Septoria tritici* (*Mycosphaerella graminicola*) infections in winter wheat crops in the UK. *Plant Pathology*, *38*(1), 35–43.
https://doi.org/10.1111/j.1365-3059.1989.tb01425.x

Skylakakis, G. (1981). Effects of alternating and mixing pesticides on the buildup of fungal resistance. *Phytopathology* 71, 1119-1121.

Sofianos, G., Samaras, A., & Karaoglanidis, G. (2023). Multiple and multidrug resistance in *Botrytis cinerea*: molecular mechanisms of MLR/MDR strains in Greece and effects of co-existence of different resistance mechanisms on fungicide sensitivity. *Frontiers in Plant Science*, *14*.
https://doi.org/10.3389/fpls.2023.1273193

Steinberg, G., & Gurr, S.J. (2020). Fungi, fungicide discovery and global food security. *Fungal Genetics and Biology*, *144*, 103476.
https://doi.org/10.1016/j.fgb.2020.103476

Taylor, N.P., & Cunniffe, N.J. (2023a). Modelling quantitative fungicide resistance and breakdown of resistant cultivars: Designing integrated disease management strategies for Septoria of winter wheat. *PLOS Computational Biology*, *19*(3), e1010969. https://doi.org/10.1371/journal.pcbi.1010969

Taylor, N.P., & Cunniffe, N.J. (2023b). Optimal Resistance Management for Mixtures of High-Risk Fungicides: Robustness to the Initial Frequency of Resistance and Pathogen Sexual Reproduction. *Phytopathology*, *113*(1), 55–69. https://doi.org/10.1094/PHYTO-02-22-0050-R

te Beest, D.E., Paveley, N.D., Shaw, M.W., & van den Bosch, F. (2013). Accounting for the Economic Risk Caused by Variation in Disease Severity in Fungicide Dose Decisions, Exemplified for *Mycosphaerella graminicola* on Winter Wheat. *Phytopathology®*, *103*(7), 666–672. https://doi.org/10.1094/PHYTO-05-12-0119-R

Torriani, S.F., Brunner, P.C., McDonald, B.A., & Sierotzki, H. (2009). QoI resistance emerged independently at least 4 times in European populations of *Mycosphaerella graminicola*. *Pest Management Science*, *65*(2), 155–162. https://doi.org/10.1002/ps.1662

Trkulja, N.R., Milosavljević, A.G., Mitrović, M.S., Jović, J.B., Toševski, I.T., Khan, M.F.R., & Secor, G.A. (2017). Molecular and experimental evidence of multi-resistance of *Cercospora beticola* field populations to MBC, DMI and QoI fungicides. *European Journal of Plant Pathology*, *149*(4), 895–910. https://doi.org/10.1007/s10658-017-1239-0

UN (2024). Global Issues: Population. Available at: https://www.un.org/en/global-issues/population [Accessed 22 November 2024].

van den Berg, F., Paveley, N.D., & van den Bosch, F. (2016). Dose and number of applications that maximize fungicide effective life exemplified by *Zymoseptoria tritici* on wheat – a model analysis. *Plant Pathology*, *65*(8), 1380–1389. https://doi.org/10.1111/ppa.12558

van den Berg, F., van den Bosch, F., & Paveley, N.D. (2013). Optimal Fungicide Application Timings for Disease Control Are Also an Effective Anti-Resistance Strategy: A Case Study for *Zymoseptoria tritici* (*Mycosphaerella graminicola*) on Wheat. *Phytopathology®*, *103*(12), 1209–1219. https://doi.org/10.1094/PHYTO-03-13-0061-R

van den Bosch, F., Blake, J., Gosling, P., Helps, J.C., & Paveley, N. (2020). Identifying when it is financially beneficial to increase or decrease fungicide dose as resistance develops: An evaluation from long-term field experiments. *Plant Pathology*, *69*(4), 631–641. https://doi.org/10.1111/ppa.13155

van den Bosch, F., & Gilligan, C.A. (2008). Models of Fungicide Resistance Dynamics. *Annual Review of Phytopathology*, *46*(1), 123–147. https://doi.org/10.1146/annurev.phyto.011108.135838

van den Bosch, F., Lopez-Ruiz, F., Oliver, R., Paveley, N., Helps, J., & van den Berg, F. (2018). Identifying when it is financially beneficial to increase or decrease fungicide dose as resistance develops. *Plant Pathology*, *67*(3), 549–560. https://doi.org/10.1111/ppa.12787

van den Bosch, F., Oliver, R., van den Berg, F., & Paveley, N. (2014a). Governing Principles Can Guide Fungicide-Resistance Management Tactics. *Annual Review of Phytopathology*, *52*(1), 175–195. https://doi.org/10.1146/annurev-phyto-102313-050158

van den Bosch, F., Paveley, N., van den Berg, F., Hobbelen, P., & Oliver, R. (2014b). Mixtures as a Fungicide Resistance Management Tactic. *Phytopathology®*, *104*(12), 1264–1273. https://doi.org/10.1094/PHYTO-04-14-0121-RVW

van den Bosch, F., Paveley, N., Shaw, M., Hobbelen, P., & Oliver, R. (2011). The dose rate debate: does the risk of fungicide resistance increase or decrease with dose? *Plant Pathology*, *60*(4), 597–606. https://doi.org/10.1111/j.1365-3059.2011.02439.x

van den Bosch, F., Smith, J., Wright, P., Milne, A., van den Berg, F., Kock-Appelgren, P. et al. (2022). Maximizing realized yield by breeding for disease

tolerance: A case study for Septoria tritici blotch. *Plant Pathology*, *71*(3), 535–543. https://doi.org/10.1111/ppa.13509

Vincent, C., Rancourt, B., & Carisse, O. (2004). Apple leaf shredding as a non-chemical tool to manage apple scab and spotted tentiform leafminer. *Agriculture, Ecosystems & Environment*, *104*(3), 595–604. https://doi.org/10.1016/j.agee.2004.01.027

Yorinori, J.T. (2021). CHAPTER 5: Difficulties Controlling Soybean Rust. In *Soybean Rust: Lessons Learned from the Pandemic in Brazil* (pp. 75–86). The American Phytopathological Society. https://doi.org/10.1094/9780890546642.05

Young, C., Boor, T., Corkley, I., Fraaije, B., Clark, B., Havis, N. et al. (2021). Managing resistance evolving concurrently against two or more modes of action to extend the effective life of fungicides. AHDB Project Report No. 637, pp 1–91. Available at: https://projectblue.blob.core.windows.net/media/Default/Research%20Papers/Cereals%20and%20Oilseed/2021/PR637%20final%20project%20report.pdf [Accessed: 1 August 2024].

Zhan, J., Pettway, R.E., & McDonald, B.A. (2003). The global genetic structure of the wheat pathogen Mycosphaerella graminicola is characterized by high nuclear diversity, low mitochondrial diversity, regular recombination, and gene flow. *Fungal Genetics and Biology*, *38*(3), 286–297. https://doi.org/10.1016/S1087-1845(02)00538-8

Chapter 2

Fungicide resistance management: Maximising the effective life of plant protection products

I. Corkley[1,2,3], B. Fraaije[4], N. Hawkins[4]

[1]ADAS, Wolverhampton, UK. [2]Rothamsted Research, Harpenden, UK. [3]University of Reading, Reading, UK. [4]NIAB, Cambridge, UK.

The following review paper was published in *Plant Pathology* **71**(1):150-169 in September 2021. I **summarise existing research on resistance management strategies, covering the effects of dose rates, application timing, and use of mixtures or alternations of different fungicides**.

The review highlights the **fundamental role of IPM as part of fungicide resistance management, including cultural control** and use of resistant crop cultivars, to reduce pathogen growth rates and the intensity of fungicide application required, thereby reducing selection for resistant pathogen strains.

Information gaps for the management of concurrent evolution of resistance are identified, including **variability in the benefits of mixture depending on mixture components**, and a **lack of modelling evidence on the relative benefits of mixture and alternation as resistance management strategies in fungal pathogens with a life cycle including a sexual reproduction stage**.

The **potential for mixtures of fungicides with partial cross-resistance to contribute to resistance management** is introduced and experimental evidence reviewed; no modelling evidence was found.

I also consider **barriers to uptake of resistance management strategies** in the section 'Principle Versus Practice'. For successful uptake, tactics must be economic, practically achievable and clearly and consistently communicated.

2.1   Abstract

Effective crop protection is vital to safeguard food security, but growers are reliant on a limited toolbox in the face of diverse and evolving pathogens. New crop

protection methods need to be developed, but it is also important to prolong the effective life of existing products through resistance management.

Some core principles in fungicide resistance management, such as using different modes of action and limiting repeat applications of any single mode of action, are long established. However, other aspects have been long debated, such as using higher or lower dose rates, mixtures or alternations, and whether to spray protectively or only if a disease threshold is reached.

Continuing research into these questions uses a range of approaches, including modelling, experimental trials, and ongoing monitoring of pathogen populations. Molecular diagnostics allow higher-throughput monitoring and earlier detection of emerging resistance. Resistance management guidelines must also be continually updated as new fungicides, and other crop protection measures, are introduced.

However, designing optimal resistance management strategies is only half of the story, because a strategy will only be effective if growers follow it in practice. This is more difficult where there are hard trade-offs between reducing selection for resistance in the future and achieving greater disease control in the present, or where there is a choice between a strategy that would be optimal on average or one that minimises the risk of control failure in any year. Therefore, communication with farmers is an aspect of resistance management that must not be overlooked.

2.2   Introduction

Over a third of potential crop production worldwide is lost pre-harvest to pests and diseases (Oerke and Dehne, 2004), with pathogen-related spoilage also contributing to post-harvest food waste. Without effective crop protection, it has been estimated that pre-harvest losses would double (Popp et al., 2013).

Crop protection against plant pathogens relies heavily on fungicide use in addition to varietal resistance. However, repeated use of single-site fungicides with the same mode of action (MoA) can lead to the evolution of resistance. The total economic cost of resistance against all pesticides in the US was calculated at $1.5 billion USD in 2005, primarily due to additional pesticide use in order to control pests resistant to previously-effective treatments (Pimentel, 2005).

The first site-specific fungicides were the methyl benzimidazole carbamates (MBCs), and in their 50 years of use, resistance has been reported in almost 100 plant pathogen species (Hawkins and Fraaije, 2016; FRAC, 2020b). In some pathogens, resistance emerged after just two years of fungicide use (Grimmer et

al., 2015). Azole resistance has been reported in 30 plant pathogens (FRAC, 2020b), in over 60 countries (Fisher et al., 2018). Quinone outside inhibitor (QoI) resistance has been reported in almost 50 species (FRAC, 2020b) after two decades of use, but in one pathogen, resistance emerged after just one year of use (Grimmer et al., 2015). Resistance has evolved against all major single-site fungicide classes, and in the case of the grey mould pathogen *Botrytis cinerea*, resistance against 15 different fungicide classes has been reported in a single pathogen species (FRAC, 2020b; Hahn, 2014) and resistance to seven modes of action in single isolates (Fernandez Ortuno et al., 2014).

With the loss of effective fungicides due to resistance, as well as public concerns about potential environmental and health impacts of agrochemicals, there is an increasing focus on developing non-chemical control measures and using integrated pest management (IPM) strategies (Birch et al., 2011; Pertot et al., 2017). However, for many crops, chemical control is still likely to be a necessary part of crop protection for the foreseeable future (Popp, 2011), so fungicide resistance management strategies must be deployed in order to extend the effective lifespan of available products.

Concerns about resistance, and the need to develop consistent guidelines for resistance management, led to the formation of the Fungicide Resistance Action Committee (FRAC) by CropLife International, a consortium of agrochemical companies, because multiple companies produce fungicides with the same mode of action and so coordinated guidelines are needed (Brent and Hollomon, 2007). In addition, regional groups, such as FRAG-UK in the United Kingdom (Burnett, 2011) and NORBARAG (Kudsk, 2010) in the Nordic-Baltic region, include researchers and regulators as well as industry, and produce local guidelines. Regional Plant Protection Organisations (RPPOs), such as the European and Mediterranean Plant Protection Organisation (EPPO), are intergovernmental organisations producing guidelines and regulatory frameworks for plant health, including resistance management (EPPO, 2015).

The major classes of fungicides are listed in Table 2.1, along with their target sites and reported resistance mechanisms. In most cases, cross-resistance applies across fungicides within a single mode of action (Heaney et al., 2000), but there are some exceptions. For azoles and succinate dehydrogenase (sdh) inhibitors (SDHIs), some target site mutations confer incomplete cross-resistance across the group, with some mutations conferring higher levels of resistance against some

compounds but lesser or even negative cross-resistance to others (Leroux et al., 2000, Sierotzki and Scalliet, 2013). Conversely, some efflux pumps confer a multi-drug resistant phenotype, or MDR (Omrane et al., 2015).

The term "fungicides" is used throughout, but similar resistance problems and management strategies apply for compounds used to control oomycete pathogens such as powdery mildews and potato blight, including phenylamides (PAs), carboxylic acid amides (CAAs) and first-generation quinone inside inhibitors (QiIs) (FRAC, 2020a, FRAC, 2020b), and some fungicides such as QoIs and some multisite inhibitors are active against oomycetes as well as fungi. In the grapevine downy mildew *Plasmopara viticola*, resistance has been reported against five fungicide classes including phenylamides, CAAs and QoIs (FRAC, 2020b). More broadly, similar principles apply for all pesticides.

2.3   The "One Health" Context

The "One Health" framework recognises that human, animal and environmental health are inextricably linked, in areas including antimicrobial resistance (Robinson et al., 2016), and it is now increasingly recognised that plant health should be included too (van Bruggen et al., 2019), since plants are essential both in healthy ecosystems and for human nutrition.

Antimicrobial resistance is a universal problem across human, animal and plant health, including antibiotic resistance in livestock, human disease and plant pathogens (Robinson et al., 2016; Sundin and Wang, 2018), and fungicide resistance in fungal pathogens of humans and plants (Fisher et al., 2018). Pesticide resistance can affect insecticides, nematicides, rodenticides and herbicides as well as fungicides (Jutsum et al., 1998). Similar evolutionary drivers (Allen et al., 2017; Hawkins et al., 2019), and similar options for resistance management in practice, apply across the different pests and pathosystems (Beckie et al., 2021; Jutsum et al., 1998; Raymond, 2019).

Crop protection also directly affects human health and nutrition (Swanton et al., 2011). Crop diseases threaten food security, reducing food availability through yield losses, and reducing food access, safety and nutritional quality due to food spoilage and mycotoxin production (Savary et al., 2017). Therefore, pathogen control failure due to the evolution of fungicide resistance or the breakdown of host plant resistance will exacerbate these problems (McDonald and Stukenbrock, 2016).

Table 2.1: Major classes of fungicides

Fungicide group	Examples[a]	Target site	Resistance mechanisms
Benzimidazoles / MBCs (methyl benzimidazole carbamates)	Benomyl, carbendazim	B-Tubulin	Target site mutations
Azoles / DMIs (demethylation inhibitors)	Tebuconazole, Epoxiconazole, Prothioconazole	CYP51 (sterol demethylase)	Target site mutations, target site overexpression, efflux, paralogue number variants
Strobilurins / QoIs (Quinone outside inhibitors)	Azoxystrobin, Picoxystrobin	Cytochrome *b* (quinone outside binding site)	Target-site mutations, AOX overexpression (not confirmed *in planta*), efflux
SDHIs (succinate dehydrogenase inhibitors)	Bixafen, fluxapyroxam, fluopyram	Succinate dehydrogenase (subunits B, C, D)	Target-site mutations, efflux, paralogue number variants
QiIs (Quinone inside inhibitors)	Fenpicoxamid; Amisulbrom	Cytochrome *b* (quinone inside binding site)	No field resistance in fungi yet (possible cross-resistance in efflux pump over-expressing strains); target site mutations in oomycetes
Dicarboximides	Iprodione, vinclozolin	os-1 (histidine kinase: signal transduction in osmoregulation)	Target site, efflux
Morpholines / amines	Fenpropimorph, spiroxamine	erg2 and erg24 (sterol reductase and isomerase)	Unknown (very rare)
Multisite inhibitors	Chlorothalonil, Folpet	Multiple	Unknown (very rare)
CAAs (carboxylic acid amides)	Dimethomorph, Mandipropamid	Cellulose synthase	Target site
PAs (phenylamides)	Metalaxyl, benalaxyl	RNA polymerase I	Unknown (polygenic)

[a]Illustrative examples only; comprehensive list available in (FRAC, 2020a) or subsequent updates.

However, there have also been concerns about negative effects of plant protection products on human health (Swanton et al., 2011). Research is ongoing into the potential role of agricultural use of azole fungicides in the selection of resistance to clinical antifungal drugs in *Aspergillus fumigatus* (Verweij et al., 2013), especially in heavily-treated cropping systems such as flower bulb production (Dunne et al., 2017) or the associated composting of fungicide-containing residues (Verweij et al., 2020), so improving resistance management and IPM in these systems would have benefits beyond plant health. Concerns about the toxicological effects of pesticides on humans and the environment (Lamichhane et al., 2015b) have resulted in some active substances being lost due to regulatory changes, reducing the chemical diversity available and increasing both the importance and the difficulty of resistance management for the remaining modes of action (AHDB, 2020). Conversely, the loss of highly target-specific compounds due to resistance would only leave compounds with wider off-target effects. A broader toolbox of crop protection options is needed to safeguard food security in a way that is both sustainable environmentally and durable in the face of evolving pathogen populations (Birch et al., 2011).

2.4   Resistance Risk

The evolution of resistance is a potential risk for all fungicides, but the risk of resistance and the speed at which resistance is likely to evolve varies between fungicide classes. Resistance risk also varies between pathogens, and between agronomic systems due to differing intensity of fungicide use and other practices affecting disease pressure (Brent and Hollomon, 2007b; EPPO, 2015). The black Sigatoka pathogen *Pseudocercospora fijiensis* has rapidly evolved resistance to several fungicide classes, as its host crop, banana, is typically treated with fungicides up to 50 times per year. However, different pathogens on the same crop may have different levels of resistance risk: for example, the barley pathogen *Ramularia collo-cygni* has rapidly evolved resistance against multiple fungicide groups (Rehfus et al., 2019) whereas *Rhynchosporium commune* has only medium resistance risk. Cereal powdery mildews have higher resistance risk than cereal rusts (Brent and Hollomon, 2007b), although rust fungi may not be low risk for all fungicides (Oliver, 2014). Resistance tends to evolve more rapidly in host-specialist, polycyclic pathogens, and in pathogens of crops grown in protected rather than outdoor systems (Grimmer et al., 2015).

Resistance risk is far higher for site-specific than multisite fungicides, but differences in resistance risk between the site-specific fungicide classes have been harder to predict (Grimmer et al., 2014). Fungicides with higher molecular complexity, or higher molecular weight as a surrogate measure, may have higher resistance risk due to higher specificity in target site binding, for which small changes in the target site can cause a drastic reduction in fungicide binding (Grimmer et al., 2015).

Experimental methods for predicting the resistance risk of a new fungicide class include *in vitro* selection, often with ultraviolet light (UV) mutagenesis. This generates a range of potential mutations; readily generating one or more mutations with very high resistance factors can be indicative of high resistance risk, although not all mutations identified in laboratory mutants will go on to emerge in the field (Hawkins and Fraaije, 2016). Mutagenesis is generally more relevant than baseline screening in the case of fungicides, since fungicide resistance and especially target site resistance has been found, in most cases investigated so far, to evolve from *de novo* mutations rather than selection from standing variation (Hawkins et al., 2019), with very few known exceptions (Steinhauer et al., 2019).

In the case of the SDHI fungicides, mutagenesis studies identified several target site mutations in sdh-B, C and D that subsequently emerged in the field, although some highly resistant mutations, notably sdhC-H152R, did not rapidly reach high frequencies in the field. Experimental evolution, in which resistant mutants evolved within a competing population, demonstrated that this is likely to be due to fitness penalties: H152R was only selected at high fungicide concentrations, at which other mutants, with intermediate resistance but higher competitive fitness, could not survive (Gutiérrez-Alonso et al., 2017). Lalève et al. (2014) used a functional genetics approach to demonstrate fitness penalties associated with several sdhB mutations, most strongly for sdhB-H272R, but they also found some evidence of compensatory mechanisms so fitness penalties will not always prevent a mutation from emerging. However, the relative fitness of different pathogen genotypes may depend on environmental conditions, varying between different field sites and years, as shown by Hagerty et al. (2017) for CYP51 alleles in the septoria tritici blotch pathogen *Zymoseptoria tritici*, as well as between laboratory and field conditions.

Once the first case of resistance has emerged against a fungicide class, usually in a high-risk pathogen, the time from introduction of the fungicide class to

emergence of resistance, and the level of resistance involved, can give a clearer indication of the resistance risk for further pathogen species. Of the major fungicide classes, the MBCs and QoIs are considered high risk; the SDHIs and dicarboximides, and predictions for new QiIs, are medium-high risk; azoles medium risk; morpholines medium-low risk; and multisite inhibitors low risk (FRAC, 2020a). A high resistance risk means effective resistance management is essential, otherwise loss of control will occur very rapidly, but even lower risk fungicides can lose effectiveness over time so continued monitoring is needed. In Europe, the European and Mediterranean Plant Protection Organization (EPPO) Standard for Resistance risk analysis comprises assessment of the resistance risk that would be posed by "unrestricted use", which then determines what "modifiers", such as limited numbers of applications per season or use only in mixtures, are needed to reduce the risk to an acceptable level (EPPO, 2015). Furthermore, the resistance factors, cross-resistance patterns, and fitness costs (or absence thereof) associated with the most likely resistance mechanisms against a fungicide class are all important in determining the most appropriate resistance management strategies.

2.5   Resistance Management

The ideal resistance management strategy would entirely prevent the emergence and spread of resistance, while maintaining effective disease control. Although theoretically achievable in limited circumstances: aided by fitness costs of resistance (Hawkins and Fraaije, 2018; Mikaberidze et al., 2014), or negative cross-resistance between different fungicides (Brent and Hollomon, 2007a): in many cases these dual aims result in an irreconcilable trade-off. Even in relatively favourable circumstances for resistance management, fungal plant pathogens have proven to be immensely adaptable, developing compensatory mutations to overcome fitness costs (Hawkins and Fraaije, 2018), or overcoming negative cross-resistance through alternative mechanisms (Hahn, 2014; Leroux et al., 2002). Large population sizes and numbers of generations in each growing season provide an ample supply of mutations (Mikaberidze et al., 2017). A more pragmatic aim for fungicide resistance management, therefore, is to slow down the emergence and spread of resistance for as long as possible, while maintaining the necessary level of disease control (Shaw, 2006; van den Bosch et al., 2014a). The effective life of a fungicide against a pathogen in this context is the number of seasons for which it continues to provide control of the pathogen, or at least continues to contribute to control in combination with other measures.

Effective fungicide resistance management is often a battle against an invisible enemy, with the greatest gains in effective life to be made during emergence of resistance while the frequency of the resistance gene is very low. By the time that a resistance gene is sufficiently common to be detected in population sampling and data on its sensitivity phenotype and fitness costs collected, further selection can rapidly select for high frequencies of the resistance gene (Milgroom and Fry, 1988; van den Bosch et al., 2014a). However, advances in molecular diagnostics are lowering the detection limits, enabling earlier warnings of emerging resistance alleles (Dodhia et al., 2021).

A set of general resistance management practices, based on governing principles of evolution and tested against experimental evidence, have proven useful across a wide range of pathosystems (van den Bosch et al., 2014a). Modelling studies demonstrate that strategies that minimise the total difference in the population growth rates of resistant and sensitive strains over the course of the growing season thereby minimise selection for resistant strains (Milgroom and Fry, 1988; van den Bosch and Gilligan, 2008). This can be achieved by reducing the growth rates of both sensitive and resistant strains; by reducing the growth rate of the resistant strain relative to that of the sensitive strain; and by minimising exposure of the pathogen to the fungicide, thereby reducing the length of time for which a difference in population growth rates exists (van den Bosch et al., 2014a) (Figure 2.1).

The first pillar of fungicide resistance management is to use non-chemical control methods, such as resistant crop cultivars, to reduce pathogen growth rates and the need for use of fungicides, and therefore reduce selection for resistant strains (Jørgensen et al., 2014). However, in many cases fungicides may still be required for disease control, particularly in high pressure seasons (Jørgensen et al., 2017), and also to reduce selection for pathogen strains with increased virulence against resistant cultivars (Carolan et al., 2017). In designing a fungicide programme with resistance management in mind, decisions include the total number of fungicide applications required, the timing and dose rate of those applications, which MoAs to use and whether different MoA will be mixed or alternated (Brent and Hollomon, 2007a). The evidence available to support each of these decisions is reviewed in the following sections, and the main components of resistance management programmes are summarised in Figure 2.2.
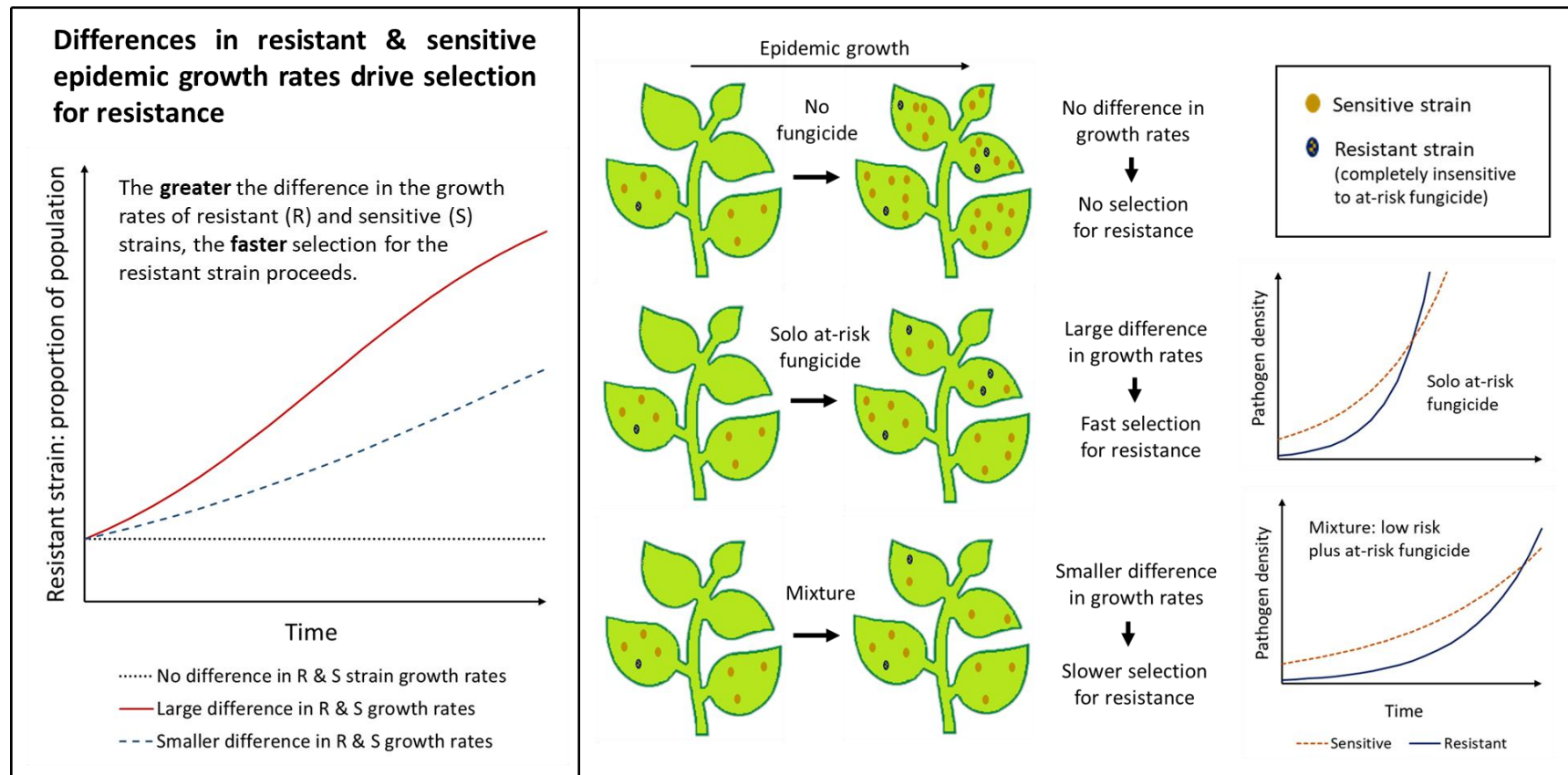
Figure 2.1: General principles of fungicide resistance management: reducing the rate of selection of resistant strains
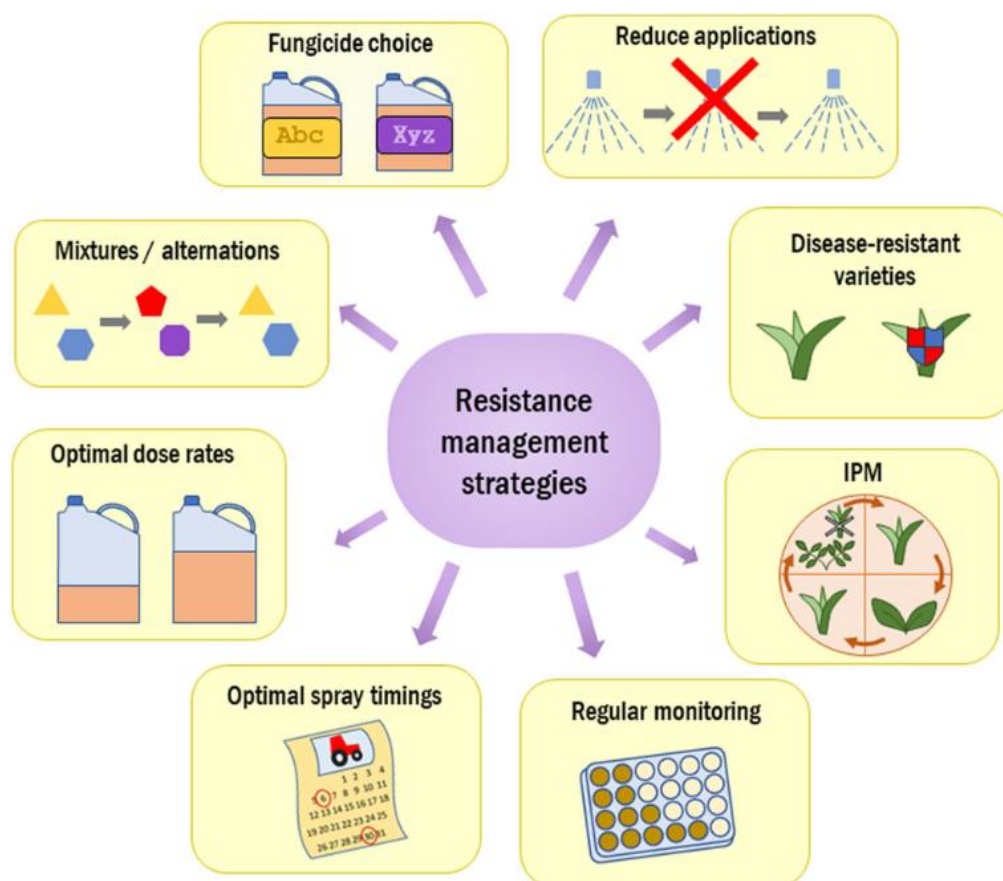
Figure 2.2: Key elements of fungicide resistance management strategies

2.5.1 Dose rates

A consensus has not yet been reached regarding the impact of dose rates on the evolution of fungicide resistance. Theoretically, high dose rates can keep pathogen populations small, reducing the supply of new mutations and thereby slowing the emergence of resistance (Hobbelen et al., 2014; Milgroom, 1990; van den Bosch et al., 2011). Sublethal doses could also increase the risk of resistance emergence due to stress-induced mutagenesis (Amaradasa and Everhart, 2016). In addition, higher dose rates could reduce the risk of polygenic resistance evolution (Brent and Hollomon, 2007a), where the accumulation of multiple minor genes causes a gradual increase in resistance; this could be prevented by dose rates sufficiently high to eliminate partially-resistant pathogen strains. Evidence from a range of other systems supports these principles, in particular clinical and modelling studies of cancer (Foo and Michor, 2010) and of antibiotic resistance (Opatowski et al., 2010; Roberts et al., 2008; Schrag et al., 2001), where high-dose, short regimens have been shown to reduce the risk of resistance. Reduced herbicide rates enabled development of increasing levels of resistance in *Lolium rigidum* in pot experiments, whereas higher herbicide doses would have been lethal to individuals

carrying each single resistance gene before multiple genes could accumulate (Manalil et al., 2011).

However, there is limited evidence in support of these principles in agricultural field settings. It has been demonstrated *in vitro,* but not confirmed *in planta*, that sublethal doses of some fungicides can increase rates of stress-induced mutagenesis in fungal pathogens (Amaradasa and Everhart, 2016; Schnabel and Chen, 2013). A reduced dose rate of herbicide was shown to select for resistance in a field experiment (Amaradasa and Everhart, 2016), but the full label rate was not used for comparison. Use of high doses to kill heterozygotes with intermediate resistance, in combination with non-treated refugia as a source of susceptible homozygote immigrants, has been credited with delaying resistance to Bt crops in insect pests (Tabashnik et al., 2013). However, for many fungal pathogens, fungicide treatments predominantly take place during haploid stages of the life cycle, so intermediate sensitivity in heterozygotes is not relevant (van den Bosch et al., 2011). A modelling study showed that high insecticide dose rates could supress major-gene resistance in cases where there is a high rate of immigration into the population, but that in most cases the effective life of insecticides would instead be increased by reducing doses where major gene resistance is the main threat (Helps et al., 2017). Experimental evolution *in vitro* of *Z. tritici* showed that higher dose rates selected for mutations conferring higher levels of resistance (Gutiérrez-Alonso et al., 2017). Manufacturers' recommended dose rates are generally set at a level that ensures disease control in high pressure seasons (Jørgensen et al., 2017), but complete population kill cannot be achieved in field conditions, so these dose rates may be equivalent to the 'intermediate' dose in some clinical or *in vitro* studies.

There are also mechanisms by which higher dose rates could increase selection for resistance. For highly resistant strains able to survive even high doses, increasing the dose will increase the difference in growth rate between the resistant and sensitive strains, leading to faster evolution of resistance (van den Bosch et al., 2011). In addition, many pathogen population growth rates are limited by the supply of host tissue for infection, so higher doses can increase the growth rate of resistant strains by reducing competition from fungicide-sensitive strains, hastening both emergence of, and selection for, resistance (Hobbelen et al., 2014; van den Bosch and Gilligan, 2008). Even for strains considered only partially resistant, the doses required to achieve full control may be higher than current recommended full label rates, so overall, selection for resistance would be reduced

by using lower dose rates (Mikaberidze et al., 2017). A model of polygenically-controlled fungicide resistance predicted that shifts in sensitivity would proceed approximately independently of fungicide concentration so long as fungicide doses are high enough to exert some selection pressure, but this was based on an assumption that the proportional difference in the growth rates of strains in the presence of fungicide is independent of fungicide concentration (Shaw, 1989a). Furthermore, resistance against site-specific fungicides is commonly due to target-site mutations with high resistance factors, in contrast to herbicide resistance where polygenic metabolic resistance appears to be more common (Hawkins et al., 2019). In addition, population size may be so large for some fungal pathogens, such as *Z. tritici*, that mutational supply is not limiting for resistance evolution (Mikaberidze et al., 2017), especially given extensive gene flow at regional and wider scales (Garnault et al., 2021).

The majority of experimental evidence, including in-field studies, suggests that higher fungicide doses increase selection for resistance (van den Bosch et al.; 2011, van den Bosch et al., 2014a). Such experimental evidence is mostly limited to the selection phase, tracking known mutations, rather than the initial emergence of resistance mutations (Blanquart, 2019). Comparison of the speed of emergence and spread of resistance in different regions and countries indicates that resistance evolution has progressed faster where higher fungicide rates are applied (Garnault et al., 2021; Jørgensen et al., 2017). However, the effect of dose rate is potentially confounded with disease pressure, as higher rates of fungicide may be applied in response to higher disease levels.

Although the choice of dose rate per application remains a contentious topic in fungicide resistance management, advice that the total number of applications of an at-risk fungicide should be minimised (whilst maintaining disease control) is less controversial and is supported by evidence from field and modelling studies (Hobbelen et al., 2014; van den Berg et al., 2016; van den Bosch et al., 2014a). Each application increases the exposure time of the pathogen to the fungicide, and therefore increases overall selection during a growing season. Even if the total dose of a single application is 'split' into two applications at half the dose rate, in most cases the effect of increased exposure time outweighs the effect of reduced dose (van den Bosch et al., 2014a): considering typical dose response curves, halving the dose usually less than halves the fungicide efficacy.

There is a need for improved understanding of how pathogen life history traits determine whether higher or lower dose rates are likely to improve management of both major-gene and polygenic resistance for each fungal pathogen. Pathogens for which a sufficiently high dose to keep the population size extremely small can be achieved in-field, without incurring unacceptable levels of phytotoxicity and environmental and economic costs, are the best candidates for high-dose strategies. However, this is rarely the case in practice, especially where target site mutations are associated with high resistance factors. In the absence of pathosystem-specific evidence on the relative risks of high and low dose rates, the weight of experimental and modelling evidence to date suggests that, in general, higher fungicide dose rates increase the speed of selection for resistant strains in-field, and that the use of the lowest dose required to achieve acceptable control is unlikely to be detrimental and may be beneficial to fungicide resistance management, even if it is lower than the manufacturer-recommended dose (Jørgensen et al., 2017).

2.5.2 Timing

Fungicides can be applied as a prophylactic, protectant treatment to prevent the establishment of infection, or as a curative treatment when the crop is infected. Whilst unnecessary fungicide applications can be avoided by only spraying when a disease is present or once a certain damage threshold is reached, this means that when treatments are needed, they will be applied at a curative rather than a preventative timepoint. Applying fungicides curatively may have negative consequences for both disease control (Angelotti et al., 2014; Blake et al., 2018; Sanatkar et al., 2015) and resistance management, and FRAC guidance for resistance management recommends avoiding curative applications wherever possible (Brent and Hollomon, 2007a). In a curative situation, higher doses may be required to achieve disease control (Blake et al., 2018; Cohen et al., 2018), increasing selection for resistance, and some mixing partners such as multisite fungicides may only have protectant activity, reducing the resistance management benefits of mixtures. In addition, a larger population size will have been reached before the treatment is applied, increasing the potential for new mutations and therefore the speed of resistance emergence (van den Bosch et al., 2014a). In the case of the azole fungicides, increasing levels of resistance are removing the option of curative treatment, with long-term monitoring showing a steeper decline in curative activity compared to protectant activity of azoles against *Z. tritici* as less-sensitive genotypes accumulate in the population (Blake et al., 2018).

There is limited experimental evidence to validate the theoretical principle of minimising curative applications. A review found that early spray timings increased selection in some experimental trials but decreased selection in others: the effects appear to depend on the characteristics of individual pathosystems (van den Bosch et al., 2014a). For some fungal pathogens, including *Z. tritici*, a spray timing that is protectant for newly emerging leaves will be curative on older leaves, blurring the distinction between prophylactic and curative applications. Modelling the effect of spray timings on selection for resistance in *Z. tritici* indicated that earlier spraying reduced selection, but at the cost of reduced efficacy (van den Berg et al., 2016). The authors concluded that optimizing the spray timing for disease control could help resistance management by achieving control at a lower dose rate.

The optimal spray timing for disease control will fluctuate from season to season, depending on the environmental factors affecting the timing of infection. Decision-support systems have been developed for a number of fungal pathogens to inform application timing and/or dose (Gent et al., 2013), with thresholds for treatment relying on an estimate of weather-related risk (Jørgensen et al., 2020a; te Beest et al., 2009), spore-trapping (Rogers et al., 2009, West and Kimber, 2015), or a combination of agronomic, weather and other risk factors (Fernando et al, 2021; Main et al., 2001). Thresholds for treatment must be carefully set; an inappropriate indication of 'high' risk can lead to unnecessary fungicide applications (Gent et al., 2013), but a high threshold for treatment may increase the proportion of curative applications, a factor which may have contributed to the development of fungicide resistance in *Venturia inaequalis* (apple scab) (Beckerman et al., 2015). Reliable disease forecasting would aid disease control and resistance management, enabling fungicides to be applied only when likely to be needed but still at protectant timing. However, with a changing climate, the accuracy of predictive models will need to be evaluated on an ongoing basis to ensure that recommended application timings remain optimal (Sanatkar et al., 2015).

2.5.3 Mixtures or alternations

Repeated use of a single mode of action (MoA) should be avoided, either through use of mixture of two or more MoAs, or alternation between them (Brent and Hollomon, 2007a). Mixture offers dual benefits for resistance management (van den Bosch et al., 2014b). Firstly, when strains with resistance to one MoA are sensitive to the second, the difference in the growth rates of resistant and sensitive strains is reduced, therefore reducing selection for resistance. Secondly, the dose

rate of each mixing partner may be reduced without sacrificing treatment efficacy, further reducing selection for resistance. Mixtures can also provide some insurance against loss of disease control if resistance to one fungicide is present at a higher level than anticipated (Shaw, 2006), but the other mixing partner will then be the sole effective product in use, increasing the risk of resistance evolving against that fungicide too. Mixtures are also used to give broad spectrum control of multiple pathogens, but for resistance management purposes it is important that more than one mixing partner is effective against the pathogen in question.

Introducing alternations as additional applications in between an unchanged number of sprays of the at-risk MoA will not reduce selection for resistant strains if there is no overlap in the time of efficacy of each spray, as there will be no change in the difference between the growth rates of the resistant and sensitive strains during the period that the at-risk MoA is exerting selection (van den Bosch et al., 2014a). The only potential benefit of such an alternation strategy would be to exert additional disease control, reducing the overall population size and therefore the initial risk of resistance mutations occurring. However, as discussed in section 2.5.1, reducing the population size also reduces competition between strains, so the implications for resistance management are not straightforward. In contrast, if alternation is implemented by replacing an application of an at-risk MoA, this will reduce the number of applications and therefore the exposure time during which selection for resistance occurs. Evidence from experimental studies supports the distinction between these two types of alternation strategy (van den Bosch et al., 2014a).

Whether mixture or alternation is optimal will vary from case to case. If achieving mixture requires splitting the dose of a high-risk fungicide across more applications, the increased exposure time may outweigh the benefit of mixture and the reduced dose per application, so alternations may be more effective (van den Bosch et al., 2014a). A modelling study of *Z. tritici* and *Erysiphe necator* comparing the relative success of mixture and alternation programmes for resistance management showed that mixture rather than alternation maximised lifetime yield, if the dose of each mixing partner was optimised according to resistance risk (Elderfield et al., 2018).

The mixture partner may either be a multisite fungicide or another single-site fungicide. A multisite fungicide is at lower risk of itself succumbing to resistance, but a fungicide with higher efficacy in disease control will also be more effective in

reducing the selection pressure exerted by others in the mixture. Programmes that minimise the dose of a high-risk fungicide, applying only as much as required for disease control, whilst applying a maximum dose of low-risk fungicide, provide the longest effective life for the high-risk fungicide (Elderfield et al., 2018; Fernando et al., 2021). Modelling has shown that if there are fitness costs of resistance, mixtures of high-risk and low-risk fungicides in an optimal ratio could potentially achieve disease control whilst avoiding selection for resistance altogether (Mikaberidze et al., 2014).

If both mixing partners are single-site fungicides, there is a risk of resistance evolving concurrently to both fungicides, introducing potential trade-offs as the optimal strategy for one may not be optimal for the other. For example, in field trials, applying a mixture of the DMI fungicide epoxiconazole and the SDHI fungicide isopyrazam slowed selection for *Z. tritici* resistance to epoxiconazole but did not slow selection for resistance to isopyrazam, relative to solo applications of the mixture components (Dooley et al., 2016). In such cases, setting the doses such that the level of control provided by each fungicide is approximately equal may help to balance resistance management for both (FRAG-UK, 2020).

Whether mixture or alternation is preferable for management of concurrent resistance also depends on the relative efficacy and persistence of the fungicidal mixture partners. A modelling study tracked selection for resistance in a *Z. tritici* population containing a strain sensitive to both fungicides, two single-resistant strains each resistant to one or the other, and a double-resistant strain. It concluded that use of a mixture would result in a longer effective life than alternation, partly through better control of single-resistant strains, but both mixture and alternation would achieve a longer effective life than a spatial mosaic of solo fungicides (Hobbelen et al., 2013). However, this study did not consider the effects of sexual reproduction, which may hasten the emergence of double-resistant strains through recombination (Chen and McDonald, 1996; Zhan et al., 2003). Management of the concurrent evolution of resistance to multiple modes of action is becoming increasingly important as multisite fungicide use is restricted by regulatory changes.

There may be further benefits to mixture if the combined efficacy of fungicides is multiplicative rather than additive (Shaw, 1989b). Under the additive dose model, the effects of the doses of each fungicide on pathogen growth are added together such that, on a normalised scale of fungicide efficacy, the dose of one fungicide

could be substituted for the other and the same level of control achieved; this is thought to apply for mixtures of fungicides with a shared mode of action (Morse, 1978). The multiplicative survival model instead implies that the proportional reductions in pathogen growth should be multiplied together to predict the effect of the mixture (Paveley et al., 2003); this is thought to apply to mixtures of different modes of action, especially if they affect different aspects of the pathogen's biology or life cycle (Shaw, 1989b). The more multiplicative the joint action, the more likely mixture will be preferable to alternation for resistance management, as lower doses can be used. Experimental work to measure the effects of fungicides on individual aspects of pathogen biology, such as germination, infection, growth or sporulation, combined with an exploration of the sensitivity of model conclusions to assumptions about which aspects are affected by each fungicide in the mixture, could improve choice of optimal mixture partners for resistance management.

Both additive and multiplicative models describe non-interacting effects, but interacting effects are also possible. The interaction may either be synergistic (achieving greater control than expected when considering the individual effects of each mixture component) or antagonistic (control is less than expected) (Kosman and Cohen, 1996). In cases of complete resistance, synergism will increase control of the sensitive strain but not the resistant strain, and so increase selection for resistance (Mikaberidze et al., 2014; Shaw, 1993). However, synergism may also enable control with lower doses (Shaw, 1993). Conversely, antagonism between mixture partners reduces the difference in resistant and sensitive strain growth rates and therefore reduces selection for resistance, but may compromise disease control and is unlikely to be economically attractive for growers (Mikaberidze et al., 2014; Shaw, 1993). These theoretical conclusions have been demonstrated experimentally for antibiotic resistance (Chait et al., 2007). The effects of synergistic or antagonistic interaction in the case of partial resistance may be more complex, depending on the nature of the change in the fungicide dose response curve.

A major factor in the choice of mixing partners is whether pathogens show cross-resistance to the different fungicides. If there is positive cross-resistance between two fungicides, then strains that are more resistant to one fungicide are also more resistant to the other. Positive cross-resistance is most common for fungicides with the same mode of action and therefore the same target site (Heaney et al., 2000), but resistance mechanisms such as enhanced efflux can affect fungicides across different classes (Omrane et al., 2015). Fungicides with positive cross-resistance

are not suitable for mixture or alternation with each other because they will both select for the same resistance mechanism, whereas fungicides without cross-resistance (sometimes referred to as neutral cross-resistance) are more suitable (Oliver, 2016). Negative cross-resistance, in which the strains that are more resistant to one fungicide are more sensitive to the other, is theoretically ideal for resistance management, but rarely found in practice. The grey mould pathogen *B. cinerea* initially showed negative cross-resistance between *N*-phenylcarbamates and benzimidazole fungicides (Elad et al., 1988). However, when a mixture of the fungicides was used, the F200Y substitution conferring resistance to both fungicide classes was rapidly selected instead (Yarden and Katan, 1993).

Positive cross-resistance may be complete, meaning that there is very strong correlation between resistance factors against two fungicides, or partial if the correlation is weaker or less consistent between strains. For example, *Z. tritici* shows a pattern of partial cross-resistance against azole fungicides among strains with different sterol 14α-demethylase (CYP51) haplotypes (Fraaije et al., 2007, Jørgensen et al., 2020b; Leroux et al., 2007). If the number of modes of action available for use in fungicide programmes against a pathogen are very limited, then partial cross-resistance may also be of some benefit for resistance management. Mixtures of azoles improved control of *Z. tritici* compared to solo azole application in field trials carried out across several European countries (Jørgensen et al., 2018). However, levels of *Z. tritici* resistance to all azole fungicides are increasing, with some strains combining several target-site mutations in combination with target-site overexpression and enhanced efflux (Huf et al., 2018; Kildea et al., 2019). Therefore, even when fungicides individually select for mutations with partial or negative cross-resistance, their combined use may instead select for generalised resistance mechanisms.

In addition, resistance to additional fungicide classes has been shown to develop more quickly in strains of *V. inaequalis* (Koller and Wilcox, 2001) and *Monilinia fructicola* (Luo and Schnabel, 2008) that have already developed resistance to an unrelated mode of action, despite similar initial sensitivity to the newer fungicide, suggesting selection for increased mutability that enables faster evolution of resistance to additional fungicides. This could be due to increased individual mutation rate, or life cycle characteristics such as shorter generation time or increased sporulation that increase the total speed of mutational supply in the population. The potential for this mechanism to increase the speed of resistance evolution should be further investigated in modelling, laboratory and field studies

to understand how widespread this is and how resistance management strategies are affected.

The effects of timing on fungicide efficacy should be accounted for when choosing mixture partners, ensuring that all are effective at the time they are applied. For example, some multisite fungicides are only effective at protectant timings. Fungicide persistence is also an important consideration in choosing mixture partners: if the mixture partners have very different decay rates, or the efficacy of one mixture partner is sustained at lower concentrations, then one mixture partner will be left acting effectively solo once the effect of the other mixture partner has decayed. Therefore, mixture partners with similar persistence should be chosen (FRAG-UK, 2020). This is especially important if both mixture partners are at high risk of resistance development. If only one mixture partner is high-risk, the low-risk mixture partner should have similar or longer persistence (Shaw, 1989b), but similar persistence is preferable since it is still prudent to practice resistance management for lower risk fungicides.

2.5.4 Combining control measures

In addition to mixing or alternating multiple fungicides, fungicides should be combined with other control measures including resistant crop varieties. The same principles apply as when combining two non-cross-resistant fungicides; the additional control measure decreases growth of both sensitive and resistant strains, so resistance selection is slowed, as well as reducing the population size in which mutations can arise (Carolan et al., 2017). The heavy reliance on fungicides and consequent resistance problems in black Sigatoka *Pseudocercospora fijiensis* has been attributed, in part, to the low genetic diversity and lack of effective host resistance in banana (Isaza et al., 2016).

As with fungicide mixtures where concurrent resistance is a risk, combining fungicides with resistant crop cultivars risks the selection of pathogen strains with both fungicide resistance and host virulence. Selective sweeps of both fungicide resistance and virulence alleles have been detected in plant pathogens including *Z. tritici* (Hartmann et al., 2018) and *Pyrenophora teres* (Ellwood et al., 2019). In *Z. tritici* isolates from Denmark, differences in fungicide resistance allele frequencies were seen between two different wheat varieties, but there was also evidence of pathogen adaptation to wheat variety over time (Vagndorf et al., 2018). Asian soybean rust *Phakopsora pachyrhizi* has evolved virulence against available host resistance genes, and resistance to multiple fungicides (Langenbach et al., 2016).

Use of resistant varieties means effective control can be achieved with lower fungicide doses or fewer fungicide treatments, but reduced use of fungicides will increase the selection pressure for virulent strains to emerge (Carolan et al., 2017). Therefore, the optimal combination should be designed to maximise the effective life of both components, and monitoring programmes should cover both virulence and fungicide resistance in the pathogen population. Once concurrent resistance and virulence has emerged, the combination of fungicide and variety will then select for those strains, and so both alternative fungicides and varieties with a different genetic basis of resistance would be needed to restore effective control with resistance/virulence management.

When combining multiple control measures, cross resistance must be considered. Host resistance has a very different mode of action from fungicides but interacting effects of resistance mechanisms are possible in some cases. Some efflux pumps have been shown to contribute both to reduced fungicide sensitivity and to virulence, likely due to efflux of substrates including both fungicides and plant defence compounds. Transporter genes associated with both fungicide resistance and virulence include *PdMFS1* in the citrus post-harvest pathogen *Penicillium digitatum* (de Ramon-Carbonell et al., 2019); *AaMFS54* in *Alternaria alternata* (Lin et al., 2018); and *BcatrB* in *B. cinerea*, for which virulence effects may be mediated by efflux of the phytoalexin resveratrol (Schoonbeek et al., 2001).

Other mechanisms contributing both to virulence and fungicide resistance include generalised stress response pathways, such as melanisation in the barley pathogen *R. commune* (Zhu et al., 2018). In *B. cinerea*, genes in the HOG signal transduction pathway are involved in responses to various osmotic and cell wall stresses; the target sites of both the phenylpyrrole and dicarboximide fungicides are involved in osmotic signal transduction; and the pathway is involved in both fungicide stress responses and pathogenicity (Yang et al., 2020). However, it is not clear whether such responses would be differentially selected by resistant varieties or if they are involved in a more general host infection pathway.

Negative trade-offs are also possible, for example if fungicide resistance is associated with fitness costs including reduced virulence. Reduced virulence has been reported in fungicide-resistant isolates in some cases (Hagerty and Mundt, 2016), but this is likely to be a general reduction in pathogenic fitness or aggressiveness rather than the loss of cultivar-specific compatibility.

The most durable crop protection strategy combines multiple modes of action within as well as between each type of control measure (Bourguet et al., 2016). Resistant cultivars should still be treated with fungicide mixtures, and varietal resistance should be based on more than one resistance gene. This can be achieved by pyramiding of resistance within varieties, and minor resistance genes are often more durable (Mundt, 2018). Multiple resistance genes can also be deployed through cultivar mixtures, although so far this has been less popular in practice due to agronomic and market requirements for uniform crop structure, phenology and produce quality. Mixing varieties has been shown to reduce selection for fungicide resistance (Kristoffersen et al., 2020), demonstrating that increased diversity across all control measures can increase the effective life of each component.

Integrated pest management is widely promoted as key to durable crop protection, although definitions vary as to what precisely this involves. Threshold-based spraying is not always beneficial for resistance management since it may result in more curative applications, as discussed in section 2.5.2; whereas combining a wider range of control measures, including cultural control, will reduce the selection exerted by each single measure. Cultural control, such as wheat stubble management to remove *Z. tritici* (McDonald and Mundt, 2016), removing volunteer plants, or covering potato discard piles with plastic to contain *P. infestans* (Cooke et al., 2011), can reduce primary inoculum. Disease pressure can also be reduced by changes to sowing date, cropping density, crop rotations, fertiliser inputs and tillage (Jørgensen et al., 2014), although there will be some trade-offs with yield.

2.6 Measuring Effectiveness

Resistance management strategies can be designed based on general principles, but they must be tested in the field for each pathosystem and fungicide group. Empirical evidence of the effectiveness of resistance management practices can come from field trials of different disease control programs, as well as wider monitoring of resistance levels in pathogen populations.

Previously, testing for resistance has been a reactive step after control failure, but now more pre-emptive screening programmes are in place (Massi et al., 2021), carried out by the fungicide industry and reported to the Fungicide Resistance Action Committee, by national bodies such as the UK's Agriculture and Horticulture Development Board (AHDB), by agronomy companies or extension organisations.

Different monitoring strategies are needed to detect the early emergence of resistance or to monitor further selection to higher frequencies (Massi et al., 2021).

Resistance can be detected by phenotypic testing of isolates, or molecular diagnostics. Phenotypic testing can detect sensitivity shifts regardless of the mechanisms involved, but testing individual isolates limits the numbers that can be screened, and to go from plant material, to bulked single-spore inoculum, to final assay result, can take considerable time, especially for slow growing or obligately biotrophic pathogens. Standard assay methods and reference isolates ensure that resistance factors from different labs are comparable (FRAC, 2021). Even in pathogens that are amendable to higher throughput *in vitro* testing, some *in planta* confirmation is needed so resistance factors measured in laboratory assays can be correlated with impacts on disease control levels in the field. For *Z. tritici*, shifts in azole EC_{50} values measured in laboratory assays were correlated with decline in control in the field, whereas all QoI-resistant isolates were highly resistant in all sensitivity assays but the severity of control loss in the field depended on the frequency of resistant isolates in the population (Blake et al., 2018).

Molecular assays can be used for bulk population screening, so may allow earlier detection (while still at lower frequency), but until now this has only been possible once the likely mutations are already known, having been predicted in lab or having already emerged in other pathogen species or other geographical regions (Barres et al., 2016). Newer methods include high-throughput next-generation amplicon sequencing (Pieczul and Wasowska, 2017), digital PCR (Zulak et al., 2018), and isothermal amplification such as loop-mediated isothermal amplification (LAMP) (Duan et al., 2015; Fraaije and Cools, 2013). Each has different advantages, suiting it to different applications. LAMP is faster and potentially portable depending on DNA purification requirements, and rapid in-field allele-specific qPCR has been developed (Dodhia et al., 2021); digital PCR and amplicon sequencing have lower detection limits. Amplicon sequencing can be used for multiple and unexpected SNPs within the sequenced gene, but some phenotypic monitoring will still be needed for less predictable, non-target-site resistance mechanisms, and phenotypic confirmation of resistance levels will be needed for any mutations initially detected through molecular methods.

Resistance monitoring in the general pathogen population can indicate whether prevalent management practices, over the spatial scale at which fungal populations mix, are selecting for resistance, and whether resistance has reached

a level likely to affect disease control (Jørgensen et al., 2020b). However, to assess the impact of specific treatments on selection for resistance, or to compare different management practices, requires experimental testing in field trials, comparing the levels of resistance selected under each treatment.

A multi-year trial of *B. cinerea* in vineyards compared treated and untreated areas. Increased frequencies of resistance against the fungicide used were selected in the treated plots. In this case, an observable decrease in resistance frequency took place in untreated plots, indicating fitness penalties associated with the resource cost of MDR efflux pump overexpression (Matusinsky et al., 2017; Walker et al., 2017).

A *Z. tritici* field trial compared various different spray programmes, assessing disease control and selection of resistance. Treatments included different numbers of fungicide doses, and mixtures or alternations of different modes of actions. The number of sprays gave a trade-off between reduced selection for resistance with fewer sprays and more effective disease control with more sprays. However, diversified spray programmes, both mixing and alternating different products, reduced the selection of any one resistance mutation whilst maintaining good levels of disease control (Heick et al., 2017).

Inoculated field trials could be used to look at selection from a specific starting pool of isolates rather than the naturally occurring population. This approach has been used to test selection for host specialisation in *Z. tritici*, *Parastagonospora nodorum* and *R. commune* on susceptible, partially resistant and mixed host cultivars (Zhan and McDonald, 2013). A similar approach could be used to test selection of specific fungicide resistance alleles under different management strategies.

Experimental evolution has been used to investigate antibiotic resistance strategies such as mixtures (combination therapy) or alternations (cycling) (Nichol et al., 2019). *In vitro* selection experiments for fungicide resistance so far have focused on potential resistance mechanisms (Gutiérrez-Alonso et al., 2017), but there is also potential for testing fundamental principles of resistance management, such as fitness costs and compensatory mechanisms, or the effects of mixing or alternating under different cross-resistance scenarios (Ballu et al., 2021), in plant pathogenic fungi.

2.7   Principle Versus Practice

Any strategy for resistance management can only be successful if growers put it into practice. Numerous stumbling blocks, in the form of practical realities, imperfect understanding and conflicting priorities, may prevent full implementation on farm.

Such obstacles include market and regulatory conditions. For example, fungicide seed treatments can contribute to selection for resistance (Brent et al., 1989; Porter et al., 2009) and therefore count as an additional fungicide application for resistance management purposes (Kitchen et al., 2016), and so like any other fungicide treatment they should be applied only where the disease pressure necessitates their use (Lamichhane et al., 2019). However, farmers may not have the choice to use non-treated seeds, for example in Australia where some imported seeds must be fungicide-treated as a biosecurity measure (Van de Wouw et al., 2021). Regulations also restrict the range of fungicides available, such that the recommended degree of mixture and alternation may not be possible. The number of fungicides registered for use on minor crops is often particularly limited (Lamichhane et al., 2015a), and this may become more common even for major crops as compounds are withdrawn due to new regulations (Hillocks, 2012; Nishimoto, 2019) especially affecting lower resistance risk multi-site inhibitors (Anastassiadou et al., 2020), and as rising costs and regulatory hurdles limit the pipeline of new fungicides (Bryson and Brix, 2019).

The number of available effective fungicide classes is also limited as resistance evolves against ever more fungicides. Pathogens for which multiple resistance is a particular concern include *B. cinerea* (Kretschmer et al., 2009), *Z. tritici* (Omrane et al., 2015), *Sclerotinia homeocarpa* (Sang et al., 2019), *R. collo-cygni* (Rehfus et al., 2019), *P. teres* (Rehfus et al., 2016) and *P. fijiensis* (Aguilar-Barragan et al., 2014). This can leave too few effective MoAs for an optimal programme of mixing and alternating. For higher-risk fungicide groups, the number of applications permitted per season is limited in order to reduce the resistance risk for that MoA (EPPO, 2015), further limiting options for mixtures and alternations with other fungicide classes. Furthermore, fungicide programmes in practice are of course limited to those fungicides that are available: whilst the ideal mixing partner would be highly effective at any required timing but also at very low risk of resistance itself, nearly all site-specific fungicides have medium or high resistance risk, whereas low-risk multisite fungicides are often limited to protectant activity.

Therefore, practical guidelines must be developed based on available, licensed, effective products, and updated as available products and resistance levels change.

Similarly, recommendations to reduce overall fungicide use through IPM approaches favouring resistant varieties, cultural control and other non-chemical measures can only be followed when such alternative control measures are available, practicable and sufficiently effective; otherwise the 'last resort' of chemical control will still be the default (Lamichhane et al., 2015b).

Recommendations must also be updated to reflect new knowledge. For example, QoI fungicides were initially predicted to be at moderate risk of resistance, but in fact resistance developed very quickly (Lucas, 2003), and uptake by growers of voluntary resistance management guidelines was slow (Burnett, 2011). Any change in guidance around dose rates would require careful communication, as a recommendation to use the lowest necessary dose would directly contradict the widespread recommendation, and in some countries a legal requirement, to adhere to full label rates. Use of dose rates lower than the manufacturer-recommended dose is already widespread (Jørgensen et al., 2017), but this choice is likely driven mostly by cost saving rather than resistance management decisions. In addition, increasing dose rates is a common adaptive measure used by growers to maintain control in the presence of partial resistance (van den Bosch et al., 2020), but this 'adaptation phase' (van den Bosch et al., 2011) is a matter of resistance mitigation rather than resistance management.

Some positive progress towards uptake of resistance management principles has been made. In a survey of 590 grain farmers in Norway, 89% of farmers responded that they combined different modes of action with the aim of preventing resistance development (Steiro et al., 2020). The high level of uptake may be partially explained by the benefits mixtures can offer besides resistance management, including risk management against the failure of any one component (Shaw, 2006) and broad-spectrum control against multiple pathogens (Brent and Hollomon, 2007a). In a smaller survey of Scottish barley growers and agronomists, a majority of respondents indicated that they were concerned about fungicide use leading to resistance (Stetkiewicz et al., 2018). A survey of 252 members of the USA grape industry revealed a high level of understanding of several resistance management principles and awareness of FRAC MoA codes amongst a majority of respondents (Oliver et al., 2021).

However, implementing resistance management may involve increased management complexity with associated time costs, identified as a barrier to uptake of herbicide resistance management in a survey of German farmers (Ulber and Rissel, 2018). This complexity is increased where the optimal strategy for one pathogen is not suitable for another. QoI fungicides are an effective mixing partner for brown rust control, but not for *Z. tritici* control in the UK (FRAG-UK, 2020). Late sowing of winter wheat decreases the risk of a severe *Z. tritici* epidemic, but can increase the risk of powdery mildew and yellow rust (Jørgensen et al., 2014). Removal of crop debris can reduce the inoculum of pathogens including *Z. tritici* in wheat (McDonald and Mundt, 2016) and *Leptosphaeria maculans* in oilseed rape (Van de Wouw et al., 2021), whereas minimum tillage may be better for suppression of the wheat diseases spot blotch *Bipolaris sorokiniana* and take-all *Gaeumannomyces tritici* (Montanari et al., 2006). Biosecurity measures to prevent the spread of invasive diseases may also contradict resistance management guidelines if the aim is elimination rather than minimal treatment, for example requiring treatment of all imported seed (Van de Wouw et al., 2021).

Furthermore, when disease levels and forecasts indicate that a fungicide treatment is not necessary for a particular pathogen, it may still be necessary for the control of other diseases, and so all pathogens present in the field will still be exposed to the same fungicide selection. This incidental exposure has resulted in some cases of resistance in pathogens that were not the original intended target of the fungicides. The emerging barley pathogen *R. collo-cygni* has become a major pathogen in recent years, but as it rose to prominence it was found to be already resistant to multiple fungicide groups, having already been present at lower levels when those fungicides were applied mainly to treat other barley diseases such as Rhynchosporium or net blotch (Fountaine et al., 2014). The selection of resistance in non-target pathogens is likely to be under-reported, since resistance monitoring programmes tend to focus on key target pathogens.

Conversely, in some cases the same pathogen species occurs on multiple different crops. For example, *B. cinerea* is a pathogen of vineyards, various soft fruits, some vegetables and ornamental plants, and there is evidence of multiple-fungicide-resistant strains moving between different host crops (Rupp et al., 2017). Brassica pathogens such as *Pyrenopeziza brassicae* can infect both oilseed rape (a broad acre arable crop) and vegetable brassicas, and *Sclerotinia sclerotiorum* can infect oilseed rape, soya and a range of vegetable crops across multiple plant families. This presents challenges in applying resistance management across the whole

pathogen population. For example, minor crops may have fewer plant protection products authorised, increasing pressure on those that are available, and high-value and ornamental crops may be treated more intensively as even superficial cosmetic damage could cause major financial losses, whereas broad-acre crops are likely to comprise the vast majority of host plant and active-substance-treated area. The availability of resistant cultivars and other non-chemical control measures will also differ between crops.

It is also important to acknowledge that resistance management is only one factor in growers' decision-making, which is likely to be weighted towards profitability, business viability and risk-aversion in protecting valuable crops against disease. Effective mixtures and alternations may require the use of more expensive fungicides within a programme. As resistance develops, short-term profitability may be maximised by maintaining or even increasing fungicide dose and number of applications (Burnett, 2011; van den Bosch et al., 2020), especially in cases where the quality and value of the crop is strongly affected by disease severity, for example powdery mildew (*Erysiphe necator*) of wine grapevines (van den Bosch et al., 2020), or turfgrass diseases on golf courses with expectations of blemish-free turf (Stowell and Gelernter, 2003), but this will increase further selection for resistance. Additionally, the ongoing viability of a farm business could be threatened by heavy crop losses in a single year, so risk-averse farmers may opt to apply higher fungicide doses than the long-term economic optimum, to insure against years in which disease severity is much higher than average (te Beest et al., 2013). Crop insurance schemes would need to be redesigned to overcome this: they currently require farmers to show that all possible crop protection measures have been used, rather than reasonable measures within sustainable use and resistance management guidelines (Lefebvre et al., 2015). Risk aversion could also be mitigated by improved disease forecasting (te Beest et al., 2013), and risks reduced by the use of other control measures including resistant varieties.

Some growers and advisors may underestimate the threat to farm business profitability posed by resistance development, due to a belief that new pesticides will be developed to replace those lost to resistance (Dentzman et al., 2016). This belief may only change once farmers have experienced a crisis point in pest control: for example, following control failures of insecticide-resistant cotton bollworm (*Helicoverpa armigera*) in Australia, farmers' perceptions and uptake of IPM strategies have improved (Wilson et al., 2018). Farmers may also overestimate the financial benefit of fungicide applications: the measured long-

term average effect of fungicide treatment on Scottish spring barley yields was lower than the expected yield response indicated by a survey of farmers and agronomists (Stetkiewicz et al., 2018, 2019).

Furthermore, some farmers may believe that they are following resistance management and IPM guidelines, but their actions do not match the claimed level of uptake. In a survey of Scottish spring barley growers, a high proportion of farmers reported selecting highly resistant varieties, but in fact the varieties chosen were mostly not highly resistant. In the same survey, the vast majority of farmers stated that they used crop rotations, but two thirds of farmers reported that they often or always sow barley in the same field for two or more consecutive seasons (Stetkiewicz et al., 2018). In another survey, onion farmers reported they were using action thresholds to determine treatment timings for onion thrip control, but their application timings appeared to follow a standard insecticide programme (Leach et al., 2019). Inconsistent guidance can leave growers unsure of what resistance management guidelines are: for example, where product labels state a permitted number of applications per growing season, but some local guidelines or even legal limits in some countries specify a lower number. Growers may also have difficulty in identifying mixing partners with different modes of action amidst a plethora of product names, especially in countries where literacy rates are low, so members of the industry body CropLife International have undertaken to include MoA information (icons and FRAC group numbers) on product labels by 2023. Ongoing communication, education and engagement with growers, including use of communication technology such as smartphone apps (Schnabel et al., 2018), is likely to improve implementation of IPM and resistance management (Leach et al., 2019; Pacilly et al., 2019).

Farmers' motivation may also be undermined by the belief or knowledge that neighbouring growers are not following good resistance management practices: an individual farmer bearing economic costs of resistance management in the short term may not benefit in the longer term if resistance evolves due to other farmers' poorer practices. A lack of cooperation and trust between farmers can therefore lead to a 'tragedy of the commons' where each farmer chooses to maximise their own short-term profits at the cost of faster evolution of resistance (Evans et al., 2018; Llewellyn and Allen, 2006). Some pests, such as black-grass (*Alopecurus myosuroides*), have limited dispersal between fields, so resistance status of fields is correlated with historical pesticide applications (Hicks et al., 2018) and farmers can expect to see a direct impact of resistance management on their own land. In

contrast, resistance in pathogens with airborne spores can only be effectively managed at a landscape scale. A modelling study showed that selection for fungicide resistance in pathogens with a large dispersal distance occurs on a regional scale, commensurate with the fraction of crop area sprayed with fungicide (Parnell et al., 2006). A statistical model fitted to regional *Z. tritici* resistance monitoring data from France showed that the main driver of resistance was the intensity of fungicide use over a regional scale, whilst smaller unsprayed areas were insufficient to noticeably delay resistance (Garnault et al., 2021).

A co-ordinated approach across government, industry and researchers is needed to support adoption of best practice and to increase co-operation between farmers on this 'common resource pool' problem (Barrett et al., 2016; Ervin et al., 2019). Successful co-operation between farmers may be best achieved by promoting local grower networks, with support from extension services (Gould et al., 2018). This may be more challenging for broad host range pathogens, requiring coordination across different agricultural sectors. Legislation could include taxes or subsidies (Barrett et al., 2016), or changes to fungicide label requirements so recommendations become mandatory (Burnett, 2011). Deploying resistance management strategies over wider spatial scales may also increase their effectiveness: a modelling study concluded that if a sufficient area at a landscape scale is not treated with fungicide but managed with other IPM measures, the evolution of resistant strains could be slowed or prevented altogether (Parnell et al., 2006).

Farmers' decisions on pesticide applications are influenced by sources of information and advice including other farmers, public or private extension services, online information and specialist publications, and decision support systems. A survey of Swiss fruit growers found that growers who were influenced by advice from public extension sources were more likely to use non-chemical preventative measures, and less likely to use synthetic insecticides, against the invasive pest *Drosophila suzukii*, than growers influenced by advice from private extension services affiliated with pesticide suppliers (Wuepper et al., 2021), and a survey of Danish agronomic advisors found that independent advisors were more likely to recommend lower dose rates than supplier-affiliated advisors (Pedersen et al., 2019). However, even where they do not earn direct commission from pesticide sales, advisors employed directly by farmers are likely to show similar risk aversion, and pride in producing a "clean' crop", to the farmers themselves.

Therefore, as resistance management is a public good, independent sources of advice are essential.

Decision support systems are often developed with an aim of avoiding unnecessary fungicide applications, for cost savings, as well as any environmental or resistance management benefits. However, analysis of fungicide use under different decision support systems has revealed very variable results between systems, depending partly on whether they are aiming to optimise for yield, costs or margin. In a study comparing five systems for *Z. tritici*, some resulted in reduced fungicide use compared to standard programme, but others led to increases (Burke and Dunne, 2008).

There is also a need to ensure that advice to growers is kept up to date, not only based on new knowledge but also due to changes to target pathogens. For example, climate change may result in the need for more or earlier fungicide sprays (Kaczmarek et al., 2016; Kremer et al., 2016), so optimal spray number and timing to balance resistance management and disease control must be reconsidered. Emerging pathogens may take over as the main targets of control programmes (Fones et al., 2017), so new advice will need to reflect the resistance risk and general biology of these pathogen species. However, alongside the emergence of new threats, new control measures are also being developed, so new resistance management guidelines will need to be developed for these new control measures in order to maximise their effective life.

2.8 New Crop Protection Methods

As new crop protection methods are developed, they are often promoted as a solution to the loss of fungicide to resistance. However, the principles of resistance management apply to any crop protection measure. For example, in resistant cultivars, single major resistance genes are vulnerable to rapid breakdown by evolving pathogens just as single site-specific fungicides are high risk. A high-profile case of the breakdown of a disease resistance gene due to the evolution of virulence in the pathogen population is the Ug99 race of stem rust of wheat *Puccinia graminis* f. sp. *tritici*, affecting all wheat varieties reliant on the Sr31 gene for stem rust resistance (Wanyera et al., 2006). Earlier in the twentieth century, other stem rust resistance genes had been broken down after being deployed as the only effective resistance gene in widely grown varieties (Ellis et al., 2014). The key resistance gene overcome by Ug99, Sr31, had actually been deployed in combination within other resistance genes, but over time, the other resistance

genes in the stack had broken down, with Sr31 the latest of many virulence alleles in the Ug99 rust lineage (Jin et al., 2007).

Similarly, soybean rust *P. pachyrrhizi* populations in South America include strains with virulence against all current major resistance genes in commercial soybean varieties, but pyramiding multiple resistance genes conferred effective resistance (Yamanaka et al., 2015). This effectiveness will only be durable if multiple resistance genes within the pyramid are effective against each pathotype, so differential sets of soybean genotypes have been developed (Kashiwa et al., 2020): as with fungicide mixtures, it is important that multiple mixing partners are effective, and monitoring programmes must check whether the breakdown of one component is being masked in the field by the continued effectiveness of another.

These previous experiences of varietal resistance breakdown have shown that combining multiple effective resistance genes, akin to mixtures of fungicides, is necessary for durable resistance. However, just as there has been debate over the relative merits of mixing or alternating fungicide modes of action, research is ongoing into the best way to deploy multiple resistance genes: whether through stacking (or pyramiding) multiple genes in a single variety, or deploying multiple varieties with different resistance genes in temporal rotations, spatial mosaics, or within-field varietal mixtures of different compositions (Bourguet et al., 2016; Mikaberidze et al., 2015).

The need for durable deployment will continue to apply to novel resistance genes, whether they are introduced through new crosses with crop wild relatives (Chen et al., 2018), or through transgenic (Zhu et al., 2012) or gene editing technologies (Langner et al., 2018). Precision breeding can rapidly introduce a single resistance gene into the desired genetic background, but can also be used to pyramid multiple resistance genes in a single variety to increase durability (Jones et al., 2014).

Genetic control of plant pathogens through gene drives has also been proposed, for example by releasing a gene drive element that spreads through pathogen populations in place of a gene necessary for pathogenicity (Gardiner et al., 2020). However, resistance to gene drives may emerge either through naturally-occurring mismatch mutations in the target region in the non-modified pathogen population, or by non-homologous end-joining (NHEJ) of DNA cleaved during the gene drive process itself (Unckless et al., 2017). The risk of mismatch mutations may be reduced by selecting more conserved targets, whereas NHEJ-derived resistance would need to be managed in the same way as any other resistance: by using in

combination with other effective control measures, thereby reducing the reproductive rate of gene-drive resistant as well as susceptible or modified individuals. A mixture-type strategy, multiplexing guide RNAs with different targets, may also be possible (Champer et al., 2018). Furthermore, gene drives spread through sexual crosses, so clonal pathogen populations are not susceptible.

Another potential future control method is RNAi, either spray-based (Koch et al., 2016) or through host-induced gene silencing (HIGS) by transgenic plants (Koch et al., 2013). Koch et al. (2013, 2016) used a double-stranded (ds) RNA construct comprising stacked fragments of three target genes, but in this case the target genes were paralogues with some functional redundancy, so this was not necessarily designed as an anti-resistance strategy. More work is needed to quantify the number of mutations that would be needed to confer target-site resistance, and to understand the intrinsic non-susceptibility of some pathogen species (Kettles et al., 2019) and whether initially susceptible species could evolve similar mechanisms for non-target-site resistance.

Whichever crop protection measures are developed in future, the same core principles of resistance management will apply: assume any control measure will exert a selection pressure for resistance, avoid over-reliance on any single measure, and use within an IPM strategy.

2.9   Acknowledgements

2.10   References

Aguilar-Barragan, A., García-Torres, A. E., Odriozola-Casas, O., Macedo-Raygoza, G., Ogura, T., Manzo-Sánchez, G. et al. (2014). Chemical management in fungicide sensitivity of *Mycosphaerella fijiensis* collected from banana fields in México. *Brazilian Journal of Microbiology* 45: 359-364.

AHDB (2020). *Spotlight on the loss of active substances* [Online]. Agriculture and Horticulture Development Board, UK. Available at:

https://ahdb.org.uk/knowledge-library/extension-of-authorisation-for-minor-use-eamu/spotlight-loss-active-substances [Accessed 21st February 2020].

Allen, R. C., Engelstadter, J., Bonhoeffer, S., McDonald, B. A. & Hall, A. R. (2017). Reversing resistance: different routes and common themes across pathogens. *Proceedings of the Royal Society B-Biological Sciences* 284**:** 10.

Amaradasa, B. S. & Everhart, S. E. (2016). Effects of Sublethal Fungicides on Mutation Rates and Genomic Variation in Fungal Plant Pathogen, Sclerotinia sclerotiorum. *PLoS One* 11**:** e0168079.

Anastassiadou, M., Bernasconi, G., Brancato, A., Cabrera, L. C., Ferreira, L., Greco, L. et al. (2020) Evaluation of confirmatory data following the Article 12 MRL review for chlorothalonil, including assessments for import tolerances for banana, papaya and peanuts. *EFSA Journal* 18**:** 48.

Angelotti, F., Buffara, C. R. S., Tessamnn, D. J., Vieira, R. A. & Vida, J. B. (2014). Protective, curative and eradicative activities of fungicides against grapevine rust. *Ciencia Rural* 44**:** 1367-1370.

Ballu, A., Despréaux, P., Duplaix, C., Dérédec, A., Carpentier, F., Walker, A.-S. (2021). I alternate therefore I generalize: how the intrinsic resistance risk of fungicides counterbalances their durability. *bioRxiv*, 2021.07.11.451819 https://doi.org/10.1101/2021.07.11.451819

Barres, B., Micoud, A., Corio-Costet, M. F., Debieu, D., Fillinger, S., Walker, A. S., et al. (2016). Trends and Challenges in Pesticide Resistance Detection. *Trends in Plant Science* 21**:** 834-853.

Barrett, M., Soteres, J. & Shaw, D. (2016). Carrots and Sticks: Incentives and Regulations for Herbicide Resistance Management and Changing Behavior. *Weed Science* 64**:** 627-640.

Beckerman, J. L., Sundin, G. W. & Rosenberger, D. A. (2015). Do some IPM concepts contribute to the development of fungicide resistance? Lessons learned from the apple scab pathosystem in the United States. *Pest Management Science* 71**:** 331-342.

Beckie, H.J., Busi, R., Lopez-Ruiz, F.J. & Umina, P.A. (2021). Herbicide resistance management strategies: how do they compare with those for insecticides, fungicides and antibiotics? *Pest Management Science* 77: 3049-3056.

Birch, A. N. E., Begg, G. S. & Squire, G. R. (2011). How agro-ecological research helps to address food security issues under new IPM and pesticide reduction policies for global crop production systems. *Journal of Experimental Botany* 62**:** 3251-3261.

Blake, J. J., Gosling, P., Fraaije, B. A., Burnett, F. J., Knight, S. M., Kildea, S. et al. (2018). Changes in field dose-response curves for demethylation inhibitor (DMI) and quinone outside inhibitor (QoI) fungicides against *Zymoseptoria tritici*, related to laboratory sensitivity phenotyping and genotyping assays. *Pest Management Science* 74: 302-313.

Blanquart, F. (2019). Evolutionary epidemiology models to predict the dynamics of antibiotic resistance. *Evolutionary Apllications* 12: 365-383.

Bourguet, D., Delmotte, F., Franck, P., Guillemaud, T., Reboud, X., Vacher, C. et al. (2016). Combining Selective Pressures to Enhance the Durability of Disease Resistance Genes. *Frontiers in Plant Science,* 7**,** 8.

Brent, K. J., Carter, G. A., Hollomon, D. W., Hunter, T., Locke, T. & Proven, M. (1989). Factors affecting build-up of fungicide resistance in powdery mildew in spring barley. *Netherlands Journal of Plant Pathology* 95**:** 31-41.

Brent, K. J. & Hollomon, D. W. (2007a). *Fungicide resistance in crop pathogens: how can it be managed?* FRAC Monographs, Fungicide Resistance Action Committee.

Brent, K. J. & Hollomon, D. W. (2007b). *Fungicide resistance: the assessment of risk.* FRAC Monographs, Fungicide Resistance Action Committee.

Bryson, R., and Brix, H.D. (2019). Challenges and prospects for fungicidal control of wheat diseases. In: Oliver, R.P. (Ed.) *Integrated diseases management of wheat and barley*. Cambridge, UK: Burleigh Dodds Science Publicing Limited, pp. 219-231.

Burke, J.J. & Dunne, B. (2008). Field testing of six decision support systems for scheduling fungicide applications to control *Mycosphaerella graminicola* on winter wheat crops in Ireland. *Journal of Agricultural Science* 146: 415-428.

Burnett, F. (2011). FRAG-UK (Fungicide Resistance Action Group – UK) – A Review of the Context, Work and Aims of this UK Resistance Action Group. *Outlooks on Pest Management* 22**:** 62-63.

Carolan, K., Helps, J., van den Berg, F., Bain, R., Paveley, N. & van den Bosch, F. (2017). Extending the durability of cultivar resistance by limiting epidemic growth rates. *Procedings of the Royal Society B- Biological Scienes* 284: 20170828.

Chait, R., Craney, A. & Kishony, R. (2007). Antibiotic interactions that select against resistance. *Nature* 446: 668-671.

Champer, J., Liu, J., Oh, S. Y., Reeves, R., Luthra, A., Oakes, N., et al. (2018). Reducing resistance allele formation in CRISPR gene drive. *Proceedings of the National Academy of Sciences* 115: 5522-5527.

Chen, R. S. & McDonald, B. A. (1996). Sexual reproduction plays a major role in the genetic structure of populations of the fungus *Mycosphaerella graminicola*. *Genetics* 142: 1119-1127.

Chen, S., Guo, Y., Briggs, J., Dubach, F., Chao, S., Zhang, W. et al. (2018). Mapping and characterization of wheat stem rust resistance genes SrTm5 and Sr60 from *Triticum monococcum*. *Theoretical and Applied Genetics* 131**: 625-635.

Cohen, Y., Rubin, A. E. & Galperin, M. (2018). Oxathiapiprolin-based fungicides provide enhanced control of tomato late blight induced by mefenoxam-insensitive *Phytophthora infestans*. *Plos One* 13: e0204523.

Cooke, L. R., Schepers, H. T. A. M., Hermansen, A., Bain, R. A., Bradshaw, N. J., Ritchie, F. et al. (2011). Epidemiology and Integrated Control of Potato Late Blight in Europe. *Potato Research* 54: 183-222.

de Ramon-Carbonell, M., Lopez-Perez, M., Gonzalez-Candelas, L. & Sanchez-Torres, P. (2019). PdMFS1 Transporter Contributes to Penicilliun digitatum Fungicide Resistance and Fungal Virulence during Citrus Fruit Infection. *Journal of Fungi* 5**: 100**.

Dentzman, K., Gunderson, R. & Jussaume, R. (2016). Techno-optimism as a barrier to overcoming herbicide resistance: Comparing farmer perceptions of the future potential of herbicides. *Journal of Rural Studies* 48: 22-32.

Dodhia, K. N., Cox, B. A., Oliver, R. P. & Lopez-Ruiz, F. J. (2021). Rapid *in situ* quantification of the strobilurin resistance mutation G143A in the wheat pathogen *Blumeria graminis* f. sp. *tritici*. *Scientific Reports* 11: 4526.

Dooley, H., Shaw, M. W., Spink, J. & Kildea, S (2016). The effect of succinate dehydrogenase inhibitor/azole mixtures on selection of *Zymoseptoria tritici* isolates with reduced sensitivity. *Pest Management Science* 72: 1150-1159.

Duan, Y. B., Yang, Y., Wang, J. X., Liu, C. C., He, L. L. & Zhou, M. G. (2015). Development and application of loop-mediated isothermal amplification for detecting the highly benzimidazole-resistant isolates in *Sclerotinia sclerotiorum*. *Scientific Reports* 5: 11.

Dunne, K., Hagen, F., Pomeroy, N., Meis, J. F. & Rogers, T. R. (2017). Intercountry Transfer of Triazole-Resistant *Aspergillus fumigatus* on Plant Bulbs. *Clinical Infectious Diseases* 65**: 147-149.

Elad, Y., Shabi, E. & Katan, T. (1988). Negative cross resistance between benzimidazole and N-phenylcarbamate fungicides and control of *Botrytis cinerea* on grapes. *Plant Pathology* 37: 141-147.

Elderfield, J. A. D., Lopez-Ruiz, F. J., van den Bosch, F. & Cunniffe, N. J. (2018). Using Epidemiological Principles to Explain Fungicide Resistance Management Tactics: Why do Mixtures Outperform Alternations? *Phytopathology* 108: 803-817.

Ellis, J. G., Lagudah, E. S., Spielmeyer, W. & Dodds, P. N. (2014). The past, present and future of breeding rust resistant wheat. *Frontiers in plant science* 5**:** 641-641.

Ellwood, S. R., Piscetek, V., Mair, W. J., Lawrence, J. A., Lopez-Ruiz, F. J. & Rawlinson, C. (2019). Genetic variation of Pyrenophora teres f. teres isolates in Western Australia and emergence of a Cyp51A fungicide resistance mutation. *Plant Pathology* 68: 135-142.

EPPO. (2015). PP 1/213 (4) Resistance risk analysis. *EPPO Bulletin* 4: 371-387.

Ervin, D. E., Breshears, E. H., Frisvold, G. B., Hurley, T., Dentzman, K. E., Gunsolus, J. L. et al. (2019). Farmer Attitudes Toward Cooperative Approaches to Herbicide Resistance Management: A Common Pool Ecosystem Service Challenge. *Ecological Economics* 157**:** 237-245.

Evans, J. A., Williams, A., Hager, A. G., Mirsky, S. B., Tranel, P. J. & Davis, A. S. (2018). Confronting herbicide resistance with cooperative management. *Pest Management Science* 74**:** 2424-2431.

Fernandez Ortuno, D., Grabke, A., Li, X. & Schnabel, G. (2014). Independent emergence of resistance to seven chemical classes of fungicides in *Botrytis cinerea*. *Phytopathology* 105: 424-32.

Fernando, W. G. D., Oghenekaro, A. O., Tucker, J. R. & Badea, A. (2021). Building on a foundation: advances in epidemiology, resistance breeding, and forecasting research for reducing the impact of fusarium head blight in wheat and barley. *Canadian Journal of Plant Pathology*, 43: 495-526.

Fisher, M. C., Hawkins, N. J., Sanglard, D. & Gurr, S. J. (2018). Worldwide emergence of resistance to antifungal drugs challenges human health and food security. *Science* 360**:** 739-742.

Fones, H. N., Fisher, M. C. & Gurr, S. J. (2017). Emerging Fungal Threats to Plants and Animals Challenge Agriculture and Ecosystem Resilience. *Microbiology Spectrum* 5: doi: 10.1128/microbiolspec.FUNK-0027-2016

Foo, J. & Michor, F. (2010). Evolution of resistance to anti-cancer therapy during general dosing schedules. *Journal of Theoretical Biology* 263**:** 179-188.

Fountaine, J., Piotrowska, M., Havis, N. & Burnett, F. (2014). Fungicide resistance in *Ramularia collo-cygni*. *The Dundee Conference. Crop Protection in*

Northern Britain 2014, Dundee, UK, 25-26 February 2014. The Association for Crop Protection in Northern Britain, pp. 101-106.

Fraaije, B. A. & Cools, H. J. (2013). Detection of azole insensitive *CYP51* over-expressing strains of *Mycosphaerella graminicola* using loop-mediated isothermal amplification (LAMP) assays. *Acta Phytopathologica Sinica* 43**:** 289.

Fraaije, B. A., Cools, H. J., Kim, S. H., Motteram, J., Clark, W. S. & Lucas, J. A. (2007). A novel substitution I381V in the sterol 14 alpha-demethylase (CYP51) of *Mycosphaerella graminicola* is differentially selected by azole fungicides. *Molecular Plant Pathology* 8**:** 245-254.

FRAC. (2020a). FRAC Code List 2020: Fungal control agents sorted by cross resistance pattern and mode of action. Fungicide Resistance Action Committee. Available at:

https://cpb-us-w2.wpmucdn.com/u.osu.edu/dist/b/28945/files/2020/02/frac-code-list-2020-final.pdf [Accessed 2nd September 2021].

FRAC. (2020b). List of First Confirmed Cases of Plant Pathogenic Organisms Resistant to Disease Control Agents. Fungicide Resistance Action Committee. Available at:

https://cpb-us-w2.wpmucdn.com/u.osu.edu/dist/b/28945/files/2020/02/frac-code-list-2020-final.pdf [Accessed 2nd September 2021].

FRAC. (2021). *Monitoring Methods* [Online]. https://www.frac.info/knowledge-database/monitoring-methods. [Accessed 3rd March 2021].

Fungicide Resistance Action Group (FRAG)- UK. (2020). *Fungicide resistance management in cereals* [Online]. Fungicide Resistance Action Group UK. Available: https://cereals.ahdb.org.uk/frag [Accessed 2nd September 2021].

Gardiner, D. M., Rusu, A., Barrett, L., Hunter, G. C. & Kazan, K. (2020). Can natural gene drives be part of future fungal pathogen control strategies in plants? *New Phytologist* 228**:** 1431-1439.

Garnault, M., Duplaix, C., Leroux, P., Couleaud, G., David, O., Walker, A. S. et al. (2021). Large-scale study validates that regional fungicide applications are major determinants of resistance evolution in the wheat pathogen *Zymoseptoria tritici* in France. *New Phytologist* 229: 3508-3521.

Gent, D. H., Mahaffee, W. F., McRoberts, N. & Pfender, W. F. (2013). The Use and Role of Predictive Systems in Disease Management. *Annual Review of Phytopathology* 51: 267-289

Gould, F., Brown, Z. S. & Kuzma, J. (2018). Wicked evolution: Can we address the sociobiological dilemma of pesticide resistance? *Science* 360**:** 728-732.

Grimmer, M. K., van den Bosch, F., Powers, S. J. & Paveley, N. D. (2014). Evaluation of a matrix to calculate fungicide resistance risk. *Pest Management Science* 70**:** 1008-16.

Grimmer, M. K., van den Bosch, F., Powers, S. J. & Paveley, N. D. (2015). Fungicide resistance risk assessment based on traits associated with the rate of pathogen evolution. *Pest Management Science* 71: 207-215.

Gutiérrez-Alonso, O., Hawkins, N. J., Cools, H. J., Shaw, M. W. & Fraaije, B. A. (2017). Dose-dependent selection drives lineage replacement during the experimental evolution of SDHI fungicide resistance in Zymoseptoria tritici. *Evolutionary Applications* 10: 1055-1066.

Hagerty, C. H., Graebner, R. C., Sackett, K. E. & Mundt, C. C. (2017). Variable competitive effects of fungicide resistance in field experiments with a plant pathogenic fungus. *Ecological Applications* 27: 1305-1316.

Hagerty, C. H. & Mundt, C. C. (2016). Reduced Virulence of Azoxystrobin-Resistant Zymoseptoria tritici Populations in Greenhouse Assays. *Phytopathology* 106: 884-889.

Hahn, M. (2014). The rising threat of fungicide resistance in plant pathogenic fungi: Botrytis as a case study. *Journal of Chemical Biology* 7**:** 133-41.

Hartmann, F. E., McDonald, B. A. & Croll, D. (2018). Genome-wide evidence for divergent selection between populations of a major agricultural pathogen. *Molecular Ecology* 27: 2725-2741.

Hawkins, N. J., Bass, C., Dixon, A. & Neve, P. (2019). The evolutionary origins of pesticide resistance. *Biological Reviews* 94**:** 135-155.

Hawkins, N. J. & Fraaije, B. A. (2016). Predicting Resistance by Mutagenesis: Lessons from 45 Years of MBC Resistance. *Frontiers in Microbiology* 7**:** 1814.

Hawkins, N. J. & Fraaije, B. A. (2018). Fitness Penalties in the Evolution of Fungicide Resistance. *Annual Review of Phytopathology* 56: 339-360.

Heaney, S. P., Hall, A., Davies, S. A. & Olaya, G. (2000). Resistance to fungicides in the QoI-STAR cross-resistance group: current perspectives. In: *The BCPC Conference: pests and diseases, volume 2. Proceedings of an International Conference, Brighton, UK, 13-16 November 2000.* Farnham: British Crop Protection Council, pp. 755-762.

Heick, T. M., Justesen, A. F. & Jørgensen, L. N. (2017). Anti -resistance strategies for fungicides against wheat pathogen Zymoseptoria tritici with focus on DMI fungicides. *Crop Protection* 99: 108-117.

Helps, J. C., Paveley, N. D. & van den Bosch, F. (2017). Identifying circumstances under which high insecticide dose increases or decreases resistance selection. *Journal of Theoretical Biology* 428**:** 153-167.

Hicks, H. L., Comont, D., Coutts, S. R., Crook, L., Hull, R., Norris, K. et al. (2018). The factors driving evolved herbicide resistance at a national scale. *Nature Ecology & Evolution* 2**:** 529-536.

Hillocks, R. J. (2012). Farming with fewer pesticides: EU pesticide review and resulting challenges for UK agriculture. *Crop Protection* 31: 85-93.

Hobbelen, P. H. F., Paveley, N. D., Oliver, R. P. & van den Bosch, F. (2013). The Usefulness of Fungicide Mixtures and Alternation for Delaying the Selection for Resistance in Populations of *Mycosphaerella graminicola* on Winter Wheat: A Modeling Analysis. *Phytopathology* 103**:** 690-707.

Hobbelen, P. H. F., Paveley, N. D. & van den Bosch, F. (2014). The Emergence of Resistance to Fungicides. *Plos One,* 9**:** e91910.

Huf, A., Rehfus, A., Lorenz, K. H., Bryson, R., Voegele, R. T. & Stammler, G. (2018). Proposal for a new nomenclature for *CYP51* haplotypes in *Zymoseptoria tritici* and analysis of their distribution in Europe. *Plant Pathology* 67;:1706-1712.

Isaza, R. E. A., Diaz-Trujillo, C., Dhillon, B., Aerts, A., Carlier, J., Crane, C. F. et al. (2016). Combating a Global Threat to a Clonal Crop: Banana Black Sigatoka Pathogen *Pseudocercospora fijiensis* (Synonym *Mycosphaerella fijiensis*) Genomes Reveal Clues for Disease Control. *PLoS Genetics* 12: e1005876.

Jin, Y., Singh, R. P., Ward, R. W., Wanyera, R., Kinyua, M., Njau, P. et al. (2007). Characterization of Seedling Infection Types and Adult Plant Infection Responses of Monogenic Sr Gene Lines to Race TTKS of *Puccinia graminis* f. sp. *tritici. Plant Disease* 91: 1096-1099.

Jones, J. D. G., Witek, K., Verweij, W., Jupe, F., Cooke, D., Dorling, S. et al. (2014). Elevating crop disease resistance with cloned genes. *Philosophical Transactions of the Royal Society B: Biological Sciences* 369**:** 20130087.

Jørgensen, L. N., Hovmoller, M. S., Hansen, J. G., Lassen, P., Clark, B., Bayles, R. et al. (2014). IPM Strategies and Their Dilemmas Including an Introduction to www.eurowheat.org. *Journal of Integrative Agriculture* 13: 265-281.

Jørgensen, L. N., Matzen, N., Ficke, A., Nielsen, G. C., Jalli, M., Ronis, A. et al. (2020a). Validation of risk models for control of leaf blotch diseases in wheat in the Nordic and Baltic countries. *European Journal of Plant Pathology* 157: 599-613.

Jørgensen, L. N., Matzen, N., Hansen, J. G., Semaskiene, R., Korbas, M., Danielewicz, J. et al. (2018). Four azoles' profile in the control of Septoria, yellow rust and brown rust in wheat across Europe. *Crop Protection* 105**:** 16-27.

Jørgensen, L. N., Matzen, N., Heick, T. M., Havis, N., Holdgate, S., Clark, B. et al. (2020b). Decreasing azole sensitivity of *Z. tritici* in Europe contributes to reduced and varying field efficacy. *Journal of Plant Diseases and Protection* 128: 287–301.

Jørgensen, L. N., van den Bosch, F., Oliver, R. P., Heick, T. M. & Paveley, N. D. (2017). Targeting Fungicide Inputs According to Need. *Annual Review of Phytopathology* 55**:** 181-203.

Jutsum, A. R., Heaney, S. P., Perrin, B. M. & Wege, P. J. (1998). Pesticide resistance: Assessment of risk and the development and implementation of effective management strategies. *Pesticide Science* 54**:** 435-446.

Kaczmarek, J., Kedziora, A., Brachaczek, A., Latunde-Dada, A. O., Dakowska, S., Karg, G. et al. (2016). Effect of climate change on sporulation of the teleomorphs of Leptosphaeria species causing stem canker of brassicas. *Aerobiologia* 32: 39-51.

Kashiwa, T., Muraki, Y. & Yamanaka, N. (2020). Near-isogenic soybean lines carrying Asian soybean rust resistance genes for practical pathogenicity validation. *Scientific Reports* 10: 13270.

Kettles, G. J., Hofinger, B. J., Hu, P. S., Bayon, C., Rudd, J. J., Balmer, D. et al. (2019). sRNA Profiling Combined With Gene Function Analysis Reveals a Lack of Evidence for Cross-Kingdom RNAi in the Wheat - *Zymoseptoria tritici* Pathosystem. *Frontiers in Plant Science* 10: 892.

Kildea, S., Heick, T.M., Grant, J., Mehenni-Ciz, J. & Dooley, H. (2019). A combination of target-site alterations, overexpression and enhanced efflux activity contribute to reduced azole sensitivity present in the Irish *Zymoseptoria tritici* population. *European Journal of Plant Pathology* 154**:** 529-540.

Kitchen, J. L., van den Bosch, F., Paveley, N. D., Helps, J. & van den Berg, F. (2016). The Evolution of Fungicide Resistance Resulting from Combinations of Foliar-Acting Systemic Seed Treatments and Foliar-Applied Fungicides: A Modeling Analysis. *PLoS One* 11**:** e0161887.

Koch, A., Biedenkopf, D., Furch, A., Weber, L., Rossbach, O., Abdellatef, E. et al. (2016). An RNAi-Based Control of *Fusarium graminearum* Infections Through

Spraying of Long dsRNAs Involves a Plant Passage and Is Controlled by the Fungal Silencing Machinery. *PLoS Pathogens* 12**:** e1005901.

Koch, A., Kumar, N., Weber, L., Keller, H., Imani, J. & Kogel, K.-H. (2013). Host-induced gene silencing of cytochrome P450 lanosterol C14α-demethylase–encoding genes confers strong resistance to *Fusarium* species. *Proceedings of the National Academy of Sciences* 110: 19324-19329.

Koller, W. & Wilcox, W. F. (2001). Evidence for the predisposition of fungicide-resistant isolates of *Venturia inaequalis* to a preferential selection for resistance to other fungicides. *Phytopathology* 91**:** 776-781.

Kosman, E. & Cohen, Y. (1996). Procedures for calculating and differentiating synergism and antagonism in action of fungicide mixtures. *Phytopathology* 86**:** 1263-1272.

Kremer, P., Schluter, J., Racca, P., Fuchs, H. J. & Lang, C. (2016). Possible impact of climate change on the occurrence and the epidemic development of cercospora leaf spot disease (*Cercospora beticola* sacc.) in sugar beets for Rhineland-Palatinate and the southern part of Hesse. *Climatic Change* 137**:** 481-494.

Kretschmer, M., Leroch, M., Mosbach, A., Walker, A. S., Fillinger, S., Mernke, D. et al. (2009). Fungicide-Driven Evolution and Molecular Basis of Multidrug Resistance in Field Populations of the Grey Mould Fungus *Botrytis cinerea*. *Plos Pathogens* 5**:** e1000696.

Kristoffersen, R., Heick, T. M., Møller, G., Eriksen, L.B., Nielsen, G. C., Jørgensen, L. N. (2020). The potential of cultivar mixtures to reduce fungicide input and mitigate fungicide resistance development. Agronomy for Sustainable Development 40:36

Kudsk, P. (2010). Norbarag (Nordic Baltic Resistance Action Group) – a new resistance action group covering Denmark, Estonia, Finland, Latvia, Lithuania, Norway and Sweden. *Outlooks on Pest Management* 21: 223-224.

Lalève, A., Fillinger, S. & Walker, A. S. (2014). Fitness measurement reveals contrasting costs in homologous recombinant mutants of *Botrytis cinerea* resistant to succinate dehydrogenase inhibitors. *Fungal Genetics and Biology* 67: 24-36.

Lamichhane, J. R., Arendse, W., Dachbrodt-Saaydeh, S., Kudsk, P., Roman, J. C., Van Bijsterveldt-Gels, J. E. M. et al. (2015a). Challenges and opportunities for integrated pest management in Europe: A telling example of minor uses. *Crop Protection* 74**:** 42-47.

Lamichhane, J. R., Dachbrodt-Saaydeh, S., Kudsk, P. & Messéan, A. (2015). Toward a Reduced Reliance on Conventional Pesticides in European Agriculture. *Plant Disease* 100: 10-24.

Lamichhane, J. R., You, M. P., Laudinot, V., Barbetti, M. J. & Aubertot, J.-N. (2019). Revisiting Sustainability of Fungicide Seed Treatments for Field Crops. *Plant Disease,* 104**,** 610-623.

Langenbach, C., Campe, R., Beyer, S. F., Mueller, A. N. & Conrath, U. (2016). Fighting Asian Soybean Rust. *Frontiers in Plant Science* 7**:** 797.

Langner, T., Kamoun, S. & Belhaj, K. (2018). CRISPR Crops: Plant Genome Editing Toward Disease Resistance. *Annual Review of Phytopathology* 56: 479-512.

Leach, A. B., Hoepting, C. A. & Nault, B. A. (2019). Grower adoption of insecticide resistance management practices increase with extension-based program. *Pest Management Science* 75**:** 515-526.

Lefebvre, M., Langrell, S. R. H. & Gomez-Y-Paloma, S. (2015). Incentives and policies for integrated pest management in Europe: a review. *Agronomy for Sustainable Development* 35: 27-45.

Leroux, P., Albertini, C., Gautier, A., Gredt, M. & Walker, A. S. (2007). Mutations in the CYP51 gene correlated with changes in sensitivity to sterol 14 alpha-demethylation inhibitors in field isolates of *Mycosphaerelia graminicola*. *Pest Management Science* 63: 688-698.

Leroux, P., Chapeland, F., Arnold, A. & Gredt, M. (2000). New cases of negative cross-resistance between fungicides, including sterol biosynthesis inhibitors. *Journal of General Plant Pathology* 66: 75-81.

Leroux, P., Fritz, R., Debieu, D., Albertini, C., Lanen, C., Bach, J., et al. (2002). Mechanisms of resistance to fungicides in field strains of *Botrytis cinerea*. *Pest Management Science* 58: 876-888.

Lin, H. C., Yu, P. L., Chen, L. H., Tsai, H. C. & Chung, K. R. (2018). A Major Facilitator Superfamily Transporter Regulated by the Stress-Responsive Transcription Factor Yap1 Is Required for Resistance to Fungicides, Xenobiotics, and Oxidants and Full Virulence in *Altemaria altemata*. *Frontiers in Microbiology* 9**:** 2229.

Llewellyn, R. S. & Allen, D. M. (2006). Expected mobility of herbicide resistance via weed seeds and pollen in a Western Australian cropping region. *Crop Protection* 25**:** 520-526.

Lucas, J. (2003). Resistance to QoI fungicides: implications for cereal disease management in Europe. *Pesticide Outlook* 14**:** 268-270.

Luo, C. X. & Schnabel, G. (2008). Adaptation to fungicides in *Monilinia fructicola* isolates with different fungicide resistance phenotypes. *Phytopathology* 98**:** 230-238.

Main, C. E., Keever, T., Holmes, G. J., & Davis, J.M. (2001). Forecasting Long-Range Transport of Downy Mildew Spores and Plant Disease Epidemics. *APSnet Features,* doi: 10.1094/APSnetFeature-2001-0501.

Manalil, S., Busi, R., Renton, M. & Powles, S. B. (2011). Rapid Evolution of Herbicide Resistance by Low Herbicide Dosages. *Weed Science* 59**:** 210-217.

Massi, F., Torriani, S. F. F., Borghi, L. & Toffolatti, S. L. (2021). Fungicide Resistance Evolution and Detection in Plant Pathogens: *Plasmopara viticola* as a Case Study. *Microorganisms* 9**:** 119.

Matusinsky, P., Svacinova, I., Jonaviciene, A. & Tvaruzek, L. (2017). Long-term dynamics of causative agents of stem base diseases in winter wheat and reaction of Czech *Oculimacula* spp. and *Microdochium* spp. populations to prochloraz. *European Journal of Plant Pathology* 148**:** 199-206.

McDonald, B. A. & Mundt, C. C. (2016). How Knowledge of Pathogen Population Biology Informs Management of Septoria Tritici Blotch. *Phytopathology* 106: 948-955.

McDonald, B. A. & Stukenbrock, E. H. (2016). Rapid emergence of pathogens in agro-ecosystems: global threats to agricultural sustainability and food security. *Philosophical Transactions of the Royal Society B: Biological Sciences,* 371: 20160026.

Mikaberidze, A., McDonald, B. A. & Bonhoeffer, S. (2014). Can High-Risk Fungicides be Used in Mixtures Without Selecting for Fungicide Resistance? *Phytopathology* 104: 324-331.

Mikaberidze, A., McDonald, B. A. & Bonhoeffer, S. (2015). Developing smarter host mixtures to control plant disease. *Plant Pathology* 64**:** 996-1004.

Mikaberidze, A., Paveley, N., Bonhoeffer, S. & van den Bosch, F. (2017). Emergence of Resistance to Fungicides: The Role of Fungicide Dose. *Phytopathology* 107**:** 545-560.

Milgroom, M. G. (1990). A stochastic-model for the initial occurrence and development of fungicide resistance in plant pathogen populations. *Phytopathology* 80**:** 410-416.

Milgroom, M. G. & Fry, W. E. (1988). A simulation analysis of the epidemiological principles for fungicide resistance management in pathogen populations. *Phytopathology* 78**:** 565-570.

Montanari, A., Innocenti, G. & Toderi, G. (2006). Effects of cultural management on the foot and root disease complex of durum wheat. *Journal of Plant Pathology* 88**:** 149-156.

Morse, P. M. (1978). Some Comments on the Assessment of Joint Action in Herbicide Mixtures. *Weed Science* 26**:** 58-71.

Mundt, C. C. (2018). Pyramiding for Resistance Durability: Theory and Practice. *Phytopathology* 108**:** 792-802.

Nichol, D., Rutter, J., Bryant, C., Hujer, A. M., Lek, S., Adams, M. D. et al. (2019). Antibiotic collateral sensitivity is contingent on the repeatability of evolution. *Nature Communications,* 10: 334.

Nishimoto, R. (2019). Global trends in the crop protection industry. *Journal of Pesticide Science* 44**:** 141-147.

Oerke, E. C. & Dehne, H. W. (2004). Safeguarding production - losses in major crops and the role of crop protection. *Crop Protection* 23**:** 275-285.

Oliver, C. L., Cooper, M. L., Ivey, M. L. L., Brannen, P. M., Miles, T. D., Mahaffee, W. F. et al. (2021). Assessing the United States Grape Industry's Understanding of Fungicide Resistance Mitigation Practices. *American Journal of Enology and Viticulture* 72: 181-193.

Oliver, R. P. (2014). A reassessment of the risk of rust fungi developing resistance to fungicides. *Pest Management Science* 70**:** 1641-1645.

Oliver, R. (2016). Fungicide resistance management in practice; mixtures, alternations and cross resistance patterns. *Journal of Plant Pathology* 98: S11.

Omrane, S., Sghyer, H., Audéon, C., Lanen, C., Duplaix, C., Walker, A.-S. et al. (2015). Fungicide efflux and the MgMFS1 transporter contribute to the MDR phenotype in *Zymoseptoria tritici* field isolates. *Environmental Microbiology* 17: 2805-2823.

Opatowski, L., Mandel, J., Varon, E., Boelle, P. Y., Temime, L. & Guillemot, D. (2010). Antibiotic Dose Impact on Resistance Selection in the Community: a Mathematical Model of beta-Lactams and *Streptococcus pneumoniae* Dynamics. *Antimicrobial Agents and Chemotherapy* 54**:** 2330-2337.

Pacilly, F. C. A., Van Bueren, E. T. L., Groot, J. C. J. & Hofstede, G. J. (2019). Moving perceptions on potato late blight control: Workshops with model-based scenarios. *Crop Protection* 119**:** 76-87.

Parnell, S., van den Bosch, F. & Gilligan, C. A. (2006). Large-Scale Fungicide Spray Heterogeneity and the Regional Spread of Resistant Pathogen Strains. *Phytopathology* 96**:** 549-555.

Paveley, N. D., Thomas, J. M., Vaughan, T. B., Havis, N. D. & Jones, D. R. (2003). Predicting effective doses for the joint action of two fungicide applications. *Plant Pathology* 52**:** 638-647.

Pedersen, A. B., Nielsen, H. Ø., Christensen, T., Ørum, J. E. & Martinsen, L. (2019). Are independent agricultural advisors more oriented towards recommending reduced pesticide use than supplier-affiliated advisors? *Journal of Environmental Management* 242: 507-514.

Pertot, I., Caffi, T., Rossi, V., Mugnai, L., Hoffmann, C., Grando, M. S. et al. (2017). A critical review of plant protection tools for reducing pesticide use on grapevine and new perspectives for the implementation of IPM in viticulture. *Crop Protection* 97**:** 70-84.

Pieczul, K. & Wasowska, A. (2017). The application of next-generation sequencing (NGS) for monitoring of *Zymoseptoria tritici* QoI resistance. *Crop Protection* 92**:** 143-147.

Pimentel, D. (2005). Environmental and Economic Costs of the Application of Pesticides Primarily in the United States. *Environment, Development and Sustainability* 7**:** 229-252.

Popp, J. (2011). Cost-benefit analysis of crop protection measures. *Journal für Verbraucherschutz und Lebensmittelsicherheit* 6**:** 105-112.

Popp, J., Peto, K. & Nagy, J. (2013). Pesticide productivity and food security. A review. *Agronomy for Sustainable Development* 33**:** 243-255.

Porter, L. D., Hamm, P. B., David, N. L., Gieck, S. L., Miller, J. S., Gundersen, B. et al. (2009). Metalaxyl-M-Resistant *Pythium* Species in Potato Production Areas of the Pacific Northwest of the USA. *American Journal of Potato Research* 86: 315-326.

Raymond, B. (2019). Five rules for resistance management in the antibiotic apocalypse, a road map for integrated microbial management. *Evolutionary Applications* 12**:** 1079-1091.

Rehfus, A., Matusinsky, P., Strobel, D., Bryson, R. & Stammler, G. (2019). Mutations in target genes of succinate dehydrogenase inhibitors and demethylation inhibitors in *Ramularia collo-cygni* in Europe. *Journal of Plant Diseases and Protection* 126**:** 447-459.

Rehfus, A., Miessner, S., Achenbach,J., Strobel, D., Bryson, R. & Stammler, G. (2016). Emergence of succinate dehydrogenase inhibitor resistance of *Pyrenophora teres* in Europe. Pest Managmeent Science 72: 447-459.

Roberts, J. A., Kruger, P., Paterson, D. L. & Lipman, J. (2008). Antibiotic resistance - What's dosing got to do with it? *Critical Care Medicine* 36**:** 2433-2440.

Robinson, T. P., Bu, D. P., Carrique-Mas, J., Fevre, E. M., Gilbert, M., Grace, D. et al. (2016). Antibiotic resistance is the quintessential One Health issue. *Transactions of the Royal Society of Tropical Medicine and Hygiene* 110**:** 377-380.

Rogers, S. L., Atkins, S. D. & West, J. S. (2009). Detection and quantification of airborne inoculum of *Sclerotinia sclerotiorum* using quantitative PCR. *Plant Pathology* 58**:** 324-331.

Rupp, S., Weber, R. W. S., Rieger, D., Detzel, P. & Hahn, M. (2017). Spread of Botrytis cinerea Strains with Multiple Fungicide Resistance in German Horticulture. *Frontiers in Microbiology* 7: 2075.

Sanatkar, M. R., Scoglio, C., Natarajan, B., Isard, S. A. & Garrett, K. A. (2015). History, Epidemic Evolution, and Model Burn-In for a Network of Annual Invasion: Soybean Rust. *Phytopathology* 105**:** 947-955.

Sang, H., Popko, J. T. & Jung, G. (2019). Evaluation of a *Sclerotinia homoeocarpa* Population with Multiple Fungicide Resistance Phenotypes Under Differing Selection Pressures. *Plant Disease* 103**:** 685-690.

Savary, S., Bregaglio, S., Willocquet, L., Gustafson, D., Mason D'croz, D., Sparks, A. et al. (2017). Crop health and its global impacts on the components of food security. *Food Security* 9**:** 311-327.

Schnabel, G. & Chen, F. (2013). Fungicide-induced mutagenesis in *Monilinia fructicola* and implications for resistance management. *Phytopathology* 103**:** 128-128.

Schnabel, G., Hu, M.J., Edison, G., & Pargas, R. (2018). Communication of FRAC code principles with fruit producers via smartphone. In: Deising, H.B., Fraaije, B., Mehl, A., Oerke, E.C., Sierotzki, H. & Stammler, G. (Eds.) *Modern fungicide and antifungal compounds VIII. Proceedings of the 18th International Reinhardsbrunn Symposium 2016.* Braunschweig, Germany: Verlag der Deutschen Phytomedizinischen Gesellschaft, pp. 73-76.

Schoonbeek, H., Del Sorbo, G. & De Waard, M. A. (2001). The ABC transporter BcatrB affects the sensitivity of *Botrytis cinerea* to the phytoalexin resveratrol and the fungicide fenpiclonil. *Molecular Plant-Microbe Interactions* 14**:** 562-571.

Schrag, S. J., Pena, C., Fernandez, J., Sanchez, J., Gomez, V., Perez, E. et al. (2001). Effect of short-course, high-dose amoxicillin therapy on resistant pneumococcal carriage - A randomized trial. *JAMA- Journal of the American Medical Association* 286**:** 49-56.

Shaw, M. W. (1989a). A model of the evolution of polygenically controlled fungicide resistance. *Plant Pathology* 38**:** 44-55.

Shaw, M. W. (1989b). Independent action of fungicides and its consequences for strategies to retard the evolution of fungicide resistance. *Crop Protection* 8**:** 405-411.

Shaw, M. W. (1993). Theoretical analysis of the effect of interacting activities on the rate of selection for combined resistance to fungicide mixtures. *Crop Protection* 12**:** 120-126.

Shaw, M. W. (2006). Is there such a thing as a resistance management strategy? A modeller's perspective. *Aspects of Applied Biology* 78**:** 95-103.

Sierotzki, H. & Scalliet, G. (2013). A Review of Current Knowledge of Resistance Aspects for the Next-Generation Succinate Dehydrogenase Inhibitor Fungicides. *Phytopathology* 103: 880-887.

Steinhauer, D., Salat, M., Frey, R., Mosbach, A., Luksch, T., Balmer, D. et al. (2019). A dispensable paralog of succinate dehydrogenase subunit C mediates standing resistance towards a subclass of SDHI fungicides in *Zymoseptoria tritici. PLoS Pathogens* 15: e1007780.

Steiro, A. L., Kvakkestad, V., Breland, T. A. & Vatn, A. (2020). Integrated Pest Management adoption by grain farmers in Norway: A novel index method. *Crop Protection,* 135: 105201.

Stetkiewicz, S., Bruce, A., Burnett, F. J., Ennos, R. A. & Topp, C. F. E. (2018). Perception vs practice: Farmer attitudes towards and uptake of IPM in Scottish spring barley. *Crop Protection* 112**:** 96-102.

Stetkiewicz, S., Burnett, F. J., Ennos, R. A. & Topp, C. F. E. (2019). The impact of fungicide treatment and Integrated Pest Management on barley yields: Analysis of a long term field trials database. *European Journal of Agronomy* 105**:** 111-118.

Stowell, L.J. & Gelernter, W. (2003). Barriers to adoption of pesticide resistance management programs. *PACE Insights* 9**:** 1-9.

Sundin, G. W. & Wang, N. (2018). Antibiotic Resistance in Plant-Pathogenic Bacteria. *Annual Review of Phytopathology* 56**:** 161-180.

Swanton, C. J., Mashhadi, H. R., Solomon, K. R., Afifi, M. M. & Duke, S. O. (2011). Similarities between the discovery and regulation of pharmaceuticals and pesticides: in support of a better understanding of the risks and benefits of each. *Pest Management Science* 67**:** 790-797.

Tabashnik, B. E., Brevault, T. & Carriere, Y. (2013). Insect resistance to Bt crops: lessons from the first billion acres. *Nature Biotechnology* 31**:** 510-521.

te Beest, D. E., Paveley, N. D., Shaw, M. W. & van den Bosch, F (2013). Accounting for the Economic Risk Caused by Variation in Disease Severity in Fungicide Dose Decisions, Exemplified for *Mycosphaerella graminicola* on Winter Wheat. *Phytopathology* 103**:** 666-672.

te Beest, D. E., Shaw, M. W., Paveley, N. D. & van den Bosch, F. (2009). Evaluation of a predictive model for *Mycosphaerella graminicola* for economic and environmental benefits. *Plant Pathology* 58: 1001-1009.

Ulber, L. & Rissel, D. (2018). Farmers' perspective on herbicide-resistant weeds and application of resistance management strategies: results from a German survey. *Pest Management Science* 74**:** 2335-2345.

Unckless, R. L., Clark, A. G. & Messer, P. W. (2017). Evolution of Resistance Against CRISPR/Cas9 Gene Drive. *Genetics* 205**:** 827-841.

Vagndorf, N., Heick, T. M., Justensen, A. F., Andersen, J. R., Jahoor, A., Jørgensen, L. N. et al. (2018). Population structure and frequency differences of CYP51 mutations in Zymoseptoria tritici populations in the Nordic and Baltic regions. European Journal of Plant Pathology, 152, 327-341.

van Bruggen, A. H. C., Goss, E. M., Havelaar, A., Van Diepeningen, A. D., Finckh, M. R. & Morris, J. G. (2019). One Health - Cycling of diverse microbial communities as a connecting force for soil, plant, animal, human and ecosystem health. *Science of the Total Environment,* 664**:** 927-937.

Van de Wouw, A. P., Marcroft, S. J., Sprague, S. J., Scanlan, J. L., Vesk, P. A. & Idnurm, A. (2021). Epidemiology and management of blackleg of canola in response to changing farming practices in Australia. *Australasian Plant Pathology* 50**:** 137-149.

van den Berg, F., Paveley, N. D. & van den Bosch, F (2016). Dose and number of applications that maximize fungicide effective life exemplified by *Zymoseptoria tritici* on wheat - a model analysis. *Plant Pathology* 65**:** 1380-1389.

van den Bosch, F., Blake, J., Gosling, P., Helps, J. C. & Paveley, N. (2020). Identifying when it is financially beneficial to increase or decrease fungicide dose as resistance develops: An evaluation from long-term field experiments. *Plant Pathology* 69**:** 631-641.

van den Bosch, F. & Gilligan, C. A. (2008). Models of fungicide resistance dynamics. *Annual Review of Phytopathology* 46**:** 123-147.

van den Bosch, F., Oliver, R., van den Berg, F. & Paveley, N. (2014a). Governing Principles Can Guide Fungicide-Resistance Management Tactics. *Annual Review of Phytopathology* 52**:** 175-195.

van den Bosch, F., Paveley, N., Shaw, M., Hobbelen, P. & Oliver, R. (2011). The dose rate debate: does the risk of fungicide resistance increase or decrease with dose? *Plant Pathology* 60**:** 597-606.

van den Bosch, F., Paveley, N., van den Berg, F., Hobbelen, P. & Oliver, R. (2014b). Mixtures as a Fungicide Resistance Management Tactic. *Phytopathology* 104**:** 1264-1273.

Verweij, P. E., Kema, G. H. J., Zwaan, B. & Melchers, W. J. G. (2013). Triazole fungicides and the selection of resistance to medical triazoles in the opportunistic mould Aspergillus fumigatus. *Pest Management Science* 69**:** 165-170.

Verweij, P. E., Lucas, J. A., Arendrup, M. C., Bowyer, P., Brinkmann, A. J. F., Denning, D. W. et al. (2020). The one health problem of azole resistance in *Aspergillus fumigatus*: current insights and future research agenda. *Fungal Biology Reviews* 34**:** 202-214.

Walker, A. S., Ravigne, V., Rieux, A., Ali, S., Carpentier, F. & Fournier, E. (2017). Fungal adaptation to contemporary fungicide applications: the case of *Botrytis cinerea* populations from Champagne vineyards (France). *Molecular Ecology* 26**:** 1919-1935.

Wanyera, R., Kinyua, M. G., Jin, Y. & Singh, R. P. (2006). The Spread of Stem Rust Caused by *Puccinia graminis* f. sp. *tritici*, with Virulence on Sr31 in Wheat in Eastern Africa. *Plant Disease* 90**:** 113-113.

West, J. S. & Kimber, R. B. E. (2015). Innovations in air sampling to detect plant pathogens. *Annals of Applied Biology* 166**:** 4-17.

Wilson, L. J., Whitehouse, M. E. A. & Herron, G. A. (2018). The Management of Insect Pests in Australian Cotton: An Evolving Story. *Annual Review of Entomology* 63: 215-237.

Wuepper, D., Roleff, N. & Finger, R. (2021). Does it matter who advises farmers? Pest management choices with public and private extension. *Food Policy* 99**:** 101995.

Yamanaka, N., Morishita, M., Mori, T., Lemos, N. G., Hossain, M. M., Akamatsu, H. et al. (2015). Multiple Rpp-gene pyramiding confers resistance to Asian soybean rust isolates that are virulent on each of the pyramided genes. *Tropical Plant Pathology* 40**:** 283-290.

Yang, Q. Q., Song, L. M., Miao, Z. G., Su, M. L., Liang, W. X. & He, Y. W. (2020). Acetylation of BcHpt Lysine 161 Regulates *Botrytis cinerea* Sensitivity to Fungicides, Multistress Adaptation and Virulence. *Frontiers in Microbiology* 10: 2965.

Yarden, O. & Katan, T. (1993). Mutations leading to substitutions at amino acids 198 and 200 of Beta-tubulin that correlate with benomyl resistance phenotypes of field strains of *Botrytis cinerea. Phytopathology* 83: 1478-1483.

Zhan, J. & McDonald, B. A. (2013). Field-based experimental evolution of three cereal pathogens using a mark-release-recapture strategy. *Plant Pathology* 62**:** 106-114.

Zhan, J., Pettway, R. E. & McDonald, B. A. (2003). The global genetic structure of the wheat pathogen *Mycosphaerella graminicola* is characterized by high nuclear diversity, low mitochondrial diversity, regular recombination, and gene flow. *Fungal Genetics and Biology* 38**:** 286-297.

Zhu, S. X., Li, Y., Vossen, J. H., Visser, R. G. F. & Jacobsen, E. (2012). Functional stacking of three resistance genes against *Phytophthora infestans* in potato. *Transgenic Research* 21**:** 89-99.

Zhu, W., Zhan, J. S. & McDonald, B. A. (2018). Evidence for local adaptation and pleiotropic effects associated with melanization in a plant pathogenic fungus. *Fungal Genetics and Biology* 115**:** 33-40.

Zulak, K. G., Cox, B. A., Tucker, M. A., Oliver, R. P. & Lopez-Ruiz, F. J. (2018). Improved Detection and Monitoring of Fungicide Resistance in *Blumeria graminis* f. sp *hordei* With High-Throughput Genotype Quantification by Digital PCR. *Frontiers in Microbiology,* 9: 706.

Chapter 3

Delaying infection through phytosanitary soybean-free periods contributes to fungicide resistance management in *Phakopsora pachyrhizi*: A modelling analysis

I. Corkley[1,2,3], J. Helps[1], F. van den Bosch[4,5,1], N.D. Paveley[6], A.E. Milne[1], A. Mikaberidze, H. Sierotzki[7], D.J. Skirvin[2]

[1]Net Zero and Resilient Farming, Rothamsted Research, Harpenden, UK. [2]Sustainable Agricultural Systems, ADAS, Wolverhampton, UK. [3]School of Agriculture, Policy and Development, University of Reading, Reading, UK. [4]Quantitative Biology & Epidemiology Group, Plant Pathology Department (Visiting Scholar), University of California, Davis, USA. [5]Sustainable Agricultural Systems, ADAS, Rosemaund, UK. [6]Sustainable Agricultural Systems, ADAS, High Mowthorpe, UK. [7]Syngenta Crop Protection AG, Basel, Switzerland.

A cornerstone principle of fungicide resistance management is to use IPM methods that can reduce disease pressure and so the intensity of fungicide application required. However, the resistance management benefits of cultural control methods are not well-quantified. In this chapter, I investigate the resistance management value of a phytosanitary cultural control method, the 'soybean-free period', in the asexual pathogen *P. pachyrhizi*.

The soybean-free period aims to remove local sources of inoculum to delay infection of soybean crops by *P. pachyrhizi* and so reduce yield losses. Using evolution of resistance to an SDHI fungicide as an example, I investigate the resistance management value of a delay in infection timing, exploring interactions with use of mixtures of different MoA, varying dose rates and number and timings of applications. I describe the development of a novel model of *P. pachyrhizi* infection of soybean crops, and the parameterisation and validation of fungicide dose response curves from efficacy data collected as part of commercial field trials.

The following manuscript was published in *Plant Pathology* **74**(4):1078-1096 in March 2025.

3.1   Abstract

Fungicide resistance threatens control of Asian soybean rust (*Phakopsora pachyrhizi*) in Brazilian soybean crops: deployment of sound resistance management tactics is crucial to prolong the effective life of new fungicides. A key integrated pest management (IPM) strategy in Brazil is the delay of *P. pachyrhizi* inoculum influx through soybean-free periods, mandated through restrictions on sowing dates. We developed an epidemiological model of fungicide resistance evolution in *P. pachyrhizi* to explore the impact of delayed inoculum influx on selection for resistance to a succinate dehydrogenase inhibitor (SDHI) fungicide, and to compare the relative benefits of alternative mixture partners. We fitted model parameters describing the efficacy of fungicides using disease severity data from field trials and validated our approach using a separate dataset from trials of solo and mixture products. Our results suggest that mixture with a multi-site acting fungicide such as mancozeb or chlorothalonil could slow the rate of selection for resistant strains and more than double the number of years for which effective disease control can be maintained. We show how cultural control measures to delay inoculum arrival contribute to resistance management. Delaying infection timing relative to crop emergence reduced selection for fungicide-resistant strains and increased fungicide effective life, through a reduction in the length of time of pathogen exposure to the fungicide and decreased disease pressure. The fungicide resistance management benefits of IPM strategies will be highest in cases where these keep to a minimum the level of fungicide treatment required to maintain effective disease control.

3.2   Introduction

Brazil is the world's largest producer of soybean (*Glycine max* (L.) Merrill). Production has expanded rapidly over the past 25 years and soybean is now Brazil's main crop (FAOSTAT, 2023). This increase in production has been achieved despite the arrival of a highly damaging pathogen, Asian soybean rust (*Phakopsora pachyrhizi*). An obligate biotrophic fungus with rapid asexual reproduction, *P. pachyrhizi* can cause yield losses of up to 80% when untreated (Dalla Lana et al., 2015; Hartman et al., 1991; Kumudini et al., 2008). Since the disease was first recorded in Brazil in 2001, soybean management has been adjusted to aid control of the disease through a variety of methods, including adoption of resistant cultivars, implementation of 90-day soybean-free periods ('vazio sanitário') (Godoy et al., 2016; Yorinori, 2021a) and an increased reliance

on fungicides. Calendar-based application of two to five fungicide sprays per growing season is widespread (Beruski et al., 2020, Yorinori, 2021a). However, increasing fungicide resistance in *P. pachyrhizi* threatens the sustainability of the current crop system (Barro et al., 2021; Dalla Lana et al., 2018). Sound fungicide resistance management tactics are needed, integrated effectively with other measures for disease control such as soybean-free periods, to safeguard fungicides as a tool for disease management.

The successful introduction and enforcement of the soybean-free period is estimated to have saved US$1.0 billion in the Mato Grosso region of Brazil in a single season alone through reduced yield losses and reduction in fungicide application requirements (Yorinori, 2021a), although this estimate did not account for the cost of implementation or yield variability. It is enforced through regulatory restrictions on the sowing date of soybean crops, with the aim of delaying and limiting infection of the next season's soybean crop by eliminating soybean 'green bridges' that enable survival of *P. pachyrhizi* inoculum in the off-season. This approach has successfully reduced, but not eliminated, the need for fungicide application, and is estimated to delay the first onset of infection by a month on average (Godoy et al., 2016; Yorinori, 2021a). The effectiveness of the soybean-free period is currently limited by imperfect control of volunteer soybean weeds in cotton crops, fallow fields and along roadsides, and by a lack of coordination between Brazilian states, and with neighbouring South American countries in controlling long-range inoculum sources, both from soybean crops and the perennial weed kudzu (*Pueraria montana*) (Reis et al., 2021; Yorinori, 2021b). Addressing these issues where feasible would potentially increase use of herbicides and require significant monetary and political investment. We aim to provide additional information for cost-benefit assessments by quantifying the potential resistance management benefits of delaying inoculum arrival through the soybean-free period.

Fungicides with modes of action (MoA) that target a single biochemical site are at a higher risk of fungicide resistance development than multi-site acting fungicides such as mancozeb. One mutation at the target site can lead to full or partial resistance to a single-site fungicide (Brent & Hollomon, 2007). *Phakopsora pachyrhizi* strains carrying resistance mutations reducing the efficacy of quinone outside inhibitor (QoI) and demethylation inhibitor (DMI) fungicides have become widespread (Dalla Lana et al., 2018; Müller et al., 2021). Succinate dehydrogenase inhibitor (SDHI) fungicides were introduced for *P. pachyrhizi* control in Brazil in

2012, with a strong level of efficacy relative to other products available at the time (Barro et al., 2021; Godoy et al., 2016; Machado et al., 2022). However, a decline in efficacy of commercial QoI and SDHI premixes has since been reported (Barro et al., 2021), likely associated with the increasingly widespread SdhC-I86F mutation (de Mello et al., 2021, Simões et al., 2018), which affects SDHI fungicides with resistance factors ranging from 4 to 26 (Müller et al., 2021). Resistance factors are defined as the EC_{50} of the resistant strain divided by the EC_{50} dose required to inhibit the growth rate of sensitive strains by 50%.

Many studies have explored strategies that can slow selection for fungicide resistance. One way to manage fungicide resistance is to combine fungicides with other control measures that reduce the growth rate of both fungicide-resistant and fungicide-sensitive pathogen subpopulations (van den Bosch et al., 2014). Reducing the growth rate of the pathogen population as a whole reduces the difference in growth rates between resistant and sensitive strains when a fungicide is applied, slowing selection. For example, the use of disease-resistant cultivars and cultivar mixtures can limit epidemic growth rates and delay the development of fungicide resistance (Kristoffersen et al., 2020; Taylor & Cunniffe, 2023a). Reducing the exposure time of the pathogen population to the fungicide also reduces selection for resistance (van den Bosch et al., 2014). Integrated pest management (IPM) involves the combination of a wide range of control methods, minimising reliance on any single control measure and therefore limiting the potential of the pathogen population to adapt (Corkley et al., 2022). We hypothesise that phytosanitary cultural control methods that delay the onset of disease, such as the soybean-free period, can contribute to fungicide resistance management by limiting the exposure time of the pathogen population to the fungicide and by keeping to a minimum the fungicide input required for disease control. Our analysis focuses on minimising selection for fungicide resistance within the constraint of maintaining effective disease control against *P. pachyrhizi*. The minimum fungicide input required will also be determined by the economics of disease control (te Beest et al., 2013; van den Bosch et al., 2018, 2020) and the need to control other damaging pathogens and disease complexes.

A number of existing statistical and epidemiological models have been developed for prediction of *P. pachyrhizi* disease risk, infection efficiency and disease severity (Del Ponte et al., 2006a), including epidemiological models parameterised for Taiwan (Yang et al., 1991) and Brazil (Kassie et al., 2023; Rodrigues et al., 2012; Tabonglek et al., 2019), but none of these models simulate the effect of fungicides

or the evolution of resistance. To represent the effect of fungicides on the pathogen growth rate, a quantitative method is needed to describe the relative effectiveness and activity of different fungicides. Epidemiological models that simulate the effect of fungicides on pathogen growth rates or life cycle parameters can be used to compare alternative resistance management strategies, such as options for mixing the at-risk fungicide with a different fungicidal mode of action, and choice of fungicide dose rates (van den Bosch et al., 2014). This approach has been previously applied in several pathosystems including potato blight (*Phytophthora infestans*) (Carolan et al., 2017; Levy et al., 1991), powdery mildew (*Blumeria. graminis* f. sp. *hordei)* in barley (Hobbelen et al., 2011a), grapevine powdery mildew (*Erysiphe nectator*) (Elderfield et al., 2018) and most extensively in septoria leaf blotch (*Zymoseptoria tritici*) of wheat (Elderfield et al., 2018; Hobbelen et al., 2011b; Hobbelen et al., 2013; Kitchen et al., 2016; Mikaberidze et al., 2017; Taylor & Cunniffe, 2023b; van den Berg et al., 2016), but not in *P. pachyrhizi*.

To derive most benefit for resistance management from epidemiological models, they must be used as early as possible to guide tactics before fungicide resistance spreads (Corkley et al., 2022), but often there is limited data available for model parameterisation when a new fungicide product first enters the market. Field efficacy trials conducted by fungicide manufacturers are usually the earliest source of information on the effects of new fungicides on pathogens, so utilising this data source can provide more timely guidance for resistance management tactics, even though there can be challenges in estimating parameters for a model using data collected for other purposes. For example, data for different fungicides may have been collected in different years and locations, meaning that environmental factors affecting the severity of the epidemic may vary. The dose rates and timing of fungicide sprays relative to the arrival of pathogen inoculum may also vary between trials. This presents a challenge to ensure a fair comparison of fungicide efficacy. Methods are therefore needed to extract information on the relative effectiveness of fungicides even when data is limited and comes from disparate sources.

We developed an epidemiological compartmental 'Susceptible-Exposed-Infectious-Removed' 'SEIR' model of *P. pachyrhizi* epidemics in Brazil, modelling the spread of a pathogen strain with resistance to an SDHI fungicide (benzovindiflupyr (Guicherit et al., 2014)), and the effect of mixture with different fungicidal modes of action (MoA). We focus on resistance management for SDHI fungicides because they play an important role in fungicide programmes for control

of *P. pachyrhizi*, but are at risk from the evolution of resistance. Our approach can be summarised as the following series of steps:

1. Build and parameterise a model describing the growth of the soybean leaf canopy and the life cycle of *P. pachyrhizi*.

2. Fit model parameters describing the efficacy of fungicides, using examples from several MoA: an SDHI fungicide (benzovindiflupyr), a QoI fungicide (azoxystrobin), a DMI fungicide (cyproconazole) and two multi-site acting fungicides, a dithiocarbamate fungicide (mancozeb) and a chloronitrile fungicide (chlorothalonil), using data from field trials.

3. Validate the fitted fungicide dose response using disease severity data from field trials of solo and mixture products.

4. Run model simulations to compare the efficacy and resistance management benefits of alternative fungicide programmes under a range of potential scenarios.

We use the model to compare the relative resistance management benefits of alternative mixture partners, considering the balance between effective disease control and minimising selection for resistance to maximise effective life. We explore the impact of the timing of first infection on effective life and the interaction with spray timing, spray number and fungicide dose, to quantify the value for fungicide resistance management of delaying disease inoculum through soybean-free periods.

3.3 Materials and methods

3.3.1 The soybean rust model

Phakopsora pachyrhizhi infection is initiated by urediniospores which germinate on host leaves in warm, moist conditions and penetrate the leaf cuticle using an appressorial peg structure. Following a mostly cryptic latent period, visible uredinia form and erupt into sporulating pustules on the leaf surface (Marchetti et al., 1975). Dispersal of the urediniospores completes the cycle of infection.

We developed a model of *P. pachyrhizi* infection of soybean, describing the effect of fungicides on the growth rate of the pathogen through a series of ordinary differential equations ('ODEs'). The model describes a system with two asexual haploid *P. pachyrhizi* strains: the wildtype 'sensitive' strain (denoted 's') and a 'resistant' strain (denoted 'R') that has a degree of resistance to one fungicide mode of action. We describe results for the spread of a strain with a degree of insensitivity

to an SDHI fungicide. We do not represent demographic or environmental stochasticity within the model, which was calibrated for 'typical' growing conditions in Brazil, using crop growth, disease severity and fungicide dose response data collected in Brazil over multiple years. The model was implemented in MATLAB R2022b (The MathWorks Inc., 2022) using built-in function 'ode45' for the solution of the ODEs.

The model outputs two measures of success for resistance management: 'T50', the number of growing seasons a treatment programme can be used until the frequency of the resistant strain exceeds 50%, and 'effective life', the number of growing seasons for which a fungicide programme was predicted to maintain effective disease control. In consultation with local agronomists, we defined 'effective control' as a 65% or greater reduction of the area under the disease progress curve (AUDPC), relative to the AUDPC in untreated crops in an average epidemic, i.e. with the mean inoculum influx timing). An 'effective dose' is a fungicide dose that achieves an equal or greater level of disease control than this threshold. The choice of threshold is flexible, but affects which fungicide programmes and dose rate combinations are considered to provide an acceptable level of control throughout the period of the simulation. The effective control threshold we used (65% disease control), has been shown to correspond to a yield gain of approximately 33% over untreated soybean crops (Alves et al., 2021; Hikishima et al., 2010).

3.3.1.1 State equations

The soybean crop total leaf area index (LAI), denoted as A in our equations, is the total planar leaf area of the crop per unit ground area. The equations track the growth of A from an initial LAI, A_0, on the day of emergence (assumed to be 10 days after planting), to a maximum LAI, A_{Max}, at a rate controlled by the soybean growth rate, r (rate of increase of LAI per unit time):

$$\frac{dA}{dt} = rA\left(1 - \frac{A}{A_{\text{Max}}}\right) \tag{1}$$

The healthy (uninfected and not senesced) LAI, H, increases as the crop grows, and decreases due to senescence and infection by *P. pachyrhizi* spores. The rate of senescence is defined by a constant γ and the time remaining until complete senescence at time t_γ. θ is the proportion of primary inoculum that is resistant, $\Omega(t)$ is the primary inoculum release rate at time t, I_S and I_R are the leaf area indices of infectious host tissue infected by *P. pachyrhizi* strains that are sensitive and

resistant to the SDHI respectively, and $\psi_S(t)$ and $\psi_R(t)$ are the transmission rate of the sensitive and resistant *P. pachyrhizi* strains respectively at time *t*:

$$\frac{dH}{dt} = rA\left[1 - \frac{A}{A_{\text{Max}}}\right] - H\left[e^{\gamma(t-t_\gamma)}\right] - \frac{H}{A}\left[(1-\theta)\Omega(t) + I_S\right]\psi_S(t) - \frac{H}{A}\left[\theta\Omega(t) + I_R\right]\psi_R(t) \quad (2)$$

The area indices of host tissue latently infected by *P. pachyrhizi* strains that are sensitive and resistant to the SDHI, L_S and L_R respectively, increase as *P. pachyrhizi* spores infect healthy crop area, and decrease as latently infected host tissue senesces, or transitions to infectious tissue at a rate determined by the latent period (in days) at time *t*, $p_S(t)$ and $p_R(t)$ for the sensitive and resistant *P. pachyrhizi* strains respectively:

$$\frac{dL_S}{dt} = \frac{H}{A}\left[(1-\theta)\Omega(t) + I_S\right]\psi_S(t) - \frac{L_S}{p_S(t)} - L_S\left[e^{\gamma(t-t_\gamma)}\right] \quad (3)$$

$$\frac{dL_R}{dt} = \frac{H}{A}\left[\theta\Omega(t) + I_R\right]\psi_R(t) - \frac{L_R}{p_R(t)} - L_R\left[e^{\gamma(t-t_\gamma)}\right] \quad (4)$$

The area indices of infectious host tissue, I_S and I_R, increase as latently infected host tissue transitions to infectious tissue, and decrease as infectious host tissue senesces, or reaches the end of the infectious sporulation period at a rate determined by the infectious period (in days), ω, which we assume is unaffected by the application of fungicide:

$$\frac{dI_S}{dt} = \frac{L_S}{p_S(t)} - \frac{I_S}{\omega} - I_S\left[e^{\gamma(t-t_\gamma)}\right] \quad (5)$$

$$\frac{dI_R}{dt} = \frac{L_R}{p_R(t)} - \frac{I_R}{\omega} - I_R\left[e^{\gamma(t-t_\gamma)}\right] \quad (6)$$

The dose of fungicide i, D_i is expressed as a proportion of the maximum permitted individual dose ('full label dose', as defined on the product label), $D_{i\,\text{Max}}$, and is assumed to decay over time at rate v_i:

$$\frac{dD_i}{dt} = -v_i D_i \quad (7)$$

3.3.1.2 Primary inoculum arrival

The primary inoculum release rate at time *t*, $\Omega(t)$, is 0 when $t < t_{\text{Inoc}}$, where t_{Inoc} is the time at which the first *P. pachyrhizi* spores (primary inoculum) arrive. We therefore assume that *P. pachyrhizi* inoculum is completely absent until the influx

of spores that initiates the epidemic arrives at t_{Inoc}. After t_{Inoc}, a constant rate of spore influx is assumed, $\Omega(t) = \Omega_0$:

$$\Omega(t) = \begin{cases} 0, t < t_{\text{Inoc}} \\ \Omega_0, t \geq t_{\text{Inoc}} \end{cases} \tag{8}$$

3.3.1.3 Transmission rate and latent period

The transmission rate, ψ, is the conversion rate of inoculum load (measured by the LAI of infectious host tissue in combination with primary inoculum) into latently infected LAI; ψ_0 is the transmission rate in the absence of fungicides. The transmission rate is reduced by the action of fungicides. The effect of a fungicide, F_i, is described by a dose-response function, with asymptote parameters q_{S_i} and q_{R_i} which define the maximum fractional reduction of the transmission rate (i.e. at infinite dose) of the sensitive and the resistant strain respectively, and the curvature parameters for the sensitive and the resistant strain respectively, k_{S_i} and k_{R_i}, defining how quickly the fractional reduction declines from the asymptote as the dose of the fungicide decreases:

$$\psi_S(t) = \psi_0 \left[1 - q_{S_i}\left(1 - e^{-k_{S_i}D_i}\right) \right] \tag{9}$$

$$\psi_R(t) = \psi_0 \left[1 - q_{R_i}\left(1 - e^{-k_{R_i}D_i}\right) \right] \tag{10}$$

When a fungicide application consists of more than one mode of action being applied simultaneously in a mixture, we assume that the joint action of the fungicides is described by a multiplicative survival model (Bliss, 1939; Paveley et al., 2003) based on the efficacy of each of the active substances on the transmission rate of the pathogen. The equation below shows how the transmission rate is calculated for the sensitive strain when a fungicide application consists of two active substances, Fungicide 1 (F_1) and Fungicide 2 (F_2):

$$\psi_S(t) = \psi_0 \left[1 - q_{S_1}\left(1 - e^{-k_{S_1}D_1}\right) \right]\left[1 - q_{S_2}\left(1 - e^{-k_{S_2}D_2}\right) \right] \tag{11}$$

The latent period, p, is increased from the default latent period, p_0, by the application of a systemic fungicide. The single-site SDHI, DMI and QoI fungicides are assumed to act systemically, whereas the protectant multi-site dithiocarbamate and chloronitrile fungicides are assumed to have no effect on the *P. pachyrhizi* latent period. The action of fungicides on the latent period is described as for the transmission rate, using parameters q_{S_i}, q_{R_i}, k_{S_i} and k_{R_i} (ideally individual values of q and k would be fitted for each of the transmission rate and latent period, but

there is a lack of data on the effects of individual fungicides on particular life cycle parameters that could inform such an approach):

$$p_S(t) = \frac{p_0}{\left[1 - q_{S_i}\left(1 - e^{-k_{S_i} D_i}\right)\right]} \tag{12}$$

$$p_R(t) = \frac{p_0}{\left[1 - q_{R_i}\left(1 - e^{-k_{R_i} D_i}\right)\right]} \tag{13}$$

3.3.1.4 Disease severity

Disease severity at time t, *Z(t)*, is calculated as the proportion of the non-senesced LAI that is infectious (latent host tissue does not show visible signs of infection until shortly before the end of the latent period (Danelli & Reis, 2016), so latent tissue is unlikely to be included in field assessments of *P. pachyrhizi* severity):

$$Z(t) = \frac{I_S + I_R}{H + L_S + L_R + I_S + I_R} \tag{14}$$

3.3.1.5 Change in frequency of the resistant strain

At the end ($t = t_\gamma$) of each growing season, the proportion of primary inoculum that is resistant, θ, is updated to the proportion of infected LAI that is resistant at t_γ. It is assumed that the pathogen overwinters (or infects the next crop in areas where there are two growing seasons in one year) without further change in the fraction θ. The fraction of the primary inoculum that is resistant in the following year, θ_{n+1}, is therefore calculated as:

$$\theta_{n+1} = \frac{I_R(t_\gamma)}{I_R(t_\gamma) + I_S(t_\gamma)} \tag{15}$$

3.3.2 Data and parameterisation

Four datasets were sourced from various experimental field trials to fit parameters and validate the model (Table 3.1). Dataset A, comprising LAI measurements from planting to senescence of early-, midseason- and late-maturing soybean cultivars (Moreira et al., 2015), was used to fit the soybean crop growth parameters A_0, A_{Max}, r, γ and t_γ. Datasets B, C and D included measurements from multiple assessment dates of *P. pachyrhizi* disease severity, assessed based on a diagrammatic scale (Godoy et al., 2006). Dataset B, comprising *P. pachyrhizi* disease severity progress in field trials of susceptible soybean cultivars in the absence of fungicides, was used to fit *P. pachyrhizi* life-cycle parameters t_{Inoc}, Ω_0

and ψ_0. Dataset C was used to fit fungicide parameters q_s and k for examples of several fungicide MoAs: an SDHI (benzovindiflupyr), a QoI (azoxystrobin), a DMI (cyproconazole), a chloronitrile (chlorothalonil) and a dithiocarbamate (mancozeb). Dataset D was used for validation (see Section 3.3.2.1). The values of the decay rate, v, for each fungicide and the length of the default latent period, p_0, and infectious period, ω, were based on a literature search (Table 3.2).

Dataset C comprised all available trials with measurements of *P. pachyrhizi* disease severity following applications of three or more non-zero solo fungicide dose rates and an untreated control, as required to fit the dose response parameters. Dataset D consisted of trial data that did not meet the criteria for inclusion in Dataset C (so the validation did not reduce the size of the dataset available for parameterisation): measurements of *P. pachyrhizi* disease severity following applications of one or two non-zero dose rates of a solo fungicide, or trials where the treatment programme involved two or more fungicides, and disease severity in the untreated control. Trial data was not included in Datasets C or D if a fungicide other than benzovindiflupyr, azoxystrobin, cyproconazole, chlorothalonil and/or mancozeb had been applied.

Parameters were fitted to the data using least squares optimisation. For the crop growth model, maturity-group-specific values of A_{Max} and t_γ, and values of A_0, r and γ common to all maturity groups were fitted simultaneously using function 'nls.lm' (Elzhov *et al*., 2016) in R 3.4.4 (R Core Team, 2018), with package 'deSolve' (Soetaert et al., 2010) used for the solution of the ODEs. We assumed that soybean emergence occurred ten days after planting for all cultivars, based on the timing of the first non-zero measurements of LAI collected by Moreira et al. (2015). The parameter values for the mid-maturing cultivar were used to fit the *P. pachyrhizi* life cycle and fungicide parameters, and as the model default for simulations. The *P. pachyrhizi* life cycle and fungicide parameters were fitted using the function 'lsqcurvefit' in MATLAB. Detailed descriptions of how data was used in the parameterisation process are provided in Appendix 3.A.

Table 3.1: Datasets used in model fitting and validation of fungicide parameterisation. Dataset A consists of soybean leaf area index measurements from planting to senescence. Datasets B, C and D comprise measurements of *P. pachyrhizi* disease severity progress over time.

Dataset	Source	Number of trials	Number of unique site/years	Number of datapoints	Use of dataset
A	Mato Grosso, Brazil, 2009-2011. Crops planted in October and November. (Moreira et al., 2015).	2	2	60	Parameterisation of soybean crop model: A_0, A_{Max}, r, γ and t_γ.
B	Syngenta, Brazil, 2012–2016.	146	68	994	Parameterisation of infection of the crop by *P. pachyrhizi*: t_{Inoc}, Ω_0 and ψ_0.
C	Syngenta, Brazil, 2015–2017.	20	17	820	Parameterisation of the effect of fungicides on *P. pachyrhizi* life cycle: parameters q_s and k for each fungicide.
D	Syngenta, Brazil, 2015–2016.	31	19	1219	Validation of fungicide parameterisation.

We used R^2 and root mean squared error (RMSE) as a measure of the overall model fit to the LAI data in Dataset A and the disease severity data in Dataset B. The fit to individual trials in Dataset B was also checked through comparison of the observed and fitted AUDPC, and comparison of the observed and fitted severity (%) at around soybean growth stage R6 (Fehr et al., 1971) which has been shown to be a good predictor of yield loss due to *P. pachyrhizi* (Dalla Lana et al., 2015). Since Dataset B did not include observed growth stages, the first disease assessment on or after 80 days after emergence (DAE), up to a maximum of 89 DAE, was used as an estimate of R6 timing. We compared the fit for trials in the north and south of Brazil, with 'north' comprising trials from states Minas Gerais, Mato Grosso, Goiás and Tocantins, and 'south' comprising trials from states Rio Grande Do Sul, Paraná and São Paulo.

The model fit for the fungicide dose response was assessed using R^2 and RMSE for the disease severity values in Dataset C, and through comparison of the overall observed and fitted fungicide efficacy for each trial, where fungicide efficacy was expressed as the proportional reduction in the area under the disease progress curve (rAUDPC) in fungicide-treated plots relative to the untreated plots.

3.3.2.1 Validation of model parameterisation of fungicide efficacy

Dataset D (Table 3.1) was used to validate the parameterisation of fungicide efficacy. Individual values of t_{Inoc} and ψ_0 were estimated for each trial, using the disease severity data from the untreated control plots (as described in Appendix 3.A (Section 3.A.2)). These trial-specific parameter values were then used in combination with the fitted fungicide efficacy parameters (Table 3.2) to produce model predictions of the disease severity on the disease assessment dates for each trial and fungicide programme. Observed and predicted fungicide efficacy was compared, with fungicide efficacy expressed as rAUDPC (as defined in section 3.3.2).

3.3.3 Modelled scenarios

The model was used to explore the consequences of the choice of fungicide programme and inoculum arrival times on the efficacy of disease control and the evolution of resistance to the SDHI over up to 20 growing seasons, for a mid-maturing cultivar. The initial proportion of primary inoculum resistant to the SDHI at the beginning of the first growing season, θ_0, was set at 1×10^{-6}. The asymptote parameter for the efficacy of the SDHI against the resistant strain was set as $q_{R_1} =$

$0.5q_{S_1}$, a 50% 'sensitivity shift'. The comparisons tested are described in the following sections.

3.3.3.1 Comparison of resistance management benefits of alternative mixture partners

The resistance management benefits of using the multi-site chloronitrile or dithiocarbamate fungicides or the DMI fungicide as mixture partners with an SDHI + QoI formulated mixture ('Elatus' is a formulated mixture of benzovindiflupyr and azoxystrobin in a 1:2 ratio of grams active ingredient (g.a.i.), Syngenta) were compared for programmes with two fungicide applications at 32 and 47 DAE, for the 'Medium' inoculum arrival timing t_{Inoc} = 44 DAE. The effect of varying the dose of the SDHI + QoI formulated mixture and the mixture partner in increments of 10% of full label dose from zero dose to a full dose was simulated, for all combinations of the SDHI + QoI formulated mixture and the mixture partner dose rate, with the same combination of dose rates used in each application.

3.3.3.2 Impact of the timing of rust inoculum arrival on resistance management

The interaction of the timing of rust inoculum arrival (t_{Inoc}), spray timing and fungicide dose was explored for mixtures of the SDHI + QoI formulated mixture and the dithiocarbamate at three dose rate combinations, corresponding to the minimum label dose ('minimum recommended dose') and full label dose rates of each product:

a. SDHI + QoI formulated mixture at full dose rate and the dithiocarbamate at full dose rate.

b. SDHI + QoI formulated mixture at 67% of full dose rate and the dithiocarbamate at full dose rate.

c. SDHI + QoI formulated mixture at 67% of full dose rate and the dithiocarbamate at 50% of full dose rate.

Each dose rate combination was simulated for fungicide programmes with a single application in a season and programmes with two applications (both applications at the same dose rate).

Values of t_{Inoc} between 32 DAE and 52 DAE were simulated in two-day increments, and the date of the first fungicide application was also varied in two-day increments between 32 DAE and 52 DAE, for all combinations of t_{Inoc} and first fungicide application. For programmes with two applications, the second fungicide application was 15 days after the first application.

3.3.3.3 Sensitivity to model parameters

Level of sensitivity shift to the SDHI

The effect of a range of sensitivity shifts was simulated for a mixture of the SDHI + QoI formulated mixture and the dithiocarbamate, for sensitivity shifts of 25%, 50%, 75% and 100%, where a 100% sensitivity shift would result in a strain completely resistant to the SDHI.

Reduced mixture partner efficacy

Due to covariance between the fungicide dose response parameters, the standard error (S.E.) for these parameters can be relatively large. The effect of the uncertainty in the fungicide efficacy parameterisation of k and q for the DMI, chloronitrile and dithiocarbamate fungicides for their potential performance as mixture partners was explored for a conservative scenario in which the efficacy of each fungicide was the minimum of the likely range indicated by the available data. In this scenario, for each fungicide, the shape parameter k was fixed at 1 S.E. below the mean fitted value, and the asymptote parameter q was refitted given the fixed value of k, with the refitted value of $q - 1S.E.$ used for the sensitivity analysis for reduced mixture partner efficacy.

SDHI decay rate

Fungicide decay rates, v_i, were parameterised using an average based on a literature review of measured foliar half-lives. However, the foliar concentration half-life of a fungicide can be very variable depending on the crop and environmental conditions (Fantke et al., 2014), and there is usually limited information on the foliar decay rate of new fungicides when a product first becomes available. Therefore, we explored the effect of parameterising the dose response parameters for the SDHI using one of the longest (16.1 days: Chang et al., 2023) and shortest (4 days: ECHA, 2014) foliar half-life values reported in literature for benzovindiflupyr.

3.4 Results

3.4.1 Model parameterisation and validation

The fitted model parameters describing soybean crop growth and infection by *P. pachyrhizi* are summarised in Table 3.2. The fitted parameters for model simulation of crop growth and senescence achieved a close fit to the LAI data in Dataset A (R^2=95.1%, RMSE=0.321; Figure A.1). The combination of model parameters

describing *P. pachyrhizi* disease progress in the absence of fungicides also achieved an excellent fit to observed disease severity (R^2=95.3%, RMSE=8.61%) and AUDPC (Figure 3.1a, R^2=98.6%, RMSE=98.8%-days). Overall, model fit to disease severity at R6 was very good (Figure 3.1b, R^2=93.7%, RMSE=8.78%), although there was slight overestimation of observed severities in the approximate range 25%-40% and slight underestimation of observed severities in the approximate range 80%-100%. Disease levels were higher on average in trials in the south of Brazil, compared to the north; the model fit was good for trials in both regions.

The fitted fungicide dose response parameters (Table 3.2) successfully represented the rank order of fungicide efficacy (Figure 3.2). Overall the parameters, fitted as an average across all trials for each fungicide, achieved a good fit to Dataset C on disease severity following fungicide application (R^2=80.6%, RMSE=13.0%). The closest fits were achieved for the single-site fungicides: R^2 and RMSE values for individual fungicide fits are provided in Appendix 3.A (Table 3.A.5). The validation using Dataset D confirmed that the fitted fungicide dose response parameters gave a good prediction of average fungicide efficacy in solo and mixture programmes (Figure 3.3).

Table 3.2: Fitted model parameters describing the growth of soybean leaf area index (LAI), infection by *P. pachyrhizi* and the effect of fungicides on *P. pachyrhizi*. [1]S.E. given in parentheses for those parameters fitted as a mean based on Datasets A, B and C. Variance-covariance matrices included in Appendix 3.A. [2]A_{Max} and t_γ parameters for midseason-maturing cultivar used for parameterisation of *P. pachyrhizi* infection and fungicide efficacy, and model simulations.

| Parameter		Description	Value (S.E.[1])	Dataset/citation
Growth of soybean LAI[2]				
	A_0	Initial LAI on day of emergence	0.0894 (0.0374)	A
	r	Rate of increase of LAI (days^{-1})	0.134 (0.017)	
	γ	Coefficient controlling rate of senescence of LAI (days^{-1})	0.0891 (0.0141)	
Mid-season maturing	A_{Max}	Maximum LAI	3.76 (0.17)	
	t_γ	Time of complete senescence (days)	121 (5.2)	
Early-season maturing	A_{Max}	Maximum LAI	3.18 (0.20)	
	t_γ	Time of complete senescence (days)	109 (5.2)	
Late-season maturing	A_{Max}	Maximum LAI	3.99 (0.12)	
	t_γ	Time of complete senescence (days)	139 (6.4)	
Infection of crop by *P. pachyrhizi*				
	p_0	Latent period (days)	9	Danelli & Reis, 2016; Marchetti et al., 1975; Melching et al., 1979; Pivonia & Yang, 2006; Vittal et al., 2014; Yeh et al., 1982
	ω	Infectious period (days)	28	Marchetti et al., 1975; Pivonia & Yang, 2006; Yeh et al., 1982
Early	t_{Inoc}	Time at which the first *P. pachyrhizi* spores (primary inoculum) arrive (days)	32	
Medium	t_{Inoc}		44	
Late	t_{Inoc}		52	B
	Ω_0	Primary inoculum release rate	4.6x10^{-6}	
	ψ_0	Transmission rate	2.78 (0.77)	

θ_0	Initial proportion of primary inoculum that is insensitive	1×10^{-6}		Not applicable

Effect of fungicides on *P. pachyrhizi*

SDHI	$D_{1\,Max}$	Full label dose rate (in SDHI + QoI formulated mixture) (g.a.i.)	45	
	v_1	Decay rate (days^{-1})	0.0745	Chang et al., 2023; ECHA, 2014; He et al., 2016; Katagi, 2016
	q_{S_1}	Dose-response asymptote for the sensitive strain	0.2634 (0.0194)	C
	k_1	Dose-response curvature	16.51 (6.07)	
QoI	$D_{2\,Max}$	Full label dose rate (in SDHI + QoI formulated mixture) (g.a.i.)	90	
	v_2	Decay rate (days^{-1})	0.1980	Chen et al., 2004; Fantke et al., 2014; Hobbelen et al., 2011a; Hou et al., 2016
	q_2	Dose-response asymptote	0.0534 (0.0634)	C
	k_2	Dose-response curvature	10.05 (39.67)	
DMI	$D_{3\,Max}$	Full label dose rate (g.a.i)	45	
	v_3	Decay rate (days^{-1})	0.1540	Fantke et al., 2014; Papadopoulou-Mourkidou et al., 1995; Wu et al., 2015
	q_3	Dose-response asymptote	0.3092 (0.1148)	C
	k_3	Dose-response curvature	2.36 (1.71)	
Chloronitrile	$D_{4\,Max}$	Full label dose rate (g.a.i)	1500	
	v_4	Decay rate (days^{-1})	0.0990	Fantke et al., 2014; Hobbelen et al., 2011b
	q_4	Dose-response asymptote	0.4761 (0.0632)	C
	k_4	Dose-response curvature	6.22 (2.86)	
Dithiocarbamate	$D_{5\,Max}$	Full label dose rate (g.a.i)	2250	
	v_5	Decay rate (days^{-1})	0.1333	Fantke et al., 2014; Hughes & Tate, 1982; Kumar & Agarwal, 1992; Sarkar et al., 2005; Sharma et al., 1994
	q_5	Dose-response asymptote	0.4751 (0.0433)	
	k_5	Dose-response curvature	17.24 (6.43)	C
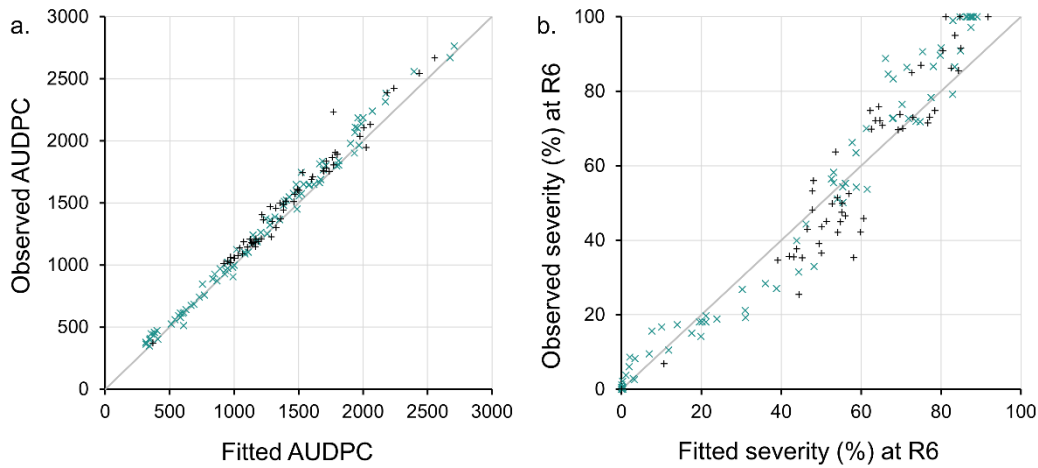
Figure 3.1: Scatter plots of fitted vs. observed a. AUDPC (%-days) and b. severity (%) at R6, for trials in Dataset B. Trials carried out in north Brazil plotted as green 'x', trials in south Brazil plotted as black '+', solid grey line denotes 1:1 line.
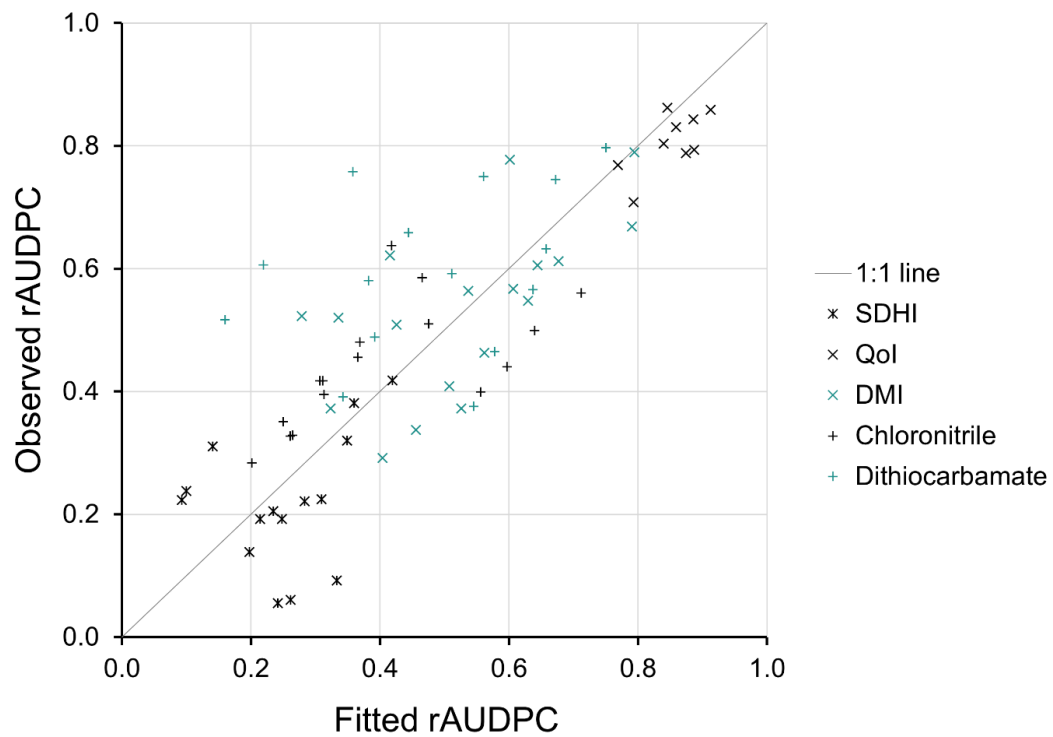
Figure 3.2: Scatter plot of fitted vs. observed proportional reduction in AUDPC relative to untreated trials (rAUDPC) for fungicide trials in Dataset C. R^2=63.1%, RMSE=0.138.
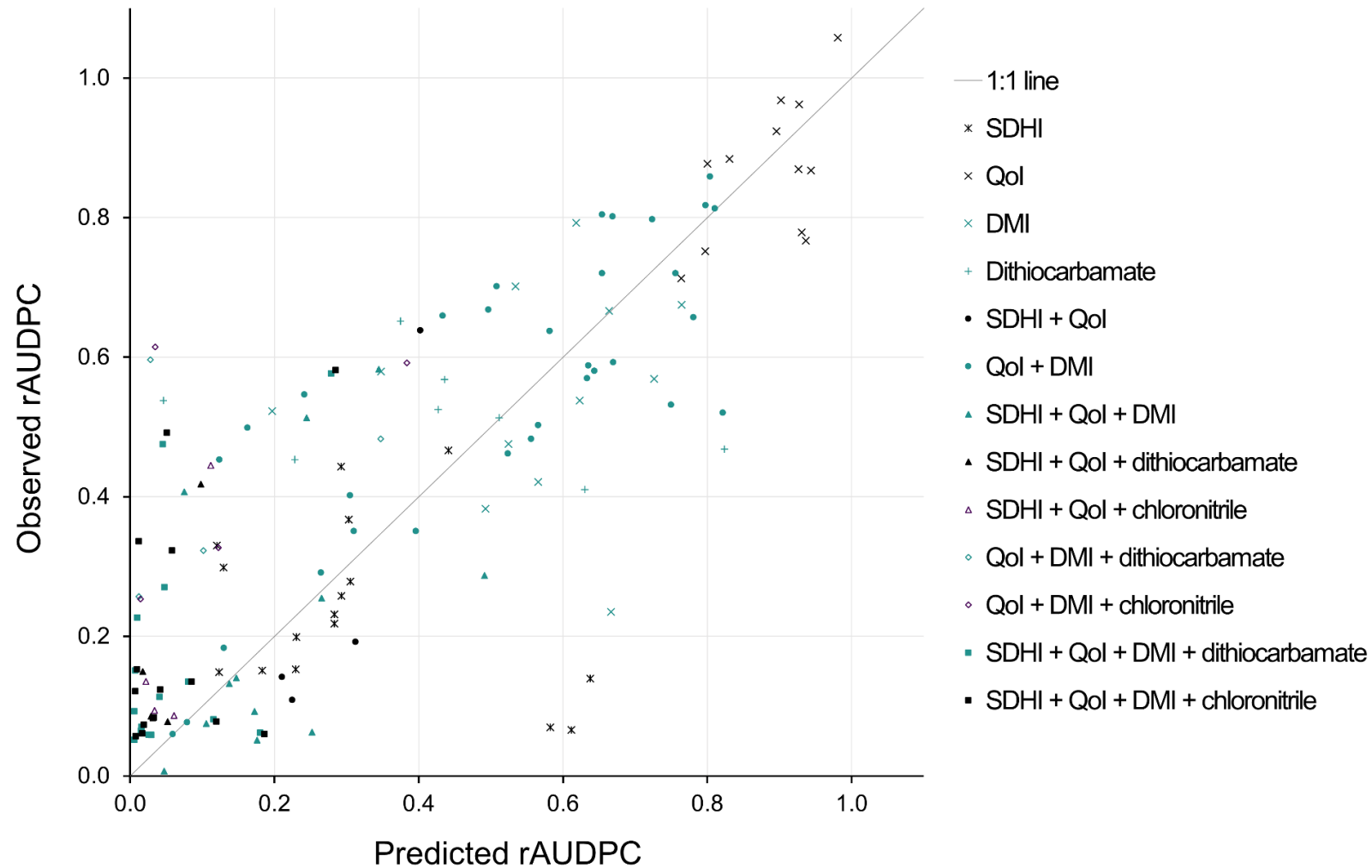
Figure 3.3: Scatter plot of predicted versus observed proportional reduction in AUDPC relative to untreated trials (rAUDPC) for fungicide trials in validation Dataset D. R^2=61.2%, RMSE=0.194.

3.4.2 Model simulations

3.4.2.1 Notes on interpretation of simulation results

We report the model output as number of years of effective life (the number of growing seasons for which a fungicide programme is predicted to maintain 'effective control') or T50 (time until 50% of the population is resistant), up to a maximum of 20 growing seasons. However, the absolute number of years predicted by the model depends on model assumptions about the initial proportion of primary inoculum resistant to the SDHI at the beginning of the first growing season, θ_0, the type and level of resistance modelled (a 50% 'asymptote shift') and the use of average values for *P. pachyrhizi* life cycle parameters, in addition to the effects of the alternative fungicide programmes and timing of rust inoculum arrival considered in the modelled scenarios. The results should therefore be interpreted as the relative effects of different fungicide programmes and inoculum arrival timing on selection for resistance.

We assumed a low starting frequency of resistance to the single-site SDHI fungicide, as is expected to be the case when resistance management strategies are used at an early stage following release of a new MoA. Our results show that using a multi-site mixture partner and reducing disease pressure through soybean-free periods can enable use of the SDHI fungicide to be kept to the minimum necessary for effective control, reducing selection pressure for resistance to the SDHI and therefore maximising resistance management benefits. However, SDH-mutant *P. pachyrhizi* strains conferring partial resistance to SDHI fungicides are now widespread in Brazil (FRAC, 2024). The fungicide dose rates required to maintain effective control following the spread of a partially resistant strain will depend on the level of resistance (see Section 3.4.2.4 and Appendix 3.B (Figure 3.B.1)). Control of other diseases is also an important factor in choosing fungicide dose rates and timing. We highlight results within the range of dose rates specified on the current product label for the SDHI + QoI mixture (Syngenta, 2024): 67%-100% of full label dose rate; a maximum of two applications per crop.

3.4.2.2 Comparison of resistance management benefits of alternative mixture partners

The use of a mixture partner slowed selection for the resistant strain, increasing both T50 and effective life (Figure 3.4). The mixture partner supresses the growth rates of both the resistant and sensitive pathogen strains. Assuming the

multiplicative survival model applies (Equation 11), the mixture partner reduces the difference in the growth rates of the resistant and sensitive strains, and therefore reduces selection for the resistant strain (van den Bosch et al., 2014). T50 was shorter for higher doses of the SDHI, due to stronger selection pressure for the resistant strain: the higher the SDHI dose, the larger the cumulative difference in the growth rates of the resistant and sensitive strains. Whilst avoiding the use of the SDHI altogether maximised T50, this is not a practical solution: use of the SDHI was required to maintain effective control in all of the programmes modelled for an average disease pressure season ('Medium' inoculum arrival timing). Overall, within the range of doses and spray programmes that provided effective control in the first season, use of the minimum effective dose of the SDHI with a higher dose of the mixture partner maximised both effective life and T50.

Based on the fungicide efficacy levels parameterised from the 2015–2017 field experiments, the dithiocarbamate and the chloronitrile were better mixture partners for resistance management than the DMI (Figure 3.4). Comparing programmes that provided effective control in the first season, mixture with the chloronitrile or the dithiocarbamate increased effective life by up to 186%, and T50 by up to 129% or 143% respectively at the 'Medium' inoculum arrival timing. The increase in T50 is due to a combination of the mixture effect and the potential to use the disease control offered by the mixture partner to maintain effective control with the minimum recommended dose of the SDHI + QoI formulated mixture, reducing selection for strains resistant to the SDHI. For a two-spray programme of the SDHI + QoI formulated mixture at the lowest recommended application rate (67% of full label dose), addition of the dithiocarbamate at 50-100% of full dose rate increased T50 by approximately 14%. A mixture of the SDHI + QoI formulated mixture with either the chloronitrile or the dithiocarbamate could maintain effective control in an average disease pressure season even when the resistant strain simulated here (50% sensitivity shift) had exceeded 50% of the population.

The effective life represents the balance between selection rate and disease control. For some lower doses of the DMI, effective life was longer for higher doses of the SDHI + QoI formulated mixture, due to improved control of both the sensitive and partially resistant strains by a higher dose of the SDHI, despite the increased rate of selection. However, the effective life of mixtures of the DMI with the SDHI + QoI formulated mixture was longest for combinations using the DMI at or just below full dose rate with the minimum effective dose of the SDHI + QoI formulated mixture.
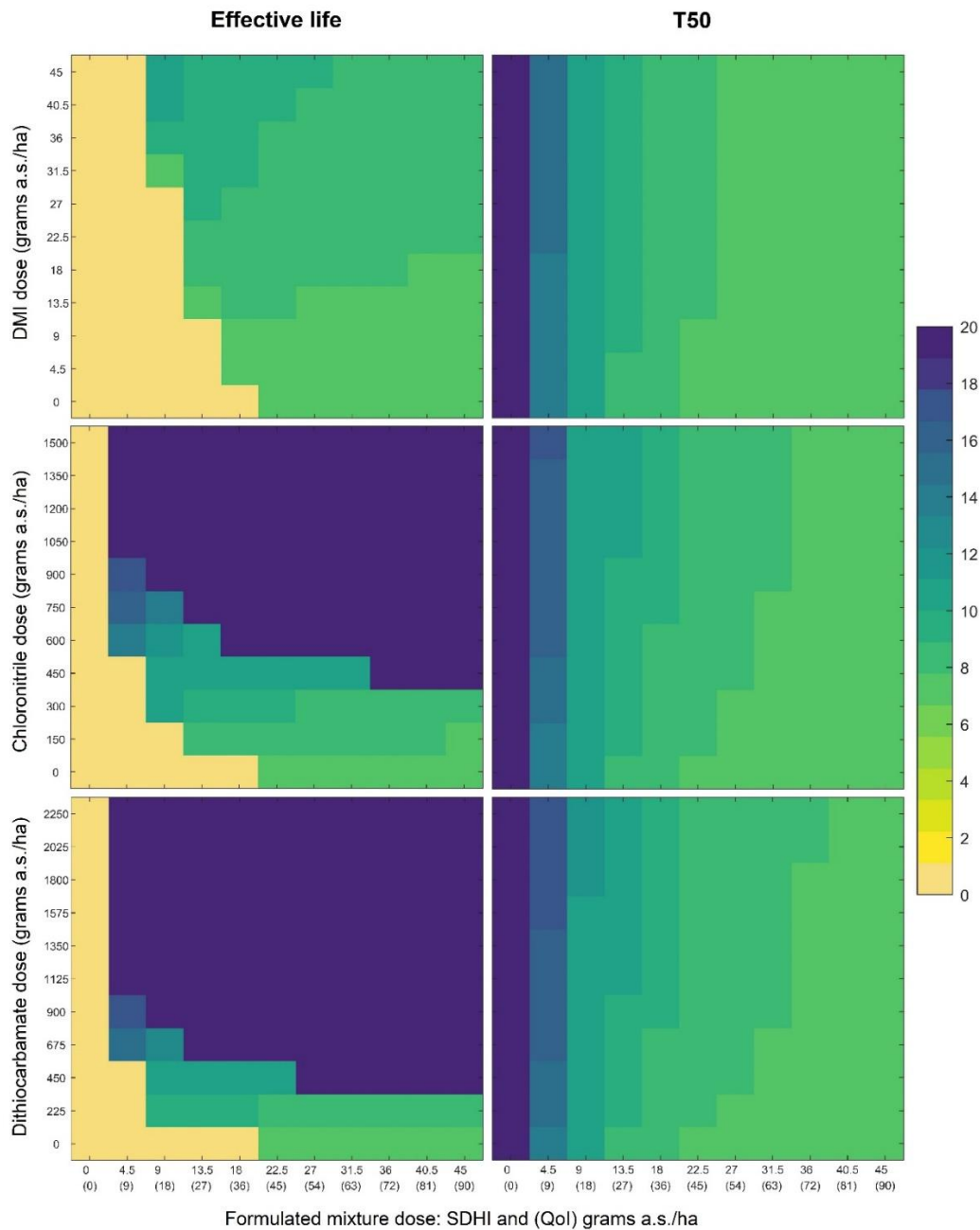
Figure 3.4: Effective life (years/number of growing seasons) and time until 50% of the population is insensitive to the SDHI (T50, years) for two-application programmes of the SDHI + QoI formulated mixture with a mixture partner (DMI, chloronitrile or dithiocarbamate) at varying dose rates (expressed as grams of active substance/ha). The x-axis label shows the dose of the SDHI with the dose of the QoI in brackets (the SDHI and the QoI are in a 1:2 ratio). Inoculum arrival timing t_{Inoc} = 44 DAE. An effective life of 20 years indicates that effective control was maintained throughout the period simulated. A T50 of 20 years indicates that the population did not reach 50% frequency of the insensitive strain in the period simulated.

3.4.2.3 Impact of the timing of rust inoculum arrival on resistance management

Effective life and T50 was prolonged by delayed *P. pachyrhizi* inoculum arrival (Figure 3.5). Later inoculum arrival reduced the exposure time of the pathogen to the fungicide, reducing the length of time for which the resistant strain had a fitness advantage compared to the sensitive strain and therefore reducing selection for resistance. In addition, disease pressure was lower when inoculum arrival was later in the season, enabling effective control to be maintained with the minimum recommended application rate of the SDHI + QoI formulated mixture, potentially even with a single fungicide application (Figure 3.6). Keeping the SDHI dose and number of sprays to a minimum reduced the strength of selection for resistance to the SDHI and increased T50 values. Prompt fungicide application was particularly important for disease control when inoculum arrived early in the growing season, with slightly greater flexibility when inoculum arrival was delayed.

For a two-spray programme of the SDHI + QoI formulated mixture at the lowest recommended application rate (67% of full label dose) and the dithiocarbamate at 50–100% of full dose rate, with the first application made at 32 DAE, 'Medium' timing for inoculum arrival (44 DAE) increased T50 by approximately 14% relative to 'Early' inoculum arrival, for approximately a 10–12 day delay in inoculum arrival. An additional delay of approximately 8 days to 'Late' inoculum arrival (52 DAE) increased T50 by 29% relative to 'Early' inoculum arrival.

For a one-spray programme of the SDHI + QoI formulated mixture at the lowest recommended application rate and the dithiocarbamate at 50–100% of full dose rate, with a choice of spray timing that provided effective control for the full 20 seasons simulated by the model, 'Medium' inoculum arrival timing increased T50 between 14–43%, and 'Late' inoculum arrival by between 29–71%, relative to the two-spray programmes required to provide effective control for 'Early' inoculum arrival.

Selection for resistance was increased, and T50 reduced, when the timing of the first application in a two-spray programme, or the timing of the single application in a one-spray programme, more closely matched inoculum arrival (Figure 5, Figure 6), as this meant that the fungicide dose was highest at the time when the pathogen population was growing most rapidly due to a lack of density dependence effects. However, closely matching the spray timing to inoculum arrival also improved disease control and therefore increased effective life overall, and the increase in selection was offset in some cases where an optimal spray timing for disease

control made it possible to reduce the dose rate or number of applications of the SDHI + QoI formulated mixture. These results are in agreement with the conclusions of van den Berg et al. (2013). Overall the resistance management benefits of delaying inoculum arrival were maximised by using a one-spray programme with spray timing approximately matching 'Medium' inoculum arrival, enabling effective control with shorter exposure time and a lower total fungicide dose.
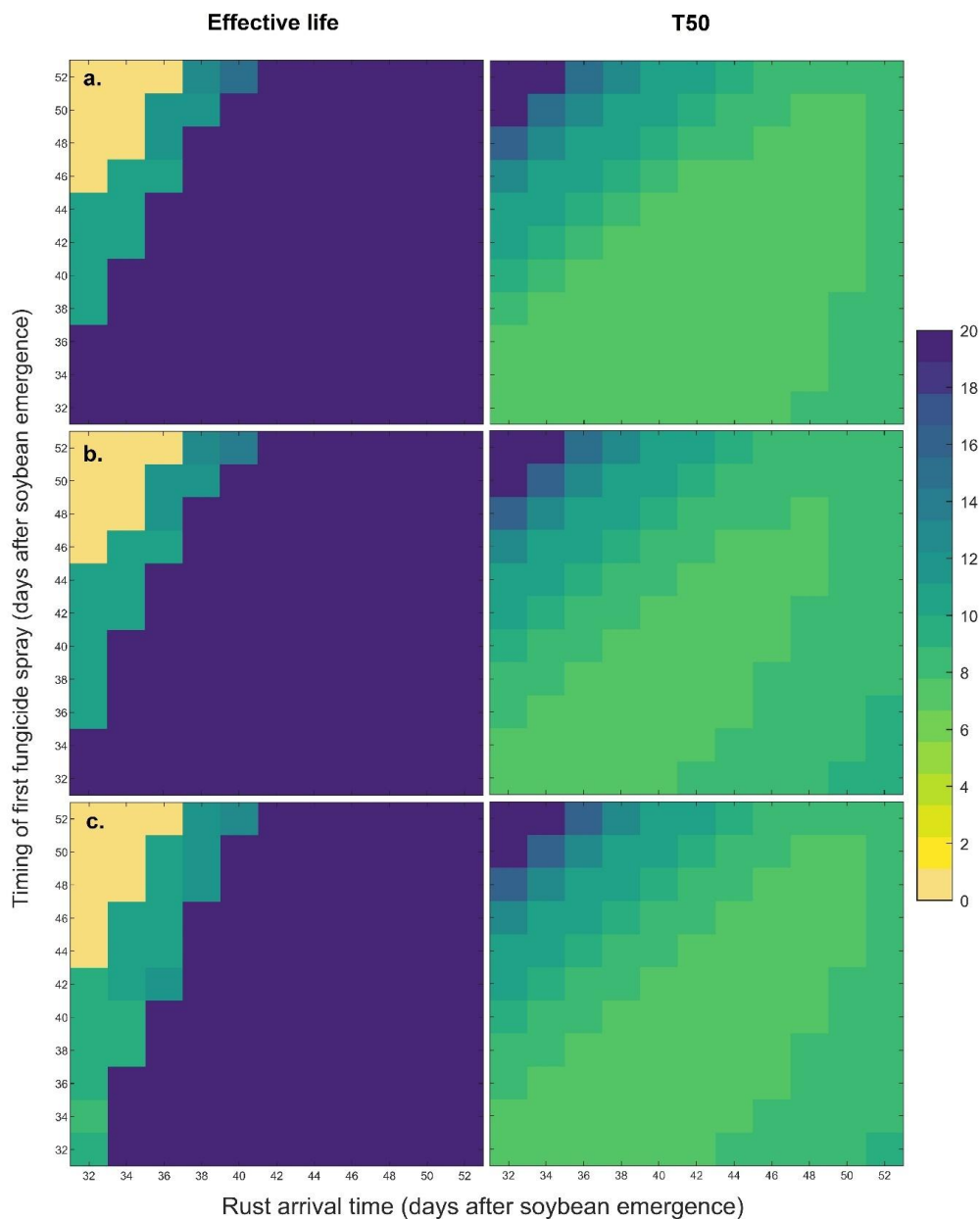
Figure 3.5: Effective life (years/number of growing seasons) and time until 50% of the population is insensitive to the SDHI (T50, years) for two-application mixture

programmes and with varying rust inoculum arrival time (t_{Inoc}) and timing of the first fungicide application (second application made 15 days after the first). Applications of SDHI + QoI formulated mixture with the dithiocarbamate at a. 100% SDHI + QoI and 100% dithiocarbamate full dose rate; b. 67% SDHI + QoI and 100% dithiocarbamate full dose rate; c. 67% SDHI + QoI and 50% dithiocarbamate full dose rate. An effective life of 20 years indicates that effective control was maintained throughout the period simulated. A T50 of 20 years indicates that the population did not reach 50% frequency of the insensitive strain in the period simulated.
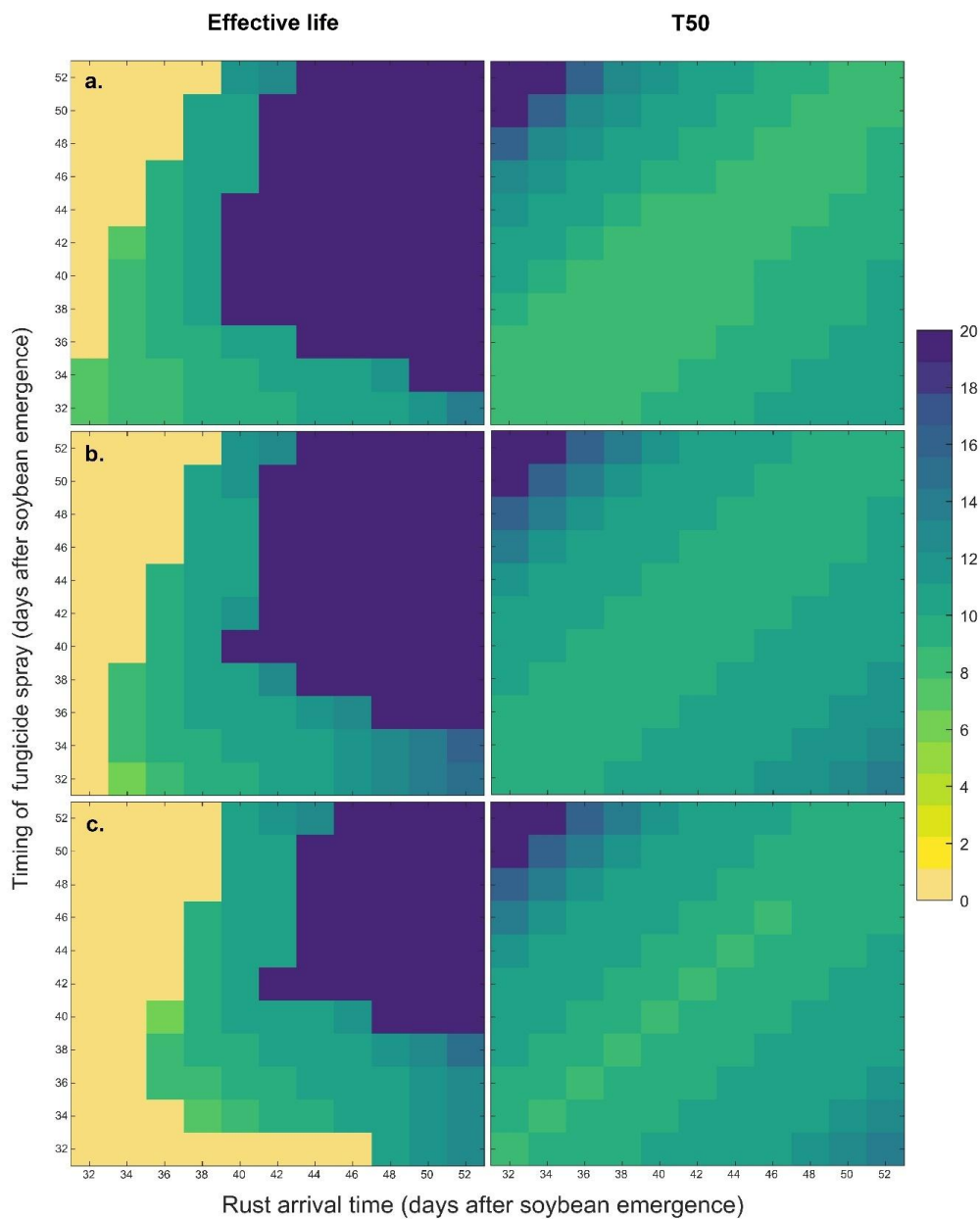
Figure 3.6: Effective life (years/number of growing seasons) and time until 50% of the population is insensitive to the SDHI (T50, years) for one-application

mixture programmes, with varying rust inoculum arrival time (t_{Inoc}) and timing of the fungicide application. SDHI + QoI formulated mixture applied with the dithiocarbamate at a. 100% SDHI + QoI and 100% dithiocarbamate full dose rate; b. 67% SDHI + QoI and 100% dithiocarbamate full dose rate; c. 67% SDHI + QoI and 50% dithiocarbamate full dose rate. An effective life of 20 years indicates that effective control was maintained throughout the period simulated. A T50 of 20 years indicates that the population did not reach 50% frequency of the insensitive strain in the period simulated.

3.4.2.4 Sensitivity to model parameters

Level of sensitivity shift to the SDHI

The greater the sensitivity shift, the stronger the selective advantage of the resistant strain. Therefore, relative to a sensitivity shift of 50%, T50 was shorter for sensitivity shifts of 75% and 100%, and longer for a sensitivity shift of 25%. The greater the sensitivity shift, the higher the doses of the SDHI + QoI formulated mixture and the mixture partner required to maintain effective control once the resistant strain has become the dominant strain in the population. Additional details in Appendix 3.B (Figure 3.B.1).

Reduced mixture partner efficacy

In a scenario in which the efficacy of each fungicide was the minimum of the likely range indicated by the available data, the resistance management benefits of mixture partners and delaying inoculum arrival were very similar to the results reported in sections 3.4.2.2 and 3.4.2.3, albeit with a slightly reduced range of dose rates and spray timings that provided effective control. There was less change in the results for the dithiocarbamate than for the chloronitrile. Compared to the chloronitrile, a greater range of dose rates of the dithiocarbamate were predicted to maintain effective control for all growing seasons simulated. Additional details in Appendix 3.B (Figures 3.B.2-3.B.4).

SDHI decay rate

The predicted *T50* was slightly increased by using a short SDHI half-life value and re-fitting parameters q_{S_1} and k_1, but in this scenario the range of dose rate and spray timing combinations that were predicted to provide effective control was slightly reduced. Using a longer SDHI half-life had the opposite effect. Additional details in Appendix 3.B (Figures 3.B.5-3.B.10).

3.5   Discussion

3.5.1 Model parameterisation and use to compare the benefits of alternative mixture partners

We presented and validated a method for extracting information on the effectiveness of fungicides from disease severity data. Our method is generic and achievable for other new-to-market products, including in other pathosystems. Our approach models both fungicide efficacy and selection for fungicide resistance to predict which fungicide programmes are likely to be optimum in the longer-term by comparing the effective life and T50 of programmes relative to one another. We showed that *P. pachyrhizi* evolution of resistance to a single-site fungicide could be slowed, and fungicide programme effective life increased substantially, through mixture of the single-site fungicide with other effective fungicides.

Model validation is important to increase confidence in model scenario predictions. Our validation dataset consisted of data that was not suitable for parameterisation of fungicide efficacy, avoiding a trade-off between reserving data for validation and maximising the size of the training dataset for robust parameterisation. Overall, the validation showed that our fitted fungicide dose response parameters gave a good prediction of average fungicide efficacy in solo and mixture programmes. The model fit to disease progress curves was excellent and compares well to similar models (Batchelor et al., 1997; Del Ponte et al., 2006b; Kassie et al., 2023; Kim et al., 2005; Yang et al., 1991), albeit with slight underestimation of the highest severity values >70% for both treated and untreated trials. This may be partially attributable to measurement errors in the assessed values at high levels of severity. Godoy et al. (2006) note a tendency for overestimation of severity through visual assessment, even with use of the diagrammatic scale by experienced raters, which represents a maximum severity of 78.5%. Values above this are likely to be difficult to distinguish: Franceschi et al. (2020) showed that severity values above 80% were nearly all overestimated by visual assessment. In addition, disease severity on an almost completely defoliated plant would often be recorded as 100%, whereas the model estimates the severity on any remaining leaves.

The crop growth model was parameterised using data from crops that had been infected by *P. pachyrhizi* which were likely to have experienced early defoliation and senescence as a result. This may cause the model to underestimate total healthy area duration (HAD) loss compared to a completely healthy crop canopy.

Ideally, the model of canopy growth would be parameterised using data on LAI over the course of the growing season in the absence of disease, where a suitable dataset is available. A mechanistic representation of defoliation as a result of *P. pachyrhizi* infection could improve model predictions but would require increased model complexity and additional data for parameterisation.

Our comparison of the likely disease control and resistance management benefits of alternative mixture partners and dose rates shows that when the SDHI fungicide is used in mixture with another effective fungicide, it should be possible to maintain effective control in an average season using the mixture even if the *P. pachyrhizi* population has evolved partial resistance to the SDHI. However, resistance management is still crucial to reduce selection for any new highly resistant strains which may emerge and to minimise the level of resistance to single-site fungicides for as long as possible, enabling control to be maintained in high-pressure seasons and cases where curative control is required. The best resistance management strategies may not be the most profitable option in the short term, but the longer-term costs of rapid development of resistance should also be considered. A model of profitability considering multiple disease pressure scenarios (Alves et al., 2021) highlighted the benefits for long-term profitability of limiting the rate of decline of fungicide efficacy.

Our results show that it is a good resistance management tactic to use the maximum dose of a low-risk mixture partner with the minimum effective dose of the at-risk fungicide required for disease control, which is consistent with previous studies (Hobbelen et al., 2011b). However, this tactic needs to be tailored to specific pathosystem requirements, in particular balancing resistance management with the costs of control (Alves et al., 2021; Machado et al., 2022). The economically optimum dose ('EcOptD') varies with the sensitivity of the pathogen population: a higher dose will generally give better disease control if partial resistance develops, driving an increase in the EcOptD, whereas if highly resistant strains are present the EcOptD may decrease (van den Bosch et al., 2018, 2020). High or unpredictable disease pressure also increase the EcOptD (te Beest et al., 2013; van den Bosch et al., 2018). In addition, dose rates need to take into account the potential need for curative control, environmental concerns relating to the use of high doses of multi-site fungicides (Ayer et al., 2021; Yang et al., 2011), and requirements for control of other crop diseases targeted by the same fungicide applications.

Our comparison of alternative mixture partners did not include the potential for concurrent resistance evolution, but the risk of this occurring is greater for the single-site DMI fungicide than for the two multi-site fungicides. On the basis of current efficacy alone, our results suggest that the dithiocarbamate or the chloronitrile are stronger mixture partner choices for resistance management than the DMI fungicide. Cyproconazole, tebuconazole and epoxiconazole were among the earliest fungicide active ingredients to be deployed against soybean rust in Brazil. A substantial population sensitivity shift to DMI fungicides occurred over the first decade of use (Dalla Lana et al., 2018), but average control efficacy for mixtures containing DMI fungicides has been stable for several years following this sensitivity shift (Barro et al., 2021). If using our method to model newer DMI and quinone inside inhibitor (QiI) fungicides as potential mixture partners, it would be prudent to simulate concurrent resistance evolution. The model structure used here can be extended for application to systems with several insensitive strains, including systems where competing strains are each insensitive to a single fungicide, and/or where a strain is insensitive to multiple fungicides (Taylor & Cunniffe, 2023b). The model could also be expanded to represent the effect of cultivar resistance and the evolution of virulence, but care and ample data would be needed to represent suitably the effect of cultivar resistance on the *P. pachyrhizi* life cycle, especially considering any role of crop architecture (Negrisoli et al., 2022) and maturity group (Moreira et al., 2015).

3.5.2 Resistance management benefits of delaying infection

The value of sanitation practices for disease control is theoretically low if they are used alone to control polycyclic pathogens such as *P. pachyrhizi*, which have a high epidemic growth rate and a short latent period (Zadoks & Schein, 1979; Nutter, 2007). However, the soybean-free period has proved very successful in reducing the impact of *P. pachyrhizi* on soybean yields in Brazil (Godoy et al., 2016; Yorinori, 2021a). Sanitation does not need to be complete to be useful, especially when used in combination with fungicides and cultivar resistance. Early onset of *P. pachyrhizi* in vegetative or early reproductive stages of growth is particularly damaging to yield (Dalla Lana et al., 2015; Kumudini et al., 2008), so a delay in infection is economically useful. Importantly, our model results demonstrate the additional value of non-fungicide-based sanitation practices such as the soybean-free period for fungicide resistance management. For a two-spray programme of the SDHI + QoI formulated mixture at the lowest recommended application rate and the dithiocarbamate at 50–100% of full dose rate, the impact on T50 of a 10-

day delay in inoculum arrival after the R1 growth stage was approximately equal to the impact on T50 of using the dithiocarbamate as a mixture partner.

Selection for resistance was reduced by later inoculum arrival due to a shorter exposure time of the pathogen to the fungicide. In addition, disease pressure was lower when inoculum arrival was delayed, enabling effective control to be maintained with lower fungicide intensity and substantially increasing the range of programmes that provided effective control for the full 20 seasons simulated. Our modelling results are supported by recent experimental evidence that orchard sanitation practices such as leaf shredding can reduce selection for resistance to DMI fungicides in apple scab (*Venturia inaequalis*) (Meitz-Hopkins et al., 2023).

The length of the delay in inoculum arrival due to the soybean-free period cannot be measured precisely, as the timing of the epidemic onset will be determined by a combination of weather conditions and phytosanitary efforts. Godoy et al. (2016) compared reports of *P. pachyrhizi* incidence in growing seasons before and after the introduction of the soybean-free period, illustrating an average delay in the first onset of infection of approximately a month. The range of infection timings we simulated correspond roughly to growth stages R1 to R4, based on the interquartile range of approximate inoculum arrival timing in the years 2012–2016 (after the introduction of the soybean-free period). Avoiding infection in the vegetative stage of growth before R1 is known to be important to minimise yield losses. Our results show that delaying infection onset after R1 offers benefits for fungicide resistance management. This evidence supports efforts to maintain and improve the soybean-free period, for example through improved management of volunteer soybean. Our results also indicate that the sowing-date limit imposed in some states of Brazil to minimise early infection of late-sown crops by high densities of inoculum is likely to be of value for resistance management.

We assumed that *P. pachyrhizi* inoculum is completely absent until the influx of spores that initiates the epidemic arrives at t_{Inoc}. If a low level of *P. pachyrhizi* infection is present prior to t_{Inoc}, prophylactic sprays would exert more selection pressure than estimated by our model results. We assumed a constant rate of spore influx from outside the crop canopy following t_{Inoc}; this rate is likely to vary with meteorological conditions (Andrade et al., 2009; Wen et al., 2017), but following initial infection the epidemic is largely driven by secondary infection from within the crop. We also assumed a constant transmission rate in the absence of fungicides, ψ_0, whereas this will in fact vary with plant and leaf age (Xavier et al.,

2017) and with weather conditions such as temperature and dew period (Yang et al., 1991), and could interact with inoculum arrival timing. Factors affecting the transmission rate could also impact on fungicide decay rate and efficacy. Additional experimental data would be needed to support further model exploration of these complex interactions.

The resistance management benefits of delaying *P. pachyrhizi* infection were maximised by using the minimum number of fungicide applications required for effective control. Enabling a reduction in pesticide applications whilst retaining control through use of alternative control strategies is a core aim of IPM, with sanitary practices playing an important role. For example, a two-year or longer crop rotation can reduce the number of fungicide applications required to control leaf blight in carrot (Gugino et al., 2007). On average, growers are estimated to make one less fungicide application per season as a result of the soybean-free period, leaving an average of 2.5 applications per season (Yorinori, 2021a). Our results suggest that a well-timed single fungicide application could provide effective control in combination with the delay of *P. pachyrhizi* inoculum arrival through the soybean-free period. However, as *P. pachyrhizi* can be a devastating pathogen and prompt application is needed to maintain control when inoculum arrives early, many growers take a risk-averse approach (Yorinori, 2021a). Improving growers' confidence to keep the number of fungicide applications to the minimum necessary for effective control is therefore crucial. A combination of field monitoring of *P. pachyrhizi* and other diseases of soybean (Yorinori, 2021a) and improved disease forecasting through models (Del Ponte et al., 2006a) could be used to help growers to minimise fungicide intensity and maximise the resistance management benefits of the soybean-free period.

3.6 Supporting Information

Appendix 3.A: Further details on model parameterisation
Appendix 3.B: Further details on sensitivity of model results to parameter values

3.7 Acknowledgements

3.8   Data availability statement

Research data are not shared due to commercial confidentiality.

3.9   Author contributions

Isabel Corkley: Conceptualization, Data Curation, Investigation, Methodology, Software, Validation, Visualization, Writing – Original Draft, Writing – Review & Editing. **Joseph Helps:** Conceptualization, Investigation, Methodology, Software, Visualization, Writing – Review & Editing. **Frank van den Bosch:** Conceptualization, Funding acquisition, Methodology, Supervision, Writing – Review & Editing. **Neil D Paveley:** Conceptualization, Funding acquisition, Supervision, Writing – Review & Editing. **Alice E Milne:** Supervision, Writing – Review & Editing. **Alexey Mikaberidze:** Supervision, Writing – Review & Editing. **Helge Sierotzki:** Conceptualization, Funding acquisition, Resources, Writing – Review & Editing. **David J Skirvin:** Conceptualization, Funding acquisition, Methodology, Software, Supervision, Visualization, Writing – Review & Editing.

3.10   References

Alves, K.S., Barro, J.P., Guimarães, M. & Del Ponte, E.M. (2021). Profitability of fungicide applications for managing soybean rust in scenarios of variable efficacy and costs: A stochastic simulation. *Plant Pathology*, *70*(6), 1354–1363. https://doi.org/10.1111/ppa.13396

Andrade, D., Pan, Z., Dannevik, W., & Zidek, J. (2009). Modeling Soybean Rust Spore Escape from Infected Canopies: Model Description and Preliminary Results. *Journal of Applied Meteorology and Climatology*, *48*(4), 789–803. https://doi.org/10.1175/2008JAMC1917.1

Ayer, K.M., Strickland, D.A., Choi, M. & Cox, K.D. (2021). Optimizing the Integration of a Biopesticide (*Bacillus subtilis* QST 713) with a Single-Site Fungicide (Benzovindiflupyr) to Reduce Reliance on Synthetic Multisite Fungicides (Captan and Mancozeb) for Management of Apple Scab. *Plant Disease*, *105*(11), 3545–3553. https://doi.org/10.1094/PDIS-02-21-0426-RE

Barro, J.P., Alves, K.S., Godoy, C.V., Dias, A.R., Forcelini, C.A., Utiamada, C.M. et al. (2021). Performance of dual and triple fungicide premixes for managing soybean rust across years and regions in Brazil: A meta-analysis. *Plant Pathology*, *70*(8), 1920–1935. https://doi.org/10.1111/ppa.13418

Batchelor, W.D. Yang, X.B. & Tschanz, A.T. (1997). Development of a Neural Network for Soybean Rust Epidemics. *Transactions of the ASAE*, *40*(1), 247–252. https://doi.org/10.13031/2013.21237

Beruski, G.C., Del Ponte, E.M., Pereira, André. B., Gleason, M.L., Câmara, G.M.S. et al. (2020). Performance and Profitability of Rain-Based Thresholds for Timing Fungicide Applications in Soybean Rust Control. *Plant Disease*, *104*(10), 2704–2712. https://doi.org/10.1094/PDIS-01-20-0210-RE

Bliss, C.I. (1939). The Toxicity of Poisons Applied Jointly. *Annals of Applied Biology*, 26(3), 585–615. https://doi.org/10.1111/j.1744-7348.1939.tb06990.x

Brent, J.K. & Hollomon, D.W. (2007). Fungicide resistance: the assessment of risk. Fungicide Resistance Action Committee. FRAC Monograph No. 2.

Carolan, K., Helps, J., van den Berg, F., Bain, R., Paveley, N., & van den Bosch, F. (2017). Extending the durability of cultivar resistance by limiting epidemic growth rates. *Proceedings of the Royal Society B: Biological Sciences*, *284*(1863), 20170828. https://doi.org/10.1098/rspb.2017.0828

Chang, H., Wang, L., Huang, C., Zhou, R., Wu, T. & Li, B. (2023). Residue analysis, dissipation dynamics, and dietary risk assessment of benzovindiflupyr in peanut field environment by LC-MS. *Journal of Food Composition and Analysis*, *123*, 105552. https://doi.org/10.1016/j.jfca.2023.105552

Chen, M.-F., Chien, H.-P., Wong, S.-S. & Li, G.-C. (2004). Dissipation of the fungicide azoxystrobin in Brassica vegetables. *Plant Protection Bulletin* 46: 123-130.

Corkley, I., Fraaije, B. & Hawkins, N. (2022). Fungicide resistance management: Maximizing the effective life of plant protection products. *Plant Pathology*, *71*(1). https://doi.org/10.1111/ppa.13467

Dalla Lana, F., Paul, P.A., Godoy, C.V., Utiamada, C.M., Da Silva, L.H.C.P., Siqueri, F.V. et al. (2018). Meta-analytic modeling of the decline in performance of fungicides for managing soybean rust after a decade of use in Brazil. *Plant Disease*, *102*(4), 807–817. https://doi.org/10.1094/PDIS-03-17-0408-RE

Dalla Lana, F., Ziegelmann, P.K., De Maia, A.H.N., Godoy, C.V. & Del Ponte, E.M. (2015). Meta-analysis of the relationship between crop yield and soybean rust severity. *Phytopathology*, *105*(3), 307–315. https://doi.org/10.1094/PHYTO-06-14-0157-R

Danelli, A.L.D. & Reis, E.M. (2016). Quantification of incubation, latent and infection periods of Phakopsora pachyrhizi in soybean, according to chronological time and degree-days. *Summa Phytopathologica*, *42*(1), 11–17. https://doi.org/10.1590/0100-5405/1920

de Mello, F.E., Mathioni, S.M., Fantin, L.H., Rosa, D.D., Antunes, R.F.D., Filho, N.R.C. et al. (2021). Sensitivity assessment and SDHC-I86F mutation frequency of *Phakopsora pachyrhizi* populations to benzovindiflupyr and fluxapyroxad fungicides from 2015 to 2019 in Brazil. *Pest Management Science*, *77*(10), 4331–4339. https://doi.org/10.1002/ps.6466

Del Ponte, E.M., Godoy, C.V, Canteri, M.G., Reis, E.M. & Yang, X.B. (2006a). Models and Applications for Risk Assessment and Prediction of Asian Soybean Rust Epidemics. In *Fitopatol. Bras* (Vol. 31, Issue 6).

Del Ponte, E.M., Godoy, C.V., Li, X. & Yang, X.B. (2006b). Predicting Severity of Asian Soybean Rust Epidemics with Empirical Rainfall Models. *Phytopathology®*, *96*(7), 797–803. https://doi.org/10.1094/PHYTO-96-0797

ECHA (2014). Annex 1. Background document to the Opinion proposing harmonized classification and labelling at Community level of Benzovindiflupyr (ISO). CAS number: 1072957-71-1.

Elderfield, J.A.D., Lopez-Ruiz, F.J., van den Bosch, F. & Cunniffe, N.J. (2018). Using Epidemiological Principles to Explain Fungicide Resistance Management Tactics: Why do Mixtures Outperform Alternations? *Phytopathology®*, *108*(7), 803–817. https://doi.org/10.1094/PHYTO-08-17-0277-R

Elzhov, T.V., Mullen, K.M., Spiess, A. & Bolker, B. (2016). minpack.lm: R Interface to the Levenberg-Marquardt Nonlinear Least-Squares Algorithm Found in MINPACK, Plus Support for Bounds. R package. version 1.2-1, https://CRAN.R-project.org/package=minpack.lm.

Fantke, P., Gillespie, B.W., Juraske, R. & Jolliet, O. (2014). Estimating Half-Lives for Pesticide Dissipation from Plants. *Environmental Science & Technology*, *48*(15), 8588–8602. https://doi.org/10.1021/es500434p

FAOSTAT (2024). Crops and livestock products. https://www.fao.org/faostat/en/#data/TCL

Fehr, W.R., Caviness, C.E., Burmood, D.T. & Pennington, J.S. (1971). Stage of Development Descriptions for Soybeans, *Glycine Max* (L.) Merrill [1]. *Crop Science*, *11*(6), 929–931. https://doi.org/10.2135/cropsci1971.0011183X001100060051x

FRAC (2024). FRAC Recommendations for SDHI fungicides. https://www.frac.info/frac-teams/working-groups/sdhi-fungicides/recommendations-for-sdhi

Franceschi, V.T., Alves, K.S., Mazaro, S.M., Godoy, C.V., Duarte, H.S.S. & Del Ponte, E.M. (2020). A new standard area diagram set for assessment of

severity of soybean rust improves accuracy of estimates and optimizes resource use. *Plant Pathology*, *69*(3), 495–505. https://doi.org/10.1111/ppa.13148

Godoy, C.V., Seixas, C.D.S., Soares, R.M., Marcelino-Guimarães, F.C., Meyer, M.C. & Costamilan, L.M. (2016). Asian soybean rust in Brazil: past, present, and future. *Pesquisa Agropecuária Brasileira*, *51*(5), 407–421. https://doi.org/10.1590/S0100-204X2016000500002

Godoy, C.V., Koga, L.J. & Canteri, M.G. (2006). Diagrammatic scale for assessment of soybean rust severity. *Fitopatologia Brasileira*, *31*(1), 63–68. https://doi.org/10.1590/S0100-41582006000100011

Gugino, B.K., Carroll, J.E., Widmer, T.L., Chen, P. & Abawi, G.S. (2007). An IPM Program for Managing Fungal Leaf Blight Diseases of Carrot in New York. *Plant Disease*, *91*(1), 59–65. https://doi.org/10.1094/PD-91-0059

Guicherit, E., Bartlett, D., Dale, S.M., Haas, H.-U., Scalliet, G. & Walter, H. (2014). Solatenol - The second generation benzonorbornene SDHI carboxamide with outstanding performance against key crop diseases. In: Dehne HW; Deising HB; Fraaije B; Gisi U; Hermann D; Mehl A; Oerke EC; Russell PE; Stammler G; Kuck KH; Lyr H (Eds), "Modern Fungicides and Antifungal Compounds", Vol. VII, pp. 67-72. © 2014 Deutsche Phytomedizinische Gesellschaft, Braunschweig, ISBN: 978-3-941261-13-6.

Hartman, G.L., Wang, T.C. & Tschanz, A.T. (1991). Soybean Rust Development and the Quantitative Relationship Between Rust Severity and Soybean Yield. *Plant Disease*, *75*(6), 596. https://doi.org/10.1094/PD-75-0596

He, M., Jia, C., Zhao, E., Chen, L., Yu, P., Jing, J. et al. (2016). Concentrations and dissipation of difenoconazole and fluxapyroxad residues in apples and soil, determined by ultrahigh-performance liquid chromatography electrospray ionization tandem mass spectrometry. *Environmental Science and Pollution Research*, *23*(6), 5618–5626. https://doi.org/10.1007/s11356-015-5750-6

Hikishima, M., Canteri, M.G., Godoy, C.V, Koga, L.J. & Silva, A.J. da. (2010). Quantificação de danos e relações entre severidade, medidas de refletância e produtividade no patossistema ferrugem asiática da soja. *Tropical Plant Pathology*, *35*(2), 96–103. https://doi.org/10.1590/S1982-56762010000200004

Hobbelen, P.H.F., Paveley, N.D., Fraaije, B.A., Lucas, J.A. & van den Bosch, F. (2011a). Derivation and testing of a model to predict selection for fungicide resistance. *Plant Pathology*, *60*(2), 304–313. https://doi.org/10.1111/j.1365-3059.2010.02380.x

Hobbelen, P.H.F., Paveley, N.D., Oliver, R.P. & van den Bosch, F. (2013). The Usefulness of Fungicide Mixtures and Alternation for Delaying the Selection for Resistance in Populations of *Mycosphaerella graminicola* on Winter Wheat: A Modeling Analysis. *Phytopathology®, 103*(7), 690–707. https://doi.org/10.1094/PHYTO-06-12-0142-R

Hobbelen, P.H.F., Paveley, N.D. & van den Bosch, F. (2011b). Delaying selection for fungicide insensitivity by mixing fungicides at a low and high risk of resistance development: A modeling analysis. *Phytopathology, 101*(10), 1224–1233. https://doi.org/10.1094/PHYTO-10-10-0290

Hou, Z., Wang, X., Zhao, X., Wang, X., Yuan, X. & Lu, Z. (2016). Dissipation rates and residues of fungicide azoxystrobin in ginseng and soil at two different cultivated regions in China. *Environmental Monitoring and Assessment, 188*(7), 440. https://doi.org/10.1007/s10661-016-5449-2

Hughes, J.T. & Tate, K.G. (1982). Dithiocarbamate spray residues on lettuces, tomatoes, berryfruits, and apples. *New Zealand Journal of Experimental Agriculture, 10*(3), 301–304. https://doi.org/10.1080/03015521.1982.10427887

Kassie, B.T., Onstad, D.W., Koga, L., Hart, T., Clark, R. & van der Heijden, G. (2023). Modeling the early phases of epidemics by Phakospora pachyrhizi in Brazilian soybean. *Frontiers in Agronomy, 5*. https://doi.org/10.3389/fagro.2023.1214038

Katagi, T. (2016). Pesticide behavior in modified water-sediment systems. In *Journal of Pesticide Science* (Vol. 41, Issue 4, pp. 121–132). Pesticide Science Society of Japan. https://doi.org/10.1584/jpestics.D16-060

Kim, K.S., Wang, T.C. & Yang, X.B. (2005). Simulation of Apparent Infection Rate to Predict Severity of Soybean Rust Using a Fuzzy Logic System. *Phytopathology®, 95*(10), 1122–1131. https://doi.org/10.1094/PHYTO-95-1122

Kitchen, J.L., van den Bosch, F., Paveley, N.D., Helps, J. & van den Berg, F. (2016). The Evolution of Fungicide Resistance Resulting from Combinations of Foliar-Acting Systemic Seed Treatments and Foliar-Applied Fungicides: A Modeling Analysis. *PLOS ONE, 11*(8), e0161887. https://doi.org/10.1371/journal.pone.0161887

Kristoffersen, R., Heick, T.M., Müller, G.M., Eriksen, L.B., Nielsen, G.C. & Jørgensen, L.N. (2020). The potential of cultivar mixtures to reduce fungicide input and mitigate fungicide resistance development. *Agronomy for*

Sustainable Development, *40*(5), 36. https://doi.org/10.1007/s13593-020-00639-y

Kumar, U. & Agarwal, H.C. (1992). Fate of [[14] C] Mancozeb in Egg Plants (*Solanum melongena* L.) during Summer under Sub-tropical Conditions. *Pesticide Science*, *36*(2), 121–125. https://doi.org/10.1002/ps.2780360207

Kumudini, S., Godoy, C.V., Board, J.E., Omielan, J. & Tollenaar, M. (2008). Mechanisms involved in soybean rust-induced yield reduction. *Crop Science*, *48*(6), 2334–2342. https://doi.org/10.2135/cropsci2008.01.0009

Levy, Y., Cohen, Y. & Benderly, M. (1991). Disease Development and Buildup of Resistance to Oxadixyl in Potato Crops Inoculated with Phytophthora infestans as Affected by Oxadixyl and Oxadixyl Mixtures: Experimental and Simulation Studies. *Journal of Phytopathology*, *132*(3), 219–229. https://doi.org/10.1111/j.1439-0434.1991.tb00114.x

Machado, F.J., Barro, J.P., Godoy, C.V., Dias, A.R., Forcelini, C.A., Utiamada, C.M. et al. (2022). Is tank mixing site-specific premixes and multi-site fungicides effective and economic for managing soybean rust? a meta-analysis. *Crop Protection*, *151*. https://doi.org/10.1016/j.cropro.2021.105839

Marchetti, M.A., Uecker, F.A. & Bromfield, K.R. (1975). Uredial Development of Phakopsora pachyrhizi in Soybeans. *Phytopathology*, *65*(7), 822. https://doi.org/10.1094/Phyto-65-822

Meitz-Hopkins, J.C., von Diest, S.G., Koopman, T.A., Tobutt, K.R., Xu, X. & Lennox, C.L. (2023). Leaf shredding as an alternative strategy for managing apple scab resistance to demethylation inhibitor fungicides. *Frontiers in Horticulture*, *2*. https://doi.org/10.3389/fhort.2023.1175168

Melching, J.S., Bromfield, K.R. & Kingsolver, C.H. (1979). Infection, Colonization, and Uredospore Production on Wayne Soybean by Four Cultures of *Phakopsora pachyrhizi,* the Cause of Soybean Rust. *Phytopathology*, *69*(12), 1262. https://doi.org/10.1094/Phyto-69-1262

Mikaberidze, A., Paveley, N., Bonhoeffer, S. & van den Bosch, F. (2017). Emergence of Resistance to Fungicides: The Role of Fungicide Dose. *Phytopathology*, *107*(5), 545–560. https://doi.org/10.1094/PHYTO-08-16-0297-R

Moreira, E.N., Vale, F.X.R., Paul, P.A., Rodrigues, F.A. & Jesus Júnior, W.C. (2015). Temporal Dynamics of Soybean Rust Associated With Leaf Area Index in Soybean Cultivars of different Maturity Groups. *Plant Disease*, *99*(9), 1216–1226. https://doi.org/10.1094/PDIS-10-14-1029-RE

Müller, M.A., Stammler, G. & May De Mio, L.L. (2021). Multiple resistance to DMI, QoI and SDHI fungicides in field isolates of Phakopsora pachyrhizi. *Crop Protection*, *145*, 105618. https://doi.org/10.1016/j.cropro.2021.105618

Negrisoli, M.M., Silva, F.N. da, Negrisoli, R.M., Lopes, L. da S., Souza Júnior, F. de S., Freitas, B.R. de et al. (2022). Impact of Fungicide Application Timing Based on Soybean Rust Prediction Model on Application Technology and Disease Control. *Agronomy*, *12*(9), 2119. https://doi.org/10.3390/agronomy12092119

Nutter, F.W. (2007). The Role of Plant Disease Epidemiology in Developing Successful Integrated Disease Management Programs. In *General Concepts in Integrated Pest and Disease Management* (pp. 45–79). Springer Netherlands. https://doi.org/10.1007/978-1-4020-6061-8_3

Papadopoulou-Mourkidou, E., Kotopoulou, A., Papadopoulos, G. & Hatziphanis, C. (1995). Dissipation of cyproconazole and quinalphos on/in grapes. *Pesticide Science*, *45*(2), 111–116. https://doi.org/10.1002/ps.2780450204

Paveley, N. D., Thomas, J. M., Vaughan, T. B., Havis, N. D. & Jones, D. R. (2003). Predicting effective doses for the joint action of two fungicide applications. *Plant Pathology*, *52*(5), 638–647. https://doi.org/10.1046/j.1365-3059.2003.00881.x

Pivonia, S. & Yang, X.B. (2006). Relating epidemic progress from a general disease model to seasonal appearance time of rusts in the United States: Implications for soybean rust. *Phytopathology*, *96*(4), 400–407. https://doi.org/10.1094/PHYTO-96-0400

R Core Team (2018). R: A language and environment for statistical computing. R Foundation for Statistical Computing, Vienna, Austria. https://www.R-project.org/

Reis, E.M., Guerra, W.D., Zanatta, M. & Zambolim, L. (2021). An Overview of the Epidemiology of Phakopsora pachyrhizi in the State of Mato Grosso, Brazil. *Journal of Agricultural Science*, *13*(6), 110. https://doi.org/10.5539/jas.v13n6p110

Rodrigues, R. de Á., Pedrini, J.E., Fraisse, C.W., Fernandes, J.M.C., Justino, F.B., Heinemann, A.B. et al. (2012). Utilization of the cropgro-soybean model to estimate yield loss caused by Asian rust in cultivars with different cycle. *Bragantia*, *71*(2), 308–317. https://doi.org/10.1590/S0006-87052012000200021

Sarkar, M.A., Pal, R., Das, P. & Chowdhury, A. (2005). Studies on residues and persistence/dissipation of Mancozeb in whole onion plant (Allium cepo) and soil following application of 75 WP formulation. *Pestology* 29(2): 17-20.

Sharma, I.D., Nath, A. & Dubey, J.K. (1994). Persistence of mancozeb (dithane M-45) in some vegetables and efficacy of decontamination processes. *Journal of Food Science and Technology* 31(3): 215-218.

Simões, K., Hawlik, A., Rehfus, A., Gava, F. & Stammler, G. (2018). First detection of a SDH variant with reduced SDHI sensitivity in Phakopsora pachyrhizi. *Journal of Plant Diseases and Protection*, *125*(1), 21–26. https://doi.org/10.1007/s41348-017-0117-5

Soetaert, K., Petzoldt, T. & Setzer, R.W. (2010). Solving Differential Equations in R : Package deSolve. Journal of Statistical Software, 33(9). https://doi.org/10.18637/jss.v033.i09

Syngenta (2024). Elatus [product label]. Available at: https://maisagro.syngenta.com.br/wp-content/uploads/2024/08/Bula_ELATUS_20.03.24.pdf [Accessed: 21 August 2024].

Tabonglek, S., Humphries, U. & van den Bosch, F. (2019). *Development of an epidemiological model for soybean rust*. *AIP Conf. Proc.* 21 August 2019; 2138 (1): 050030. https://doi.org/10.1063/1.5121135

Taylor, N.P. & Cunniffe, N.J. (2023a). Modelling quantitative fungicide resistance and breakdown of resistant cultivars: Designing integrated disease management strategies for Septoria of winter wheat. *PLOS Computational Biology*, *19*(3), e1010969. https://doi.org/10.1371/journal.pcbi.1010969

Taylor, N.P. & Cunniffe, N.J. (2023b). Optimal Resistance Management for Mixtures of High-Risk Fungicides: Robustness to the Initial Frequency of Resistance and Pathogen Sexual Reproduction. *Phytopathology*, *113*(1), 55–69. https://doi.org/10.1094/PHYTO-02-22-0050-R

te Beest, D. E., Paveley, N. D., Shaw, M. W. & van den Bosch, F. (2013). Accounting for the Economic Risk Caused by Variation in Disease Severity in Fungicide Dose Decisions, Exemplified for Mycosphaerella graminicola on Winter Wheat. Phytopathology®, 103(7), 666–672. https://doi.org/10.1094/PHYTO-05-12-0119-R

The MathWorks Inc. (2022). MATLAB version: 9.13.0 (R2022b), Natick, Massachusetts: The MathWorks Inc. https://www.mathworks.com

van den Berg, F., Paveley, N.D. & van den Bosch, F. (2016). Dose and number of applications that maximize fungicide effective life exemplified by

Zymoseptoria tritici on wheat – a model analysis. *Plant Pathology*, *65*(8), 1380–1389. https://doi.org/10.1111/ppa.12558

van den Berg, F., van den Bosch, F., & Paveley, N. D. (2013). Optimal Fungicide Application Timings for Disease Control Are Also an Effective Anti-Resistance Strategy: A Case Study for *Zymoseptoria tritici* (*Mycosphaerella graminicola*) on Wheat. *Phytopathology®*, *103*(12), 1209–1219. https://doi.org/10.1094/PHYTO-03-13-0061-R

van den Bosch, F., Blake, J., Gosling, P., Helps, J.C. & Paveley, N. (2020). Identifying when it is financially beneficial to increase or decrease fungicide dose as resistance develops: An evaluation from long-term field experiments. *Plant Pathology*, *69*(4), 631–641. https://doi.org/10.1111/ppa.13155

van den Bosch, F., Lopez-Ruiz, F., Oliver, R., Paveley, N., Helps, J. & van den Berg, F. (2018). Identifying when it is financially beneficial to increase or decrease fungicide dose as resistance develops. Plant Pathology, 67(3), 549–560. https://doi.org/10.1111/ppa.12787

van den Bosch, F., Oliver, R., van den Berg, F. & Paveley, N. (2014). Governing Principles Can Guide Fungicide-Resistance Management Tactics. *Annual Review of Phytopathology*, *52*(1), 175–195. https://doi.org/10.1146/annurev-phyto-102313-050158

Vittal, R., Paul, C., Hill, C.B. & Hartman, G.L. (2014). Characterization and Quantification of Fungal Colonization of *Phakopsora pachyrhizi* in Soybean Genotypes. *Phytopathology*, *104*(1), 86–94. https://doi.org/10.1094/PHYTO-12-12-0334-R

Wen, L., Bowen, C. R., & Hartman, G. L. (2017). Prediction of Short-Distance Aerial Movement of Phakopsora pachyrhizi Urediniospores Using Machine Learning. *Phytopathology*, *107*(10), 1187–1198. https://doi.org/10.1094/PHYTO-04-17-0138-FI

Wu, X., Ma, J., Zhang, J., Wang, H., Shi, L., Zhou, J. et al. 2015. Analysis of wheat and soil cyproconazole dissipation under field conditions and risk for dietary residue intake. Chinese Journal of Eco-Agriculture 3: 337-344. https://doi.org/10.13930/j.cnki.cjea.140798

Xavier, S.A., Martins, D.C., Fantin, L.H. & Canteri, M.G. (2017). Older leaf tissues in younger plants are more susceptible to soybean rust. *Acta Scientiarum. Agronomy*, *39*(1), 17. https://doi.org/10.4025/actasciagron.v39i1.30638

Yang, C., Hamel, C., Vujanovic, V. & Gan, Y. (2011). Fungicide: Modes of Action and Possible Impact on Nontarget Microorganisms. *ISRN Ecology*, *2011*, 1–8. https://doi.org/10.5402/2011/130289

Yang, X.B., Dowler, W.M. & Tschanz, A.T. (1991). A Simulation Model for Assessing Soybean Rust Epidemics. *Journal of Phytopathology*, *133*(3), 187–200. https://doi.org/10.1111/j.1439-0434.1991.tb00153.x

Yeh, C., Sinclair, J. & Tschanz, A. (1982). Phakopsora pachyrhizi: uredial development, urediospore production and factors affecting teliospore formation on soybeans. *Australian Journal of Agricultural Research*, *33*(1), 25. https://doi.org/10.1071/AR9820025

Yorinori, J.T. (2021a). CHAPTER 5: Difficulties Controlling Soybean Rust. In *Soybean Rust: Lessons Learned from the Pandemic in Brazil* (pp. 75–86). The American Phytopathological Society. https://doi.org/10.1094/9780890546642.05

Yorinori, J.T. (2021b). CHAPTER 6: Hosts and Sources of Inoculum of Soybean Rust. In *Soybean Rust: Lessons Learned from the Pandemic in Brazil* (pp. 87–91). The American Phytopathological Society. https://doi.org/10.1094/9780890546642.06

Zadoks, J.C. & Schein, R.D. (1979). *Epidemiology and plant disease management*. Oxford University Press, New York. 427 pp.

Chapter 4

Dose splitting increases selection for both target-site and non-target-site fungicide resistance – a modelling analysis

I. Corkley[1,2,3], A. Mikaberidze[2], N. Paveley[4], F. van den Bosch[5,6], M.W. Shaw[2], A.E. Milne[1]

[1]*Net Zero and Resilient Farming, Rothamsted Research, Harpenden, UK.* [2]*School of Agriculture, Policy and Development, University of Reading, Reading, UK.* [3]*Sustainable Agricultural Systems, ADAS, Wolverhampton, UK.* [4]*Sustainable Agricultural Systems, ADAS, High Mowthorpe, UK.* [5]*Quantitative Biology & Epidemiology Group, Plant Pathology Department (Visiting Scholar), University of California, Davis, USA.* [5]*Sustainable Agricultural Systems, ADAS, Rosemaund, UK.*

Dose splitting may be required to enable use of mixtures of different MoA due to increasing limitation of the number of MoA available for use due to regulation and existing resistance. Previous modelling studies have predicted that dose splitting will increase selection for resistance, but did not show how the effect of dose splitting varies with fungicide properties and the type and magnitude of resistance. The balance between the effects on selection of increased exposure time due to dose splitting, the reduced dose rate of each fungicide at each application timing and the effect of mixing different MoA will determine whether splitting and mixing is beneficial for management of concurrent evolution of resistance. In this chapter, I investigate variability in the effects of dose-splitting, to improve understanding of this key trade-off for management of concurrent evolution of resistance. The following manuscript was published in *Plant Pathology* **74**(4):1152-1167 in March 2025.

4.1   Abstract

Fungicide resistance management principles recommend that farmers avoid splitting the total dose applied of a fungicidal mode of action (MoA) across multiple applications per season ('dose splitting'). However, dose splitting may sometimes be needed to make another proven resistance management tactic - application in

mixture with a different MoA - practically achievable, especially in cases where there are limited MoAs available for disease control. Variable effects of dose splitting on selection for resistance have been observed in field experiments, and its effect on selection for partial resistance in fungal pathogens is not well studied. An improved understanding of whether the effect of dose splitting depends on fungicide properties and type of fungicide resistance is required. We developed a compartmental epidemiological model of septoria leaf blotch (STB) (*Zymoseptoria tritici*) to investigate the effect of dose splitting on selection for both complete and partial target-site and non-target-site resistance. To measure solely the effects of dose splitting, we restricted the analysis to solo fungicide application (solo use is not recommended in practice). Our results show variable effects of dose splitting: in general, it increased selection for both target-site and non-target-site resistance. Within the range of dose response parameters expected for commercial fungicides, dose splitting increased selection most for partial resistance mechanisms that result in a reduction in fungicide efficacy at low fungicide concentrations but not at high concentrations. We predict that dose splitting of a succinate dehydrogenase inhibitor (SDHI) fungicide (solo) will increase selection for target-site and non-target-site resistance by between 20-35%.

4.2   Introduction

The effectiveness of fungicides for control of plant diseases is threatened by the evolution of resistance (Corkley et al., 2022). The risk of resistance is particularly high for polycyclic foliar fungal pathogens, such as septoria tritici blotch (STB) *(Zymoseptoria tritici)* in wheat, grey mould (*Botrytis cinerea*) in many hosts, potato late blight (*Phytophthora infestans*), and net blotch (*Pyrenophora teres*) and powdery mildew (*Blumeria hordei*) diseases of barley. These pathogens have large population sizes and many generations per year, enabling rapid evolution of resistance (Grimmer et al., 2015; McDonald et al., 2022), and have the potential to cause large economic losses. Fungicide resistance management tactics include minimising the dose and number of applications, and applying in mixture with a different mode of action (MoA) (Corkley et al., 2022; Elderfield et al., 2018; Mikaberidze et al., 2017; van den Berg et al., 2016; van den Bosch et al., 2014a, 2014b). However, the number of effective MoA available for use is increasingly restricted by regulation (especially of multi-site fungicides) and resistance which has already evolved. This poses challenges for implementation of current resistance management strategies.

Fungicides with a MoA affecting a single pathogen target site are at particular risk of resistance development because a single point mutation affecting the target site gene ('target-site resistance') may confer a large fitness advantage. Target-site mutations may confer either complete or partial resistance. If a target-site mutation substantially prevents fungicide binding, for example through a change in the shape of the fungicide binding site, this can fully restore cellular or enzyme function and result in a high level of complete resistance. For example, the G143A mutation prevents quinone outside inhibitor (QoI) fungicides from binding to the cytochrome b mitochondrial protein, restoring its function in respiration (Dorigan et al., 2023). Target-site resistance may involve a single point mutation, or a combination of multiple mutations on the target gene, each conferring partial resistance, but potentially leading to highly resistant phenotypes in combination. For example, *Z. tritici* has accumulated multiple mutations in the CYP51 gene, leading to gradually increasing levels of resistance to demethylation inhibitor (DMI) fungicides (Cools & Fraaije, 2013; Hawkins & Fraaije, 2021; Leroux & Walker, 2011). In addition to target-site mutations, other mechanisms of fungicide resistance in pathogens include target-site overexpression, and non-target-site resistance such as increased efflux, detoxification and alternative metabolism (Dorigan et al., 2023; Hawkins & Fraaije, 2021; Hu & Chen, 2021). These mechanisms may cause partially or highly resistant strains, especially in combination with one another or with target-site resistance. Metabolic resistance pathways such as efflux pumps are also implicated in multi-drug resistant fungal strains (Kretschmer et al., 2009; Omrane et al., 2017; Patry-Leclaire et al., 2023).

To predict the impact of fungicide resistance management tactics on selection, it is helpful to consider pathogen epidemics in terms of the *per capita* rate of increase or 'growth rate' (*r*) of each strain: a number which combines the repeating stages of lesion establishment, growth and sporulation into a single measure of the success of a strain at a given point in time. Pathogen strains with resistance to the action of a fungicide have higher growth rates in the presence of that fungicide than strains that are sensitive to the fungicide. The greater the difference in the *per capita* growth rates of resistant and sensitive strains, the faster the rate of selection for resistance (van den Bosch et al., 2014a). The impact of any given fungicide dose on the *per capita* growth rate of a pathogen strain can be represented in models by its effect on important parts of the pathogen life cycle, such as a reduction in the pathogen transmission rate. Assuming that the applied dose decays exponentially over time, it is possible to track the 'effective dose' remaining

at any point in time. The impact of the fungicide on the pathogen life cycle is greatest at high effective doses, where the maximum effect is defined by an 'asymptote parameter', and the rate at which the effect decreases with reducing fungicide doses is defined by a 'curvature parameter'. The effect of resistance on the dose response to a fungicide may be observed either as a complete or partial reduction in the maximum effect of the fungicide on the pathogen growth rate even at very high effective doses, or as a reduction in the efficacy of lower effective doses of the fungicide. We will refer to these types of resistance as 'asymptote shift' and 'curvature shift' respectively, to reflect their effect on the fungicide dose response (Figure 4.1(a), 4.1(b)). Resistance resulting from an asymptote shift is sometimes referred to as 'type I' resistance, and resistance resulting from a curvature shift as 'type II' resistance (Elderfield, 2018; Mikaberidze et al., 2017; Taylor & Cunniffe, 2023a).

Let us consider which resistance mechanisms are likely to lead to either a partial asymptote shift or a curvature shift. Some fungicides bind competitively directly to the enzyme active site: for example, DMI fungicides bind competitively to the CYP51 protein which catalyses a step in ergosterol biosynthesis (Hargrove et al., 2015), occupying the P450 active site and preventing substrate binding. A target-site mutation that causes a small to moderate reduction in the affinity of the enzyme for the fungicide will reduce fungicide efficacy at low fungicide concentrations, but not at high fungicide concentrations. This case is therefore best represented by a curvature shift. A curvature shift will also be representative of other resistance mechanisms that reduce fungicide efficacy at low fungicide concentrations but are overwhelmed by high fungicide concentrations. These may include target-site overexpression and non-target-site, metabolic resistance mechanisms such as increased expression of efflux pumps and detoxification. A partial asymptote shift could result from a target-site mutation that reduces the maximum effect at any dose rate of fungicides which bind allosterically and non-competitively to an enzyme. These fungicides change the structure of the enzyme in a way that inhibits enzyme function or reduces access or binding of the substrate to the enzyme active site. An example is the cyanoacrylate phenamacril which is used against a number of *Fusarium* species (Wollenberg et al., 2020). The maximum effect of these fungicides could be partially reduced by a target-site mutation which changes the shape of the enzyme-fungicide complex, partially restoring enzyme function.

Multiple fungicide applications per year are often useful to avoid economically damaging epidemics of polycyclic foliar fungal pathogens such as *Z. tritici*. If the

number of MoA available for programmes is limited, use of mixtures may require splitting the total dose of a fungicide across two or more applications, reducing the dose of each MoA per application but increasing the exposure time of the pathogen to each fungicide, with counteracting (but not necessarily equal) effects on selection for resistance. If resistance is evolving 'concurrently' to two or more MoA at the same time, this situation introduces complex trade-offs for resistance management. Whether 'splitting and mixing' is a good or a poor choice of strategy for management of concurrent evolution of resistance will depend on the balance between the effects of mixture and dose splitting on selection. However, variation in the effects of dose splitting is not well understood. van den Bosch et al. (2014a) hypothesise that dose splitting will, overall, increase selection for strains with an asymptote shift against a fungicide. They highlight several experimental studies that support this theory, but the effect of dose splitting on selection for partially resistant strains with a curvature shift has not been explicitly considered in previous modelling studies, to our knowledge. Field trials carried out between 2018 and 2020 to measure the effect of dose splitting on selection for SDH-mutants showed variable results (Paveley et al., 2020; Young et al., 2021). An improved understanding of how fungicide properties and type of resistance determine the effect of dose splitting on selection for resistant pathogen strains is needed to inform tactics for management of concurrent evolution of resistance.

To investigate the effect of dose splitting on selection, we developed a model of fungicide resistance evolution in *Z. tritici*. *Zymoseptoria tritici* is one of the most common, widespread and damaging pathogens affecting winter wheat crops in the UK and worldwide. It has evolved resistance to QoIs, DMIs and SDHIs (Cools & Fraaije, 2013; Dooley et al., 2016; Huf et al., 2018; Rehfus et al., 2018; Torriani et al., 2009), with a corresponding decline in disease control (Blake et al., 2018). The model simulates a typical UK epidemic of STB*,* describing the seasonal growth and senescence of the upper crop canopy of winter wheat under average temperature conditions in the UK, key processes in the pathogen life cycle (sporulation, infection and growth) and their interaction with fungicides. In the UK, initial infection of wheat crops by *Z. tritici* occurs in autumn or spring through airborne ascospores or by splash-dispersed conidia from wheat stubble. After penetrating the leaf stomata, the fungus develops slowly during a symptomless latent period, following which necrotic lesions form on the leaf surface. These produce asexual haploid pycnidiospores which spread to the upper leaf canopy through contact and rain splash, driving the majority of secondary infections within the growing season with

the potential for rapid increases in disease severity (Ponomarenko et al., 2011; Suffert et al., 2011). STB is associated with a reduction in crop quality and yield losses of up to 50% if uncontrolled (Fones and Gurr, 2015).

Through model simulations, we compared the effects on selection for a resistant *Z. tritici* strain of applying a fungicide solo in either a single application at full label rate or in two applications, each at half the full label rate. It should be noted that use of solo MoA is not recommended in practice. However, restricting the analysis to dose splitting of a solo fungicide enabled us to measure solely the effects of dose splitting, rather than the combined effects of 'splitting and mixing', giving a clearer picture of the drivers in variation of the effects of dose splitting. We used the model to investigate how the effect of dose splitting on selection for resistance depends on: (a) fungicide properties (foliar concentration half-life; asymptote and curvature dose response parameters for the sensitive strain); (b) the type of resistance (asymptote shift or curvature shift); and (c) the magnitude of the asymptote or curvature shift.

4.3   Materials and Methods

4.3.1 Model background and approach

Our model has the same functional form as one developed by Hobbelen *et al.* (2011a, b). However, the rate of crop senescence in that model was parameterised using data on spring barley (*Hordeum vulgare*) (Hobbelen et al., 2011a), and the simulated timing of senescence could impact on model predictions of the effects of dose splitting on selection for resistant strains. We therefore re-parameterised the model (see Section 4.3.3) using a dataset of green leaf area index (GLAI) and *Z. tritici* infection of the top three leaves of wheat crops from 14 site-years (Milne et al., 2003, described as 'Data set 1'; te Beest et al., 2009).

We follow the approach of (Hobbelen et al., 2011b), modelling the leaf area index (LAI; a dimensionless measure of leaf density, defined as the total amount of one-sided leaf area of the canopy (m^2) per unit ground area (m^2)) and infection by *Z. tritici* pycnidiospores on the top three leaves of the wheat canopy only. Yield loss due to *Z. tritici* occurs due to a reduction in healthy leaf area duration (HAD) and the resulting loss of interception of photosynthetically active radiation (PAR) on the upper three leaves during grain-filling: the level of disease on the upper canopy is a good predictor of yield loss (Parker et al., 2004; Shaw & Royle, 1989). Fungicide applications targeted against *Z. tritici* are therefore mostly applied to the upper leaf

canopy. Although there will be some fungicide exposure on lower leaves, previous modelling results suggest that it is on the upper leaf canopy that selection for resistance primarily occurs (van den Berg et al., 2013).

The dynamics of the epidemic in the model are driven by the growth and senescence of the crop, which determines the leaf area available for infection, and the effect of a fungicide on the pathogen life cycle over time. The leaf area can pass sequentially through healthy, latent (infected but not yet sporulating), infectious (sporulating) and post-infectious stages; healthy and latent leaf area may also senesce due to leaf age. The infectious leaf area generates new infections on healthy leaf area. The model simulates the LAI of both the latent and infectious stages of a sensitive strain and a resistant strain of *Z. tritici*.

4.3.2 Model equations

4.3.2.1 Growth and senescence of wheat leaf canopy

It is assumed that the growth rate of the total leaf area of the upper canopy is not affected by *Z. tritici* severity, so the total leaf area index (LAI) and uninfected healthy green leaf area index (GLAI) are tracked separately (Hobbelen et al., 2011b). In the absence of disease the rates of change of the total LAI (A) and the total healthy GLAI (H) are given by:

$$\frac{\mathrm{d}A}{\mathrm{d}t} = \begin{cases} 0, & t < t_0 \\ \gamma(A_{\mathrm{Max}} - A), & t > t_0 \end{cases} \tag{1}$$

$$\frac{\mathrm{d}H}{\mathrm{d}t} = \gamma(A_{\mathrm{Max}} - A) - \beta(t)H \tag{2}$$

$$\text{where } \beta(t) = \begin{cases} 0, & t < t_{\beta_0} \\ \tau\left(\dfrac{t - t_{\beta_0}}{t_{\beta_T} - t_{\beta_0}}\right) + \varphi e^{\omega\left(t_{\beta_T} - t\right)}, & t_{\beta_0} \leq t \leq t_{\beta_T} \end{cases} \tag{3}$$

where t_0 is the time at which leaf 3 emerges and growth of the upper canopy commences, A_{Max} is the maximum LAI, γ is the growth rate of the leaf area, $\beta(t)$ is the rate of senescence at time t, t_{β_0} is the time of onset of senescence, t_{β_T} is the time at which the canopy has fully senesced, and τ, φ *and* ω are coefficients controlling the rate at which senescence occurs in relation to the length of time after the onset of senescence. Time is measured in degree days (base 0°C), 'zero-degree days' (see Section 4.3.3).

4.3.2.2 Infection of crop by *Zymoseptoria tritici*

The development of the STB epidemic is described in the model by tracking the LAI of latent and infectious lesions of the resistant and sensitive strains.

It is assumed that the epidemic on the upper leaves is initiated by an influx of spores from infectious lesions on lower leaves. The density of infectious lesions on lower leaves, C, diminishes over time at rate λ, as lower leaves senesce and infectious lesions on the lower leaves reach the end of the infectious period. The LAI of infectious lesions on lower leaves at time t, $C(t)$, is calculated as:

$$C(t) = C_0 e^{-\lambda t} \tag{4}$$

A fraction, $\theta_{\rho \text{Start}}$, of the initial influx C from lower leaves is assumed to be spores of the resistant strain, with the sensitive strain fraction $\theta_{\sigma \text{Start}} = 1 - \theta_{\rho \text{Start}}$. It is assumed that $\theta_{\rho \text{Start}}$ and $\theta_{\sigma \text{Start}}$ are not affected by fungicide application after the start of the model simulation at GS31. The initial influx is denoted as C_σ and C_ρ for the sensitive and resistant strains respectively.

The influx of spores, C, and infectious LAI on the upper canopy, I, are converted into new latent lesions on the upper canopy, at transmission rate ε, i.e. the overall rate at which infectious lesion density is converted into new latent lesions on a given density of healthy leaf area. Latent lesions mature into infectious, sporulating lesions, at a rate δ, where $1/\delta$ is the average latent period. Infectious lesions die at a rate μ, where $1/\mu$ is the average infectious period. Leaf senescence affects latent LAI, but not infectious LAI as the leaf tissue is already killed by the necrotic process of lesions becoming infectious (Hobbelen et al., 2011b; Kema et al., 1996). The following set of equations track the area index of healthy (H), latently infected (L) and infectious (I) leaf area over time, with L_ρ and L_σ denoting the area index of latent lesions and I_ρ and I_σ the infectious area index of the resistant and sensitive strains respectively:

$$\frac{dH}{dt} = \gamma(A_{\text{Max}} - A) - \beta(t)H - \varepsilon\left(H/A\right)(C_\sigma + C_\rho + I_\sigma + I_\rho) \tag{5}$$

$$\frac{dL_\sigma}{dt} = \varepsilon_\sigma\left(H/A\right)(C_\sigma + I_\sigma) - \delta L - \beta(t)L_\sigma \tag{6}$$

$$\frac{dL_\rho}{dt} = \varepsilon_\rho\left(H/A\right)(C_\rho + I_\rho) - \delta L_\rho - \beta(t)L_\rho \tag{7}$$

$$\frac{\mathrm{d}I_\sigma}{\mathrm{d}t} = \delta_\sigma L_\sigma - \mu I_\sigma \tag{8}$$

$$\frac{\mathrm{d}I_\rho}{\mathrm{d}t} = \delta_\rho L_\rho - \mu I_\rho \tag{9}$$

The final fraction of the resistant strain in the population at crop senescence, $\theta_{\rho_{\text{End}}}$, is calculated as:

$$\theta_{\rho_{\text{End}}} = \frac{I_\rho(t_{\beta_T})}{I_\rho(t_{\beta_T}) + I_\sigma(t_{\beta_T})} \tag{10}$$

4.3.2.3 The effect of the fungicide on pathogen growth rate

Fungicide effects on the two strains of *Z. tritici* are simulated in the model through a dose-dependent reduction of pathogen life cycle parameters ε (transmission rate, Equations 6 and 7) and δ (the rate at which latent lesions are converted to sporulating lesions, Equations 8 and 9), slowing the rate of increase of the pathogen population. Single-site fungicides are assumed to reduce both the transmission rate and the rate of conversion of latent infections to sporulating lesions. The infectious period of sporulating lesions is assumed to be unaffected by fungicides.

The fungicide dose at time t, $D(t)$, decays exponentially over time at rate v:

$$D(t) = \begin{cases} D_0 e^{-v(t-t^*)}, & t \geq t^* \\ 0, & t < t^* \end{cases} \tag{11}$$

where D_0 is the applied dose, expressed as a proportion of the maximum permitted individual dose (as defined on the product label), D_{Max}, and t^* is the time of the first application. $D(t)$ is the 'effective dose' referred to in Section 4.2. If an additional application is made at t^{**}, the remaining dose from the application at t^* is added to the newly applied dose to calculate a total value for D_0 at t^{**}.

The fungicide reduces the pathogen life cycle parameters ε and δ by a fraction $f(t)$, which changes over time depending on the remaining fungicide dose, $D(t)$. The dose response of $f(t)$ to $D(t)$ (Figure 4.1(a), 4.1(b)) is described by a combination of an asymptote parameter, q, which is the maximum fractional reduction of the pathogen life cycle parameter (i.e. at infinite fungicide dose), and a curvature parameter, k, which defines how quickly the fractional reduction declines from the asymptote as $D(t)$ decreases:

$$f_\sigma(t) = q_\sigma\left(1 - e^{-k_\sigma D(t)}\right) \tag{12}$$

$$f_\rho(t) = q_\rho\left(1 - e^{-k_\rho D(t)}\right) \tag{13}$$

The asymptote parameters are denoted as q_σ and q_ρ, the curvature parameters as k_σ and k_ρ, and the fractional reductions as $f_\sigma(t)$ and $f_\rho(t)$ for the sensitive and resistant strains respectively. Each pathogen life cycle parameter affected by the fungicide is multiplied by $\left(1 - f(t)\right)$ to represent the effect of the fungicide on the growth rate of the pathogen population. For example, the transmission rate of the sensitive strain at time t, $\varepsilon_\sigma(t)$, is calculated as:

$$\varepsilon_\sigma(t) = \varepsilon_0\left(1 - f_\sigma(t)\right) = \varepsilon_0\left(1 - q_\sigma\left(1 - e^{-k_\sigma D(t)}\right)\right) \tag{14}$$

where ε_0 is the transmission rate in the absence of fungicides. It is assumed that there are no fitness costs of resistance. If $f_\sigma(t) > f_\rho(t)$, the density of the resistant strain will increase faster than the density of the sensitive strain, leading to an increase in the resistant strain fraction of the *Z. tritici* population.

4.3.2.4 Types of fungicide resistance

We simulate two types of fungicide resistance based on the nature of the shift in sensitivity to the fungicide ('sensitivity shift'):

- Asymptote shift, ζ_q: parameter q is reduced relative to the sensitive strain.
- Curvature shift, ζ_k: parameter k is reduced relative to the sensitive strain.

We describe the level of sensitivity shift as a percentage. For example, a 50% asymptote shift means that $q_\rho = 0.5q_\sigma$. Partial resistance could take the form of either an asymptote shift or a curvature shift, or a combination of both. An asymptote shift means that the effect of any dose $D(t)$ against the resistant strain of the pathogen is reduced (Figure 4.1(a)). For a curvature shift, the instantaneous effect of a high dose of the fungicide may still be as potent, but at lower doses it is less effective against the resistant strain than against the sensitive strain (Figure 4.1(b)). The biological significance of asymptote and curvature shifts is discussed in Section 4.2.
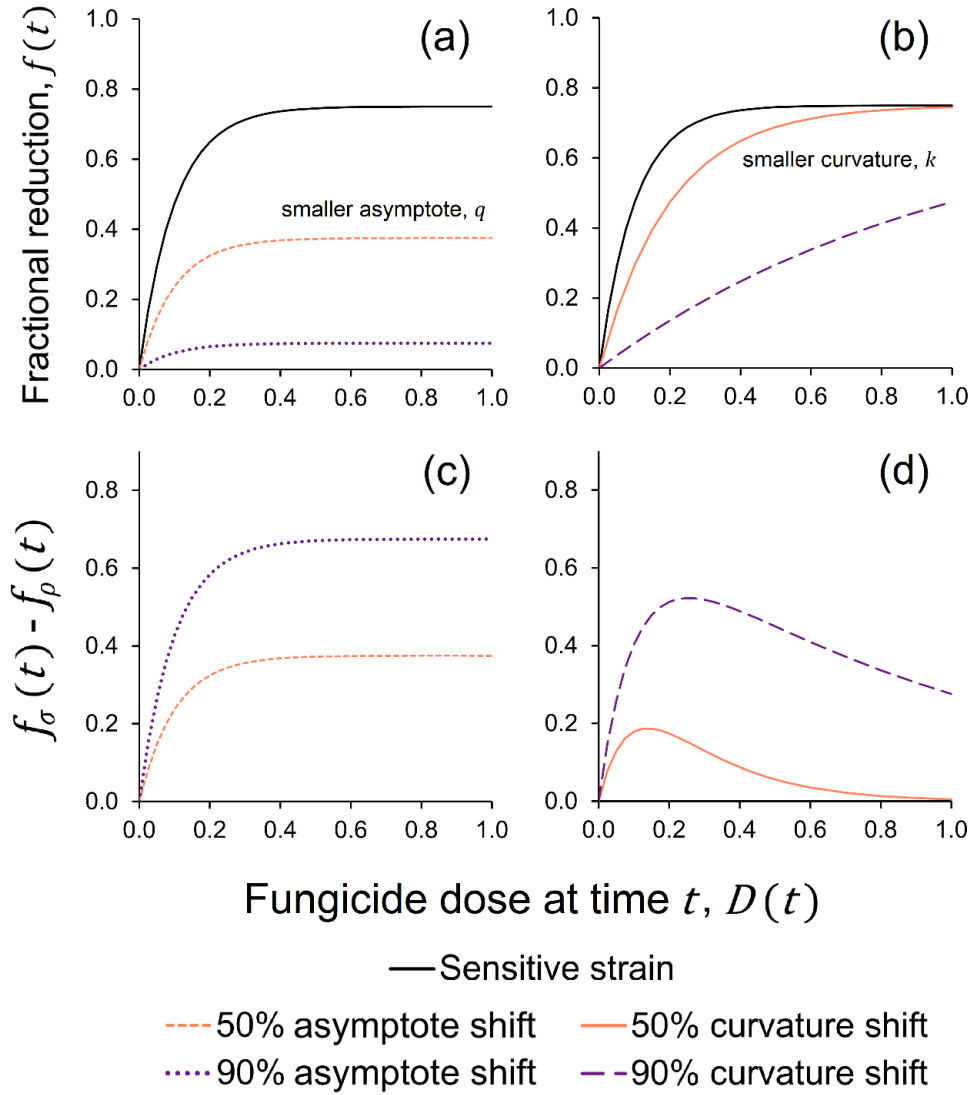
Figure 4.1: Effect of asymptote shift, ζ_q, and curvature shift, ζ_k, on the dose response to fungicide dose, $D(t)$. (a) and (b) show the fractional reduction, $f(t)$, of pathogen life cycle parameters for different levels of asymptote shift and curvature shift respectively. (c) and (d) show $f_\sigma(t) - f_\rho(t)$, the resulting difference in $f(t)$ of the sensitive strain compared to a resistant strain with an asymptote shift or a curvature shift respectively. Dose response shown for a fungicide with $q_\sigma = 0.75, k_\sigma = 10$. Solid black line: dose response of sensitive strain. Dashed orange line: $\zeta_q = 50\%$. Dotted purple line: $\zeta_q = 90\%$. Solid orange line: $\zeta_k = 50\%$. Dashed purple line: $\zeta_k = 90\%$.

A 100% asymptote and a 100% curvature shift are functionally identical: both represent strains that are completely resistant to the fungicide at any dose $D(t)$. Otherwise, for a given percentage sensitivity shift, an asymptote shift will result in a more highly resistant strain than the same level of curvature shift (as can be seen

by comparing Figures 4.1(a) and 4.1(b)). The difference in the fractional reduction of the sensitive strain compared to the resistant strain, $f_\sigma(t) - f_\rho(t)$, is greatest at high fungicide dose $D(t)$ for asymptote shifts, and greatest at intermediate fungicide dose $D(t)$ for partial (<100%) curvature shifts (Figures 4.1(c), 4.1(d)).

4.3.2.5 Calculation of the selection coefficient

We used the selection coefficient, s, to compare the rate of selection for the resistant strain in each scenario simulated (Milgroom & Fry, 1988; van den Bosch et al., 2014a). The selection coefficient is defined as the difference in fitness between the resistant and sensitive strains due to the application of the fungicide, where fitness is measured by the per capita rate of increase, r, of a population:

$$s = r_\rho - r_\sigma \tag{15}$$

where r_ρ and r_σ are the average per capita rates of increase of the resistant and sensitive strains respectively over the course of the growing season. We calculate total selection between the start of the simulation, t_0, and crop senescence, time t_{β_T}, denoting the total length of time simulated as T. Assuming exponential growth of the sensitive and resistant strains (in the absence of density dependence), the density of the sensitive strain and resistant strain at time t_{β_T}, denoted as $P_\sigma(t_{\beta_T})$ and $P_\rho(t_{\beta_T})$ respectively, can be calculated as:

$$P_\sigma(t_{\beta_T}) = P_\sigma(0)e^{r_\sigma T} \tag{16}$$

$$P_\rho(t_{\beta_T}) = P_\rho(0)e^{r_\rho T} \tag{17}$$

where $P_\sigma(0)$ and $P_\rho(0)$ are the initial densities of the sensitive and resistant strain respectively at the start of the simulation.

Rearrangement of equations (16) and (17) for r_σ and r_ρ, and substitution of equation (15) gives:

$$s = \frac{1}{T}\left(\ln\left(\frac{P_\rho(t_{\beta_T})P_\sigma(0)}{P_\rho(0)P_\sigma(t_{\beta_T})} \right) \right) \tag{18}$$

This can also be expressed in terms of the population fractions of the resistant and sensitive strains, θ_ρ and θ_σ, at the beginning of the simulation and the end of the growing season:

$$s = \frac{1}{T}\left(\ln\left(\frac{\theta_{\rho_{\text{End}}}\theta_{\sigma_{\text{Start}}}}{\theta_{\rho_{\text{Start}}}\theta_{\sigma_{\text{End}}}} \right) \right) \quad (19)$$

4.3.3 Model implementation and parameterisation

The model was implemented in MATLAB R2022b (The MathWorks Inc., 2022) using built-in function 'ode45' for the solution of the ordinary differential equations.

The model was parameterised using data on GLAI and *Z. tritici* infection over time from field trials of wheat crops grown with and without fungicide application, recorded over 14 site-years between 1993 and 1995 in England, United Kingdom, and corresponding daily weather data from meteorological stations within one kilometre of the site (Milne et al., 2003, described as 'Data set 1'; te Beest et al., 2009). We refer to data from these trials as 'Dataset 1'. For each site-year, Dataset 1 includes data on four cultivars (Riband, Apollo, Slejpner and Haven), with four replicates per cultivar.

We chose to follow previous models (Elderfield et al. 2018; Hobbelen et al. 2011b; van den Berg et al. 2013) in parameterising the model on a zero-degree days scale. Weather data for the sites was used to calculate both the thermal time (degree days base 0°C) and photo-vernal-thermal time (base 1°C) since sowing (Milne et al., 2003; Weir et al., 1984) corresponding to each observation date. The photo-thermal-vernal time gave a more consistent profile for the timings of the upper canopy growth and senescence than thermal time (see Figure 4.A.2 in Appendix 4.A for further details). Using linear regression, we derived a relationship between thermal time and photo-thermal-vernal time, t_{pvt}, and used this to convert t_{pvt} to the average thermal time in zero-degree days, t:

$$t = 1.204t_{pvt} + 778.6 \quad (20)$$

Dataset 1 was used to estimate the average number of zero-degree days per day, z.

We assumed that data from field plots that received a fungicide programme designed to provide full protection against disease (Milne et al., 2003) are representative of canopy growth in the absence of disease. We used these data to estimate the parameters controlling the growth and senescence of the wheat canopy: t_0, t_{β_0}, t_{β_T}, A_{Max}, γ, τ, φ and ω (defined in Section 4.3.2.1). The mean GLAI of the top three leaves at each observation time point was calculated for each site-year from data from all four cultivars and replicates in Dataset 1. The

parameters were fitted to data pooled from six site-years with maximum observed GLAI ranging from 3.76 to 4.90 (Cambridgeshire-1994, Devon-1994, Devon-1995, Kent-1995, Norfolk-1994, Norfolk-1995), using least squares optimisation (lsqcurvefit, MATLAB R2022b; further details in Appendix 4.A). Model zero-degree days were mapped to growth stages on Zadoks' scale (Zadoks et al., 1974), based on the fitted values of t_0, t_{β_0}, t_{β_T} and the estimated phyllochron length (see Appendix 4.A for further details).

We estimated *Z. tritici* life cycle parameters δ, μ and λ (defined in Section 4.3.2.2) based on data from a literature search (Table 4.2). In combination with C_0 (Equation 4) and ε_0 (Equations 6, 7, 14), these parameters describe the infection of crop by *Z. tritici* in the absence of a fungicide. We estimated values for C_0 and ε_0 using data on STB epidemic progress (% severity) (Dataset 1) on untreated plots on which the maximum severity of the STB epidemic exceeded 5% and the maximum cumulative severity of yellow rust, brown rust and powdery mildew did not exceed 15%. Data from cultivars that were considered moderately resistant at the time the trials were carried out were used to estimate ε_0. Data from six site-years (Devon-1994, Devon-1995, Hampshire-1995, Herefordshire-1994, Herefordshire-1995, Kent-1994) fitted these criteria. We fitted separate values of C_0 and ε_0 for each site-year-cultivar combination using least squares optimisation and calculated the average of these values (further details in Appendix A.1).

We used data from AHDB Fungicide Performance trials (AHDB, 2024a) on the observed dose response of STB severity to fluxapyroxad and isopyrazam from 2011-2012 (Dataset 2) to estimate indicative values of q_σ and k_σ for SDHI fungicides (see Appendix 4.A for further details), using an estimate of ν based on a literature search (Table 4.2).

4.3.4 Model simulations of dose splitting

We investigated the impact of dose splitting on selection for resistant strains with either an asymptote shift or a curvature shift (either partial or complete resistance), for a range of values of the fungicide parameters q_σ, k_σ and ν (Table 4.1). We compared selection for the resistant strain following a single application of the fungicide at full label rate, D_{Max}, at either growth stage 32 (GS32) or GS39, to selection for the resistant strain following a 'split dose' application of $0.5D_{\text{Max}}$ at

both GS32 and GS39. In all simulations, the total dose applied to the upper leaf canopy, D_{Total}, was equal to D_{Max}.

The foliar concentration half-lives of fungicide products can be very variable depending on the crop and environmental conditions (Fantke et al., 2014). We simulated three values of v (Table 4.1), equivalent to foliar half-lives of 3 days, 6 days and 12 days; SDHI fungicides such as fluxapyroxad, penthiopyrad and fluopyram have an average half-life of approximately 6 days (Fantke et al., 2014; He et al., 2016; Noh et al., 2019). Figure 4.2 illustrates the effect of the decay rate on the simulated fungicide dose $D(t)$ and fractional reduction $f(t)$ over time following single and split dose applications.
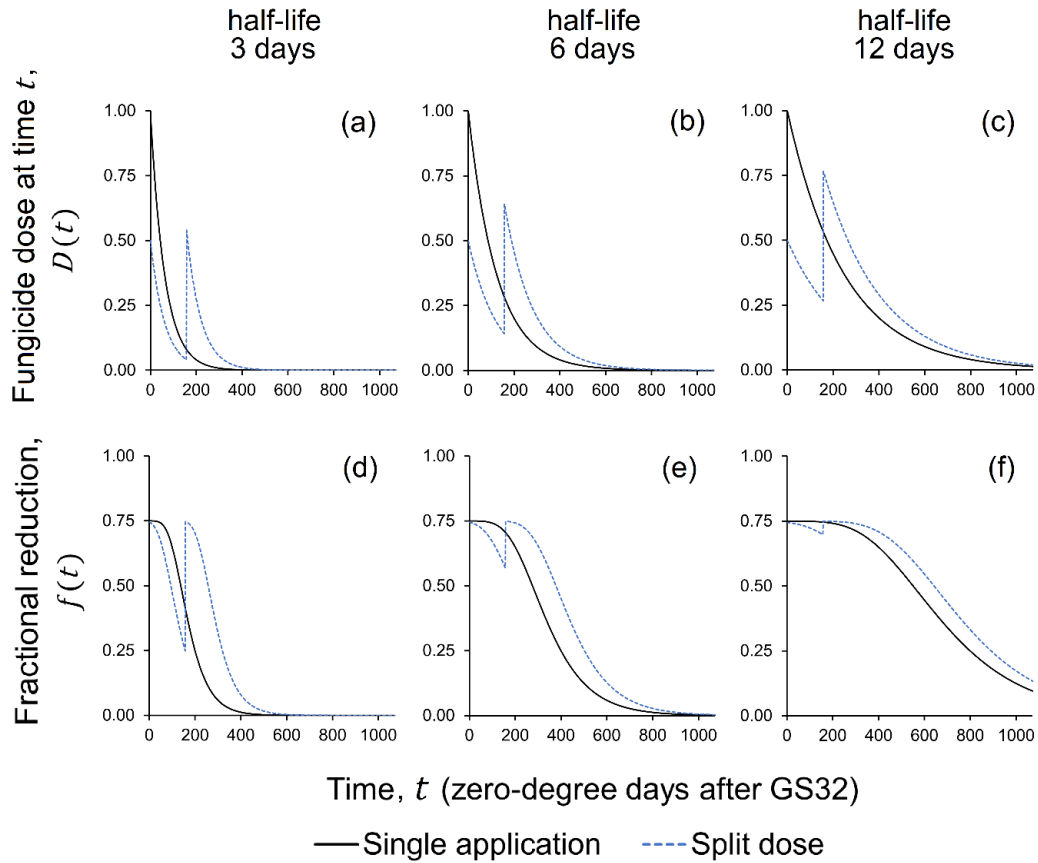
Figure 4.2: Effect of decay rate v on the simulated fungicide dose, $D(t)$, and fractional reduction, $f(t)$, over time following single (solid black line) and split dose (blue dashed line) applications of a fungicide with $q = 0.75, k = 10$. (a), (b) and (c) show $D(t)$ for $v = 0.016\ t^{-1}$, $v = 0.008\ t^{-1}$ and $v = 0.004\ t^{-1}$ respectively, corresponding to foliar half-lives of 3, 6 and 12 days respectively. (d), (e) and (f) show $f(t)$ for $v = 0.016\ t^{-1}$, $v = 0.008\ t^{-1}$ and $v = 0.004\ t^{-1}$ respectively.

Table 4.1: List of parameter values simulated. All combinations of q_σ, k_σ and ν values simulated for each value of ζ_q and ζ_k listed.

Parameter	Description	Values simulated
D_{Total}	Total fungicide dose applied to upper leaf canopy	1, i.e. D_{Max}
$\theta_{\rho\text{Start}}$	Initial fraction of inoculum C that is resistant	0.01
q_σ	Asymptote of fungicide dose response (sensitive strain)	0.05, 0.1, 0.25, 0.5, 0.75, 0.8, 0.95, 1
k_σ	Curvature of fungicide dose response (sensitive strain)	0, 0.25, 0.5, 0.75, 1, 1.5, 2, 4, 5, 7.5, 10, 15, 20, 30
ν	Decay rate (t^{-1})	0.01605, 0.00802, 0.00401
ζ_q	Asymptote shift of resistant strain	0, 1, 5, 10, 25, 50, 75, 90, 100
ζ_k	Curvature shift of resistant strain	0, 1, 5, 10, 25, 50, 75, 90, 100
GS32	Timing of GS32 application (zero-degree days)	1495
GS39	Timing of GS39 applications (zero-degree days)	1653

We included very low and high values of parameters q_σ and k_σ in the analysis to understand the extremes of the range of possible effects of dose-splitting. In practice, these parameter values are unlikely in a commercially available fungicide: fungicides with very low values of q_σ or k_σ would not be effective, whilst very high values are more likely to be associated with an unacceptable toxicity profile. We compared our results to those obtained using our fitted parameter values for SDHI fungicides to understand the most likely range of effects of dose splitting on selection for resistance to commercial fungicides.

We assumed that $\theta_\rho(0) = 0.01$, i.e. 1% of the inoculum initiating the epidemic was the resistant *Z. tritici* strain, whilst the remaining 99% of the population was sensitive to the fungicide. The simulations were run for a single growing season from the start of the leaf growth of the upper canopy, t_0, to complete canopy senescence, t_{β_T}. For each combination of parameter values simulated, the selection coefficient for the resistant strain, s, was calculated (Equation 19). The percentage change in the selection coefficient due to dose splitting, η, was then calculated as:

$$\eta = 100 \times \frac{\left(s_{\text{Split}} - s_{\text{Single}}\right)}{s_{\text{Single}}} \tag{21}$$

where s_{Single} is the selection coefficient for a single application at D_{Total} and s_{Split} is the selection coefficient for the resistant strain for a split dose application.

4.4   Results

4.4.1 Model parameterisation

The fitted model parameters are summarised in Table 4.2. The model fit to observed GLAI in the absence of disease was good (Figure 4.3(a); n=76, R^2 = 76.9%, RMSE = 0.76). For the cultivar-site-year combinations used to fit ε_0, the transmission rate in the absence of fungicide, the overall fit to observed disease severity progress was excellent (n=293, R^2 = 88.4%, RMSE = 2.8%); fitted values of ε_0 ranged from 0.0136 to 0.0364, with a mean value of 0.0211. In the absence of a fungicide, the model predicts STB severity of 9.5% (Figure 4.3(b)) at GS75 (medium milk), which is approximately equivalent to the expected average severity on a cultivar with an AHDB resistance rating of 6 (AHDB, 2024b).
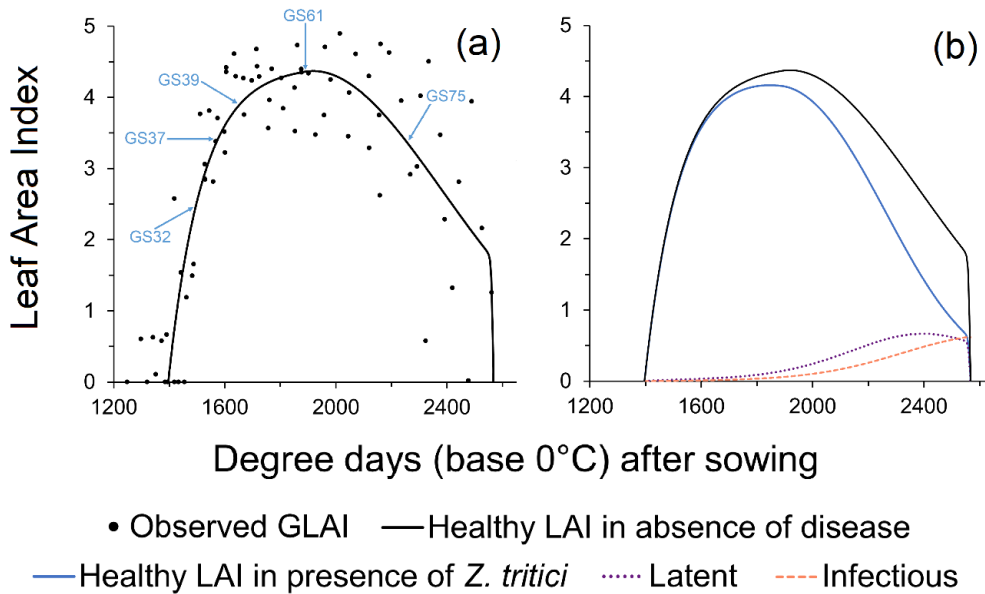
Figure 4.3: Model simulation of the growth, senescence and infection by *Z. tritici* of the upper wheat canopy. (a) Model simulation of healthy LAI in the absence of disease (solid line) and observed green leaf area index (GLAI) measurements used for parameterisation of wheat canopy (points) (n=76, from 6 sites from Dataset 1). The simulated timings of growth stages 32, 37, 39, 61 and 75 are

indicated (blue arrows). (b) Model simulation of healthy (not latently infected) LAI in the presence of *Z. tritici*, latently infected LAI and infectious LAI for an average untreated epidemic of STB in the UK.

Table 4.2: Fitted parameter values. Time, t is measured in degree days (base 0°C) after sowing. [a]Estimate based on 'Data set 1' from Milne et al., 2003; [b]Shaw, 1990; Suffert et al., 2013; [c]Boixel, 2020; Eyal, 1971; [d]Hobbelen et al., 2011b; [e]Estimate based on data from AHDB Fungicide Performance field trials; [f]Fantke et al., 2014; He et al., 2016; Noh et al., 2019.

Parameter	Definition	Units	Fitted value	Source
t_0, GS31	Timing of start of growth of leaf 3	t	1396	a
GS32	Timing of GS32: leaf 3 fully emerged	t	1495	a
GS37	Timing of GS37: leaf 2 fully emerged	t	1574	a
GS39	Timing of GS39: flag leaf fully emerged	t	1653	a
t_{β_0}, GS61	Timing of anthesis & start of leaf 3 senescence	t	1891	a
t_{β_T}, GS87	Timing of end of grainfill & complete senescence of wheat canopy	t	2567	a
A_{Max}	Maximum leaf area index of top three leaves of the wheat canopy	-	4.438	a
γ	Growth rate of leaf area	t^{-1}	0.0082	a
τ	Coefficients controlling the rate of senescence over time, in relation to the length of time after the onset of senescence	t^{-1}	0.0028	a
φ		t^{-1}	0.704	a
ω		t^{-1}	0.314	a
$1/\delta$	Average latent period	t	350	b
$1/\mu$	Average infectious period	t	600	c
C_0	Initial density of infectious lesions on the lower leaves	-	0.0144	a
λ	Rate at which $C(t)$ decreases	t^{-1}	0.00897	d
ε_0	Transmission rate	-	0.0211	a
z	Number of zero-degree days per day	t	14.4	a
q_σ	Asymptote parameter for an SDHI fungicide (against sensitive strain)	-	0.569	e
k_σ	Curvature parameter for an SDHI fungicide (against sensitive strain)	-	9.9	e
ν	Decay rate for an SDHI fungicide	t^{-1}	0.00802	f

4.4.2 Effect of dose splitting on selection for fungicide resistance

For the range of parameter values simulated (Table 4.1), we show results for both the overall magnitude of selection, measured by the selection coefficient s (Section 4.3.2.5), and the percentage change in selection due to dose splitting, η (Equation 21). When describing the baseline level of efficacy of a fungicide in Sections 4.4.2.1 and 0, we refer to the dose response against the sensitive strain, notated as q_σ and k_σ for the asymptote and curvature parameter respectively. For a resistant strain with an asymptote shift, $\zeta_q > 0$ but no curvature shift i.e. $\zeta_k = 0$, note that $k_\rho = k_\sigma$. For a resistant strain with a curvature shift $\zeta_k > 0$ but no asymptote shift, $q_\rho = q_\sigma$.

4.4.2.1 Magnitude of selection

The magnitude of selection for fungicide resistance, measured by the selection coefficient s, increased for both single and split dose fungicide applications with increasing values of the asymptote parameter, q_σ, curvature parameter, k_σ, asymptote shift, ζ_q or curvature shift, ζ_k, and with decreasing values of the decay rate, ν (Figure 4.4). This means that a strain with resistance against a highly effective fungicide (with high values of q_σ, k_σ and a relatively low value of ν) would spread more quickly if the fungicide was applied, compared to a strain with resistance against a fungicide with lower efficacy. The greater the effect of a fungicide on the growth rate of the sensitive strain, the greater the maximum magnitude of the cumulative difference in growth rates between the resistant and sensitive strains when the fungicide is applied. More highly resistant strains (higher values of ζ_q or ζ_k) will also spread more quickly, as they have higher growth rates in the presence of a fungicide relative to the sensitive strain.

As noted in Section 4.3.2.4, either a 100% asymptote shift or 100% curvature shift leads to a strain that is completely resistant to the fungicide at any dose $D(t)$, and an identical value of s for a given combination of q_σ, k_σ and ν. For a given sensitivity shift percentage less than 100% (e.g. 50% or 90%), s is higher for an asymptote shift than for the same level of curvature shift, as the asymptote shift corresponds to a more highly resistant strain, leading to a greater cumulative difference in growth rates between the resistant and sensitive strain when fungicide is applied.

For partial and complete asymptote shifts, s was consistently higher for split dose applications than for single applications.
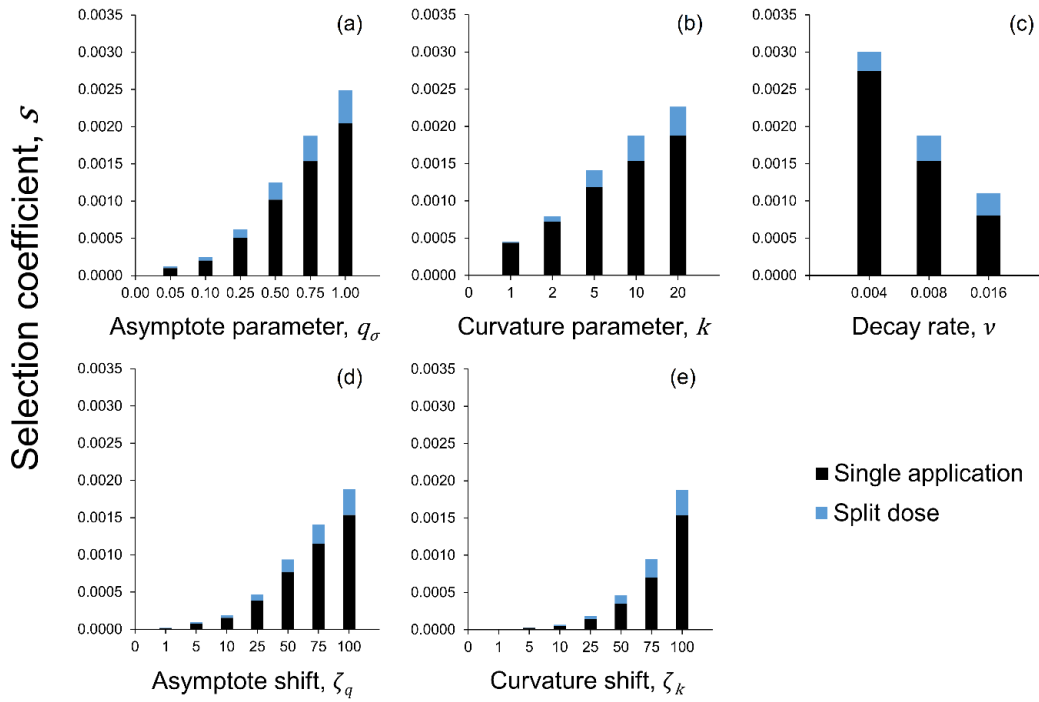
Figure 4.4: Effect of fungicide properties and resistance type on magnitude of selection for a resistant strain. Variation in selection coefficient, s with (a) asymptote parameter, q_σ; (b) curvature parameter, k; (c) decay rate, v; (d) asymptote shift, ζ_q; and (e) curvature shift, ζ_k. Only one parameter varied at a time: $v = 0.008\ t^{-1}$ for (a), (b), (d) and (e); $q_\sigma = 0.75$ for (b)–(e); $k_\sigma = 10$ for (a) and (c)–(e); $\zeta_q = 100\%$ for (a)–(c) and 0% for (e); $\zeta_k = 0\%$ for (a)–(d). s measures the magnitude of selection for a resistant strain.

4.4.2.2 Effect of dose splitting on selection for resistance, η

The values of the asymptote parameter, q_σ, and asymptote shift, ζ_q, have very little impact on the percentage change in the selection coefficient s (η in Equation 21) as a result of dose splitting (Figure 4.5). q_σ also has very little impact on η for a curvature shift (Figure 4.B.1, Appendix 4.B). This is because q_σ and ζ_q do not affect the length of time for which there is a difference in the level of control exerted by single and split dose applications. The curvature parameter, k_σ, and the decay rate, v, together control the value of η, in combination with the curvature shift, ζ_k, where relevant (Figure 4.6).
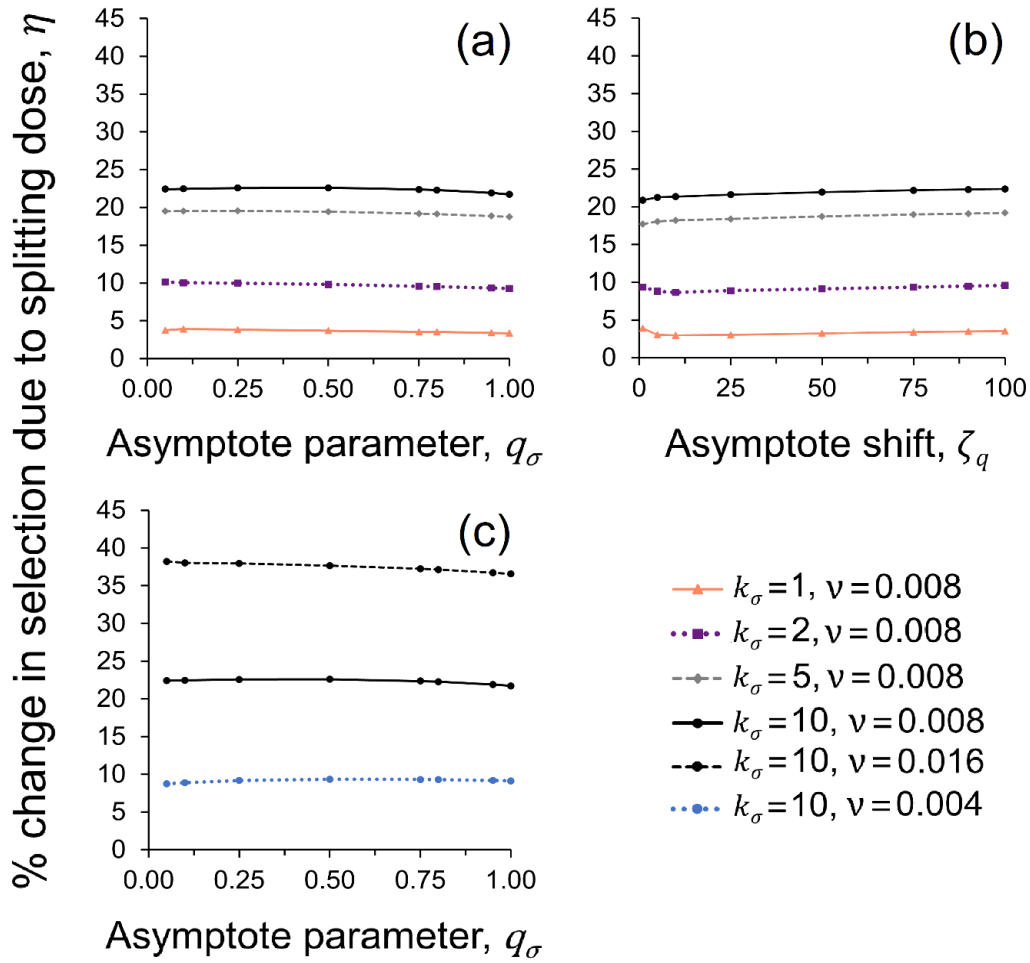
Figure 4.5: Negligible effect of asymptote parameter, q_σ, and asymptote shift, ζ_q on η, the percentage change in selection due to dose splitting. Variation in η with (a) q_σ and (b) ζ_q for $k_\sigma = 1$, 2, 5 and 10. (c) Variation in η with q_σ for decay rates $\nu = 0.004\ t^{-1}$, $0.008\ t^{-1}$ and $0.016\ t^{-1}$. η is measured as the percentage change in selection as a result of splitting a total fungicide dose D_{Total} over two applications of $0.5 D_{\text{Max}}$ at GS32 and GS39.
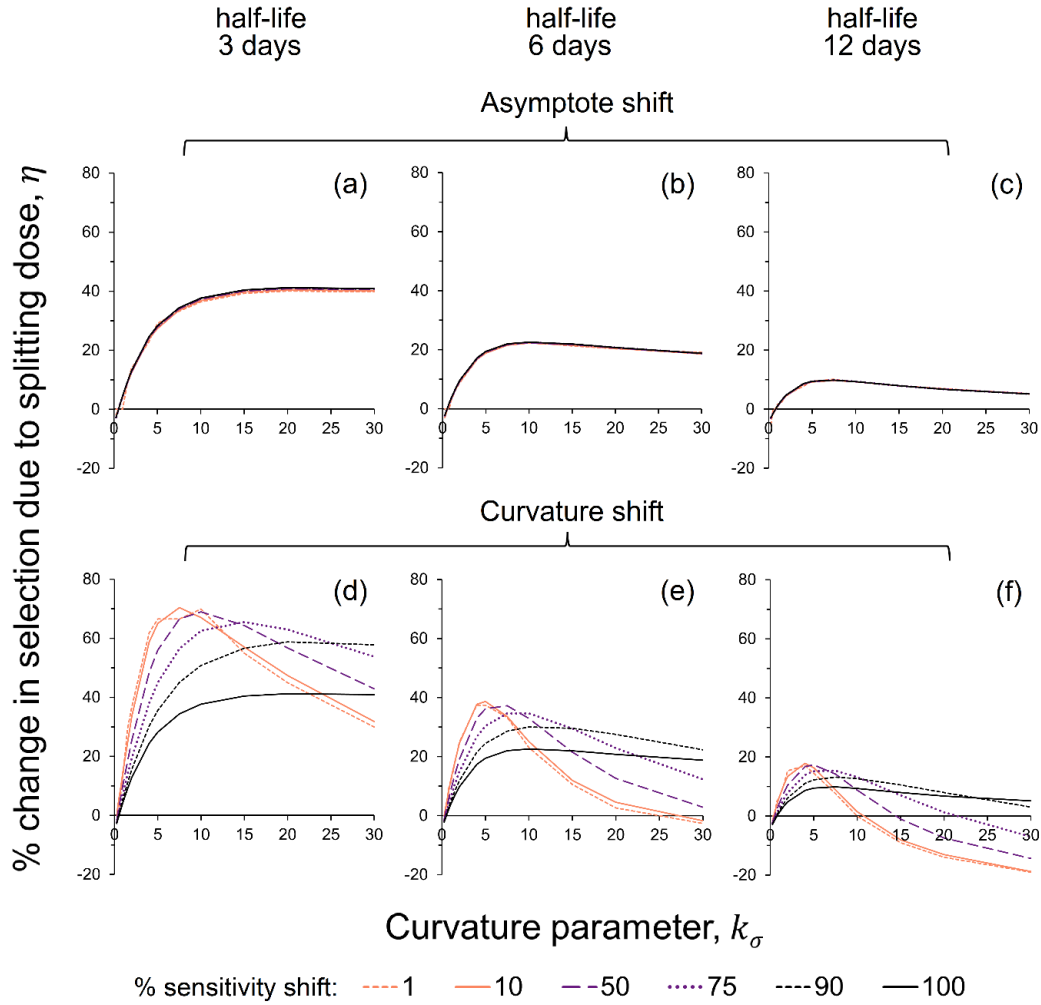
Figure 4.6: Percentage change in selection, η, as a result of dose splitting for a range of parameter values: curvature parameter, k_σ, decay rate, v, and levels of sensitivity shift, ζ_q and ζ_k. Dose splitting simulated as two applications of $0.5D_{\text{Max}}$ at GS32 and GS39, compared to a single application of D_{Max} at GS32. (a), (b) and (c) show the effect of k_σ on η for a resistant strain with an asymptote shift, ζ_q, for fungicide decay rates $v = 0.01605\ t^{-1}$, $v = 0.008\ t^{-1}$, and $v = 0.004\ t^{-1}$ respectively, corresponding to foliar half-lives of 3, 6 and 12 days respectively. (d), (e) and (f) show the effect of k_σ on η for a resistant strain with a curvature shift, ζ_k, for fungicide decay rates $v = 0.016\ t^{-1}$, $v = 0.008\ t^{-1}$, and $v = 0.004$ t^{-1} respectively. Results shown for asymptote parameter $q_\sigma = 0.5$; the effect of q_σ on η is very small (see Figure 4.5).

For any asymptote shift, dose splitting increased selection for resistance. The value of η for an asymptote shift varied from <5% to 40%, depending on the values of k_σ and v (Figure 4.6(a)-(c)). Our results suggest that splitting the dose

of a solo SDHI across two applications rather than making a single application at full dose rate could increase selection for a strain with an asymptote shift to the SDHI by approximately 20%.

For curvature shifts, η varied from -20% to 80% (Figure 4.6(d)-(f)), indicating that dose splitting can reduce selection for partially resistant strains in some cases, but in other cases it may lead to a large increase in selection for resistance, dependent on the values of k_σ, v and ζ_k. The value of η increased with the curvature parameter, k_σ, reaching an asymptote at high values of k_σ when the fungicide half-life was short (Figure 4.6(d)). For longer fungicide half-lives, the value of η initially increased with k_σ to a maximum, then decreased at very large values of k_σ (Figure 4.6(f)). For larger curvature shifts, ζ_k, the η-values approach the curves for asymptote shifts (Figure 4.6(a)-(c)). For smaller curvature shifts, ζ_k <50%, η initially increased with k_σ, to a maximum at approximately $5 \leq k_\sigma \leq 10$, and then decreased again for larger values of k_σ. For small curvature shifts, ζ_k, large curvature parameters, k_σ, and longer fungicide half-lives, η approached zero or even became negative. Our results suggest that dose splitting of a solo SDHI application would increase selection for a strain with a curvature shift to the SDHI by approximately 20-35%, with smaller curvature shifts falling towards the upper end of this range.

Dose splitting will increase selection for resistance if it leads to a larger difference in the growth rates of the sensitive strain and resistant strain for a longer time than a single application, i.e. if it increases the overall sum of the differences in fractional reduction, $\sum_{t=0}^{T} \left(f_\sigma(t) - f_\rho(t) \right)$. For an asymptote shift, the maximum difference in the growth rates of the sensitive strain and the resistant strain occurs at high fungicide doses, $D(t)$, for which the fractional reduction $f_\sigma(t)$ is close to the maximum (as defined by the asymptote q_σ) (Figure 4.1(c)). For a curvature shift, dose response curves for sensitive and resistant strains converge at high values of $D(t)$. The maximum difference in the fractional reduction and resulting growth rates of the sensitive strain and a resistant strain with a curvature shift occurs at intermediate fungicide dose $D(t)$ (Figure 4.1(d)). As discussed by Taylor & Cunniffe (2023b), the effect of dose-response convergence on selection must be considered not only at the applied dose, but across the full time span of fungicide decay. Dose splitting increases the length of time that the pathogen is exposed to intermediate fungicide doses, which

therefore increases $\sum_{t=0}^{T} \left(f_\sigma(t) - f_\rho(t) \right)$. The results in Figure 4.6 can be understood by considering how the values of k_σ, v and ζ_k affect the size and duration of the difference in the growth rates of the sensitive and resistant strain, for single and split dose applications.

Effect of decay rate, v

For both asymptote shifts and curvature shifts, η was higher for larger values of v (Figure 4.6). If the decay rate is high, the effect of a single application dissipates quickly, so a split dose application is likely to double the exposure time. If the decay rate is low, the effect of a single application at full dose rate will last for longer, so there is less difference in exposure time compared to the split dose application.

Why does η increase with k_σ for asymptote shifts?

For small values of the curvature parameter k_σ (approx. <4), the maximum reduction of the sensitive strain life cycle parameters is only achieved at a high fungicide dose, $D(t)$, and the fractional reduction reduces quickly as $D(t)$ decreases (Figure 4.B.2(a), Appendix 4.B). Therefore, the higher maximum dose applied in the single application initially achieves a much higher fractional reduction than the split dose application. Larger corresponding differences in the growth rates of the resistant and sensitive strain partially counterbalance the increased selection from the increased exposure time in the split dose application. The rate of selection from either a single or split dose application is therefore relatively similar for small values of k_σ, resulting in small values of η.

As k_σ increases, the fractional reduction remains close to the maximum fractional reduction even at lower fungicide doses ≤ 0.5 D_{Max}, so at lower values of $D(t)$, differences in the growth rates of the resistant and sensitive strain are similar to the difference at the full dose rate (Figure 4.B.2(b), Appendix 4.B). The effect of the increased exposure time from the split dose therefore dominates at higher values of k_σ, resulting in higher values of η.

Why does η exhibit a maximum vs. k_σ for asymptote shifts when v is low?

If k_σ is large and v is low, the effect of a single application persists close to the maximum fractional reduction for a long time (Figure 4.2(f); Figure 4.B.2(c), Appendix 4.B), which shifts the point at which there is a large difference in the fractional reduction from the single application and the split dose application later

in the season. Since canopy senescence begins to restrict the growth rates of both the resistant and sensitive strains later in the season, the value of η is reduced relative to the maximum at intermediate values of k_σ and lower values of ν. However, the effect of dose splitting may still be larger than for small values of k_σ.

Why does η increase with k_σ more for curvature shifts than for asymptote shifts?

As k_σ increases, the dose response curve for the sensitive strain becomes more steeply curved, resulting in a decrease in the fungicide dose $D(t)$ at which the difference $f_\sigma(t) - f_\rho(t)$ is maximised for a curvature shift. The larger the value of k_σ and the smaller the value of ζ_k, the lower the dose $D(t)$ at which the difference $f_\sigma(t) - f_\rho(t)$ is maximised (Figure 4.1; 4.B.2(d)-(f), Appendix 4.B), as resistant strains with a small curvature shift are still well controlled at high fungicide doses.

For very small values of k_σ, the maximum difference in growth rates occurs at higher values of $D(t) > 0.5D_{\mathrm{Max}}$, which may not be reached using a split dose application. The maximum difference in growth rates is reached by the higher dose rate of the single application, partially counterbalancing the increased exposure time from the split dose application. Therefore η is small for small values of k_σ for a curvature shift. For larger values of k_σ, the maximum difference in growth rates occurs at values of $D(t) < 0.5D_{\mathrm{Max}}$. A split dose application keeps $D(t)$ close to the level that maximises $f_\sigma(t) - f_\rho(t)$ for longer. In combination with the effect of increased exposure time, a split dose application increases selection more for strains with a curvature shift than for strains with an asymptote shift for intermediate values of k_σ.

Why does η become negative for small curvature shifts, large values of k_σ and small values of ν?

If k_σ is large and ζ_k is small, the maximum difference in growth rates occurs at very small values of $D(t) < 0.1D_{\mathrm{Max}}$ (Figure 4.B.2(f), Appendix 4.B). If the decay rate, ν, is also small, low values of $D(t)$ are not reached for a split dose application until late in the season, when canopy senescence restricts the growth rates of both the resistant and sensitive strains, leading to low or even negative values of η for large values of k_σ combined with small values of ν and small values of ζ_k.

It is important to note that our results do not suggest that there would be no selection for resistance in cases where η was close to 0 or even negative: on the

contrary, selection for resistance will usually be strong in cases with large values of k_σ and small values of ν (Figure 4.4), as resistance against a very effective fungicide gives a strong fitness advantage. However, in these cases dose splitting may have little effect on the strength of selection for resistance, or may even slightly decrease selection relative to a single application.

4.5 Discussion

Dose splitting is likely to increase selection for both target-site and non-target-site resistance. Our results suggest that the percentage increase in selection due to dose splitting, η, is likely to be particularly large for resistance mechanisms that cause a curvature shift, where the effect of the fungicide is reduced at lower concentrations but not at high concentrations. These mechanisms could include non-target-site resistance, target-site overexpression, and target-site mutations that affect fungicide competitive binding rates. Our results also support the hypothesis of van den Bosch et al. (2014a) that dose splitting will increase selection for target-site mutations that cause an asymptote shift.

We show that the effects of dose splitting can be very variable for both target-site and non-target-site resistance. The largest increases in selection due to dose splitting are likely to occur for fungicides with a steeply curved dose response curve (i.e. high values of k_σ) and a relatively short half-life (i.e. high values of the decay rate, ν). In these cases, dose splitting should be considered high-risk for both target-site and non-target-site resistance. Our analysis focused on dose splitting of a solo MoA, whereas resistance management guidelines recommend application in mixture with other MoA; mixture may reduce selection for resistance and change the measured effects of dose splitting (Young et al., 2021). Where use of mixture requires 'splitting and mixing' due to limited numbers of effective MoAs for use in disease control, careful choice of mixture partners will be needed for fungicides for which dose splitting is high-risk for resistance evolution.

We found a small range of parameter values – fungicides with a large curvature parameter and a low decay rate – for which dose splitting could reduce selection for a resistant strain with a small curvature shift. However, these parameter values are relatively unlikely for a commercial fungicide, unless a high level of persistence could be achieved without associated environmental toxicity that would prevent regulatory approval. We used SDHI fungicides as an example of a commercial

MoA currently available to growers. Our results suggest that dose splitting of an SDHI fungicide applied solo will increase selection for resistance by 20-35%.

Our results suggest that variability in fungicide decay rates between years and sites due to differing environmental conditions is likely to contribute to the variable selection for SDH-mutants observed in field experiments on dose splitting (Paveley et al. 2020; Young et al. 2021). We modelled the effect of a 4-fold change in fungicide half-life, which is well within the maximum range observed in field conditions (Fantke et al., 2014). Our results suggest that for a fungicide with $k_\sigma = 10$, the variation in decay rates could account for the variation in the percentage effect of dose splitting on selection, η, in the range 10-40% for an asymptote shift, or 0-70% for a curvature shift (Figures 4.6(b), 4.6(e)). The statistical power or field trials to detect the lower end of this range may be limited due to experimental noise, but our results confirm that dose splitting tends to increase selection for resistance.

There is a strong covariance between the fitted values of k_σ, q_σ, and ν for the SDHI fungicide, increasing uncertainty in the estimation of these parameters and the consequences of dose splitting. We also assumed that k_σ and q_σ were the same for the fractional reduction of the transmission rate and the rate of conversion from latent to infectious leaf tissue. Measures of fungicide foliar half-life for each trial, and laboratory investigation of the effects of different fungicide dose rates on life cycle parameters such as latent period, could provide valuable additional evidence to inform these parameter values.

In our study we assumed negligible fitness costs of fungicide resistance, which is often the case (Hawkins & Fraaije, 2018; Mikaberidze & McDonald, 2015). However, fitness costs may sometimes suppress the growth rate of the resistant strain to a level below the growth rate of the sensitive strain. This can occur in the absence of fungicide, at low fungicide doses for an asymptote shift (Mikaberidze et al., 2017), or at high fungicide doses for resistant strains with a small curvature shift. Fitness costs have been reported for some target-site and non-target-site mutations; conversely, resistant strains can also have increased virulence relative to wild-type strains (Dorigan et al., 2023).

We did not explicitly model polygenic resistance, where resistance is conferred by multiple genes and the degree of resistance can build up gradually over time as resistance mutations accumulate. At the population level, this process leads to a continuous distribution of resistance phenotypes across strains, with the average

levels of resistance increasing over time as selection for resistance continues (Shaw, 1989; Taylor & Cunniffe, 2023a). The difference between the dose response curves of partially-resistant strains may be analogous to a small curvature shift in our model, meaning that dose splitting could strongly increase the rate of selection for polygenic resistance.

The variable effect of dose splitting complicates management of resistance evolving 'concurrently' to two or more MoA at the same time. Use of mixtures may require splitting the total dose of a fungicide across two or more applications, due to a limited number of MoA available. The balance between the effects of mixture and dose splitting on selection for resistance will change depending on fungicide properties and resistance type and strength, and the optimal strategy to slow evolution of resistance to one fungicide may not be the optimal strategy for another fungicide. The efficacy of the fungicide programme also needs to be considered and, where relevant, the effects of sexual reproduction of the pathogen.

Previous modelling studies found that if it is necessary to combine two high-risk fungicides in a programme, mixture rather than alternation or concurrent use will generally present the best strategy to maximise the length of time that effective disease control can be maintained (Elderfield, 2018; Hobbelen et al., 2013). However, Eldferfield (2018) found that alternation may be a better strategy against strains with a small curvature shift. Experimental evolution *in vitro* on sensitive isolates of *Z. tritici* using mixtures of high-risk fungicides showed that the success of mixture in delaying resistance depended strongly on the mixture components, and some reduced-dose mixtures selected for generalist, multi-drug resistance (Ballu et al., 2021). These results may be explained by our finding that dose splitting increases selection more for strains with a small curvature shift – representative of non-target-site resistance – than for strains with an asymptote shift.

Since the balance between the effects of mixture and dose splitting on selection for resistance will differ for asymptote and curvature shifts, this could introduce trade-offs between tactics to reduce selection for large, target-site, asymptote shifts and alternative tactics to limit incrementally increasing levels of resistance due to mechanisms that cause a curvature shift. These trade-offs appear to occur in weed management, where use of herbicide mixtures is associated with lower prevalence of target-site resistance, but higher prevalence of metabolic resistance (Comont et al., 2020). Fungicide resistance management strategies have tended

to focus on large asymptote shifts associated with target-site mutations, as these can lead to a rapid loss of fungicide efficacy, for example as experienced in QoI fungicides for multiple pathogens (Grimmer et al., 2015). Due to their large effects, target-site mutations that result in an asymptote shift are more likely to be quickly identified and studied than individual non-target-site resistance mechanisms which may be overlooked due to the small effects of each gene (Hu and Chen, 2021). However, in combination with target-site resistance, non-target-site mechanisms may contribute to highly resistant MDR strains (Omrane et al., 2017). Synergistic interactions between resistance mechanisms could enhance the overall impact of non-target site resistance: for example, increased efflux reduces the cellular fungicide concentration and could therefore increase the effect of a target-site mutation that causes a partial curvature shift. Wherever possible, tactics should be chosen for their effectiveness against both target-site and non-target-site resistance.

4.6   Supporting Information

Appendix 4.A: Further details on model parameterisation
Appendix 4.B: Further details on model results

4.7   Acknowledgements

4.8   Data availability statement

Dataset 1: Data sharing is not applicable to this dataset as no new data were created or analysed in this study.

Dataset 2: These data are available from the Agriculture and Horticulture Development Board (AHDB). Restrictions apply to the availability of these data, which were used under license for this study. A summarized version of the data used is available at https://ahdb.org.uk/knowledge-library/a-guide-to-fungicide-performance-in-wheat-barley-and-oilseed-rape, and in Appendix 4.A (Figure 4.A.5).

4.9 References

AHDB (2024a) A guide to fungicide performance in wheat, barley and oilseed rape. Available at: https://ahdb.org.uk/knowledge-library/a-guide-to-fungicide-performance-in-wheat-barley-and-oilseed-rape [Accessed: 1 August 2024].

AHDB (2024b) Recommended Lists disease ratings. Available at: https://ahdb.org.uk/recommended-lists-disease-ratings [Accessed: 1 August 2024].

Ballu, A., Deredec, A., Walker, A.-S., & Carpentier, F. (2021) Are Efficient-Dose Mixtures a Solution to Reduce Fungicide Load and Delay Evolution of Resistance? An Experimental Evolutionary Approach. *Microorganisms* 9, 2324. https://doi.org/10.3390/microorganisms9112324

Blake, J.J., Gosling, P., Fraaije, B.A., Burnett, F.J., Knight, S.M., Kildea, S. et al. (2018) Changes in field dose–response curves for demethylation inhibitor (DMI) and quinone outside inhibitor (QoI) fungicides against *Zymoseptoria tritici*, related to laboratory sensitivity phenotyping and genotyping assays. *Pest Management Science* 74, 302–313. https://doi.org/10.1002/ps.4725

Boixel, A.-L. (2020). Environmental heterogeneity, a driver of adaptation to temperature in foliar plant pathogen populations? PhD Thesis. Université Paris-Saclay. Available at: https://pastel.hal.science/tel-03202132/document [Accessed: 1 August 2024].

Comont, D., Lowe, C., Hull, R., Crook, L., Hicks, H.L., Onkokesung, N., et al. (2020) Evolution of generalist resistance to herbicide mixtures reveals a trade-off in resistance management. *Nature Communications* 11, 3086. https://doi.org/10.1038/s41467-020-16896-0

Cools, H.J. & Fraaije, B.A. (2013) Update on mechanisms of azole resistance in *Mycosphaerella graminicola* and implications for future control. *Pest Management Science* 69, 150–155. https://doi.org/10.1002/ps.3348

Corkley, I., Fraaije, B. & Hawkins, N. (2022) Fungicide resistance management: Maximizing the effective life of plant protection products. *Plant Pathology* 71, 150-169. https://doi.org/10.1111/ppa.13467

Dooley, H., Shaw, M.W., Mehenni-Ciz, J., Spink, J. & Kildea, S. (2016) Detection of *Zymoseptoria tritici* SDHI-insensitive field isolates carrying the *SdhC* -H152R and *SdhD* -R47W substitutions. *Pest Management Science* 72, 2203–2207. https://doi.org/10.1002/ps.4269

Dorigan, A.F., Moreira, S.I., da Silva Costa Guimarães, S., Cruz-Magalhães, V. & Alves, E. (2023) Target and non-target site mechanisms of fungicide

resistance and their implications for the management of crop pathogens. *Pest Management Science* 79, 4731–4753. https://doi.org/10.1002/ps.7726

Elderfield, J.A.D. (2018) Using epidemiological principles and mathematical models to understand fungicide resistance evolution. PhD thesis, University of Cambridge. https://doi.org/10.17863/CAM.22236

Elderfield, J.A.D., Lopez-Ruiz, F.J., van den Bosch, F. & Cunniffe, N.J. (2018) Using Epidemiological Principles to Explain Fungicide Resistance Management Tactics: Why do Mixtures Outperform Alternations? *Phytopathology* 108, 803–817. https://doi.org/10.1094/PHYTO-08-17-0277-R

Eyal, Z. (1971) The kinetics of pycnospore liberation in *Septoria tritici*. *Canadian Journal of Botany* 49, 1095–1099. https://doi.org/10.1139/b71-157

Fantke, P., Gillespie, B.W., Juraske, R. & Jolliet, O. (2014). Estimating Half-Lives for Pesticide Dissipation from Plants. *Environmental Science & Technology* 48, 8588–8602. https://doi.org/10.1021/es500434p

Fones, H. & Gurr, S. (2015). The impact of Septoria tritici Blotch disease on wheat: An EU perspective. *Fungal Genetics and Biology* 79, 3–7. https://doi.org/10.1016/j.fgb.2015.04.004

Grimmer, M.K., van den Bosch, F., Powers, S.J. & Paveley, N.D. (2015) Fungicide resistance risk assessment based on traits associated with the rate of pathogen evolution. *Pest Management Science* 71, 207–215. https://doi.org/10.1002/ps.3781

Hargrove, T.Y., Wawrzak, Z., Lamb, D.C., Guengerich, F.P. & Lepesheva, G.I. (2015) Structure-Functional Characterization of Cytochrome P450 Sterol 14α-Demethylase (CYP51B) from Aspergillus fumigatus and Molecular Basis for the Development of Antifungal Drugs. *Journal of Biological Chemistry* 290, 23916–23934. https://doi.org/10.1074/jbc.M115.677310

Hawkins, N.J. & Fraaije, B.A. (2021) Contrasting levels of genetic predictability in the evolution of resistance to major classes of fungicides. *Molecular Ecology* 30, 5318–5327. https://doi.org/10.1111/mec.15877

Hawkins, N. J. & Fraaije, B. A. (2018). Fitness Penalties in the Evolution of Fungicide Resistance. *Annual Review of Phytopathology*, 56(1), 339–360. https://doi.org/10.1146/annurev-phyto-080417-050012

He, M., Jia, C., Zhao, E., Chen, L., Yu, P., Jing, J. et al. (2016) Concentrations and dissipation of difenoconazole and fluxapyroxad residues in apples and soil, determined by ultrahigh-performance liquid chromatography electrospray ionization tandem mass spectrometry. *Environmental Science and Pollution Research* 23, 5618–5626. https://doi.org/10.1007/s11356-015-5750-6

Hobbelen, P.H.F., Paveley, N.D., Fraaije, B.A., Lucas, J.A. & van den Bosch, F. (2011a) Derivation and testing of a model to predict selection for fungicide resistance. *Plant Pathology* 60, 304–313. https://doi.org/10.1111/j.1365-3059.2010.02380.x

Hobbelen, P.H.F., Paveley, N.D., Oliver, R.P. & van den Bosch, F. (2013). The Usefulness of Fungicide Mixtures and Alternation for Delaying the Selection for Resistance in Populations of *Mycosphaerella graminicola* on Winter Wheat: A Modeling Analysis. *Phytopathology* 103, 690–707. https://doi.org/10.1094/PHYTO-06-12-0142-R

Hobbelen, P.H.F., Paveley, N.D. & van den Bosch, F. (2011b). Delaying selection for fungicide insensitivity by mixing fungicides at a low and high risk of resistance development: A modeling analysis. *Phytopathology* 101, 1224–1233. https://doi.org/10.1094/PHYTO-10-10-0290

Hu, M. & Chen, S. (2021) Non-Target Site Mechanisms of Fungicide Resistance in Crop Pathogens: A Review. *Microorganisms* 9, 502. https://doi.org/10.3390/microorganisms9030502

Huf, A., Rehfus, A., Lorenz, K.H., Bryson, R., Voegele, R.T. & Stammler, G. (2018) Proposal for a new nomenclature for *CYP51* haplotypes in *Zymoseptoria tritici* and analysis of their distribution in Europe. *Plant Pathology* 67, 1706–1712. https://doi.org/10.1111/ppa.12891

Kema, G.H.J., Yu, D., Rijkenberg, F.H.J., Shaw, M.W. & Baayen, R.P. (1996) Histology of the Pathogenesis of *Mycosphaerella graminicola* in Wheat. *Phytopathology* 86, 777. https://doi.org/10.1094/Phyto-86-777

Kretschmer, M., Leroch, M., Mosbach, A., Walker, A.-S., Fillinger, S., Mernke, D. et al. (2009) Fungicide-Driven Evolution and Molecular Basis of Multidrug Resistance in Field Populations of the Grey Mould Fungus Botrytis cinerea. *PLoS Pathogens* 5, e1000696. https://doi.org/10.1371/journal.ppat.1000696

Leroux, P. & Walker, A. (2011) Multiple mechanisms account for resistance to sterol 14α-demethylation inhibitors in field isolates of *Mycosphaerella graminicola*. *Pest Management Science* 67, 44–59. https://doi.org/10.1002/ps.2028

McDonald, B.A., Suffert, F., Bernasconi, A. & Mikaberidze, A. (2022) How large and diverse are field populations of fungal plant pathogens? The case of *Zymoseptoria tritici*. *Evolutionary Applications* 15, 1360–1373. https://doi.org/10.1111/eva.13434

Mikaberidze A. & McDonald, B. A. (2015) Fitness cost of fungicide resistance - impact on management. Invited chapter in the book "Fungicide Resistance in

Plant Pathogens: Principles and a Guide to Practical Management", p. 77-89, Springer Japan, eds. Hideo Ishii & Derek Hollomon. https://doi.org/10.1007/978-4-431-55642-8 6.

Mikaberidze, A., Paveley, N., Bonhoeffer, S. & van den Bosch, F. (2017) Emergence of Resistance to Fungicides: The Role of Fungicide Dose. *Phytopathology* 107, 545–560. https://doi.org/10.1094/PHYTO-08-16-0297-R

Milgroom, M.G. & Fry, W.E. (1988) A Simulation Analysis of the Epidemiological Principles for Fungicide Resistance Management in Pathogen Populations. *Phytopathology* 78, 565. https://doi.org/10.1094/Phyto-78-565

Milne, A., Paveley, N., Audsley, E. & Livermore, P. (2003) A wheat canopy model for use in disease management decision support systems. *Annals of Applied Biology* 143, 265–274. https://doi.org/10.1111/j.1744-7348.2003.tb00294.x

Noh, H.H., Lee, J.Y., Park, H.K., Lee, J.W., Jo, S.H., Lim, J.B. et al. (2019) Dissipation, persistence, and risk assessment of fluxapyroxad and penthiopyrad residues in perilla leaf (Perilla frutescens var. japonica Hara). *PLoS One* 14, e0212209. https://doi.org/10.1371/journal.pone.0212209

Omrane, S., Audéon, C., Ignace, A., Duplaix, C., Aouini, L., Kema, G., et al. (2017) Plasticity of the *MFS1* Promoter Leads to Multidrug Resistance in the Wheat Pathogen *Zymoseptoria tritici*. *mSphere* 2: 10.1128/msphere.00393-17. https://doi.org/10.1128/mSphere.00393-17

Parker, S.R., Welham, S., Paveley, N.D., Foulkes, J. & Scott, R.K. (2004) Tolerance of septoria leaf blotch in winter wheat. *Plant Pathology* 53, 1–10. https://doi.org/10.1111/j.1365-3059.2004.00951.x

Patry-Leclaire, S., Neau, E., Pitarch, A., Walker, A.-S. & Fillinger, S. (2023) Plasticity of the MFS1 promotor is not the only driver of Multidrug resistance in Zymoseptoria tritici. *bioRxiv* 2023.12.27.573052. https://doi.org/10.1101/2023.12.27.573052

Paveley, N., Fraaije, B., van den Bosch, F., Kildea, S., Burnett, F., Clark, W. et al. (2020) Managing resistance evolving concurrently against two modes of action. In: Diesing HB; Fraaije B; Mehl A; Oerke EC; Sierotzki H; Stammler G (Eds), "Modern Fungicides and Antifungal Compounds", Vol. IX, pp.141-146. Deutsche Phytomedizinische Gesellschaft, Branschweig, ISBN: 978-3-941261-16-7.

Ponomarenko, A., Goodwin, S.B. & Kema, G.H.J. (2011) Septoria tritici blotch (STB) of wheat. Plant Health Instructor. https://doi.org/10.1094/PHI-I-2011-0407-01

Rehfus, A., Strobel, D., Bryson, R. & Stammler, G. (2018) Mutations in *sdh* genes in field isolates of *Zymoseptoria tritici* and impact on the sensitivity to various succinate dehydrogenase inhibitors. *Plant Pathology* 67, 175–180. https://doi.org/10.1111/ppa.12715

Shaw, M.W. (1990) Effects of temperature, leaf wetness and cultivar on the latent period of *Mycosphaerella graminicola* on winter wheat. *Plant Pathology* 39, 255–268. https://doi.org/10.1111/j.1365-3059.1990.tb02501.x

Shaw, M.W. (1989) A model of the evolution of polygenically controlled fungicide resistance. *Plant Pathology* 38, 44–55. https://doi.org/10.1111/j.1365-3059.1989.tb01426.x

Shaw, M.W. & Royle, D.J. (1989). Estimation and validation of a function describing the rate at which *Mycosphaerella graminicola* causes yield loss in winter wheat. *Annals of Applied Biology* 115, 425–442. https://doi.org/10.1111/j.1744-7348.1989.tb06562.x

Suffert, F., Sache, I. & Lannou, C. (2013). Assessment of quantitative traits of aggressiveness in *Mycosphaerella graminicola* on adult wheat plants. *Plant Pathology* 62, 1330–1341. https://doi.org/10.1111/ppa.12050

Suffert, F., Sache, I. & Lannou, C. (2011). Early stages of septoria tritici blotch epidemics of winter wheat: build-up, overseasoning, and release of primary inoculum. *Plant Pathology* 60, 166–177. https://doi.org/10.1111/j.1365-3059.2010.02369.x

Taylor, N.P. & Cunniffe, N.J. (2023a). Modelling quantitative fungicide resistance and breakdown of resistant cultivars: Designing integrated disease management strategies for Septoria of winter wheat. *PLoS Computational Biology* 19, e1010969. https://doi.org/10.1371/journal.pcbi.1010969

Taylor, N.P. & Cunniffe, N.J. (2023b). Coupling machine learning and epidemiological modelling to characterise optimal fungicide doses when fungicide resistance is partial or quantitative. *Journal of the Royal Society Interface* 20: 20220685 https://doi.org/10.1098/rsif.2022.0685

te Beest, D.E., Shaw, M.W., Pietravalle, S. & van den Bosch, F. (2009) A predictive model for early-warning of Septoria leaf blotch on winter wheat. *European Journal of Plant Pathology* 124, 413–425. https://doi.org/10.1007/s10658-009-9428-0

The MathWorks Inc. (2022) MATLAB version: 9.13.0 (R2022b), Natick, Massachusetts: The MathWorks Inc. https://www.mathworks.com

Torriani, S.F., Brunner, P.C., McDonald, B.A. & Sierotzki, H. (2009) QoI resistance emerged independently at least 4 times in European populations of

Mycosphaerella graminicola. *Pest Management Science* 65, 155–162. https://doi.org/10.1002/ps.1662

van den Berg, F., Paveley, N.D. & van den Bosch, F. (2016) Dose and number of applications that maximize fungicide effective life exemplified by *Zymoseptoria tritici* on wheat – a model analysis. *Plant Pathology* 65, 1380–1389. https://doi.org/10.1111/ppa.12558

van den Berg, F., van den Bosch, F. & Paveley, N.D. (2013). Optimal Fungicide Application Timings for Disease Control Are Also an Effective Anti-Resistance Strategy: A Case Study for *Zymoseptoria tritici* (*Mycosphaerella graminicola*) on Wheat. *Phytopathology* 103, 1209–1219. https://doi.org/10.1094/PHYTO-03-13-0061-R

van den Bosch, F., Oliver, R., van den Berg, F. & Paveley, N. (2014a) Governing Principles Can Guide Fungicide-Resistance Management Tactics. *Annual Review of Phytopathology* 52, 175–195. https://doi.org/10.1146/annurev-phyto-102313-050158

van den Bosch, F., Paveley, N., van den Berg, F., Hobbelen, P. & Oliver, R. (2014b) Mixtures as a Fungicide Resistance Management Tactic. *Phytopathology* 104, 1264–1273. https://doi.org/10.1094/PHYTO-04-14-0121-RVW

Weir, A.H., Bragg, P.L., Porter, J.R. & Rayner, J.H. (1984) A winter wheat crop simulation model without water or nutrient limitations. *The Journal of Agricultural Science* 102, 371–382.
https://doi.org/10.1017/S0021859600042702

Wollenberg, R.D., Donau, S.S., Taft, M.H., Balázs, Z., Giese, S., Thiel, C. et al. (2020) Undefeated—Changing the phenamacril scaffold is not enough to beat resistant Fusarium. *PLoS One* 15, e0235568.
https://doi.org/10.1371/journal.pone.0235568

Young, C., Boor, T., Corkley, I., Fraaije, B., Clark, B., Havis, N. et al. (2021) Managing resistance evolving concurrently against two or more modes of action to extend the effective life of fungicides. AHDB Project Report No. 637, pp 1–91. Available at:
https://projectblue.blob.core.windows.net/media/Default/Research%20Papers/Cereals%20and%20Oilseed/2021/PR637%20final%20project%20report.pdf [Accessed: 1 August 2024].

Zadoks, J.C., Chang, T.T. & Konzak, C.F. (1974) A decimal code for the growth stages of cereals. *Weed Research* 14, 415–421.
https://doi.org/10.1111/j.1365-3180.1974.tb01084.x

Chapter 5

Which resistance management strategies work against concurrent evolution of resistance to fungicides?

I. Corkley[1,2,3], A. Mikaberidze[2], F. van den Bosch[4,5], N.D. Paveley[6], A.E. Milne[1]

[1]Net Zero and Resilient Farming, Rothamsted Research, Harpenden, UK. [2]School of Agriculture, Policy and Development, University of Reading, Reading, UK. [3]Sustainable Agricultural Systems, ADAS, Wolverhampton, UK. [4]Quantitative Biology & Epidemiology Group, Plant Pathology Department (Visiting Scholar), University of California, Davis, USA. [5]Sustainable Agricultural Systems, ADAS, Rosemaund, UK. [6]Sustainable Agricultural Systems, ADAS, High Mowthorpe, UK.

The results in Chapter 4 showed that the effect of dose-splitting of a single mode of action ('MoA') without a mixture partner varied with fungicide properties and the type and magnitude of resistance. In general, dose-splitting increased selection for both asymptote shift and curvature shift types of resistance. These results provide insight into one key trade-off that will influence the balance between alternation or 'splitting and mixing' strategies for resistance management. I define 'splitting and mixing' as dose-splitting of the total dose of each of two MoA over multiple applications, enabling application of the MoA in mixture with one another at each application timing (the analysis presented in this chapter assumes a maximum of two applications). Alternation is defined as using one solo application of each MoA at the same total dose rate (the maximum permitted individual dose).

A potential resistance management benefit of splitting and mixing is that using another MoA as a mixture partner can improve control of strains with resistance to a single MoA ('single-resistant strains'), reducing the difference in growth rates between sensitive and resistant strains. This may therefore counterbalance the increase in selection from dose-splitting described in Chapter 4. In this chapter, I consider mixtures of two fungicides, 'A' and 'B', with different MoAs.

However, if resistance is evolving to both MoAs at the same time, there is the potential for selection for double-resistant strains that have reduced sensitivity to both MoAs. A double-resistant strain may have particularly high fitness against

155

mixtures of the two MoAs, relative to single-resistant strains and sensitive strains, but alternation may also select for double-resistant strains (Ballu et al., 2024). Sexual reproduction can generate double-resistant strains through sexual recombination of single-resistant strains with resistance to fungicide A and fungicide B respectively. If fungicide programmes select for both single-resistant strains, this will therefore also increase the rate at which the frequency of double-resistant strains increases. It is not clear whether alternation or splitting and mixing is a better strategy to minimise increases in the frequency of the double-resistant strain.

In this chapter, I adapt the model described in Chapter 4 to simulate alternation and 'splitting and mixing' programmes of two MoAs, 'A' and 'B', to which resistance is evolving concurrently. The model tracks changes in the frequency of sensitive, single-resistant and double-resistant strains, including the effects of sexual reproduction at the end of the growing season. Following the results of Chapter 4, I simulated a wide area of parameter space of fungicide efficacy and persistence (asymptote, curvature and decay rate parameters) and different magnitudes of asymptote shift or curvature shift to each MoA.

5.1   Abstract

The best strategies for managing resistance evolving 'concurrently' to two or more MoA at the same time are unclear, due to complex trade-offs. For crop pathogens such as *Zymoseptoria tritici*, multiple fungicide applications per year are often required to keep infection below damaging levels of severity, whilst the number of MoA available for disease control is increasingly limited by regulation and existing resistance. Use of mixtures may therefore require splitting the total dose of a fungicide across two or more applications, reducing the dose of each MoA per application but increasing the exposure time of the pathogen to the fungicide. We used a model of the effect of fungicides on *Z. tritici* infection of the upper leaves of winter wheat crops to explore the effect of varying fungicide properties and the magnitude and type of resistance on the rate of selection for double-resistant strains when two at-risk MoA are either mixed (with dose-splitting) or alternated (without dose-splitting). We compared results for 'asymptote shifts', where the maximum effect of the fungicide is reduced even at high fungicide concentrations (e.g. some target-site resistance), and 'curvature shifts', where efficacy is reduced only at lower fungicide concentrations (e.g. non-target-site resistance). We show that whether 'splitting or mixing' or alternation is the better strategy depends on

fungicide efficacy and decay rate and the type and magnitude of resistance. Splitting and mixing the total dose of two at-risk fungicides is most likely to be beneficial against strains with an asymptote shift, or in cases where both fungicides have strong efficacy and a high decay rate; alternation is more likely to minimise selection for strains with a curvature shift, or in cases where both fungicides are weakly or moderately effective.

5.2   Introduction

Fungicidal modes of action (MoA) with a single pathogen target site ('single-site fungicides') are at a high-risk of target-site resistance, as a single point mutation can produce pathogen strains with large resistance factors (Hollomon & Brent, 2009). Modelling and experimental evidence suggests that resistance development can be slowed by applying at-risk fungicides in mixture with a fungicide with a different MoA that the resistant strains are sensitive to: this reduces the fitness advantage of resistant strains (van den Bosch et al., 2014a, 2014b). Mixing high-risk MoAs with lower-risk (multi-site) MoAs has been recommended as an effective resistance management strategy, supported by both modelling and experimental evidence (Hobbelen et al., 2011; van den Bosch, Oliver, et al., 2014; van den Bosch, Paveley, et al., 2014). Multi-site fungicides target multiple aspects of the pathogen biology, so a single mutation is unlikely to have a large effect on growth rate and they are at lower-risk from resistance evolution, but these fungicides often lack curative action against established infections and may not be sufficiently effective on their own to maintain disease control throughout the season without the inclusion of a systemic high-risk MoA in the fungicide programme (Deising et al., 2008; van den Berg et al., 2013). However, the use of multi-site fungicides is increasingly restricted by regulation, affecting both major and minor crops. This limits options to use multi-site MoAs in mixture with high-risk MoAs as a resistance management tactic.

Strains with fungicide resistance against two or more single-site MoAs have been observed in several fungal pathogens including *Botrytis cinerea* (the cause of grey mould in multiple crops), *Cercospora beticola* (the cause of Cercospora leaf spot in sugar beet), *Venturia inaequalis* (apple scab), *Phakopsora pachyrhizi* (Asian soybean rust) and *Zymoseptoria tritici* (the causal pathogen of septoria tritici blotch (STB)) (Chapman et al., 2011; Chatzidimopoulos et al., 2022; Garnault et al., 2019; Müller et al., 2021; Omrane et al., 2017; Rupp et al., 2017; Trkulja et al., 2017). Evidence is needed for resistance management strategies for cases where low-

risk fungicides are not available and resistance is evolving concurrently to two or more MoA: what is the best way to combine two high-risk MoA in a fungicide programme?

Concurrent evolution of resistance introduces complex trade-offs for resistance management. The best strategy for one MoA may not represent the optimal strategy for a second MoA. In field trials, mixtures of a demethylation inhibitor (DMI) fungicide and a succinate dehydrogenase inhibitor (SDHI) fungicide reduced selection for resistance against the DMI fungicide, but selection for the SDHI fungicide was not reduced by mixture with the DMI fungicide (Dooley et al., 2016b). One modelling study comparing mixture and alternation tactics against complete resistance evolving to two high-risk fungicides found that the optimal tactic varied depending on the relative effectiveness and doses of the two fungicides (Elderfield, 2018); whilst another study which accounted for the effect of sexual reproduction found that mixtures would outperform alternation in the case of complete resistance (Taylor & Cunniffe, 2023). Another modelling study predicted that mixture tactics would outperform alternation across a range of scenarios of complete and partial resistance and varying fungicide efficacy (Hobbelen et al., 2013). However, in experimental evolution *in vitro,* both mixture and alternation only delayed resistance for some MoA combinations, and in some cases increased selection for generalist, multi-drug resistance (Ballu et al., 2021, 2023). It is therefore important to understand how fungicide and system properties may determine whether mixture of at-risk fungicides is a good strategy for resistance management.

Zymoseptoria tritici, one of the most common, widespread and damaging pathogens affecting winter wheat crops in the UK, Ireland and Europe (Fones & Gurr, 2015), is an important example of a fungal pathogen in which concurrent evolution of resistance to multiple MoAs is a current and increasing challenge for disease control. In most years in the UK, multiple fungicide applications are required to keep *Z. tritici* below damaging levels of severity, so use of mixture would require splitting the total dose of a fungicide across two or more applications: a 'splitting and mixing' tactic. Dose-splitting reduces the dose of each MoA per application but increases the exposure time of the pathogen to the fungicide, with counteracting effects on selection (van den Bosch et al., 2014a). The results presented in Chapter 4 (Corkley et al., 2025a) showed that dose splitting of a solo fungicide is likely to increase selection for both target-site and non-target-site resistance, but the increase in selection varies depending on fungicide dose

response properties and foliar half-life, and the type and magnitude of resistance. The effect of a mixture partner on sensitive and resistant strain growth rates will also vary with the same parameters. In which cases will the benefits of mixture outweigh the disadvantages of dose splitting?

The model described in Chapter 4 (Corkley et al., 2025a) represents the effect of fungicides on the *per capita* growth rate of sensitive and resistant pathogen strains through parameters defining the effect of the fungicide on important aspects of the pathogen life cycle, such as a reduction in pathogen transmission rate. The fungicide dose response is defined by a combination of an 'asymptote parameter', the maximum effect on the life cycle parameter at high fungicide doses, the 'curvature parameter', the rate at which this effect decreases with reducing fungicide dose, and the foliar dissipation half-life of the fungicide. The sensitivity shift as a result of the impact of resistance mutations on the fungicide dose response is represented by a reduction in either the asymptote parameter ('asymptote shift') or the curvature parameter ('curvature shift'); in Chapter 4 (Corkley et al., 2025a) we argue that an asymptote shift can be considered as broadly representative of target-site mutation that reduces the maximum effect at any dose rate of fungicides which bind allosterically and non-competitively to an enzyme. A partial curvature shift is broadly representative of target-site resistance to competitive inhibitors causing a partial reduction in binding affinity, target-site overexpression and non-target-site resistance mechanisms.

Within a single season and crop, *Z. tritici* epidemics increase primarily through asexual reproduction and the production of pycnidiospores (Eriksen & Munk, 2003), with overlapping generations consistently reproducing the same allele combinations and resistance phenotype. Sexual reproduction in *Z. tritici* occurs predominantly towards the end of the growing season, producing ascospores that disperse and infect the next season's wheat crop (Eriksen & Munk, 2003; Hunter et al., 1999; Shaw & Royle, 1989; Suffert et al., 2019). Sexual reproduction will produce new combinations of resistance alleles through reassortment and crossing over, potentially producing new multi-fungicide resistant pathogen strains or boosting the frequency of rarer strains (Chen & McDonald, 1996; Zhan et al., 2003). This is particularly relevant for concurrent evolution of resistance to two or more MoA, as the relevant alleles conferring resistance are more likely to be on separate chromosomes, or at a sufficient distance apart on the same chromosome that crossing over is likely (Lobo and Shaw, 2008; Morgan, 1911).

We extended the model described in Chapter 4 (Corkley et al., 2025a) to include sexual reproduction at the end of the growing season and to track four *Z. tritici* strains defined by their sensitivity to two fungicides 'A' and 'B': a strain sensitive to both fungicides, strains sensitive to only one fungicide ('A' and 'B' respectively) and a double-resistant strain. We used the model to investigate in which cases 'splitting and mixing' is a good or poor resistance management strategy compared to alternation (solo) at full label dose, when there is concurrent evolution of resistance. Each option introduces trade-offs, and so could either increase or reduce selection (Chapter 1 – Figure 1.4). To constrain the number of treatment combinations, we restricted our analysis to a fixed total dose of the maximum permitted individual dose for a single application for each fungicide 'A' and 'B': dose rates are partially determined by control requirements for pathogens other than *Z. tritici*. We compared the rate of selection for the double-resistant strain and the rate of erosion of disease control for each programme over a large range of foliar dissipation half-lives, asymptote and curvature parameter values and sensitivity shifts (asymptote and curvature), including parameter values representative of the activity of SDHI fungicides against *Z. tritici*. We considered the following cases of concurrent resistance evolution: (a) varying levels of asymptote shift to both fungicides 'A' and 'B'. (b) varying levels of curvature shift to both fungicides 'A' and 'B'. (c) varying levels of asymptote shift to fungicide 'A' and varying levels of curvature shift to fungicide 'B'.

5.3 Materials and Methods

5.3.1 Model of *Zymoseptoria tritici* life cycle

We used the model and parameter values described in Chapter 4 (Corkley et al., 2025a). The compartmental epidemiological model tracks the growth and senescence of the leaf area index (LAI) of the top three leaves of a wheat canopy, infection of healthy leaf area by haploid pycnidiospores, the progress of the disease through latent and infectious (sporulating) periods, and the increase in severity of the polycyclic epidemic over time. The latent and infectious areas of each pathogen strain are tracked throughout the period simulated by the model. We extended the model to track four pathogen strains defined by their sensitivity to two fungicides 'A' and 'B':

(a) 'SS' – sensitive to both fungicides

(b) 'RS' – resistant to fungicide A, sensitive to fungicide B

(c) 'SR' – sensitive to fungicide A, resistant to fungicide B

(d) 'RR' – resistant to both fungicides.

It is assumed that the epidemic on the upper leaves is initiated by an influx of spores from infectious lesions on lower leaves. The density of infectious lesions on lower leaves, C, diminishes over time at rate λ, as lower leaves senesce and infectious lesions on the lower leaves reach the end of the infectious period. The LAI of infectious lesions on lower leaves at time t, $C(t)$, is calculated as:

$$C(t) = C_0 e^{-\lambda t} \tag{1}$$

Fractions $\theta_{RS_{\text{Start}}}$ and $\theta_{SR_{\text{Start}}}$ of the initial influx C from lower leaves are assumed to be spores of the single-strains resistant to fungicide A and fungicide B respectively, with the double-resistant strain fraction calculated as $\theta_{RR_{\text{Start}}} = \theta_{RS_{\text{Start}}}\theta_{SR_{\text{Start}}}$ and the sensitive strain fraction calculated as $\theta_{SS_{\text{Start}}} = 1 - \left(\theta_{RS_{\text{Start}}} + \theta_{SR_{\text{Start}}} + \theta_{RR_{\text{Start}}}\right)$. It is assumed that these fractions are not affected by fungicide application after the start of the model simulation at growth stage 31 (GS31) (Zadoks et al., 1974), as they represent influx from elsewhere. The initial influx is denoted as C_{SS}, C_{RS} C_{SR} and C_{RR} for the sensitive, single-resistant and double-resistant strains respectively.

The influx of spores, C, and infectious LAI on the upper canopy, I, are converted into new latent lesions on the upper canopy, at transmission rate ε, i.e. the overall rate at which infectious lesion density is converted into new latent lesions on a given density of healthy leaf area. Latent lesions mature into infectious, sporulating lesions, at a rate δ , where $1/\delta$ is the average latent period. The transmission rate ε and maturation rate δ are affected by the action of fungicides, so ε_i and δ_i are calculated for each strain i. Infectious lesions die at a rate μ, where $1/\mu$ is the average infectious period. The area index of healthy (H), latently infected (L) and infectious (I) leaf area over time are tracked using the following set of equations:

$$\frac{dH}{dt} = \gamma(M_{\text{Max}} - M) - \beta(t)H - \left(H/M\right)\left(\sum \varepsilon_i\,(C_i + I_i)\right) \tag{2}$$

$$\frac{dL_i}{dt} = \varepsilon_i\left(H/M\right)(C_i + I_i) - \delta_i L_i - \beta(t)L_i \tag{3}$$

$$\frac{dI_i}{dt} = \delta_i L_i - \mu I_i \tag{4}$$

where M is the total LAI ($M = H + S + \sum(L_i + I_i)$, where S is LAI removed by either senescence or the end of the infectious period), M_{Max} is the maximum LAI, γ is

the growth rate of the leaf area, and $\beta(t)$ is the rate of senescence of healthy and latently infected LAI at time t, as detailed in Chapter 4 (Section 4.3.2.1) (Corkley et al., 2025a).

The fungicide dose of fungicide j at time t, $D_j(t)$, decays exponentially over time at rate v_j:

$$D_j(t) = \begin{cases} D_{j_0}e^{-v_j(t-t^*)}, & t \geq t^* \\ 0, & t < t^* \end{cases} \tag{5}$$

where D_{j_0} is the applied dose, expressed as a proportion of the maximum permitted individual dose (as defined on the product label), $D_{j_{\text{Max}}}$, and t^* is the time of the first application of fungicide j. If an additional application of fungicide j is made at t^{**}, the remaining dose from the application at t^* is added to the newly applied dose to calculate a total value for D_{j_0} at t^{**}.

The action of systemic fungicides reduces the pathogen life cycle parameters ε and δ by a fraction $f(t)$, which changes over time depending on the remaining fungicide dose, $D_j(t)$. The dose response of the fractional reduction of strain i, $f_i(t)$, to $D_j(t)$ is described by a combination of an asymptote parameter, q_{ij}, which is the maximum fractional reduction of the pathogen life cycle parameter (i.e. at infinite fungicide dose), and a curvature parameter, k_{ij}, which defines how quickly the fractional reduction declines from the asymptote as $D_j(t)$ decreases:

$$f_i(t) = q_{i_j}\left(1 - e^{-k_{i_j}D_j(t)}\right) \tag{6}$$

The fractional reduction as a result of the joint action of the two fungicides 'A' and 'B' is described by a multiplicative survival model (Bliss, 1939; Paveley et al., 2003). For example, the transmission rate ε_i when fungicides A and B are applied in mixture is calculated as:

$$\varepsilon_i(t) = \varepsilon\left[1 - q_{i_A}\left(1 - e^{-k_{i_A}D_A(t)}\right)\right]\left[1 - q_{i_B}\left(1 - e^{-k_{i_B}D_B(t)}\right)\right] \tag{7}$$

A shift in sensitivity to the fungicide is defined as either an asymptote shift, ζ_q, or a curvature shift, ζ_k, denoted as a percentage reduction in the fungicide parameter relative to the sensitive strain. For example, a 60% asymptote shift to fungicide A means that $q_{RS_A} = 0.4q_{SS_A}$. We assume that there are no fitness costs of resistance.

The infectious area of each strain at GS87 is used to calculate the population fraction of each strain at the time of complete senescence of the wheat canopy, denoted as $\theta_{SS_{End}}$, $\theta_{RS_{End}}$, $\theta_{SR_{End}}$ and $\theta_{RR_{End}}$ respectively. The starting population fractions of each strain in the following growing season (year *n+1*) following sexual reproduction on wheat stubble are calculated assuming Mendelian inheritance (Miko, 2008; Taylor and Cunniffe, 2023b), assuming that the alleles for resistance to fungicide A and fungicide B are on the chromosomal genome and that they are unlinked, and so are inherited independently:

$$\theta_{RS_{Start}}(n+1) = \theta_{RS_{End}}^{2} + \theta_{SS_{End}}\theta_{RS_{End}} + 0.5\theta_{RS_{End}}\theta_{SR_{End}} + \theta_{RS_{End}}\theta_{RR_{End}} + 0.5\theta_{SS_{End}}\theta_{RR_{End}} \quad (8)$$

$$\theta_{SR_{Start}}(n+1) = \theta_{SR_{End}}^{2} + \theta_{SS_{End}}\theta_{SR_{End}} + 0.5\theta_{RS_{End}}\theta_{SR_{End}} + \theta_{SR_{End}}\theta_{RR_{End}} + 0.5\theta_{SS_{End}}\theta_{RR_{End}} \quad (9)$$

$$\theta_{RR_{Start}}(n+1) = \theta_{RR_{End}}^{2} + 0.5\theta_{SS_{End}}\theta_{RR_{End}} + 0.5\theta_{RS_{End}}\theta_{SR_{End}} + \theta_{RS_{End}}\theta_{RR_{End}} + \theta_{SR_{End}}\theta_{RR_{End}} \quad (10)$$

$$\theta_{SS_{Start}}(n+1) = 1 - \left[\theta_{RS_{Start}}(n+1) + \theta_{SR_{Start}}(n+1) + \theta_{RR_{Start}}(n+1)\right] \quad (11)$$

5.3.2 Fungicide programme scenarios

Three potential fungicide programmes combining the same total dose of two systemic fungicides A and B were simulated, across multiple scenarios covering a wide range of parameter values (Table 5.1) representing variation in fungicide efficacy and longevity, and the type and magnitude of the shift in sensitivity of resistant strains:

(a). 'Alternate Fungicide A first': Fungicide A applied at full label dose rate at GS32, Fungicide B applied at full label dose rate at GS39.

(b). 'Alternate Fungicide B first': Fungicide B applied at full label dose rate at GS32, Fungicide A applied at full label dose rate at GS39.

(c). 'Split and mix': A mixture of fungicides A and B in a 50:50 ratio, each at half of full label dose, applied twice, at GS32 and GS39.

Table 5.1: List of parameter values simulated. All combinations of q_σ, k_σ, ζ_q and ζ_k values simulated for fungicides A and B, for each value of the decay rate ν.

Parameter	Description	Values simulated
$D_{j\,\text{Total}}$	Total fungicide dose of each fungicide applied	1, i.e. $D_{j\,\text{Max}}$
$\theta_{RS\text{Start}}$	Initial fraction of inoculum C that is resistant to fungicide A	0.01
$\theta_{SR\text{Start}}$	Initial fraction of inoculum C that is resistant to fungicide B	0.01
$\theta_{RR\text{Start}}$	Initial fraction of inoculum C that is resistant to fungicides A and B	0.0001
q_{SS}	Asymptote of fungicide dose response (sensitive strain)	0.2845, 0.4268, 0.5690, 0.7113, 0.8535
k_{SS}	Curvature of fungicide dose response (sensitive strain)	2.475, 4.950, 9.900, 14.850, 29.700
ν	Decay rate (t^{-1})	0.01605, 0.00802, 0.00401
ζ_q	Asymptote shift of resistant strain	1, 10, 50, 75, 100
ζ_k	Curvature shift of resistant strain	1, 10, 50, 75, 100
GS31	Timing of start of growth of leaf 3	1396
GS32	Timing of GS32 application (zero-degree days)	1495
GS39	Timing of GS39 applications (zero-degree days)	1653
GS61	Timing of anthesis	1891
GS87	Timing of end of grainfill & complete senescence of canopy	2567

The decay rates, $\nu = 0.01605\ t^{-1}$, $\nu = 0.00802\ t^{-1}$ and $\nu = 0.00401\ t^{-1}$ correspond to foliar concentration half-lives of 3, 6 and 12 days respectively. For an SDHI fungicide, we previously estimated $\nu = 0.00802\ t^{-1}$, $q_{SS} = 0.569$ and $k_{SS} = 9.9$ (Chapter 4 – Table 4.2 (Corkley et al., 2025a)).

5.3.3 Metrics used to compare resistance management strategies

5.3.3.1 Effective disease control threshold

Fungicide programmes that do not provide effective disease control are not suitable for use as part of a resistance management strategy. We follow (Hobbelen et al., 2011) in defining effective disease control as limiting the loss of healthy area duration ('HAD') to less than 5% of the HAD predicted for a healthy crop in the complete absence of disease. HAD is calculated as the area under the curve of

green leaf area index (GLAI) over time (in zero-degree-days) between GS61 and GS87; GLAI during this period is strongly correlated with yield (Bryson et al., 1997). GLAI was defined as LAI in the healthy (H) and latently-infected (L) compartments.

5.3.3.2 Rate of selection for double-resistant strain

We used the rate of selection for the double-resistant strain, 'RR', over a single growing season, as measured by the selection coefficient, *s* (Milgroom & Fry, 1988; van den Bosch et al., 2014a), to compare the success of each programme for managing concurrent evolution of resistance. Since sexual reproduction between single-resistant strains can boost the frequency of the double-resistant strain, we used $\theta_{RR_{\text{Start}}}(n+1)$ following sexual reproduction to calculate the selection coefficient, compared to the starting population fraction of 'RR' at the beginning of the first growing season, $\theta_{RR_{\text{Start}}}(n)$:

$$s = \frac{1}{T}\left(\ln\left(\frac{\theta_{RR_{\text{Start}}}(n+1)\left[1-\theta_{RR_{\text{Start}}}(n)\right]}{\theta_{RR_{\text{Start}}}(n)\left[1-\theta_{RR_{\text{Start}}}(n+1)\right]}\right)\right) \tag{12}$$

where T is the length of time simulated over a single growing season between GS31 and GS87 (Chapter 4 – Section 4.3.2.5 (Corkley et al., 2025a)). The smaller the value of *s*, the more successful the programme is at managing concurrent evolution of resistance, providing it meets the minimum threshold for effective disease control.

The ratio $\frac{s_{\text{SplitMix}}}{s_{\text{Alternate}}}$, where $s_{\text{Alternate}}$ is the minimum of $s_{\text{AlternateAFirst}}$ and $s_{\text{AlternateBFirst}}$, provides a measure of the relative rate of selection for 'RR' in splitting and mixing and alternation programmes. A value of $\frac{s_{\text{SplitMix}}}{s_{\text{Alternate}}} < 1$ indicates that splitting and mixing reduces selection for 'RR' relative to alternation, and a value > 1 indicates the reverse.

5.3.3.3 Rate of increase in HAD loss

In some cases, the rate of selection for a single-resistant strain may be more important for the overall level of programme control than selection for the double-resistant strain, such as a case where the shift in sensitivity to one fungicide has a much larger effect on programme efficacy than the shift in sensitivity to the other fungicide. We therefore compared the rate of decrease in HAD, ΔHAD, between the first growing season *n* and the following growing season *n+1*, for all fungicide programmes that met the effective control threshold in the first growing season:

$$\Delta\text{HAD} = 100 \times \frac{\text{HAD}(n+1) - \text{HAD}(n)}{\text{HAD}(n)} \tag{13}$$

The more negative the value of ΔHAD, the faster the rate of loss of disease control. Using this metric, programmes can be ranked according to the stability of the level of disease control provided.

5.4   Results

The programmes which minimised selection for the double-resistant strain in different scenarios are summarised in Figure 5.1. Each scenario is described in further detail in sections 5.4.1 to 5.4.3, and full tables of results are provided in Supplementary Materials.

For all combinations of type of sensitivity shift (asymptote shift to both, curvature shift to both, asymptote shift to Fungicide A and curvature shift to Fungicide B), splitting and mixing minimised selection for the double-resistant strain 'RR' for some fungicide dose response parameter values, and alternation minimised selection in other cases. Overall, splitting and mixing minimised selection for 'RR' most frequently when there was an asymptote shift to both fungicides, and least frequently when there was a curvature shift to both fungicides. Table 5.2 shows the distribution of the ratio $\frac{S_{\text{SplitMix}}}{S_{\text{Alternate}}}$ (Section 5.3.3.2) across all parameter values simulated. For each combination of type of sensitivity shift, there were cases where splitting and mixing strongly reduced selection for 'RR' relative to alternation, as well as cases where the reverse was true. Not all combinations of parameter values are equally likely, so the mean value of $\frac{S_{\text{SplitMix}}}{S_{\text{Alternate}}}$ over all parameter values is not necessarily indicative of the most likely outcome in each scenario, but provides a comparison of the tendency for splitting and mixing or alternation to be optimal in each scenario. It is important to note that over a large area of parameter space, the difference in selection for 'RR' between splitting and mixing and alternation was small, as indicated by the interquartile range.

(a)

Asymptote shift to Fungicide A

(b)

Curvature shift to Fungicide A

Tactic that minimised selection for double-resistant strain

- **Alt** — Alternation better
- **Alt** — Variable outcome (alternation usually better)
- **SplitM** — Splitting and mixing better

(c)

Asymptote shift to Fungicide A
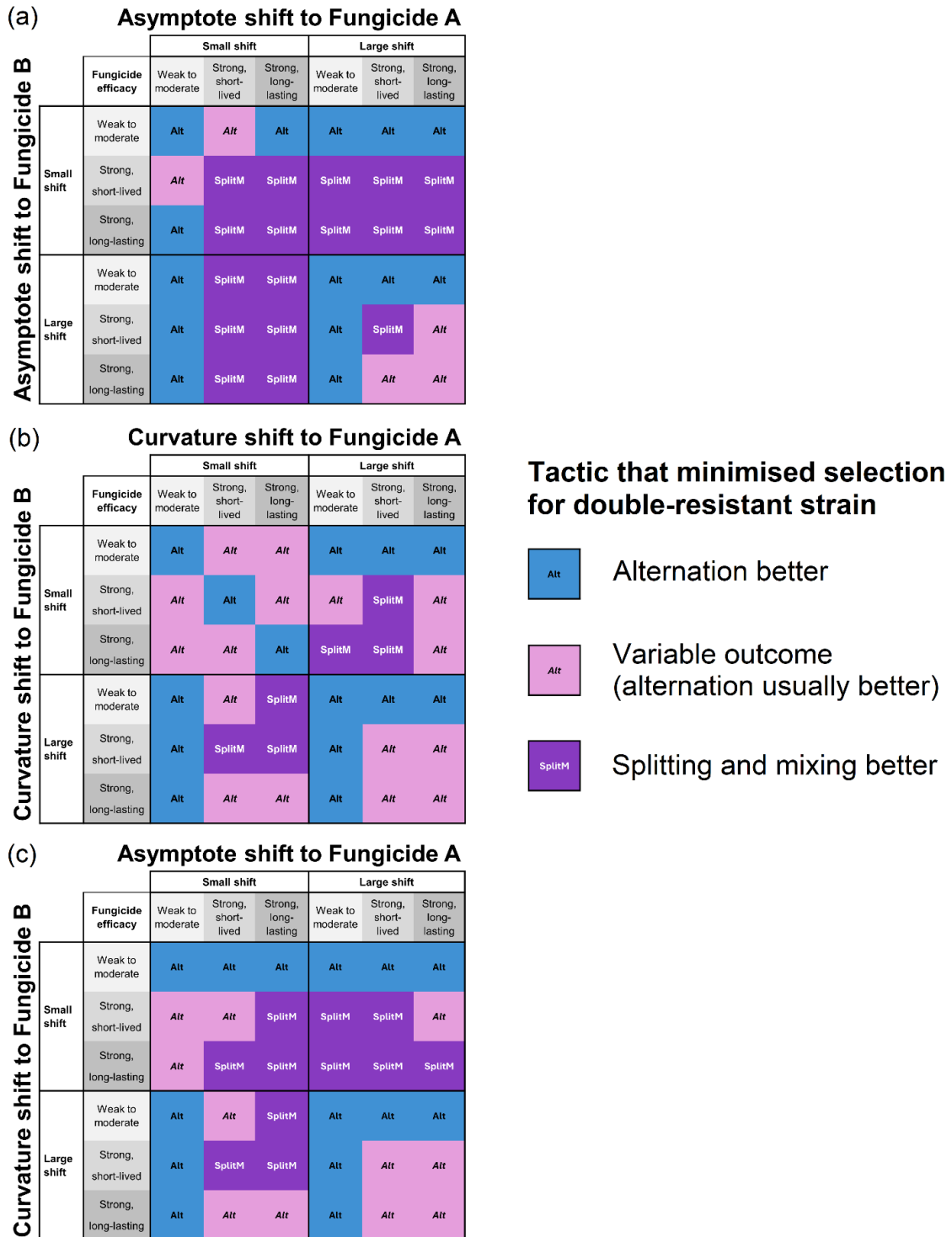
Figure 5.1: Cases where alternation or splitting and mixing tended to minimise selection for the double-resistant strain, depending on fungicide efficacy and the type and level of sensitivity shift. (a) Asymptote shifts to fungicides A and B; (b) Curvature shifts to fungicides A and B; (c) Asymptote shift to fungicide A and curvature shift to fungicide B. A 'small' sensitivity shift corresponds to $1 < \zeta < 50$ (%); for a 'large' sensitivity shift, $50 < \zeta \leq 100$ (%); a 'strong' fungicide has a large

167

asymptote parameter, $q_{SS} \geq 0.569$ approximately; 'short-lived' and 'long-lasting' fungicides have small/ large values respectively of curvature parameter, k_{SS}, and/ or high/ low values respectively of the decay rate, ν. The effects of k_{SS} and ν interact to define a 'short-lived' or 'long-lasting' effect: for example, a fungicide with $\nu = 0.00802\ t^{-1}$ and $k_{SS} < 5$ has a short-lived effect, but if $\nu > 0.00802\ t^{-1}$, larger values of k_{SS} would also define a short-lived effect.

Table 5.2: Distribution of ratio $\frac{s_{\text{SplitMix}}}{s_{\text{Alternate}}}$ across all parameter values for scenarios with (a) an asymptote shift, ζ_q, to both fungicides, (b) a curvature shift, ζ_k, to both fungicides, or (c) an asymptote shift to Fungicide A and a curvature shift to Fungicide B; $s_{\text{Alternate}}$ is the minimum of $s_{\text{AlternateAFirst}}$ and $s_{\text{AlternateBFirst}}$. The ratio $\frac{s_{\text{SplitMix}}}{s_{\text{Alternate}}}$ is a measure of the relative rate of selection for 'RR' in splitting and mixing and alternation programmes. A value of $\frac{s_{\text{SplitMix}}}{s_{\text{Alternate}}} < 1$ indicates that splitting and mixing reduces selection for 'RR' relative to alternation, and a value > 1 indicates the reverse.

Type of shift to A	Type of shift to B	Decay rate of A & B, ν (t^{-1})	Mean	Minimum	Maximum	Interquartile range
ζ_q	ζ_q		1.070	0.509	1.404	0.975 - 1.195
ζ_k	ζ_k	0.01605	1.215	0.496	2.030	1.086 - 1.358
ζ_q	ζ_k		1.132	0.496	2.004	1.020 - 1.260
ζ_q	ζ_q		1.052	0.686	1.220	0.995 - 1.133
ζ_k	ζ_k	0.00802	1.138	0.682	1.643	1.065 - 1.221
ζ_q	ζ_k		1.091	0.682	1.591	1.027 - 1.166
ζ_q	ζ_q		1.049	0.783	1.180	1.013 - 1.095
ζ_k	ζ_k	0.00401	1.085	0.841	1.256	1.049 - 1.130
ζ_q	ζ_k		1.064	0.841	1.248	1.029 - 1.110

5.4.1 Concurrent evolution of complete resistance to both fungicides

For most parameter value combinations considered, splitting and mixing increased selection for the double-resistant strain relative to alternation, as measured by the selection coefficient s (Equation 12). When there is concurrent evolution of complete resistance to both fungicides, splitting and mixing increases the fractional reduction of the sensitive ('SS') strain relative to alternation, but the growth rate of

the double-resistant ('RR') strain is completely unaffected, leading to a larger difference in growth rates (Figure 5.2(a)). Although control of single-resistant ('RS' and 'SR') strains is improved by splitting and mixing relative to alternation, overall the cumulative difference in control of sensitive and single-resistant strains is small relative to the cumulative difference in control of the sensitive and double-resistant strains, due to the effect of increased exposure time from splitting and mixing (Figure 5.2(c)). In a small number of cases, where both fungicides had a large asymptote parameter, q_{SS}, in combination with a low curvature parameter, k_{SS}, or a high decay rate, ν, splitting and mixing strongly reduced selection for single-resistant strains, outweighing the effect of increased exposure time, whilst only slightly increasing selection for the double-resistant strain during the growing season (Figure 5.2(b), 5.2(d)). For this limited set of parameter values, reduced selection for single-resistant strains 'RS' and 'SR' reduced the rate of increase in the double-resistant strain 'RR' following sexual reproduction for 'split & mix' programmes compared to alternation programmes.

In cases where alternation minimised *s*, if the decay rate of both fungicides was either low or high ($\nu = 0.00401\ t^{-1}$ and $\nu = 0.01605\ t^{-1}$ respectively), alternating the more effective fungicide second minimised *s*. The growth rate of the pathogen population is highest prior to GS39, when the canopy LAI is expanding rapidly so pathogen growth rates are not limited by density dependence, meaning the maximum difference in resistant and sensitive strain growth rates is also larger prior to GS39. However, if both fungicides had an intermediate half-life (i.e. $\nu = 0.00802\ t^{-1}$, representative of an SDHI fungicide), alternating the fungicide with the smaller curvature parameter second minimised *s*: the lower part of the dose response curve of the fungicide with the larger as an overlapping effect with the fungicide alternated first reduced the difference in the growth rates of the sensitive strain and the single-resistant strains following the second application.

In a few cases, splitting and mixing provided effective disease control when alternation did not, for example cases where the fungicides had a high decay rate and where the curvature and asymptote parameters of at least one of the fungicides were relatively low. Additionally, in cases where both fungicides had moderate to high asymptote parameters in combination with a moderate to high decay rate or low curvature parameter, the rate of loss of disease control, $\Delta\mathrm{HAD}$, was generally smaller for 'split & mix' programmes than for alternation programmes despite higher values of *s* relative to alternation, due to a higher level of control of single-resistant strains.
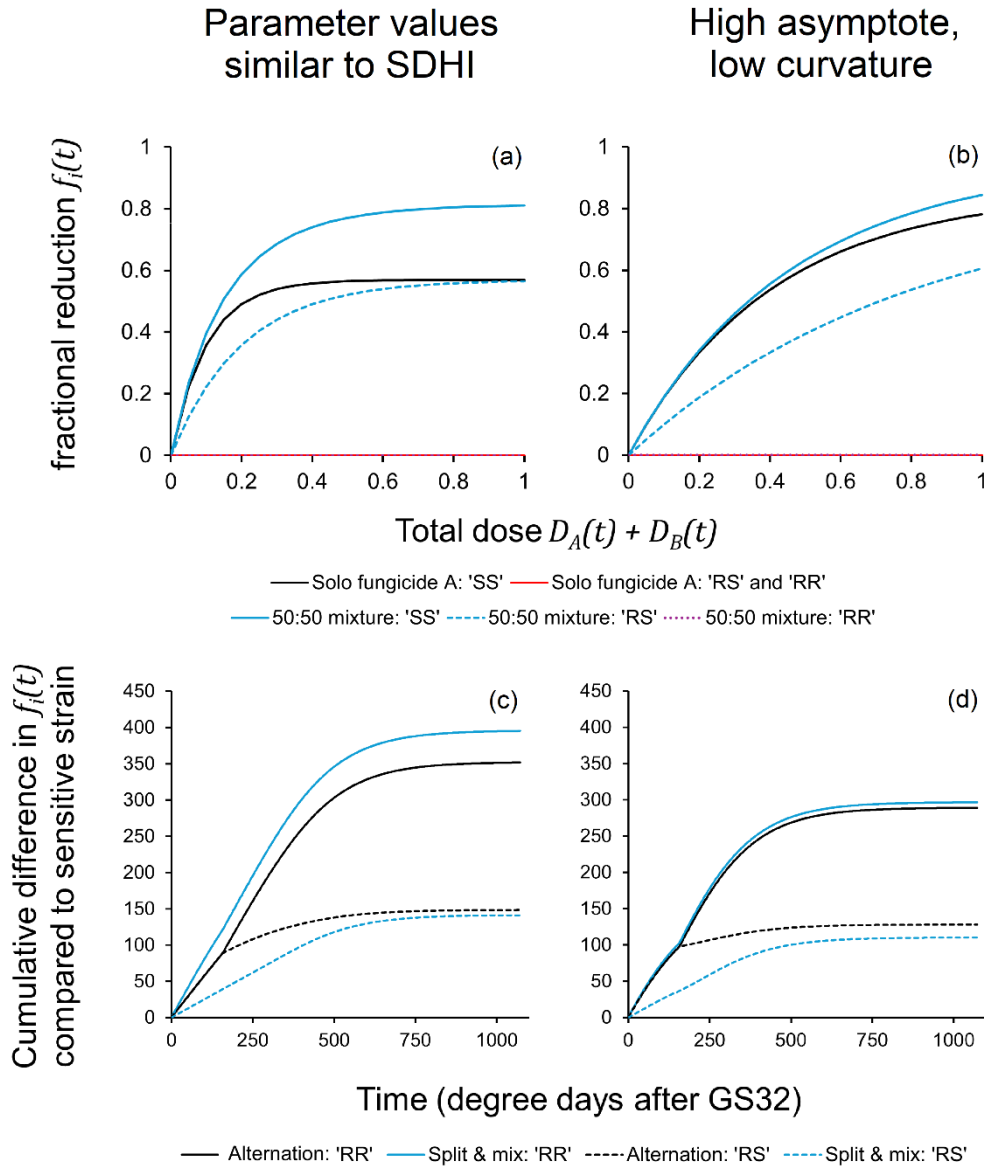
Figure 5.2: Comparison of the effect of 'splitting & mixing' and alternation on selection for double-resistant and single-resistant strains when there is concurrent evolution of complete resistance to both fungicides A and B. (a) and (b) show differences in the dose response curve of the fractional reduction, $f_i(t)$, of strains 'SS', 'RS' and 'RR' for solo fungicide A and a 50:50 mixture of fungicides A and B. (c) and (d) show the cumulative differences $\sum_{GS32}^{t}(f_{SS}(t) - f_{RS}(t))$ and $\sum_{GS32}^{t}(f_{SS}(t) - f_{RR}(t))$ for alternation and 'split & mix' programmes. In the cases shown here, both fungicides A and B have the same asymptote, curvature and decay rate parameters, so the results for strain 'SR' would be identical if fungicide B was alternated first. (a) and (c) are plotted for a pair of fungicides with parameter values representative of an SDHI fungicide (q_{SS}=0.569, k_{SS}=9.9, v=0.00802 t^{-1}); (b) and (d) are plotted for a pair of fungicides with a high asymptote parameter in

combination with a low curvature parameter (q_{SS}=0.8535, k_{SS}=2.475, v=0.00802 t^{-1}).

5.4.2 Concurrent evolution of partial resistance to both fungicides

5.4.2.1 Asymptote shift to both fungicides

For weak to moderately effective fungicides with relatively small values of the asymptote parameter q_{SS}, alternation minimised selection for the double-resistant strain (Figure 5.1(a): both fungicides weak to moderately effective) when there was a partial asymptote shift to both fungicides A and B. Splitting and mixing improves control of the sensitive strain, the single-resistant strains and the double-resistant strain. However, overall the difference in the growth rates of 'RR' and 'SS' is increased by splitting and mixing in this case, because the increase in control of the double-resistant strain is small relative to the level of control of the sensitive strain achieved by the mixture (Figure 5.3(a): compare the difference in control of strains 'SS' and 'RR' by solo fungicide A and 50:50 mixture). The difference in the growth rates of 'RS' and 'SS' is decreased by the 50:50 mixture relative to solo application of fungicide A, but the decrease is too small to outweigh the effect of increased exposure time from splitting and mixing. Therefore splitting and mixing two weak to moderately effective fungicides increases both $\sum_{GS32}^{T}(f_{SS}(t) - f_{RR}(t))$ and $\sum_{GS32}^{T}(f_{SS}(t) - f_{RS}(t))$ (Figure 5.3(c)), and therefore increases the rate of selection for the double-resistant strain.

When both fungicides were strongly effective, with a large asymptote parameter, q_{SS}, splitting and mixing reduced s for strain 'RR' relative to alternation in many cases (Figure 5.1(a)). In this case, the cumulative differences $\sum_{GS32}^{T}(f_{SS}(t) - f_{RS}(t))$ and $\sum_{GS32}^{T}(f_{SS}(t) - f_{RR}(t))$ are both smaller for the 'split & mix' programme compared to the alternation programme (Figure 5.3(b), 5.3(d)): the increase in control of the double-resistant strain by splitting and mixing is large enough relative to the increase in control of the sensitive strain that $f_{SS} - f_{RR}$ decreases overall, and the increase in control of single-resistant strains decreases $f_{SS} - f_{RS}$ and $f_{SS} - f_{SR}$ sufficiently to outweigh the effect of increased exposure time. The smaller the asymptote shift, ζ_q, the wider the range of parameter values over which this result applies. Table 3 shows the results for different levels of asymptote shift to two fungicides with parameter values representative of an SDHI fungicide.
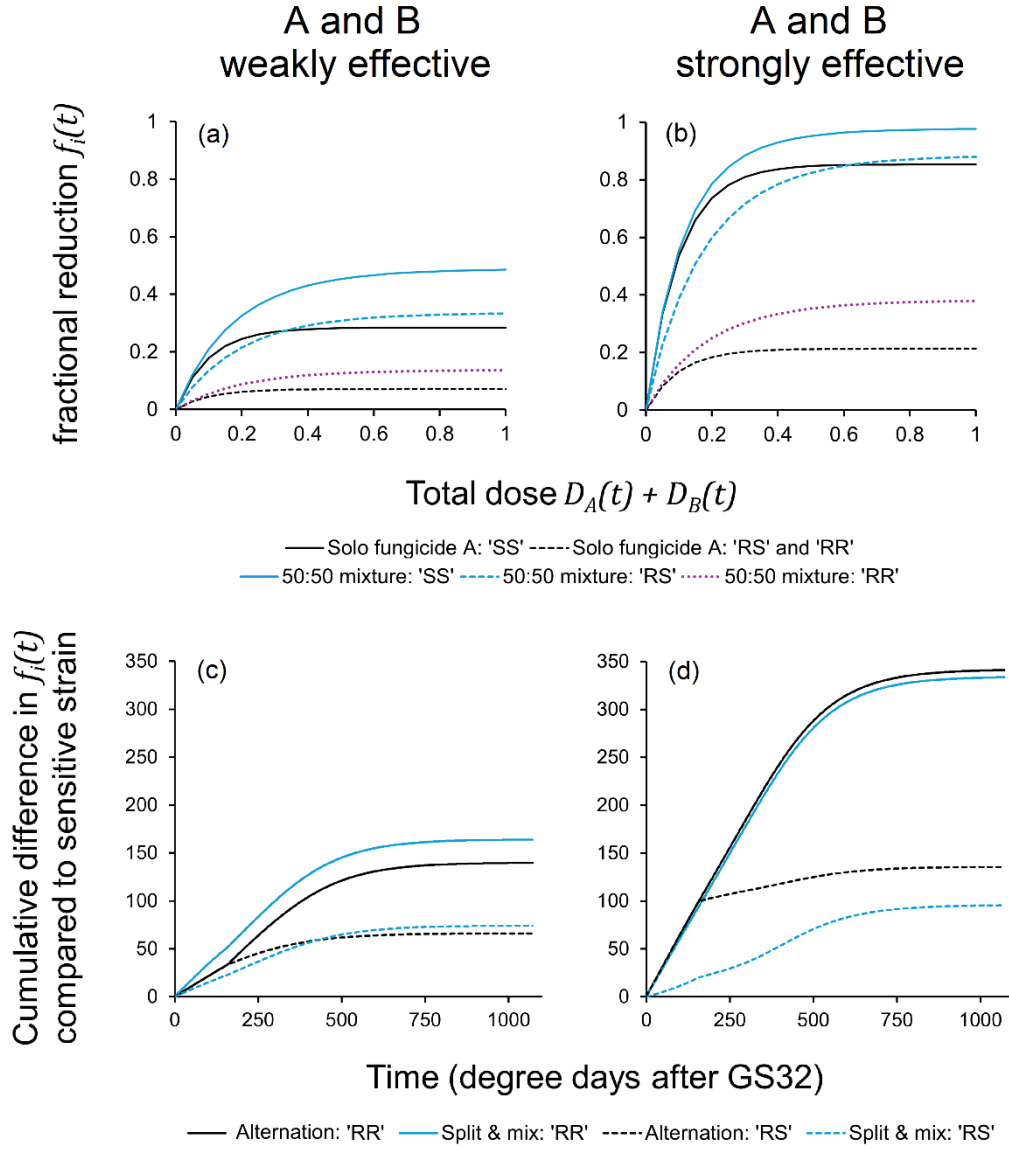
Figure 5.3: Comparison of the effect of 'splitting & mixing' and alternation on selection for double-resistant and single-resistant strains when there is concurrent evolution of a partial asymptote shift to both fungicides A and B. (a) and (b) show differences in the dose response curve of the fractional reduction, $f_i(t)$, of strains 'SS', 'RS' and 'RR' for solo fungicide A and a 50:50 mixture of fungicides A and B. (c) and (d) show the cumulative differences $\sum_{GS32}^{t}(f_{SS}(t) - f_{RS}(t))$ and $\sum_{GS32}^{t}(f_{SS}(t) - f_{RR}(t))$ for alternation and 'split & mix' programmes. In the cases shown here, both fungicides A and B have the same asymptote, curvature and decay rate parameters, and the resistant strains have the same level of asymptote shift ζ_q = 75%, so the results for strain 'SR' would be identical if fungicide B was alternated first. (a) and (c) are plotted for a pair of weakly to moderately effective fungicides (q_{SS} = 0.2845, k_{SS} = 9.9, v = 0.00802 t^{-1}); (b) and (d) are plotted for a pair of strongly effective fungicides (q_{SS} = 0.8535, k_{SS} = 9.9, v = 0.00802 t^{-1}).

Table 5.3: Fungicide programmes that minimised selection, *s*, for the double-resistant strain for different levels of asymptote shift to two fungicides 'A' and 'B' with parameter values representative of an SDHI fungicide (q_{SS} = 0.569, k_{SS} = 9.9, v = 0.00802 t^{-1}). Where an alternation programme minimised *s*, the order of alternation that minimised *s* is indicated.

		Asymptote shift to Fungicide A (%)				
		1	10	50	75	100
Asymptote shift to Fungicide B (%)	1	Split & Mix	Split & Mix	Split & Mix	Split & Mix	Split & Mix
	10	Split & Mix	Split & Mix	Split & Mix	Alternate (B first)	Alternate (B first)
	50	Split & Mix	Split & Mix	Alternate (Either)	Alternate (B first)	Alternate (B first)
	75	Split & Mix	Alternate (A first)	Alternate (A first)	Alternate (Either)	Alternate (B first)
	100	Split & Mix	Alternate (A first)	Alternate (A first)	Alternate (A first)	Alternate (Either)

When the efficacy and level of asymptote shift to fungicides A and B differed, the outcome depended on the relative level of efficacy and resistance to each fungicide (Figure 5.1(a)). If there was a large asymptote shift to the weaker fungicide (strains 'RR' and 'RS') and a small asymptote shift to the stronger fungicide (strains 'RR' and 'SR'), splitting and mixing reduced *s* for strains 'RR' and 'RS' relative to alternation (Figure 5.4(a)) because 'RR' and 'RS' are well-controlled by the mixture, but have high fitness when the weak fungicide is applied solo, whereas the fitness advantage of strain 'SR' is relatively small. Conversely, if there was a small asymptote shift to the weaker fungicide (strains 'RR' and 'RS') and a large asymptote shift to the stronger fungicide ('SR'), *s* for strain 'RR' was lower for alternation relative to splitting and mixing (Figure 5.4(b)): in this case the weaker fungicide is not a strong enough mixture partner to reduce the growth rates of 'RR' and 'SR' relative to 'SS'.

In a substantial number of cases where alternation minimised *s*, the rate of loss of disease control, ΔHAD was lower for splitting and mixing: in particular, cases where the asymptote shift to both fungicides was small, or where both fungicides had moderate to high asymptote parameters in combination with a moderate to high decay rate, v, or low curvature parameter, k_{SS}.
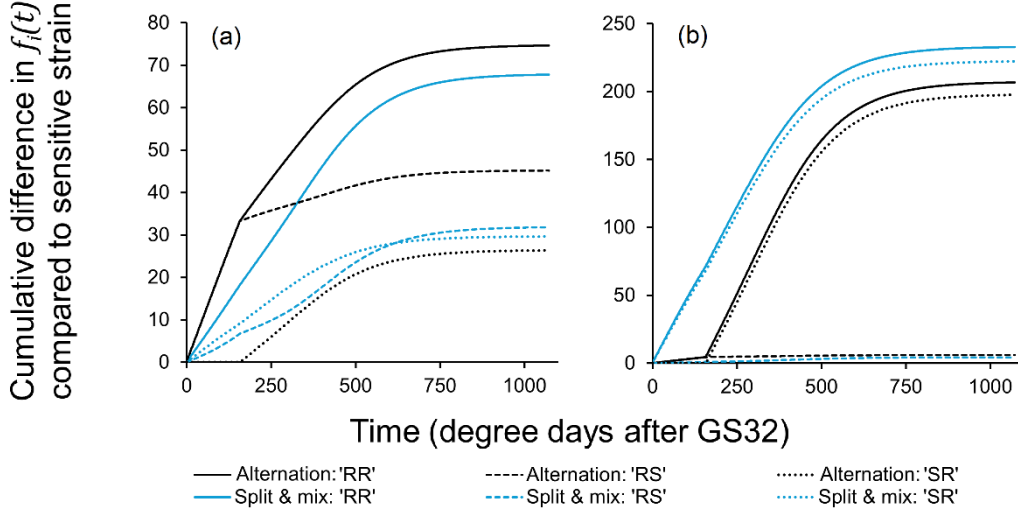
Figure 5.4: Comparison of the effect of 'splitting & mixing' and alternation on selection for double-resistant and single-resistant strains when there is concurrent evolution of a partial asymptote shift to both fungicides A and B, and the efficacy of the fungicides and level of asymptote shift to each fungicide differs. The cumulative differences $\sum_{GS32}^{t}(f_{SS}(t) - f_{RS}(t))$, $\sum_{GS32}^{t}(f_{SS}(t) - f_{SR}(t))$ and $\sum_{GS32}^{t}(f_{SS}(t) - f_{RR}(t))$ are shown. (a) Large shift to a weakly effective fungicide A and small shift to a strongly effective fungicide B (q_{SS_A} = 0.2845, ζ_{q_A} = 75%, k_{SS_A} = 9.9, v_A = 0.00802 t^{-1}; q_{SS_B} = 0.8535, ζ_{q_B} = 10%, k_{SS_B} = 9.9, v_B = 0.00802 t^{-1}). (b) Small shift to a weakly effective fungicide A and large shift to a strongly effective fungicide B (q_{SS_A} = 0.2845, ζ_{q_A} = 10%, k_{SS_A} = 9.9, v_A = 0.00802 t^{-1}; q_{SS_B} = 0.8535, ζ_{q_B} = 75%, k_{SS_B} = 9.9, v_B = 0.00802 t^{-1}).

5.4.2.2 Curvature shift to both fungicides

In most cases where resistance to both fungicides A and B took the form of a curvature shift, ζ_k, alternation programmes selected less for the double-resistant strain compared to splitting and mixing (Figure 5.1(b)). Due to converging dose response curves when ζ_k is small (Figure 5.5(a)), the effect of ζ_k is largest at intermediate fungicide dose $D_j(t)$, so splitting and mixing tends to increase $\sum_{GS32}^{T}(f_{SS}(t) - f_{RS}(t))$, $\sum_{GS32}^{T}(f_{SS}(t) - f_{SR}(t))$ and $\sum_{GS32}^{T}(f_{SS}(t) - f_{RR}(t))$ (Figure 5.5(c)). For two fungicides with parameter values representative of an SDHI fungicide, alternation reduced selection for all combinations of partial curvature shift considered (Table 5.4).
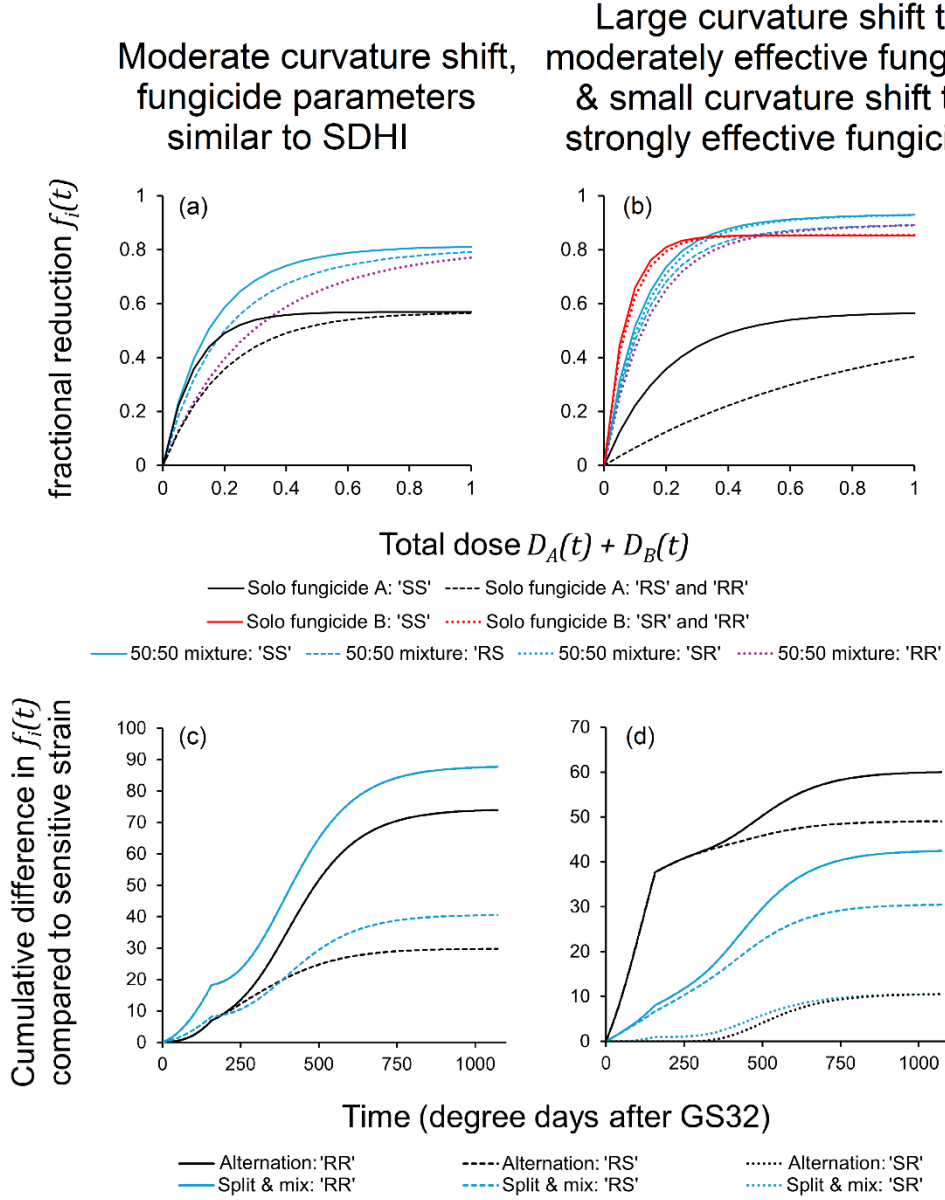
Figure 5.5: Comparison of the effect of 'splitting & mixing' and alternation on selection for double-resistant and single-resistant strains when there is concurrent evolution of a partial curvature shift to both fungicides A and B. (a) and (b) show differences in the dose response curve of the fractional reduction, $f_i(t)$, of strains 'SS', 'RS', 'SR' and 'RR' for solo fungicides A and B and a 50:50 mixture of fungicides A and B. (c) and (d) show the cumulative differences $\sum_{GS32}^{t}(f_{SS}(t) - f_{RS}(t))$, $\sum_{GS32}^{t}(f_{SS}(t) - f_{SR}(t))$ and $\sum_{GS32}^{t}(f_{SS}(t) - f_{RR}(t))$ for alternation and 'split & mix' programmes. For the case shown in (a) and (c), both fungicides A and B have the same asymptote, curvature and decay rate parameters representative of an SDHI fungicide (q_{SS} = 0.2845, k_{SS} = 9.9, ν = 0.00802 t^{-1}), and the resistant strains have the same level of curvature shift ζ_k = 50%, so the results for strain 'SR' would be identical if fungicide B was alternated first. For the case shown in (b)

175

and (d), the efficacy of and level of curvature shift to fungicides A and B varies: there is a large shift to a short-lived fungicide A and a small shift to a strong, long-lasting fungicide B (q_{SS_A} = 0.569, k_{SS_A} = 4.95, ζ_{k_A} = 75%, v_A = 0.00802 t^{-1}; q_{SS_B} = 0.8535, k_{SS_B} = 14.85, ζ_{k_B} = 10%, v_B = 0.00802 t^{-1}).

Table 5.4: Fungicide programmes that minimised selection, *s*, for the double-resistant strain for different levels of curvature shift to two fungicides 'A' and 'B' with parameter values representative of an SDHI fungicide (q_{SS} = 0.569, k_{SS} = 9.9, v = 0.00802 t^{-1}). Where an alternation programme minimised *s*, the order of alternation that minimised *s* is indicated.

		Curvature shift to Fungicide A (%)				
		1	10	50	75	100
Curvature shift to Fungicide B (%)	1	Alternate (Either)	Alternate (A first)	Alternate (A first)	Alternate (A first)	Split & Mix
	10	Alternate (B first)	Alternate (Either)	Alternate (A first)	Alternate (A first)	Alternate (B first)
	50	Alternate (B first)	Alternate (B first)	Alternate (Either)	Alternate (A first)	Alternate (B first)
	75	Alternate (B first)	Alternate (B first)	Alternate (B first)	Alternate (Either)	Alternate (B first)
	100	Split & Mix	Alternate (A first)	Alternate (A first)	Alternate (A first)	Alternate (Either)

In general, alternating the fungicide with the larger curvature shift (ζ_k) or the larger curvature parameter (k_{SS}) first minimised *s*: if the lower part of the dose response curve for the first fungicide overlaps with the effect of the second application, there is improved control of strains resistant to the first fungicide at a point where the difference in growth rates would otherwise be at a maximum due to the converging dose response curve.

Splitting and mixing reduced *s* relative to alternation in cases where there was a large curvature shift to a weakly/ moderately effective or short-lived fungicide and a small curvature shift to a strongly effective, longer-lived fungicide (Figure 5.1(b); Figure 5.5(b); 5.5(d)). In addition, ΔHAD was lower for splitting and mixing in a substantial number of cases where alternation minimised *s*, in particular cases where the curvature shift to both fungicides was small.

5.4.2.3 Asymptote shift to fungicide A and curvature shift to fungicide B

When there was concurrent evolution of an asymptote shift to fungicide A, ζ_{q_A} and a curvature shift to fungicide B, ζ_{k_B}, there were fewer cases where splitting and mixing was beneficial compared to concurrent evolution of an asymptote shift to both fungicides, but more cases than for concurrent evolution of a curvature shift to both fungicides (Figure 5.1(c)). Splitting and mixing generally minimised s in cases where (a) fungicide B had a large asymptote parameter and a small curvature shift and fungicide A had a small asymptote shift, or (b) fungicide B had a large curvature shift and fungicide A had a large asymptote parameter, a small asymptote shift, and large curvature parameter relative to fungicide B. For cases where alternation minimised s, it was generally better to alternate fungicide A second, unless fungicide A had a very large curvature parameter and fungicide B had a very small curvature parameter. Table 5.5 shows the results for different levels of asymptote shift to fungicide 'A' and curvature shift to fungicide 'B' for two fungicides with parameter values representative of an SDHI fungicide.

Table 5.5: Fungicide programmes that minimised selection, s, for the double-resistant strain for different levels of asymptote shift to fungicide 'A' and different levels of curvature shift to fungicide 'B', each with parameter values representative of an SDHI fungicide (q_{SS}=0.569, k_{SS}=9.9, v=0.00802 t^{-1}). Where an alternation programme minimised s, the order of alternation that minimised s is indicated.

| | | Asymptote shift to Fungicide A (%) | | | | |
		1	10	50	75	100
Curvature shift to Fungicide B (%)	1	Alternate (B first)	Alternate (B first)	Split & Mix	Split & Mix	Split & Mix
	10	Alternate (B first)	Alternate (B first)	Alternate (B first)	Alternate (B first)	Alternate (B first)
	50	Alternate (B first)	Alternate (B first)	Alternate (B first)	Alternate (B first)	Alternate (B first)
	75	Alternate (B first)	Alternate (B first)	Alternate (B first)	Alternate (B first)	Alternate (B first)
	100	Split & Mix	Alternate (A first)	Alternate (A first)	Alternate (A first)	Alternate (A first)

5.4.3 Concurrent evolution of complete resistance to fungicide A and partial resistance to fungicide B

When there was concurrent evolution of complete resistance to fungicide A and partial resistance to fungicide B, splitting and mixing generally minimised selection

for the double-resistant strain 'RR' in cases where fungicide B was reasonably effective (i.e. with a moderate to large asymptote parameter and curvature parameter), and the level of sensitivity shift to fungicide B (ζ_{q_B} or ζ_{k_B}) was small. If fungicide B was weakly effective or there was a large sensitivity shift to fungicide B, alternation generally minimised *s*.

5.5 Discussion

Our results reveal differences between which strategies are best for management of resistance mechanisms that result in an asymptote shift and resistance mechanisms that result in a curvature shift. Splitting and mixing the total dose of two at-risk fungicides is more likely to be beneficial against strains with an asymptote shift, whereas alternation is more likely to minimise selection for strains with a curvature shift. However, in both cases there was variability in which tactic was better for managing concurrent evolution of resistance, with dependency on fungicide properties and the magnitude of the sensitivity shift. This fits with our previous findings that dose splitting can increase selection more for partial curvature shifts than for asymptote shifts, but that the effects of dose splitting are variable (Chapter 4 (Corkley et al., 2025a)). Across all combinations of types of sensitivity shift (complete; partial asymptote shift or partial curvature shift), splitting and mixing was more likely to be beneficial when both fungicides had strong but short-lived efficacy (i.e. a combination of a high asymptote parameter with a high decay rate and/or a low curvature parameter), and the size of the sensitivity shifts to each fungicide was unequal. Alternation was more likely to minimise selection for double-resistant strains when both fungicides were weakly or moderately effective.

Our finding that the optimal strategy for combining two at-risk fungicides in a programme varies depending on fungicide efficacy, longevity and the type and magnitude of resistance underlines the value of experimental work to understand fungicide properties and likely resistance mechanisms as early as possible following development of new MoAs. This information can be used to identify pairs of fungicides for which formulation in mixture is more likely to be beneficial for resistance management, and fungicides for which alternation is likely to be a better strategy. However, this may be challenging in practice. Fungicide foliar decay rates can be measured experimentally or estimated using models (Fantke et al., 2014), but are affected by environmental factors and can be highly variable. Asymptote and curvature parameters can be estimated from field trials where the response of

disease severity to at least three dose rates of a solo fungicide and an untreated control has been measured (Chapter 3 – Section 3.3.2 (Corkley et al., 2025b)); the level of uncertainty in the estimated parameter values depends on the quantity and quality of data available. Mutagenesis studies *in vitro* and experimental evolution can be used to predict likely resistance mechanisms for any given fungicide and the relative fitness of strains with different mutations (Hawkins, 2024), whilst data gathered to fit EC_{50} dose rates (the dose that inhibits the *in vitro* growth of the pathogen by 50%) could indicate whether a resistance mechanism causes an asymptote shift or a curvature shift. The predictability of mutations varies between fungicide groups (Hawkins, 2024; Hawkins & Fraaije, 2021), but it may also be possible to predict the type and magnitude of resistance that is likely by considering fungicide binding mechanisms (Chapter 4 – Section 4.2 (Corkley et al., 2025a); Grimmer et al., 2015).

It should be noted that the difference in selection between splitting and mixing and alternation was relatively small across a substantial area of parameter space. Field trials comparing splitting and mixing with alternation of SDHI and DMI fungicides found no significant difference in selection for SDH-mutations across a range of SDHI and DMI dose rates (Young et al., 2021); any difference was small relative to experimental variability. Experimental evolution *in vitro* using SDHI and DMI fungicides found that mixtures performed moderately better than alternation against single-resistant strains, but that there was very little difference in the performance of the strategies against double-resistant strains once the 'RR' strain reached a population frequency of 5% (Ballu et al., 2024). Where differences in selection are small, and there is economic or environmental justification, there is likely to be room for flexibility in the choice of resistance management tactics, as proposed by Paveley et al. (2023), especially if additional IPM measures can be utilised to contribute to resistance management.

The measure of success for fungicide resistance management can affect which tactic appears to be optimal (Elderfield et al., 2018). We focused on the rate of selection for the double-resistant strain, for programmes that kept HAD loss below a maximum threshold, over a simulated period of two growing seasons chosen to keep model runtime tractable over the large area of parameter space explored. However, splitting and mixing tends to provide improved disease control, and in many cases the rate of loss of HAD was lower using splitting and mixing tactics even when selection for the double-resistant strain was increased compared to alternation tactics. If the choice of tactic is rigid over time, splitting and mixing may

be the pragmatic choice in general to maximise lifetime yield, lifetime profitability or effective life, as concluded by previous studies (Elderfield et al., 2018; Hobbelen et al., 2013; Taylor & Cunniffe, 2023b). However, if there is flexibility in the choice of tactics and alternation of the high-risk fungicides initially provides sufficient disease control, in some cases choosing alternation initially could delay concurrent evolution of resistance for longer, with the option to later switch to splitting and mixing as necessary for disease control. To explore these effects, it would be necessary to run the model for a larger number of seasons to estimate the length of time until breakdown of effective control. Additionally, whilst our comparison of selection rates used a single scenario of starting frequencies of the single- and double-resistant strains, these starting frequencies will vary depending on the evolutionary history of the pathogen population and can affect which strategy is optimal for maximising effective life or lifetime yield (Ballu et al., 2024; Hobbelen et al., 2013; Taylor & Cunniffe, 2023b). The existing frequencies of resistant strains would therefore need to be considered when choosing an optimal strategy for maximising effective life.

We restricted the analysis to a fixed dose rate of each high-risk fungicide: varying the dose rate of each fungicide could increase the range of scenarios in which splitting and mixing is optimal (Taylor & Cunniffe, 2023b), but dose rates can be partially determined by control requirements for pathogens other than *Z. tritici*, and risk-averse growers and fungicide manufacturers are sometimes reluctant to reduce dose rates beneath a minimum recommended dose (te Beest et al., 2013; van den Bosch et al., 2018). We also restricted our analysis to cases where the initial frequencies of the single-resistant strains were equal, and the initial frequency of the double-resistant strain was low. If the initial frequency of resistance to one fungicide is substantially higher, this may affect which strategies are optimal (Taylor & Cunniffe, 2023b) or may mean that the fungicide is a poor choice of mixture partner. If the double-resistant strain is already common, neither alternation or mixture of the high-risk fungicides is likely to extend effective life materially. If available, the introduction of a third novel or low-risk fungicide in alternation or mixture would be needed to provide control of the double-resistant strain (Ballu et al., 2024).

Our analysis used the simplifying assumption that both fungicides were systemic, affecting both the latent period and the transmission rate, and that the fractional reduction $f_{i_j}(t)$ for each strain and fungicide combination was the same for both pathogen life cycle parameters. The reality is likely to be more complex, but there

is scant data to support parameterisation of individual effects for each combination. The impact on our qualitative conclusions of differing dose response curves for the latent period and transmission rates is likely to be small for a given level of fungicide efficacy, which is defined by the overall effect on fungicide growth rate.

We also assumed that sexual reproduction only occurs at the end of the growing season, and that all infections at the start of the second growing season originated from ascospores following sexual reproduction. Some sexual reproduction also occurs in *Z. tritici* during the growing season and could accelerate concurrent evolution of resistance. The impact of ascospores on epidemic development on the upper leaf canopy is thought to be small (Eriksen et al., 2001), although ascospores may account for a greater proportion of disease on resistant cultivars where a larger area of healthy leaf area is available for infection late in the growing season (Duvivier, 2015). The impact of any sexual reproduction during the growing season will depend on the timing and the level of fungicide exposure prior to the formation of pseudothecia, but the effect on the qualitative results is likely to be small: in the cases where splitting and mixing was most beneficial, the mixture reduced the difference in the growth rates of both the single-resistant and double-resistant strains relative to the sensitive strain. Taylor & Cunniffe (2023b) explored the impact of different levels of sexual reproduction between growing seasons, showing modest differences in effective life (but not optimal strategy), between sexual proportions of 50% and 100%. The survival of pycnidiospores on surface debris left following harvest varies with climate, but infection by splash dispersal of pycnidiospores is a plausible scenario for second wheat crops sown into wheat stubble. However, it is likely that ascospores form the majority of inoculum of the new season's crop (Suffert et al., 2011), and the impact on our qualitative comparisons between splitting and mixing and alternation programmes is likely to be small.

Any application of fungicide exerts selection pressure for evolution of resistance: programmes relying solely on at-risk fungicides will be at high risk of concurrent evolution of resistance, regardless of the choice of splitting and mixing or alternation strategy. Steps should be taken to avoid relying only on programmes of at-risk fungicides for disease control wherever possible. Stacking disease control measures reduces the potential fitness advantage for the pathogen of evolving resistance to any individual measure (Corkley et al., 2022). High-risk MoA should be used in mixture or alternation with multi-sites where available (Ballu et al., 2024; Hobbelen et al., 2011). Choice of cultivars should prioritise disease resistance,

which can contribute to fungicide resistance management by reducing pathogen growth rates, reducing the fitness advantage of fungicide-resistant strains, whilst both resistant and disease-tolerant cultivars which maintain yield in the presence of diseases can reduce the intensity of chemical control required for effective disease control (Taylor & Cunniffe, 2023; van den Bosch et al., 2022). Cultural control methods should also be adopted as relevant for each crop and pathogen as part of integrated pest management ('IPM'). For *Z. tritici*, cultural control measures include delayed sowing (Morgan et al., 2021; Shaw and Royle, 1993), use of cultivar mixtures (Kristoffersen et al., 2020) and improved management of stubble to reduce inoculum survival and spread (McDonald & Mundt, 2016). Non-chemical IPM methods resulting in lower disease pressure can reduce the rate and number of fungicide applications needed for disease control, contributing to fungicide resistance management (Chapter 3 (Corkley et al., 2025b). Use of a diverse range of disease control measures is key to the generation of an evolutionary landscape that will improve the resilience of tactics against concurrent evolution of resistance.

5.6   Supporting Information

Tables of modelling results available at: https://doi.org/10.5281/zenodo.14424058

5.7   Acknowledgements

5.8   References

Ballu, A., Deredec, A., Walker, A.-S., & Carpentier, F. (2021). Are Efficient-Dose Mixtures a Solution to Reduce Fungicide Load and Delay Evolution of Resistance? An Experimental Evolutionary Approach. *Microorganisms*, *9*(11), 2324. https://doi.org/10.3390/microorganisms9112324

Ballu, A., Despréaux, P., Duplaix, C., Dérédec, A., Carpentier, F., & Walker, A.-S. (2023). Antifungal alternation can be beneficial for durability but at the cost of generalist resistance. *Communications Biology*, *6*(1), 180. https://doi.org/10.1038/s42003-023-04550-6

Ballu, A., Ugazio, C., Duplaix, C., Noly, A., Wullschleger, J., Torriani, S. F. F., Dérédec, A., Carpentier, F., & Walker, A. (2024). Preventing multiple resistance above all: New insights for managing fungal adaptation. *Environmental Microbiology*, *26*(4). https://doi.org/10.1111/1462-2920.16614

Bliss, C. I. (1939). The Toxicity of Poisons Applied Jointly. *Annals of Applied Biology*, *26*(3), 585–615. https://doi.org/10.1111/j.1744-7348.1939.tb06990.x

Bryson, R. J., Paveley, N. D., Clark, W. S., Sylvester-Bradley, R., & Scott, R. K. (1997). Use of in-field measurements of green leaf area and incident radiation to estimate the effects of yellow rust epidemics on the yield of winter wheat. *European Journal of Agronomy*, *7*(1–3), 53–62. https://doi.org/10.1016/S1161-0301(97)00025-7

Chapman, K. S., Sundin, G. W., & Beckerman, J. L. (2011). Identification of Resistance to Multiple Fungicides in Field Populations of *Venturia inaequalis*. *Plant Disease*, *95*(8), 921–926. https://doi.org/10.1094/PDIS-12-10-0899

Chatzidimopoulos, M., Zambounis, A., Lioliopoulou, F., & Vellios, E. (2022). Detection of Venturia inaequalis Isolates with Multiple Resistance in Greece. *Microorganisms*, *10*(12), 2354. https://doi.org/10.3390/microorganisms10122354

Chen, R.-S., & McDonald, B. A. (1996). Sexual Reproduction Plays a Major Role in the Genetic Structure of Populations of the Fungus *Mycosphaerella graminicola*. *Genetics*, *142*(4), 1119–1127. https://doi.org/10.1093/genetics/142.4.1119

Corkley, I., Fraaije, B., & Hawkins, N. (2022). Fungicide resistance management: Maximizing the effective life of plant protection products. *Plant Pathology*, *71*(1). https://doi.org/10.1111/ppa.13467

Corkley, I., Mikaberidze, A., Paveley, N., van den Bosch, F., Shaw, M. W., & Milne, A. E. (2025a). Dose Splitting Increases Selection for Both Target-Site and Non-Target-Site Fungicide Resistance—A Modelling Analysis. *Plant Pathology*, *74*(4), 1152–1167. https://doi.org/10.1111/ppa.14080

Corkley, I., Helps, J., van den Bosch, F., Paveley, N. D., Milne, A. E., Mikaberidze, A., Sierotzki, H., & Skirvin, D. J. (2025b). Delaying Infection Through Phytosanitary Soybean-Free Periods Contributes to Fungicide Resistance Management in *Phakopsora pachyrhizi*: A Modelling Analysis. *Plant Pathology*, *74*(4), 1078–1096. https://doi.org/10.1111/ppa.14074

Deising, H. B., Reimann, S., & Pascholati, S. F. (2008). Mechanisms and significance of fungicide resistance. *Brazilian Journal of Microbiology*, *39*, 286–295.

Dooley, H., Shaw, M. W., Spink, J., & Kildea, S. (2016). The effect of succinate dehydrogenase inhibitor/azole mixtures on selection of *Zymoseptoria tritici* isolates with reduced sensitivity. *Pest Management Science*, *72*(6), 1150–1159. https://doi.org/10.1002/ps.4093

Duvivier, M. (2015). Distribution of the airborne inoculum of wheat leaf rust and septoria tritici blotch. PhD thesis. Belgique: Université Catholique de Louvain

Elderfield, J.A.D. (2018). Using epidemiological principles and mathematical models to understand fungicide resistance evolution. PhD thesis, University of Cambridge. https://doi.org/10.17863/CAM.22236

Elderfield, J. A. D., Lopez-Ruiz, F. J., van den Bosch, F., & Cunniffe, N. J. (2018). Using Epidemiological Principles to Explain Fungicide Resistance Management Tactics: Why do Mixtures Outperform Alternations? *Phytopathology®*, *108*(7), 803–817. https://doi.org/10.1094/PHYTO-08-17-0277-R

Eriksen, L., & Munk, L. (2003). The Occurrence of *Mycosphaerella graminicola* and its Anamorph *Septoria tritici* in Winter Wheat during the Growing Season. *European Journal of Plant Pathology*, *109*(3), 253–259. https://doi.org/10.1023/A:1022851502770

Eriksen, L., Shaw, M. W., & Østergård, H. (2001). A Model of the Effect of Pseudothecia on Genetic Recombination and Epidemic Development in Populations of *Mycosphaerella graminicola*. *Phytopathology®*, *91*(3), 240–248. https://doi.org/10.1094/PHYTO.2001.91.3.240

Fantke, P., Gillespie, B. W., Juraske, R., & Jolliet, O. (2014). Estimating Half-Lives for Pesticide Dissipation from Plants. *Environmental Science & Technology*, *48*(15), 8588–8602. https://doi.org/10.1021/es500434p

Fones, H., & Gurr, S. (2015). The impact of Septoria tritici Blotch disease on wheat: An EU perspective. *Fungal Genetics and Biology*, *79*, 3–7. https://doi.org/10.1016/j.fgb.2015.04.004

Garnault, M., Duplaix, C., Leroux, P., Couleaud, G., Carpentier, F., David, O., & Walker, A. (2019). Spatiotemporal dynamics of fungicide resistance in the wheat pathogen *Zymoseptoria tritici* in France. *Pest Management Science*, *75*(7), 1794–1807. https://doi.org/10.1002/ps.5360

Grimmer, M. K., van den Bosch, F., Powers, S. J., & Paveley, N. D. (2015). Fungicide resistance risk assessment based on traits associated with the rate of pathogen evolution. Pest Management Science, 71(2), 207–215. https://doi.org/10.1002/ps.3781

Hawkins, N. J. (2024). Assessing the predictability of fungicide resistance evolution through in vitro selection. *Journal of Plant Diseases and Protection*, *131*(4), 1257–1264. https://doi.org/10.1007/s41348-024-00906-0

Hawkins, N. J., & Fraaije, B. A. (2021). Contrasting levels of genetic predictability in the evolution of resistance to major classes of fungicides. *Molecular Ecology*, *30*(21), 5318–5327. https://doi.org/10.1111/mec.15877

Hobbelen, P. H. F., Paveley, N. D., Oliver, R. P., & van den Bosch, F. (2013). The Usefulness of Fungicide Mixtures and Alternation for Delaying the Selection for Resistance in Populations of *Mycosphaerella graminicola* on Winter Wheat: A Modeling Analysis. *Phytopathology®*, *103*(7), 690–707. https://doi.org/10.1094/PHYTO-06-12-0142-R

Hobbelen, P. H. F., Paveley, N. D., & van den Bosch, F. (2011). Delaying selection for fungicide insensitivity by mixing fungicides at a low and high risk of resistance development: A modeling analysis. *Phytopathology*, *101*(10), 1224–1233. https://doi.org/10.1094/PHYTO-10-10-0290

Hollomon, D. W., & Brent, K. J. (2009). Combating plant diseases—the Darwin connection. *Pest Management Science*, *65*(11), 1156–1163. https://doi.org/10.1002/ps.1845

Hunter, Coker, & Royle. (1999). The teleomorph stage, *Mycosphaerella graminicola* , in epidemics of septoria tritici blotch on winter wheat in the UK. *Plant Pathology*, *48*(1), 51–57. https://doi.org/10.1046/j.1365-3059.1999.00310.x

Kristoffersen, R., Heick, T. M., Müller, G. M., Eriksen, L. B., Nielsen, G. C., & Jørgensen, L. N. (2020). The potential of cultivar mixtures to reduce fungicide input and mitigate fungicide resistance development. *Agronomy for Sustainable Development*, *40*(5), 36. https://doi.org/10.1007/s13593-020-00639-y

Lobo, I., Shaw, K. (2008). Thomas Hunt Morgan, Genetic Recombination, and Gene Mapping. *Nature Education* 1(1): 205.

McDonald, B. A., & Mundt, C. C. (2016). How Knowledge of Pathogen Population Biology Informs Management of Septoria Tritici Blotch. *Phytopathology®*, *106*(9), 948–955. https://doi.org/10.1094/PHYTO-03-16-0131-RVW

Miko, I. (2008) Gregor Mendel and the principles of inheritance. *Nature Education* 1(1):134

Milgroom, M. G., & Fry, W. E. (1988). A Simulation Analysis of the Epidemiological Principles for Fungicide Resistance Management in Pathogen Populations. *Phytopathology*, *78*(5), 565. https://doi.org/10.1094/Phyto-78-565

Morgan, C., Wright, P., Blake, J., Corkley, I., Knight, S., Burnett, F. (2021). Combining agronomy, variety and chemistry to maintain control of septoria tritici in wheat. AHDB Project Report No. 634, pp 1-113. Available at: https://projectblue.blob.core.windows.net/media/Default/Research%20Paper s/Cereals%20and%20Oilseed/2021/PR634%20final%20project%20report.p df [Accessed: 17 November 2024].

Morgan, T.H. (1911). Random segregation versus coupling in Mendelian inheritance. *Science* 34, 384.

Müller, M. A., Stammler, G., & May De Mio, L. L. (2021). Multiple resistance to DMI, QoI and SDHI fungicides in field isolates of Phakopsora pachyrhizi. *Crop Protection*, *145*, 105618. https://doi.org/10.1016/j.cropro.2021.105618

Omrane, S., Audéon, C., Ignace, A., Duplaix, C., Aouini, L., Kema, G., Walker, A.-S., & Fillinger, S. (2017). Plasticity of the *MFS1* Promoter Leads to Multidrug Resistance in the Wheat Pathogen *Zymoseptoria tritici*. *MSphere*, *2*(5). https://doi.org/10.1128/mSphere.00393-17

Paveley, N. D., Thomas, J. M., Vaughan, T. B., Havis, N. D., & Jones, D. R. (2003). Predicting effective doses for the joint action of two fungicide applications. *Plant Pathology*, *52*(5), 638–647. https://doi.org/10.1046/j.1365-3059.2003.00881.x

Paveley, N., Young, C., Fraaije, B.., van den Bosch, F., Kildea, S., Burnett, F. et al. (2023). Choice of resistance management tactics: how flexible should we be? In: Deising HB; Fraaije B; Mehl A; Oerke EC; Sierotzki H; Stammler G (Eds), "Modern Fungicides and Antifungal Compounds", Vol. X, pp. 205-211. © 2023. Deutsche Phytomedizinische Gesellschaft, Braunschweig, ISBN: 978-3-941261-17-4

Rupp, S., Weber, R. W. S., Rieger, D., Detzel, P., & Hahn, M. (2017). Spread of Botrytis cinerea Strains with Multiple Fungicide Resistance in German Horticulture. *Frontiers in Microbiology*, 7, 2075. https://doi.org/10.3389/fmicb.2016.02075

Shaw, M. W., & Royle, D. J. (1989). Airborne inoculum as a major source of *Septoria tritici* (*Mycosphaerella graminicola*) infections in winter wheat crops in the UK. *Plant Pathology*, *38*(1), 35–43. https://doi.org/10.1111/j.1365-3059.1989.tb01425.x

Shaw, M.W., Royle, D.J., 1993. Factors determining the severity of epidemics of *Mycosphaerella graminicola* (*Septoria tritici*) on winter wheat in the UK. *Plant Pathology* 42, 882–899. https://doi.org/10.1111/j.1365-3059.1993.tb02674.x

Suffert, F., Delestre, G., & Gélisse, S. (2019). Sexual Reproduction in the Fungal Foliar Pathogen Zymoseptoria tritici Is Driven by Antagonistic Density Dependence Mechanisms. *Microbial Ecology*, *77*(1), 110–123. https://doi.org/10.1007/s00248-018-1211-3

Suffert, F., Sache, I., & Lannou, C. (2011). Early stages of septoria tritici blotch epidemics of winter wheat: build-up, overseasoning, and release of primary inoculum. *Plant Pathology*, *60*(2), 166–177. https://doi.org/10.1111/j.1365-3059.2010.02369.x

Taylor, N. P., & Cunniffe, N. J. (2023a). Modelling quantitative fungicide resistance and breakdown of resistant cultivars: Designing integrated disease management strategies for Septoria of winter wheat. *PLOS Computational Biology*, *19*(3), e1010969. https://doi.org/10.1371/journal.pcbi.1010969

Taylor, N. P., & Cunniffe, N. J. (2023b). Optimal Resistance Management for Mixtures of High-Risk Fungicides: Robustness to the Initial Frequency of Resistance and Pathogen Sexual Reproduction. *Phytopathology*, *113*(1), 55–69. https://doi.org/10.1094/PHYTO-02-22-0050-R

te Beest, D. E., Paveley, N. D., Shaw, M. W., & van den Bosch, F. (2013). Accounting for the Economic Risk Caused by Variation in Disease Severity in Fungicide Dose Decisions, Exemplified for *Mycosphaerella graminicola* on Winter Wheat. *Phytopathology®*, *103*(7), 666–672. https://doi.org/10.1094/PHYTO-05-12-0119-R

Trkulja, N. R., Milosavljević, A. G., Mitrović, M. S., Jović, J. B., Toševski, I. T., Khan, M. F. R., & Secor, G. A. (2017). Molecular and experimental evidence of multi-resistance of Cercospora beticola field populations to MBC, DMI and QoI fungicides. *European Journal of Plant Pathology*, *149*(4), 895–910. https://doi.org/10.1007/s10658-017-1239-0

van den Berg, F., van den Bosch, F., & Paveley, N. D. (2013). Optimal Fungicide Application Timings for Disease Control Are Also an Effective Anti-Resistance Strategy: A Case Study for *Zymoseptoria tritici* (*Mycosphaerella graminicola*) on Wheat. *Phytopathology®*, *103*(12), 1209–1219. https://doi.org/10.1094/PHYTO-03-13-0061-R

van den Bosch, F., Lopez-Ruiz, F., Oliver, R., Paveley, N., Helps, J., & van den Berg, F. (2018). Identifying when it is financially beneficial to increase or decrease fungicide dose as resistance develops. *Plant Pathology*, *67*(3), 549–560. https://doi.org/10.1111/ppa.12787

van den Bosch, F., Oliver, R., van den Berg, F., & Paveley, N. (2014a). Governing Principles Can Guide Fungicide-Resistance Management Tactics. *Annual*

Review of Phytopathology, *52*(1), 175–195. https://doi.org/10.1146/annurev-phyto-102313-050158

van den Bosch, F., Paveley, N., van den Berg, F., Hobbelen, P., & Oliver, R. (2014b). Mixtures as a Fungicide Resistance Management Tactic. *Phytopathology®, 104*(12), 1264–1273. https://doi.org/10.1094/PHYTO-04-14-0121-RVW

van den Bosch, F., Smith, J., Wright, P., Milne, A., van den Berg, F., Kock-Appelgren, P., Foulkes, J., & Paveley, N. (2022). Maximizing realized yield by breeding for disease tolerance: A case study for Septoria tritici blotch. *Plant Pathology*, *71*(3), 535–543. https://doi.org/10.1111/ppa.13509

Young, C., Boor, T., Corkley, I. Fraaije, B., Clark, B., Havis N. et al. (2021). Managing resistance evolving concurrently against two or more modes of action to extend the effective life of new fungicides. AHDB Project Report No. 637, pp 1-91. Available at:

https://projectblue.blob.core.windows.net/media/Default/Research%20Papers/Cereals%20and%20Oilseed/2021/PR637%20final%20project%20report.pdf [Accessed: 16 November 2024].

Zadoks, J. C., Chang, T. T., & Konzak, C. F. (1974). A decimal code for the growth stages of cereals. *Weed Research*, *14*(6), 415–421. https://doi.org/10.1111/j.1365-3180.1974.tb01084.x

Zhan, J., Pettway, R. E., & McDonald, B. A. (2003). The global genetic structure of the wheat pathogen Mycosphaerella graminicola is characterized by high nuclear diversity, low mitochondrial diversity, regular recombination, and gene flow. *Fungal Genetics and Biology*, *38*(3), 286–297. https://doi.org/10.1016/S1087-1845(02)00538-8

Chapter 6

Azole mixtures: Modelling resistance management benefits of incomplete cross-resistance within a fungicide mode of action group

I. Corkley[1,2,3], N.D. Paveley[4], B.A. Fraaije[5], J. Helps[1], M.W. Shaw[3], A.E. Milne[1], N.J. Hawkins[6], F. van den Bosch[7,8]

[1]*Net Zero and Resilient Farming, Rothamsted Research, Harpenden, UK.* [2]*Sustainable Agricultural Systems, ADAS, Wolverhampton, UK.* [3]*School of Agriculture, Policy and Development, University of Reading, Reading, UK.* [4]*Sustainable Agricultural Systems, ADAS, High Mowthorpe, UK.* [5]*BU Biointeractions and Plant Health, Wageningen Plant Research, Wageningen University and Research, Wageningen, The Netherlands.* [6]*NIAB, Cambridge, UK.* [7]*Quantitative Biology & Epidemiology Group, Plant Pathology Department (Visiting Scholar), University of California, Davis, USA.* [8]*Sustainable Agricultural Systems, ADAS, Rosemaund, UK.*

The level of cross-resistance in a pathogen population to two fungicides is measured by the correlation of the sensitivity of pathogen strains to each fungicide. Strong positive cross-resistance implies that pathogen strains that are sensitive to one fungicide are also sensitive to the second fungicide, pathogen strains that are moderately resistant to the first fungicide are also moderately resistant to the second, and pathogen strains that are highly resistant to one fungicide are also highly resistant to the second fungicide. Low cross-resistance implies that there is little to no correlation between the sensitivity of pathogen strains to each fungicide.

Most existing modelling studies of the evolution of resistance assume that there is complete cross-resistance between fungicides with the same MoA, and a complete lack of cross-resistance between fungicides with different MoA, in the case of single-resistant strains, with these cases modelled using an additive dose model (ADM) or a multiplicative survival model (MSM) respectively. In Chapter 5, I modelled strains that had resistance to two MoA due to a combination of two resistance genes with independent inheritance: the MSM modelling approach was

suitable for this case. However, there are important examples of incomplete cross-resistance within a MoA, including azole fungicides in the demethylation inhibitor (DMI) group: a large number of combinations of target-site mutations in the target CYP51 enzyme have led to pathogen strains with variable resistance profiles against different azoles. Neither the ADM or MSM modelling approaches are appropriate for this case.

There is some limited experimental evidence that using azole programmes with a diverse range of active substances with the same MoA but incomplete cross-resistance could contribute to fungicide resistance management (Heick et al., 2017), but it is unclear how these benefits vary with the choice of azole fungicide, the level of incomplete cross-resistance between azoles, the number of azole active substances available, or the way that active substance diversity is deployed (mixture, alternation within-year or between years, or mosaic at a landscape level).

In this chapter, I describe the development of a mathematical population genetic model that represents the joint target-site action of fungicides with the same MoA but incomplete cross-resistance. I investigate how the resistance management benefits of mixtures of fungicides with the same MoA but incomplete cross-resistance vary with the number of active substances and the degree of cross-resistance between fungicides included in the mixture. In the supporting information, I compare the performance of programmes utilising mixture, alternation or mosaic within a MoA with incomplete cross-resistance. The supporting information was published as a short paper, 'Modelling resistance management benefits of diversity with a fungicidal mode of action with incomplete cross-resistance: the azoles example' has been published in "Modern Fungicides and Antifungal Compounds", Vol. X (2023), the Proceedings Volume of the 20th International Reinhardsbrunn Symposium on Modern Fungicides and Antifungal Compounds, held in April 2023.

6.1   Abstract

Mixing fungicides with different modes of action (MoA) is a well-established resistance management tactic which relies on the general absence of cross-resistance between MoAs. Mixtures of fungicides with the same MoA and complete cross-resistance do not contribute to resistance management. However, in some cases cross-resistance is only partial within a MoA, for example azole fungicides in the demethylation inhibitor (DMI) group (FRAC Code 3). We developed and used a mathematical population genetic model to explore possible resistance

management benefits of mixtures of fungicides with the same MoA with incomplete cross-resistance. An important example in agriculture is the deployment of DMIs against the wheat pathogen *Zymoseptoria tritici*. We modelled selection for known *Z. tritici* CYP51 haplotypes following application of solo azoles or two, three or four-way mixtures of epoxiconazole, prothioconazole, prochloraz and tebuconazole (all programmes having the same total dose as a proportion of full label rate). We measured the rate of resistance development as the resulting rate of change in the pathogen population growth rate, $\Delta \bar{r}$, and compared disease control against a minimum threshold. We focused on within-MoA programmes to investigate resistance management benefits of within-MoA active substance diversity; in practice azoles should be used in combination with other MoA wherever possible. Our results show that mixtures of fungicides with incomplete cross-resistance within a MoA can contribute to resistance management, achieving greater stability in disease control over time. Increasing the number of azole active substances in a mixture reduced $\Delta \bar{r}$ on average, but with diminishing returns. A generalised linear model fitted to the population genetic model results showed that $\Delta \bar{r}$ increased with the average level of disease control and with the maximum variance in haplotype sensitivity to an individual azole component. Azole combinations with low or negative cross-resistance maximised resistance management benefits, but any degree of incomplete cross-resistance was useful.

6.2   Introduction

Azoles, part of the demethylation inhibitor (DMI) group of fungicides (FRAC Code 3), have played an important role in crop protection since their introduction in the 1970s. Over time, increasing levels of partially resistant pathogen strains have reduced the efficacy of some azole fungicides, but modern azole compounds are still an important component of fungicide programmes for a wide variety of crops and plant diseases (Cools et al., 2013; Jørgensen and Heick, 2021). It has been hypothesized that azole mixtures could contribute to fungicide resistance management (Dooley et al., 2016b; EPPO Workshop, 2010), because of incomplete cross-resistance between some azole fungicides. Use of azole mixtures has been shown to improve disease control compared to use of a single azole and to provide a more consistent level of disease control across different locations (Jørgensen et al., 2018), and azole mixtures may also be chosen by commercial growers to improve broad-spectrum control against a range of plant pathogens (Dooley et al., 2016). However, all azoles share the same mode of action (MoA) with a single target-site: inhibition of the sterol 14a-demethylase

(CYP51) enzyme which catalyses the conversion of lanosterol into ergosterol, an essential component of fungal cell membranes (Rodrigues, 2018). Mixture of active substances within a MoA is not usually recommended for resistance management, as there is typically strong positive cross-resistance of pathogen strain sensitivity between active substances in the same MoA: isolates that are resistant to one active substance in the MoA tend to be resistant to other active substances in the same MoA, and vice versa.

Use of mixtures of fungicides with different MoAs is a proven resistance management tactic to slow the rate of pathogen evolution (Corkley et al., 2022; van den Bosch et al., 2014a, 2014b). This tactic works because there is generally a lack of cross-resistance between MoA. Strains with a high resistance factor to one MoA are therefore controlled by the other MoA, resulting in similar population growth rates for both resistant and sensitive strains and reducing the strength of selection for resistance. This holds particularly if resistance occurs primarily by target-site mutations or overexpression of the fungicide target gene. Efflux mechanisms create a degree of cross-resistance between single-site acting MoA, but the resistance factors in fungal pathogens resulting from efflux mechanisms have been low thus far, as high resistance factors have occurred only where efflux has combined with target-site alterations or upregulation of the fungicide target protein (Leroux & Walker, 2013; Omrane et al., 2015).

Patterns of cross-resistance between fungicides in the demethylation inhibitor (DMI) group include both cases described above – an absence of cross-resistance and strong positive cross-resistance – in addition to weak positive cross-resistance and negative cross-resistance (Dooley et al., 2016; Fraaije et al., 2007; Jørgensen et al., 2021; Leroux et al., 2000; Leroux and Walker, 2011). The primary cause of azole resistance in many pathogens is CYP51 target-site alternation, although target-site overexpression and increased non-target-site efflux pump activity are also implicated (Cools et al., 2013; Cools & Fraaije, 2013). The effects of these target-site mutations vary between azole fungicides due to structural differences at a molecular level and variation in the binding activity of different azole ligands with regions involved in or bordering the CYP51 enzyme active site (Mullins et al., 2011; Xiao et al., 2004); in some cases, a mutation that increases resistance to some azoles increases sensitivity to others. For example, the alteration I381V decreases pathogen sensitivity to tebuconazole, but has little effect on sensitivity to epoxiconazole, and increases sensitivity to prochloraz (Fraaije et al., 2007; Mullins et al., 2011; Stammler et al., 2008). Interactions between multiple CYP51 mutations

can also affect the sensitivity phenotype. *Zymoseptoria tritici,* a polycyclic foliar fungal pathogen which causes septoria leaf blotch (STB) in wheat, has accumulated large numbers of target-site alterations of the CYP51 protein. The *Z. tritici* population is composed of multiple strains, each with different combinations of these target-site mutations and differing levels of sensitivity to each azole active substance.

Differential effects of azoles on selection for strains with different CYP51 combinations have been observed in *Z. tritici*, *Phakopsora pachyrhizi* (the cause of Asian soybean rust) and *Cercospora beticola* (the cause of Cercospora leaf spot of sugar beet) (Heick et al., 2017; Kayamori et al., 2021; Stammler et al., 2008; Stilgenbauer et al., 2023). It has therefore been hypothesised that azole mixtures could contribute to resistance management. However, there is limited existing evidence to show whether mixtures of active substances with incomplete cross-resistance within a MoA can provide resistance management benefits, or how within-MoA mixtures could best be deployed to maximise any such benefits. Mixtures of epoxiconazole and metconazole did not reduce selection for *Z. tritici* strains with reduced sensitivity when compared to solo application (at the same total azole dose) of either fungicide (Dooley et al., 2016), but increased diversity of azole active substances in application programmes has been shown to reduce selection overall for CYP51 alterations (Heick et al., 2017). There are no previous modelling studies of the effect on selection for resistance of within-MoA mixtures with incomplete cross-resistance.

To model the resistance management benefit of a fungicide mixture, an estimate of the effect of the mixture on pathogen growth rates is needed, as the difference in the growth rates of resistant and sensitive strains determines the strength of selection for resistance (van den Bosch et al., 2014a). Existing models of the joint action in mixture of two or more fungicides on pathogen growth rates typically use either an additive dose model (ADM) or a multiplicative survival model (MSM). These describe alternative methods of combining the dose-response curves of the fungicides (when applied solo) to estimate the effect of the mixture. In ADMs, the effects of the doses of each fungicide in the mixture are added together. Dose rates of each fungicide calculated from the solo dose-response curves as giving equivalent levels of control could be substituted for each other with no change in the overall level of control of the mixture. In the MSM, the effects of each fungicide on the pathogen growth rate are multiplied together. The ADM is typically applied to mixtures within a MoA, and the MSM to mixtures of different MoA (Corkley et al.,

2022; Morse, 1978; Paveley et al., 2003). If cross-resistance within a MoA is close to complete, then the additive dose model is appropriate: i.e. mixtures within the MoA are the equivalent of mixing the same product with itself and so do not contribute to resistance management (Oliver, 2016). If cross-resistance is weak, then the benefits of active substance diversity within a MoA would be close to the benefits of diversity between MoA, as described by the MSM. The joint target-site action of fungicides within a MoA with incomplete cross-resistance, as observed for azole fungicides, cannot be adequately described by either the ADM or MSM.

Of the many pathogens targeted by azole programmes, *Z. tritici* is one of the most common and economically damaging disease of winter wheat crops in Europe and worldwide, associated with reduced crop quality and yield losses of up to 50% in severe epidemics (Fones & Gurr, 2015). Due to its importance and proven potential for rapid evolution of fungicide resistance (Cools & Fraaije, 2013; Dooley et al., 2016a; McDonald et al., 2022, 2019; Rehfus et al., 2018; Torriani et al., 2009), it is also one of the most intensively studied crop pathogens. The datasets generated through sampling and study of *Z. tritici* isolates make this pathogen an excellent case study for parameterisation of a model of the effects of within-MoA mixtures. *Zymoseptoria tritici* has both sexual and asexual reproductive cycles, but the majority of infection during the growing season is driven by asexual haploid pycnidiospores, spread between leaves by contact and rain splash (Ponomarenko et al., 2011; Shaw & Royle, 1993). We can therefore consider the effect of the haploid CYP51 genotype ('haplotype') on the growth rate of strains in the presence of fungicides – i.e. the effect of singular chromosomes rather than pairs of chromosomes. We refer to singular CYP51 variants as 'haplotypes'. A few key CYP51 haplotypes typically comprise a high proportion of the *Z. tritici* population in any season (Glaab et al., 2024; Kildea et al., 2023). The laboratory sensitivities of these key haplotypes to contrasting azoles have been determined (Cools et al., 2011; Huf et al., 2018; Kildea et al., 2019, 2023; Kirikyali et al., 2017), and recent analysis of long-term datasets has related laboratory to field sensitivities (Blake et al., 2018), enabling parameterisation of the field sensitivities of haplotypes for a population genetic approach.

We introduce a population genetic model that tracks CYP51 haplotype frequencies in the pathogen population under a range of azole fungicide treatment programmes. This model was developed from known population genetic theory (Crow & Kimura, 1977), with a sub-model introduced to account for the joint target-site action of multiple azoles. Our approach explicitly models the growth of

individual haplotypes and fungicide dose decay, enabling modelling of a wide range of fungicide programmes. The model and its application to simulate azole mixture, alternation and mosaic programmes were described in brief in Corkley et al. (2023) (see Appendix 6.E). Here we describe the model derivation and parameterisation for *Z. tritici* CYP51 haplotypes in full, and use the model to investigate resistance management benefits of mixtures within a MoA with incomplete cross-resistance, aiming to answer the following questions:

(a) Are there resistance management benefits of mixture within the same mode of action?

(b) Are there resistance management benefits of additional active substances within a mode of action ('azole diversity')?

(c) How do resistance management benefits vary with the degree of cross-resistance between active substances?

6.3   Materials and Methods

6.3.1 Measuring resistance management benefits

6.3.1.1 Selection for fungicide resistance: rate of change in epidemic growth rate

Each CYP51 haplotype has its own population growth rate, r_i, under an azole fungicide treatment regime (Figure 6.1a). These differences in population growth rate cause the frequencies of the haplotypes in the pathogen population to change. A haplotype that has a larger growth rate than the average of the entire population will increase in frequency, whilst a haplotype that has a lower growth rate will decrease in frequency. Haplotypes with lower sensitivity to a fungicide will have the highest growth rates in the present of fungicide.

The population growth of each haplotype can be calculated and the frequency of it in the total pathogen population tracked through time. Such ensembles of haplotypes and their population dynamics are of interest to plant pathologists and theoretical biologists. However, growers are interested in the growth rate of the entire pathogen population, $\bar{r}$, since this determines the level of damage to the crop (Figure 6.1b). $\bar{r}$ is the average population growth rate of the pathogen including all pathogen strains.

Since fungicide applications select for the strains that are less sensitive to fungicide, over time they select for an increase in the average epidemic growth rate, $\bar{r}$. Resistance management aims to minimise this increase. We therefore use the rate of change in $\bar{r}$ from one year to the next, $\Delta\bar{r}$, as a measure of selection for

fungicide resistance. Denoting the growth rate of the pathogen population in year n as $\bar{r}_n$, the rate of resistance development is measured as:

$$\Delta\bar{r} = \frac{\overline{r_{n+1}} - \bar{r}_n}{\bar{r}_n} \tag{1}$$

a. What the plant pathologist sees   b. What the grower sees
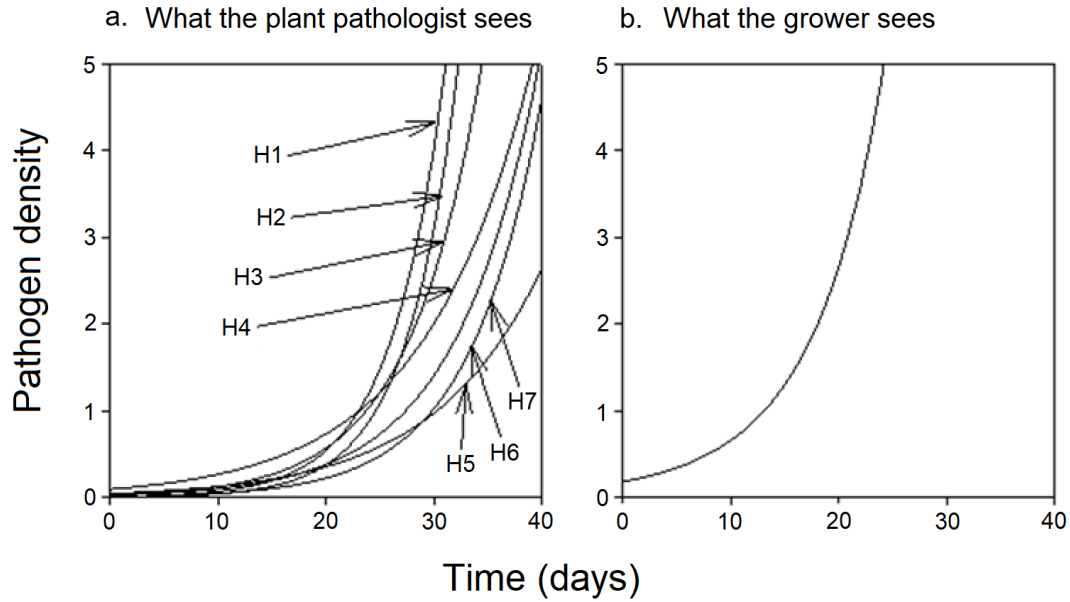
Figure 6.1: Epidemic growth rates: what a plant pathologist sees versus what a grower sees. (a). Sub-populations of seven pathogen haplotypes (H1 to H7), each with a different initial density and a different sub-population growth rate, r_i, are shown. (b). The epidemic the grower observes in the field is the sum of the densities of all haplotypes, with average growth rate $\bar{r}$.

6.3.1.2 Threshold for effective disease control

An effective fungicide programme is one that prevents economically damaging levels of disease. We follow previous studies (Gladders et al., 2001; Pietravalle et al., 2003; te Beest et al., 2009) in defining a damaging epidemic as one where *Z. tritici* severity on the upper three leaves exceeds 5% at growth stage 75 (GS75) on Zadok's scale (Zadoks et al., 1974). We therefore use 5% severity at GS75 as a threshold value, S_{Max}, to measure whether a fungicide programme provides adequate disease control.

6.3.2 The population genetic model

6.3.2.1 CYP51 and the azole dose-response curve

The CYP51 enzyme takes part in the conversion of lanosterol into ergosterol by removal of the 14α-methyl group from sterol substrates (Zhang et al., 2019).

Ergosterol is an essential building block of cell membranes and acts to maintain membrane integrity (Rodrigues, 2018). Azole fungicides affect pathogen fitness by targeting the CYP51 enzyme. We assume that azole fungicides act as competitive CYP51 inhibitors which bind to the enzyme and occupy the P450 active site, preventing binding of lanosterol and its conversion into ergosterol (Hargrove et al., 2015, 2018). The resulting reduction in ergosterol production reduces the fungal growth rate.

Lanosterol binds to the enzyme at rate k_1, and either unbinds from the enzyme at rate k_{-1}, or is converted to ergosterol at rate k_2. The binding of an azole molecule to the enzyme at rate k_3 is reversible, so the azole molecule can unbind at rate k_{-3} (Figure 6.A.1, Appendix 6.A). Assuming this process is in steady-state (Michaelis & Menten, 1913; Murray, 1991), we can calculate the rate of ergosterol production, V, from Hill's equation (Hill, 1913) as used in enzyme kinetics studies and as a dose-response curve in fungicide resistance models (Mikaberidze et al., 2017):

$$V = \frac{A}{1 + BD} \tag{2}$$

where $A = \frac{k_1 L E_0}{k_{-1} + k_2 + k_1 L}$ and $B = \frac{k_3}{k_{-3}} \frac{k_{-1} + k_2}{k_{-1} + k_2 + k_1 L}$, where L is the concentration of lanosterol, E_0 is the total concentration of CYP51 enzyme (free and bound), B is the dose-response parameter for the azole fungicide and D is the fungicide dose.

Assuming competitive binding of azole molecules, meaning that when an azole molecule is bound to the CYP51 enzyme, other azole molecules cannot bind to that CYP51 molecule, we generalise equation (2) for the rate of ergosterol production, V, to mixtures of azoles:

$$V = \frac{A}{1 + B_1 D_1 + B_2 D_2} \tag{3}$$

where B_1 and B_2 are the dose-response parameters for azole 1 and azole 2 respectively and D_1 and D_2 are the doses of azole 1 and azole 2 respectively. An illustration of the dose-response curve of the ergosterol production rate, V, to a mixture of two azoles for varying values of B_1 and $B_2 = 1$ is shown in Figure 6.A.2 in Appendix 6.A. Note that although we show here the derivation of the dose-response curve for competitive inhibition, the form of the dose-response curve is the same for non-competitive inhibition (see Section 6.A.1 in Appendix 6.A).

We generalise equation (3) to include more than two azoles and multiple pathogen haplotypes:

$$V_i = \frac{A}{1 + \sum_{j=1}^{jmax} B_{ij}D_j} \qquad (4)$$

where V_i is the rate of ergosterol production of pathogen haplotype i, the subscript j denotes each azole fungicide, and the number of azoles used is $jmax$. For haplotypes with one or more mutations in the gene coding for the CYP51 enzyme, binding of the azole to CYP51 will be more difficult, and/or make unbinding easier, equating to a smaller value of B_{ij} (i.e. less inhibition of the enzyme function).

For the purpose of modelling the application of azole fungicides, we assume that the only process varying between haplotypes is the ergosterol production rate. We can therefore describe the fungal population growth rate as affected by azole fungicides:

$$r_i = \frac{r_0}{1 + \sum_{j=1}^{jmax} B_{ij}D_j} \qquad (5)$$

where r_i is the population growth rate of fungal haplotype i, r_0 is the growth rate of the pathogen when no fungicide is applied, D_j is the dose of azole j and B_{ij} describes the effect of azole j on the growth rate of haplotype i. We assume that that there is no fitness cost due to the development of resistance, so r_0 is the same for all haplotypes: i.e. when no fungicide is present, all pathogen haplotypes have the same population growth rate. Equation (5) thus defines the dose-response curve for the growth rate of all pathogen haplotypes and all azole treatments.

6.3.2.2 The growth rate of the sub-population of a haplotype following azole application

The model defines the fungicide dose as a function of time, so that applications can be simulated at several points during the crop growing season. We assume that the concentration of the fungicide immediately following application is the applied dose, or the applied dose plus any residual concentration from the previous application. After the spray we assume that the fungicide decays exponentially due to processes such as plant metabolism and UV degradation:

$$D_j(t) = \begin{cases} D_{j_0}e^{-\alpha(t-t^*)}, & t \geq t^* \\ 0, & t < t^* \end{cases} \qquad (6)$$

where $D_j(t)$ is the dose of azole j at time t, t^* is the time of the first application of azole j, D_{j0} is the application dose of azole j, expressed as a proportion of the

maximum permitted individual dose (as defined on the product label), and α is the decay rate of the fungicide. If an additional application of fungicide j is made at t^{**}, the remaining dose from the application at t^* is added to the dose from t^{**} to calculate the total remaining dose.

In field experiments, dose-response curves are usually plotted as the severity of the epidemic (after an interval of time following fungicide application) as a function of fungicide dose. Assuming that the pathogen population grows exponentially in time (i.e. that density dependence does not limit growth during the period relevant for fungicide activity), we can calculate the severity of the epidemic at any point in time, t. The fungicide dose determines the pathogen sub-population growth rate, r_i, which in turn determines the population size/severity of the epidemic (Figure 6.1).

6.3.2.2.1 Haplotype severity following application of a single azole

From equation (5), the growth rate of haplotype i as affected by fungicide dose $D_j(t)$ is:

$$r_i\left(D_j(t)\right) = \frac{r_0}{1 + B_{ij}D_j(t)} \tag{7}$$

The dynamics of the pathogen sub-population of haplotype i is given by:

$$\frac{d\,S_i(t)}{d\,t} = r_i\left(D_j(t)\right)S_i(t) \tag{8}$$

where $S_i(t)$ is the disease severity caused by haplotype i at time t.

This model can be solved (see Section 6.A.2 in Appendix 6.A) to calculate the severity at the end of the growing season, $t = T$.

For one fungicide application at dose D_{j0} at time t^*, the disease severity caused by haplotype i at the end of the growing season, $S_i(T)$, is given by:

$$S_i(T) = S_i(0)e^{r_0 t^*}\left(\frac{B_{ij}D_{j0} + e^{\alpha(T-t^*)}}{B_{ij}D_{j0} + 1}\right)^{\frac{r_0}{\alpha}} \tag{9}$$

where $S_i(0)$ is the severity of haplotype i at the start of the simulation. For two applications at dose D_{j0}, one at t^*, the second at t^{**}:

$$S_i(T) = S_i(0)e^{r_0 t^*}\left(\frac{B_{ij}D_{j0} + e^{\alpha(t^{**}-t^*)}}{B_{ij}D_{j0} + 1}\right)^{\frac{r_0}{\alpha}}\left(\frac{B_{ij}D_{j0}\left(1 + e^{-\alpha(t^{**}-t^*)}\right) + e^{\alpha(T-t^{**})}}{B_{ij}D_{j0}\left(1 + e^{-\alpha(t^{**}-t^*)}\right) + 1}\right)^{\frac{r_0}{\alpha}} \tag{10}$$

6.3.2.2.2 Haplotype severity following application of multiple azoles

The equations in Section 6.3.2.2.1 can be generalised to include more than one azole. In the case of mixing azoles, equation (7), combined with equation (6) for fungicide dose decay, becomes:

$$r_i\big(D_1(t), D_2(t)\big) = \frac{r_0}{1 + B_{i1}D_{10}e^{-\alpha_1 t} + B_{i2}D_{20}e^{-\alpha_2 t}} \tag{11}$$

If $\alpha_1 \neq \alpha_2$, it is not straightforward to solve the model equation (8), and recourse to numerical solutions is required. In the case that the fungicide decay rates are equal, $\alpha_1 = \alpha_2$, the model is solved with a generalisation of equations (9) and (10) using the term $\sum_{j=1}^{jmax} B_{ij}D_j$ as in equation (5):

One application of an azole mixture at time t^*:

$$S_i(T) = S_i(0)e^{r_0 t^*}\left(\frac{\sum_{j=1}^{jmax} B_{ij}D_j + e^{\alpha(T - t^*)}}{\sum_{j=1}^{jmax} B_{ij}D_j + 1}\right)^{\frac{r_0}{\alpha}} \tag{12}$$

Two applications of an azole mixture, one at t^*, the second at t^{**}:

$$S_i(T) = S_i(0)e^{r_0 t^*}\left(\frac{\sum_{j=1}^{jmax} B_{ij}D_j + e^{\alpha(t^{**} - t^*)}}{\sum_{j=1}^{jmax} B_{ij}D_j + 1}\right)^{\frac{r_0}{\alpha}}\left(\frac{\sum_{j=1}^{jmax} B_{ij}D_j\left(1 + e^{-\alpha(t^{**} - t^*)}\right) + e^{\alpha(T - t^{**})}}{\sum_{j=1}^{jmax} B_{ij}D_j\left(1 + e^{-\alpha(t^{**} - t^*)}\right) + 1}\right)^{\frac{r_0}{\alpha}} \tag{13}$$

6.3.2.3 Growth rate of the overall pathogen population

The total pathogen population growth rate, $\bar{r}$, is calculated as the average growth rate over all the haplotypes in the population:

$$\bar{r} = \frac{\ln(\theta_1 e^{r_1 T} + \theta_2 e^{r_2 T} + \cdots + \theta_M e^{r_M T})}{T} \tag{14}$$

where θ_i is the frequency of haplotype i, r_i is the sub-population growth rate of haplotype i, M is the total number of haplotypes in the population and T is the length of time simulated (see section 6.3.3.1). The larger the difference between the sub-population growth rate of a haplotype, r_i, and the mean total pathogen population growth rate, $\bar{r}$, the greater the rate of selection for or against that haplotype.

The sub-population growth rate of a haplotype is interpreted as the mean growth rate over the cropping season, $\bar{r_i}$. As the sub-population growth rate of a haplotype varies during the growing season, due to the application and subsequent decay of the fungicide, we calculate the mean haplotype growth rate using the expressions:

$$S_i(T) = S_i(0)e^{\bar{r_i}T} \text{ and } S_i(T) = S_i(0)G_i \qquad (15)$$

Where the term G_i can be derived from equation (12) or (13) depending on the number of azole applications. The severity of haplotype i at the start of the simulation, $S_i(0)$, can be calculated from the initial severity of the overall pathogen population at $t = 0$, I_0, and the proportion of haplotype i in the initial infection of the crop, $\theta_{i_{\text{start}}}$:

$$S_i(0) = I_0\theta_{i_{\text{start}}} \qquad (16)$$

It follows that:

$$\bar{r_i} = \frac{1}{T}\ln\left(\frac{S_i(T)}{S_i(0)}\right) = \frac{1}{T}\ln(G_i) \qquad (17)$$

The mean total population growth rate/fitness in the first growing season is given by:

$$\overline{r_{y1}} = \frac{1}{T}\ln\left(\sum_{i=1}^{M}\theta_{i_{\text{start}}}e^{\bar{r_i}T}\right) \qquad (18)$$

At the end of the first growing season, the haplotype frequencies are:

$$\theta_{i_{\text{end}}} = \frac{\theta_{i_{\text{start}}}G_i}{\sum_{i=1}^{M}\theta_{i_{\text{start}}}G_i} \qquad (19)$$

The mean population growth rate in the second year is therefore:

$$\overline{r_{y2}} = \frac{1}{T}\ln\left(\sum_{i=1}^{M}\theta_{i_{\text{end}}}e^{\bar{r_i}T}\right) \qquad (20)$$

Our measure of selection for fungicide resistance, the rate of increase in total population growth rate, $\Delta\bar{r}$, can therefore be calculated by substituting equations (18) and (20) into equation (1).

The overall disease severity at time T, $S(T)$, our measure of disease control for comparison to the threshold value for effective disease control (see Section 6.3.1.2) is calculated as:

$$S(T) = \sum_{i=1}^{M}S_i(T) \qquad (21)$$

6.3.3 Model parameterisation

The model was implemented in R version 4.2.0 (R Core Team, 2022) and parameterised for *Zymoseptoria tritici* on wheat, an important pathogen for which the epidemiology and haplotype composition of the population have been

extensively studied. We used a literature search to estimate values of r_0, T, I_0 (Section 6.3.3.1) and α (Section 6.3.3.2). We used a dataset of CYP51 haplotype frequencies over time and the sensitivity of each haplotype to four azoles (epoxiconazole, prothioconazole, tebuconazole and prochloraz) (Tables 6.B.2, 6.B.3 and 6.B.4 in Appendix 6.B) to estimate values of θ_{i_start} and the dose-response parameters for each haplotype-azole combination, B_{ij}.

6.3.3.1 Parameterisation of r_0, T and I_0

Pathogen population growth rate when no fungicide is applied, r_0

Epidemic growth rates in the absence of fungicide vary from year to year, depending on weather conditions amongst other factors (Gladders et al., 2001). We used an estimate of the average growth rate, r_0 = 0.1173 t^{-1}, that was calculated from a dataset of disease severity on untreated plots from multiple sites and years (Hobbelen et al., 2011; te Beest et al., 2009).

Timing of fungicide applications and end of the growing season, T

We set the start of the simulation, t = 0, to correspond to GS32. We estimate T = 53 days, approximately corresponding to the timing of GS75 relative to GS32 (Chapter 4 - Table 4.2; Chapter 4 - Appendix 4.A (Corkley et al., 2025)). We assume that the haplotype composition at GS75 will be representative of the haplotype frequencies at the start of the following growing season, as the wheat leaf canopy rapidly senesces after GS75, limiting epidemic growth rate due to density dependence and a lack of green leaf area.

Initial severity of the overall pathogen population, I_0

The mean untreated disease severity at GS75 was estimated as 25.0% by van den Bosch et al. (2020), from a dataset of UK field trials covering 21 years and 80 site-years. We used this estimate in combination with the values of r_0 and T to estimate a value for the initial severity of the overall pathogen population, I_0:

$$I_0 = \frac{0.25}{e^{\,r_0 T}} \tag{22}$$

6.3.3.2 Fungicide decay rate, α

The fungicide decay rate, α, is calculated from the foliar dissipation half-life ('DT50') of the fungicide, which we estimated from information available in public domain sources, from a range of crops for tebuconazole, epoxiconazole, prochloraz and the active metabolite of prothioconazole, prothioconazole-desthio

(Table 6.1). There is large variability in the DT50 values estimated in experimental studies. However, the mean values are quite similar for all azoles considered in this study, between 7.09 and 7.93 days, with an overall average of 7.5 days. We therefore used an estimate of 7.5 days for all azoles in this study. The decay rate, α, is then calculated as:

$$\alpha = \frac{-\ln(0.5)}{\text{DT50}} = 0.0924 \; t^{-1} \tag{23}$$

Table 6.1: Foliar dissipation half-life ('DT50') of the azoles considered in this study.

Fungicide	Foliar half-life (days): values in published sources						Mean
Tebuconazole	6.4[a]	7.7[b]	7.75[c]	7.76[d]	7.83[e]	10.12[f]	7.93
Epoxiconazole	3.1[g]	5.25[h]	5.3[i]	9.84[j]	13.31[d]		7.36
Prochloraz	3.4[k]	3.5[l]	6.85[m]	10.2[n]	11.5[o]		7.09
Prothioconazole-desthio	2.9[c]	6.7[p]	12.21[q]				7.27

Published sources indicated by letter superscripts. [a]Dong & Hu, 2014; [b]Lin et al., 2014; [c]Lehoczki-Krjak et al., 2012; [d]Fantke et al., 2014; [e]Feng et al., 2020; [f]He et al., 2008; [g]Rao et al., 2013; [h]Wu et al., 2017; [i]Yan et al., 2015; [j]Liu et al., 2007; [k]Han et al., 2005. [l]Liu et al., 2009; [m]Feng et al., 2019; [n]Yuan et al., 2016. [o]Anonymous, 1983. [p]Dong et al., 2019. [q]Lin et al., 2017.

6.3.3.3 Initial haplotype frequencies, $\theta_{i\,\text{start}}$

As shown by equations (17) to (19), we can calculate the selection rate, $\Delta \bar{r}$, when the initial haplotype composition of the pathogen population is known. The initial frequency, $\theta_{i\,\text{start}}$, of each *Z. tritici* haplotype, i, was estimated from a dataset of isolates sampled in fields around Rothamsted Research, UK in each of the years 2003 and 2010-2019 (Figure 6.2; Tables 6.B.2 and 6.B.4 in Appendix 6.B). We ran simulations using each year's estimated relative haplotype frequencies for all haplotypes for which *in vitro* EC$_{50}$ dose-response measurements were available, with the aim of representing realistic starting haplotype compositions.
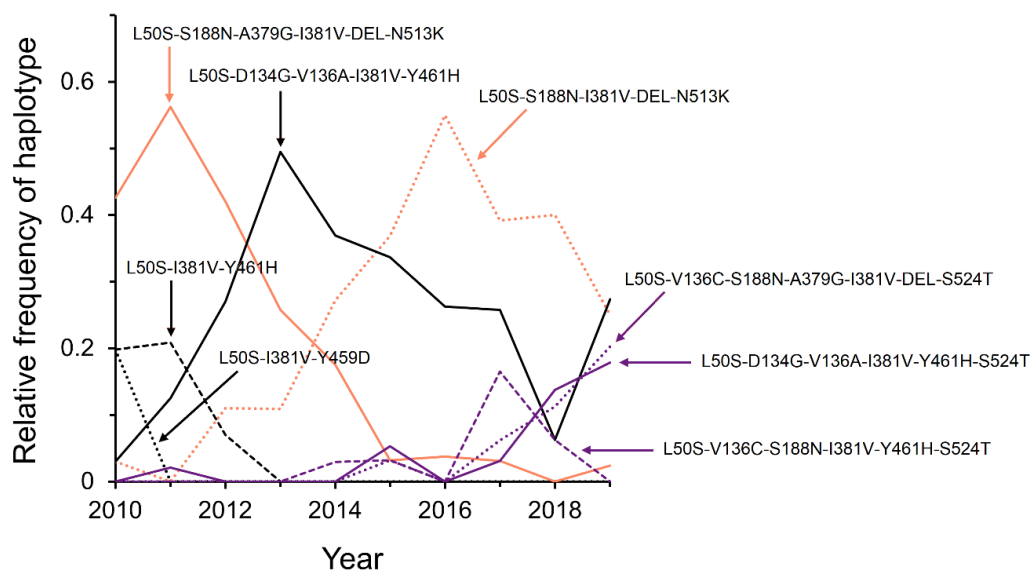
Figure 6.2: Relative frequencies of CYP51 haplotype frequencies for which *in vitro* EC$_{50}$ dose-response measurements were available, as sampled from the *Zymoseptoria tritici* population in fields around Rothamsted Research, Harpenden, UK, in 2010 to 2019. Haplotypes that reached a minimum frequency of 0.15 in one or more years from 2010 to 2019 shown.

6.3.3.4 Fungicide dose-response of each haplotype, B_{ij}

We used *in vitro* EC$_{50}$ dose-response measurements (Table 6.B.3 in Appendix 6.B) to parameterise the fungicide dose-response parameter, B_{ij}, for each of 116 haplotype-azole combinations (29 haplotypes and 4 azoles). To calculate B_{ij}, a measure of the field dose-response is needed. Blake et al. (2018) developed log-log relationships between lab-EC$_{50}$ and field-ED$_{50}$ values for epoxiconazole and prothioconazole-desthio. We used these relationships to convert lab-EC$_{50}$ values into field-ED$_{50}$ values for each haplotype. The relationship developed for epoxiconazole was used for tebuconazole and prochloraz (see Section 6.A.3 in Appendix 6.A).

EC$_{50}$ data for all four azole fungicides modelled were available for the majority of the haplotypes found in the sample, although there was insufficient data to include a haplotype commonly found with variable numbers of promoter insertions associated with CYP51 overexpression, L50S-I381V-S188N-DEL-N513K-CYP↑, which reached high frequencies >30% in a number of later years included in the analysis. A small number of other haplotypes with frequencies <15% in any single year were also excluded from the analysis due to insufficient EC$_{50}$ data (Table 6.B.2 in Appendix 6.B).

The ED_{50} measure of field dose-response represents the applied fungicide dose, D_{j0}, that would, on average, reduce the disease severity by 50% relative to an untreated ($D_{j0} = 0$) epidemic. B_{ij} can be calculated from these field-ED_{50} values in combination with equation (9), defining dose D_{j0} as a proportion of the full label field dose. For the calculation of the B_{ij} values, we set T to equal the duration between treatment and assessment of the field experiments, estimated as 31.5 days, the average of the two assessment timings at three and six weeks post-application (Blake et al., 2018). Since field-ED_{50} is the dose, $D_{ij_{50}}$, at which $S_i(T) = 0.5S_{i0}e^{r_0T}$, it follows that:

$$0.5S_{i0}e^{r_0T} = S_{i0}\left(\frac{B_{ij}D_{ij_{50}} + e^{\alpha T}}{B_{ij}D_{ij_{50}} + 1}\right)^{\frac{r_0}{\alpha}} \tag{24}$$

which gives:

$$B_{ij} = \frac{a - e^{\alpha T}}{D_{ij_{50}}(1 - a)} \tag{25}$$

where $a = (0.5e^{r_0T})^{\frac{\alpha}{r_0}}$.

6.3.4 Fungicide application scenarios

For this study we simulated a maximum of two applications of azole fungicides per growing season, in solo or mixture application. We set the timing of the first fungicide application to GS32, i.e. $t^* = 0$, and of the second application as $t^{**} = 20$ days, approximately corresponding to GS39. We modelled solo application and two-way, three-way and four-way azole mixtures, with the total azole dose kept constant across all scenarios (Table 6.2). All possible combinations of the four azoles tebuconazole, epoxiconazole, prochloraz and prothioconazole were modelled. We modelled additional application rates for a case study of two-way mixtures of epoxiconazole and prochloraz (using starting haplotype frequencies from 2015), changing the proportion of each azole in the mixture in 0.05 increments between 0.05 j_1 + 0.95 j_2 to 0.95 j_1 + 0.05 j_2. We measured the rate of increase in the epidemic growth rate, $\Delta\bar{r}$, over two years, with the assumption that $\theta_{i_{start}}$ in year 2 = $\theta_{i_{end}}$ in year 1 (Equation 20).

Table 6.2: Example fungicide application scenarios (except for the case study, all possible combinations of the four azoles at the dose rates presented in this table were simulated). 1.0 j_1 denotes a full label dose of azole 1.

Application scenario	Spray 1	Spray 2
Solo	1.0 j_1	1.0 j_1
Two-way mixture	0.5 j_1 + 0.5 j_2	0.5 j_1 + 0.5 j_2
Three-way mixture	0.33 j_1 + 0.33 j_2 + 0.33 j_3	0.33 j_1 + 0.33 j_2 + 0.33 j_3
Four-way mixture	0.25 j_1 + 0.25 j_2 + 0.25 j_3 + 0.25 j_4	0.25 j_1 + 0.25 j_2 + 0.25 j_3 + 0.25 j_4
Case study	$x\,j_1$ + (1 − x) j_2, 0.05 ≤ x ≤ 0.95	$x\,j_1$ + (1 − x) j_2

6.3.5 Estimating the impact of the degree of cross-resistance on resistance management benefits of azole mixtures

To investigate to what extent the model predictions of $\Delta\bar{r}$ for each fungicide programme and starting haplotype frequency (year) scenario can be explained by the degree of cross-resistance and other explanatory variables, we fitted generalised linear models ('GLMs') with a log link function using Genstat statistical software (VSN International, 2024). We chose explanatory variables that can be calculated directly from model inputs without a need to run the full model simulation.

The explanatory variables considered were three alternative measures of the degree of cross-resistance (Section 6.3.5.1), a measure of average programme efficacy (Section 6.3.5.2), and a measure of the maximum variance in haplotype sensitivity to any azole component of each mixture (Section 6.3.5.3). We fitted separate GLMs for each measure of cross-resistance to determine which was most informative. The measure of cross-resistance was the first explanatory variable term included in each model, with the order of other terms determined through forward stepwise regression. In addition, we fitted individual GLMs for each explanatory variable, and checked the level of correlation between explanatory variables.

We checked for significant interactions between each of the explanatory variables and the number of azoles included in each programme, to determine whether separate GLMs should be fitted for solo azoles, two-way, three-way and four-way mixtures.

6.3.5.1 Measuring the degree of cross-resistance

We measured cross-resistance in a group of haplotypes to two azole fungicides as the frequency-weighted correlation coefficient of the ED_{50} values expressed as a proportion of the full label field dose, $D_{ij_{50}}$. We denote the weighted correlation coefficient as cc_w.

$$cc_w = \frac{\sum_{i=1}^{M} \theta_{i_{\text{start}}}(D_{i1_{50}} - m_1)(D_{i2_{50}} - m_2)}{\sqrt{\sum_{i=1}^{M} \theta_{i_{\text{start}}}(D_{i1_{50}} - m_1)^2 \sum_{i=1}^{M} \theta_{i_{\text{start}}}(D_{i2_{50}} - m_2)^2}} \tag{26}$$

where $m_1 = \sum_{i=1}^{M} \theta_{i_{\text{start}}} D_{i1_{50}}$ and $m_2 = \sum_{i=1}^{M} \theta_{i_{\text{start}}} D_{i2_{50}}$, i.e. the frequency-weighted mean ED_{50} for each azole.

Levels of cross-resistance between fungicide active substances are typically measured using the unweighted Pearson's correlation coefficient or Spearman's rank correlation coefficient, for example as used in (Jørgensen et al., 2021; Kiiker et al., 2021; Kildea et al., 2024, 2023). We denote these measures as cc_u and cc_z respectively. We tested these measures of correlation between the ED_{50} values of each azole as alternative inputs to the generalised linear model.

In addition to two-azole cases (Figure 6.3), we modelled programmes with three and four azoles, for which there are multiple correlation coefficients, one for each combination pair of azoles (e.g. for four azoles there are 6 combination pairs of azoles and thus 6 correlation coefficients). As a simple measure of overall cross-resistance in the pathogen population to the azoles used in each programme, we used the average of the relevant correlation coefficients.

a. $cc_w = 0.657$

b. $cc_w = -0.199$

Sampled frequency of haplotype (%)   ● 30 - 40   ● 5-10   • < 5
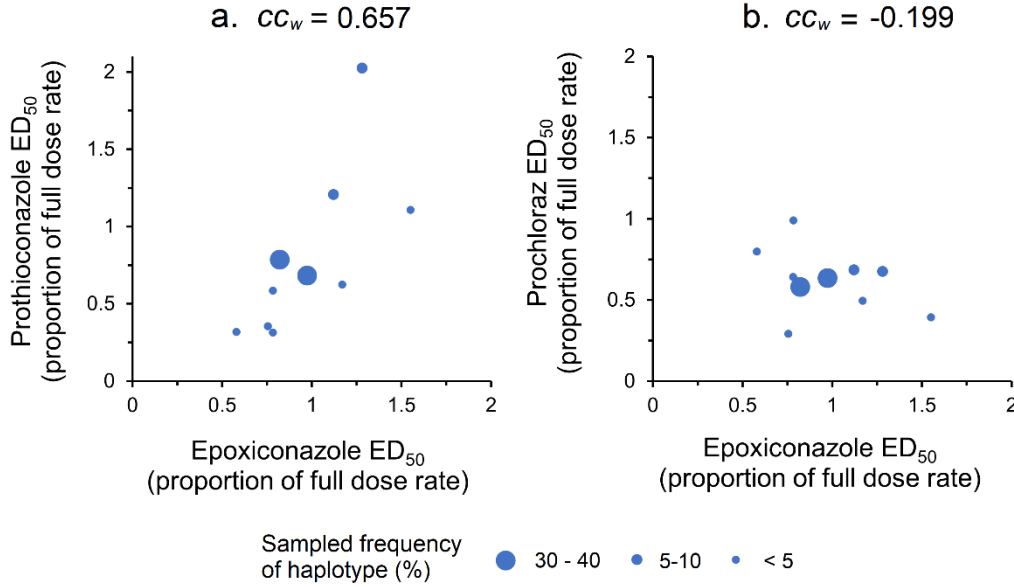
Figure 6.3: Examples of patterns of cross-resistance between two azoles, as measured by the weighted correlation coefficient, cc_w, of the ED_{50} values of CYP51 haplotypes, based on sampled haplotype frequencies in 2015 (n=37). (a). Positive cross-resistance between epoxiconazole and prothioconazole: $cc_w = 0.657$. (b). Weak negative cross-resistance between epoxiconazole and prochloraz: $cc_w = -0.199$. Each point on the graph represents a unique CYP51 haplotype. The width of each point represents the initial frequency of the haplotype; note that the displayed widths are not strictly proportional to frequency, to ensure visibility of all points. The sampled frequencies represented are as follows: large points: 30-40%; medium points 5-10%; small points: <5%.

6.3.5.2 Average programme efficacy

The rate of selection will be greatest when applying the fungicide results in a large difference in the growth rates of highly/moderately resistant strains and more sensitive strains. The more effective the fungicide programme against sensitive haplotypes, the larger the potential difference in haplotype growth rates. Therefore, the average efficacy of the azole programme can affect the strength of selection. We measured the average efficacy of each programme as $\bar{f}_{\text{start}}$, the average fractional reduction of the pathogen growth rate at the applied dose rate, weighted by the initial haplotype frequencies:

$$\bar{f}_{\text{start}} = 1 - \sum_{i=1}^{M} \theta_{i\,\text{start}} \frac{1}{\sum_{j=1}^{jmax} B_{ij}D_j + 1} \tag{27}$$

6.3.5.3 Variance in haplotype sensitivity

The larger the genetic variance in the ED_{50} values of the haplotypes, the greater the potential shift in resistance following application of the azole fungicide (Fisher, 1930; Lande, 1979; see Appendix 6.C). For each starting haplotype composition scenario (year), we calculated the variance, Var_j, in the relative growth rates of each haplotype i at the full label field dose of each solo azole j, $D_{j_{\text{Max}}} = 1$. Relative growth rates were calculated by setting $r_0 = 1\ t^{-1}$. Var_j is then calculated for a population of M haplotypes as:

$$Var_j = \frac{\sum_{i=1}^{M}\left(\frac{1}{B_{ij}+1} - \frac{\sum_{i=1}^{M}\frac{1}{B_{ij}+1}}{M}\right)^2}{M} \tag{28}$$

We used $Var_{j_{\text{Max}}}$, the maximum value of Var_j for any azole component in the mixture, as a potential explanatory variable in the generalised linear model.

It should be noted that the variance of the relative growth rates of each haplotype under each mixture application scenario, Var_{App}, could be calculated by replacing the $\frac{1}{B_{ij}+1}$ terms with $\frac{1}{\sum_{j=1}^{jmax} B_{ij}D_j + 1}$. Var_{App} is likely to be a useful variable for predicting $\Delta\bar{r}$, but it is partially dependent on the level of cross-resistance between azole mixture components. Since the purpose of fitting the generalised linear model was to determine the impact of the degree of cross-resistance on resistance management benefits of azole mixtures, we chose not to include Var_{App} as a potential explanatory variable.

6.4   Results

Table 6.3 summarises the definitions and values of the fitted model parameters, model variables and generalised linear model variables. Model results and generalized linear model inputs for each starting haplotype composition scenario and application scenario (excluding the case study) and are given in Table 6.D.1 (Appendix 6.D).

Table 6.3: Definitions of model parameters, model variables and GLM variables.

	Definition	Units	Details	Value/s
Parameter				
r_0	Average pathogen growth rate without fungicide	t^{-1}	Equation 5	0.1173
t	Time: t = 0 corresponds to GS32.	days	Section 6.3.3.1	-
t^*	Timing of first azole application (GS32)	days	Section 6.3.4	0
t^{**}	Timing of first azole application (GS39)	days	Section 6.3.4	20
T	Timing of GS75	days	Section 2.3.1	53
B_{ij}	Dose-response of haplotype i to azole j	-	Equation 5; Section 6.3.2.1	See Table 6.B.4[1]
D_{j0}	Applied dose of azole j	Proportion of full label rate	Equation 6	See Table 6.2
α	Decay rate of azole fungicides	t^{-1}	Equation 6; Section 6.3.3.2	0.0924
M	Total number of haplotypes in the population	-	Equation 14	See Table 6.B.4[1]
$\theta_{i\,\text{start}}$	Proportion of haplotype i at t = 0	-	Equation 17; Section 6.3.3.3	See Table 6.B.4[1]
S_0	Initial severity of the total pathogen population at $t = 0$	Proportion of leaf area	Equation 22	4.989 x 10^-4
S_{Max}	Threshold value of $S(T)$ for effective disease control	Proportion of leaf area	Section 6.3.1.2	0.05
Variable				
$\bar{r}_n$	Average growth rate of the pathogen population in year n	t^{-1}	Equation 1; Section 6.3.2.3	
$\Delta\bar{r}$	Rate of resistance development	-	Equation 1	See Table 6.D.1[2]
r_i	Growth rate of haplotype i	t^{-1}	Equation 5; Equation 16	
$D_j(t)$	Dose of azole j remaining at time t	Proportion of full label rate	Equation 6	
$\theta_{i\,\text{end}}$	Proportion of haplotype i at time T	-	Equation 19	
$S(T)$	Disease severity at GS75	Proportion of leaf area	Equation 21	See Table 6.D.1[2]
GLM variable				
cc_w	Average level of cross-resistance of haplotypes to two or more azoles	-	Equation 26; Section 6.3.5.1	See Table 6.D.1[2]
$\bar{f}_{\text{start}}$	Initial (frequency-weighted) programme efficacy at applied dose rate	Fractional reduction in growth rate	Equation 27	See Table 6.D.1[2]
$\text{Var}_{j\,\text{Max}}$	Maximum variance of haplotype sensitivity to a single component of mixture	t^{-2}	Section 6.3.5.3	See Table 6.D.1[2]

[1]Table 6.B.4 (Appendix 6.B).

[2]Table 6.D.1 (Appendix 6.D).

6.4.1 Case study: resistance management benefit of mixture within the same mode of action

A case-study of two-way mixtures of epoxiconazole and prochloraz, with starting haplotype frequencies based on a sample taken in 2015 from Harpenden, UK, demonstrates the potential resistance management benefits of mixture within the same mode of action when there is incomplete or negative cross-resistance. In this scenario, there was negative cross-resistance between epoxiconazole and prochloraz, as cc_w = -0.199 (Equation 26, Figure 6.3). Some haplotypes that were among the most resistant to epoxiconazole were well-controlled by prochloraz, and vice-versa (Figure 6.4, Table 6.4): for example, haplotype L50S-V136C-S188N-A379G-I381V-DEL-S524T was resistant to epoxiconazole but was well-controlled by prochloraz, and L50S-V136A-S188N-DEL-S524T was the least sensitive to prochloraz of the haplotypes present, but among the most sensitive to epoxiconazole. Therefore, the use of a 50:50 mixture of epoxiconazole and prochloraz reduced the differences in the relative growth rates of the haplotypes, compared with applying epoxiconazole or prochloraz solo (Figure 6.4), so the selective advantage of the fittest haplotypes was smaller for the mixture. This led to a smaller rate of selection for the mixture ($\Delta\bar{r}$ = 0.0071) than for application of solo epoxiconazole ($\Delta\bar{r}$ = 0.0148) or solo prochloraz ($\Delta\bar{r}$ = 0.0182) (Table 6.4).

In this scenario, either prochloraz (solo) or the 50:50 mixture of prochloraz and epoxiconazole were predicted to provide an adequate level of disease control over the full two-year simulation period, but epoxiconazole (solo) was not. Out of the three fungicide programmes, prochloraz (solo) gave the highest level of control, both against the initial haplotype composition and after two years of selection. However, erosion of the level of control was also fastest for prochloraz (solo). The level of control achieved with the mixture programme was slightly lower, but more stable.

The values of $\bar{f}_{\mathrm{end}}$, the average fractional reduction of the pathogen growth rate at the applied dose rate weighted by the final haplotype frequencies at the end of two years of selection, are shown for each for each fungicide programme (Table 6.4). A higher level of control would be obtainable with prochloraz (solo) following two years of use of the mixture programme compared to following two years' use of prochloraz (solo). In contrast, there would be little difference in the level of control obtainable with the mixture following two years' use of mixture versus two years' use of prochloraz (solo). These results suggest that use of azole mixtures can help
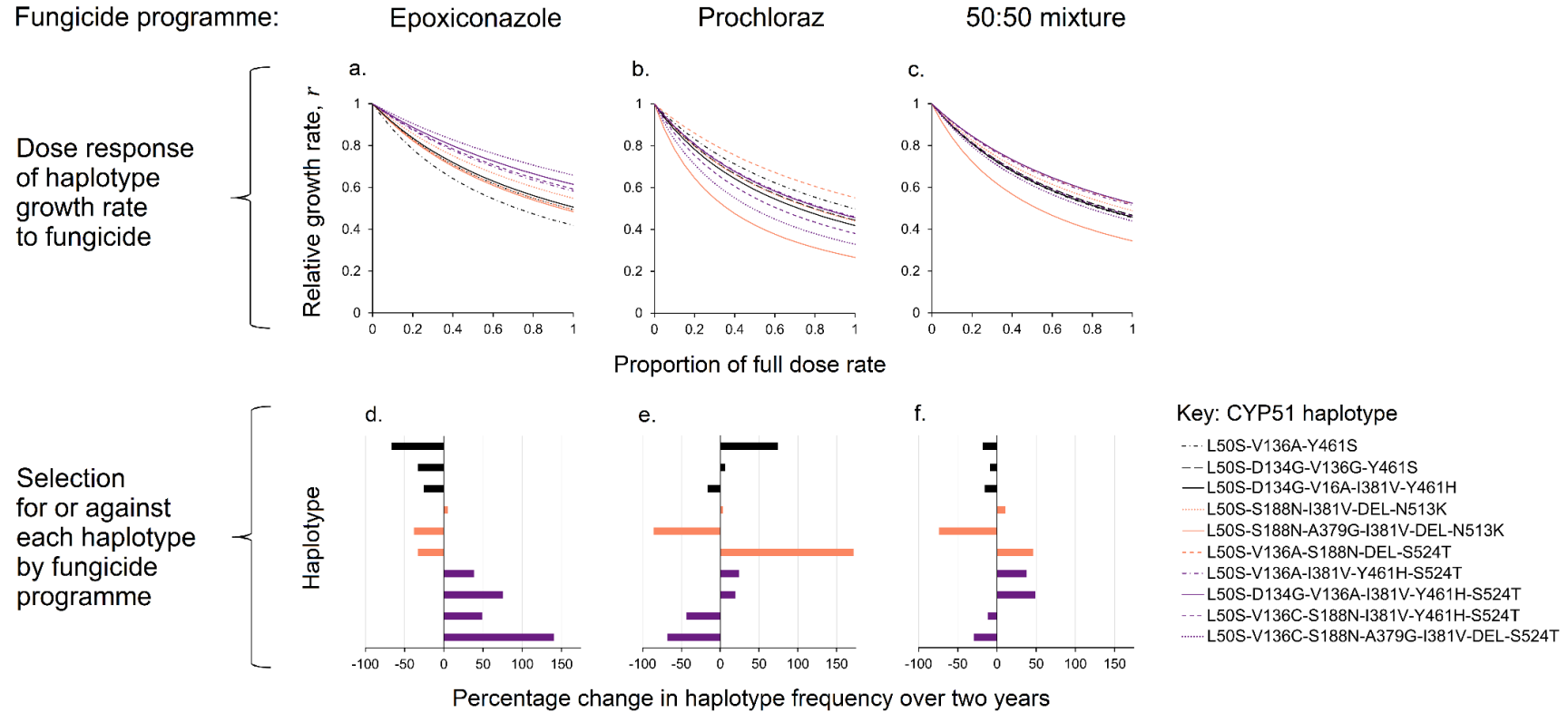
Figure 6.4: Dose-responses of individual CYP51 haplotypes to (a) epoxiconazole; (b) prochloraz and (c) a 50:50 mixture of epoxiconazole and prochloraz, and the resulting changes in haplotype frequency over 2 years for (d)-(f) epoxiconazole, prochloraz and the 50:50 mixture respectively. We plot relative growth rates by setting $r_0 = 1\ t^{-1}$. Fungicide dose is expressed as a proportion of the full label field dose $D_{j\,\text{Max}}$, where the full label field dose for the 50:50 mixture is equal to $0.5D_{1\,\text{Max}} + 0.5D_{2\,\text{Max}}$. Haplotypes shown are those present in 2015 scenario (based on the sampled population from Harpenden, UK).

Table 6.4: Comparison of the effects of two years of application of epoxiconazole (solo), prochloraz (solo) or a 50:50 mixture of epoxiconazole and prochloraz on selection of individual CYP51 haplotypes, and the overall resulting change in fungicide programme efficacy, for initial haplotype frequencies based on a sample from 2015 from Harpenden, UK. $\bar{f}_{start}$ is a measure of average programme efficacy weighted by the initial haplotype frequencies: the average fractional reduction of the pathogen growth rate at the applied dose rate (Equation 27). $\Delta \bar{r}$ measures the rate of change of the pathogen population growth rate for each programme (Equation 1). $\bar{f}_{end}$ is the average programme efficacy weighted by the final haplotype frequencies following two years of fungicide application.

Haplotype	Initial frequency (%)	ED$_{50}$		Fungicide programme		
				Epoxiconazole	Prochloraz	Mixture
		Epoxiconazole	Prochloraz	Percentage change in frequency		
L50S-V136A-Y461S	3.16	0.579	0.799	-66.5	**+74.7**	-18.3
L50S-D134G-V136G-Y461S	3.16	0.782	0.642	-33.2	**+6.7**	-8.7
L50S-D134G-V136A-I381V-Y461H	33.68	0.823	0.580	-25.5	-16.2	-15.9
L50S-S188N-I381V-DEL-N513K	36.84	0.974	0.634	**+5.5**	**+3.7**	**+10.4**
L50S-S188N-A379G-I381V-DEL-N513K	3.16	0.755	0.293	-38.3	-85.6	-73.9
L50S-V136A-S188N-DEL-S524T	3.16	0.784	0.990	-32.9	**+171.9**	**+45.9**
L50S-V136A-I381V-Y461H-S524T	5.26	1.122	0.686	**+38.3**	**+24.4**	**+37.8**
L50S-D134G-V136A-I381V-Y461H-S524T	5.26	1.281	0.675	**+75.6**	**+19.7**	**+49.0**
L50S-V136C-S188N-I381V-Y461H-S524T	3.16	1.170	0.494	**+49.4**	-43.3	-11.6
L50S-V136C-S188N-A379G-I381V-DEL-S524T	3.16	1.550	0.394	**+140.2**	-68.2	-29.9
$\bar{f}_{start}$ **for fungicide programme**				0.466	0.570	0.526
$\bar{r}$ **for fungicide programme at start of year 1** (t^{-1})				0.0900	0.0813	0.0850
$\bar{r}$ **for fungicide programme at end of year 2** (t^{-1})				0.0913	0.0828	0.0856
$\Delta \bar{r}$				0.0148	0.0182	0.0071
$\bar{f}_{end}$ **for epoxiconazole (solo)**				0.448	0.470	0.461
$\bar{f}_{end}$ **for prochloraz (solo)**				0.573	0.553	0.562
$\bar{f}_{end}$ **for mixture**				0.522	0.517	0.518

to protect the efficacy of the individual components of the mixture.

For this case study the proportion of each azole j in the mixture was simulated in 0.05 increments between $0.05\,j_1 + 0.95\,j_2$ to $0.95\,j_1 + 0.05\,j_2$ (Figure 6.5). The lowest rate of selection, measured by $\Delta\bar{r}$, was achieved with mixtures between a 50:50 prochloraz to epoxiconazole ratio and a 25:75 prochloraz to epoxiconazole ratio; the 50:50 ratio provided better disease control than a 25:75 ratio. A 75:25 prochloraz to epoxiconazole ratio improved disease control, but at the cost of a higher rate of selection.
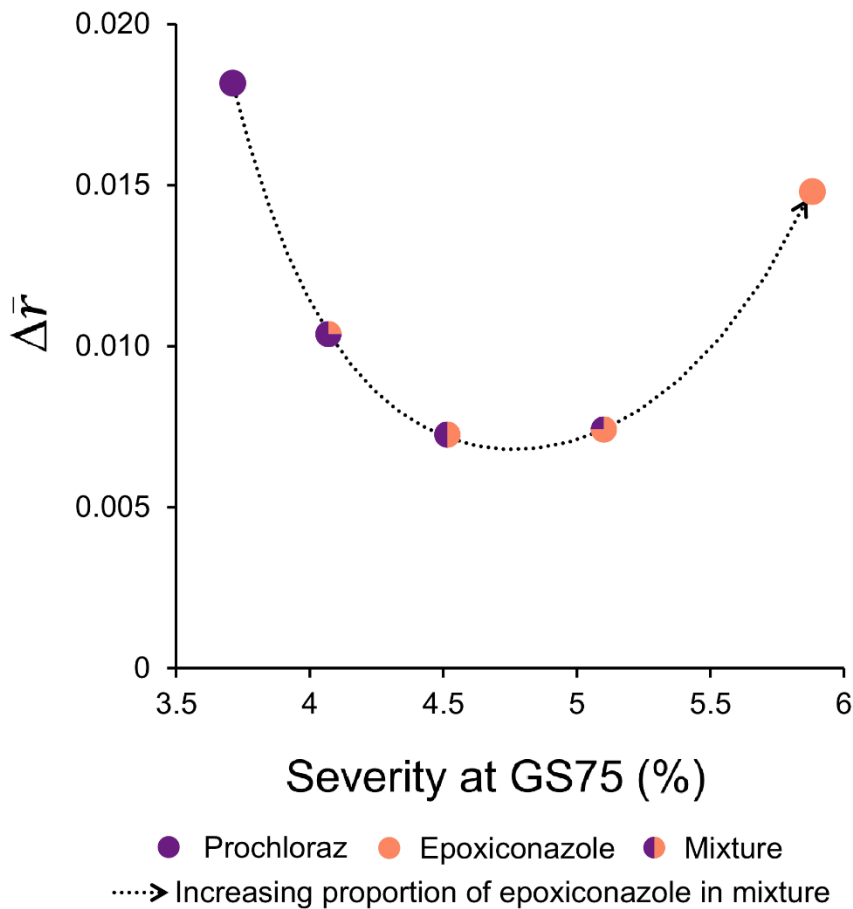
Figure 6.5: Variation in the rate of resistance development, $\Delta\bar{r}$, and epidemic severity with the ratio of two azoles in a mixture: prochloraz and epoxiconazole, for a *Z. tritici* population with the CYP51 haplotype frequencies sampled in 2015 in Harpenden, UK. Points are plotted as pie charts indicating the ratio of prochloraz and epoxiconazole in the mixture: prochloraz – purple; epoxiconazole – orange. In addition to solo prochloraz and solo epoxiconazole, the proportion of each azole j in the mixture was simulated in 0.05 increments between $0.05\,j_1 + 0.95\,j_2$ to $0.95\,j_1 + 0.05\,j_2$; points shown here are for 0.25 increments for visual clarity.

6.4.2 Resistance management benefit of additional active substances within a mode of action

Disease control

In most years, there were several azole mixture programmes incorporating two, three or four azoles that kept disease severity below the 5% threshold for effective control, in addition to some solo azole programmes (Figure 6.6a). From 2016 to 2019, when the average level of azole resistance of the pathogen population was higher, the four-way mixture did not provide effective disease control, and in 2018 there were no three-way mixtures that provided effective disease control. In all year scenarios simulated, there were at least 2 two-way mixtures and at least 1 solo azole programme that achieved effective control.

Selection for fungicide resistance

The greater the number of azole active substances included in the mixture, the lower the rate of selection for resistance, as measured by the average $\Delta\bar{r}$ of programmes meeting the threshold for effective disease control (Figure 6.6b). Although there were some solo and two-way mixture programmes for which $\Delta\bar{r}$ was very low, the values of $\Delta\bar{r}$ were more variable for solo and two-way mixtures, whereas $\Delta\bar{r}$ was consistently relatively low for three-way and four-way mixtures (Figure 6.6a, 6b). On average, having a diversity of azole active substances available enables mixture programmes that can lower selection, but there are diminishing returns of additional active substances, as a well-chosen combination of two azoles can provide the same benefit.

$\Delta\bar{r}$ was highest in the earlier years simulated (Figure 6.6b), when there were large differences in growth rates between sensitive and resistant haplotypes. The average level of azole resistance of the population was higher in later years and the differences in growth rates between different resistant haplotypes was smaller, leading to a slower rate of selection for further increases in resistance.
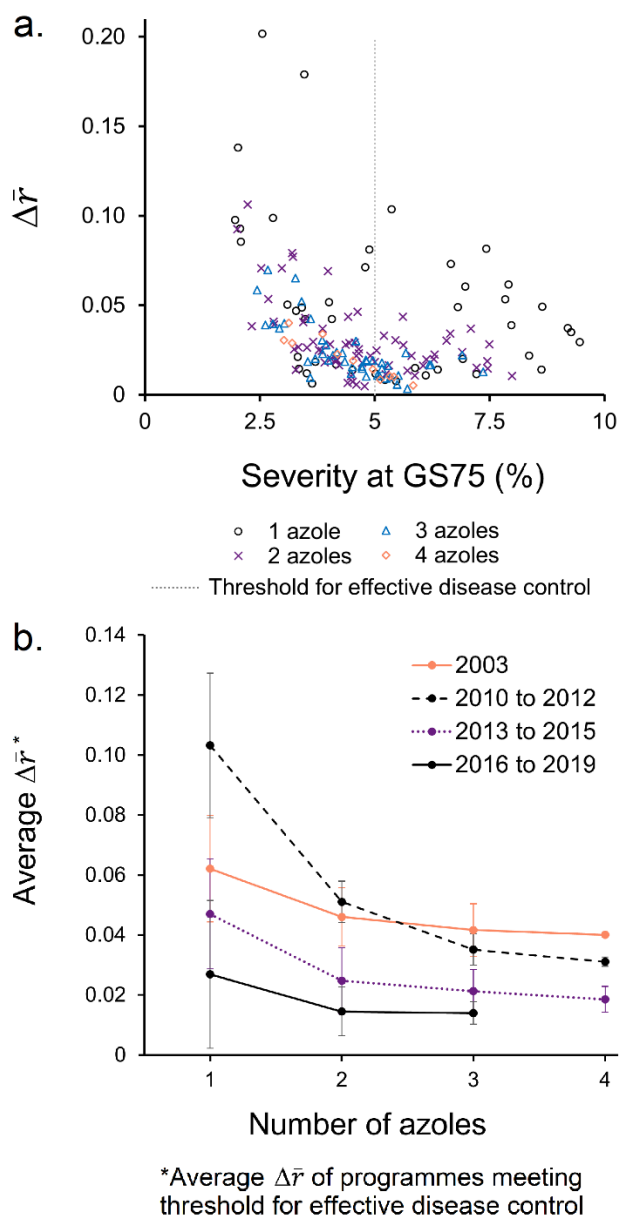
Figure 6.6: Variation in the rate of resistance development, $\Delta\bar{r}$, with the number of azoles included in the mixture ('within-MoA diversity'). (a). $\Delta\bar{r}$ over 2 years of application and level of disease control, measured as severity (%) at GS75 in the first year of application, in the first year of application, for all azole mixture programmes and initial haplotype frequency scenarios (years) modelled. The target for resistance management is programmes that combine effective disease control and a low rate of resistance development, $\Delta\bar{r}$. Number of azoles in each programme indicated by: 1 azole: black circle; 2 azoles: purple cross; 3 azoles: blue triangle; 4 azoles: orange diamond. The 5% severity threshold for effective disease control is indicated by the grey dotted line. (b). Variation with number of azoles and time of the average $\Delta\bar{r}$ of programmes meeting the threshold for

effective disease control (<5% severity at GS75). Results grouped together for years (initial haplotype frequency scenarios), indicated as follows: 2003: orange solid line; 2010-2012: black dashed line; 2013-2016: purple dotted line; 2016-2019: black solid line. Error bars show ±1 standard error of the mean; in cases where only one azole programme in the category met the threshold for effective disease control, these are plotted as points without an error bar. Averages are joined by point-to-point lines to aid interpretation.

6.4.3 Impact of the degree of cross-resistance on resistance management benefits of azole mixtures

Generalised linear models ('GLMs') of the rate of selection for resistance, $\Delta\bar{r}$, showed that there were significant interactions between the number of azoles and the fitted coefficients (see Tables 6.D.2 and 6.D.3 in Appendix 6.D). We therefore fitted individual GLMs of $\Delta\bar{r}$ for solo azoles, two-way, three-way and four-way mixtures (Table 6.5; full ANOVA results in Tables 6.D.5 to 6.D.8, Appendix 6.D).

Out of the three measures of cross-resistance, cc_w, the frequency-weighted correlation coefficient of the ED_{50} values (defined in Equation 26), was the best predictor for $\Delta\bar{r}$ (Table 6.5). The GLMs using cc_w as the measure of cross-resistance achieved adjusted R^2 values of 83.0%, 84.0% and 88.2% respectively for 2-, 3- and 4-azole programmes (Figure 6.7a, Table 6.5). The degree of cross-resistance, cc_w explained 36.6%, 38.6% and 36.0% of the variance in $\Delta\bar{r}$ respectively for 2-, 3- and 4-azole programmes (Table 6.5). The cross-resistance of an azole with itself is always equal to 1: a GLM fitted for solo azole programmes only, using $\mathrm{Var}_{j_{\mathrm{Max}}}$ and $\bar{f}_{\mathrm{start}}$ as explanatory variables, achieved an adjusted R^2 of 80.1% (Figure 6.D.1, Appendix 6.D).

Table 6.5: Percentage variance in $\Delta\bar{r}$ explained by individual variates included in generalised linear models (GLMs) with a log link function for 1, 2, 3 and 4-azole programmes. Explanatory variables are listed in the order that terms were added to each GLM: cross-resistance was always included first, whilst the inclusion and order of other terms was determined by forwards stepwise regression.

Number of azoles in programme	Explanatory variable	% variance explained by variate in GLM [1]Measure of cross-resistance		
		cc_w	cc_u	cc_z
1	Cross-resistance	[4]N/A	[4]N/A	[4]N/A
	[3]$\text{Var}_{j_{\text{Max}}}$	44.6		
	[2]$\bar{f}_{\text{start}}$	36.4		
2	Cross-resistance	36.6	22.9	11.3
	[2]$\bar{f}_{\text{start}}$	35.0	38.5	46.6
	[3]$\text{Var}_{j_{\text{Max}}}$	12.1	14.0	13.5
3	Cross-resistance	38.6	25.6	7.8
	$\bar{f}_{\text{start}}$	40.2	46.2	61.9
	$\text{Var}_{j_{\text{Max}}}$	6.4	6.6	5.7
4	Cross-resistance	36.0	42.4	1.6 ([5]NS)
	$\bar{f}_{\text{start}}$	48.7	42.1	85.5
	$\text{Var}_{j_{\text{Max}}}$	7.1	0.0 ([5]NS)	0.6 ([5]NS)

[1]Measures of cross-resistance calculated using ED_{50} field doses are the frequency-weighted correlation coefficient, unweighted Pearson's correlation coefficient and the Spearman's rank correlation coefficient, denoted as cc_w, cc_u and cc_z respectively (see Section 6.3.5.1).

[2]Average programme efficacy measured as $\bar{f}_{\text{start}}$, the average fractional reduction of the pathogen growth rate at the applied dose rate, weighted by the initial haplotype frequencies (see Section 6.3.5.2).

[3]Maximum variance in haplotype sensitivity for a single azole component of the mixture, measured as $\text{Var}_{j_{\text{Max}}}$ (see Section 6.3.5.3).

[4]Cross-resistance is not an informative term for 1-azole programmes, as the cross-resistance of an azole with itself is always equal to 1.

[5]NS denotes terms that were not significant (F-test). All other terms shown were significant.

$\Delta \bar{r}$ was predicted to increase with increasing levels of cross-resistance, cc_w, average programme efficacy, $\bar{f}_{\text{start}}$, and maximum variance in haplotype sensitivity to a single azole component of the mixture, $\text{Var}_{j_{\text{Max}}}$ (Table 6.6, Figure 6.7b). Figure 6.7b shows the variation in $\Delta \bar{r}$ predicted by the general linear model for 2-azole mixtures with varying levels of cross-resistance, programme efficacy and maximum variance in haplotype sensitivity. For programmes with a combination of high programme efficacy and high $\text{Var}_{j_{\text{Max}}}$, there is a steep decrease in $\Delta \bar{r}$ as the degree of cross-resistance between azoles in the mixture decreases, although in these cases $\Delta \bar{r}$ is still relatively high even for mixtures of azoles with negative cross-resistance. Relatively low values of $\bar{f}_{\text{start}}$ and $\text{Var}_{j_{\text{Max}}}$ are associated with lower values of $\Delta \bar{r}$, but in these cases there is a shallower gradient between cc_w and $\Delta \bar{r}$: the rate of selection is still minimised by low or negative cross-resistance, but the predicted change in $\Delta \bar{r}$ is smaller.

Several combinations of azole active substances consistently minimised or maximised $\Delta \bar{r}$ for several years in a row, in addition to meeting the threshold for effective disease control (Table 6.7). This suggests that some azole mixtures can provide stable resistance management benefits, despite variation in the values of cc_w, $\bar{f}_{\text{start}}$ and $\text{Var}_{j_{\text{Max}}}$ for each azole programme between each starting year scenario due to differences in haplotype composition. On average, azole mixtures that consistently minimised $\Delta \bar{r}$ had negative or low levels of positive cross-resistance between azole components, and relatively low levels of programme efficacy close to the threshold for effective disease control.

a.

b.

Figure 6.7: Generalised linear model (GLM) predictions of $\Delta\bar{r}$ for azole mixtures based on the degree of cross-resistance between azole components, cc_w, average programme efficacy, $\bar{f}_{\text{start}}$, and the maximum variance in haplotype sensitivity for a single azole component of the mixture, $\text{Var}_{j_{\text{Max}}}$. (a). Comparison of epidemiological model values vs. GLM fitted values of $\Delta\bar{r}$ for 2-, 3- and 4-azole mixtures (denoted as purple cross, blue triangle and orange diamond respectively); solid black line denotes 1:1 line. (b). Variation in $\Delta\bar{r}$ of 2-azole mixtures with the degree of cross-resistance, cc_w, and high and low values of $\bar{f}_{\text{start}}$ and $\text{Var}_{j_{\text{Max}}}$. The higher and lower values of $\bar{f}_{\text{start}}$ correspond to final disease severity at GS75 of 2-

3.5% and 4.5-5.5% respectively. GLM predictions are denoted as follows for the different levels of $\bar{f}_{\text{start}}$ (higher = 0.62; lower = 0.51) and $\text{Var}_{j_{\text{Max}}}$ (high = 0.019 t^{-2}; low = 0.0075 t^{-2}): high efficacy and high $\text{Var}_{j_{\text{Max}}}$: solid black line; high efficacy and low $Var_{j_{\text{Max}}}$: dashed black line; lower efficacy and high $\text{Var}_{j_{\text{Max}}}$: solid orange line; lower efficacy and low $\text{Var}_{j_{\text{Max}}}$. Epidemiological model results for similar categories of $\bar{f}_{\text{start}}$ (higher: 0.585 < $\bar{f}_{\text{start}}$ < 0.687; lower: 0.485 < $\bar{f}_{\text{start}}$ < 0.526) and $Var_{j_{\text{Max}}}$ (high: 0.0165 t^{-2} < $\text{Var}_{j_{\text{Max}}}$ < 0.0275 t^{-2}; low: 0.0021 t^{-2} < $\text{Var}_{j_{\text{Max}}}$ < 0.0118 t^{-2}) are denoted as follows: high efficacy and high $\text{Var}_{j_{\text{Max}}}$: black circle; high efficacy and low $\text{Var}_{j_{\text{Max}}}$: black square; low efficacy and high $\text{Var}_{j_{\text{Max}}}$: pink circle; low efficacy and low $\text{Var}_{j_{\text{Max}}}$: pink square.

Table 6.6: Fitted parameter values for generalised linear models with a log link function for 1, 2, 3 and 4-azole programmes.

Number of azoles	1	2	3	4
Parameter		Estimate (S.E)		
Intercept	-6.545 (0.384)	-7.213 (0.280)	-8.702 (0.440)	-9.799 (0.943)
cc_w	N/A	0.697 (0.084)	0.774 (0.125)	1.769 (0.689)
$\bar{f}_{\text{start}}$	5.353 (0.602)	5.835 (0.456)	8.137 (0.720)	9.32 (1.49)
$\text{Var}_{j_{\text{Max}}}$	63.96 (5.43)	28.00 (4.03)	22.86 (5.27)	31.3 (11.8)

Table 6.7: Azole programmes meeting the threshold for effective control that tended to minimise or maximise $\Delta\bar{r}$ most frequently for the scenarios modelled (i.e. sampled haplotype starting frequencies by year), and range of values of cross-resistance (cc_w), programme efficacy ($\bar{f}_{start}$) and maximum variance in haplotype sensitivity ($\text{Var}_{j_{\text{Max}}}$) over the years relevant for each programme. [1]Programmes were defined as maximising or minimising $\Delta\bar{r}$ in a year if they had one of the highest 3 or lowest 3 $\Delta\bar{r}$ values respectively within the year of programmes meeting the threshold for effective control. In years when fewer than 6 programmes met threshold for effective control (2016, 2018, 2019), programmes with the highest/lowest 1 or 2 $\Delta\bar{r}$ values were considered to maximise/minimise $\Delta\bar{r}$ respectively. [2]Prochloraz minimised $\Delta\bar{r}$ in 2016.

Fungicide programme	[1]Years minimised / maximised $\Delta\bar{r}$	cc_w	$\bar{f}_{\text{start}}$	$\text{Var}_{j_{\text{Max}}}$ (t^{-2})
Programmes that tended to minimise $\Delta\bar{r}$				
Prochloraz, Epoxiconazole & Tebuconazole	2003, 2010-2014	-0.241 - 0.169	0.514 - 0.578	0.0087 - 0.0167
Prochloraz & Epoxiconazole	2003, 2014-2019	-0.601 - 0.309	0.513 - 0.598	0.0021 - 0.0070
Four-way mixture	2012-2015	0.114 - 0.204	0.507 - 0.564	0.0101 - 0.0274
Programmes that tended to maximise $\Delta\bar{r}$				
Prothioconazole (solo)	2003, 2010-2015, 2017	1	0.516 - 0.692	0.0036 - 0.0274
Prothioconazole & Prochloraz	2010-2019	-0.061 - 0.656	0.522 - 0.687	0.0101 - 0.0274
[2]Prochloraz (solo)	2010-2014, 2017, 2019	1	0.590 - 0.689	0.0038 - 0.0107

6.5   Discussion

We have described a novel method for modelling the joint action of active substances within a MoA with incomplete cross-resistance, where the dose response can be parameterised based on measured lab EC_{50} values. We applied this method to the case of CYP51 haplotypes, where the resistance phenotype can be estimated from combination of mutations on a single gene. Our results show that there can be resistance management benefits of mixture within a MoA, which are maximised by low or negative cross-resistance between the active substances in the mixture. We show that use of azole mixtures can help to protect the efficacy of the individual components of the mixture and provide a more stable level of control than solo application. We focused on within-MoA programmes for the purpose of investigating the benefit of azole diversity, but it is important to note that in practice azoles should be used in combination with other MoAs when possible.

Our analysis focused on azole products with a long history of use, but our findings are of relevance for the newer azole product mefentrifluconazole which has low cross-resistance with prothioconazole (Heick et al., 2020; Kildea et al., 2024). The method we introduce for modelling the joint target-site action of multiple active substances within a MoA is also likely to be applicable to other MoA, although the model may require adaptation for cases other than azole fungicides. For example, there are varying levels of positive cross-resistance between SDHI fungicides (Alzohairy et al., 2023; Veloukas et al., 2013; Zhu et al., 2022). Resistance to succinate dehydrogenase inhibitor (SDHI) fungicides can occur due to target-site mutations on the *sdhb*, *sdhc*, and *sdhd* genes which code for subunits of the succinate dehydrogenase enzyme. Some isolates can also carry an additional sdhc paralog, named alt-SDHC, conferring high levels of insensitivity to stretched heterocycle amide SDHIs (SHA-SDHIs), a subclass of chemically-related SDHIs (Steinhauer et al., 2019; Yamashita & Fraaije, 2018). To model resistance evolution following application of SDHI mixtures in pathogens with a sexual stage, it would be necessary to include the effect of sexual reproduction, with phenotype depending on the combination of mutations on more than one SDH- subunit and/or presence of additional SDHC paralogs (Gutiérrez-Alonso et al., 2017; Sun et al., 2022). It would also be necessary to account for the effects of sexual reproduction if extending the model to account for the combined effects of target-site mutations and non-target-site resistance mechanisms such as efflux pumps.

We show that greater diversity of active substances is helpful to enable use of mixtures that reduce selection, but with diminishing returns as some two-way mixtures minimized selection (but some did not). Our results are consistent with the findings of both Dooley et al. (2016b), where no resistance management benefits were seen from mixture of two azoles with relatively strong positive cross-resistance were seen, and those of Heick et al. (2017), who showed that more diverse azole programmes reduced selection overall for CYP51 alterations. The resistance management benefits of additional active substances within a MoA are likely to be greater for fungicides with low cross-resistance with other active substances and a similar level of efficacy. It should be noted that one of the active substances included in our analysis, tebuconazole, provided relatively poor disease control of *Z. tritici* compared to the other azoles in our analysis. The resistance management benefits of additional active substances that are newer to market may be greater if they offer improved disease control and have low cross-resistance with other azoles.

We used sampled haplotype frequencies to inform the starting points for population composition in the scenarios modelled. Some individual haplotype EC_{50} values were larger than the average population EC_{50} used by Blake et al. (2018) to calculate EC_{50} to ED_{50} values, requiring some extrapolation beyond the fitted relationship. Our estimates of B_{ij} are therefore more uncertain for some highly resistant haplotypes present in the later years simulated. A small number of haplotypes that appeared in the samples could not be included in the analysis due to insufficient EC_{50} data; most of these were only found at very low frequencies and so would have minimal impact on the overall value of $\Delta\bar{r}$ calculated for the two-year period simulated. One haplotype which could not be included in the analysis, L50S-I381V-S188N-DEL-N513K-CYP↑, was associated with variable levels of CYP51 overexpression and sensitivity. This haplotype reached frequencies >25% of the population from 2014 onwards, so could have had a larger impact on the outcomes for years in which it was present. We restricted our analysis to the effect of selection on haplotypes that were already present, and did not estimate the likelihood of the emergence of novel haplotypes over the course of the two-year period simulated. The repeatability of CYP51 mutations in the field is low (Hawkins & Fraaije, 2021), so it is very difficult to predict which new haplotypes might emerge in response to different azole programmes. However, selective pressures on emerging strains could be affected by the use of azole mixtures, potentially selecting for different haplotypes that were not seen in the sampled dataset.

Overreliance on within-MoA diversity and incomplete cross-resistance for resistance management could increase selection for generalized mechanisms of azole resistance, as noted by Dooley et al. (2016b). For example, target-site overexpression can reduce sensitivity to all azole fungicides; some non-target-site resistance mechanisms, such as overexpression of efflux pumps, are also associated with an increased risk of multi-drug-resistance (Omrane et al., 2015). Data on the frequency and heritability of different levels of CYP51 overexpression and efflux mechanisms in combination with CYP51 haplotype could enable exploration of the effects of target-site overexpression and non-target-site resistance in combination with the target-site mutations modelled in this analysis.

Our results show a trade-off between efficacy and selection: the rate of selection is increased by higher programme efficacy and higher variability in the fitness of haplotypes against mixture components. If azole fungicides are being used in mixture with other single-site/at-risk MoA, it may be necessary to choose azole active substances which do not minimise $\Delta\bar{r}$ for azole programmes alone, to ensure that the efficacy of both mixture partners is balanced. Out of all azole mixture programmes that we predicted to provide effective disease control, our results suggest that some azole combinations would have consistently minimised selection for a minimum of 4-5 years, despite some fluctuation in the level of cross-resistance between azoles over time. Our approach could therefore be useful to identify combinations of azole active substances that can provide resistance management benefits over multiple growing seasons. Overall, choosing azole mixture partners with low or negative cross-resistance, only aiming for the minimum level of disease control required to protect yield and profitability, and where possible avoiding use of active substances for which there is a large variance in haplotype sensitivity will help to maximise the resistance management benefits of within-MoA diversity and keep azole fungicides effective for longer.

6.6   Supporting Information

Appendix 6.A: Further details on the population genetic model

Appendix 6.B: CYP51 haplotype frequencies and sensitivity to four azole active substances

Appendix 6.C: Lande's model of the effect of genetic variance on the rate of selection

Appendix 6.D: Further details on model results

Appendix 6.E: Offprint of Corkley et al. (2023)

6.7   Acknowledgements

6.8   References

Alzohairy, S.A., Heger, L., Nikzainalalam, N. & Miles, T.D. (2023). Cross-Resistance of Succinate Dehydrogenase Inhibitors (SDHI) in *Botrytis cinerea* and Development of Molecular Diagnostic Tools for SDHI Resistance Detection. *Phytopathology* 113, 998–1009. https://doi.org/10.1094/PHYTO-09-22-0346-R

Anonymous (1983). Data and recommendations of the joint meeting of the FAO Panel of Experts on Pesticide Residues in Food and the Environment and the WHO Expert Group on Pesticide Residues Geneva, 5 - 14 December 1983. https://www.inchem.org/documents/jmpr/jmpmono/v83pr37.htm

Blake, J.J., Gosling, P., Fraaije, B.A., Burnett, F.J., Knight, S.M., Kildea, S. et al. (2018). Changes in field dose–response curves for demethylation inhibitor (DMI) and quinone outside inhibitor (QoI) fungicides against *Zymoseptoria tritici*, related to laboratory sensitivity phenotyping and genotyping assays. *Pest Management Science* 74, 302–313. https://doi.org/10.1002/ps.4725

Cools, H.J. & Fraaije, B.A. (2013). Update on mechanisms of azole resistance in *Mycosphaerella graminicola* and implications for future control. *Pest Management Science* 69, 150–155. https://doi.org/10.1002/ps.3348

Cools, H.J., Hawkins, N.J. & Fraaije, B.A. (2013). Constraints on the evolution of azole resistance in plant pathogenic fungi. *Plant Pathology* 62, 36–42. https://doi.org/10.1111/ppa.12128

Cools, H.J., Mullins, J.G.L., Fraaije, B.A., Parker, J.E., Kelly, D.E., Lucas, J.A. et al. (2011). Impact of Recently Emerged Sterol 14α-Demethylase (CYP51) Variants of Mycosphaerella graminicola on Azole Fungicide Sensitivity. *Applied and Environmental Microbiology* 77, 3830–3837. https://doi.org/10.1128/AEM.00027-11

Corkley, I., Fraaije, B. & Hawkins, N. (2022). Fungicide resistance management: Maximizing the effective life of plant protection products. *Plant Pathology* 71. https://doi.org/10.1111/ppa.13467

Corkley, I., Mikaberidze, A., Paveley, N., van den Bosch, F., Shaw, M. W., & Milne, A. E. (2025). Dose Splitting Increases Selection for Both Target-Site and Non-Target-Site Fungicide Resistance—A Modelling Analysis. *Plant Pathology*, *74*(4), 1152–1167. https://doi.org/10.1111/ppa.14080

Corkley, I., van den Bosch, F., Fraaije, B.A., Shaw, M.W., Helps, J. Mikaberidze A. et al. (2023). Modelling resistance management benefits of diversity within a fungicidal mode of action with incomplete cross-resistance: the azoles example. In: Deising HB; Fraaije B; Mehl A; Oerke EC; Sierotzki H; Stammler G (Eds), "Modern Fungicides and Antifungal Compounds", Vol. X, pp. 291-296. © 2023. Deutsche Phytomedizinische Gesellschaft, Braunschweig, ISBN: 978-3-941261-17-4

Dooley, H., Shaw, M.W., Mehenni-Ciz, J., Spink, J. & Kildea, S. (2016a). Detection of *Zymoseptoria tritici* SDHI-insensitive field isolates carrying the *SdhC* - H152R and *SdhD* -R47W substitutions. *Pest Management Science* 72, 2203–2207. https://doi.org/10.1002/ps.4269

Dooley, H., Shaw, M.W., Spink, J. & Kildea, S. (2016b). Effect of azole fungicide mixtures, alternations and dose on azole sensitivity in the wheat pathogen *Zymoseptoria tritici*. *Plant Pathology* 65, 124–136. https://doi.org/10.1111/ppa.12395

Dong, B. & Hu, J. (2014). Dissipation and residue determination of fluopyram and tebuconazole residues in watermelon and soil by GC-MS. *International Journal of Environmental Analytical Chemistry*, *94*(5), 493–505. https://doi.org/10.1080/03067319.2013.841152

Dong, X., Tong, Z., Chu, Y., Sun, M., Wang, M., Gao, T. et al. (2019). Dissipation of Prothioconazole and Its Metabolite Prothioconazole-Desthio in Rice Fields and Risk Assessment of Its Dietary Intake. *Journal of Agricultural and Food Chemistry*, *67*(23), 6458–6465. https://doi.org/10.1021/acs.jafc.8b06788

EPPO (2010). Workshop on Azole fungicides and Septoria leaf blotch control Conference Centre, Rothamsted Research, Harpenden (GB), 2010-12-07/09

Fantke, P., Gillespie, B.W., Juraske, R. & Jolliet, O. (2014). Estimating Half-Lives for Pesticide Dissipation from Plants. *Environmental Science & Technology*, *48*(15), 8588–8602. https://doi.org/10.1021/es500434p

Feng, Y., Han, J., Qi, X., Wang, X., Pan, J., Jin, J. et al. (2019). Residue and Safety Use of 45% Prochloraz EW in Ginger. *Plant Disease and Pests* 10(5/6):28-30. https://doi.org/10.19579/j.cnki.plant-d.p.2019.05-06.008

Feng, Y., Qi, X., Wang, X., Liang, L. & Zuo, B. (2020). Residue dissipation and dietary risk assessment of trifloxystrobin, trifloxystrobin acid, and tebuconazole in wheat under field conditions. *International Journal of Environmental Analytical Chemistry*, *102*(7), 1598–1612. https://doi.org/10.1080/03067319.2020.1739667

Fisher, R. A. (1930). The genetical theory of natural selection. Clarendon Press. https://doi.org/10.5962/bhl.title.27468

Fones, H. & Gurr, S. (2015). The impact of Septoria tritici Blotch disease on wheat: An EU perspective. *Fungal Genetics and Biology* 79, 3–7. https://doi.org/10.1016/j.fgb.2015.04.004

Fraaije, B.A., Cools, H.J., Kim, S., Motteram, J., Clark, W.S. & Lucas, J.A. (2007). A novel substitution I381V in the sterol 14α-demethylase (CYP51) of *Mycosphaerella graminicola* is differentially selected by azole fungicides. *Molecular Plant Pathology* 8, 245–254. https://doi.org/10.1111/j.1364-3703.2007.00388.x

Glaab, A., Weilacher, X., Hoffmeister, M., Strobel, D. & Stammler, G. (2024). Occurrence and distribution of CYP51 haplotypes of Zymoseptoria tritici in recent years in Europe. *Journal of Plant Diseases and Protection* 131, 1187–1194. https://doi.org/10.1007/s41348-024-00897-y

Gladders, P., Paveley, N.D., Barrie, I.A., Hardwick, N.V, Hims, M.J., Langton, S. et al. (2001). Agronomic and meteorological factors affecting the severity of leaf blotch caused by Mycosphaerella graminicola in commercial wheat crops in England. *Annals of Applied Biology* 138, 301–311. https://doi.org/10.1111/j.1744-7348.2001.tb00115.x

Gutiérrez-Alonso, O., Hawkins, N.J., Cools, H.J., Shaw, M.W. & Fraaije, B.A. (2017). Dose-dependent selection drives lineage replacement during the experimental evolution of SDHI fungicide resistance in *Zymoseptoria tritici*. *Evolutionary Applications* 10, 1055–1066. https://doi.org/10.1111/eva.12511

Han, L., Qian, C., Jiang, C. & Wang, W. (2005). Residue Detection and Degradation of Prochloraz and its Metabolites in Rice. *Chinese Journal of Pesticide Science* 7(1): 54-58.

Hargrove, T.Y., Wawrzak, Z., Fisher, P.M., Child, S.A., Nes, W.D., Guengerich, F.P. et al. (2018). Binding of a physiological substrate causes large-scale

conformational reorganization in cytochrome P450 51. *Journal of Biological Chemistry* 293, 19344–19353. https://doi.org/10.1074/jbc.RA118.005850

Hargrove, T.Y., Wawrzak, Z., Lamb, D.C., Guengerich, F.P. & Lepesheva, G.I. (2015). Structure-Functional Characterization of Cytochrome P450 Sterol 14α-Demethylase (CYP51B) from Aspergillus fumigatus and Molecular Basis for the Development of Antifungal Drugs. *Journal of Biological Chemistry* 290, 23916–23934. https://doi.org/10.1074/jbc.M115.677310

Hawkins, N.J. & Fraaije, B.A. (2021). Contrasting levels of genetic predictability in the evolution of resistance to major classes of fungicides. *Molecular Ecology* 30, 5318–5327. https://doi.org/10.1111/mec.15877

He, L., Gong, D., Zuo, C. & Ma, H. (2010). Residue and degradation dynamics of tebuconazole SYP-1620 20%SC in rice field. *Agrochemicals* 7:506-509.

Heick, T.M., Justesen, A.F. &Jørgensen, L.N. (2017). Anti-resistance strategies for fungicides against wheat pathogen Zymoseptoria tritici with focus on DMI fungicides. *Crop Protection* 99, 108–117. https://doi.org/10.1016/j.cropro.2017.05.009

Heick, T.M., Matzen, N. & Jørgensen, L.N. (2020). Reduced field efficacy and sensitivity of demethylation inhibitors in the Danish and Swedish *Zymoseptoria tritici* populations. *European Journal of Plant Pathology* 157, 625–636. https://doi.org/10.1007/s10658-020-02029-2

Hill, A.V. (1913). The Combinations of Haemoglobin with Oxygen and with Carbon Monoxide. I. *Biochemical Journal* 7, 471–480. https://doi.org/10.1042/bj0070471

Hobbelen, P.H.F., Paveley, N.D. & van den Bosch, F. (2011). Delaying selection for fungicide insensitivity by mixing fungicides at a low and high risk of resistance development: A modeling analysis. *Phytopathology* 101, 1224–1233. https://doi.org/10.1094/PHYTO-10-10-0290

Huf, A., Rehfus, A., Lorenz, K.H., Bryson, R., Voegele, R.T. & Stammler, G. (2018). Proposal for a new nomenclature for *CYP51* haplotypes in *Zymoseptoria tritici* and analysis of their distribution in Europe. *Plant Pathology* 67, 1706–1712. https://doi.org/10.1111/ppa.12891

Jørgensen, L.N. & Heick, T.M. (2021). Azole Use in Agriculture, Horticulture, and Wood Preservation – Is It Indispensable? *Frontiers in Cellular and Infection Microbiology* 11. https://doi.org/10.3389/fcimb.2021.730297

Jørgensen, L.N., Matzen, N., Hansen, J.G., Semaskiene, R., Korbas, M., Danielewicz, J. et al. (2018). Four azoles' profile in the control of Septoria,

yellow rust and brown rust in wheat across Europe. *Crop Protection* 105, 16–27. https://doi.org/10.1016/j.cropro.2017.10.018

Jørgensen, L.N., Matzen, N., Heick, T.M., Havis, N., Holdgate, S., Clark, B. et al. (2021). Decreasing azole sensitivity of Z. tritici in Europe contributes to reduced and varying field efficacy. *Journal of Plant Diseases and Protection* 128, 287–301. https://doi.org/10.1007/s41348-020-00372-4

Kayamori, M., Zakharycheva, A., Saito, H. & Komatsu, K. (2021). Resistance to demethylation inhibitors in Cercospora beticola, a pathogen of sugar beet in Japan, and development of unique cross-resistance patterns. *European Journal of Plant Pathology* 160, 39–52. https://doi.org/10.1007/s10658-021-02219-6

Kiiker, R., Juurik, M., Heick, T.M. & Mäe, A. (2021). Changes in DMI, SDHI, and QoI Fungicide Sensitivity in the Estonian *Zymoseptoria tritici* Population between 2019 and 2020. *Microorganisms* 9, 814. https://doi.org/10.3390/microorganisms9040814

Kildea, S., Dooley, H. & Byrne, S. (2023). A note on the impact of CYP51 alterations and their combination in the wheat pathogen *Zymoseptoria tritici* on sensitivity to the azole fungicides epoxiconazole and metconazole. *Irish Journal of Agricultural and Food Research* 62. https://doi.org/10.15212/ijafr-2023-0103

Kildea, S., Hellin, P., Heick, T.M., Byrne, S. & Hutton, F. (2024). Mefentrifluconazole sensitivity amongst European *Zymoseptoria tritici* populations and potential implications for its field efficacy. *Pest Management Science* 80, 533–543. https://doi.org/10.1002/ps.7795

Kildea, S., Marten-Heick, T., Grant, J., Mehenni-Ciz, J. & Dooley, H. (2019). A combination of target-site alterations, overexpression and enhanced efflux activity contribute to reduced azole sensitivity present in the Irish *Zymoseptoria tritici* population. *European Journal of Plant Pathology* 154, 529–540. https://doi.org/10.1007/s10658-019-01676-4

Kirikyali, N., Diez, P., Luo, J., Hawkins, N. & Fraaije, B.A. (2017). Azole and SDHI sensitivity status of *Zymoseptoria tritici* field populations sampled in France, Germany and the UK during 2015. In: Deising HB, Fraaije BA, Mehl A, Oerke EC, Sierotzki H and Stammler G (Eds), "Modern Fungicides and Antifungal Compounds" Vol VIII, pp. 153–158. Deutsche Phytomedizinische Gesellschaft, Braunschweig, Germany.

Lande, R. (1979). Quantitative genetic analysis of a multivariate evolution, applied to brain: body size allometry. *Evolution* 33: 402-416. https://doi.org/10.1111/j.1558-5646.1979.tb04694.x

Lehoczki-Krsjak, S., Varga, M., Szabó-Hevér, Á. & Mesterházy, Á. (2013). Translocation and degradation of tebuconazole and prothioconazole in wheat following fungicide treatment at flowering. *Pest Management Science*, *69*(11), 1216–1224. https://doi.org/10.1002/ps.3486

Leroux, P., Chapeland, F., Arnold, A. & Gredt, M. (2000). New Cases of Negative Cross-resistance between Fungicides, Including Sterol Biosynthesis Inhibitors. *Journal of General Plant Pathology* 66, 75–81. https://doi.org/10.1007/PL00012925

Leroux, P. & Walker, A. (2011). Multiple mechanisms account for resistance to sterol 14α-demethylation inhibitors in field isolates of *Mycosphaerella graminicola*. *Pest Management Science* 67, 44–59. https://doi.org/10.1002/ps.2028

Leroux, P. & Walker, A.-S. (2013). Activity of fungicides and modulators of membrane drug transporters in field strains of Botrytis cinerea displaying multidrug resistance. *European Journal of Plant Pathology* 135, 683–693. https://doi.org/10.1007/s10658-012-0105-3

Lin, H., Dong, B., & Hu, J. (2017). Residue and intake risk assessment of prothioconazole and its metabolite prothioconazole-desthio in wheat field. *Environmental Monitoring and Assessment*, 189(5), 236. https://doi.org/10.1007/s10661-017-5943-1

Lin, J., Zhang, Y., Han, B.-J. & Lyu, D. (2014). Residue dynamics of tebuconazole in different tissues of banana. *Journal of Southern Agriculture* 45(9), 1599. doi.10.3969/j:issn.2095-1191.2014.9.1599

Liu, L., Xu, Y., Huang, Y., Sun, Y. & Lin, D. (2007). Residue Dynamics of Epoxiconazole in Apples and Soil. *Modern Scientific Instruments*, 1: 61-63.

Liu, X., Shen, M., Li, S. & Chen, H. (2009). Residue Dynamics of Prochloraz and its Metabolite2,4,6-Trichlorophenol in Mushroom and Soil. *Chinese Journal of Pesticide Science* 11(3): 362-366

McDonald, B.A., Suffert, F., Bernasconi, A. & Mikaberidze, A. (2022). How large and diverse are field populations of fungal plant pathogens? The case of *Zymoseptoria tritici*. *Evolutionary Applications* 15, 1360–1373. https://doi.org/10.1111/eva.13434

McDonald, M.C., Renkin, M., Spackman, M., Orchard, B., Croll, D., Solomon, P.S. et al. (2019). Rapid Parallel Evolution of Azole Fungicide Resistance in Australian Populations of the Wheat Pathogen *Zymoseptoria tritici*. *Applied and Environmental Microbiology* 85. https://doi.org/10.1128/AEM.01908-18

Michaelis L. & Menten M.L. (1913). Die Kinetik der Invertinwirkung. *Biochemische Zeitschrift*, 49:333-369.

Mikaberidze, A., Paveley, N., Bonhoeffer, S. & van den Bosch, F. (2017). Emergence of Resistance to Fungicides: The Role of Fungicide Dose. *Phytopathology* 107, 545–560. https://doi.org/10.1094/PHYTO-08-16-0297-R

Morse, P.M. (1978). Some Comments on the Assessment of Joint Action in Herbicide Mixtures. *Weed Science* 26, 58–71. https://doi.org/10.1017/S0043174500032690

Mullins, J.G.L., Parker, J.E., Cools, H.J., Togawa, R.C., Lucas, J.A., Fraaije, B.A. et al. (2011). Molecular Modelling of the Emergence of Azole Resistance in Mycosphaerella graminicola. *PLoS One* 6, e20973. https://doi.org/10.1371/journal.pone.0020973

Murray J.D. (1991). Mathematical Biology. Biomathematics Texts volume 19. Springer-Verlag Berlin Heidelberg. 767pp.

Oliver, R. (2016). Fungicide resistance management in practice; mixtures, alternations and cross resistance patterns. *Journal of Plant Pathology* 98 (4).

Omrane, S., Sghyer, H., Audéon, C., Lanen, C., Duplaix, C., Walker, A. et al. (2015). Fungicide efflux and the MgMFS1 transporter contribute to the multidrug resistance phenotype in *Zymoseptoria tritici* field isolates. *Environmental Microbiology* 17, 2805–2823. https://doi.org/10.1111/1462-2920.12781

Paveley, N.D., Thomas, J.M., Vaughan, T.B., Havis, N.D. & Jones, D.R. (2003). Predicting effective doses for the joint action of two fungicide applications. *Plant Pathology* 52, 638–647. https://doi.org/10.1046/j.1365-3059.2003.00881.x

Pietravalle, S., Shaw, M.W., Parker, S.R. & van den Bosch, F. (2003). Modeling of Relationships Between Weather and *Septoria tritici* Epidemics on Winter Wheat: A Critical Approach. *Phytopathology* 93, 1329–1339. https://doi.org/10.1094/PHYTO.2003.93.10.1329

Ponomarenko, A., Goodwin, S.B. & Kema, G.H.J. (2011). Septoria tritici blotch (STB). *Plant Health Instructor*, 10.

R Core Team (2022). R: A language and environment for statistical computing. R Foundation for Statistical Computing, Vienna, Austria. https://www.R-project.org/

Rao, T.N., Reddy, E.S., Reddy, G.R., Sreenivasulu, D. & Ramesh, J. (2013). Persistence study of pyraclostrobin and epoxiconazole fungicide formulation

in groundnut plant followed by HPLC-UV method. *International Journal of Current Microbiology and Applied Sciences*, *2*(9), 5-13.

Rehfus, A., Strobel, D., Bryson, R. & Stammler, G. (2018). Mutations in *sdh* genes in field isolates of *Zymoseptoria tritici* and impact on the sensitivity to various succinate dehydrogenase inhibitors. *Plant Pathology* 67, 175–180. https://doi.org/10.1111/ppa.12715

Rodrigues, M.L. (2018). The Multifunctional Fungal Ergosterol. *mBio* 9:10.1128/mbio.01755-18. https://doi.org/10.1128/mBio.01755-18

Shaw, M.W. & Royle, D.J. (1993). Factors determining the severity of epidemics of *Mycosphaerella graminicola (Septoria tritici)* on winter wheat in the UK. *Plant Pathology* 42, 882–899. https://doi.org/10.1111/j.1365-3059.1993.tb02674.x

Stammler, G., Carstensen, M., Koch, A., Semar, M., Strobel, D. & Schlehuber, S. (2008). Frequency of different CYP51-haplotypes of Mycosphaerella graminicola and their impact on epoxiconazole-sensitivity and -field efficacy. *Crop Protection* 27, 1448–1456. https://doi.org/10.1016/j.cropro.2008.07.007

Steinhauer, D., Salat, M., Frey, R., Mosbach, A., Luksch, T., Balmer, D. et al. (2019). A dispensable paralog of succinate dehydrogenase subunit C mediates standing resistance towards a subclass of SDHI fungicides in *Zymoseptoria tritici*. *PLoS Pathogens* 15: e1007780. https://doi.org/10.1371/journal.ppat.1007780

Stilgenbauer, S., Simões, K., Craig, I.R., Brahm, L., Steiner, U. & Stammler, G. (2023). New CYP51-genotypes in Phakopsora pachyrhizi have different effects on DMI sensitivity. *Journal of Plant Diseases and Protection* 130, 973–983. https://doi.org/10.1007/s41348-023-00757-1

Sun, B., Zhu, G., Xie, X., Chai, A., Li, L., Shi, Y. et al. (2022). Double Mutations in Succinate Dehydrogenase Are Involved in SDHI Resistance in *Corynespora cassiicola*. *Microorganisms* 10, 132. https://doi.org/10.3390/microorganisms10010132

te Beest, D.E., Shaw, M.W., Pietravalle, S. & van den Bosch, F. (2009). A predictive model for early-warning of Septoria leaf blotch on winter wheat. *European Journal of Plant Pathology* 124, 413–425. https://doi.org/10.1007/s10658-009-9428-0

Torriani, S.F., Brunner, P.C., McDonald, B.A. & Sierotzki, H. (2009). QoI resistance emerged independently at least 4 times in European populations of *Mycosphaerella graminicola*. *Pest Management Science* 65, 155–162. https://doi.org/10.1002/ps.1662

van den Bosch, F., Blake, J., Gosling, P., Helps, J.C. & Paveley, N. (2020). Identifying when it is financially beneficial to increase or decrease fungicide dose as resistance develops: An evaluation from long-term field experiments. *Plant Pathology* 69, 631–641. https://doi.org/10.1111/ppa.13155

van den Bosch, F., Oliver, R., van den Berg, F. & Paveley, N. (2014a). Governing Principles Can Guide Fungicide-Resistance Management Tactics. *Annual Review of Phytopathology* 52, 175–195. https://doi.org/10.1146/annurev-phyto-102313-050158

van den Bosch, F., Paveley, N., van den Berg, F., Hobbelen, P. & Oliver, R. (2014b). Mixtures as a Fungicide Resistance Management Tactic. *Phytopathology* 104, 1264–1273. https://doi.org/10.1094/PHYTO-04-14-0121-RVW

Veloukas, T., Markoglou, A.N. & Karaoglanidis, G.S. (2013). Differential Effect of *Sdh* B Gene Mutations on the Sensitivity to SDHI Fungicides in *Botrytis cinerea*. *Plant Disease* 97, 118–122. https://doi.org/10.1094/PDIS-03-12-0322-RE

VSN International (2024). Genstat *for Windows* 24th Edition. VSN International, Hemel Hempstead, UK. https://vsni.co.uk/software/genstat

Wu, X., Ma, J., Wang, H., Zhou, L., Li, T., An, L. et al. (2017). Residue and dissipation of epoxiconazole in *Triticum aestivum* L. and soil under field conditions. *Chinese Journal of Pesticide Science*, 2017, 19(4): 474-481. https://doi.org/10.16801/j.issn.1008-7303.2017.0062

Xiao, L., Madison, V., Chau, A.S., Loebenberg, D., Palermo, R.E. & McNicholas, P.M. (2004). Three-Dimensional Models of Wild-Type and Mutated Forms of Cytochrome P450 14α-Sterol Demethylases from *Aspergillus fumigatus* and *Candida albicans* Provide Insights into Posaconazole Binding. *Antimicrobial Agents and Chemotherapy* 48, 568–574.
https://doi.org/10.1128/AAC.48.2.568-574.2004

Yamashita, M. & Fraaije, B. (2018). Non-target site SDHI resistance is present as standing genetic variation in field populations of Zymoseptoria tritici. *Pest Management Science* 74: 672-681. https://doi.org/10.1002/ps.4761

Yan, B., Ye, F. & Gao, D. (2015). Residues of the fungicide epoxiconazole in rice and paddy in the Chinese field ecosystem. *Pest Management Science*, *71*(1), 65–71. https://doi.org/10.1002/ps.3763

Yuan, X.-Y., Peng, Z., Zhou, H.-P. & Liu, C. (2016). Degradation dynamics and safety evaluation of prochloraz in banana. *Journal of Food Safety and Quality* 7(1): 209-214.

Zadoks, J.C., Chang, T.T. & Konzak, C.F. (1974). A decimal code for the growth stages of cereals. *Weed Research* 14, 415–421. https://doi.org/10.1111/j.1365-3180.1974.tb01084.x

Zhang, J., Li, L., Lv, Q., Yan, L., Wang, Y. & Jiang, Y. (2019). The Fungal CYP51s: Their Functions, Structures, Related Drug Resistance, and Inhibitors. *Frontiers in Microbiology* 10. https://doi.org/10.3389/fmicb.2019.00691

Zhu, J., Li, J., Ma, D., Gao, Y., Cheng, J., Mu, W. et al. (2022). SDH mutations confer complex cross-resistance patterns to SDHIs in *Corynespora cassiicola*. *Pesticide Biochemistry and Physiology* 186, 105157. https://doi.org/10.1016/j.pestbp.2022.105157

Chapter 7

Discussion

This thesis describes the use of epidemiological modelling to investigate which strategies are likely to provide both good resistance management and robust disease control in cases where there is concurrent evolution of resistance to two or more fungicides. The thesis starts with a review of existing evidence (Chapter 2), which mostly relates to strategies against resistance evolving to a single mode of action (MoA) at any given time. In this discussion, I summarise the main findings of my research, discuss their implications for design of resistance management strategies for current and future MoA and identify potential areas for further research.

7.1 What is the value of phytosanitary cultural control for fungicide resistance management?

Any application of fungicide will exert selection pressure for resistance. Integrated Pest Management ('IPM') methods that can reduce disease pressure and the intensity of fungicide application required are therefore key to fungicide resistance management, but the value of these methods for resistance management is rarely quantified and may be overlooked or underestimated. In Chapter 3, I considered the value of a phytosanitary cultural control method, the 'soybean-free period' for fungicide resistance management for a succinate dehydrogenase inhibitor (SDHI) fungicide used to control *Phakopsora pachyrhizi* (Asian soybean rust).

My results show that phytosanitary cultural control can contribute to fungicide resistance management. Delaying infection timing relative to crop emergence both reduced selection for fungicide-resistant *P. pachyrhizi* strains and increased fungicide effective life, for two reasons:

(a) There was a reduction in the length of exposure time of the pathogen to fungicide.

(b) There was a reduction in the total disease pressure over time. This enabled effective control to be maintained with lower fungicide inputs, reducing the difference between the growth rates of resistant and sensitive strains. In addition, since the level of fungicide efficacy needed to maintain effective control was

reduced, a wider range of fungicide programmes provided effective control even after increases in frequency of partially resistant strains.

The value for resistance management of IPM measures that reduce the rate of growth of pathogens is already recognised. For example, some disease-resistance genes have been shown to enable the plant to actively combat infection by a pathogen and so reduce the growth rate of avirulent pathogen strains (Saintenac et al., 2018). These resistant cultivars can effectively act 'in mixture' with fungicides and reduce the difference in growth rates between fungicide-sensitive and resistant strains (Taylor & Cunniffe, 2023b). The results presented in Chapter 3 show that delaying disease onset can also have substantial benefits for resistance management, even if the growth rate of the pathogen is not affected. In model simulations, delay in inoculum arrival due to phytosanitary cultural control increased the time until 50% of the population was resistant ('T50') by between 14–71%. For a 10-day delay in inoculum arrival, the increase in 'T50' was approximately equal to the increase in 'T50' resulting from use of a multi-site (dithiocarbamate) mixture partner.

The magnitude of the resistance management benefit of the soybean-free period was somewhat surprising: in theory, the value of sanitation practices for disease control of polycyclic foliar pathogens such as *P. pachyrhizi* with high epidemic growth rates and short latent periods is expected to be low, as the epidemic quickly builds to damaging levels (Nutter, 2007; Zadoks & Schein, 1979). However, it appears that for *P. pachyrhizi*, even a relatively modest delay in the onset of infection can be useful for resistance management and disease control, especially when used in combination with fungicides. The introduction of the soybean-free period in Brazil has indeed proved valuable, reducing the loss of soybean yields to *P. pachyrhizi* and reducing the average number of fungicide applications required for disease control (Yorinori, 2021).

These findings are applicable in other systems where IPM methods reduce disease pressure through delaying disease onset. For example, covering potato discard heaps limits sources of *Phytophthora infestans* (late blight) inoculum (Cooke et al., 2011). Wheat stubble management such as straw removal, burning or burial can be useful to reduce *Zymoseptoria tritici* (septoria tritici blotch) inoculum, or an autumn-sown cover crop can trap ascospores and prevent infection of neighbouring fields (McDonald & Mundt, 2016). In addition, plant defence is not always attributable to genetic mechanisms that reduce pathogen growth rates:

measured differences in disease severity can also be due to differences in the crop architecture of different cultivars that affect the timing of infection (disease escape). For example, the location of different leaf layers affects the risk of infection by *Z. tritici* and *Mycosphaerella pinodes* (ascochyta blight) in wheat and pea cultivars respectively (Le May et al., 2009; Lovell et al., 2004).

Use of tolerant cultivars that maintain yield levels at higher levels of disease (van den Bosch et al., 2022) neither reduces pathogen growth rates nor delays disease onset, but does reduce the required level of disease control, acting in a similar way to the reduction in disease pressure noted as the second mechanism by which the soybean-free period contributed to increased *T50* and effective life. For this reason, cultivar tolerance is also likely to contribute to resistance management.

The resistance management benefits of delaying *P. pachyrhizi* infection were maximised by using the minimum number of fungicide applications required for effective control after taking into account the reduction in disease levels due to the soybean-free period. Resistance management benefits therefore rely on growers adapting their fungicide application practices based on the reduced disease risk, but in some years the risk may still be high if weather conditions are favourable for inoculum dispersal and pathogen growth. If the disease risk is unknown, growers may choose not to reduce fungicide applications to avoid the risk of heavy yield losses in years with high disease pressure (te Beest et al., 2013). Decision support systems (DSS) that incorporate information on the dependence of infection risk on weather can provide guidance about cases where a reduction in fungicide input can be achieved with limited increased risk of yield loss to disease (Lázaro et al., 2021). Some models and DSS already include the effects of cultivar resistance and tolerance on the fungicide dose required for effective disease control (e.g. Grimmer et al., 2024; Prahl et al., 2022; Small et al., 2015; Taylor & Cunniffe, 2023b; te Beest et al., 2009). Our results suggest that to maximise the resistance management benefits of IPM, there is a need for DSS with the flexibility to account for a wider range of IPM measures taken by growers, such as choice of sowing date and phytosanitary cultural control.

7.2   How does the impact of dose splitting vary with fungicide properties and the type and magnitude of resistance?

Dose splitting presents a key trade-off for management of the concurrent evolution of resistance to two different fungicidal modes of action (MoA), since use of two fungicides in mixture may require splitting the total dose of each fungicide across multiple applications, increasing the exposure time to each fungicide. In Chapter 4, I used a compartmental epidemiological model of *Z. tritici* to explore variation in the effect of dose-splitting with fungicide efficacy, persistence and the type and magnitude of resistance. I found that dose-splitting increased selection for both target-site and non-target-site resistance, but the effect of dose-splitting was variable and depended on the combination of fungicide and resistant strain properties.

Fungicide efficacy and persistence were defined by the combination of an asymptote parameter (the maximum effect of the fungicide at high dose rates), a curvature parameter (defining the rate of decrease in efficacy from the asymptote with decreasing dose) and the foliar concentration decay rate of the fungicide. Resistance mechanisms were defined as causing either an 'asymptote shift' or a or a 'curvature shift', a reduction in the asymptote or curvature parameter respectively. My results show that the percentage increase in selection due to dose splitting is likely to be particularly large for 'curvature shift' resistance mechanisms, and highest for small curvature shifts. Mechanisms likely to result in a partial curvature shift include target-site mutations that reduce fungicide competitive binding rates, target-site overexpression and generalist non-target-site resistance mechanisms such as enhanced efflux activity.

The effects of dose splitting also depend on fungicide properties: the largest increases in selection due to dose splitting were predicted for fungicides with a steeply curved dose response curve and a relatively short foliar concentration half-life. SDHI fungicides were used as an example of a commercial MoA currently available to growers: the results show that dose splitting of an SDHI fungicide applied solo is likely to increase selection for resistance by approximately 20–35%. However, accounting for potential variability in decay rates suggests a wider range of 10–40% for an asymptote shift, or 0–70% for a curvature shift. Variability in fungicide decay rates between years and sites due to differing environmental conditions may therefore explain the variable rate of selection for SDH-mutants

reported from field experiments on dose splitting (Paveley et al. 2020; Young et al. 2021).

The results from Chapter 4 provide insights for the modelling analysis presented in Chapter 5, where I investigated how the balance between increased selection from dose splitting and the benefits of mixture varies with fungicide properties and the type and magnitude of resistance. In cases where dose splitting increases selection for resistance most strongly, this trade-off may outweigh the benefits of mixture.

7.3 Which is the better strategy against concurrent evolution of resistance: alternation or splitting and mixing?

In Chapter 5, I used a model of *Z. tritici* to investigate how interactions between the effects of fungicide efficacy, persistence and the type and magnitude of resistance determine whether alternation or splitting and mixing is a better strategy against concurrent evolution of resistance to two at-risk MoAs. The model included the effects of sexual reproduction on the frequencies of single- and double-resistant strains. Fungicide properties and types of resistance were defined in the same way as described in Chapter 4. I considered the rate of selection for a strain with resistance to both MoAs for scenarios where there was (a) an asymptote shift to both MoAs; (b) a curvature shift to both MoAs; or (c) an asymptote shift to fungicide A and a curvature shift to fungicide B.

I found that splitting and mixing the total dose of two at-risk fungicides minimised selection for the double-resistant strain more often when there was an asymptote shift to both MoAs, whereas if there was a curvature shift to both MoAs, alternation was more likely to minimise selection. These results are partially explained by the findings presented in Chapter 4, which showed that dose splitting can increase selection more for partial curvature shifts than for asymptote shifts.

However, for all scenarios of resistance type considered, the tactic that minimised selection for the double-resistant strain varied with fungicide properties (asymptote parameter, curvature parameter and decay rate) and the magnitude of the sensitivity shift: neither splitting and mixing nor alternation was consistently better. In addition, across much of the parameter space explored, the difference in selection between splitting and mixing and alternation was small. Overall, for all resistance type scenarios, splitting and mixing was more likely to outperform alternation for resistance management when both fungicides had strong efficacy

with a high decay rate and/or a low curvature parameter, and the magnitude of resistance differed between MoAs. Alternation was more likely to minimise selection for double-resistant strains when both fungicides were weakly or moderately effective.

The variability in which strategy minimised selection for double-resistant strains poses a challenge for management of the concurrent evolution of resistance. Fungicide and resistant strain properties are often uncertain or unknown, especially when a new MoA is first released to the market. Whilst experimental data can be used to estimate fungicide foliar decay rates and dose-response parameters, the level of uncertainty in the estimated parameter values can be high, as discussed in Chapter 3. Mutagenesis studies *in vitro* and experimental evolution can be used to predict likely resistance mechanisms for any given fungicide and the relative fitness of strains with different mutations, but do not always closely predict which mutations emerge and spread through pathogen populations following the release of a new MoA (Hawkins, 2024).

Splitting and mixing generally gave improved disease control initially relative to alternation, and often minimised the rate of loss of healthy leaf area index duration (HAD) between the first and second year of the fungicide programme. Splitting and mixing may therefore maintain effective disease control for longer, despite higher rates of selection for double-resistant strains compared to alternation tactics. However, effective control could potentially be maintained for longer by initially minimising selection using alternation tactics (which also provide sufficient disease control initially), and then switching to splitting and mixing when necessary to maintain disease control. The modelling analysis could be extended to compare longer-term strategies to maximise effective life or lifetime yield. If the choice of tactic is not flexible over time, splitting and mixing may be the better choice to maximise lifetime yield, lifetime profitability or effective life, as found in previous studies (Elderfield et al., 2018; Hobbelen et al., 2013; Taylor & Cunniffe, 2023c).

My analysis considered pathogen strains with either an asymptote or a curvature shift. However, the potential for target-site resistance to evolve to a MoA does not preclude the possibility of non-target-site resistance evolving to the same MoA. Focusing on minimising selection for strains with asymptote shifts may come at the expense of an increased risk of selection for generalist resistance. For example, in weed management, use of herbicide mixtures is associated with lower prevalence of target-site resistance but higher prevalence of metabolic resistance (Comont et

al., 2020). Selection for generalist resistance mechanisms by use of mixtures has also been demonstrated in *Z. tritici* and the bacterium *Pseudomonas aeruginosa* (Ballu et al., 2021; Vestergaard et al., 2016). A pragmatic choice of resistance management tactics may require weighing 'the lesser of two evils': an asymptote shift due to target-site resistance is more likely to cause a large, rapid loss in efficacy, whereas it may initially be possible to control generalist resistance by increasing fungicide dose rates as resistance develops (Taylor & Cunniffe, 2023a; van den Bosch et al., 2020). Since the pipeline of future MoAs is limited, there are clear economic benefits to prolonging the effective life of current MoAs. However, efflux and other non-target-site mechanisms can contribute to multi-drug-resistant (MDR) strains and could reduce the baseline sensitivity of the pathogen to novel MoA, making future disease control more difficult.

7.4   Can incomplete cross-resistance within a fungicidal mode of action be useful for resistance management?

As the number of MoAs available for disease control is becoming increasingly limited due to regulation and existing resistance, the use of mixtures or alternations of fungicides with the same MoA but incomplete cross-resistance has been proposed as a potential resistance management strategy. For example, patterns of partial cross-resistance have been observed for azole fungicides in the demethylation inhibitor (DMI) group (FRAC Code 3) (Dooley et al., 2016; Fraaije et al., 2007; Leroux & Walker, 2011; Sykes et al., 2017), and use of azole mixtures has been shown to improve disease control compared to single azoles (Heick et al., 2017). However, the resistance management value of within-MoA mixtures with incomplete cross-resistance was unclear, and previous modelling approaches representing the joint action of fungicides (multiplicative survival model and additive dose model) had not adequately represented this case. In Chapter 6, I used a novel model of the joint target-site action of multiple azole fungicides group to investigate how the resistance management benefits of within-MoA mixtures vary with the degree of incomplete cross-resistance and the number of active substances available within a MoA.

The growth rates and changes in population fraction of multiple pathogen strains with different CYP51 haploid genotypes ('haplotypes') were simulated for scenarios where fungicide applications comprised single azoles or two-, three- or four-way azole mixtures. The model was parameterised for the sensitivity of known *Z. tritici* CYP51 haplotypes to the DMI fungicides epoxiconazole, prothioconazole,

prochloraz and tebuconazole. Scenarios of initial haplotype population compositions were estimated from a dataset of isolates sampled from the *Z. tritici* populations in fields around Rothamsted Research, UK in 2003 and each year from 2010–2019. It was assumed that the entire CYP51 haplotype was inherited from one generation to the next: the potential for intragenic recombination (Brunner et al., 2008) was not included in the model. The epidemic growth rate of the pathogen was calculated as the frequency-weighted average growth rate of all haplotypes, $\bar{r}$. The rate of selection for fungicide resistance was measured by the rate of change of $\bar{r}$ from one year to the next, $\Delta\bar{r}$. Programmes that had low values of $\Delta\bar{r}$ and provided effective disease control (total severity <5% on the upper leaf canopy at growth stage 75) were considered to have the greatest resistance management benefits.

My results show that there are resistance management benefits of using mixtures, alternation or mosaics of azole active substances with incomplete cross-resistance. The best method of deployment (mixture, alternation or mosaic) varied between years and depended on exact product combinations and pathogen population haplotype composition. However, the disease control provided by mixtures and within-year alternation was more resilient than mosaics and between-year alternation to declines in fungicide efficacy as resistant strain frequencies increased.

On average, across all scenarios simulated, programmes with more azole active substances resulted in a lower rate of selection for resistance, although there were diminishing returns as additional azoles were added to the programme, and some two-way azole combinations had the same or lower $\Delta\bar{r}$ as three- or four-way combinations. My analysis showed that fungicide programmes with stronger efficacy selected more strongly for resistance. In addition, $\Delta\bar{r}$ was higher for azole combinations for which there was and higher variability in the fitness of haplotypes against individual mixture components. Mixtures of azoles with low or negative cross-resistance maximised resistance management benefits, but any degree of incomplete cross-resistance was useful. If the approximate CYP51 haplotype composition of a population is known prior to fungicide application, these principles can guide choice of which combinations of azoles could usefully contribute to fungicide resistance management as part of a fungicide programme.

Although my analysis focused on the example of azole fungicides, a similar approach could be used to model varying levels of cross-resistance within other

MoA groups. For example, varying levels of positive cross-resistance have been reported for SDHI fungicides in the pathogens *Botrytis cinerea* (grey mould), *Alternaria alternata* (Alternaria leaf spot), pathogens of cucumber *Corynespora cassiicola* (Corynespora leaf spot) and *Podosphaera xanthii* (powdery mildew), and *Z. tritici (*(Alzohairy et al., 2023; Förster et al., 2022; Ishii et al., 2011; Miyamoto et al., 2020; Veloukas et al., 2013; Yamashita & Fraaije, 2018; Zhu et al., 2022). However, it may be necessary to account for the effects of sexual reproduction if the sensitivity phenotype is determined by mutations on multiple genes or intragenic recombination. Cross-resistance patterns to SDHI fungicides depend on which target-site mutations are present on three genes (*sdhb*, *sdhc* and *sdhd*) coding for subunits of the succinate dehydrogenase enzyme, and the presence or absence of an additional sdhc paralog (Scalliet et al., 2012; Steinhauer et al., 2019; Yamashita & Fraaije, 2018). The approach could also be adapted to model cases of incomplete cross-resistance within MoA groups in other biological systems, such as pyrethroid insecticides (Moyes et al., 2021), and in antibiotic, antiviral and cancer treatments (Butaye et al., 2000; Hazuda et al., 2004; Sonpavde et al., 2015).

My analysis focused on within-MoA programmes, but in practice azoles should be used in mixture or alternation with other MoA wherever possible, as relying on fungicides within a single MoA group will select strongly for strains with low sensitivity to all active substances within the MoA group and lead to increasing levels of positive cross-resistance within the MoA. This effect has been observed in *Z. tritici* for both DMI and SDHI fungicides (Dooley et al., 2016; Hagerty et al., 2021; Kildea et al., 2024; Rehfus et al., 2018). The mutation S524T is particularly implicated in increasing levels of positive cross-resistance between azole fungicides, in combination with generalised resistance resulting from inserts in the MFS1 region (Kildea et al., 2023; Omrane et al., 2017), whilst the C-H152R mutation results in strains with high resistance factors to many SDHI fungicides (Rehfus et al., 2018). However, options to maintain diversity between MoA in a programme are becoming increasingly limited; my results demonstrate that incomplete cross-resistance within a MoA can offer additional options for resistance management.

The model could be extended to investigate the effect of mixture programmes of multiple fungicides with incomplete cross-resistance within a MoA in addition to a fungicide from a different MoA. It would be valuable to investigate to what extent incomplete cross-resistance between two mixture components with the same MoA

could contribute to reduced selection for resistance to a third mixture component with a different MoA. There may be differences in which azole active substances and dose rates are optimal in a three-way mixture including a different MoA. There was often higher variance in haplotype sensitivity to azole fungicides with higher average efficacy, so $\Delta\bar{r}$ was higher for these azoles. However, azole fungicides with higher average efficacy may nevertheless be better mixture partners for a fungicide with a different MoA, due to a closer balance in the disease control provided by each mixture component.

7.5 Recommendations for Further Research

7.5.1 Emergence of resistance

My thesis focuses on the effects of resistance management strategies on the 'selection phase', for cases in which resistance mutations were already present at high enough frequencies that they were unlikely to be lost from the population through chance. However, prior to the selection phase there is an 'emergence phase', in which the frequency of strains with the resistance mutation is so small that it may become extinct due to the stochastic chances of survival of small numbers of resistant lesions (Mikaberidze et al., 2017). Strategies that increase the time to emergence of resistance will extend the effective life of fungicides, potentially for longer than attempts to reduce selection once resistant strains have emerged, as the selection phase can be very rapid (Deising et al., 2008). It would therefore be useful to extend the analysis presented in Chapter 5 to consider the relative effects of alternation and splitting and mixing on the risk of concurrent emergence of resistance to two MoA.

Previous modelling studies of resistance evolving to a single MoA have considered the emergence phase for strains with asymptote or curvature shifts, incorporating stochastic sub-models for the dynamics of a resistant strain in the emergence phase. Hobbelen et al. (2014) showed that mixtures of a high-risk and low-risk fungicide delayed the emergence phase as well as the selection phase for a strain with resistance to the high-risk fungicide. Mikaberidze et al. (2017) showed that high fungicide doses generally accelerate the emergence phase; although their analysis shows that high doses could theoretically delay the emergence phase for some mutations causing a curvature shift. However, they argue that the *Z. tritici* populations are typically very large even after fungicide application, and that it is therefore unlikely that even the highest field dose rates will reduce the population sufficiently that mutational supply limits the rate of emergence. Taylor & Cunniffe

(2023b) developed a model of quantitative fungicide resistance (analogous to a curvature shift) incorporating the effect of mutation on a continuous distribution of resistance phenotypes over time, and additionally considered concurrent evolution of virulence to resistant host cultivars, although demographic stochasticity in the emergence phase was not considered. Their results showed that using fewer fungicide applications per year (minimising pathogen exposure time) maximised yield over longer-term timescales. The results of these studies show that strategies that prolong the selection phase will also often prolong the emergence phase, increasing fungicide effective lives.

The emergence of new resistant strains is also relevant to the analysis presented in Chapter 6. It would be interesting to investigate how different azole combinations and programme type (mixture; alternation within-years; alternation between-years; mosaic) influence the rate of emergence of different CYP51 haplotypes. In Chapter 6, I considered selection only for haplotypes present in population samples taken in individual years. An extended analysis could consider the presence of additional known CYP51 haplotypes at low frequencies, or allow for new CYP51 haplotypes to emerge through mutation or intragenic recombination. However, the level of predictability of individual CYP51 mutations in the field is low: 75% of CYP51 mutations found in the field have been reported only in a single species (Hawkins & Fraaije, 2021). The existence of a given mutation may increase or decrease the likelihood of particular CYP51 mutations arising in the same strain, due to interactions in the effects of individual CYP51 mutations on enzyme structure conferring fitness advantages or penalties (Hawkins & Fraaije, 2018; Mullins et al., 2011). The likelihood of intragenic recombination will vary between CYP51 mutations depending on their proximity on the gene. The likelihood of new CYP51 mutations or haplotypes arising may therefore depend on genetic background (Hawkins & Fraaije, 2018), so previous selection for particular haplotypes could influence the future course of evolution. A realistic representation of the emergence of new CYP51 haplotypes would therefore be highly complex.

The length of time for resistance to emerge is likely to be reduced in a genetic background with a higher mutation rate. Fungicide applications could therefore indirectly select for an increase in pathogen mutation rates over time, or an increased frequency of hypermutator strains (Gambhir et al., 2022). Although there are often fitness costs of a higher mutation rate due to increased numbers of deleterious mutations, the fitness advantage of fungicide resistance is also large. Additionally, in a sexually reproducing population, beneficial resistance alleles

generated by hypermutator strains present at a low frequency could quickly recombine into a genetic background without deleterious mutations. Hypermutator strains have been found in several fungal pathogens of humans, including *Aspergillus fumigatus* (dos Reis et al., 2019; Gambhir et al., 2022).

It would be useful to model the effect of different fungicide programmes on selection for increased mutation rates in plant pathogens. The use of more diverse fungicide programmes such as mixtures or alternation generates a more challenging adaptive landscape for pathogens, which could increase selection for hypermutator strains. For example, a modelling study of the bacteria *Escherichia coli* showed that the likelihood of fixation of mutator alleles increasing the mutation rate by 10- to 100-fold increased as the number of mutations required for adaptation increased, although this analysis assumed equal fitness gain with each mutation (Tenaillon et al., 1999). Hypermutator strains have been shown to increase the risk of multi-drug resistance to antibiotics in *E. coli*, both following combination (mixture) and single-drug treatment, with increased expression of multi-drug efflux pumps (Gifford et al., 2023).

An increase in mutation rates could occur across the whole pathogen genome, or could be localised to areas of the genome that are under directional selection from fungicide application, minimising deleterious mutations in other areas of the genome. Epigenetic modifications have been shown to affect local mutation rates and gene duplication rates in *Z. tritici*, whilst mutation rates were found to be higher on accessory chromosomes (Habig et al., 2021). Gene duplication could directly increase resistance levels through target-site or efflux-pump overexpression, or could increase the likelihood of adaptive mutations and reduce purifying selection on deleterious mutations due to redundancy (Pegueroles et al., 2013). These mechanisms for localised increases in mutation rate would be of relevance for modelling the effect of fungicide programmes on mutation rates. Collections of *Z. tritici* isolates with different CYP51 haplotypes now span decades: it would be informative to compare the mutation rates of these isolates of different areas of the genome, to test for changes over time and with CYP51 haplotype.

7.5.2 Timing and proportion of sexual reproduction

In Chapter 5, I used the simplifying assumption that the epidemic proceeded through asexual reproduction throughout the growing season, with sexual reproduction and formation of ascospores occurring only at the end of the growing season. However, there is evidence from spore trapping, field observations and

molecular markers that sexual recombination occurs at a low level in *Z. tritici* throughout the growing season, followed by a strong increase in the rate of sexual reproduction towards the end of the growing season (Chen & McDonald, 1996; Duvivier, 2015; Eriksen & Munk, 2003; Hassine et al., 2019; Hunter et al., 1999; Zhan et al., 1998). Sexual reproduction in *Z. tritici* is density-dependent, with ascospore production reaching a maximum at a disease severity of 30 to 45% (Suffert et al., 2019).

Eriksen et al. (2001) modelled the relative contribution of pycnidiospores and ascospores to epidemics of septoria tritici blotch, and concluded that most of the increase in disease severity is attributable to infection by asexual pycnidiospores. They note that the number of pycnidiospores produced by a single lesion is orders of magnitude larger than the number of ascospores contained in a single pseudothecium. The latent periods for the development of pseudothecia and for the establishment of infection following infection with ascospores are also longer compared to pycnidia and pycnidiospores (Eriksen et al., 2001; Morais et al., 2015). However, Eriksen et al. (2001) also showed that sexual recombination within the season could affect the genetic composition of the population during the season, with larger effects if the pathogen population experienced dry weather that reduced the rate of infection by pycnidiospores due to decreased dispersal rates. This model could be adapted to investigate whether accounting for sexual reproduction prior to the end of the growing season affects the comparison of alternation and splitting and mixing as strategies against concurrent evolution of resistance to two MoA.

A model comparing the contribution of ascospores to epidemic growth on susceptible and resistant crop cultivars predicted that ascospores may account for a greater proportion of infections on resistant cultivars (Duvivier, 2015). This was explained by the escape of resistant cultivars from infection earlier in the growing season, leaving a greater area of healthy leaf area available for new infection by ascospores late in the growing season (when ascospore numbers are highest) compared to susceptible cultivars. If resistant cultivars are more likely to be infected by ascospores released from another crop that was treated with fungicides, there may be an increased frequency of double-resistant strains on resistant cultivars, with potential implications for resistance management. For example, this may affect the choice of fungicide programme for applications to the upper leaf canopy of resistant cultivars. This phenomenon may also be of relevance for management of cultivar mixtures within the same field.

I also assumed that all between-season reproduction was sexual, and only considered a single scenario of the starting frequencies of the single- and double-resistant strains. The impact of different levels of sexual reproduction between seasons could be explored in more detail: a study by Taylor & Cunniffe (2023c) showed that a higher rate of sexual reproduction increased the rate of production of double-resistant strains when the frequency of the double-resistant strain was low, but subsequently suppressed higher frequencies of the double-resistant strain. Ascospores are thought to contribute the majority of initial infections in the next season's crops (Suffert et al., 2011), and the effect on qualitative comparisons between splitting and mixing and alternation is likely to be minimal (as discussed in Section 5.5). However, consideration of potential variation in the level of sexual reproduction between seasons in combination with multiple scenarios of the starting frequencies of single- and double-resistant strains would be informative for estimates of programme effective life or lifetime yield. Such estimates would also require running the model for a larger number of growing seasons to estimate the length of time before disease control breaks down.

7.5.3 Representation of the dose response to fungicides

In Chapters 3-5, the effect of fungicide application on the pathogen was described in terms of changes to the pathogen transmission rate and latent period. These life cycle parameters affect the overall growth rate of the pathogen population. The fungicide dose response is described by a combination of an asymptote parameter, q, a curvature parameter, k, and the fungicide decay rate (Figure 4.1). This approach is compatible with the use of compartmental epidemiological models, with healthy, latently infected, infectious and senesced leaf area index tracked separately. Fungicide decay rates were estimated from values available in published literature, whilst disease progress data from multiple field trials provided sufficient degrees of freedom to fit the two dose response parameter values q and k. However, there is strong covariance between the values of q and k (for example, see Section 3.A.3), which can increase the standard error for these parameter values.

A different approach was used in Chapter 6, where the dose response to mixtures of azole fungicides with the same mode of action is described in terms of a direct effect on the pathogen population growth rate, as it is derived by considering the mode of action of azole fungicides as CYP51 inhibitors reducing the rate of production of ergosterol, and thereby limiting the population growth rate (Section

6.3.2.1). The fungicide dose response for each haplotype i and azole j is described by a combination of parameter B_{ij} and the fungicide decay rate. A simplifying assumption of exponential pathogen population growth was used, with no representation of density dependence, in contrast to the more detailed compartmental models used in Chapters 3-5. Data on the mean EC_{50} of isolates of each haplotype was used to fit the dose response parameter B_{ij}. It should be noted that there was limited data available for parameterisation for a number of haplotypes and azoles (in some cases only a single isolate), so there would be insufficient degrees of freedom to parameterise two dose response parameters as used in Chapters 3-5.

Cunniffe et al. (2012) demonstrate how compartmental models with multiple latent and infectious compartments can be linearised around the pathogen-free equilibrium to obtain an expression for the pathogen growth rate, r. This approach could potentially be exploited to map the effect of azole mixtures on the pathogen growth rate to an effect on an individual pathogen life cycle parameter (latent period or transmission rate), or multiple parameters subject to assumptions on the relative effects of the fungicides on each of these life cycle parameters.

In Chapters 3-5, I used the simplifying assumption that the fungicide dose response parameters for a systemic fungicide would be the same for their effect on the transmission rate and the latent period, and additionally I assumed that multisite fungicides affect only the transmission rate. The reality is likely to be more complex, but it is not possible to accurately parameterise this from field data alone, and there is also a lack of suitable laboratory data. It would be interesting to explore the impact of these assumptions on the modelling results. However, a previous modelling analysis suggests that these assumptions may have little impact on qualitative model results (Mikaberidze et al., 2014).

7.5.4 Variation in pathogen life cycle parameters

In this thesis, I used modelling approaches that assumed a constant average latent period, infectious period and transmission rate over time (before accounting for the effects of density dependence and fungicide application). However, there is strong empirical evidence that these pathogen life cycle parameters are not constant over time. For example, spore dispersal and germination rates in many pathogens depend on weather conditions including rainfall, wind, humidity and temperature. Latent periods can also vary, even when measured over thermal time, depending on optimum temperatures for pathogen growth, fluctuating leaf temperature and

host growth stage and leaf age (Bernard et al., 2013; Shaw, 1990; Suffert & Thompson, 2018). The rate of release of spores is not constant over the infectious period of a lesion (Cunniffe et al., 2012; Eyal, 1971).

Variability in pathogen life cycle parameters is relevant to all of the pathosystems modelled in this thesis. However, it would be particularly useful to explore the effect of variable pathogen life cycle parameters on the results presented in Chapter 3, which showed that there were resistance management benefits of delaying inoculum arrival using a phytosanitary 'soybean-free period'. There could be potential interactions of the effects of delaying infection with variation in pathogen life cycle parameters due to weather conditions.

Decision-support systems often use weather data as inputs to provide predictions of disease risk and severity (González-Domínguez et al., 2023). Many decision-support systems provide threshold-based assessments of risk, such as the 'Irish Rules' and 'Nærstad' models of *P. infestans* (Cucak et al., 2019; Hjelkrem et al., 2021). More complex epidemiological models that incorporate the effect of environmental variables on pathogen development can provide good predictions of disease progress over time, for example as implemented in models of *Z. tritici*, *P. pachyrhizi*, *Puccinia striiformis* (yellow rust), and *Fusicladium eriobotryae* (loquat scab) (Audsley et al., 2005; Chaloner et al., 2019; González-Domínguez et al., 2014; Kassie et al., 2023; Savary et al., 2015).

Many biological processes are inherently variable even after accounting for large numbers of explanatory factors, so pathogen life cycle parameter values may be best represented by a frequency distribution. Cunniffe et al. (2012) proposed a method to extend basic susceptible, exposed infection and removed (SEIR) compartmental models by increasing the number of latent and infectious compartments included in the model, enabling improved simulation of empirically-observed frequency distributions.

The approaches described above could be incorporated into the modelling approaches described in this thesis to provide a better simulation of disease severity progress. High-quality data would be required to parameterise and run the model, and to check for the effects of environmental variability on model outcomes. Improved simulation of disease progress in the absence of fungicide could reduce the uncertainty in the parameterisation of the fungicide dose-response curve, as a lack of fit to disease progress curves may account for some apparent differences in fungicide efficacy between trials. If modelling effects of environmental variability

on pathogen life cycle parameters, the effect of these factors on fungicide foliar decay rate should also be modelled, but data availability is currently limited (Fantke et al., 2014). If weather data or parameter values for the effects of environmental variables are uncertain, there is a risk that the added model complexity will simply add another source of uncertainty, or cause unexpected and misleading model behaviour that may be difficult to detect.

I did not consider the effect of fitness costs of resistance, which can be represented by their effects on pathogen life cycle parameters. Resistant strains with a fitness cost will have slower population growth rates than sensitive strains in the absence of fungicide (and possibly at low fungicide effective doses, depending on the fungicide dose response curve and the type and magnitude of sensitivity shift). This can affect which fungicide programmes are optimal (Mikaberidze et al., 2014, 2017), at least in the short term. However, fitness costs can be transient due to compensatory mutations, so resistance management strategies cannot rely on fitness costs of resistance (Hawkins & Fraaije, 2018).

7.5.5 Modelling the effect of efflux mechanisms and incomplete cross-resistance between MoA

The modelling approach in Chapter 6 accounted implicitly for interactions between different target-site mutations, based on the laboratory-measured EC_{50} sensitivities of different CYP51 haplotypes. However, the dataset did not allow for parameterisation of the effect of enhanced efflux in combination with target-site mutations. It would be interesting to extend the analysis in Chapters 4, 5 and 6 to investigate interactions between enhanced efflux and other resistance mechanisms, if suitable data were available for model parameterisation. Genotyping of multi-drug resistant (MDR) isolates suggests that there are multiple genes responsible for enhanced efflux (Omrane et al., 2015; Patry-Leclaire et al., 2023) which may be inherited independently of target-site mutations and one another, so it would be necessary to account for the effects of sexual reproduction.

Membrane transporters actively reduce the pathogen's cellular concentration of fungicide through drug efflux, reducing the effective dose. This could interact with changes in the dose response curve due to an asymptote or curvature shift arising through a target-site mutation. Figure 7.1 shows theoretical dose response curves for strains with enhanced efflux in combination with a target-site mutation causing an asymptote shift or a curvature shift respectively, assuming that efflux reduces the intracellular fungicide concentration up to a fixed percentage of a full label dose

rate. The combination would lead to a more highly resistant strain in both cases, but the decrease in sensitivity is more dramatic for the strain with a target-site mutation causing a curvature shift. There is experimental evidence that combinations of target-site mutations with enhanced efflux mechanisms can lead to more highly resistant phenotypes in *B. cinerea* and *Z. tritici* (Kildea et al., 2019; Sofianos et al., 2023), and synergistic effects between efflux mechanisms and permeability barriers have been observed in Gram-negative bacteria (Krishnamoorthy et al., 2017; Li et al., 2015).

In the modelling analysis presented in Chapter 5, I assumed that the resistance mechanism causing a sensitivity shift to one MoA ('Fungicide A') did not affect sensitivity to the second MoA ('Fungicide B'), and vice versa, i.e. that there was a complete absence of cross-resistance between the single-resistant strains. However, generalist resistance mechanisms including enhanced drug efflux can cause cross-resistance to multiple MoA (Omrane et al., 2015, 2017; Patry-Leclaire et al., 2023). It would therefore be useful to extend the model to represent the effect of efflux mechanisms on the dose response to mixtures of different MoAs, to understand whether this affects the comparison between splitting and mixing and alternation strategies. However, additional data would be needed to parameterise the effect of efflux mechanisms on a fungicide mixture. The effects vary between MoAs (Omrane et al., 2015), potentially because of differences in fungicide molecular size or the binding affinity of membrane transporters to different fungicides. If fungicide concentrations overwhelm the capacity of membrane transporters, it is not clear whether there would be preferential efflux of one fungicide in a mixture, or whether the rate of efflux of each fungicide would be mostly determined by their relative intracellular concentrations. Molecular modelling or direct measurements of efflux rates would therefore be useful to inform parameterisation of a model of the effect of MDR efflux mechanisms on fungicide mixtures.
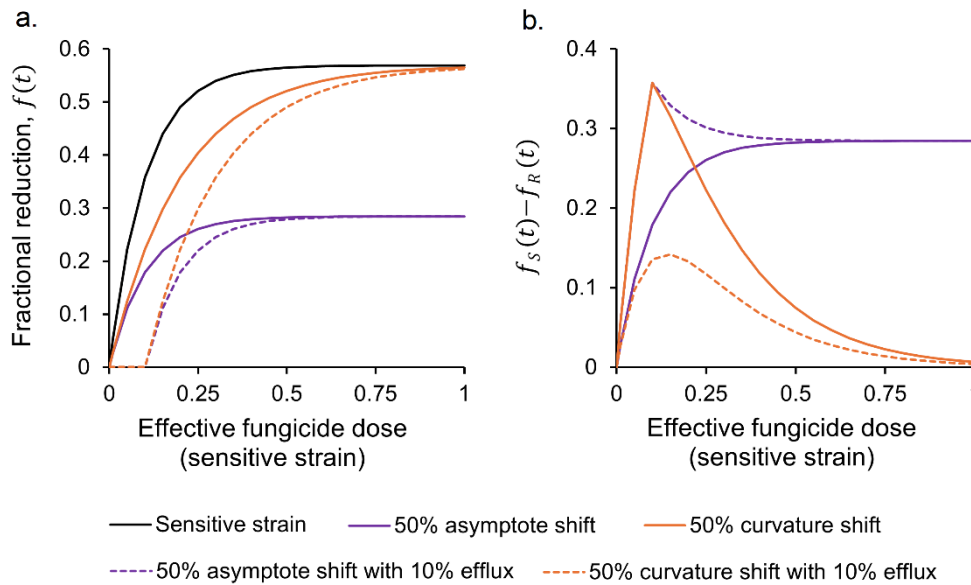
Figure 7.1: Theoretical dose response curves of (a) the fractional reduction in pathogen life cycle parameters, $f(t)$, and (b) the difference in the fractional reduction of sensitive and resistant strains, $f_S(t) - f_R(t)$, for strains with enhanced efflux in combination with a target-site mutation causing a 50% asymptote shift or 50% curvature shift. The dose response is compared with a sensitive strain and strains with a target-site mutation with no enhanced efflux. It is assumed that efflux reduces intracellular fungicide concentrations by up to a maximum of 10% of a full label dose rate.

7.6 Are there any universal strategies against concurrent evolution of resistance?

Successful implementation of resistance management strategies requires consistent, clear messaging on which tactics work, to build industry consensus and enable growers to integrate these strategies into decision-making on-farm (Chapter 2 – Section 2.7). Unfortunately, my results have identified variation in the best way to combine fungicidal MoAs in fungicide programmes when resistance is evolving concurrently to both MoAs, which increases the complexity of the message to be communicated, making it more difficult to build consensus. There may be no universal tactic for how to combine MoAs in a fungicide programme in this case. My results suggest that the suitability of resistance management tactics may need to be assessed for individual fungicide active substances and MoAs, taking into consideration fungicide properties, likely resistance risks, and the dynamics of individual pathosystems.

The results of this thesis add to evidence from previous studies that the optimal fungicide resistance strategy can depend on the choice of fungicide active substances and the frequency of strains with resistance to one or both active substances (Ballu et al., 2024; Taylor & Cunniffe, 2023c). A comparison with other biological systems is also informative. Helps et al. (2020) compared the effective lives of reduced-dose mixtures, label-dose mixtures, alternation and sequential application of two insecticides in a modelling study covering a wide range of life-history traits and parameter values. They showed that reduced dose mixture was optimal in the majority of cases with sexual reproduction, and second to sequential application for asexual insects, but the optimal strategy was variable in all cases, and the relative efficacies of each insecticide were important. Trade-offs between selection for target-site resistance and generalist resistance to antibiotics have been demonstrated in the bacterium *P. aeruginosa* (Vestergaard et al., 2016). Non-target-site, metabolic resistance is particularly common in weeds (Hawkins et al., 2019). There is evidence that use of reduced-rate herbicide mixtures is a poor strategy for herbicide resistance management, and that mixtures can increase selection for generalist resistance (Comont et al., 2020; Lagator et al., 2013). However, a recent modelling study suggests that full-label rate herbicide mixtures can be more effective than alternation, even against generalist non-target-site resistance (Renton et al., 2024).

Overall, the most universal resistance management strategy is to reduce reliance on chemical control. This can be achieved through use of IPM strategies including cultural control measures and use of resistant and tolerant cultivars. However, individual IPM measures may not be universal: a measure that reduces the risk of some pests and diseases may increase the risk of others, and agronomic factors can affect whether a measure is viable on a particular farm. For example, delayed sowing can help with *Z. tritici* and *Alopecurus myosuroides* (black-grass) control (Morgan et al., 2021; Neale, 2012; Vandersteen et al., 2011), but may increase the risk of *P. striiformis* in susceptible cultivars (Gladders et al., 2007) and make the crop less resilient to attack by wheat bulb fly (AHDB, 2024). On wet soils, delayed drilling may not be a practical option: it can negatively impact crop establishment, with the potential to reduce yields or require increased nitrogen application, with associated increases in cost, potential water quality impacts and greenhouse gas emissions (AHDB, 2023; Jarecki, 2024; Menegat et al., 2022). A holistic approach is therefore needed to assess the costs and benefits of IPM measures at a local scale. Where there are economic costs associated with increased use of non-

chemical IPM, there may be a role for the use of economic incentives and regulation to counteract 'future discounting'. Since the rate of development and approval of new MoAs is limited, swift adoption of a diverse range of IPM strategies is vital to aid fungicide resistance management, improve the resilience of the farming system and safeguard future food security.

7.7   References

AHDB (2023). Wheat growth guide. Available at: https://projectblue.blob.core.windows.net/media/Default/Imported%20Public ation%20Docs/AHDB%20Cereals%20&%20Oilseeds/General/Wheat%20gr owth%20guide%20(2023).pdf [Accessed: 8 December 2024].

AHDB (2024). How to manage wheat bulb fly risk in cereals. Available at: https://ahdb.org.uk/knowledge-library/how-to-manage-wheat-bulb-fly-risk-in-cereals [Accessed: 8 December 2024].

Alzohairy, S. A., Heger, L., Nikzainalalam, N., & Miles, T. D. (2023). Cross-Resistance of Succinate Dehydrogenase Inhibitors (SDHI) in *Botrytis cinerea* and Development of Molecular Diagnostic Tools for SDHI Resistance Detection. *Phytopathology®, 113*(6), 998–1009. https://doi.org/10.1094/PHYTO-09-22-0346-R

Audsley, E., Milne, A., & Paveley, N. (2005). A foliar disease model for use in wheat disease management decision support systems. *Annals of Applied Biology, 147*(2), 161–172. https://doi.org/10.1111/j.1744-7348.2005.00023.x

Ballu, A., Deredec, A., Walker, A.-S., & Carpentier, F. (2021). Are Efficient-Dose Mixtures a Solution to Reduce Fungicide Load and Delay Evolution of Resistance? An Experimental Evolutionary Approach. *Microorganisms*, *9*(11), 2324. https://doi.org/10.3390/microorganisms9112324

Ballu, A., Ugazio, C., Duplaix, C., Noly, A., Wullschleger, J., Torriani, S. F. F. et al. (2024). Preventing multiple resistance above all: New insights for managing fungal adaptation. *Environmental Microbiology, 26*(4). https://doi.org/10.1111/1462-2920.16614

Bernard, F., Sache, I., Suffert, F., & Chelle, M. (2013). The development of a foliar fungal pathogen does react to leaf temperature! *New Phytologist, 198*(1), 232–240. https://doi.org/10.1111/nph.12134

Brunner, P. C., Stefanato, F. L., & McDonald, B. A. (2008). Evolution of the *CYP51* gene in *Mycosphaerella graminicola* : evidence for intragenic recombination and selective replacement. *Molecular Plant Pathology, 9*(3), 305–316. https://doi.org/10.1111/j.1364-3703.2007.00464.x

Butaye, P., Devriese, L. A., & Haesebrouck, F. (2000). Incomplete Cross Resistance Against Ionophores in *Enterococcus faecium* and *Enterococcus faecalis* Strains from Pigs and Poultry. *Microbial Drug Resistance*, *6*(1), 59–61. https://doi.org/10.1089/mdr.2000.6.59

Chaloner, T. M., Fones, H. N., Varma, V., Bebber, D. P., & Gurr, S. J. (2019). A new mechanistic model of weather-dependent Septoria tritici blotch disease risk. *Philosophical Transactions of the Royal Society B: Biological Sciences*, *374*(1775), 20180266. https://doi.org/10.1098/rstb.2018.0266

Chen, R.-S., & McDonald, B. A. (1996). Sexual Reproduction Plays a Major Role in the Genetic Structure of Populations of the Fungus *Mycosphaerella graminicola*. *Genetics*, *142*(4), 1119–1127. https://doi.org/10.1093/genetics/142.4.1119

Comont, D., Lowe, C., Hull, R., Crook, L., Hicks, H. L., Onkokesung, N. et al. (2020). Evolution of generalist resistance to herbicide mixtures reveals a trade-off in resistance management. *Nature Communications*, *11*(1), 3086. https://doi.org/10.1038/s41467-020-16896-0

Cooke, L. R., Schepers, H. T. A. M., Hermansen, A., Bain, R. A., Bradshaw, N. J., Ritchie, F. et al. (2011). Epidemiology and Integrated Control of Potato Late Blight in Europe. *Potato Research*, *54*(2), 183–222. https://doi.org/10.1007/s11540-011-9187-0

Cucak, M., Sparks, A., Moral, R., Kildea, S., Lambkin, K., & Fealy, R. (2019). Evaluation of the 'Irish Rules': The Potato Late Blight Forecasting Model and Its Operational Use in the Republic of Ireland. *Agronomy*, *9*(9), 515. https://doi.org/10.3390/agronomy9090515

Cunniffe, N. J., Stutt, R. O. J. H., van den Bosch, F., & Gilligan, C. A. (2012). Time-Dependent Infectivity and Flexible Latent and Infectious Periods in Compartmental Models of Plant Disease. *Phytopathology®*, *102*(4), 365–380. https://doi.org/10.1094/PHYTO-12-10-0338

Deising, H. B., Reimann, S., & Pascholati, S. F. (2008). Mechanisms and significance of fungicide resistance. *Brazilian Journal of Microbiology*, *39*, 286–295.

Dooley, H., Shaw, M. W., Spink, J., & Kildea, S. (2016). Effect of azole fungicide mixtures, alternations and dose on azole sensitivity in the wheat pathogen *Zymoseptoria tritici*. *Plant Pathology*, *65*(1), 124–136. https://doi.org/10.1111/ppa.12395

Duvivier, M. (2015). Distribution of the airborne inoculum of wheat leaf rust and septoria tritici blotch. PhD thesis. Belgique: Université Catholique de Louvain

dos Reis, T. F., Silva, L. P., de Castro, P. A., do Carmo, R. A., Marini, M. M., da Silveira, J. F. et al. (2019). The Aspergillus fumigatus Mismatch Repair *MSH2* Homolog Is Important for Virulence and Azole Resistance. *MSphere*, *4*(4). https://doi.org/10.1128/mSphere.00416-19

Elderfield, J. A. D., Lopez-Ruiz, F. J., van den Bosch, F., & Cunniffe, N. J. (2018). Using Epidemiological Principles to Explain Fungicide Resistance Management Tactics: Why do Mixtures Outperform Alternations? *Phytopathology®*, *108*(7), 803–817. https://doi.org/10.1094/PHYTO-08-17-0277-R

Eriksen, L., & Munk, L. (2003). The Occurrence of *Mycosphaerella graminicola* and its Anamorph *Septoria tritici* in Winter Wheat during the Growing Season. *European Journal of Plant Pathology*, *109*(3), 253–259. https://doi.org/10.1023/A:1022851502770

Eriksen, L., Shaw, M. W., & Østergård, H. (2001). A Model of the Effect of Pseudothecia on Genetic Recombination and Epidemic Development in Populations of *Mycosphaerella graminicola*. *Phytopathology®*, *91*(3), 240–248. https://doi.org/10.1094/PHYTO.2001.91.3.240

Eyal, Z. (1971). The kinetics of pycnospore liberation in *Septoria tritici*. *Canadian Journal of Botany*, *49*(7), 1095–1099. https://doi.org/10.1139/b71-157

Fantke, P., Gillespie, B. W., Juraske, R., & Jolliet, O. (2014). Estimating Half-Lives for Pesticide Dissipation from Plants. *Environmental Science & Technology*, *48*(15), 8588–8602. https://doi.org/10.1021/es500434p

Förster, H., Luo, Y., Hou, L., & Adaskaveg, J. E. (2022). Mutations in *Sdh* Gene Subunits Confer Different Cross-Resistance Patterns to SDHI Fungicides in *Alternaria alternata* Causing Alternaria Leaf Spot of Almond in California. *Plant Disease*, *106*(7), 1911–1918. https://doi.org/10.1094/PDIS-09-21-1913-RE

Fraaije, B. A., Cools, H. J., Kim, S., Motteram, J., Clark, W. S., & Lucas, J. A. (2007). A novel substitution I381V in the sterol 14α-demethylase (CYP51) of *Mycosphaerella graminicola* is differentially selected by azole fungicides. *Molecular Plant Pathology*, *8*(3), 245–254. https://doi.org/10.1111/j.1364-3703.2007.00388.x

Gambhir, N., Harris, S. D., & Everhart, S. E. (2022). Evolutionary Significance of Fungal Hypermutators: Lessons Learned from Clinical Strains and Implications for Fungal Plant Pathogens. *MSphere*, *7*(3). https://doi.org/10.1128/msphere.00087-22

Gifford, D. R., Berríos-Caro, E., Joerres, C., Suñé, M., Forsyth, J. H., Bhattacharyya, A. et al. (2023). Mutators can drive the evolution of multi-resistance to antibiotics. *PLOS Genetics*, *19*(6), e1010791. https://doi.org/10.1371/journal.pgen.1010791

Gladders, P., Langton, S. D., Barrie, I. A., Hardwick, N. V., Taylor, M. C., & Paveley, N. D. (2007). The importance of weather and agronomic factors for the overwinter survival of yellow rust (*Puccinia striiformis*) and subsequent disease risk in commercial wheat crops in England. *Annals of Applied Biology*, *150*(3), 371–382. https://doi.org/10.1111/j.1744-7348.2007.00131.x

González-Domínguez, E., Armengol, J., & Rossi, V. (2014). Development and Validation of a Weather-Based Model for Predicting Infection of Loquat Fruit by *Fusicladium eriobotryae*. *PLoS ONE*, *9*(9), e107547. https://doi.org/10.1371/journal.pone.0107547

González-Domínguez, E., Caffi, T., Rossi, V., Salotti, I., & Fedele, G. (2023). Plant Disease Models and Forecasting: Changes in Principles and Applications over the Last 50 Years. *Phytopathology®*, *113*(4), 678–693. https://doi.org/10.1094/PHYTO-10-22-0362-KD

Grimmer, M., Sokolidi, A., Corkley, I. (2024). Impact of fungicide programmes on the performance of cereals and oilseeds varieties (scoping review). ADAS report to AHDB, Research Review 99. Available at: https://projectblue.blob.core.windows.net/media/Default/Research%20Paper s/Cereals%20and%20Oilseed/2024/RR99%20final%20report.pdf [Accessed 29 November 2024].

Habig, M., Lorrain, C., Feurtey, A., Komluski, J., & Stukenbrock, E. H. (2021). Epigenetic modifications affect the rate of spontaneous mutations in a pathogenic fungus. *Nature Communications*, *12*(1), 5869. https://doi.org/10.1038/s41467-021-26108-y

Hagerty, C. H., Klein, A. M., Reardon, C. L., Kroese, D. R., Melle, C. J., Graber, K. R. et al. (2021). Baseline and Temporal Changes in Sensitivity of *Zymoseptoria tritici* Isolates to Benzovindiflupyr in Oregon, U.S.A., and Cross-Sensitivity to Other SDHI Fungicides. *Plant Disease*, *105*(1), 169–174. https://doi.org/10.1094/PDIS-10-19-2125-RE

Hassine, M., Siah, A., Hellin, P., Cadalen, T., Halama, P., Hilbert, J.-L. et al. (2019). Sexual reproduction of Zymoseptoria tritici on durum wheat in Tunisia revealed by presence of airborne inoculum, fruiting bodies and high levels of genetic diversity. *Fungal Biology*, *123*(10), 763–772. https://doi.org/10.1016/j.funbio.2019.06.006

Hawkins, N. J. (2024). Assessing the predictability of fungicide resistance evolution through in vitro selection. *Journal of Plant Diseases and Protection*, *131*(4), 1257–1264. https://doi.org/10.1007/s41348-024-00906-0

Hawkins, N. J., Bass, C., Dixon, A., & Neve, P. (2019). The evolutionary origins of pesticide resistance. *Biological Reviews*, *94*(1), 135–155. https://doi.org/10.1111/brv.12440

Hawkins, N. J., & Fraaije, B. A. (2018). Fitness Penalties in the Evolution of Fungicide Resistance. *Annual Review of Phytopathology*, *56*(1), 339–360. https://doi.org/10.1146/annurev-phyto-080417-050012

Hawkins, N. J., & Fraaije, B. A. (2021). Contrasting levels of genetic predictability in the evolution of resistance to major classes of fungicides. *Molecular Ecology*, *30*(21), 5318–5327. https://doi.org/10.1111/mec.15877

Hazuda, D. J., Anthony, N. J., Gomez, R. P., Jolly, S. M., Wai, J. S., Zhuang, L. et al. (2004). A naphthyridine carboxamide provides evidence for discordant resistance between mechanistically identical inhibitors of HIV-1 integrase. *Proceedings of the National Academy of Sciences*, *101*(31), 11233–11238. https://doi.org/10.1073/pnas.0402357101

Heick, T. M., Justesen, A. F., & Jørgensen, L. N. (2017). Anti-resistance strategies for fungicides against wheat pathogen Zymoseptoria tritici with focus on DMI fungicides. *Crop Protection*, *99*, 108–117. https://doi.org/10.1016/j.cropro.2017.05.009

Helps, J. C., Paveley, N. D., White, S., & van den Bosch, F. (2020). Determinants of optimal insecticide resistance management strategies. *Journal of Theoretical Biology*, *503*, 110383. https://doi.org/10.1016/j.jtbi.2020.110383

Hjelkrem, A.-G. R., Eikemo, H., Le, V. H., Hermansen, A., & Nærstad, R. (2021). A process-based model to forecast risk of potato late blight in Norway (The Nærstad model): model development, sensitivity analysis and Bayesian calibration. *Ecological Modelling*, *450*, 109565. https://doi.org/10.1016/j.ecolmodel.2021.109565

Hobbelen, P. H. F., Paveley, N. D., Oliver, R. P., & van den Bosch, F. (2013). The Usefulness of Fungicide Mixtures and Alternation for Delaying the Selection for Resistance in Populations of *Mycosphaerella graminicola* on Winter Wheat: A Modeling Analysis. *Phytopathology®*, *103*(7), 690–707. https://doi.org/10.1094/PHYTO-06-12-0142-R

Hobbelen, P. H. F., Paveley, N. D., & van den Bosch, F. (2014). The Emergence of Resistance to Fungicides. *PLoS ONE*, *9*(3), e91910. https://doi.org/10.1371/journal.pone.0091910

Hunter, T., Coker, R. R., & Royle, D. J. (1999). The teleomorph stage, *Mycosphaerella graminicola* , in epidemics of septoria tritici blotch on winter wheat in the UK. *Plant Pathology*, *48*(1), 51–57. https://doi.org/10.1046/j.1365-3059.1999.00310.x

Ishii, H., Miyamoto, T., Ushio, S., & Kakishima, M. (2011). Lack of cross-resistance to a novel succinate dehydrogenase inhibitor, fluopyram, in highly boscalid-resistant isolates of *Corynespora cassiicola* and *Podosphaera xanthii*. *Pest Management Science*, *67*(4), 474–482. https://doi.org/10.1002/ps.2092

Jarecki, W. (2024). Response of Winter Wheat to Delayed Sowing and Varied Nitrogen Fertilization. *Agriculture*, *14*(1), 121. https://doi.org/10.3390/agriculture14010121

Kassie, B. T., Onstad, D. W., Koga, L., Hart, T., Clark, R., & van der Heijden, G. (2023). Modeling the early phases of epidemics by Phakospora pachyrhizi in Brazilian soybean. *Frontiers in Agronomy*, *5*. https://doi.org/10.3389/fagro.2023.1214038

Kildea, S., Dooley, H., & Byrne, S. (2023). A note on the impact of CYP51 alterations and their combination in the wheat pathogen *Zymoseptoria tritici* on sensitivity to the azole fungicides epoxiconazole and metconazole. *Irish Journal of Agricultural and Food Research*, *62*(1). https://doi.org/10.15212/ijafr-2023-0103

Kildea, S., Hellin, P., Heick, T. M., Byrne, S., & Hutton, F. (2024). Mefentrifluconazole sensitivity amongst European *Zymoseptoria tritici* populations and potential implications for its field efficacy. *Pest Management Science*, *80*(2), 533–543. https://doi.org/10.1002/ps.7795

Kildea, S., Marten-Heick, T., Grant, J., Mehenni-Ciz, J., & Dooley, H. (2019). A combination of target-site alterations, overexpression and enhanced efflux activity contribute to reduced azole sensitivity present in the Irish Zymoseptoria tritici population. *European Journal of Plant Pathology*, *154*(3), 529–540. https://doi.org/10.1007/s10658-019-01676-4

Krishnamoorthy, G., Leus, I. V., Weeks, J. W., Wolloscheck, D., Rybenkov, V. V., & Zgurskaya, H. I. (2017). Synergy between Active Efflux and Outer Membrane Diffusion Defines Rules of Antibiotic Permeation into Gram-Negative Bacteria. *MBio*, *8*(5). https://doi.org/10.1128/mBio.01172-17

Lagator, M., Vogwill, T., Mead, A., Colegrave, N., & Neve, P. (2013). Herbicide mixtures at high doses slow the evolution of resistance in experimentally evolving populations of *Chlamydomonas reinhardtii* . *New Phytologist*, *198*(3), 938–945. https://doi.org/10.1111/nph.12195

Lázaro, E., Makowski, D., & Vicent, A. (2021). Decision support systems halve fungicide use compared to calendar-based strategies without increasing disease risk. *Communications Earth & Environment*, *2*(1), 224. https://doi.org/10.1038/s43247-021-00291-8

Le May, C., Ney, B., Lemarchand, E., Schoeny, A., & Tivoli, B. (2009). Effect of pea plant architecture on spatiotemporal epidemic development of ascochyta blight (*Mycosphaerella pinodes*) in the field. *Plant Pathology*, *58*(2), 332–343. https://doi.org/10.1111/j.1365-3059.2008.01947.x

Leroux, P., & Walker, A. (2011). Multiple mechanisms account for resistance to sterol 14α-demethylation inhibitors in field isolates of *Mycosphaerella graminicola*. *Pest Management Science*, *67*(1), 44–59. https://doi.org/10.1002/ps.2028

Li, X.-Z., Plésiat, P., & Nikaido, H. (2015). The Challenge of Efflux-Mediated Antibiotic Resistance in Gram-Negative Bacteria. *Clinical Microbiology Reviews*, *28*(2), 337–418. https://doi.org/10.1128/CMR.00117-14

Lovell, D. J., Parker, S. R., Hunter, T., Welham, S. J., & Nichols, A. R. (2004). Position of inoculum in the canopy affects the risk of septoria tritici blotch epidemics in winter wheat. *Plant Pathology*, *53*(1), 11–21. https://doi.org/10.1046/j.1365-3059.2003.00939.x

McDonald, B. A., & Mundt, C. C. (2016). How Knowledge of Pathogen Population Biology Informs Management of Septoria Tritici Blotch. *Phytopathology®*, *106*(9), 948–955. https://doi.org/10.1094/PHYTO-03-16-0131-RVW

Menegat, S., Ledo, A., & Tirado, R. (2022). Greenhouse gas emissions from global production and use of nitrogen synthetic fertilisers in agriculture. *Scientific Reports*, *12*(1), 14490. https://doi.org/10.1038/s41598-022-18773-w

Mikaberidze, A., McDonald, B. A., & Bonhoeffer, S. (2014). Can High-Risk Fungicides be Used in Mixtures Without Selecting for Fungicide Resistance? *Phytopathology®*, *104*(4), 324–331. https://doi.org/10.1094/PHYTO-07-13-0204-R

Mikaberidze, A., Paveley, N., Bonhoeffer, S., & van den Bosch, F. (2017). Emergence of Resistance to Fungicides: The Role of Fungicide Dose. *Phytopathology®*, *107*(5), 545–560. https://doi.org/10.1094/PHYTO-08-16-0297-R

Miyamoto, T., Hayashi, K., Okada, R., Wari, D., & Ogawara, T. (2020). Resistance to succinate dehydrogenase inhibitors in field isolates of Podosphaera xanthii on cucumber: Monitoring, cross-resistance patterns and molecular characterization. *Pesticide Biochemistry and Physiology*, *169*, 104646.

https://doi.org/10.1016/j.pestbp.2020.104646

Morais, D., Laval, V., Sache, I., & Suffert, F. (2015). Comparative pathogenicity of sexual and asexual spores of *Zymoseptoria tritici* (septoria tritici blotch) on wheat leaves. *Plant Pathology*, *64*(6), 1429–1439. https://doi.org/10.1111/ppa.12372

Morgan, C., Wright, P., Blake, J., Corkley, I., Knight, S., Burnett, F. (2021). Combining agronomy, variety and chemistry to maintain control of septoria tritici in wheat. AHDB Project Report No. 634, pp 1-113. Available at: https://projectblue.blob.core.windows.net/media/Default/Research%20Paper s/Cereals%20and%20Oilseed/2021/PR634%20final%20project%20report.p df [Accessed: 17 November 2024].

Moyes, C. L., Lees, R. S., Yunta, C., Walker, K. J., Hemmings, K., Oladepo, F. et al. (2021). Assessing cross-resistance within the pyrethroids in terms of their interactions with key cytochrome P450 enzymes and resistance in vector populations. *Parasites & Vectors*, *14*(1), 115. https://doi.org/10.1186/s13071-021-04609-5

Mullins, J. G. L., Parker, J. E., Cools, H. J., Togawa, R. C., Lucas, J. A., Fraaije, B. A. et al. (2011). Molecular Modelling of the Emergence of Azole Resistance in Mycosphaerella graminicola. *PLoS ONE*, *6*(6), e20973. https://doi.org/10.1371/journal.pone.0020973

Neale, D. (2012). Optimising the cultural control of black-grass (*Alopecurus Myosuroides*). In: Orson J (ed) *Crop protection in southern Britain*. *Proceedings of an AAB conference, Peterborough, UK, 27-28 November 2012. Aspects of Applied Biology* 117, 7-10.

Nutter, F. W. (2007). The Role of Plant Disease Epidemiology in Developing Successful Integrated Disease Management Programs. In *General Concepts in Integrated Pest and Disease Management* (pp. 45–79). Springer Netherlands. https://doi.org/10.1007/978-1-4020-6061-8_3

Omrane, S., Audéon, C., Ignace, A., Duplaix, C., Aouini, L., Kema, G. et al. (2017). Plasticity of the *MFS1* Promoter Leads to Multidrug Resistance in the Wheat Pathogen *Zymoseptoria tritici*. *MSphere*, *2*(5). https://doi.org/10.1128/mSphere.00393-17

Omrane, S., Sghyer, H., Audéon, C., Lanen, C., Duplaix, C., Walker, A. et al. (2015). Fungicide efflux and the *MgMFS*1 transporter contribute to the multidrug resistance phenotype in *Zymoseptoria tritici* field isolates. *Environmental Microbiology*, *17*(8), 2805–2823. https://doi.org/10.1111/1462-2920.12781

Patry-Leclaire, S., Neau, E., Pitarch, A., Walker, A.-S., & Fillinger, S. (2023). Plasticity of the MFS1 promotor is not the only driver of Multidrug resistance in *Zymoseptoria tritici*. *BioRxiv*, 2023.12.27.573052. https://doi.org/10.1101/2023.12.27.573052

Paveley, N., Fraaije, B., van den Bosch, F., Kildea, S., Burnett, F., Clark, W. et al. (2020). Managing resistance evolving concurrently against two modes of action. In: Diesing HB; Fraaije B; Mehl A; Oerke EC; Sierotzki H; Stammler G (Eds), "Modern Fungicides and Antifungal Compounds", Vol. IX, pp.141-146. Deutsche Phytomedizinische Gesellschaft, Branschweig, ISBN: 978-3-941261-16-7.

Pegueroles, C., Laurie, S., & Albà, M. M. (2013). Accelerated Evolution after Gene Duplication: A Time-Dependent Process Affecting Just One Copy. *Molecular Biology and Evolution*, *30*(8), 1830–1842. https://doi.org/10.1093/molbev/mst083

Prahl, K. C., Klink, H., Hasler, M., Hagen, S., Verreet, J.-A., & Birr, T. (2022). Can Decision Support Systems Help Improve the Sustainable Use of Fungicides in Wheat? *Sustainability*, *14*(23), 15599. https://doi.org/10.3390/su142315599

Rehfus, A., Strobel, D., Bryson, R., & Stammler, G. (2018). Mutations in *sdh* genes in field isolates of *Zymoseptoria tritici* and impact on the sensitivity to various succinate dehydrogenase inhibitors. *Plant Pathology*, *67*(1), 175–180. https://doi.org/10.1111/ppa.12715

Renton, M., Willse, A., Aradhya, C., Tyre, A., & Head, G. (2024). Simulated herbicide mixtures delay both specialist monogenic and generalist polygenic resistance evolution in weeds. *Pest Management Science*, *80*(11), 5983–5994. https://doi.org/10.1002/ps.8331

Saintenac, C., Lee, W.-S., Cambon, F., Rudd, J. J., King, R. C., Marande, W. et al. (2018). Wheat receptor-kinase-like protein Stb6 controls gene-for-gene resistance to fungal pathogen *Zymoseptoria tritici*. *Nature Genetics*, *50*(3), 368–374. https://doi.org/10.1038/s41588-018-0051-x

Savary, S., Stetkiewicz, S., Brun, F., & Willocquet, L. (2015). Modelling and mapping potential epidemics of wheat diseases—examples on leaf rust and Septoria tritici blotch using EPIWHEAT. *European Journal of Plant Pathology*, *142*(4), 771–790. https://doi.org/10.1007/s10658-015-0650-7

Scalliet, G., Bowler, J., Luksch, T., Kirchhofer-Allan, L., Steinhauer, D., Ward, K. et al. (2012). Mutagenesis and Functional Studies with Succinate

Dehydrogenase Inhibitors in the Wheat Pathogen *Mycosphaerella graminicola*. *PLoS ONE*, *7*(4), e35429. https://doi.org/10.1371/journal.pone.0035429

Shaw, M. W. (1990). Effects of temperature, leaf wetness and cultivar on the latent period of *Mycosphaerella graminicola* on winter wheat. *Plant Pathology*, *39*(2), 255–268. https://doi.org/10.1111/j.1365-3059.1990.tb02501.x

Small, I. M., Joseph, L., & Fry, W. E. (2015). Development and implementation of the BlightPro decision support system for potato and tomato late blight management. *Computers and Electronics in Agriculture*, *115*, 57–65. https://doi.org/10.1016/j.compag.2015.05.010

Sofianos, G., Samaras, A., & Karaoglanidis, G. (2023). Multiple and multidrug resistance in Botrytis cinerea: molecular mechanisms of MLR/MDR strains in Greece and effects of co-existence of different resistance mechanisms on fungicide sensitivity. *Frontiers in Plant Science*, *14*. https://doi.org/10.3389/fpls.2023.1273193

Sonpavde, G., Pond, G. R., Mullane, S., Qu, A. Q., Di Lorenzo, G., Federico, P. et al. (2015). Incomplete Cross-Resistance Between Taxanes for Advanced Urothelial Carcinoma: Implications for Clinical Practice and Trial Design. *Clinical Genitourinary Cancer*, *13*(3), 250–256. https://doi.org/10.1016/j.clgc.2014.10.005

Steinhauer, D., Salat, M., Frey, R., Mosbach, A., Luksch, T., Balmer, D. et al. (2019). A dispensable paralog of succinate dehydrogenase subunit C mediates standing resistance towards a subclass of SDHI fungicides in *Zymoseptoria tritici*. *PLOS Pathogens*, *15*(12), e1007780. https://doi.org/10.1371/journal.ppat.1007780

Suffert, F., Delestre, G., & Gélisse, S. (2019). Sexual Reproduction in the Fungal Foliar Pathogen Zymoseptoria tritici Is Driven by Antagonistic Density Dependence Mechanisms. *Microbial Ecology*, *77*(1), 110–123. https://doi.org/10.1007/s00248-018-1211-3

Suffert, F., Sache, I., & Lannou, C. (2011). Early stages of septoria tritici blotch epidemics of winter wheat: build-up, overseasoning, and release of primary inoculum. *Plant Pathology*, *60*(2), 166–177. https://doi.org/10.1111/j.1365-3059.2010.02369.x

Suffert, F., & Thompson, R. N. (2018). Some reasons why the latent period should not always be considered constant over the course of a plant disease epidemic. *Plant Pathology*, *67*(9), 1831–1840. https://doi.org/10.1111/ppa.12894

Sykes, E. M., Sackett, K. E., Severns, P. M., & Mundt, C. C. (2017). Sensitivity variation and cross-resistance of Zymoseptoria tritici to azole fungicides in North America. *European Journal of Plant Pathology*. https://doi.org/10.1007/s10658-017-1370-y

Taylor, N. P., & Cunniffe, N. J. (2023a). Coupling machine learning and epidemiological modelling to characterise optimal fungicide doses when fungicide resistance is partial or quantitative. *Journal of The Royal Society Interface*, *20*(201). https://doi.org/10.1098/rsif.2022.0685

Taylor, N. P., & Cunniffe, N. J. (2023b). Modelling quantitative fungicide resistance and breakdown of resistant cultivars: Designing integrated disease management strategies for Septoria of winter wheat. *PLOS Computational Biology*, *19*(3), e1010969. https://doi.org/10.1371/journal.pcbi.1010969

Taylor, N. P., & Cunniffe, N. J. (2023c). Optimal Resistance Management for Mixtures of High-Risk Fungicides: Robustness to the Initial Frequency of Resistance and Pathogen Sexual Reproduction. *Phytopathology*, *113*(1), 55–69. https://doi.org/10.1094/PHYTO-02-22-0050-R

te Beest, D. E., Paveley, N. D., Shaw, M. W., & van den Bosch, F. (2013). Accounting for the Economic Risk Caused by Variation in Disease Severity in Fungicide Dose Decisions, Exemplified for *Mycosphaerella graminicola* on Winter Wheat. *Phytopathology®*, *103*(7), 666–672. https://doi.org/10.1094/PHYTO-05-12-0119-R

te Beest, D. E., Shaw, M. W., Pietravalle, S., & van den Bosch, F. (2009). A predictive model for early-warning of Septoria leaf blotch on winter wheat. *European Journal of Plant Pathology*, *124*(3), 413–425. https://doi.org/10.1007/s10658-009-9428-0

Tenaillon, O., Toupance, B., Le Nagard, H., Taddei, F., & Godelle, B. (1999). Mutators, Population Size, Adaptive Landscape and the Adaptation of Asexual Populations of Bacteria. *Genetics*, *152*(2), 485–493. https://doi.org/10.1093/genetics/152.2.485

van den Bosch, F., Blake, J., Gosling, P., Helps, J. C., & Paveley, N. (2020). Identifying when it is financially beneficial to increase or decrease fungicide dose as resistance develops: An evaluation from long-term field experiments. *Plant Pathology*, *69*(4), 631–641. https://doi.org/10.1111/ppa.13155

van den Bosch, F., Smith, J., Wright, P., Milne, A., van den Berg, F., Kock-Appelgren, P. et al. (2022). Maximizing realized yield by breeding for disease tolerance: A case study for Septoria tritici blotch. *Plant Pathology*, *71*(3), 535–543. https://doi.org/10.1111/ppa.13509

Vandersteen, J., Jaunard, D., Mahy, G., Bizoux, J.-P., Monty, A., Henriet, F. et al. (2011). Dynamics of black-grass populations depending on the sowing time of winter wheat. *Communications in Agricultural and Applied Biological Sciences, 76* (3), 485-490.

Veloukas, T., Markoglou, A. N., & Karaoglanidis, G. S. (2013). Differential Effect of *Sdh* B Gene Mutations on the Sensitivity to SDHI Fungicides in *Botrytis cinerea*. *Plant Disease*, *97*(1), 118–122. https://doi.org/10.1094/PDIS-03-12-0322-RE

Vestergaard, M., Paulander, W., Marvig, R. L., Clasen, J., Jochumsen, N., Molin, S. et al. (2016). Antibiotic combination therapy can select for broad-spectrum multidrug resistance in Pseudomonas aeruginosa. *International Journal of Antimicrobial Agents*, *47*(1), 48–55.
https://doi.org/10.1016/j.ijantimicag.2015.09.014

Yamashita, M., & Fraaije, B. (2018). Non-target site SDHI resistance is present as standing genetic variation in field populations of *Zymoseptoria tritici*. *Pest Management Science*, *74*(3), 672–681. https://doi.org/10.1002/ps.4761

Yorinori, J. T. (2021). CHAPTER 5: Difficulties Controlling Soybean Rust. In *Soybean Rust: Lessons Learned from the Pandemic in Brazil* (pp. 75–86). The American Phytopathological Society.
https://doi.org/10.1094/9780890546642.05

Young, C., Boor, T., Corkley, I., Fraaije, B., Clark, B., Havis, N. et al. (2021). Managing resistance evolving concurrently against two or more modes of action to extend the effective life of fungicides. AHDB Project Report No. 637, pp 1–91. Available at:
https://projectblue.blob.core.windows.net/media/Default/Research%20Papers/Cereals%20and%20Oilseed/2021/PR637%20final%20project%20report.pdf [Accessed: 1 August 2024].

Zadoks, J.C. & Schein, R.D. (1979). *Epidemiology and plant disease management*. Oxford University Press, New York. 427 pp.

Zhan, J., Mundt, C. C., & McDonald, B. A. (1998). Measuring Immigration and Sexual Reproduction in Field Populations of *Mycosphaerella graminicola*. *Phytopathology®, 88*(12), 1330–1337.
https://doi.org/10.1094/PHYTO.1998.88.12.1330

Zhu, J., Li, J., Ma, D., Gao, Y., Cheng, J., Mu, W. et al. (2022). SDH mutations confer complex cross-resistance patterns to SDHIs in Corynespora cassiicola. *Pesticide Biochemistry and Physiology*, *186*, 105157.
https://doi.org/10.1016/j.pestbp.2022.105157

Managing concurrent evolution of resistance to fungicides

Supplementary Material

A thesis submitted for the degree of Doctor of Philosophy

School of Agriculture, Policy and Development, University of Reading

Net Zero and Resilient Farming, Rothamsted Research

Isabel Corkley

December 2024

Supplementary Material: Chapter 3

Delaying infection through phytosanitary soybean-free periods contributes to fungicide resistance management in Phakopsora pachyrhizi: A modelling analysis

Appendix 3.A: Further details on model parameterisation

Sections 3.A.1, 3.A.2 and 3.A.3 include further information on the data used in the parameterisation process, and in addition provide summary statistics describing the distribution of the fitted *P. pachyrhizi* life cycle parameter values and variance-covariance matrices for the fitted crop growth and fungicide parameters. These can be used to generate stochastic combinations of parameters within a realistic range. The variance-covariance matrices are colour-coded to indicate the degree of correlation between parameter values (Table 3.A.1). Please refer to Table 3.2 and Sections 843.3.1.1 – 3.3.1.3 for full parameter definitions.

Table 3.A.1: Colour-coding key for variance-covariance matrices.

Correlation between parameters (range)
-1.00 ≤ ρ ≤ -0.50
-0.50 < ρ ≤ -0.25
-0.25 < ρ ≤ 0.00
0.00 < ρ ≤ 0.25
0.25 < ρ ≤ 0.50
0.50 < ρ ≤ 1.00

3.A.1 Parameterisation of the soybean crop growth model

Ideally, the values of the crop growth parameters, A_0 (initial LAI), A_{Max} (maximum LAI), r (rate of increase of LAI), γ (rate of senescence of LAI) and t_γ (time of complete crop senescence), would be fitted using time series data on the leaf area index (LAI) of healthy crops not infected by *P. pachyrhizi* or any other diseases (for example, crops fully protected from disease by fungicide applications). To our knowledge, there was no such dataset available for soybean growth in Brazil

covering the full time series from sowing date to senescence. The crop model was therefore parameterised using data on the LAI of three soybean cultivars of different maturity groups (early-, mid- and late-maturing), sourced from a study carried out in Mato Grosso, Brazil (Table 3.1 - 'Dataset A' (Moreira et al., 2015)), in which *P. pachyrhizi* infection did occur (the implications of this are addressed in Section 3.5.1). The data came from experiments carried out during the 2009/2010 and 2010/2011 growing seasons, where LAI was measured at intervals ranging from 5 to 21 days. Data for the mean LAI averaged across four blocks for each cultivar in each experiment were available; data from crops planted in October and November in each season were used to fit the soybean crop growth model (Figure 3.A.1, Table 3.A.2).
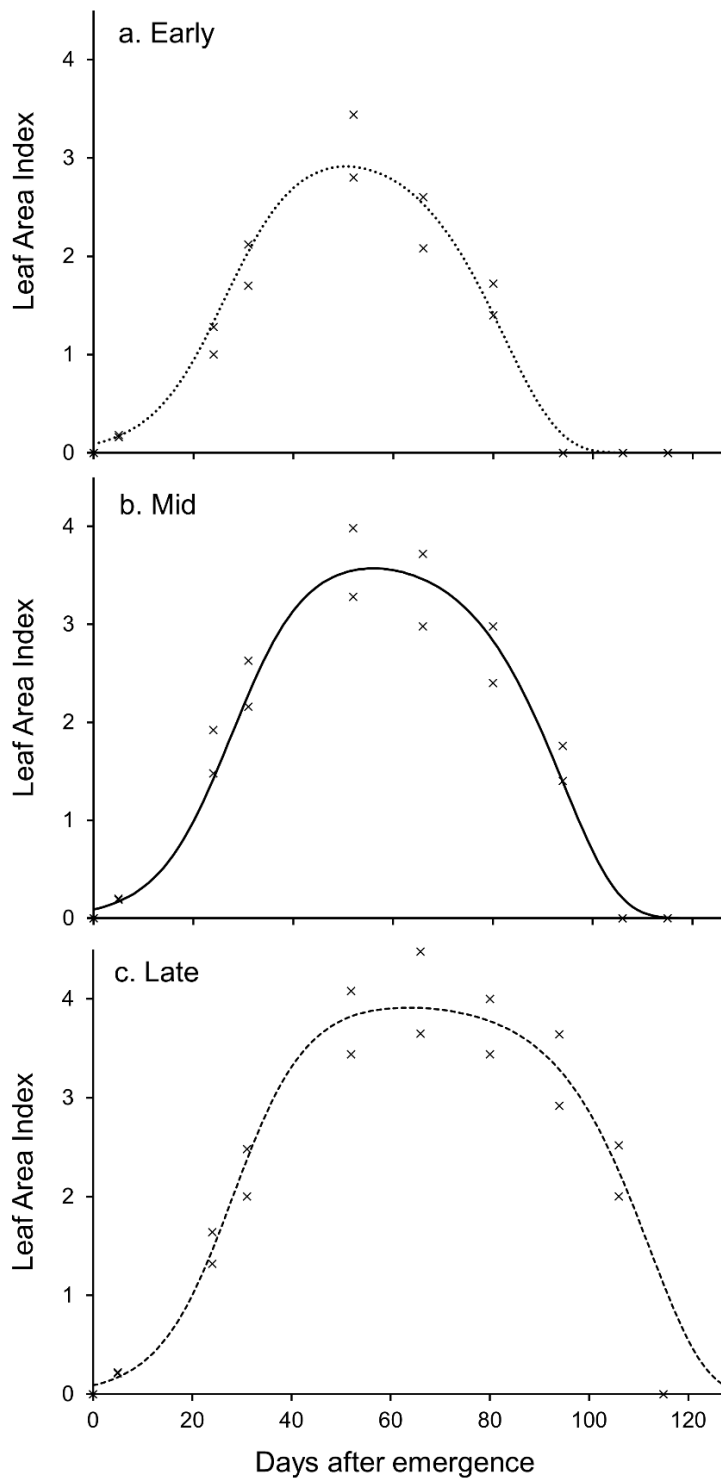
Figure 3.A.1: Dataset A of observed soybean leaf area index (LAI) over time (Moreira et al., 2015), and model simulation of LAI for a. Early-maturing, b. Mid-maturing and c. Late-maturing cultivars. Dataset A datapoints shown as black 'x' and fitted model shown as black lines.

Table 3.A.2: Variance-covariance matrix for fitted crop growth model parameters.

Parameter	A_0	r	γ	A_{Max} (Early)	A_{Max} (Mid)	A_{Max} (Late)	t_γ (Early)	t_γ (Mid)	t_γ (Late)
A_0	0.0014	-0.0006	-0.0001	0.0023	0.0023	0.0016	0.0407	0.0425	0.0518
r	-0.0006	0.0003	0.0001	-0.0012	-0.0012	-0.0008	-0.0219	-0.0231	-0.0282
γ	-0.0001	0.0001	0.0002	-0.0015	-0.0015	-0.0008	-0.0625	-0.0642	-0.0787
A_{Max} (Early)	0.0023	-0.0012	-0.0015	0.0406	0.0167	0.0095	0.432	0.607	0.745
A_{Max} (Mid)	0.0023	-0.0012	-0.0015	0.0167	0.0303	0.0090	0.563	0.503	0.714
A_{Max} (Late)	0.0016	-0.0008	-0.0008	0.0095	0.0090	0.0149	0.296	0.307	0.298
t_γ (Early)	0.0407	-0.0219	-0.0625	0.432	0.563	0.296	27.3	25.1	30.8
t_γ (Mid)	0.0425	-0.0231	-0.0642	0.607	0.503	0.307	25.1	27.4	31.7
t_γ (Late)	0.0518	-0.0282	-0.0787	0.745	0.714	0.298	30.8	31.7	41.0

3.A.2 Parameterisation of the soybean crop growth model

The life cycle parameters p_0 (latent period) and ω (infectious period) were estimated based on a literature review of the biology of soybean rust in Brazil (Table 3.2). The parameters t_{Inoc} (time of arrival of the first *P. pachyrhizi* spores causing primary infection), Ω_0 (primary inoculum release rate) and ψ_0 (transmission rate) were fitted using data on soybean rust disease severity on susceptible soybean cultivars in the absence of fungicides (Table 3.1– Dataset 'B').

The trials in Dataset B were carried out between 2012 and 2016 in Minas Gerais, Mato Grosso, Goiás, Tocantins, Rio Grande Do Sul, Paraná and São Paulo states (Table 3.A.2). The disease severity measured was an average value based on assessments of multiple leaves in the plant canopy, measured as the percentage of leaf area infected by *P. pachyrhizi*. Trials were included in the dataset if they met all of the following criteria designed to ensure that the progress of the epidemic had been captured in sufficient detail to enable parameterisation: data on disease severity was available for at least five separate dates; the earliest disease assessment had a severity <5%, the trial had assessments on at least three dates where the severity was between (not including) 0% and 100%, at least one date where the severity was ≤50%, and at least one date where the severity was >50% (indicating moderate or high disease pressure seasons (Dalla Lana et al., 2015).

The parameters t_{Inoc}, Ω_0 and ψ_0 were fitted individually for each trial. The value of t_{Inoc} for each trial was estimated based on the assessment day in which soybean rust was first observed in each trial. If a severity of 0% had been observed, t_{Inoc} was estimated as nine days prior to the latest assessment date with an observed severity of 0%, based on the estimated latent period of the disease. If disease had been observed on all assessment dates, but the earliest assessment date had a severity <5%, t_{Inoc} was estimated as sixteen days prior to the earliest assessment date. The lower quartile ('Early'), median ('Medium') and upper quartile ('Late') values of t_{Inoc} were used for model simulations to represent a range of *P. pachyrhizi* inoculum arrival timings.

There is an interaction between the values of Ω_0 or ψ_0 which makes a simultaneous fitting process unstable: an increase in the value of either Ω_0 or ψ_0 increases the rate at which the rust severity increases, so an increase in one parameter can be counteracted by a decrease in the other. Therefore a two-stage fitting process was used. Firstly, Ω_0 and ψ_0 were fitted simultaneously for each trial using the function 'lsqcurvefit' in MATLAB, using the value of t_{Inoc} estimated for the individual trial. In

the second stage, the value of Ω_0 was fixed at the median value from the simultaneous fitting process, and ψ_0 was then fitted for each individual trial given the fixed value of Ω_0. The value of ψ_0 used for model simulations was fitted as the mean value of ψ_0 for trials within the interquartile range of t_{Inoc} (Table 3.A.4).

Figure 3.A.2a. shows the fit to all disease severity data in Dataset B, whilst Figures 3.A.2b. – d. illustrate model fits to disease progress curves for selected individual trials. Figure 3.1a. shows the model fit to the observed area under the disease progress curve (AUDPC) for all 146 trials.
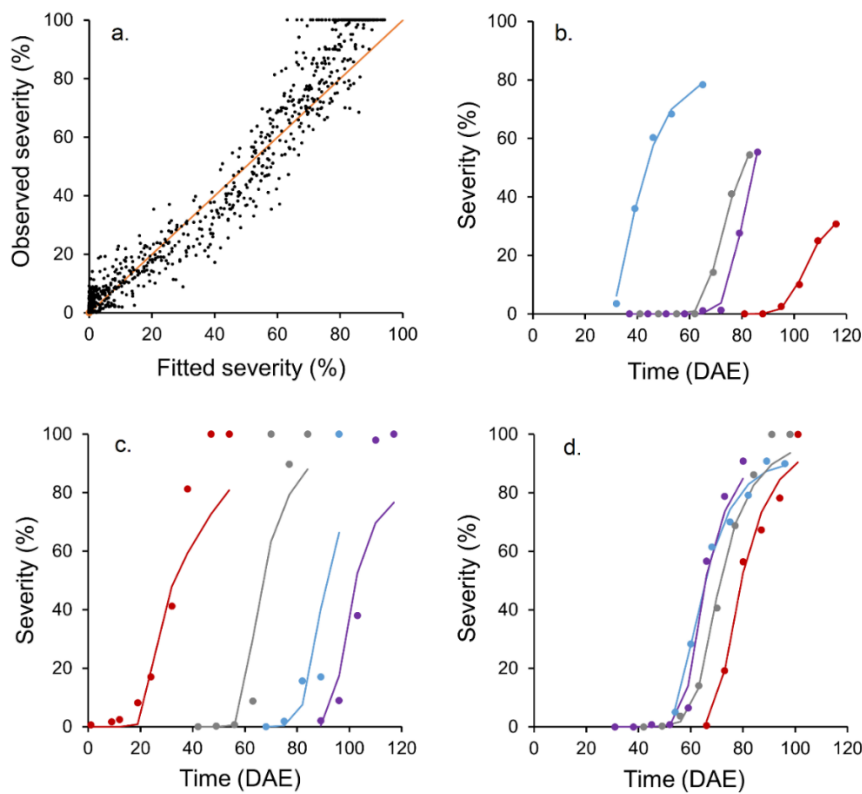
Figure 3.A.2: a. Scatter plot of fitted vs. observed *P. pachyrhizi* severity (%) at all assessment timings. b. – d. Illustration of model fits to disease severity progress data from individual trials. Points indicate observed severity data at each assessment timing (number of days after soybean emergence), and lines indicate model fitted values. Colours are used within each plot to distinguish individual trials. b. Trials for which the closest fit was obtained (based on sum of squares of differences of all observed severity (%) values for the trial). c. Trials with the poorest model fit obtained. d. Trials with maximum severity >90% for which the closest fit was obtained.

274

Table 3.A.3: Dataset B: Year and location within Brazil of trials used for parameterisation of *P. pachyrhizi* life cycle. 'North' comprises states Minas Gerais, Mato Grosso, Goiás and Tocantins; 'South' comprises states Rio Grande Do Sul, Paraná and São Paulo.

Year	Number of trials			Number of sites		
	Total	North	South	Total	North	South
2012	23	21	2	10	9	1
2013	13	8	5	10	5	5
2014	10	9	1	8	7	1
2015	32	24	8	15	9	6
2016	68	27	41	25	13	12
All	146	89	57	68	43	25

Table 3.A.4: Distribution of fitted *P. pachyrhizi* life cycle parameter values across 146 trials.

Summary statistic	Parameter			
	t_{Inoc} (DAE)	Ω_0: simultaneous fitting	ψ_0: all trials, $\Omega_0 = 4.6 \times 10^{-6}$	ψ_0: trials in t_{Inoc} interquartile range, $\Omega_0 = 4.6 \times 10^{-6}$
Mean	43.4	2.5×10^{-3}	2.94	2.78
Median	44.0	4.6×10^{-6}	2.79	2.78
Lower quartile	32.0	2.8×10^{-8}	1.90	2.26
Upper quartile	52.0	2.5×10^{-4}	3.55	3.23
Minimum	0.0	4.0×10^{-9}	0.99	1.32
Maximum	79.0	7.9×10^{-2}	8.12	5.82

3.A.3 Parameterisation of the effect of fungicides on P. pachyrhizi

The model was parameterised to describe the efficacy of fungicides, using examples from several MoA: an SDHI fungicide (benzovindiflupyr), a QoI fungicide (azoxystrobin), a DMI fungicide (cyproconazole) and two multi-site acting fungicides, a dithiocarbamate fungicide (mancozeb) and a chloronitrile fungicide (chlorothalonil). The average fungicide decay rates, ν_i, for each fungicide F_i, were estimated through a literature review of foliar concentration half-lives (Table 3.2). The decay rate is calculated from the half-life assuming first-order kinetics: $\nu = \frac{-ln(0.5)}{half-life}$. The asymptote, q_{S_i} and shape parameter k_{S_i}, for each fungicide F_i, were fitted using data from field trials of fungicide efficacy (Table 3.1 – 'Dataset C'), carried across north and south Brazil in 2015, 2016 and 2017 (Table 3.A.5). In all trials included in Dataset C, disease progress was measured as the observed *P. pachyrhizi* severity (measured as the percentage of leaf area infected) at several time points following applications of three or more non-zero dose rates of the solo fungicide, and disease progress in the untreated control. The severity data for benzovindiflupyr, azoxystrobin, cyproconazole and chlorothalonil were averages across all replicates. Data for mancozeb included replicates from three blocks at each site.

Individual values of t_{Inoc} were estimated for each trial as described in Section 3.A.2. Then, for each fungicide F_i, individual values of ψ_0 for each trial and average values of q_{S_i} and k_{S_i} common to all trials were fitted in MATLAB simultaneously, using the function 'lsqcurvefit'. Most trials provided data for one fungicide and data on disease progress in the absence of fungicidal control. The field trials of solo azoxystrobin efficacy also included data on the efficacy of solo cyproconazole applications, with a common trial ID and dataset for severity in the absence of fungicide applications. Therefore, a single value of ψ_0 was fitted for each trial consisting of both azoxystrobin and cyproconazole dose response data, and the QoI and DMI dose response parameters were fitted simultaneously. The variance-covariance matrices are shown in Tables 3.A.6 to 3.A.9. Figure 3.A.3 gives an example of the estimated dose response curve for each fungicide.

Table 3.A.5: Year and location within Brazil of trials used for parameterisation of the effect of fungicides on *P. pachyrhizi* life cycle, and the model fit to the data for each fungicide. [1]'North' comprises states Minas Gerais, Mato Grosso and Goiás; 'South' comprises states Rio Grande Do Sul, Paraná and São Paulo. [2]Number of datapoints for the dithiocarbamate includes replicates from three blocks at each site. [3]QoI and DMI dose responses were fitted simultaneously, so a joint R^2 and RMSE and number of datapoints for untreated plots is reported for these fungicides.

Number of trials	Fungicide				
	SDHI	QoI	DMI	Chloronitrile	Dithiocarbamate
North[1]	2	1	3	2	2
South[1]	3	2	3	2	3
2015	0	0	3	0	0
2016	5	3	3	4	0
2017	0	0	0	0	5
Total	5	3	6	4	5
Number of datapoints[2]					
Fungicide	102	54	112	112	261
Untreated plots[3]	35	29		28	87
Model fit[3]					
R^2 (%)	88.5	93.8		77.9	73.7
RMSE (% severity)	8.96	8.46		12.55	16.13

Table 3.A.6: Variance-covariance matrix for fitted SDHI dose response parameters. $\psi_{0_i} \ldots \psi_{0_v}$ denotes the transmission rate (in the absence of fungicides) in each of the trials used to fit the SDHI dose response.

Parameter	q_1	k_1	ψ_{0_i}	$\psi_{0_{ii}}$	$\psi_{0_{iii}}$	$\psi_{0_{iv}}$	ψ_{0_v}
q_1	0.0004	-0.0635	0.0021	0.0004	0.0006	0.0005	0.0004
k_1	-0.0635	36.784	-0.0422	0.0437	0.0490	0.0600	0.0203
ψ_{0_i}	0.0021	-0.0422	0.0335	0.0038	0.0054	0.0046	0.0034
$\psi_{0_{ii}}$	0.0004	0.0437	0.0038	0.0112	0.0014	0.0013	0.0009
$\psi_{0_{iii}}$	0.0006	0.0490	0.0054	0.0014	0.0038	0.0018	0.0013
$\psi_{0_{iv}}$	0.0005	0.0600	0.0046	0.0013	0.0018	0.0070	0.0011
ψ_{0_v}	0.0004	0.0203	0.0034	0.0009	0.0013	0.0011	0.0017

Table 3.A.7: Variance-covariance matrix for fitted QoI and DMI dose response parameters. q_2 and k_2 are the dose response parameters for the QoI, and q_3 and k_3 are the dose response parameters for the DMI. $\psi_{0_i} \dots \psi_{0_{vi}}$ denotes the transmission rate (in the absence of fungicides) in each of the trials used to fit the QoI and DMI dose responses.

Parameter	q_2	q_3	k_2	k_3	ψ_{0_i}	$\psi_{0_{ii}}$	$\psi_{0_{iii}}$	$\psi_{0_{iv}}$	ψ_{0_v}	$\psi_{0_{vi}}$
q_2	0.0132	0.0002	-0.1889	-0.2792	-0.0017	-0.0010	2×10^{-5}	-0.0017	0.0006	-0.0051
q_3	0.0002	0.0040	0.0014	-2.2906	0.0008	2×10^{-5}	0.0006	0.0007	0.0003	0.0009
k_2	-0.1889	0.0014	2.9119	6.3947	0.0582	0.0316	0.0106	0.0613	0.0040	0.1229
k_3	-0.2792	-2.2906	6.3947	1537.6	0.7566	0.6950	0.0448	0.4634	0.1412	0.6917
ψ_{0_i}	-0.0017	0.0008	0.0582	0.7566	0.0125	0.0037	0.0022	0.0062	0.0021	0.0089
$\psi_{0_{ii}}$	-0.0010	2×10^{-5}	0.0316	0.6950	0.0037	0.0039	0.0011	0.0031	0.0010	0.0045
$\psi_{0_{iii}}$	2×10^{-5}	0.0006	0.0106	0.0448	0.0022	0.0011	0.0013	0.0019	0.0007	0.0026
$\psi_{0_{iv}}$	-0.0017	0.0007	0.0613	0.4634	0.0062	0.0031	0.0019	0.0357	0.0023	0.0095
ψ_{0_v}	0.0006	0.0003	0.0040	0.1412	0.0021	0.0010	0.0007	0.0023	0.0021	0.0030
$\psi_{0_{vi}}$	-0.0051	0.0009	0.1229	0.6917	0.0089	0.0045	0.0026	0.0095	0.0030	0.0269

Table 3.A.8: Variance-covariance matrix for fitted chloronitrile dose response parameters. $\psi_{0_i} \ldots \psi_{0_{iv}}$ denotes the transmission rate (in the absence of fungicides) in each of the trials used to fit the chloronitrile dose response.

Parameter	q_4	k_4	ψ_{0_i}	$\psi_{0_{ii}}$	$\psi_{0_{iii}}$	$\psi_{0_{iv}}$
q_4	0.0040	-0.0729	0.0116	0.0139	0.0066	0.0259
k_4	-0.0729	8.2023	0.2877	0.3541	0.1793	0.6338
ψ_{0_i}	0.0116	0.2877	0.1023	0.0843	0.0409	0.1553
$\psi_{0_{ii}}$	0.0139	0.3541	0.0843	0.1749	0.0495	0.1877
$\psi_{0_{iii}}$	0.0066	0.1793	0.0409	0.0495	0.0367	0.0911
$\psi_{0_{iv}}$	0.0259	0.6338	0.1553	0.1877	0.0911	0.7009

Table 3.A.9: Variance-covariance matrix for fitted dithiocarbamate dose response parameters. $\psi_{0_i} \ldots \psi_{0_v}$ denotes the transmission rate (in the absence of fungicides) in each of the trials used to fit the dithiocarbamate dose response.

Parameter	q_5	k_5	ψ_{0_i}	$\psi_{0_{ii}}$	$\psi_{0_{iii}}$	$\psi_{0_{iv}}$	ψ_{0_v}
q_5	0.0019	-0.0651	0.0085	0.0146	0.0053	0.0180	0.0019
k_5	-0.0651	41.405	0.3889	0.8241	0.3745	0.9783	0.0819
ψ_{0_i}	0.0085	0.3889	0.0961	0.0901	0.0337	0.1100	0.0111
$\psi_{0_{ii}}$	0.0146	0.8241	0.0901	0.3042	0.0600	0.1948	0.0197
$\psi_{0_{iii}}$	0.0053	0.3745	0.0337	0.0600	0.0325	0.0732	0.0074
$\psi_{0_{iv}}$	0.018	0.9783	0.1100	0.1948	0.0732	0.5975	0.0240
ψ_{0_v}	0.0019	0.0819	0.0111	0.0179	0.0074	0.0240	0.0079
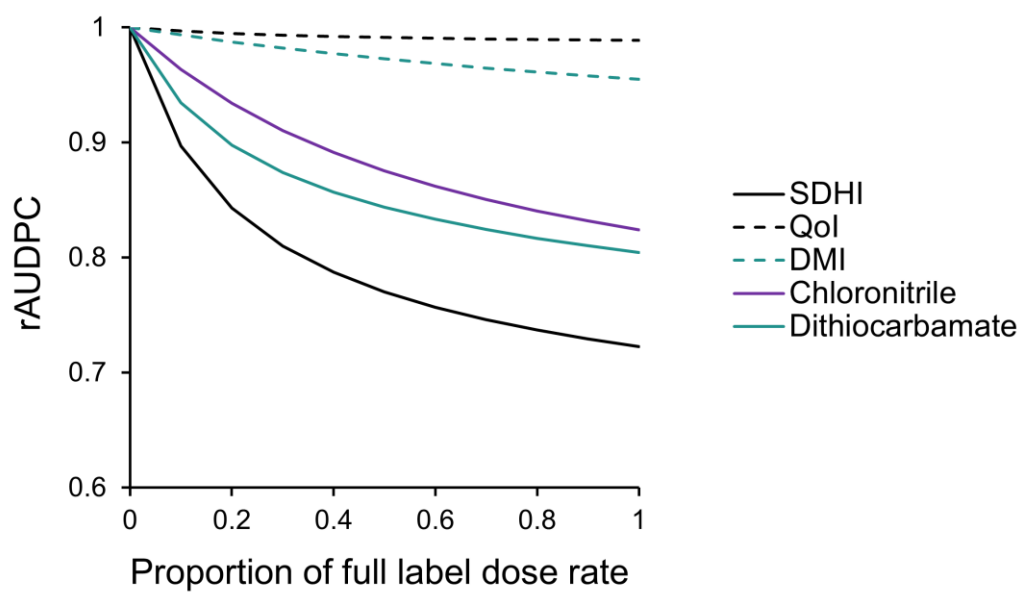
Figure 3.A.3: Dose response curve of proportional reduction in AUDPC relative to untreated crop (rAUDPC) for each fungicide, for a single application of the fungicide at t = 47 DAE, for an epidemic with t_{Inoc} = 44 DAE.

Appendix 3.B: Further details on sensitivity of model results to parameter values

3.B.1 Level of sensitivity shift to the SDHI

The effect of varying levels of sensitivity shift to the SDHI on effective life and T50 is illustrated in Figure 3.B.1. The greater the level of sensitivity shift, the greater the selection for resistance and the less control the SDHI would contribute following selection for the resistant strain. Therefore, as the level of sensitivity shift increases, T50 and effective life values decrease for most dose rates. Note that the model predicts that, when t_{Inoc} = 44 DAE, effective control will be maintained for a mixture of the dithiocarbamate at the full dose rate and a high dose rate of the SDHI + QoI formulated mixture even when the *P. pachyrhizi* population has become completely insensitive to the SDHI. This is because of the combined efficacy of the dithiocarbamate and the QoI component of the SDHI + QoI formulated mixture. A mixture of the dithiocarbamate and the SDHI would not provide effective control after the spread of a *P. pachyrhizi* strain with a 100% sensitivity shift to the SDHI.

Figure 3.B.1 (Figure on page 276): Effective life (years/number of growing seasons) and time until 50% of the population is insensitive to the SDHI (T50, years) for two-application programmes of the SDHI + QoI formulated mixture with the dithiocarbamate at varying dose rates, for resistant strains with varying levels of sensitivity shift to the SDHI (25%, 50%, 75% and 100%, where 100% indicates completely insensitivity). The x-axis label shows the dose of the SDHI with the dose of the QoI in brackets (the SDHI and the QoI are in a 1:2 ratio). Inoculum arrival timing t_{Inoc} = 44 DAE. Note that a high dose of the QoI is contributing to disease control, which is the reason that the SDHI + QoI formulated mixture continues to contribute to disease control even in a case where a 100% sensitivity shift has occurred.
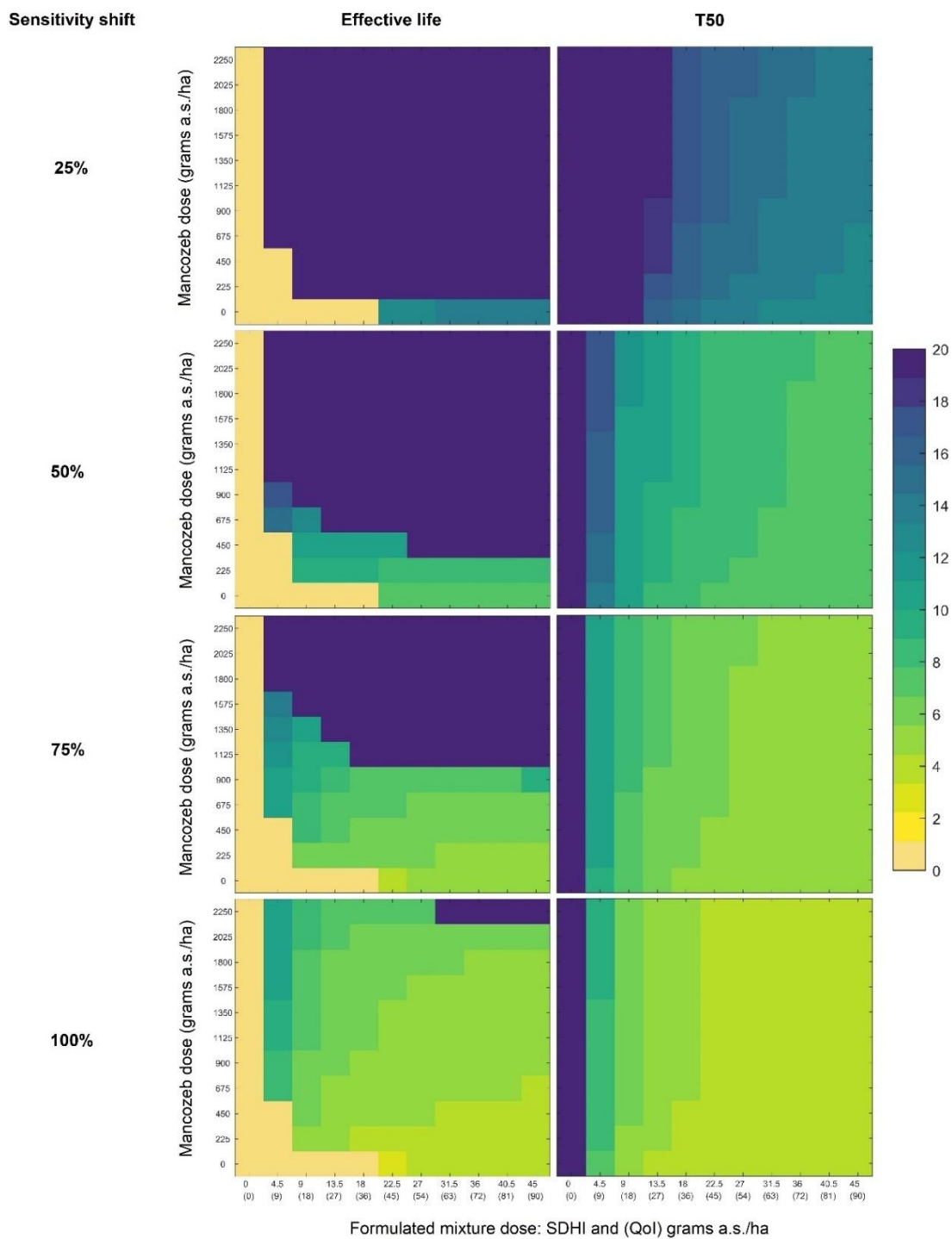
Figure 3.B.1: Figure legend on page 275.

283

3.B.2 Reduced mixture partner efficacy

The fungicide parameter values used to represent a conservative scenario in which the efficacy of the mixture partner was the minimum of the likely range indicated by the data are given in Table 3.B.1. The effective life and T50 predicted in this scenario for two-application programmes of the SDHI + QoI formulated mixture with a mixture partner at a range of dose rates are shown in Figure 3.B.2. This shows a reduced range of dose rate combinations that maximise effective life and T50, requiring higher mixture partner doses to achieve this in comparison to a scenario based on the average mixture partner efficacy (Figure 3.4). Similarly, considering the combination of rust inoculum arrival time and fungicide spray timing in this scenario (Figures 3.B.3 to 3.B.4), a smaller range of combinations maximise effective life and T50, and a greater delay in inoculum arrival is needed to maximise effective life or enable control with one application compared to the scenario with average mixture partner efficacy (Figure 3.5 and 3.6).

Table 3.B.1: Fungicide parameter values fitted for scenario in which mixture partner efficacy is the minimum of the likely range indicated by available data.

Fungicide	q_{Low}	k_{Low}
DMI	0.6177	0.66
Chloronitrile	0.4572	3.35
Dithiocarbamate	0.4340	10.81

Figure 3.B.2 (figure on page 278): Effective life (years/number of growing seasons) and time until 50% of the population is insensitive to the SDHI (T50, years) for two-application programmes of the SDHI + QoI formulated mixture with a mixture partner (DMI, chloronitrile or dithiocarbamate) at varying dose rates, for a scenario in which the mixture partner efficacy is the minimum of the likely range indicated by available data. The x-axis label shows the dose of the SDHI with the dose of the QoI in brackets (the SDHI and the QoI are in a 1:2 ratio). Inoculum arrival timing t_{Inoc} = 44 DAE, sensitivity shift =50%.
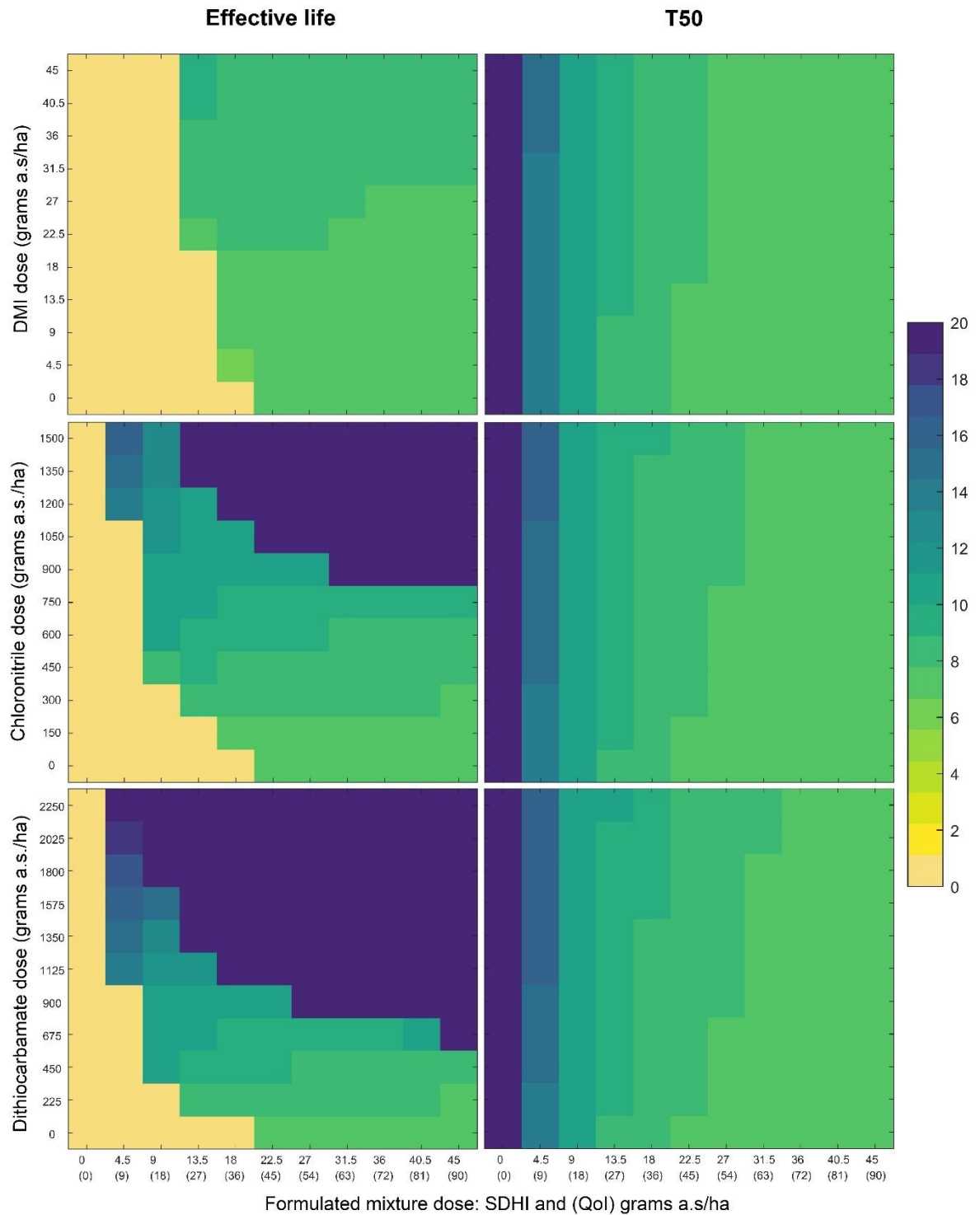
Figure 3.B.2: Figure legend on page 277.
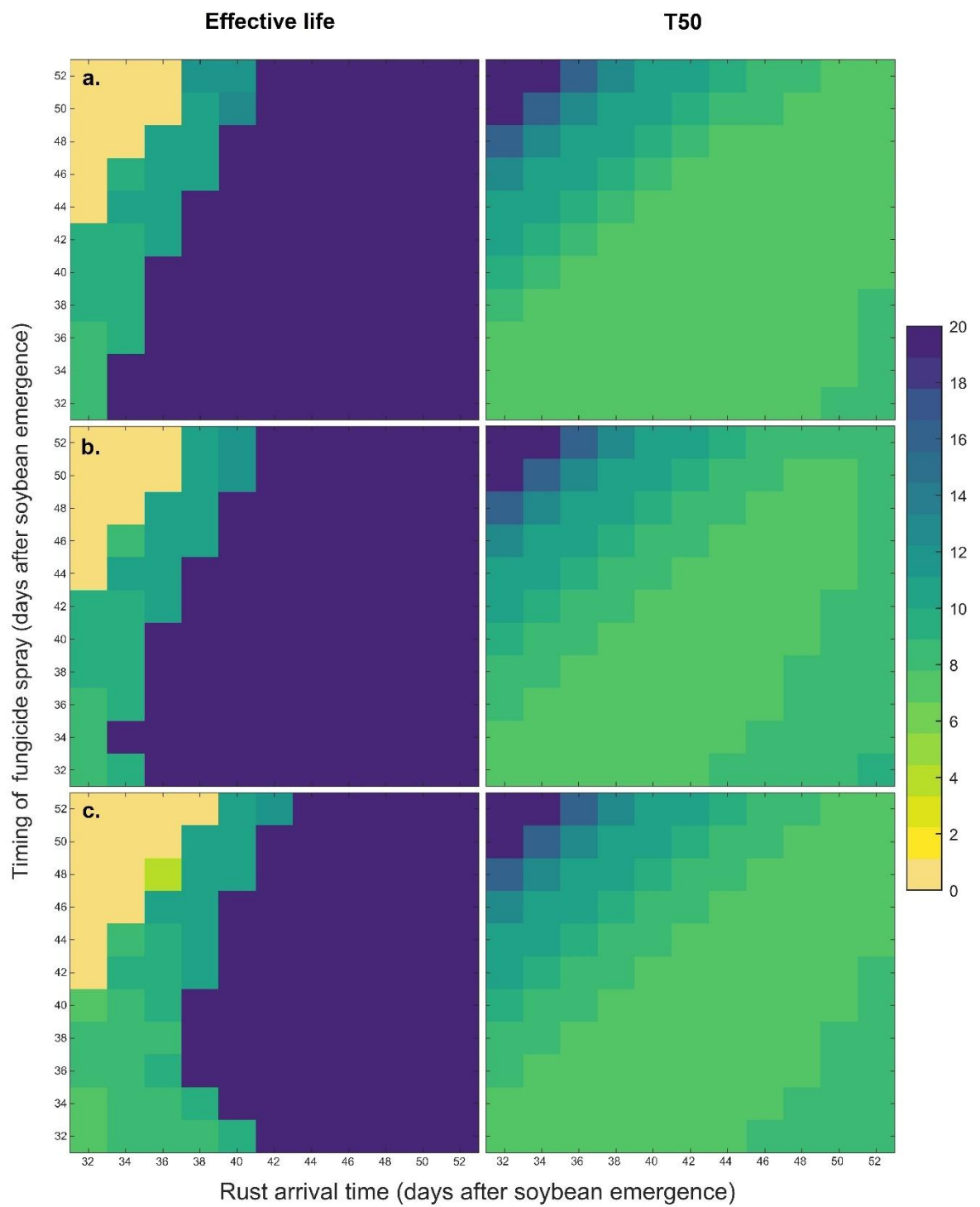
Figure 3.B.3: Figure legend on page 281.
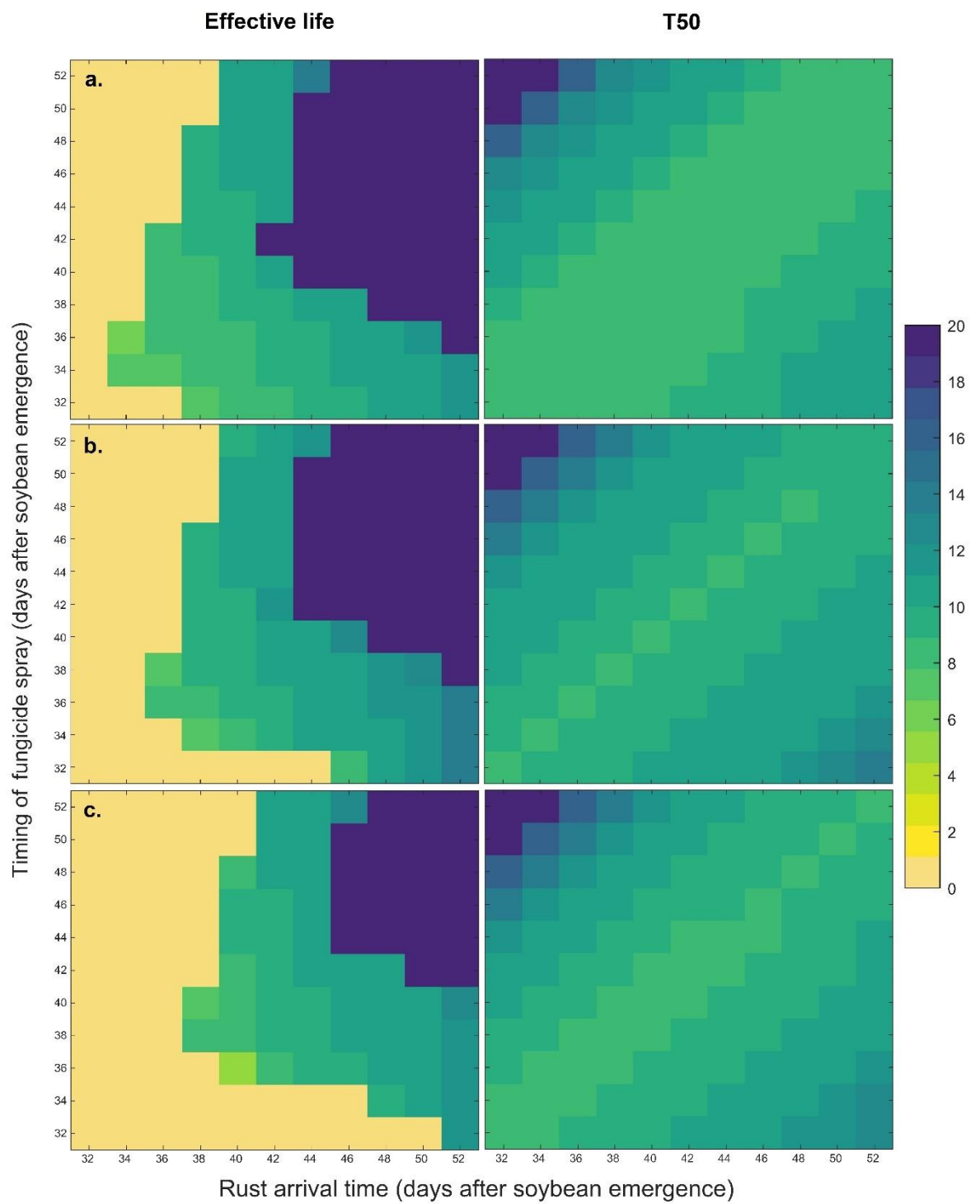
Figure 3.B.4: Figure legend on page 281.

Figure 3.B.3 (figure on page 279): Effective life (years/number of growing seasons) and time until 50% of the population is insensitive to the SDHI (T50, years) for two-application programmes of the SDHI + QoI formulated mixture with the dithiocarbamate at a. 100% SDHI + QoI and 100% dithiocarbamate full dose rate; b. 67% SDHI + QoI and 100% dithiocarbamate full dose rate; c. 67% SDHI + QoI and 50% dithiocarbamate full dose rate, for a scenario in which dithiocarbamate efficacy is the minimum of the likely range indicated by available data, and for varying rust inoculum arrival time (t_{Inoc}) and timing of the first fungicide application (second application made 15 days after the first).

Figure 3.B.4 (figure on page 280): Effective life (years/number of growing seasons) and time until 50% of the population is insensitive to the SDHI (T50, years) for one-application programmes of the SDHI + QoI formulated mixture with the dithiocarbamate at a. 100% SDHI + QoI and 100% dithiocarbamate full dose rate; b. 67% SDHI + QoI and 100% dithiocarbamate full dose rate; c. 67% SDHI + QoI and 50% dithiocarbamate full dose rate, for a scenario in which dithiocarbamate efficacy is the minimum of the likely range indicated by available data, and for varying rust inoculum arrival time (t_{Inoc}) and timing of the fungicide application.

3.B.3 SDHI decay rate

The parameter values fitted for the SDHI assuming a long, average or short foliar half-life (based on the range reported in literature) are shown in Table 3.B.2. In this scenario we used the average fungicide efficacy parameterisation for mixture partners, as given in Chapter 3, and modelled selection for a partially resistant strain (50% sensitivity shift). The effective life and T50 predicted for two-application programmes of the SDHI + QoI formulated mixture with a mixture partner at a range of dose rates for scenarios where the SDHI has a long / short half-life are illustrated in Figures 3.B.5 and 3.B.6 respectively. T50 is generally longer in the short half-life scenario, but a smaller range of dose rate combinations provide a long effective life, as the overall efficacy of the SDHI against sensitive and resistant strains is lower in this scenario. The opposite effect is observed for the long half-life scenario, whilst the average half-life scenario (Figure 3.4) is intermediate. A similar effect is observed on effective life and T50 for the results showing the impact of rust inoculum arrival time and fungicide spray timing (Figures 3.B.7–3.B.10).

Table 3.B.2: Fungicide parameter values fitted for a range of SDHI foliar concentration half-life values.

Foliar half-life (days)	v (days^{-1})	q	k
16.1	0.0431	0.2542	11.34
9.3	0.0745	0.2634	16.51
4.0	0.1733	0.3139	44.16

Figure 3.B.5 (figure on page 284): Effective life (years/number of growing seasons) and time until 50% of the population is insensitive to the SDHI (T50, years) for two-application programmes of the SDHI + QoI formulated mixture with a mixture partner (DMI, chloronitrile or dithiocarbamate) at varying dose rates, for a scenario where the foliar half-life of the SDHI is one of the highest values reported in literature for benzovindiflupyr (16.1 days). The x-axis label shows the dose of the SDHI with the dose of the QoI in brackets (the SDHI and the QoI are in a 1:2 ratio). Inoculum arrival timing t_Inoc = 44 DAE, sensitivity shift=50%.

Figure 3.B.6 (Figure on page 285): Effective life (years/number of growing seasons) and time until 50% of the population is insensitive to the SDHI (T50, years) for two-application programmes of the SDHI + QoI formulated mixture with a mixture partner (DMI, chloronitrile or dithiocarbamate) at varying dose rates, for a scenario where the foliar half-life of the SDHI is one of the lowest values reported in literature for benzovindiflupyr (4 days). The x-axis label shows the dose of the SDHI with the dose of the QoI in brackets (the SDHI and the QoI are in a 1:2 ratio). Inoculum arrival timing t_Inoc = 44 DAE, sensitivity shift=50%.

Figure 3.B.7 (figure on page 286): Effective life (years/number of growing seasons) and time until 50% of the population is insensitive to the SDHI (T50, years) for two-application programmes of the SDHI + QoI formulated mixture with the dithiocarbamate at a. 100% SDHI + QoI and 100% dithiocarbamate full dose rate; b. 67% SDHI + QoI and 100% dithiocarbamate full dose rate; c. 67% SDHI + QoI and 50% dithiocarbamate full dose rate, for a scenario where the foliar half-life of the SDHI is one of the highest values reported in literature for benzovindiflupyr (16.1 days), and for varying rust inoculum arrival time (t_Inoc) and timing of the first fungicide application (second application made 15 days after the first).

Figure 3.B.8 (figure on page 287): Effective life (years/number of growing seasons) and time until 50% of the population is insensitive to the SDHI (T50, years) for two-application programmes of the SDHI + QoI formulated mixture with the dithiocarbamate at a. 100% SDHI + QoI and 100% dithiocarbamate full dose

rate; b. 67% SDHI + QoI and 100% dithiocarbamate full dose rate; c. 67% SDHI + QoI and 50% dithiocarbamate full dose rate, for a scenario where the foliar half-life of the SDHI is one of the lowest values reported in literature for benzovindiflupyr (4 days), and for varying rust inoculum arrival time (t_{Inoc}) and timing of the first fungicide application (second application made 15 days after the first).

Figure 3.B.9 (figure on page 288): Effective life (years/number of growing seasons) and time until 50% of the population is insensitive to the SDHI (T50, years) for one-application programmes of the SDHI + QoI formulated mixture with the dithiocarbamate at a. 100% SDHI + QoI and 100% dithiocarbamate full dose rate; b. 67% SDHI + QoI and 100% dithiocarbamate full dose rate; c. 67% SDHI + QoI and 50% dithiocarbamate full dose rate, for a scenario where the foliar half-life of the SDHI is one of the highest values reported in literature for benzovindiflupyr (16.1 days), and for varying rust inoculum arrival time (t_{Inoc}) and timing of the fungicide application.

Figure 3.B.10 (figure on page 289): Effective life (years/number of growing seasons) and time until 50% of the population is insensitive to the SDHI (T50, years) for one-application programmes of the SDHI + QoI formulated mixture with the dithiocarbamate at a. 100% SDHI + QoI and 100% dithiocarbamate full dose rate; b. 67% SDHI + QoI and 100% dithiocarbamate full dose rate; c. 67% SDHI + QoI and 50% dithiocarbamate full dose rate, for a scenario where the foliar half-life of the SDHI is one of the lowest values reported in literature for benzovindiflupyr (4 days), and for varying rust inoculum arrival time (t_{Inoc}) and timing of the fungicide application.
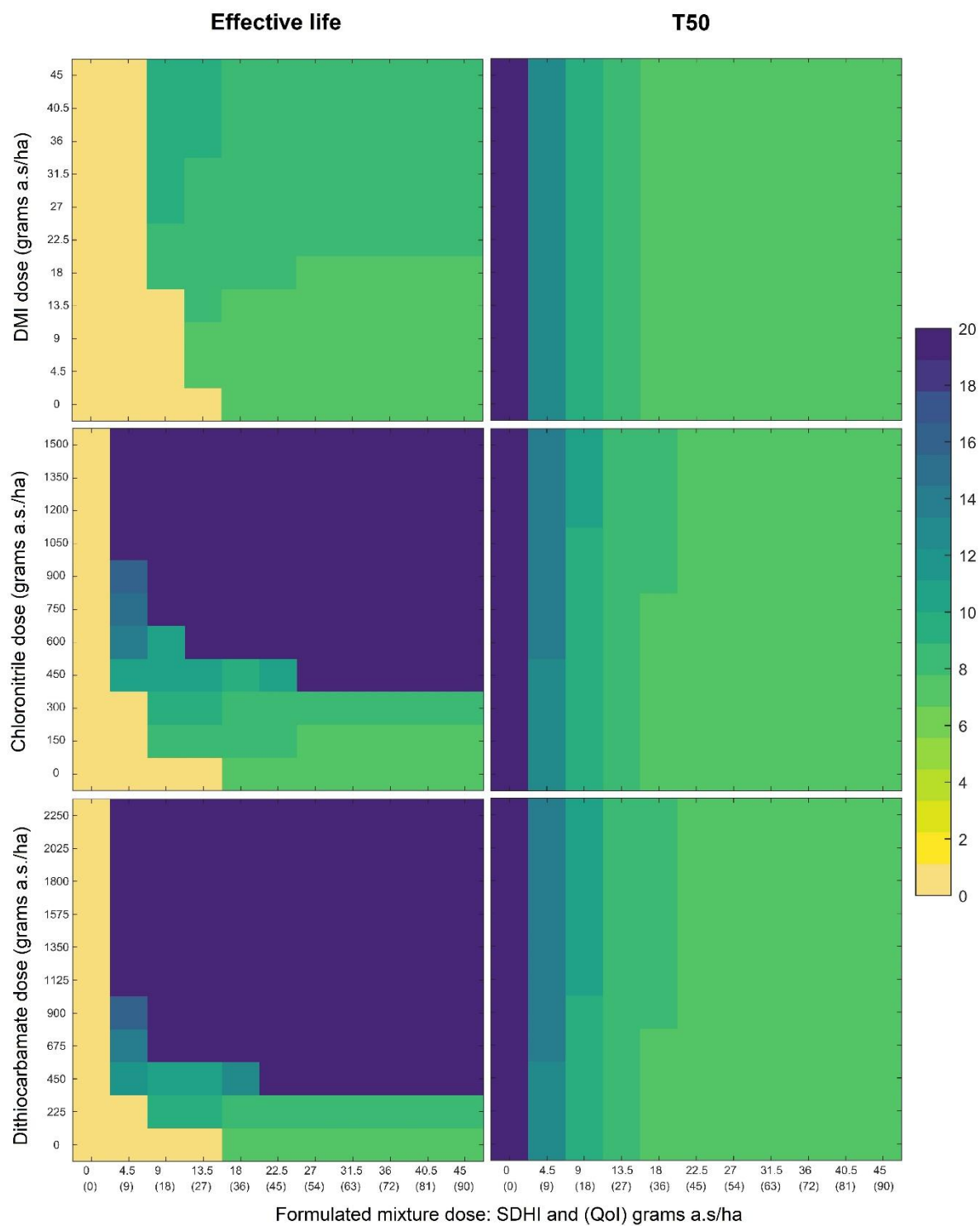
Figure 3.B.5: Figure legend on page 282.
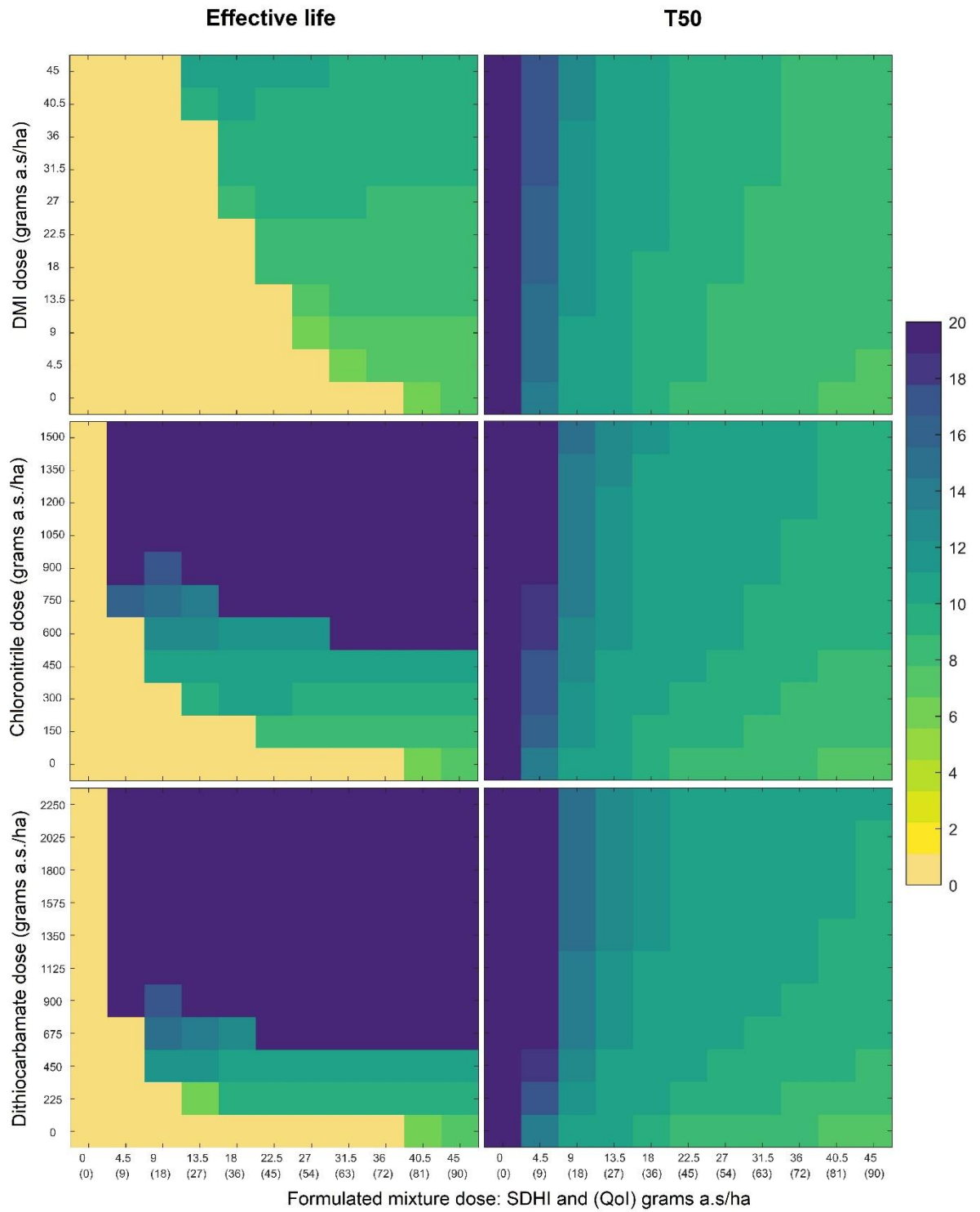
Figure 3.B.6: Figure legend on page 282.
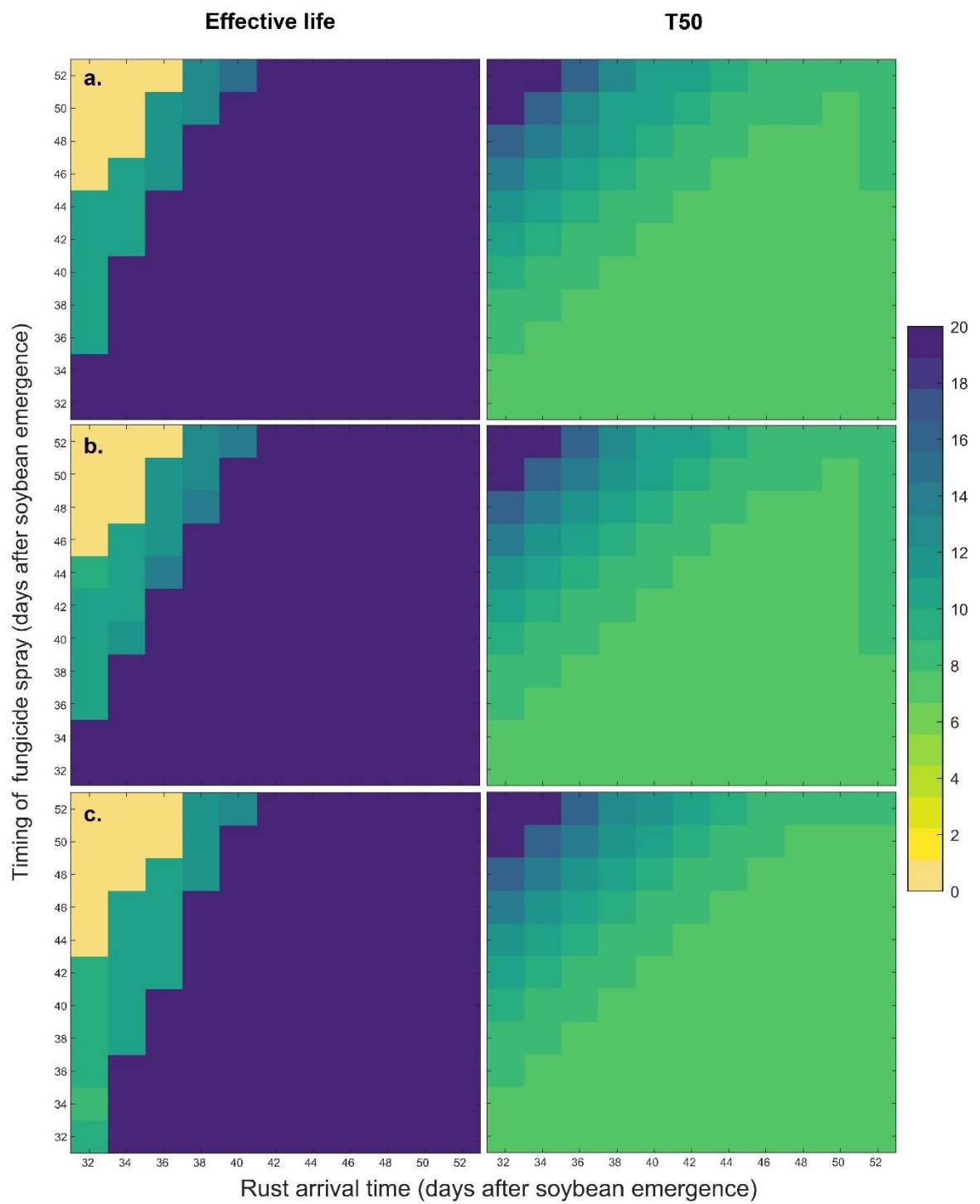
Figure 3.B.7: Figure legend on page 282.
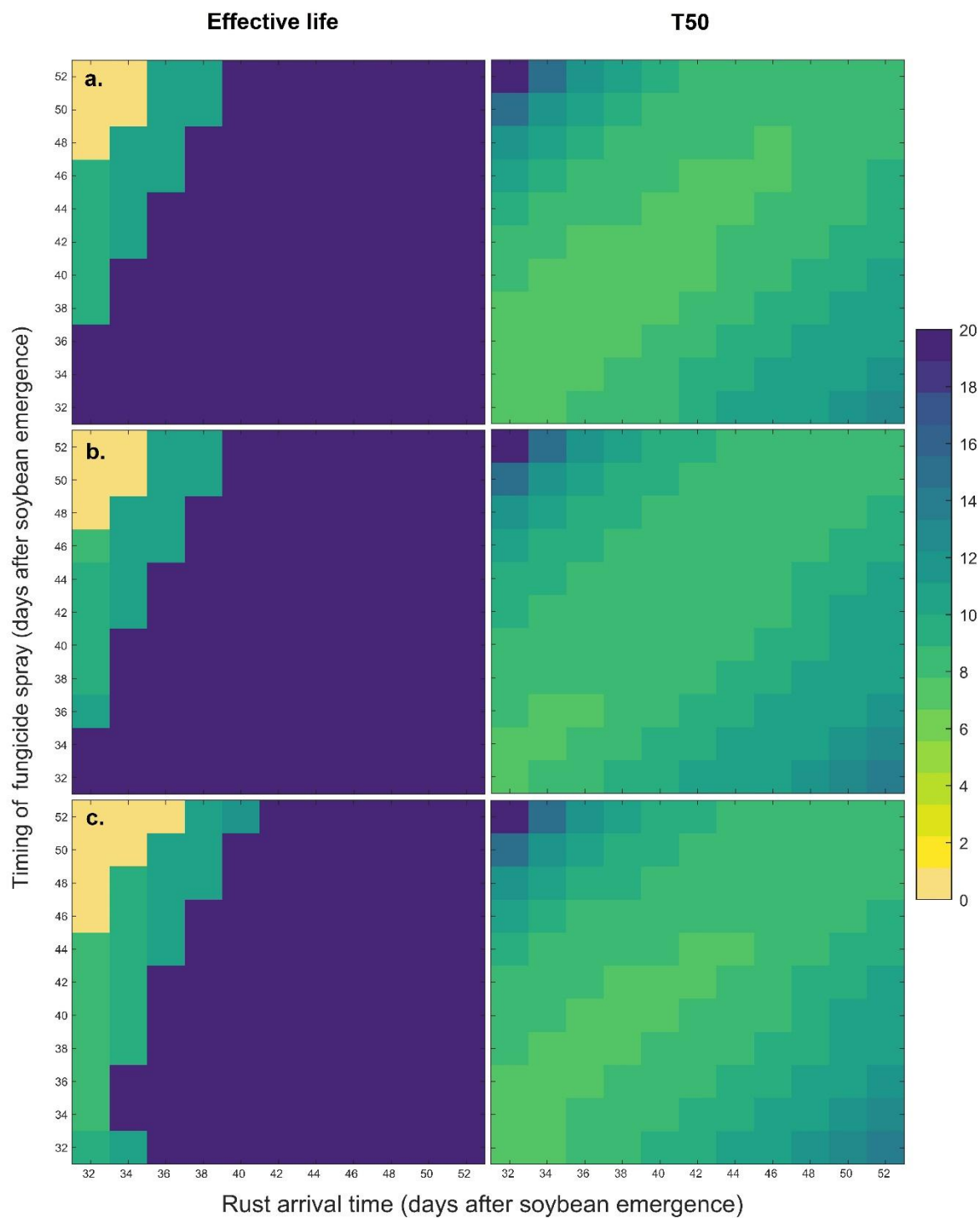
Figure 3.B.8: Figure legend on page 282.
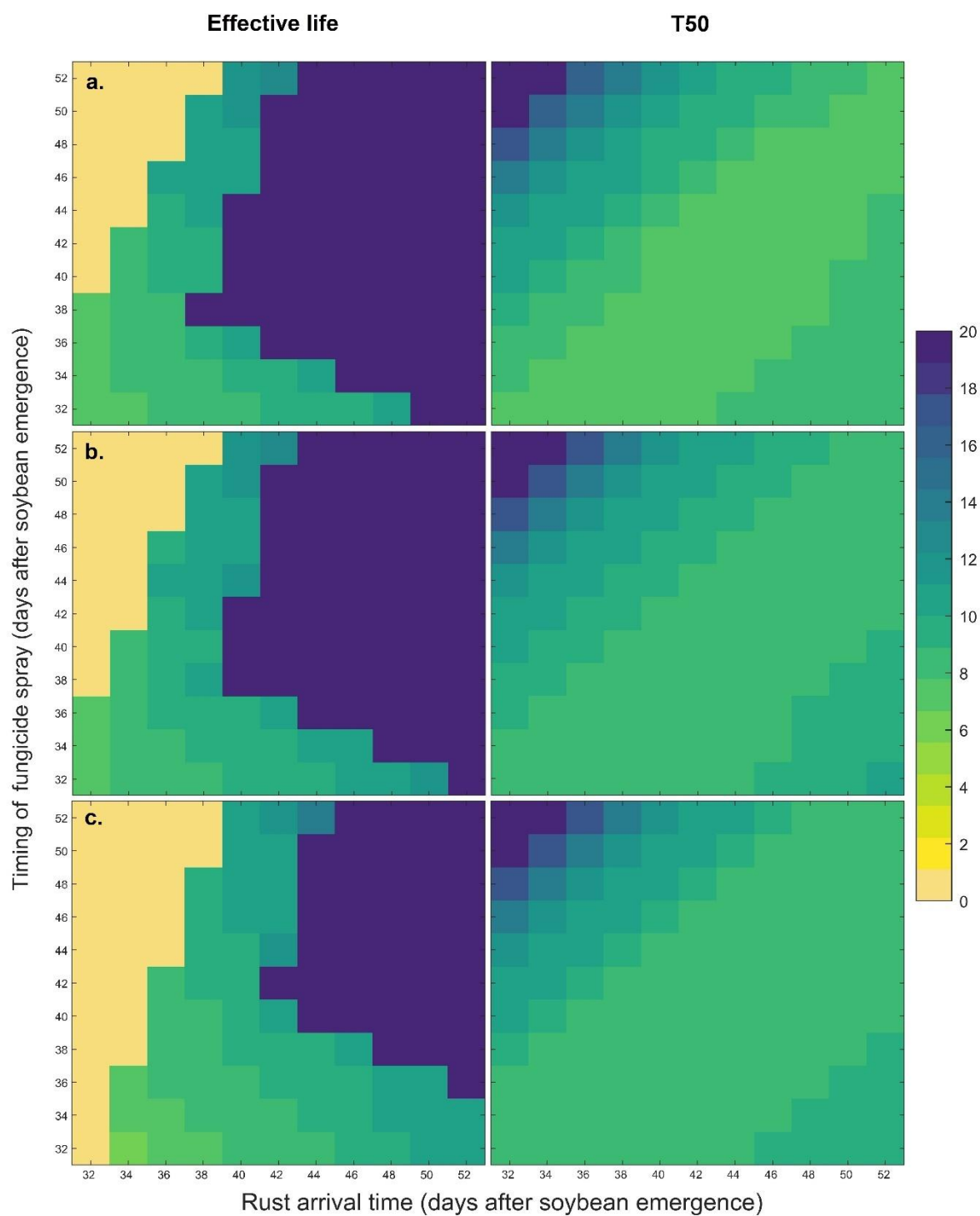
Figure 3.B.9: Figure legend on page 283.
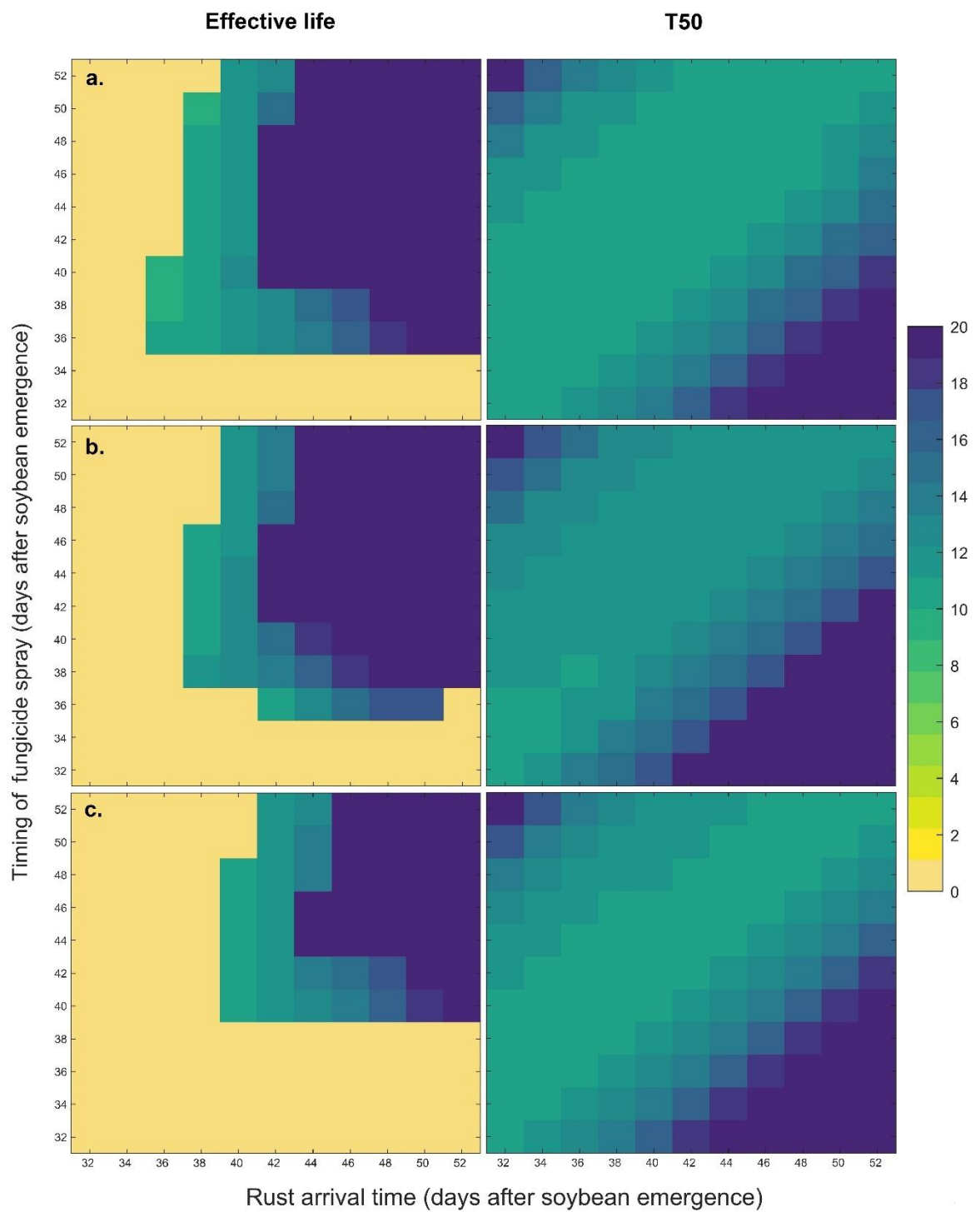
Figure 3.B.10: Figure legend on page 283.

Supplementary Material: Chapter 4

Dose splitting increases selection for both target-site and non-target-site fungicide resistance – a modelling analysis

Appendix 4.A: Further details on model parameterisation

Model parameterisation is described in brief in Sections 1324.3.3 and 4.4.1. Sections 4.A.1 to 4.A.4 give further details on the data and methods used to parameterise the model.

4.A.1 Parameterisation of wheat canopy growth and senescence

Figure 4.A.1 shows the relationship between thermal time (base 0°C) and photo-thermal-vernal time (base 1°C), t_{pvt}. The fitted regression was used to convert t_{pvt} to the average thermal time in zero-degree days, t, for each observed time point. The observed green leaf area index (GLAI) over time was compared for 12 site-years. The average thermal time estimated from t_{pvt} gave a more consistent profile for the timings of upper canopy growth and senescence than the thermal time (base 0°C) calculated without adjusting for the effects of daylength and vernalisation (Figure 4.A.2).

The starting values used for fitting parameter values for t_0, t_{β_0}, t_{β_T}, A_{Max}, γ, τ, φ and ω were based on values used in previous models and averages derived from the experimental dataset (Table 4.A.1). The fits to individual site-year data are shown in Table 4.A.2.

Table 4.A.1: Initial values used in parameterisation of wheat canopy growth and senescence.

Parameter	t_0	t_{β_0}	t_{β_T}	A_{Max}	γ	τ	φ	ω
Units	t	t	t	-	t^{-1}	t^{-1}	t^{-1}	t^{-1}
Initial value	1380	2066	2500	4.1	0.0126	0.005	0.1	0.02
Source	a, b, c	c	b	a, b	a	a	a	a

[a]Hobbelen et al., 2011; [b]Estimate based on 'Data set 1' from Milne et al., 2003; [c]van den Berg et al., 2013

The average number of zero-degree days per day was estimated by using the fitted model values of t_0 (leaf 3 emergence) and t_{β_T} (complete senescence of upper canopy) (Table 4.2) and the dates of the corresponding observed photo-thermal-vernal time to estimate the number of days between emergence and senescence for each site-year (Table 4.A.3). The model estimate of the total number of zero-degree days between upper canopy emergence and senescence was adjusted for any mismatch between t_0, t_{β_T} and the observed photo-thermal-vernal time at the start and end of the emergence and senescence dates respectively (to account for 'overshooting' the required photo-thermal-vernal time due to using daily average weather data). Then the estimated total number of zero-degree days between upper canopy emergence and senescence was divided by the total number of days, to estimate z for each site-year. The mean value of z was calculated across eleven site-years, excluding one site-year for which the model fit was relatively poor.
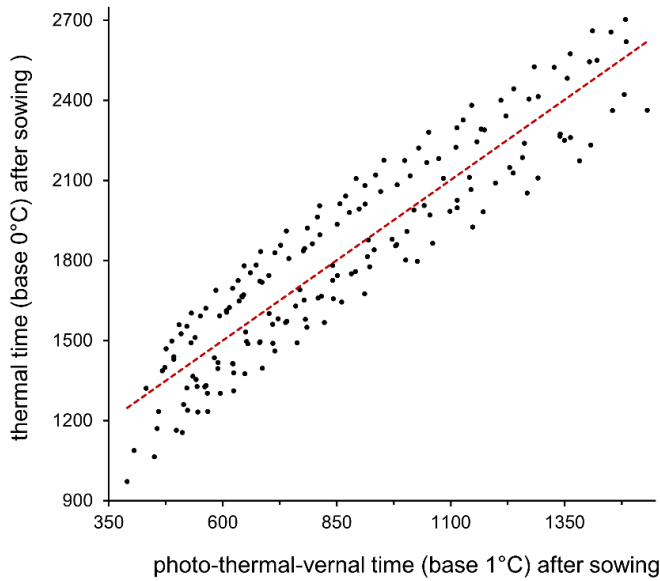
Figure 4.A.1: Linear regression between photo-thermal-vernal time (base 1°C), t_{pvt}, and thermal time (base 0°C), t. Round black points show the time points used to fit the regression, corresponding to time points at which observations of wheat green leaf area index (GLAI) were made for 12 site-years. Dashed line shows the fitted regression line: $t = 1.204\, t_{pvt} + 778.6$. n=179, R^2 = 84.8%, RMSE = 149 degree days (base 0°C).
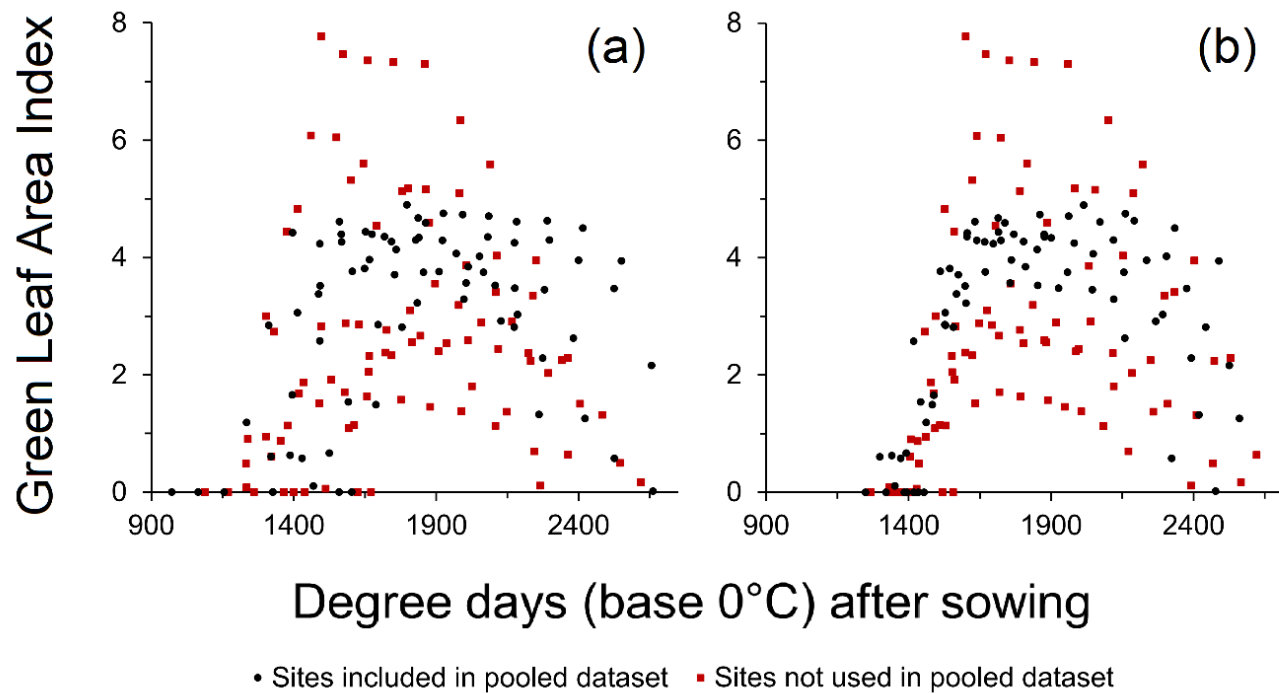
Figure 4.A.2: Comparison between the profile of the Green Leaf Area Index growth and senescence of upper wheat canopy for (a) thermal time (base 0°C) calculated without adjusting for daylength and vernalisation, and (b) thermal time (base 0°C) calculated from photo-thermal-vernal time, t_{pvt}, using the equation derived through simple linear regression (Equation 20, Chapter 4). Using the average thermal time calculated from t_{pvt} gives more consistent timings of upper canopy growth and senescence for use in model parameterisation. Round points (black) show data from the six sites included in the pooled dataset used for parameterisation of the model. Square points (red) show data from the eight sites not included in the pooled dataset.

Table 4.A.2: Fitted parameter values for the wheat canopy model for individual site-years, number of observation time points for each site-year (n), and R^2 for the model fit to each site-year. Data used to fit the model comprised the mean GLAI of the top three leaves at each observation time point, averaged all four cultivars and replicates in Dataset 1. The values used for model simulations (Table 4.2) were fitted to the 'Pooled' dataset, comprised of the first six site-years listed below.

Site and year	Maximum Observed GLAI	t_0 (t)	t_{β_0} (t)	t_{β_T} (t)	A_{Max} (-)	γ (t^{-1})	τ (t^{-1})	φ (t^{-1})	ω (t^{-1})	n	R^2 (%)
Pooled dataset (6 sites)	4.898	1396	1891	2567	4.438	0.0082	0.0028	0.704	0.314	76	76.9
Devon, 1995	3.758	1413	1947	2482	3.704	0.0096	0.0070	0.251	0.017	13	98.8
Boxworth, Cambridgeshire, 1994	4.270	1454	1645	2461	4.166	0.0167	0.0016	0.326	0.056	10	98.9
Kent, 1995	4.351	1357	2074	2617	4.440	0.0067	0.0036	0.076	0.748	14	96.8
Devon, 1994	4.615	1460	1709	2537	4.535	0.0154	0.0017	0.157	0.024	12	94.8
Norfolk, 1995	4.733	1334	2022	2748	4.793	0.0080	0.0012	0.060	0.810	14	97.2
Norfolk, 1994	4.898	1364	2040	2608	5.183	0.0047	0.0042	0.085	0.251	13	96.1
Ely, Cambridgeshire, 1995	1.706	1437	1864	2543	1.556	0.0309	0.0065	0.642	0.013	11	66.7
Boxworth, Cambridgeshire, 1995	2.668	1479	1500	2631	2.622	0.0191	0.0004	0.054	0.010	13	99.6
Hampshire, 1995	2.761	1424	1931	2655	2.744	0.0076	0.0046	0.073	0.847	14	94.5
Yorkshire, 1995	2.882	1426	1868	2491	2.709	0.0218	0.0061	0.266	0.023	13	94.2
Herefordshire, 1995	3.558	1456	1803	2686	3.368	0.0108	0.0062	0.103	1.205	11	95.8
Ely, Cambridgeshire, 1994	5.137	1449	1888	2510	4.621	0.0119	0.0026	0.235	0.362	10	81.8
Herefordshire, 1994	6.080	1433	1912	2532	5.814	0.0130	0.0036	0.065	0.973	13	97.2
Kent, 1994	7.773	1425	1736	2535	7.764	0.0124	0.0024	0.207	0.230	14	98.7

Table 4.A.3: Comparison of model estimation of dates of leaf 3 emergence and complete senescence of upper canopy with recorded dates for 12 site-years (Dataset 1), and estimation of the average number of zero-degree days per day, z, based on model estimates of the number of days between emergence and senescence at each site. [a]Model estimates for each site based on the dates of observed photo-thermal-vernal time corresponding to the fitted parameter values of t_0 (leaf 3 emergence) and t_{β_T} (complete senescence of upper canopy) (Table 4.2). [b]Data from Ely, Cambridgeshire, 1995 were not used in the final estimate of z.

Site and year[a]	Date leaf 3 emergence recorded	Date of final observation	Model estimate of leaf 3 emergence date	Model estimate of date of complete senescence	Model estimate of number of days between upper canopy emergence and senescence	Model estimate: Average number of zero-degree days per day, z
Devon, 1995	29/04/95	12/07/95	23/04/95	17/07/95	86	13.7
Boxworth, Cambridgeshire, 1994	14/05/94	13/07/94	06/05/94	21/07/94	77	15.4
Kent, 1995	25/04/95	17/07/95	26/04/95	19/07/95	85	13.8
Devon, 1994	10/05/94	20/07/94	01/05/94	21/07/94	82	14.4
Norfolk, 1995	01/05/95	17/07/95	29/04/95	21/07/95	84	14.1
Norfolk, 1994	17/05/94	19/07/94	12/05/94	25/07/94	75	15.7
Boxworth, Cambridgeshire, 1995	03/05/95	19/07/95	01/05/95	20/07/95	81	14.7
Hampshire, 1995	28/04/95	18/07/95	24/04/95	19/07/95	87	13.7
Yorkshire, 1995	20/05/95	26/07/95	09/05/95	03/08/95	87	13.5
Herefordshire, 1995	28/04/95	14/07/95	24/04/95	19/07/95	87	13.5
Herefordshire, 1994	13/05/94	29/07/94	10/05/94	27/07/94	79	15.0
Kent, 1994	12/05/94	21/07/94	06/05/94	23/07/94	79	14.9
Ely, Cambridgeshire, 1994	19/05/94	07/07/94	02/05/94	21/07/94	81	14.7
Ely, Cambridgeshire, 1995[b]	11/05/95	20/07/95	09/05/95	19/08/95	103	11.5

Model zero-degree days were mapped to growth stages on Zadoks' scale (AHDB, 2023; Zadoks et al., 1974).The fitted values of t_0, t_{β_0}, t_{β_T} indicate the timings of GS31 (start of growth of leaf 3), GS61 (anthesis) and GS87 (end of grainfill) respectively. We estimated the timing of GS39 (flag leaf fully emerged) as 1653 zero-degree days, the median time at which the flag leaf was first observed to have reached at least 90% of its maximum observed size, for the six site-years included in the pooled dataset from Dataset 1 (Table 4.A.4).

We followed the approach of Milne et al. (2003) in using phyllochron length, l, to estimate the timings of other growth stages before GS39. The phyllochron is the accumulated thermal time between the emergence of consecutive leaves. There is approximately one phyllochron between GS32 (leaf 3 fully emerged) and GS37 (leaf 2 fully emerged), and between GS37 and GS39, so the timing of GS37 can be estimated as GS39 $- l$, and the timing of GS32 as GS39 $-2l$. There are approximately three phyllochrons between GS39 and GS61 (Milne et al., 2003), so l can be estimated as:

$$l = (\mathrm{GS}61 - \mathrm{GS}39)/3 \qquad\qquad (4.A.1)$$

Our estimated value of l was 79.3 zero-degree days. We assumed that the timings (in zero-degree days) of growth stages could be linearly interpolated between GS32 and GS37, GS37 and GS39, GS39 and GS61, and GS61 and GS87.The estimated timings of GS32 (1495 zero-degree days) and GS37 (1574 zero-degree days) were very similar to the average observed timings of leaf 3 and leaf 2 full emergence across the twelve site-years in Dataset 1 (Table 4.A.4). The mapped growth stages were used to determine the timing of fungicide applications in model simulations (Section 4.3.4).

Table 4.A.4: Observed timing (in zero-degree days, converted from t_{pvt}) of leaf emergence across 12 site-years.

Site and year	Leaf 3 >90% emerged	Leaf 2 >90% emerged	Leaf 1 >90% emerged
Devon, 1995	1483	1558	1669
Boxworth, Cambridgeshire, 1994	1528	1528	1667
Kent, 1995	1527	1574	1639
Devon, 1994	1488	1633	1633
Norfolk, 1995	1418	1511	1714
Norfolk, 1994	1529	1529	1605
Boxworth, Cambridgeshire, 1995	1510	1553	1717
Hampshire, 1995	1542	1589	1751
Yorkshire, 1995	1431	1564	1564
Herefordshire, 1995	1493	1552	1675
Herefordshire, 1994	1495	1559	1639
Kent, 1994	1457	1527	1600
Ely, Cambridgeshire, 1994	1479	1623	1623
Ely, Cambridgeshire, 1995	1460	1633	1719

4.A.2 Contribution of individual leaves to total upper canopy area

In addition to the overall model fit described in Section 4.A.1, which describes the total GLAI of the upper canopy (top three leaves), we also fitted the growth and senescence model parameters individually for each leaf 1–3. This was necessary to obtain an estimate of the proportional contribution of each leaf to the overall non-senesced LAI of the upper wheat canopy, which is useful for the parameterisation of fungicide dose response parameters, as it can be used to weight estimates of average disease severity (Section 4.A.4). Fungicide dose response data on disease severity does not always include data on the LAI of each leaf, and an unweighted average of disease severity on each leaf 1–3 may give a biased estimate of the overall percentage severity on the upper canopy: for example, *Z. tritici* severity is often higher on leaf 3 than on leaf 1 and 2, whilst the LAI of leaf 3 is typically smaller than leaves 1 and 2 (van den Berg et al., 2013).

We assumed that the values of t_0 and t_{β_0} for Leaf 3 and t_{β_T} for Leaf 1 corresponded to the fitted values of t_0, t_{β_0} and t_{β_T} for the entire upper canopy (Table 4.2: Fitted parameter values) respectively. We assumed that the growth rate, γ, was the same for all leaves (Milne et al., 2003), and so could be estimated from the timings of GS31 and GS32 in degree days:

$$\gamma = \frac{2\ln 3}{GS32 - GS31} \qquad (4.A.2)$$

The values of t_0 for leaf 2 and leaf 1 were estimated as GS37 – $\frac{2\ln 3}{\gamma}$ and GS39 – $\frac{2\ln 3}{\gamma}$ respectively. The onset of senescence, t_{β_0}, of leaves 2 and 1 was assumed to occur $7l$ and $6l$ after GS37 and GS39 respectively, based on their relative leaf area (van den Berg 2013).

Data on the GLAI of each of leaves 3, 2 and 1 at the six site-years included in the 'pooled' dataset (Table 4.A.2) were used to fit individual values of A_{Max} for each leaf, t_{β_T} for leaves 3 and 2, and values of τ, φ and ω common to all leaves.

The fitted parameter values for leaves 1, 2 and 3 are shown in Table 4.A.5. The fitted and observed proportional contribution of each leaf to the total GLAI of the upper canopy is compared in Figure 4.A.3. The sum of the simulated GLAI of all three leaves was very similar to the GLAI simulated by the fit to the total GLAI of the upper canopy (Figure 4.A.4).

Table 4.A.5: Fitted parameter values for growth and senescence of individual leaves in the upper wheat canopy.

Leaf	Parameter							
	t_0	t_{β_0}	t_{β_T}	A_{Max}	γ	τ	φ	ω
3	1396	1891	2443	1.350				
2	1475	2127	2534	1.555	0.2219	0.0038	0.0909	1.466
1	1554	2127	2567	1.410				
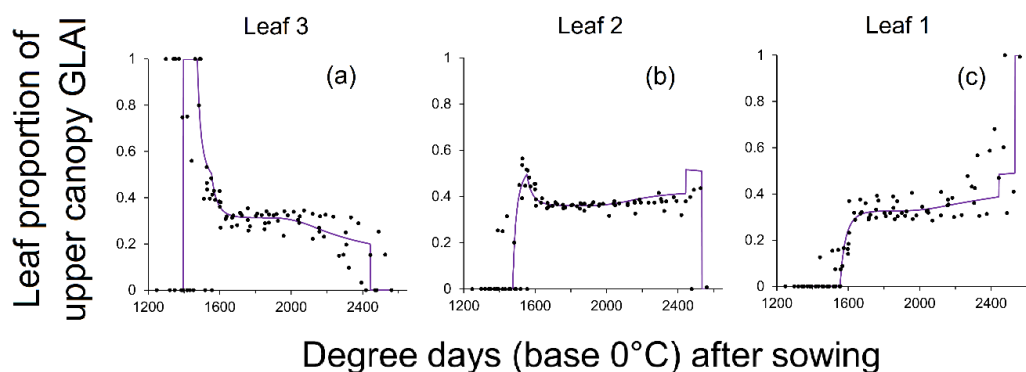
Figure 4.A.3: Observed (black points) and fitted (purple lines) proportional contribution of each leaf 1-3 to the overall green leaf area index (GLAI) of the upper wheat canopy. Observed data (black points) from six site-years included in the 'pooled' dataset (Table 4.A.2).
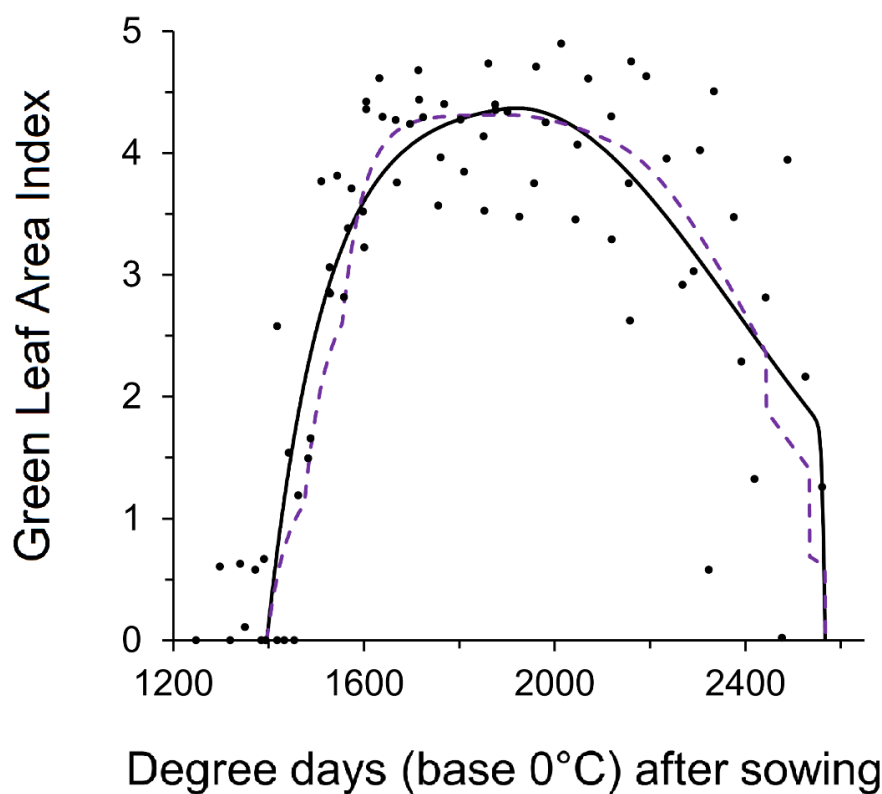
Figure 4.A.4: Model simulation of the overall upper wheat canopy green leaf area index (GLAI) in the absence of disease, comparing the model fitted to total upper canopy GLAI (solid black line) with the model simulation summing the fitted GLAI of individual leaves 1–3 (dashed purple line), and with observed total GLAI measurements used for parameterisation of wheat canopy (points) (n=76, from 6 sites from Dataset 1).

4.A.3 Parameterisation of Zymoseptoria tritici life cycle parameters

The value of λ (Equation 4, Chapter 4) estimated by Hobbelen et al. (2011) was recalculated based on the fitted value of z.

We estimated values for C_0 and ε_0 using data on *Z. tritici* epidemic progress (% severity) (Dataset 1) on untreated plots on which the maximum severity of the Z. tritici epidemic exceeded 5% and the maximum cumulative severity of yellow rust, brown rust and powdery mildew did not exceed 15% (Table 4.A.6). Data on *Z. tritici* severity and LAI for each leaf 1-3 were available, so the average severity over all three leaves was calculated using the LAI of each leaf as a weighting factor.

As an increase in the value of either C_0 or ε_0 can increase disease severity, an increase in one parameter can be counteracted by a decrease in the other, so a two-stage fitting process was used. Firstly, C_0 and ε_0 were fitted simultaneously for each site-year-cultivar combination using least squares optimisation (lsqcurvefit, MATLAB 2022), assuming canopy growth and senescence as fitted to the 'pooled' dataset (parameters shown in Table 4.2). The median value of C_0 was calculated across all site-year-cultivar combinations, and ε_0 refitted for each site-year-cultivar using the fixed value of C_0. The mean value of ε_0 from cultivars that were considered moderately resistant at the time the trials were carried out was used for model simulations.

In the absence of a fungicide, using the fitted values of C_0 and ε_0 (Table 4.2) the model predicts septoria severity of 9.5% at GS75, which is approximately equivalent to the expected average severity on a cultivar with an AHDB resistance rating of 6 (AHDB, 2024b).

Riband at the time of the trials was highly susceptible to septoria. We fitted a separate value of ε_0 for Riband: this could be used to represent susceptible cultivars in future model simulations. For the susceptible cultivar (Riband), values of ε_0 ranged from 0.0183 to 0.0800, with a mean value of 0.0357, corresponding to a prediction of 24.1% septoria severity at GS75, equivalent to an AHDB resistance rating of approximately 3–4 (AHDB, 2024b).

Table 4.A.6: Site-year-cultivar combinations used (✓) and excluded (✗) from parameterisation of septoria infection model, and reasons for exclusion where relevant ('LS' denotes exclusion because the maximum severity of the septoria epidemic was ≤5%; 'OD' denotes exclusion because the maximum cumulative severity of diseases other than *Z. tritici* exceeded 15%. All 4 replicates were used for each site-year-cultivar combination, unless one replicate did not meet the criteria for inclusion (these cases are noted as '3 reps', indicating data from 3 replicates was used). The value of ε_0 used for model simulations was fitted to data from cultivars Apollo, Slejpner and Haven.

Site and year	Cultivar			
	Riband	Apollo	Slejpner	Haven
Devon, 1994	✓	✗ LS	✓ (3 reps)	✓
Devon, 1995	✓	✗ LS	✓ (3 reps)	✗ LS
Hampshire, 1995	✓	✓	✗ OD	✓
Herefordshire, 1994	✓	✗ LS	✓	✓ (3 reps)
Herefordshire, 1995	✓	✗ LS	✓	✓
Kent, 1994	✓	✗OD	✗OD	✓
Kent, 1995	✓ (3 reps)	✗ LS	✗ LS	✗ LS
Boxworth, Cambridgeshire, 1994	✗ LS	✗ LS	✗ LS	✗ LS
Boxworth, Cambridgeshire, 1995	✗ LS	✗ LS	✗ LS	✗ LS
Ely, Cambridgeshire, 1994	✗ LS	✗LS	✗ LS	✗ LS
Ely, Cambridgeshire, 1995	✗OD	✗OD	✗ OD	✗ LS
Norfolk, 1994	✗ LS	✗ LS	✗ LS	✗ LS
Norfolk, 1995	✗ LS	✗ LS	✗ LS	✗ LS
Yorkshire, 1995	✗ LS	✗ LS	✗ LS	✗ LS

4.A.4 Parameterisation of fungicide dose response parameters for SDHI fungicides

We used a literature search to estimate an average decay rate, ν, for SDHI fungicides, and data from AHDB Fungicide Performance Trials (AHDB, 2024a) on the observed dose response of *Z. tritici* severity to fluxapyroxad and isopyrazam from 2011-2012 to fit indicative values of q_σ and k_σ (Section 4.3.2.3). The dose response data consisted of the *Z. tritici* severity, averaged over three replicates for each site-year, on leaves 1, 2 and 3 following a single application of fluxapyroxad or isopyrazam at 0.25, 0.5, 1 or 2 times the full label dose, and on untreated plots (note that applying more than the full label dose is not recommended in practice,

but is included in the experimental protocol for the AHDB Fungicide Performance trials to enable a better estimation of the fungicide dose response).

We sourced gridded weather data were sourced via the Agri4cast Resources Portal (JRC, 2024) to estimate the thermal time (base 0°C) between treatment and assessment timings. We calculated the average severity over all three leaves, weighted by the average contribution of each leaf to the overall canopy at the assessment timing. Data were included in the parameterisation if the average severity on the corresponding untreated plots was >5% and ≤70% (Table 4.A.7).

Table 4.A.7: Data used in parameterisation of SDHI fungicide dose response parameters.

Fungicide	Number of sites			Number of datapoints		
	2011	2012	Total	2011	2012	Total
Isopyrazam	3	3	6	17	18	35
Fluxapyroxad	0	3	3	0	18	18
Both	3	3	6	17	36	53

An individual value of ε_0 was fitted for each site-year based on the severity on the untreated plots. Cross-site values of q_σ and k_σ for each SDHI fungicide (Table 4.A.8) were then fitted to the observed severity data for fluxapyroxad (n=18) and isopyrazam (n=35) using least-squares optimisation (lsqcurvefit, MATLAB 2022). The model achieved a very good fit to the observed disease severity data (n=53, R^2 = 91.3%, RMSE = 5.6 % severity). The cross-site observed and fitted dose response for fluxapyroxad in 2012 is shown in Figure 4.A.5. The averages of the fitted values of q_σ and k_σ for fluxapyroxad and isopyrazam were used as indicative parameter values for an SDHI fungicide for the purpose of interpreting model simulation results (Table 4.2).

As an additional check to ensure that the parameterisation was robust to our assumptions around the average contribution of each leaf to the overall canopy over time, we also fitted q_σ and k_σ using the unweighted average severity over all three leaves. The results were similar, but with slightly lower values of q_σ and slightly higher values of k_σ (Table 4.A.8).

Table 4.A.8: Fitted dose response parameters q_σ and k_σ for SDHI fungicides.

Fungicide	Fitted parameters: weighted average severity		Fitted parameters: unweighted average severity	
	q_σ	k_σ	q_σ	k_σ
Isopyrazam	0.5280	10.0	0.5076	10.9
Fluxapyroxad	0.6091	9.7	0.5804	10.5
Average	0.5686	9.9	0.5440	10.7
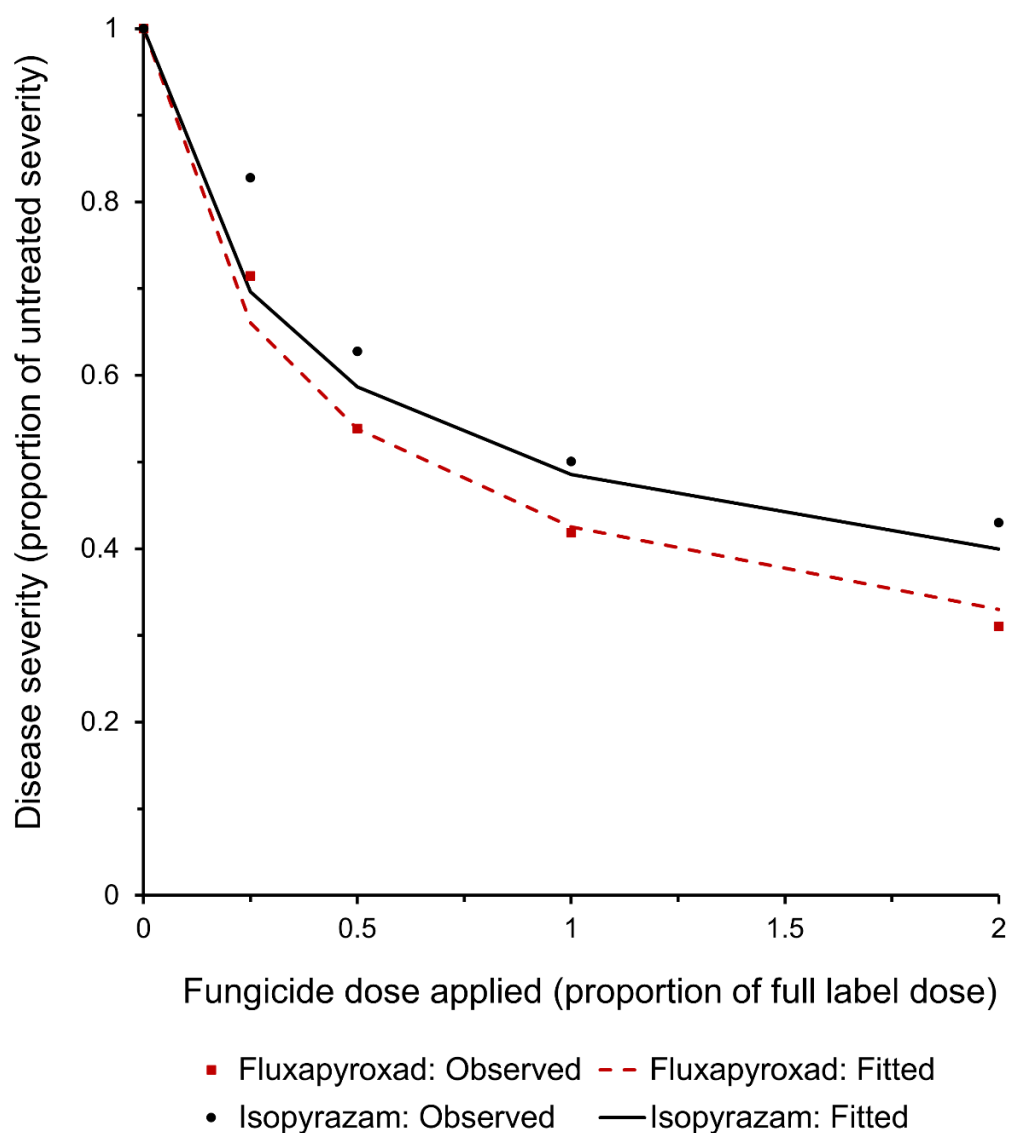
Figure 4.A.5: Observed and fitted fungicide dose response for fluxapyroxad and Isopyrazam. Average disease severity for each fungicide dose rate expressed as a proportion of the untreated severity. Points (isopyrazam – black, round; fluxapyroxad – red, square) show the average observed dose response in 2012 (n=36 across 3 sites). Lines show the average fitted dose response at the same three (2012) sites for isopyrazam (black solid line, parameters fitted to 6 site-years,

2011-2012) and fluxapyroxad (red dashed line, parameters fitted to 3 site-years, 2012). Note that applying more than the full label dose is not recommended in practice, but a higher dose rate is included in the experimental protocol for the AHDB Fungicide Performance trials to enable a better estimation of the fungicide dose response.

4.A.5 References

AHDB (2023). Wheat growth guide. Available at: https://ahdb.org.uk/knowledge-library/wheat-growth-guide [Accessed 6 August 2024].

AHDB (2024a). A guide to fungicide performance in wheat, barley and oilseed rape. Available at: https://ahdb.org.uk/knowledge-library/a-guide-to-fungicide-performance-in-wheat-barley-and-oilseed-rape [Accessed 6 August 2024].

AHDB (2024b). Recommended Lists disease ratings. Available at: https://ahdb.org.uk/recommended-lists-disease-ratings [Accessed 6 August 2024].

Hobbelen, P.H.F., Paveley, N.D., van den Bosch, F. (2011). Delaying selection for fungicide insensitivity by mixing fungicides at a low and high risk of resistance development: A modeling analysis. *Phytopathology* 101, 1224–1233. https://doi.org/10.1094/PHYTO-10-10-0290

Joint Research Centre (JRC) of the European Commission (EC) (2024). Gridded Agro-Meteorological Data in Europe. Available at: https://agri4cast.jrc.ec.europa.eu/DataPortal/Index.aspx?o=

The MathWorks Inc. (2022). MATLAB version: 9.13.0 (R2022b), Natick, Massachusetts: The MathWorks Inc. https://www.mathworks.com

Milne, A., Paveley, N., Audsley, E., Livermore, P. (2003). A wheat canopy model for use in disease management decision support systems. *Annals of Applied Biology* 143, 265–274. https://doi.org/10.1111/j.1744-7348.2003.tb00294.x

van den Berg, F., van den Bosch, F., Paveley, N.D. (2013). Optimal Fungicide Application Timings for Disease Control Are Also an Effective Anti-Resistance Strategy: A Case Study for *Zymoseptoria tritici* (*Mycosphaerella graminicola*) on Wheat. *Phytopathology* 103, 1209–1219. https://doi.org/10.1094/PHYTO-03-13-0061-R

Zadoks, J.C., Chang, T.T., Konzak, C.F. (1974). A decimal code for the growth stages of cereals. *Weed Research* 14, 415–421. https://doi.org/10.1111/j.1365-3180.1974.tb01084.x

Appendix 4.B: Further details on model results

This section provides further illustration of some of the results described in Section 4.4.2.2. Figure 4.B.1 shows that the asymptote parameter, q_σ, has very little impact on η for a curvature shift. Figure 4.B.2 shows how curvature parameter, k_σ, asymptote shift, ζ_q, and curvature shift, ζ_k, affect the fungicide concentration, $D(t)$, that maximises the difference in growth rates of the sensitive and resistant strain, demonstrating the driver of the results shown in Figure 4.6.
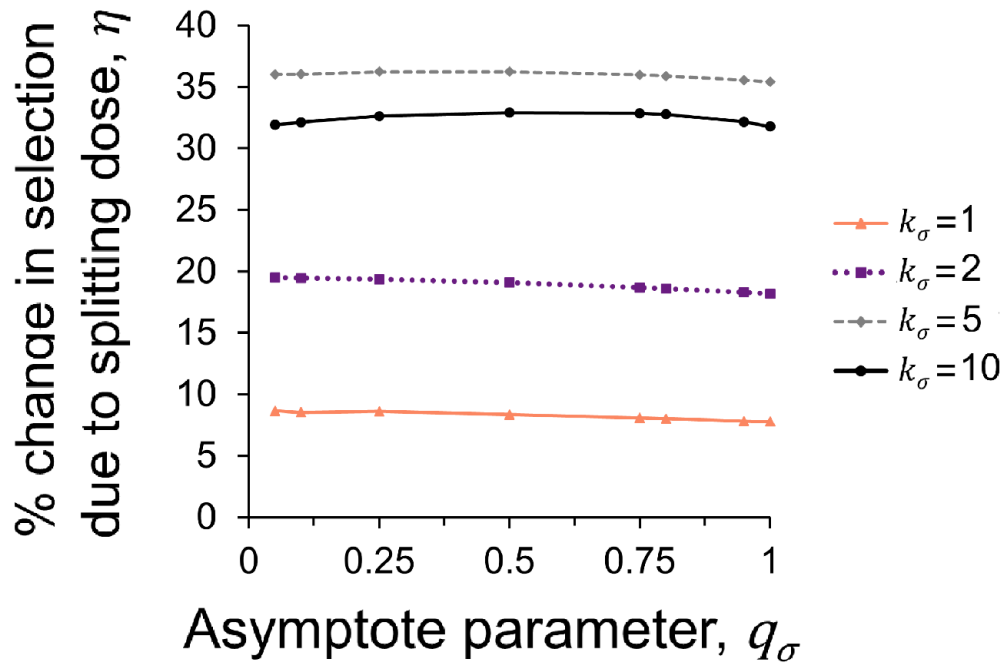
Figure 4.B.1: Negligible variation in η, the percentage change in selection due to dose splitting with asymptote parameter q_σ for strains with a curvature shift, ζ_k (see Section 4.4.2.2). For the example shown here, $\zeta_k = 50\%$ and $\nu = 0.008\ t^{-1}$.
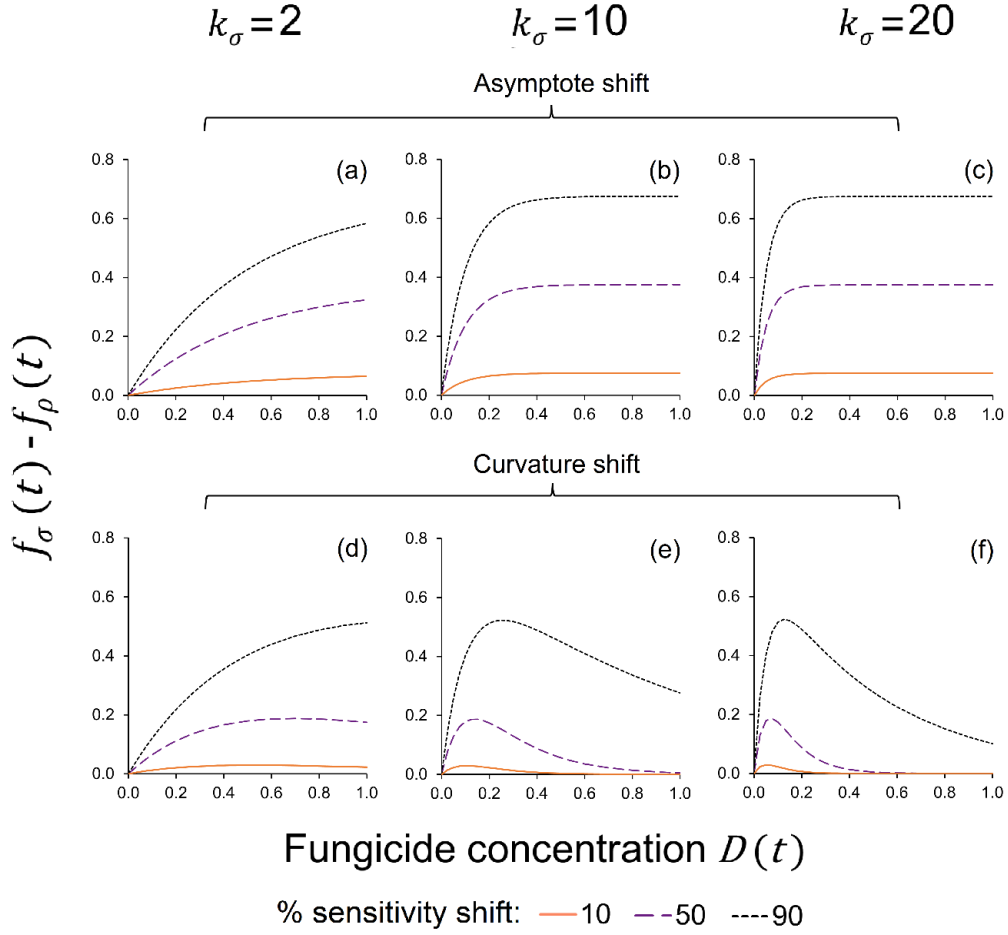
Figure 4.B.2: Effect of curvature parameter, k_σ, and sensitivity shift, ζ_q or ζ_k, on the fungicide concentration $D(t)$ that maximises $f_\sigma(t) - f_\rho(t)$, the difference in the fractional reduction $f(t)$ of pathogen life cycle parameters of the sensitive strain compared to a resistant strain. (a), (b) and (c) show $f_\sigma(t) - f_\rho(t)$ for different levels of asymptote shift, ζ_q, for $k_\sigma = 2$, 10 and 20 respectively. (d), (e) and (f) show $f_\sigma(t) - f_\rho(t)$ for different levels of curvature shift, ζ_k, for $k_\sigma = 2$, 10 and 20 respectively. For a curvature shift, the smaller the value of ζ_k and the larger the value of k_σ, the smaller the concentration $D(t)$ at which $f_\sigma(t) - f_\rho(t)$ is at a maximum. Dashed black line: sensitivity shift = 90%. Dashed purple line: sensitivity shift = 50%. Solid orange line: sensitivity shift = 10%.

Supplementary Material: Chapter 5

Which resistance management strategies work against concurrent evolution of resistance to fungicides?

Tables of modelling results are available at Corkley, I. (2024). Supplementary Information to Chapter 5 of the PhD thesis entitled "Managing concurrent evolution of resistance to fungicides". (Version v1) [Data set].
Zenodo. https://doi.org/10.5281/zenodo.14424058

List of Supplementary Tables:

Table S.1: Modelling results for scenarios with asymptote shifts to both fungicide A and fungicide B, where fungicides A and B have a foliar concentration half-life of 3 days (v = 0.01605 t^{-1}).

Table S.2: Modelling results for scenarios with curvature shifts to both fungicide A and fungicide B, where fungicides A and B have a foliar concentration half-life of 3 days (v = 0.01605 t^{-1}).

Table S.3: Modelling results for scenarios with an asymptote shift to fungicide A and a curvature shift to fungicide B, where fungicides A and B have a foliar concentration half-life of 3 days (v = 0.01605 t^{-1}).

Table S.4: Modelling results for scenarios with asymptote shifts to both fungicide A and fungicide B, where fungicides A and B have a foliar concentration half-life of 6 days (v = 0.00802 t^{-1}).

Table S.5: Modelling results for scenarios with curvature shifts to both fungicide A and fungicide B, where fungicides A and B have a foliar concentration half-life of 6 days (v = 0.00802 t^{-1}).

Table S.6: Modelling results for scenarios with an asymptote shift to fungicide A and a curvature shift to fungicide B, where fungicides A and B have a foliar concentration half-life of 6 days (v = 0.00802 t^{-1}).

Table S.7: Modelling results for scenarios with asymptote shifts to both fungicide A and fungicide B, where fungicides A and B have a foliar concentration half-life of 12 days ($v = 0.00401\ t^{-1}$).

Table S.8: Modelling results for scenarios with curvature shifts to both fungicide A and fungicide B, where fungicides A and B have a foliar concentration half-life of 12 days ($v = 0.00401\ t^{-1}$).

Table S.9: Modelling results for scenarios with an asymptote shift to fungicide A and a curvature shift to fungicide B, where fungicides A and B have a foliar concentration half-life of 12 days ($v = 0.00401\ t^{-1}$).

Supplementary Material: Chapter 6

Azole mixtures: Modelling resistance management benefits of incomplete cross-resistance within a fungicide mode of action group

Appendix 6.A: Further details on the population genetic model

6.A.1 Further details on modelling the azole dose-response curve
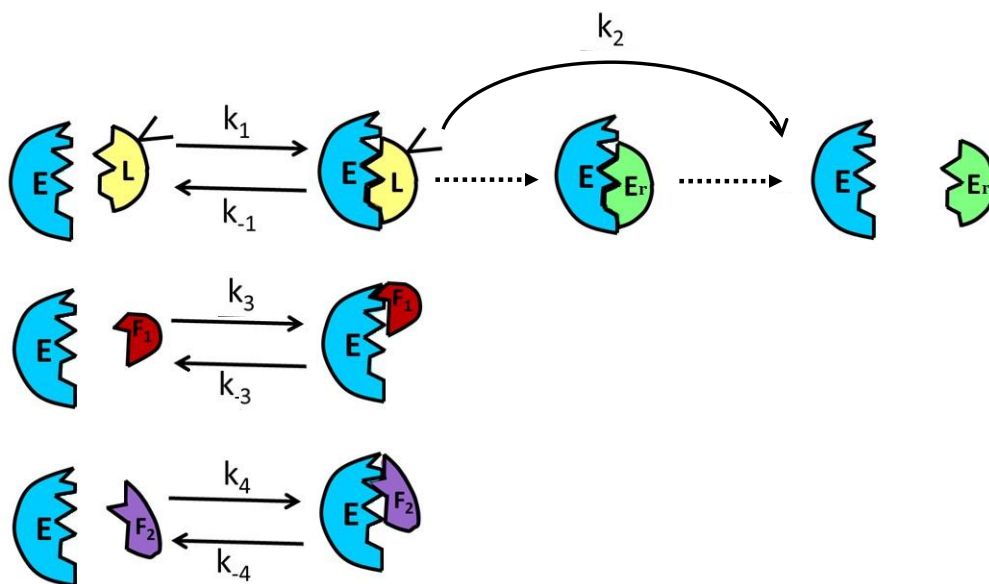
Figure 6.A.1: The process of converting lanosterol into ergosterol, top row, and competitive binding and release of two azole fungicides to the CYP51 enzyme. Enzyme, E, blue. Lanosterol molecule, L, yellow. Ergosterol molecule, Er, green. Azole 1 molecule, F_1, red. Azole 2 molecule, F_2, purple. k_a is the rate of binding and k_{-a} is the unbinding rate for each process. Rate k_2 denotes the combined rate of conversion of lanosterol to ergosterol and unbinding of the product from the enzyme.
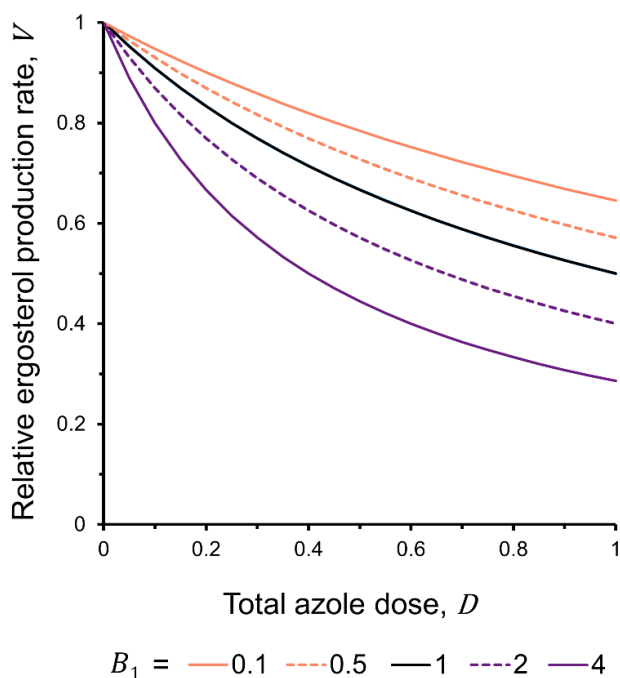
Figure 6.A.2: Ergosterol production rate, *V*, as a function of the total azole dose, *D*, of two azoles in a 1:1 ratio ($D_1 = D_2$), for a range of values of dose response parameter B_1 and $B_2 = 1$. We plot relative rates by setting $A = 1$ t^{-1}. See Equation 3, Section 6.3.2.1.

Assumption that azoles bind competitively to the CYP51 enzyme

In the derivation of the dose-response curve we have assumed that azole molecules bind competitively to the CYP51 enzyme. There is an ongoing debate about the binding dynamics of azoles to the CYP51 molecule. We thank Dr Marcus Fehr for his insights into the debate. Several authors say that azoles bind non-competitively to the CYP51 molecule (e.g. Parker et al., 2011). They make this claim because of the observed effect of the substrate concentration on the rate of product development. This is however an indirect observation. Direct observations on the binding dynamics, such as those carried out by Hargrove et al. (2018), suggest that binding is of the competitive type.

Using competitive inhibition or non-competitive inhibition does affect the rate of product formation as dependent on the substrate concentration. However, to model the dose-response the substrate concentration is not relevant, only the effect of inhibitor concentration.

Wang (2014) derived both cases step by step and the reader is referred to those lecture notes. In his notation, which is slightly different from ours, Wang shows that the rate of product formation for the case of competitive binding is given by:

$$V = \frac{k_2 E_0 S}{K_m \left(1 + \frac{I}{K_I}\right) + S} \tag{A.1}$$

And in the case of non-competitive binding by:

$$V = \frac{k_2 E_0 S}{\left(1 + \frac{I}{K_I}\right)(K_m + S)} \tag{A.2}$$

where S is the substrate concentration and I is the inhibitor concentration, and the rest of the symbols are other parameters. It is clear from Equations (A.1) and (A.2) that the effect of substrate concentration on product formation is different, but also that the effect of the inhibition concentration on product formation is the same as both equations can be written as $V = \frac{A}{1 + BI}$, which is the form of our dose-response curve (Equation 2, Chapter 6).

6.A.2 Solving the model for $S_i(T)$

The dose dynamics of a fungicide spray, dose response curve, and dynamics of disease severity (lesion density) are described by Equations (6), (7) and (6) and (8), and the season length is defined as T. (Section 6.3.2.2; Section 6.3.2.2.1). We can use these to derive equations for the severity of haplotype i at time T, $S_i(T)$, after one or two applications of fungicide j.

Consider one application of dose D_{j0} at $t = 0$:

$$\frac{dS_i(t)}{dt} = \frac{r_0}{1 + B_{ij}D_{j0}e^{-\alpha t}} S_i(t) \;\rightarrow\; \frac{1}{S_i(t)} \frac{dS_i(t)}{dt} = \frac{r_0}{1 + B_{ij}D_{j0}e^{-\alpha t}} \tag{A.3}$$

Integrating with respect to time from $t = 0$ to $t = T$:

$$\int_0^T \frac{1}{S_i(t)} dS_i(t) = \int_0^T \frac{r_0}{1 + B_{ij}D_{j0}e^{-\alpha t}} dt \rightarrow \ln\big(S_i(t)\big) - \ln\big(S_i(0)\big) = \int_0^T \frac{r_0}{1 + B_{ij}D_{j0}e^{-\alpha t}} dt =$$

$$\frac{r_0}{\alpha} \int_0^T \frac{\alpha e^{\alpha t}}{B_{ij}D_{j0} + e^{\alpha t}} dt \tag{A.4}$$

To solve the integral at the right-hand side, we define $u = B_{ij}D_{j0} + e^{\alpha t}$. Then $u' = \alpha e^{\alpha t}$.

$$\frac{r_0}{\alpha}\int_0^T \frac{\alpha e^{\alpha t}}{B_{ij}D_{j0} + e^{\alpha t}}\,dt = \frac{r_0}{\alpha}\int_0^T \frac{u'}{u}\,dt = \frac{r_0}{\alpha}\int_0^T \frac{1}{u}\,du = \frac{r_0}{\alpha}\ln(u)\Big|_0^T$$

$$= \frac{r_0}{\alpha}\ln\left(B_{ij}D_{j0} + e^{\alpha t}\right)\Big|_0^T \tag{A.5}$$

Therefore:

$$\frac{r_0}{\alpha}\int_0^T \frac{\alpha e^{\alpha t}}{B_{ij}D_{j0} + e^{\alpha t}}\,dt = \frac{r_0}{\alpha}\ln\left(B_{ij}D_{j0} + e^{\alpha t}\right) - \frac{r_0}{\alpha}\ln\left(B_{ij}D_{j0} + 1\right) \tag{A.6}$$

Substituting $S_i(t)$ into equation (A.6) gives:

$$\ln\left(S_i(t)\right) - \ln\left(S_i(0)\right) = \frac{r_0}{\alpha}\ln\left(B_{ij}D_{j0} + e^{\alpha t}\right) - \frac{r_0}{\alpha}\ln\left(B_{ij}D_{j0} + 1\right) \tag{A.7}$$

$$S_i(t) = S_i(0)\left(\frac{B_{ij}D_{j0} + e^{\alpha t}}{B_{ij}D_{j0} + 1}\right)^{\frac{r_0}{\alpha}} \tag{A.8}$$

If there is a time period t^* between $t = 0$ and the spray application, and the season length is $t = T$, then:

$$S_i(T) = S_i(t^*)\left(\frac{B_{ij}D_{j0} + e^{\alpha(T-t^*)}}{B_{ij}D_{j0} + 1}\right)^{\frac{r_0}{\alpha}} \tag{A.9}$$

Since $S_i(t^*) = S_i(0)e^{r_0 t^*}$, we find Equation 9 (Chapter 6):

$$S_i(T) = S_i(0)e^{r_0 t^*}\left(\frac{B_{ij}D_{j0} + e^{\alpha(T-t^*)}}{B_{ij}D_{j0} + 1}\right)^{\frac{r_0}{\alpha}}$$

Consider two applications, one at t^* and one at t^{**}. First it is necessary to calculate what dose remains at time t^{**} from the first application at time t^*, following dose decay over the time period $t^{**} - t^*$; this dose is added to the application dose at t^{**}, D_{j0}:

$$D(t^{**}) = D_{j0}e^{-\alpha(t^{**}-t^*)} + D_{j0} \tag{A.10}$$

Therefore for a two-spray programme, we find Equation 10 (Chapter 6):

$$S_i(T) = S_i(0)e^{r_0 t^*}\left(\frac{B_{ij}D_{j0} + e^{\alpha(t^{**}-t^*)}}{B_{ij}D_{j0} + 1}\right)^{\frac{r_0}{\alpha}}\left(\frac{B_{ij}D_{j0}\left(1 + e^{-\alpha(t^{**}-t^*)}\right) + e^{\alpha(T-t^{**})}}{B_{ij}D_{j0}\left(1 + e^{-\alpha(t^{**}-t^*)}\right) + 1}\right)^{\frac{r_0}{\alpha}}$$

6.A.3 Relationships between lab-EC_{50} and field-ED_{50} values

We used relationships between lab-EC_{50} and field-ED_{50}, developed by Blake et al. (2018), to convert lab-EC_{50} measurements of haplotype sensitivity (in (μg/ml)) to each azole into the field-ED_{50} values used for parameterisation of the B_{ij} dose-response parameters for each haplotype-azole combination. For epoxiconazole y=0.3128x-0.007, where y=log(ED_{50}) and x=log(EC_{50}). For prothioconazole, y=3.812x+0.246 with y=log(prothioconazole ED_{50}) and x=log(prothioconazole-desthio EC_{50}). We used these relationships to calculate epoxiconazole and prothioconazole ED_{50} values respectively for each haplotype-azole combination. The fitted relationships differ between epoxiconazole and prothioconazole. We therefore assessed which, if any relationship was likely to be appropriate for converting tebuconazole and prochloraz EC_{50} values to ED_{50} values.

The antifungal action from an applied dose of prothioconazole is caused by its active metabolite prothioconazole-desthio (Parker et al., 2013). We compared the results of studies that measured the proportion of the applied dose of prothioconazole, epoxiconazole and tebuconazole that is successfully transferred onto or into plant leaves: the relevant comparison for prothioconazole is the proportion of applied prothioconazole that is transferred onto or into plant leaves as prothioconazole-desthio. When tebuconazole and prothioconazole were applied at the same rate, approximately 3.5g tebuconazole was measured on/in the flag leaf for every 1g of prothioconazole-desthio, a ratio of 3.5:1 (Lehoczki-Krsjak et al., 2013, 2015). From similar studies, we estimated this ratio as 4.7:1 for epoxiconazole vs. prothioconazole-desthio (Lichiheb et al., 2015; Lin et al., 2017; Zhang et al., 2018). Applying this ratio as a correction factor explains the differences between epoxiconazole and prothioconazole in the observed relationships between EC_{50} and ED_{50}. We therefore assumed that the relationship between EC_{50} and ED_{50} is consistent for other azole fungicides, and used the relationship between EC_{50} and ED_{50} for epoxiconazole as an estimate for the relationship between EC_{50} and ED_{50} for tebuconazole and prochloraz.

For any haplotypes which had a direct measurement of lab-EC_{50} for prothioconazole-desthio, we used the mean value of prothioconazole-desthio EC_{50} measurements across all isolates with that haplotype. However, seven haplotypes included in the analysis did not have EC_{50} measurements for prothioconazole-desthio, but did have EC_{50} measurements for prothioconazole (Table 6.B.4). For

some isolates EC$_{50}$ measurements were available for both prothioconazole-desthio and prothioconazole (Table 6.B.3). We fitted a relationship between the lab-EC$_{50}$ measurements of prothioconazole-desthio and prothioconazole (Figure 6.A.3) and used this to estimate prothioconazole-desthio EC$_{50}$ from prothioconazole EC$_{50}$ measurements in cases where there were no EC$_{50}$ measurements for prothioconazole-desthio. For prothioconazole-desthio, y=0.7152x-4.3645, where y=log(prothioconazole-desthio EC$_{50}$) and x=log(prothioconazole EC$_{50}$).
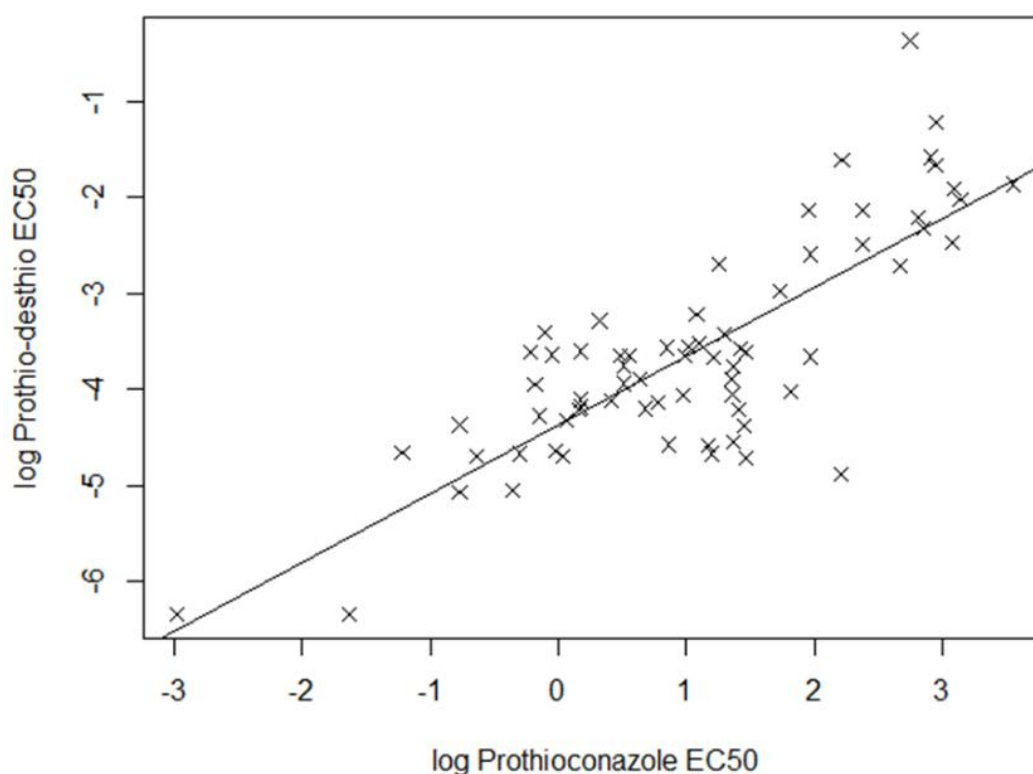
Figure 6.A.3: Fitted relationship between log(prothioconazole EC$_{50}$) (log (μg/ml)) and log(prothioconazole-desthio EC$_{50}$) (log (μg/ml)). Adjusted R^2 = 63.95%.

6.A.4 References

Blake, J.J., Gosling, P., Fraaije, B.A., Burnett, F.J., Knight, S.M., Kildea, S. et al. (2018). Changes in field dose–response curves for demethylation inhibitor (DMI) and quinone outside inhibitor (QoI) fungicides against *Zymoseptoria tritici*, related to laboratory sensitivity phenotyping and genotyping assays. *Pest Management Science* 74, 302–313. https://doi.org/10.1002/ps.4725

Hargrove, T.Y., Wawrzak, Z., Fisher, P.M., Child, S.A., Nes, W.D., Guengerich, F.P. et al. (2018). Binding of a physiological substrate causes large-scale

conformational reorganization in cytochrome P450 51. *Journal of Biological Chemistry* 293, 19344–19353. https://doi.org/10.1074/jbc.RA118.005850

Lehoczki-Krsjak, S., Varga, M. & Mesterházy, Á. (2015). Distribution of prothioconazole and tebuconazole between wheat ears and flag leaves following fungicide spraying with different nozzle types at flowering. *Pest Management Science*, 71(1), 105–113. https://doi.org/10.1002/ps.3774

Lehoczki-Krsjak, S., Varga, M., Szabó-Hevér, Á. & Mesterházy, Á. (2013). Translocation and degradation of tebuconazole and prothioconazole in wheat following fungicide treatment at flowering. *Pest Management Science*, 69(11), 1216–1224. https://doi.org/10.1002/ps.3486

Lichiheb, N., Bedos, C., Personne, E., Benoit, P., Bergheaud, V., Fanucci, O. et al. (2015). Measuring Leaf Penetration and Volatilization of Chlorothalonil and Epoxiconazole Applied on Wheat Leaves in a Laboratory-Scale Experiment. *Journal of Environmental Quality*, *44*(6), 1782–1790. https://doi.org/10.2134/jeq2015.03.0165

Lin, H., Dong, B. & Hu, J. (2017). Residue and intake risk assessment of prothioconazole and its metabolite prothioconazole-desthio in wheat field. *Environmental Monitoring and Assessment*, *189*(5), 236. https://doi.org/10.1007/s10661-017-5943-1

Parker, J.E., Warrilow, G.S., Cools, H.J., Martel, C.M., Nes, W.D., Fraajie, B.A. et al. (2011). Mechanism of binding of prothioconazole to *Mycosphaerella graminicola* CYP51 differs from that of other azole antifungals. *Applied and Environmental Microbiology* 77: 1460-1465. https://doi.org/10.1128/AEM.01332-10

Parker, J. E., Warrilow, A. G., Cools, H. J., Fraaije, B. A., Lucas, J. A., Rigdova, K. et al. (2013). Prothioconazole and prothioconazole-desthio activities against *Candida albicans* sterol 14-α-demethylase. *Applied and environmental microbiology*, *79*(5), 1639–1645. https://doi.org/10.1128/AEM.03246-12

Wang, N.S. (2014). Enzyme inhibition. Course notes. https://terpconnect.umd.edu/~nsw/chbe482/inhibit.pdf [Accessed 17 September 2024].

Zhang, M., Dong, B., Qiao, Y., Shi, C., Yang, H., Wang, Y. et al. (2018). Yield and water use responses of winter wheat to irrigation and nitrogen application in the North China Plain. *Journal of Integrative Agriculture*, *17*(5), 1194–1206. https://doi.org/10.1016/S2095-3119(17)61883-5

Appendix 6.B: CYP51 haplotype frequencies and sensitivity to four azole active substances

Table 6.B.1: Dataset metadata for Tables 6.B.2, 6.B.3 and 6.B.4.

People & Organisations				
List of people involved with the dataset generation				
Name	Affiliation	Email	ORCID	Role
Bart Fraaije	Wageningen University & Research	bart.fraaije@wur.nl	https://orcid.org/0000-0001-8176-2258	Principal Investigator
Nichola Hawkins	NIAB	nichola.hawkins@niab.com	https://orcid.org/0000-0003-3389-0436	Data Collector
Isabel Corkley	Rothamsted Research, RSK ADAS Ltd	isabel.corkley@rothamsted.ac.uk	https://orcid.org/0000-0003-3783-3180	Data Curator
Funder & Project information				
Funder name	Award (Grant) code	Award title	Project name	
BBSRC	BBS/OS/CP/000001	Smart Crop Protection		
BBSRC	BB/X010953/1; BBS/E/RH/230003C	Growing Health		
BBSRC	BB/S018867/2	BBRSC-FAPESP AMR and Insecticide Pest Resistance in Livestock and Agriculture		
AHDB	21120062	AHDB PhD Studentship	Managing concurrent evolution of resistance to fungicides	
BASF plc	1020280		Assessing the benefits of azole diversity to resistance management	
AHDB	PR475	AHDB project grant	Understanding evolution and selection of azole resistance mechanisms in UK populations of *Mycosphaerella graminicola*	
AHDB	PR619	AHDB project grant	Azole and SDHI fungicide sensitivity monitoring of septoria populations (2011–19) and development of tools to rationalise fungicide programmes to control cereal diseases	

Table 6.B.2: Relative haplotype frequencies as sampled in Harpenden, UK in the years 2003 and 2010-2019.

Haplotype ID	CYP51 Haplotype	Sampled frequency by year										
		2003	2010	2011	2012	2013	2014	2015	2016	2017	2018	2019
3	L50S-Y461S	0.0270	0.0000	0.0000	0.0000	0.0000	0.0000	0.0000	0.0000	0.0000	0.0000	0.0000
4	L50S-Y461H	0.0541	0.0000	0.0000	0.0000	0.0000	0.0000	0.0000	0.0000	0.0000	0.0000	0.0000
6	Y137F-S524T	0.0541	0.0000	0.0000	0.0000	0.0000	0.0000	0.0000	0.0000	0.0000	0.0000	0.0000
7	L50S-V136A-Y461S	0.0000	0.0000	0.0244	0.0000	0.0000	0.0000	0.0270	0.0000	0.0000	0.0000	0.0000
9	L50S-V136A-Y461H	0.2162	0.0000	0.0000	0.0222	0.0263	0.0000	0.0000	0.0000	0.0000	0.0000	0.0000
10	V136A-S188N-DEL	0.0270	0.0000	0.0000	0.0000	0.0000	0.0000	0.0000	0.0000	0.0000	0.0000	0.0000
12	L50S-I381V-Y459D	0.0541	0.2000	0.0000	0.0000	0.0000	0.0000	0.0000	0.0000	0.0000	0.0000	0.0000
14	L50S-I381V-Y459S	0.0000	0.0250	0.0000	0.0000	0.0000	0.0000	0.0000	0.0000	0.0000	0.0000	0.0000
15	L50S-I381V-Y461H	0.1892	0.2000	0.1951	0.0667	0.0000	0.0000	0.0000	0.0000	0.0000	0.0000	0.0000
20	L50S-S188N-DEL-N513K	0.0811	0.0250	0.0000	0.0000	0.0000	0.0000	0.0000	0.0000	0.0000	0.0000	0.0000
22	D134G-V136A-S188N-DEL	0.0000	0.0000	0.0244	0.0000	0.0000	0.0000	0.0000	0.0000	0.0000	0.0000	0.0000
24	L50S-D134G-V136G-Y461S	0.0000	0.0000	0.0000	0.0000	0.0000	0.0000	0.0270	0.0000	0.0000	0.0000	0.0000
26	D107V-I381V-N513K-S524T	0.0000	0.0000	0.0244	0.0000	0.0000	0.0250	0.0000	0.0000	0.0000	0.0000	0.0000
27	L50S-S188N-I381V-DEL-N513K	0.0811	0.0250	0.0000	0.0000	0.0000	0.0000	0.0000	0.0000	0.0000	0.0000	0.0000
28	L50S-V136A-S188N-DEL-N513K	0.0270	0.0250	0.0000	0.0000	0.0000	0.0000	0.0000	0.0000	0.0000	0.0000	0.0000

29	L50S-V136C-S188N-DEL-N513K	0.0000	0.0000	0.0244	0.0000	0.0000	0.0000	0.0000	0.0000	0.0000	0.0000	0.0000
32	L50S-S188N-A379G-I381V-DEL-N513K	0.0270	0.4250	0.5366	0.4222	0.2632	0.1750	0.0270	0.0294	0.0313	0.0000	0.0213
33	L50S-S188N-A379G-I381V-DEL-S524T	0.0000	0.0000	0.0000	0.0000	0.0000	0.0000	0.0000	0.0000	0.0313	0.0000	0.0000
34	L50S-S188N-A379G-I381V-Y459D-S524T	0.0000	0.0000	0.0000	0.0000	0.0000	0.0000	0.0000	0.0000	0.0000	0.0000	0.0213
35	L50S-V136A-S188N-I381V-DEL-N513K	0.0000	0.0250	0.0000	0.0000	0.0000	0.0000	0.0000	0.0000	0.0000	0.0000	0.0000
37	L50S-V136A-S188N-DEL-S524T	0.0000	0.0000	0.0000	0.0667	0.0263	0.0750	0.0270	0.0000	0.0000	0.0000	0.0000
40	L50S-V136A-I381V-Y461H-S524T	0.0000	0.0000	0.0000	0.0222	0.0526	0.0500	0.0541	0.0294	0.0000	0.0227	0.0000
42	L50S-D134G-V136A-I381V-Y461H	0.0000	0.0250	0.1220	0.2667	0.5000	0.3750	0.3243	0.2059	0.2500	0.0455	0.2340
44	L50S-D134G-V136A-I381V-Y461H-S524T	0.0000	0.0000	0.0244	0.0000	0.0000	0.0000	0.0541	0.0000	0.0313	0.1136	0.1489
45	L50S-V136C-S188N-I381V-Y461H-S524T	0.0000	0.0000	0.0000	0.0000	0.0000	0.0250	0.0270	0.0000	0.1563	0.0455	0.0000
46	L50S-S188N-A379G-I381V-DEL-N513K-S524T	0.0000	0.0000	0.0000	0.0000	0.0263	0.0000	0.0000	0.0000	0.0000	0.0000	0.0000

49	L50S-V136C-S188N-A379G-I381V-DEL-S524T	0.0000	0.0000	0.0000	0.0000	0.0000	0.0000	0.0270	0.0000	0.0625	0.0909	0.1702
50	L50S-V136A-S188N-A379G-I381V-DEL-S524T	0.0000	0.0000	0.0000	0.0000	0.0000	0.0000	0.0000	0.0882	0.0313	0.1136	0.0213
51	L50S-V136A-S188N-A379G-I381V-DEL-N513K-S524T	0.0000	0.0000	0.0000	0.0222	0.0000	0.0000	0.0000	0.0000	0.0000	0.0455	0.0213
Total frequency of haplotypes included in model:		**0.8378**	**0.9750**	**0.9756**	**0.8889**	**0.8947**	**0.7250**	**0.5946**	**0.3529**	**0.5938**	**0.4773**	**0.6383**
CYP51 haplotypes not included in model analysis: missing required EC50 data												
Y459D		0.0541	0.0000	0.0000	0.0000	0.0000	0.0000	0.0000	0.0000	0.0000	0.0000	0.0000
V136C-I381V-Y461H-S524T		0.0000	0.0000	0.0000	0.0000	0.0000	0.0000	0.0270	0.0000	0.0000	0.0682	0.0213
L50S-I381V-S188N-DEL-N513K-CYP↑		0.0000	0.0000	0.0000	0.1111	0.1053	0.2750	0.3514	0.4412	0.3750	0.3182	0.2128
L50S-V136C-S188N-A379G-I381V-Y461H-S524T		0.0000	0.0000	0.0000	0.0000	0.0000	0.0000	0.0000	0.1471	0.0000	0.0000	0.0851
L50S-D134G-V136A-A379G-I381V-DEL-N513K-S524T		0.0000	0.0000	0.0000	0.0000	0.0000	0.0000	0.0000	0.0294	0.0313	0.0909	0.0000
Other CYP51 haplotypes, individually <5% frequency in any year		0.1081	0.0250	0.0244	0.0000	0.0000	0.0000	0.0270	0.0294	0.0000	0.0455	0.0426
TOTAL FREQUENCY:		1.0000	1.0000	1.0000	1.0000	1.0000	1.0000	1.0000	1.0000	1.0000	1.0000	1.0000
n (number of isolates in sample)		37	40	41	45	38	40	37	34	32	44	47

Table 6.B.3: Isolates of each haplotype used to estimate mean EC50 values for each haplotype-azole combination. [a]Epoxiconazole; [b]Prothioconazole; [c]Prochloraz; [d]Tebuconazole.

Isolate strain	CYP51 Haplotype	Haplotype ID	Collection year	Location & Country	EC_{50} (µg/ml)				
					Epoxi[a]	Prothio Desthio	Prothio[b]	Prochl[c]	Tebuco[d]
Bd12	L50S-Y461S	3	2006	Berdun, Aragon, Spain	0.0404		0.314	0.134	1.47
IC6	L50S-Y461S	3	2009	Ireland	0.0814		0.553	0.118	1.28
R2003-6	L50S-Y461S	3	2003	Harpenden, England	0.0401		0.556	0.212	1.68
R2003-51	L50S-Y461H	4	2003	Harpenden, England	0.032		1.25	0.063	1.11
R2003-5	L50S-Y461H	4	2003	Harpenden, England	0.064		0.554	0.077	1.26
CTRL1-01	Y137F-S524T	6	2001	Harpenden, England	0.093		0.0626	0.629	0.736
4362	Y137F-S524T	6	2007	Denmark	0.145		0.298	0.451	1.01
R2003-25	Y137F-S524T	6	2003	Harpenden, England	0.205		0.322	0.682	1.47
R2003-45	Y137F-S524T	6	2003	Harpenden, England	0.0583		0.284	0.49	0.379
R2006-31	Y137F-S524T	6	2006	Harpenden, England	0.0668		0.238	0.433	0.842
ST12/16-2	Y137F-S524T	6	2012	Fielding Manawatu, New Zealand	0.0112	0.0014		0.0446	0.179
ST12/12-1	Y137F-S524T	6	2012	Methven, New Zealand	0.0561	0.00361		0.147	0.492
SAC56.1	L50S-V136A-Y461S	7	2007	Scotland	0.239		1.39	0.103	1
IRE30	L50S-V136A-Y461S	7	2003	Carlow, Ireland	0.36	0.0093		0.742	1.68
R2003-27	L50S-V136A-Y461H	9	2003	Harpenden, England	0.147		4.11	0.261	0.075

R2003-28	L50S-V136A-Y461H	9	2003	Harpenden, England	0.188		1.44	0.351	1.02
R2003-31	L50S-V136A-Y461H	9	2003	Harpenden, England	0.339		16.8	0.822	0.12
R2003-37	L50S-V136A-Y461H	9	2003	Harpenden, England	0.227		8.96	0.381	0.088
R2003-39	L50S-V136A-Y461H	9	2003	Harpenden, England	0.277		6.96	0.677	0.146
R2003-40	L50S-V136A-Y461H	9	2003	Harpenden, England	0.061		2.3	0.2	1.43
R2003-42	L50S-V136A-Y461H	9	2003	Harpenden, England	0.174		5.32	0.366	0.071
R2006-43	L50S-V136A-Y461H	9	2006	Harpenden, England	0.224		15.1	0.581	0.133
SAC15	L50S-V136A-Y461H	9	2011	Scotland	0.024		0.577	0.0651	0.0169
RBay1	L50S-V136A-Y461H	9	2011	Harpenden, England	0.0167	0.00951	0.295	0.155	0.011
RBay9	L50S-V136A-Y461H	9	2011	Harpenden, England	0.0592	0.0149	1.18	0.359	0.032
R2003-36	V136A-S188N-DEL	10	2003	Harpenden, England	0.14		1.32	0.78	0.1
V108-6	V136A-S188N-DEL	10	2007	Kent, England	0.124		1.45	0.212	0.107
V212-2	V136A-S188N-DEL	10	2007	Kent, England	0.121		1.86	0.419	0.064
V308-4	V136A-S188N-DEL	10	2007	Kent, England	0.073		0.876	0.237	0.068
R2003-23	L50S-I381V-Y459D	12	2003	Harpenden, England	0.052		0.988	0.01	1.4
R2003-35	L50S-I381V-Y459D	12	2003	Harpenden, England	0.398		1.17	0.16	3.76
R2010-7	L50S-I381V-Y459D	12	2010	Harpenden, England	0.185		2.24	0.036	2.38
R2010-11	L50S-I381V-Y459D	12	2010	Harpenden, England	0.232		0.853	0.013	3.43

R2010-18	L50S-I381V-Y459D	12	2010	Harpenden, England	0.109		0.603	0.019	2.95
R2010-24	L50S-I381V-Y459D	12	2010	Harpenden, England	0.2		0.639	0.031	3.53
R2010-29	L50S-I381V-Y459D	12	2010	Harpenden, England	0.08		0.51	0.015	2.71
R2010-32	L50S-I381V-Y459D	12	2010	Harpenden, England	0.236		0.355	0.0699	4.12
R2010-39	L50S-I381V-Y459D	12	2010	Harpenden, England	0.105		0.891	0.015	2.08
R2010-40	L50S-I381V-Y459D	12	2010	Harpenden, England	0.108		1.26	0.016	2.9
RProl12	L50S-I381V-Y459D	12	2011	Harpenden, England	0.09	0.00917	0.528	0.0007	1.09
RProl14	L50S-I381V-Y459D	12	2011	Harpenden, England	0.144	0.00941	0.741	0.0296	0.898
R2010-1	L50S-I381V-Y459S	14	2010	Harpenden, England	0.1		0.651	0.0124	2.09
RBay10	L50S-I381V-Y459S	14	2011	Harpenden, England	0.069	0.00642	0.701	0.00054	0.619
R2003-2	L50S-I381V-Y461H	15	2003	Harpenden, England	0.239		1.6	0.052	3.45
R2003-8	L50S-I381V-Y461H	15	2003	Harpenden, England	0.176		1.44	0.041	3.33
R2003-10	L50S-I381V-Y461H	15	2003	Harpenden, England	0.157		1.33	0.023	2.69
R2003-33	L50S-I381V-Y461H	15	2003	Harpenden, England	0.247		2.27	0.052	2.09
R2003-38	L50S-I381V-Y461H	15	2003	Harpenden, England	0.15		3.03	0.024	2.52
R2003-41	L50S-I381V-Y461H	15	2003	Harpenden, England	0.153		3.29	0.066	6.07

R2003-43	L50S-I381V-Y461H	15	2003	Harpenden, England	0.336		4.68	0.065	3.71
R2006-8	L50S-I381V-Y461H	15	2006	Harpenden, England	0.459		3.06	0.23	4.87
R2010-4	L50S-I381V-Y461H	15	2010	Harpenden, England	0.348		4.82	0.0039	4.23
R2010-14	L50S-I381V-Y461H	15	2010	Harpenden, England	0.084		0.708	0.0159	2.15
R2010-15	L50S-I381V-Y461H	15	2010	Harpenden, England	0.171		0.799	0.0232	3.42
R2010-22	L50S-I381V-Y461H	15	2010	Harpenden, England	0.274		2.81	0.043	6.69
R2010-23	L50S-I381V-Y461H	15	2010	Harpenden, England	0.136		1.33	0.032	5.42
R2010-27	L50S-I381V-Y461H	15	2010	Harpenden, England	0.378		1.62	0.052	5.22
R2010-31	L50S-I381V-Y461H	15	2010	Harpenden, England	0.336		5.09	0.1	3.59
ROS75-2(2009)	L50S-I381V-Y461H	15	2009	Rosemaund, England	0.462		4.42	0.43	3.43
ROS75-10(2009)	L50S-I381V-Y461H	15	2009	Rosemaund, England	0.124		2.66	0.0855	3.11
RBay12	L50S-I381V-Y461H	15	2011	Harpenden, England	0.253	0.0272	4.32	0.0363	0.755
RBay14	L50S-I381V-Y461H	15	2011	Harpenden, England	0.148	0.026	2.68	0.0547	1.57
RBay2	L50S-I381V-Y461H	15	2011	Harpenden, England	0.109	0.0163	1.51	0.0322	1.2
RBay6	L50S-I381V-Y461H	15	2011	Harpenden, England	0.232	0.0233	3.91	0.103	1.63
ROpus10	L50S-I381V-Y461H	15	2011	Harpenden, England	0.152	0.0133	1.07	0.0232	1.21

Name	Mutation		Year	Location					
ROpus12	L50S-I381V-Y461H	15	2011	Harpenden, England	0.098	0.0262	1.74	0.0265	1.23
ROpus15	L50S-I381V-Y461H	15	2011	Harpenden, England	0.086	0.0259	1.62	0.103	1.27
RProl2	L50S-I381V-Y461H	15	2011	Harpenden, England	0.104	0.0139	0.865	0.00154	0.905
RProl5	L50S-I381V-Y461H	15	2011	Harpenden, England	0.139	0.0092	1.04	0.00008	1.15
RProl6	L50S-I381V-Y461H	15	2011	Harpenden, England	0.228	0.0375	1.38	0.093	1.61
RProl8	L50S-I381V-Y461H	15	2011	Harpenden, England	0.342	0.0173	2.64	0.0635	1.4
RProl9	L50S-I381V-Y461H	15	2011	Harpenden, England	0.084	0.0096	0.982	0.0133	0.656
RTrac27	L50S-I381V-Y461H	15	2011	Harpenden, England	0.298	0.0255	3.35	0.0252	1.75
RTrac28	L50S-I381V-Y461H	15	2011	Harpenden, England	0.201	0.0258	7.15	0.0575	1.39
RTrac29	L50S-I381V-Y461H	15	2011	Harpenden, England	0.141	0.0102	3.23	0.0155	1.26
RTrac30	L50S-I381V-Y461H	15	2011	Harpenden, England	0.1	0.0094	3.31	0.0006	1.28
RTrac31	L50S-I381V-Y461H	15	2011	Harpenden, England	0.271	0.0089	4.32	0.022	0.958
RTrac35	L50S-I381V-Y461H	15	2011	Harpenden, England	1.15	0.696	15.6		4.26
R2011-23	L50S-I381V-Y461H	15	2011	Harpenden, England	0.0544	0.00897		0.00452	0.741
R2003-34	L50S-S188N-DEL-N513K	20	2003	Harpenden, England	0.062		1.72	0.071	1.01
R2003-44	L50S-S188N-DEL-N513K	20	2003	Harpenden, England	0.073		2.79	0.128	2.26

ID	Mutations	No.	Year	Location					
R2003-46	L50S-S188N-DEL-N513K	20	2003	Harpenden, England	0.035		1.05	0.044	0.735
R2010-52	L50S-S188N-DEL-N513K	20	2010	Harpenden, England	0.181		1.81	0.034	4.85
R2011-28	D134G-V136A-S188N-DEL	22	2011	Harpenden, England	0.0266	0.0186		0.1	0.015
B1-3 (11)	L50S-D134G-V136G-Y461S	24	2012		0.48	0.0176		0.255	0.062
T2	D107V-I381V-N513K-S524T	26	2008	Crotelles, Tours, France	0.309	0.0063	0.462	0.0219	3.58
TAG74-11	D107V-I381V-N513K-S524T	26	2010	England	1.25		19.4	0.203	2.55
R2011-16	D107V-I381V-N513K-S524T	26	2011	Harpenden, England	0.307	0.0376		0.0332	0.646
R2014-31	D107V-I381V-N513K-S524T	26	2014	Harpenden, England	0.0543	0.013		0.0122	0.756
R2003-29	L50S-S188N-I381V-DEL-N513K	27	2003	Harpenden, England	0.364		22.2	0.128	4.1
R2003-54	L50S-S188N-I381V-DEL-N513K	27	2003	Harpenden, England	0.092		1.55	0.025	1.5
RBay15	L50S-S188N-I381V-DEL-N513K	27	2011	Harpenden, England	0.482	0.0282	4.14	0.0495	1.63
ROpus6	L50S-S188N-I381V-DEL-N513K	27	2011	Harpenden, England	0.055	0.0127	0.462	0.0105	0.868
TAG1-18	L50S-S188N-I381V-DEL-N513K	27	2010	England	1.17		18.6	0.382	7.23
TAG74-3	L50S-S188N-I381V-DEL-N513K	27	2010	England	0.997		16.2	0.656	22.5
V18 (09)	L50S-S188N-I381V-DEL-N513K	27	2009	England	0.723		11	0.148	21.3
ROpus7 (10)	L50S-S188N-I381V-DEL-N513K	27	2010	Harpenden, England	0.917	0.11	16.6	0.253	5.13

RProl13	L50S-S188N-I381V-DEL-N513K	27	2011	Harpenden, England	1.39	0.119	10.8	0.0843	7.16
ROS13-126-3	L50S-S188N-I381V-DEL-N513K	27	2010	Rosemaund, England	1.04		17.7	0.258	11.8
V43	L50S-S188N-I381V-DEL-N513K	27	2009	England	0.914		13.7	1.02	31.2
011226 (LA12)	L50S-S188N-I381V-DEL-N513K	27	2012	England	1.05	0.0935		0.133	18.9
105-9 (VL12)	L50S-S188N-I381V-DEL-N513K	27	2012	England	1.27	0.169		0.331	26.1
115-5 (VL12)	L50S-S188N-I381V-DEL-N513K	27	2012	England	2.38	0.229		0.526	30.5
34-07(FA12)	L50S-S188N-I381V-DEL-N513K	27	2012	Rosemaund, England	0.874	0.0749		0.206	7.51
60-02(FA12)	L50S-S188N-I381V-DEL-N513K	27	2012	Rosemaund, England	0.607	0.0779		0.104	10.7
61-04(FA12)	L50S-S188N-I381V-DEL-N513K	27	2012	Rosemaund, England	0.705	0.0518		0.136	9.82
R12-03	L50S-S188N-I381V-DEL-N513K	27	2012	Harpenden, England	0.788	0.0915		0.284	19
ROS18-1 (11)	L50S-S188N-I381V-DEL-N513K	27	2011	Rosemaund, England	0.621	0.133		0.106	11.7
210-6 (LV12)	L50S-S188N-I381V-DEL-N513K	27	2012	England	2	0.287		0.354	35
A2 (V12)	L50S-S188N-I381V-DEL-N513K	27	2012	England	0.526	0.111		0.0925	13.8
118-7 (FN12)	L50S-S188N-I381V-DEL-N513K	27	2012	Sutton Scotney, England	1.28	0.159		0.204	20.8
87-10	L50S-S188N-I381V-DEL-N513K	27	2012	England	2.02	0.0846		0.15	11.1
BC11	L50S-V136A-S188N-DEL-N513K	28	2009	England	0.208		3.59	0.602	0.123

SAC1-35 (10)	L50S-V136A-S188N-DEL-N513K	28	2010	Scotland	0.18	0.0076	9.06	0.857	0.239
SAC73-16	L50S-V136A-S188N-DEL-N513K	28	2010	Scotland	0.171		1.9	0.136	0.139
RPro10	L50S-V136A-S188N-DEL-N513K	28	2011	Harpenden, England	0.084	0.0235	1.66	0.136	0.0331
RTrac32	L50S-V136A-S188N-DEL-N513K	28	2011	Harpenden, England	0.138	0.0174	3.89	0.253	0.0349
RBay13 (10)	L50S-V136C-S188N-DEL-N513K	29	2010	Harpenden, England	0.251	0.0106	3.93	0.327	0.968
RTrac26	L50S-V136C-S188N-DEL-N513K	29	2011	Harpenden, England	0.196	0.0204	1.9	0.296	0.689
R2011-20	L50S-V136C-S188N-DEL-N513K	29	2011	Harpenden, England	0.0939	0.0136		0.0369	0.553
R2003-14	L50S-S188N-A379G-I381V-DEL-N513K	32	2003	Harpenden, England	0.156		2.36	0.001	4.35
V201-1	L50S-S188N-A379G-I381V-DEL-N513K	32	2007	Kent, England	0.385		2.75	0.026	3.38
R2010-5	L50S-S188N-A379G-I381V-DEL-N513K	32	2010	Harpenden, England	1.29		2.66	0.026	21.7
R2010-6	L50S-S188N-A379G-I381V-DEL-N513K	32	2010	Harpenden, England	0.292		7.43	0.045	14.6
R2010-8	L50S-S188N-A379G-I381V-DEL-N513K	32	2010	Harpenden, England	0.21		0.961	0.0036	7.12
R2010-19	L50S-S188N-A379G-I381V-DEL-N513K	32	2010	Harpenden, England	0.736		2.16	0.013	15.2
R2010-21	L50S-S188N-A379G-I381V-DEL-N513K	32	2010	Harpenden, England	0.181		0.752	0.0014	5.83
R2010-26	L50S-S188N-A379G-I381V-DEL-N513K	32	2010	Harpenden, England	0.218		0.906	0.0015	6.45
R2010-28	L50S-S188N-A379G-I381V-DEL-N513K	32	2010	Harpenden, England	0.327		1.62	0.0058	7.69

R2010-30	L50S-S188N-A379G-I381V-DEL-N513K	32	2010	Harpenden, England	0.983		3.08	0.011	17.6
R2010-33	L50S-S188N-A379G-I381V-DEL-N513K	32	2010	Harpenden, England	0.613		5.59	0.0113	10.9
R2010-36	L50S-S188N-A379G-I381V-DEL-N513K	32	2010	Harpenden, England	0.329		0.809	0.001	8.29
R2010-37	L50S-S188N-A379G-I381V-DEL-N513K	32	2010	Harpenden, England	0.348		2.6	0.0036	8.75
R2010-38	L50S-S188N-A379G-I381V-DEL-N513K	32	2010	Harpenden, England	0.465		3.93	0.0061	12.5
SAC45-37(2009)	L50S-S188N-A379G-I381V-DEL-N513K	32	2009	Scotland	0.224		1.08	0.0094	2.72
ROS69-16(2009)	L50S-S188N-A379G-I381V-DEL-N513K	32	2009	Rosemaund, England	0.394		3.84	0.031	3.94
SAC17	L50S-S188N-A379G-I381V-DEL-N513K	32	2011	Scotland	0.861		2.57	0.0019	7.31
TAG74-10	L50S-S188N-A379G-I381V-DEL-N513K	32	2010	England	1.22		18.6	0.0621	10
TAG74-6	L50S-S188N-A379G-I381V-DEL-N513K	32	2010	England	1.46		19.5	0.0812	17.1
RBay11	L50S-S188N-A379G-I381V-DEL-N513K	32	2011	Harpenden, England	0.197	0.016	2.17	0.000246	2.79
RBay4	L50S-S188N-A379G-I381V-DEL-N513K	32	2011	Harpenden, England	0.215	0.0284	2.34	0.00115	3.27
ROpus1	L50S-S188N-A379G-I381V-DEL-N513K	32	2011	Harpenden, England	0.425	0.027	0.804	0.00333	2.13
ROpus2	L50S-S188N-A379G-I381V-DEL-N513K	32	2011	Harpenden, England	0.563	0.0204	3.87	0.0303	3.38
ROpus4	L50S-S188N-A379G-I381V-DEL-N513K	32	2011	Harpenden, England	0.315	0.0192	0.832	0.00134	2.68
ROpus5	L50S-S188N-A379G-I381V-DEL-N513K	32	2011	Harpenden, England	0.11	0.0263	0.95	0.00215	2.79

ROpus8	L50S-S188N-A379G-I381V-DEL-N513K	32	2011	Harpenden, England	0.16	0.0273	1.19	0.000377	2.54
ROpus9	L50S-S188N-A379G-I381V-DEL-N513K	32	2011	Harpenden, England	0.462	0.0195	1.66	0.0048	2.18
ROpus13	L50S-S188N-A379G-I381V-DEL-N513K	32	2011	Harpenden, England	0.259	0.0402	2.94	0.0129	2.68
ROpus16	L50S-S188N-A379G-I381V-DEL-N513K	32	2011	Harpenden, England	0.526	0.0327	3.66	0.00077	3.11
RProl1	L50S-S188N-A379G-I381V-DEL-N513K	32	2011	Harpenden, England	0.243	0.0331	0.9	0.00064	2.81
RProl3	L50S-S188N-A379G-I381V-DEL-N513K	32	2011	Harpenden, England	0.208	0.0153	1.19	0.00153	2.09
RProl11	L50S-S188N-A379G-I381V-DEL-N513K	32	2011	Harpenden, England	0.241	0.0165	1.19	0.000409	1.78
RTrac21	L50S-S188N-A379G-I381V-DEL-N513K	32	2011	Harpenden, England	0.166	0.0126	4.29	0.00275	1.88
RTrac22	L50S-S188N-A379G-I381V-DEL-N513K	32	2011	Harpenden, England	0.479	0.018	6.16	0.00249	1.75
RTrac23	L50S-S188N-A379G-I381V-DEL-N513K	32	2011	Harpenden, England	0.874	0.0288	2.76	0.0398	2.72
RTrac33	L50S-S188N-A379G-I381V-DEL-N513K	32	2011	Harpenden, England	0.347	0.015	1.98	0.0019	2.5
B11-1 (11)	L50S-S188N-A379G-I381V-DEL-N513K	32	2011	England	0.149	0.0275		0.00129	3.45
B13-6 (11)	L50S-S188N-A379G-I381V-DEL-N513K	32	2011	England	0.123	0.00875		0.00022	3.16
B31-2 (11)	L50S-S188N-A379G-I381V-DEL-N513K	32	2011	England	0.0265	0.0169		0.000243	2.79
B31-6 (11)	L50S-S188N-A379G-I381V-DEL-N513K	32	2011	England	0.0973	0.0185		0.00296	3.73
B36-3 (11)	L50S-S188N-A379G-I381V-DEL-N513K	32	2011	England	0.708	0.123		0.386	0.908

B36-9 (11)	L50S-S188N-A379G-I381V-DEL-N513K	32	2011	England	0.238	0.0148		0.00199	3.72
SAC16-36 (11)	L50S-S188N-A379G-I381V-DEL-N513K	32	2011	England	0.426	0.0239		0.0499	6.53
TAG48 (11)	L50S-S188N-A379G-I381V-DEL-N513K	32	2011	England	0.436	0.027		0.019	3.5
ROS49-11(11)	L50S-S188N-A379G-I381V-DEL-N513K	32	2011	Rosemaund, England	1.52	0.146		0.0756	17.3
B1-5 (11)	L50S-S188N-A379G-I381V-DEL-N513K	32	2011	England	0.128	0.00929		0.00187	3.4
B5-1 (11)	L50S-S188N-A379G-I381V-DEL-N513K	32	2011	England	0.0833	0.0062		0.00422	2.6
60-7 (FA12)	L50S-S188N-A379G-I381V-DEL-N513K	32	2012	Rosemaund, England	0.129	0.0115		0.00097	4.47
TAG1-35	L50S-S188N-A379G-I381V-DEL-S524T	33	2010	England	1.31		21.6	0.0542	19.6
ROS13-150-1	L50S-S188N-A379G-I381V-Y459D-S524T	34	2010	Rosemaund, England	1.61	0.189	19	0.0569	15
R2010-53	L50S-V136A-S188N-I381V-DEL-N513K	35	2010	Harpenden, England	0.778		20.4	0.969	0.391
V10	L50S-V136A-S188N-DEL-S524T	37	2009	England	0.551		5.93	1.9	0.391
V12	L50S-V136A-S188N-DEL-S524T	37	2009	England	0.377		4.21	1.21	1.18
TAG1-16	L50S-V136A-S188N-DEL-S524T	37	2010	England	0.424		18.4	0.747	0.311
RBay7	L50S-V136A-S188N-DEL-S524T	37	2011	Harpenden, England	0.624	0.0988	17.4	0.56	0.166
RTrac25	L50S-V136A-S188N-DEL-S524T	37	2011	Harpenden, England	0.374	0.0667	14.4	0.383	0.0667
ROS33-11 (11)	L50S-V136A-S188N-DEL-S524T	37	2011	Rosemaund, England	0.55	0.101		1.32	0.368

TAG1-9 (10)	L50S-V136A-I381V-Y461H-S524T	40	2010	England	1.47	0.299	19.1	0.71	1.02
ROS41-42 (11)	L50S-V136A-I381V-Y461H-S524T	40	2011	Rosemaund, England	1.59	0.192		0.178	0.87
ROS65-06(11)	L50S-V136A-I381V-Y461H-S524T	40	2011	Rosemaund, England	1.68	0.285		0.553	0.824
ROS53-18 (11)	L50S-V136A-I381V-Y461H-S524T	40	2011	Rosemaund, England	1.35	0.239		0.163	0.397
29-6 (FN12)	L50S-V136A-I381V-Y461H-S524T	40	2012	Sutton Scotney, England	1.63	0.103		0.132	5.47
34-10 (FA12)	L50S-V136A-I381V-Y461H-S524T	40	2012	Rosemaund, England	1.54	0.272		0.219	0.476
B12 (V12)	L50S-V136A-I381V-Y461H-S524T	40	2012	England	1.38	0.373		0.253	0.788
4418	L50S-D134G-V136A-I381V-Y461H	42	2007	UK	0.603		8.21	0.257	0.492
R2010-9	L50S-D134G-V136A-I381V-Y461H	42	2010	Harpenden, England	0.91		9.89	0.263	1.13
BAY2	L50S-D134G-V136A-I381V-Y461H	42	2010	England	1.17	0.132	23.1	0.581	0.819
BAY6	L50S-D134G-V136A-I381V-Y461H	42	2010	England	0.611		28.6	0.571	0.467
ROS9-142-3	L50S-D134G-V136A-I381V-Y461H	42	2010	Rosemaund, England	1.26		20.1	0.132	0.544
TAG74-17	L50S-D134G-V136A-I381V-Y461H	42	2010	England	0.902		19.3	0.584	0.858
RBay16	L50S-D134G-V136A-I381V-Y461H	42	2011	Harpenden, England	1.36	0.206	18.4	0.417	0.326
ROpus11	L50S-D134G-V136A-I381V-Y461H	42	2011	Harpenden, England	0.0847	0.0852	21.8	0.0907	0.226
RProl4	L50S-D134G-V136A-I381V-Y461H	42	2011	Harpenden, England	0.397	0.0828	10.8	0.193	0.181

RProl7	L50S-D134G-V136A-I381V-Y461H	42	2011	Harpenden, England	0.269	0.202	9.17	0.158	0.176
RProl15	L50S-D134G-V136A-I381V-Y461H	42	2011	Harpenden, England	0.586	0.118	7.09	0.193	0.287
RTrac24	L50S-D134G-V136A-I381V-Y461H	42	2011	Harpenden, England	0.185	0.0751	7.18	0.0211	0.112
R2011-1	L50S-D134G-V136A-I381V-Y461H	42	2011	Harpenden, England	0.36	0.147		0.1	0.116
R2011-3	L50S-D134G-V136A-I381V-Y461H	42	2011	Harpenden, England	0.319	0.141		0.0658	0.0404
R2011-6	L50S-D134G-V136A-I381V-Y461H	42	2011	Harpenden, England	0.286	0.0994		0.0508	0.0726
R2011-37	L50S-D134G-V136A-I381V-Y461H	42	2011	Harpenden, England	0.322	0.184		0.0503	0.115
R2011-46	L50S-D134G-V136A-I381V-Y461H	42	2011	Harpenden, England	0.467	0.143		0.0476	0.164
B11-4 (11)	L50S-D134G-V136A-I381V-Y461H	42	2011	England	0.261	0.123		0.115	0.229
B11-6 (11)	L50S-D134G-V136A-I381V-Y461H	42	2011	England	0.266	0.125		0.05	0.194
B11-7 (11)	L50S-D134G-V136A-I381V-Y461H	42	2011	England	0.475	0.164		0.142	0.346
B11-8 (11)	L50S-D134G-V136A-I381V-Y461H	42	2011	England	0.373	0.11		0.0603	0.242
B23-3 (11)	L50S-D134G-V136A-I381V-Y461H	42	2011	England	0.332	0.21		0.113	0.301
B23-5 (11)	L50S-D134G-V136A-I381V-Y461H	42	2011	England	0.334	0.0876		0.111	0.247
B31-8 (11)	L50S-D134G-V136A-I381V-Y461H	42	2011	England	0.277	0.17		0.0687	0.205
TAG33 (11)	L50S-D134G-V136A-I381V-Y461H	42	2011	England	0.97	0.29		0.243	0.56

ROS50(11)	L50S-D134G-V136A-I381V-Y461H	42	2011	Rosemaund, England	0.622	0.152	0.206	0.433
SAC7(11)	L50S-D134G-V136A-I381V-Y461H	42	2011	Scotland	0.942	0.222	0.466	0.486
ROSU37 (11)	L50S-D134G-V136A-I381V-Y461H	42	2011	Rosemaund, England	0.947		0.216	0.375
B1-1(11)	L50S-D134G-V136A-I381V-Y461H	42	2011	England	0.633	0.119	0.125	0.486
B1-2 (11)	L50S-D134G-V136A-I381V-Y461H	42	2011	England	0.545	0.0941	0.105	0.293
B5-3 (11)	L50S-D134G-V136A-I381V-Y461H	42	2011	England	0.588	0.0956	0.117	0.332
B5-5 (11)	L50S-D134G-V136A-I381V-Y461H	42	2011	England	0.519	0.114	0.132	0.327
61-9 (FA12)	L50S-D134G-V136A-I381V-Y461H	42	2012	Rosemaund, England	0.411	0.131	0.101	0.338
75-8 (FN12)	L50S-D134G-V136A-I381V-Y461H	42	2012	Sutton Scotney, England	0.411	0.133	0.136	0.483
B1 (V12)	L50S-D134G-V136A-I381V-Y461H	42	2012	England	0.744	0.139	0.163	0.562
R2011-43	L50S-D134G-V136A-I381V-Y461H-S524T	44	2011	Harpenden, England	2.2	0.271	0.212	0.363
118-5 (FN12)	L50S-D134G-V136A-I381V-Y461H-S524T	44	2012	Sutton Scotney, England	1.66	0.479	0.515	1.06
87-7 (FA12)	L50S-D134G-V136A-I381V-Y461H-S524T	44	2012	Rosemaund, England	4.14	0.539	0.271	0.695
89-1 (FA12)	L50S-D134G-V136A-I381V-Y461H-S524T	44	2012	Rosemaund, England	2.21	0.423	0.223	0.971
75-10 (FN12)	L50S-D134G-V136A-I381V-Y461H-S524T	44	2012	Sutton Scotney, England	1.83	0.512	0.288	0.736
96-4 (FN12)	L50S-D134G-V136A-I381V-Y461H-S524T	44	2012	Sutton Scotney, England	1.91	0.575	0.285	0.92

ID	Mutations		Year	Location				
19-2 (FN12)	L50S-V136C-S188N-I381V-Y461H-S524T	45	2012	Sutton Scotney, England	2.51	0.147	0.12	4.72
16-10 (FN12)	L50S-V136C-S188N-I381V-Y461H-S524T	45	2012	Sutton Scotney, England	2.18	0.103	0.138	4.68
29-6 (FN12)	L50S-V136C-S188N-I381V-Y461H-S524T	45	2012	Sutton Scotney, England	1.63	0.103	0.132	5.47
R2014-5	L50S-V136C-S188N-I381V-Y461H-S524T	45	2014	Harpenden, England	0.634	0.0448	0.0529	3.08
TAG10(11)	L50S-S188N-A379G-I381V-DEL-N513K-S524T	46	2011	England	1.37	0.113	0.074	5.55
44-15 (BR12)	L50S-V136C-S188N-A379G-I381V-DEL-S524T	49	2012	Harpenden, England	6.32	0.263	0.0498	14.1
87-6 (FA12)	L50S-V136C-S188N-A379G-I381V-DEL-S524T	49	2012	Rosemaund, England	2.73	0.137	0.0484	15.4
B23 (V12)	L50S-V136C-S188N-A379G-I381V-DEL-S524T	49	2012	England	2.78	0.209	0.035	11.8
T560.11	L50S-V136C-S188N-A379G-I381V-DEL-S524T	49	2012		5.26	0.294	0.0818	28.4
ROS33-21 (11)	L50S-V136A-S188N-A379G-I381V-DEL-S524T	50	2011	Rosemaund, England	5.1	0.791	0.31	1.79
34-1 (FA12)	L50S-V136A-S188N-A379G-I381V-DEL-S524T	50	2012	Rosemaund, England	1.63	0.339	0.138	1.1
50-3 (FN12)	L50S-V136A-S188N-A379G-I381V-DEL-S524T	50	2012	Sutton Scotney, England	1.56	0.314	0.0466	0.645

340

B22 (V12)	L50S-V136A-S188N-A379G-I381V-DEL-S524T	50	2012	England	1.58	0.387	0.0592	1.23
105-3 (LV12)	L50S-V136A-S188N-A379G-I381V-DEL-S524T	50	2012	England	1.9	0.67	0.133	1.44
44-19 (BR12)	L50S-V136A-S188N-A379G-I381V-DEL-S524T	50	2012	Harpenden, England	5.47	0.983	0.484	2.7
306-7 (LV12)	L50S-V136A-S188N-A379G-I381V-DEL-N513K-S524T	51	2012	England	4.02	1.09	0.142	1.8
A1 (V12)	L50S-V136A-S188N-A379G-I381V-DEL-N513K-S524T	51	2012	England	1.87	0.521	0.0969	1.34
A3 (V12)	L50S-V136A-S188N-A379G-I381V-DEL-N513K-S524T	51	2012	England	2.7	0.933	0.158	1.73
A13 (V12)	L50S-V136A-S188N-A379G-I381V-DEL-N513K-S524T	51	2012	England	2.03	0.92	0.105	1.54

Table 6.B.4: Relative haplotype frequencies and dose response parameters B_{ij} used in modelling scenarios, and the mean EC_{50} values for each haplotype used to derive the field dose $D_{ij_{50}}$ and dose response parameters. [a]Epoxiconazole; [b]Prothioconazole; [c]Prochloraz; [d]Tebuconazole. [e]Prothio-desthio EC_{50} estimated from prothioconazole EC_{50} for haplotypes for which there was no data for prothio-desthio (highlighted in red text). [f]Prothioconazole $D_{ij_{50}}$ estimated from prothio-desthio EC_{50}.

Haplotype ID	Frequencies used in modelling - year scenarios										
	2003	2010	2011	2012	2013	2014	2015	2016	2017	2018	2019
3	0.03571	0	0	0	0	0	0	0	0	0	0
4	0.05952	0	0	0	0	0	0	0	0	0	0
6	0.05952	0	0	0	0	0	0	0	0	0	0
7	0	0	0.02083	0	0	0	0.03158	0	0	0	0
9	0.2619	0	0	0.02	0.0297	0	0	0	0	0	0
10	0.03571	0	0	0	0	0	0	0	0	0	0
12	0.05952	0.19802	0	0	0	0	0	0	0	0	0
14	0	0.0297	0	0	0	0	0	0	0	0	0
15	0.22619	0.19802	0.20833	0.07	0	0	0	0	0	0	0
20	0.09524	0.0297	0	0	0	0	0	0	0	0	0
22	0	0	0.02083	0	0	0	0	0	0	0	0
24	0	0	0	0	0	0	0.03158	0	0	0	0
26	0	0	0.02083	0	0	0.02913	0	0	0	0	0
27	0.09524	0.0297	0	0.11	0.10891	0.27184	0.36842	0.55	0.39175	0.4	0.25
28	0.03571	0.0297	0	0	0	0	0	0	0	0	0
29	0	0	0.02083	0	0	0	0	0	0	0	0
32	0.03571	0.42574	0.5625	0.42	0.25743	0.17476	0.03158	0.0375	0.03093	0	0.02381
33	0	0	0	0	0	0	0	0	0.03093	0	0
34	0	0	0	0	0	0	0	0	0	0	0.02381

35	0	0.0297	0	0	0	0	0	0	0	0	0
37	0	0	0	0.07	0.0297	0.07767	0.03158	0	0	0	0
40	0	0	0	0.02	0.0495	0.04854	0.05263	0.0375	0	0.025	0
42	0	0.0297	0.125	0.27	0.49505	0.36893	0.33684	0.2625	0.25773	0.0625	0.27381
44	0	0	0.02083	0	0	0	0.05263	0	0.03093	0.1375	0.17857
45	0	0	0	0	0	0.02913	0.03158	0	0.16495	0.0625	0
46	0	0	0	0	0.0297	0	0	0	0	0	0
49	0	0	0	0	0	0	0.03158	0	0.06186	0.1125	0.20238
50	0	0	0	0	0	0	0	0.1125	0.03093	0.1375	0.02381
51	0	0	0	0.02	0	0	0	0	0	0.0625	0.02381

Haplotype ID	Mean EC$_{50}$ (µg/ml)				No. of isolates included in EC$_{50}$ mean value					
	Epoxi[a]	Prothio Desthio[e]	Prochl[c]	Tebuco[d]	Total	Epoxi[a]	Prothio Desthio[e]	Prothio[b]	Prochl[c]	Tebuco[d]
3	0.054	0.007	0.155	1.477	3	3	0	3	3	3
4	0.048	0.012	0.070	1.185	2	2	0	2	2	2
6	0.091	0.003	0.411	0.730	7	7	2	5	7	7
7	0.184	0.019	0.515	0.136	2	2	0	2	2	2
9	0.158	0.012	0.383	0.286	11	11	2	11	11	11
10	0.115	0.016	0.412	0.085	4	4	0	4	4	4
12	0.162	0.009	0.035	2.604	12	12	2	12	12	12
14	0.085	0.006	0.006	1.355	2	2	1	2	2	2
15	0.234	0.054	0.058	2.562	36	36	19	35	35	36
20	0.088	0.020	0.069	2.214	4	4	0	4	4	4
22	0.027	0.019	0.100	0.015	1	1	1	0	1	1
24	0.480	0.018	0.255	0.062	1	1	1	0	1	1

343

26	0.480	0.019	0.068	1.883	4	4	3	2	4	4
27	0.968	0.115	0.245	14.319	23	23	16	11	23	23
28	0.156	0.016	0.397	0.114	5	5	3	5	5	5
29	0.180	0.015	0.220	0.737	3	3	3	2	3	3
32	0.428	0.029	0.021	5.918	48	48	29	36	48	48
33	1.310	0.115	0.054	19.600	1	1	0	1	1	1
34	1.610	0.189	0.057	15.000	1	1	1	1	1	1
35	0.778	0.110	0.969	0.391	1	1	0	1	1	1
37	0.483	0.089	1.020	0.414	6	6	3	5	6	6
40	1.520	0.252	0.315	1.406	7	7	7	1	7	7
42	0.564	0.141	0.184	0.359	35	35	29	12	35	35
44	2.325	0.467	0.299	0.791	6	6	6	0	6	6
45	1.739	0.099	0.111	4.488	4	4	4	0	4	4
46	1.370	0.113	0.074	5.550	1	1	1	0	1	1
49	4.273	0.226	0.054	17.425	4	4	4	0	4	4
50	2.873	0.581	0.195	1.484	6	6	6	0	6	6
51	2.655	0.866	0.125	1.603	4	4	4	0	4	4

Haplotype ID	B_{ij}				$D_{ij_{50}}$			
	Epoxi[a]	Prothio[b]	Prochl[c]	Tebuco[d]	Epoxi[a]	Prothio[b,f]	Prochl[c]	Tebuco[d]
3	2.036	2.929	1.464	0.723	0.395	0.272	0.549	1.112
4	2.112	2.762	1.877	0.775	0.381	0.325	0.428	1.038
6	1.730	3.145	1.079	0.901	0.465	0.180	0.745	0.892
7	1.388	2.520	1.006	1.525	0.579	0.390	0.799	0.527
9	1.455	2.748	1.102	1.209	0.552	0.329	0.729	0.665
10	1.609	2.619	1.078	1.768	0.500	0.364	0.746	0.455

12	1.445	2.856	2.339	0.605	0.556	0.296	0.344	1.327
14	1.769	2.972	3.952	0.743	0.454	0.257	0.203	1.082
15	1.287	1.775	1.995	0.609	0.625	0.580	0.403	1.321
20	1.748	2.503	1.883	0.637	0.460	0.394	0.427	1.262
22	2.540	2.536	1.678	3.038	0.316	0.386	0.479	0.265
24	1.028	2.567	1.252	1.949	0.782	0.378	0.642	0.412
26	1.028	2.525	1.897	0.670	0.782	0.389	0.424	1.199
27	0.825	1.178	1.268	0.355	0.974	0.771	0.634	2.262
28	1.460	2.613	1.091	1.612	0.551	0.366	0.737	0.499
29	1.396	2.655	1.312	0.899	0.576	0.354	0.613	0.894
32	1.065	2.264	2.748	0.468	0.755	0.455	0.293	1.716
33	0.751	1.178	2.033	0.322	1.071	0.771	0.395	2.496
34	0.704	0.832	2.002	0.350	1.142	0.934	0.401	2.296
35	0.884	1.208	0.825	1.096	0.910	0.759	0.974	0.734
37	1.025	1.375	0.812	1.076	0.784	0.700	0.990	0.747
40	0.717	0.666	1.172	0.734	1.122	1.042	0.686	1.095
42	0.977	1.025	1.387	1.125	0.823	0.835	0.580	0.714
44	0.627	0.397	1.192	0.879	1.281	1.318	0.675	0.914
45	0.687	1.286	1.626	0.511	1.170	0.731	0.494	1.574
46	0.740	1.188	1.844	0.478	1.086	0.767	0.436	1.682
49	0.519	0.726	2.038	0.334	1.550	0.999	0.394	2.406
50	0.587	0.327	1.362	0.722	1.369	1.432	0.590	1.113
51	0.602	0.227	1.563	0.705	1.336	1.668	0.514	1.140

Appendix 6.C: Lande's model of the effect of genetic variance on the rate of selection

Lande (1975, 1976, 1979) developed a model for the selection of a phenotypic character of individuals of a population that is under the control of a large number of genes. This model can also apply to a character, *Z*, that is the result of a large number of changes in one gene, as is the case for azole resistance. The model shows that the change in the numerical value of the character, ΔZ, over one generation is the product of the genetic variance, *G*, and the selection gradient, ∇r:

$$\Delta Z = G \nabla r \qquad (6.C.1)$$

For the case described here, *Z* is the average ED_{50} of the pathogen population to an azole fungicide, which changes over time due to selection through application of the azole. ∇r, the selection gradient, is the change in the average population growth rate caused by a change in the ED_{50} of the population.

Although Lande's model can be applied to the evolution of azole resistance, it does not explicitly account for the effects of dose decay on differences in haplotype growth rates over time. The population genetic model that we have introduced here models dose decay explicitly, giving greater flexibility to model a wide range of azole programmes. However, in combination with Fisher's (1930) classic text, Lande's model provides a useful insight of the role of genetic variance in driving the rate of selection.

References

Fisher, R.A. (1930). The genetical theory of natural selection. Clarendon Press. https://doi.org/10.5962/bhl.title.27468

Lande, R. (1975). The maintenance of genetic variability by mutation in a polygenic character with linked loci. *Genetic Research* 26: 221-235.

Lande, R. (1976). Natural selection and random genetic drift in phenotypic evolution. *Evolution* 30: 314-334.

Lande, R. (1979). Quantitative genetic analysis of a multivariate evolution, applied to brain: body size allometry. *Evolution* 33: 402-416.

Appendix 6.D: Further details on model results

Table 6.D.1: Model results and generalized linear model inputs for each combination of solo or mixture application scenario and starting haplotype composition scenario.

Year	Fungicide programme	Number of azoles	$\Delta\bar{r}$	$S(T)$	cc_w	cc_u	cc_z	$\bar{f}_{\text{start}}$	$\text{Var}_{j_{\text{Max}}}$ (t^{-2})
2003	Epoxiconazole	1	0.0421	0.0349	1.0000	1.0000	1.0000	0.5850	0.0040
2003	Prochloraz	1	0.0467	0.0329	1.0000	1.0000	1.0000	0.5994	0.0059
2003	Prothioconazole	1	0.0975	0.0197	1.0000	1.0000	1.0000	0.6923	0.0036
2003	Tebuconazole	1	0.0488	0.0681	1.0000	1.0000	1.0000	0.4388	0.0128
2003	EpoxiProchlMix	2	0.0253	0.0325	-0.0086	-0.0766	-0.2909	0.5976	0.0059
2003	EpoxiProthioMix	2	0.0706	0.0253	0.8909	0.8693	0.6545	0.6477	0.0040
2003	EpoxiTebucoMix	2	0.0462	0.0462	0.7522	0.7331	0.5545	0.5262	0.0128
2003	ProchlTebucoMix	2	0.0383	0.0416	-0.5027	-0.5407	-0.7727	0.5453	0.0128
2003	ProthioProchlMix	2	0.0771	0.0232	-0.1874	-0.0397	-0.2818	0.6594	0.0059
2003	ProthioTebucoMix	2	0.0186	0.0322	0.8375	0.7508	0.4455	0.6045	0.0128
2003	EpoxiProchlTebucoMix	3	0.0227	0.0387	0.0803	0.0386	-0.1697	0.5610	0.0128
2003	EpoxiProthioProchlMix	3	0.0389	0.0262	0.2316	0.2510	0.0273	0.6383	0.0059
2003	EpoxiProthioTebucoMix	3	0.0650	0.0328	0.8269	0.7844	0.5515	0.5994	0.0128
2003	ProthioProchlTebucoMix	3	0.0399	0.0304	0.0492	0.0568	-0.2030	0.6108	0.0128
2003	FourWayMix	4	0.0400	0.0313	0.2970	0.2827	0.0515	0.6051	0.0128
2010	Epoxiconazole	1	0.0169	0.0416	1.0000	1.0000	1.0000	0.5456	0.0044
2010	Prochloraz	1	0.1379	0.0203	1.0000	1.0000	1.0000	0.6887	0.0107
2010	Prothioconazole	1	0.0853	0.0209	1.0000	1.0000	1.0000	0.6809	0.0081
2010	Tebuconazole	1	0.0140	0.0864	1.0000	1.0000	1.0000	0.3670	0.0112
2010	EpoxiProchlMix	2	0.0533	0.0269	0.2538	0.5871	0.5167	0.6346	0.0107
2010	EpoxiProthioMix	2	0.0408	0.0280	0.6094	0.8632	0.8667	0.6268	0.0081
2010	EpoxiTebucoMix	2	0.0134	0.0571	0.4694	0.3027	0.2833	0.4730	0.0112
2010	ProchlTebucoMix	2	0.0925	0.0334	-0.5644	-0.3694	-0.4167	0.5913	0.0112

Year	Treatment	N							
2010	ProthioProchlMix	2	0.0263	0.0201	0.6557	0.6017	0.5500	0.6869	0.0107
2010	ProthioTebucoMix	2	0.0266	0.0353	-0.1559	0.0302	0.0500	0.5808	0.0112
2010	EpoxiProchlTebucoMix	3	0.0186	0.0355	0.0529	0.1735	0.1278	0.5784	0.0112
2010	EpoxiProthioProchlMix	3	0.0586	0.0244	0.5063	0.6840	0.6444	0.6524	0.0107
2010	EpoxiProthioTebucoMix	3	0.0202	0.0370	0.3077	0.3987	0.4000	0.5702	0.0112
2010	ProthioProchlTebucoMix	3	0.0396	0.0278	-0.0215	0.0875	0.0611	0.6276	0.0112
2010	FourWayMix	4	0.0303	0.0303	0.2113	0.3359	0.3083	0.6109	0.0112
2011	Epoxiconazole	1	0.0137	0.0452	1.0000	1.0000	1.0000	0.5269	0.0079
2011	Prochloraz	1	0.0927	0.0207	1.0000	1.0000	1.0000	0.6841	0.0049
2011	Prothioconazole	1	0.2016	0.0256	1.0000	1.0000	1.0000	0.6525	0.0213
2011	Tebuconazole	1	0.0218	0.0837	1.0000	1.0000	1.0000	0.3806	0.0167
2011	EpoxiProchlMix	2	0.0391	0.0281	0.0718	0.1693	0.0000	0.6259	0.0079
2011	EpoxiProthioMix	2	0.0792	0.0320	0.6909	0.8661	0.8095	0.6030	0.0213
2011	EpoxiTebucoMix	2	0.0108	0.0587	0.1308	0.3403	0.4286	0.4669	0.0167
2011	ProchlTebucoMix	2	0.1062	0.0328	-0.9262	-0.6690	-0.6667	0.5937	0.0167
2011	ProthioProchlMix	2	0.0248	0.0223	0.5964	0.3449	0.0238	0.6713	0.0213
2011	ProthioTebucoMix	2	0.0138	0.0378	-0.4874	-0.0400	0.3095	0.5663	0.0213
2011	EpoxiProchlTebucoMix	3	0.0096	0.0360	-0.2412	-0.0531	-0.0794	0.5747	0.0167
2011	EpoxiProthioProchlMix	3	0.0698	0.0267	0.4530	0.4601	0.2778	0.6366	0.0213
2011	EpoxiProthioTebucoMix	3	0.0192	0.0399	0.1114	0.3888	0.5159	0.5545	0.0213
2011	ProthioProchlTebucoMix	3	0.0372	0.0292	-0.2724	-0.1213	-0.1111	0.6179	0.0213
2011	FourWayMix	4	0.0288	0.0320	0.0127	0.1686	0.1508	0.5996	0.0213
2012	Epoxiconazole	1	0.0116	0.0502	1.0000	1.0000	1.0000	0.5023	0.0046
2012	Prochloraz	1	0.0987	0.0279	1.0000	1.0000	1.0000	0.6378	0.0068
2012	Prothioconazole	1	0.1788	0.0347	1.0000	1.0000	1.0000	0.5991	0.0274
2012	Tebuconazole	1	0.0387	0.0798	1.0000	1.0000	1.0000	0.3962	0.0093
2012	EpoxiProchlMix	2	0.0429	0.0349	0.3154	-0.0120	0.0000	0.5863	0.0068

2012	EpoxiProthioMix	2	0.0690	0.0398	0.7907	0.8605	0.9524	0.5606	0.0274
2012	EpoxiTebucoMix	2	0.0161	0.0605	0.1048	0.1970	0.2381	0.4591	0.0093
2012	ProchlTebucoMix	2	0.0705	0.0387	-0.5166	-0.4669	-0.5952	0.5632	0.0093
2012	ProthioProchlMix	2	0.0434	0.0298	0.3046	-0.0963	0.0000	0.6228	0.0274
2012	ProthioTebucoMix	2	0.0368	0.0443	-0.2813	-0.0570	0.0714	0.5346	0.0274
2012	EpoxiProchlTebucoMix	3	0.0239	0.0417	-0.0321	-0.0940	-0.1190	0.5458	0.0093
2012	EpoxiProthioProchlMix	3	0.0521	0.0341	0.4702	0.2507	0.3175	0.5927	0.0274
2012	EpoxiProthioTebucoMix	3	0.0300	0.0459	0.2047	0.3335	0.4206	0.5248	0.0274
2012	ProthioProchlTebucoMix	3	0.0423	0.0361	-0.1644	-0.2067	-0.1746	0.5795	0.0274
2012	FourWayMix	4	0.0340	0.0387	0.1196	0.0709	0.1111	0.5635	0.0274
2013	Epoxiconazole	1	0.0082	0.0523	1.0000	1.0000	1.0000	0.4926	0.0032
2013	Prochloraz	1	0.0503	0.0311	1.0000	1.0000	1.0000	0.6121	0.0072
2013	Prothioconazole	1	0.0515	0.0401	1.0000	1.0000	1.0000	0.5629	0.0109
2013	Tebuconazole	1	0.0603	0.0697	1.0000	1.0000	1.0000	0.4350	0.0118
2013	EpoxiProchlMix	2	0.0244	0.0385	0.2995	-0.1804	-0.1429	0.5644	0.0072
2013	EpoxiProthioMix	2	0.0288	0.0445	0.6820	0.8084	0.8571	0.5341	0.0109
2013	EpoxiTebucoMix	2	0.0217	0.0581	0.2464	0.4768	0.3929	0.4701	0.0118
2013	ProchlTebucoMix	2	0.0405	0.0403	-0.4652	-0.5496	-0.5357	0.5536	0.0118
2013	ProthioProchlMix	2	0.0254	0.0345	0.6337	0.1492	-0.0714	0.5912	0.0109
2013	ProthioTebucoMix	2	0.0281	0.0465	-0.4916	-0.0087	0.1786	0.5223	0.0118
2013	EpoxiProchlTebucoMix	3	0.0185	0.0435	0.0269	-0.0844	-0.0952	0.5357	0.0118
2013	EpoxiProthioProchlMix	3	0.0305	0.0386	0.5384	0.2590	0.2143	0.5653	0.0109
2013	EpoxiProthioTebucoMix	3	0.0187	0.0482	0.1456	0.4255	0.4762	0.5131	0.0118
2013	ProthioProchlTebucoMix	3	0.0278	0.0394	-0.1077	-0.1364	-0.1429	0.5598	0.0118
2013	FourWayMix	4	0.0225	0.0419	0.1508	0.1159	0.1131	0.5454	0.0118
2014	Epoxiconazole	1	0.0075	0.0547	1.0000	1.0000	1.0000	0.4816	0.0018
2014	Prochloraz	1	0.0485	0.0342	1.0000	1.0000	1.0000	0.5925	0.0070

Year	Treatment	Group	Val1	Val2	Val3	Val4	Val5	Val6	Val7
2014	Prothioconazole	1	0.0421	0.0407	1.0000	1.0000	1.0000	0.5566	0.0101
2014	Tebuconazole	1	0.0532	0.0784	1.0000	1.0000	1.0000	0.4047	0.0087
2014	EpoxiProchlMix	2	0.0199	0.0416	0.2866	0.0707	0.4286	0.5472	0.0070
2014	EpoxiProthioMix	2	0.0218	0.0460	0.5475	0.6406	0.7143	0.5250	0.0101
2014	EpoxiTebucoMix	2	0.0224	0.0631	0.4441	0.2711	0.0000	0.4503	0.0087
2014	ProchlTebucoMix	2	0.0295	0.0456	-0.2224	-0.4365	-0.4286	0.5277	0.0087
2014	ProthioProchlMix	2	0.0246	0.0366	0.5118	0.4352	0.5714	0.5773	0.0101
2014	ProthioTebucoMix	2	0.0290	0.0504	-0.3423	-0.2226	-0.2857	0.5044	0.0101
2014	EpoxiProchlTebucoMix	3	0.0194	0.0481	0.1695	-0.0316	0.0000	0.5142	0.0087
2014	EpoxiProthioProchlMix	3	0.0220	0.0409	0.4486	0.3822	0.5714	0.5516	0.0101
2014	EpoxiProthioTebucoMix	3	0.0177	0.0516	0.2164	0.2297	0.1429	0.4975	0.0101
2014	ProthioProchlTebucoMix	3	0.0232	0.0430	-0.0176	-0.0747	-0.0476	0.5405	0.0101
2014	FourWayMix	4	0.0190	0.0453	0.2042	0.1264	0.1667	0.5278	0.0101
2015	Epoxiconazole	1	0.0148	0.0588	1.0000	1.0000	1.0000	0.4656	0.0048
2015	Prochloraz	1	0.0182	0.0371	1.0000	1.0000	1.0000	0.5701	0.0061
2015	Prothioconazole	1	0.0711	0.0479	1.0000	1.0000	1.0000	0.5223	0.0189
2015	Tebuconazole	1	0.0614	0.0792	1.0000	1.0000	1.0000	0.4068	0.0183
2015	EpoxiProchlMix	2	0.0071	0.0452	-0.1991	-0.3712	-0.2485	0.5260	0.0061
2015	EpoxiProthioMix	2	0.0330	0.0520	0.6567	0.7134	0.8303	0.4981	0.0189
2015	EpoxiTebucoMix	2	0.0302	0.0656	0.4665	0.5928	0.5636	0.4429	0.0183
2015	ProchlTebucoMix	2	0.0202	0.0490	-0.1606	-0.6145	-0.6000	0.5104	0.0183
2015	ProthioProchlMix	2	0.0276	0.0405	0.0536	0.0153	-0.0545	0.5523	0.0189
2015	ProthioTebucoMix	2	0.0217	0.0562	-0.1330	0.1089	0.4424	0.4811	0.0189
2015	EpoxiProchlTebucoMix	3	0.0145	0.0515	0.0356	-0.1310	-0.0949	0.4974	0.0183
2015	EpoxiProthioProchlMix	3	0.0156	0.0451	0.1704	0.1192	0.1758	0.5277	0.0189
2015	EpoxiProthioTebucoMix	3	0.0234	0.0568	0.3301	0.4717	0.6121	0.4769	0.0189
2015	ProthioProchlTebucoMix	3	0.0157	0.0472	-0.0800	-0.1634	-0.0707	0.5185	0.0189

350

2015	FourWayMix	4	0.0141	0.0496	0.1140	0.0741	0.1556	0.5068	0.0189
2016	Epoxiconazole	1	0.0107	0.0612	1.0000	1.0000	1.0000	0.4550	0.0028
2016	Prochloraz	1	0.0060	0.0364	1.0000	1.0000	1.0000	0.5726	0.0048
2016	Prothioconazole	1	0.1034	0.0537	1.0000	1.0000	1.0000	0.4990	0.0222
2016	Tebuconazole	1	0.0372	0.0921	1.0000	1.0000	1.0000	0.3582	0.0086
2016	EpoxiProchlMix	2	0.0055	0.0460	0.3087	0.5745	0.7000	0.5218	0.0048
2016	EpoxiProthioMix	2	0.0435	0.0561	0.8777	0.9457	0.9000	0.4805	0.0222
2016	EpoxiTebucoMix	2	0.0150	0.0721	0.0866	-0.2002	-0.1000	0.4152	0.0086
2016	ProchlTebucoMix	2	0.0165	0.0531	0.3086	-0.2182	0.0000	0.4914	0.0086
2016	ProthioProchlMix	2	0.0198	0.0423	0.0537	0.4306	0.5000	0.5423	0.0222
2016	ProthioTebucoMix	2	0.0165	0.0629	-0.3763	-0.4007	-0.5000	0.4504	0.0222
2016	EpoxiProchlTebucoMix	3	0.0106	0.0552	0.2346	0.0520	0.2000	0.4808	0.0086
2016	EpoxiProthioProchlMix	3	0.0146	0.0473	0.4134	0.6502	0.7000	0.5170	0.0222
2016	EpoxiProthioTebucoMix	3	0.0166	0.0622	0.1960	0.1149	0.1000	0.4522	0.0222
2016	ProthioProchlTebucoMix	3	0.0103	0.0510	-0.0047	-0.0628	0.0000	0.4992	0.0222
2016	FourWayMix	4	0.0101	0.0533	0.2099	0.1886	0.2500	0.4891	0.0222
2017	Epoxiconazole	1	0.0139	0.0638	1.0000	1.0000	1.0000	0.4454	0.0032
2017	Prochloraz	1	0.0144	0.0335	1.0000	1.0000	1.0000	0.5904	0.0039
2017	Prothioconazole	1	0.0809	0.0489	1.0000	1.0000	1.0000	0.5157	0.0196
2017	Tebuconazole	1	0.0347	0.0928	1.0000	1.0000	1.0000	0.3552	0.0101
2017	EpoxiProchlMix	2	0.0065	0.0441	-0.3435	0.1645	0.1905	0.5314	0.0039
2017	EpoxiProthioMix	2	0.0304	0.0546	0.5075	0.6392	0.7143	0.4853	0.0196
2017	EpoxiTebucoMix	2	0.0188	0.0745	0.3586	0.1447	0.0952	0.4075	0.0101
2017	ProchlTebucoMix	2	0.0180	0.0500	-0.0321	-0.5343	-0.5238	0.5050	0.0101
2017	ProthioProchlMix	2	0.0197	0.0391	0.1522	0.5698	0.5000	0.5591	0.0196
2017	ProthioTebucoMix	2	0.0182	0.0612	-0.2544	-0.4751	-0.3333	0.4568	0.0196
2017	EpoxiProchlTebucoMix	3	0.0101	0.0535	-0.0057	-0.0750	-0.0794	0.4880	0.0101

2017	EpoxiProthioProchlMix	3	0.0119	0.0449	0.1054	0.4578	0.4683	0.5281	0.0196
2017	EpoxiProthioTebucoMix	3	0.0166	0.0619	0.2039	0.1029	0.1587	0.4534	0.0196
2017	ProthioProchlTebucoMix	3	0.0101	0.0481	-0.0448	-0.1466	-0.1190	0.5123	0.0196
2017	FourWayMix	4	0.0084	0.0512	0.0647	0.0848	0.1071	0.4978	0.0196
2018	Epoxiconazole	1	0.0113	0.0721	1.0000	1.0000	1.0000	0.4134	0.0021
2018	Prochloraz	1	0.0119	0.0353	1.0000	1.0000	1.0000	0.5797	0.0017
2018	Prothioconazole	1	0.0814	0.0743	1.0000	1.0000	1.0000	0.4249	0.0176
2018	Tebuconazole	1	0.0292	0.0946	1.0000	1.0000	1.0000	0.3456	0.0083
2018	EpoxiProchlMix	2	0.0048	0.0478	-0.6009	-0.5103	-0.4286	0.5130	0.0021
2018	EpoxiProthioMix	2	0.0369	0.0710	0.6119	0.5027	0.5476	0.4238	0.0176
2018	EpoxiTebucoMix	2	0.0105	0.0799	-0.1840	0.3069	0.4286	0.3862	0.0083
2018	ProchlTebucoMix	2	0.0232	0.0524	-0.2254	-0.5047	-0.5476	0.4928	0.0083
2018	ProthioProchlMix	2	0.0145	0.0465	-0.0613	0.0019	0.2143	0.5218	0.0176
2018	ProthioTebucoMix	2	0.0113	0.0746	-0.6543	-0.3817	-0.2857	0.4055	0.0176
2018	EpoxiProchlTebucoMix	3	0.0034	0.0571	-0.3368	-0.2361	-0.1825	0.4709	0.0083
2018	EpoxiProthioProchlMix	3	0.0161	0.0528	-0.0167	-0.0019	0.1111	0.4916	0.0176
2018	EpoxiProthioTebucoMix	3	0.0127	0.0736	-0.0755	0.1426	0.2302	0.4084	0.0176
2018	ProthioProchlTebucoMix	3	0.0055	0.0549	-0.3137	-0.2948	-0.2063	0.4806	0.0176
2018	FourWayMix	4	0.0051	0.0584	-0.1857	-0.0975	-0.0119	0.4659	0.0176
2019	Epoxiconazole	1	0.0198	0.0692	1.0000	1.0000	1.0000	0.4262	0.0034
2019	Prochloraz	1	0.0211	0.0333	1.0000	1.0000	1.0000	0.5933	0.0038
2019	Prothioconazole	1	0.0729	0.0666	1.0000	1.0000	1.0000	0.4473	0.0252
2019	Tebuconazole	1	0.0490	0.0865	1.0000	1.0000	1.0000	0.3783	0.0100
2019	EpoxiProchlMix	2	0.0101	0.0448	-0.4388	0.1358	0.0952	0.5282	0.0038
2019	EpoxiProthioMix	2	0.0342	0.0665	0.5267	0.6228	0.8095	0.4398	0.0252
2019	EpoxiTebucoMix	2	0.0280	0.0750	0.4439	0.1211	0.2381	0.4077	0.0100
2019	ProchlTebucoMix	2	0.0279	0.0473	-0.4528	-0.5085	-0.5476	0.5174	0.0100

2019	ProthioProchlMix	2	0.0239	0.0436	0.1819	0.3639	0.2857	0.5368	0.0252
2019	ProthioTebucoMix	2	0.0177	0.0691	-0.3078	-0.4782	-0.2143	0.4284	0.0252
2019	EpoxiProchlTebucoMix	3	0.0090	0.0524	-0.1492	-0.0839	-0.0714	0.4923	0.0100
2019	EpoxiProthioProchlMix	3	0.0191	0.0496	0.0899	0.3742	0.3968	0.5069	0.0252
2019	EpoxiProthioTebucoMix	3	0.0222	0.0690	0.2209	0.0886	0.2778	0.4278	0.0252
2019	ProthioProchlTebucoMix	3	0.0107	0.0505	-0.1929	-0.2076	-0.1587	0.5013	0.0252
2019	FourWayMix	4	0.0100	0.0541	-0.0078	0.0428	0.1111	0.4851	0.0252

6.D.1 Further details on generalised linear models of $\Delta\bar{r}$

There were significant interactions between the number of azoles and the fitted generalised linear model (GLM) coefficients for $\bar{f}_{\text{start}}$ and $\text{Var}_{j_{\text{Max}}}$ (Tables 6.D.2, 6.D.3). The percentage of the variance in $\Delta\bar{r}$ explained by $\bar{f}_{\text{start}}$ as an individual variable increased with the number of azoles included in the mixture (Table 6.D.4). For 2-azole programmes, there was no significant correlation between the explanatory variables, but for 4-azole programmes, $\bar{f}_{\text{start}}$ was positively correlated with cc_w (Spearman's correlation, r_s (9) = 0.63, p=0.039).

Table 6.D.2: Accumulated analysis of variance for a generalised linear model of $\Delta\bar{r}$ with a log link function for two and three-azole mixture programmes.

Variable	d.f.	s.s.	m.s.	v.r.	F pr.
cc_w	1	0.01483	0.01483	253.08	<.001
$\bar{f}_{\text{start}}$	1	0.01367	0.01367	233.26	<.001
$\text{Var}_{j_{\text{Max}}}$	1	0.00346	0.00346	59.04	<.001
2 vs. 3 azoles	1	0.00092	0.00092	15.64	<.001
3 azoles * $\bar{f}_{\text{start}}$	1	0.00047	0.00047	7.96	0.031
Residual	104	0.00609	0.00006		
Total	109	0.03943	0.00036		

Table 6.D.3: Accumulated analysis of variance for a generalised linear model of $\Delta\bar{r}$ with a log link function for 2-azole mixture programmes and solo azole programmes.

Variable	d.f.	s.s.	m.s.	v.r.	F pr.
cc_w	1	0.01983	0.01983	99.82	<.001
$\bar{f}_{\text{start}}$	1	0.03340	0.03340	168.15	<.001
$\text{Var}_{j_{\text{Max}}}$	1	0.04274	0.04274	215.16	<.001
2 azoles vs. solo	1	0.00219	0.00219	11.00	0.001
Solo * $\text{Var}_{j_{\text{Max}}}$	1	0.00460	0.00460	23.17	<.001
Residual	104	0.02066	0.00020		
Total	109	0.12343	0.00113		

Table 6.D.4: Percentage variance in $\Delta\bar{r}$ of 1, 2, 3 and 4-azole programmes explained by individual variables in generalised linear models (GLMs) with a log-link function, with only one explanatory variable per GLM. [1]Cross-resistance is not an informative term for 1-azole programmes, as the cross-resistance of an azole with itself is always equal to 1. [2]NS denotes variables for which there was no significant correlation (F-test). All other variables shown were significant.

Number of azoles in programme	Explanatory variable	% variance explained as single variate
1	cc_w	[1]N/A
	[3]$\mathrm{Var}_{j_\mathrm{Max}}$	43.3
	[2]$\bar{f}_\mathrm{start}$	24.8
2	cc_w	35.7
	[2]$\bar{f}_\mathrm{start}$	48.2
	[3]$\mathrm{Var}_{j_\mathrm{Max}}$	7.6
3	cc_w	37.1
	$\bar{f}_\mathrm{start}$	65.1
	$\mathrm{Var}_{j_\mathrm{Max}}$	0.0 ([2]NS)
4	cc_w	28.9 ([2]NS: p=0.051)
	$\bar{f}_\mathrm{start}$	80.1
	$\mathrm{Var}_{j_\mathrm{Max}}$	0.0 ([2]NS)

The accumulated analysis of variance tables for GLMs of $\Delta\bar{r}$ for solo azoles, two-way, three-way and four-way mixtures are shown in Tables 6.D.5, 6.D.6, 6.D.7 and 6.D.8 respectively, and a comparison of the GLM fitted values and simulation model values of $\Delta\bar{r}$ for solo azoles is shown in Figure 6.D.1.

Table 6.D.5: Accumulated analysis of variance for a generalised linear model of $\Delta\bar{r}$ with a log link function for solo azole programmes.

Variable	d.f.	s.s.	m.s.	v.r.	F pr.
$\mathrm{Var}_{j_\mathrm{Max}}$	1	0.03771	0.03771	96.24	<.001
$\bar{f}_\mathrm{start}$	1	0.03083	0.03083	78.67	<.001
Residual	41	0.01607	0.00039		
Total	43	0.08460	0.00197		

Table 6.D.6: Accumulated analysis of variance for a generalised linear model of $\Delta\bar{r}$ with a log link function for two-azole mixture programmes.

Variable	d.f.	s.s.	m.s.	v.r.	F pr.
cc_w	1	0.01025	0.01025	139.96	<.001
$\bar{f}_{\text{start}}$	1	0.00980	0.00980	133.74	<.001
$\text{Var}_{j_{\text{Max}}}$	1	0.00338	0.00338	46.19	<.001
Residual	62	0.00454	0.00007		
Total	65	0.02797	0.00043		

Table 6.D.7: Accumulated analysis of variance for a generalised linear model of $\Delta\bar{r}$ with a log link function for three-azole mixture programmes.

Variable	d.f.	s.s.	m.s.	v.r.	F pr.
cc_w	1	0.00393	0.00393	103.77	<.001
$\bar{f}_{\text{start}}$	1	0.00409	0.00409	108.09	<.001
$\text{Var}_{j_{\text{Max}}}$	1	0.00065	0.00065	17.24	<.001
Residual	40	0.00152	0.00004		
Total	43	0.01019	0.00024		

Table 6.D.8: Accumulated analysis of variance for a generalised linear model of $\Delta\bar{r}$ with a log link function for four-azole mixture programmes.

Variable	d.f.	s.s.	m.s.	v.r.	F pr.
cc_w	1	0.00050	0.00050	30.59	<.001
$\bar{f}_{\text{start}}$	1	0.00067	0.00067	41.43	0.006
$\text{Var}_{j_{\text{Max}}}$	1	0.00010	0.00010	6.00	0.044
Residual	7	0.00011	0.00002		
Total	10	0.00138	0.00014		
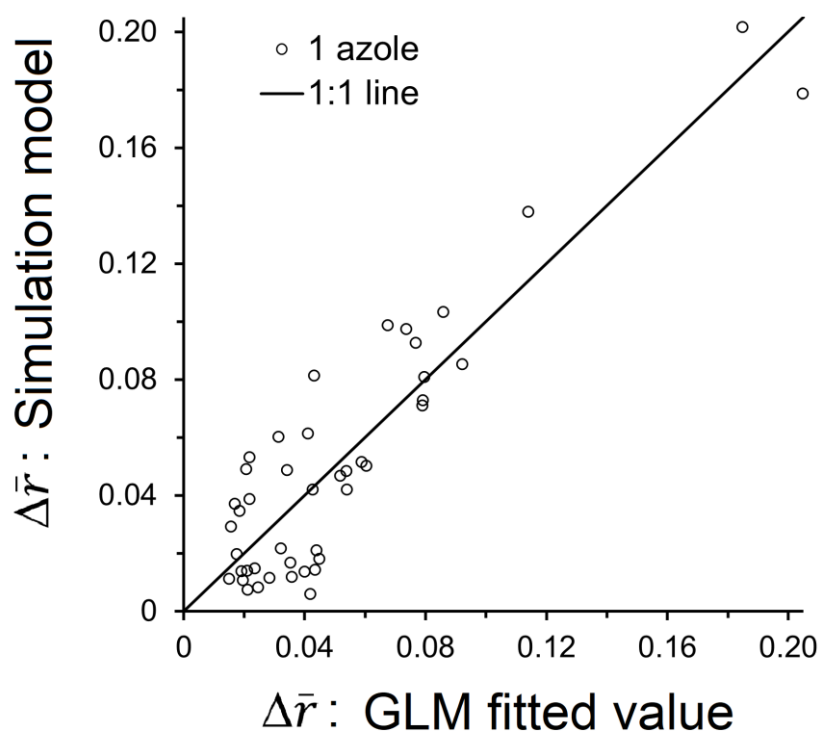
Figure 6.D.1: Comparison of epidemiological model values vs. GLM fitted values of $\Delta\bar{r}$ for solo azole applications (denoted as black circle); solid black line denotes 1:1 line.

The cross-resistance of an azole with itself is always equal to 1. Using a value of cc_w=1, the fitted parameter values for 2-azole mixtures (Table 6.6) were a moderately good predictor for the rank order of the $\Delta\bar{r}$ values of solo azole programmes (Spearman's correlation, r_s (42) = 0.57, p<.001), but there was a tendency to underpredict the highest $\Delta\bar{r}$ values. The GLM fitted for solo azole programmes was a better predictor of the rank order of the $\Delta\bar{r}$ values of solo azole programmes (Spearman's correlation, r_s (42) = 0.71, p<.001).

Appendix 6.E: Offprint of Corkley et al. (2023)

In the following short paper, I describe a modelling comparison of the use of alternations, mixtures and mosaics of azole active substances with incomplete cross-resistance, using the model described in Chapter 6. This paper was published in the Proceedings of the Reinhardsbrunn Symposium: In: Deising HB; Fraaije B; Mehl A; Oerke EC; Sierotzki H; Stammler G (Eds), "Modern Fungicides and Antifungal Compounds", Vol. X, pp. 291-296. © 2023. Deutsche Phytomedizinische Gesellschaft, Braunschweig, ISBN: 978-3-941261-17-4.

Modelling resistance management benefits of diversity within a fungicidal mode of action with incomplete cross-resistance: the azoles example

Corkley I[1,4,5], van den Bosch F[2], Fraaije BA[3], Shaw MW[4], Helps J[5], Mikaberidze A[4], Milne AE[5], Paveley ND[2]

[1]*ADAS Wolverhampton, Unit 14 Newton Court, Wolverhampton, WV9 5HB, UK.* [2]*ADAS High Mowthorpe, Duggleby, Malton, North Yorkshire, YO17 8BP, UK.* [3]*BU Biointeractions and Plant Health, Wageningen Plant Research, Wageningen University and Research, Wageningen, The Netherlands.* [4]*School of Agriculture, Policy and Development, University of Reading, Reading, UK.* [5]*Rothamsted Research, Harpenden, Hertfordshire, AL5 2JQ, UK*

6.E.1 Introduction

The resistance management benefits of having multiple fungicidal modes-of-action (MoA) available for disease control are well established. These include enabling the use of mixtures and alternation of fungicides with different MoA, and overcoming practical disease control constraints caused by limiting the number of applications of each MoA, which are proven tactics for slowing pathogen evolution (van den Bosch et al., 2014; Corkley et al., 2022). Resistance management tactics employing more than one MoA work as there is generally little cross-resistance between MoA, i.e. a high resistance factor to one MoA is not usually correlated with a high level of resistance to a second MoA. Strains with a high resistance factor to one MoA are therefore controlled by the other MoA, resulting in similar population growth rates for both resistant and sensitive strains, reducing the strength of selection for resistance and providing effective disease control.

The resistance management benefits of having a range of active substances within a MoA are not known. The benefits will depend on the degree of cross-resistance. If cross-resistance is close to complete, then mixtures and alternation are the equivalent of mixing the same product with itself and thus confer no benefit to resistance management (Oliver, 2016). If cross-resistance is weak, then the benefits of active substance diversity within a MoA would be close to the benefits of diversity between MoA. Azole fungicides in the demethylation inhibitor (DMI) group present a case between these extremes: incomplete cross-resistance.

Azole fungicides inhibit the activity of sterol 14a-demethylase (CYP51). A diverse range of CYP51 mutations associated with resistance to azole fungicides have been recorded, with resistance factors varying between azole compounds (Cools et al., 2013; Fraaije et al., 2007; Leroux et al., 2007). Differential control and shifts in the frequency of CYP51 mutations and azole sensitivity have been observed depending on which azole(s) are applied (Fraaije et al., 2007; Stilgenbauer et al., 2023; Dooley et al., 2015; Jørgensen et al., 2018).

Many CYP51 variants are now known, each with different combinations of CYP51 mutations. We refer to the haploid genotype of singular CYP51 variants as the 'haplotype'. A few key CYP51 haplotypes typically make up a high proportion of the *Z. tritici* population in any season (Huf et al., 2018). The laboratory sensitivities of these key haplotypes to contrasting azoles are known (Cools et al., 2011; Huf et al., 2018), and recent analysis of long-term datasets has related laboratory to field sensitivities (Blake et al., 2018), enabling parameterisation of the field sensitivities of haplotypes for a population genetic approach.

Applying a population genetic approach to azole fungicides and CYP51 haplotypes as a case study, we investigate:

- What is the resistance management benefit of mixture, mosaic or alternation within the same mode of action?
- What is the benefit of additional active substances within a mode of action ('azole diversity')?

6.E.2 Methods

We developed a population genetic model that explicitly models the growth of individual haplotypes and fungicide dose decay, enabling simulation of a wide

range of fungicide programmes, including mixture, alternation and mosaic programmes using two or more azoles.

Each haplotype has its own population growth rate under an azole fungicide treatment regime, leading to changes in the frequencies of haplotypes when an azole is applied, with selection for haplotypes that have a larger growth rate than the population average. Considering the growth rate and frequency of all haplotypes over time enables calculation of changes to the average epidemic growth rate of the entire pathogen population, $\bar{r}$, a value with greater relevance to the grower than individual haplotype dynamics, since the total pathogen population determines the level of damage to the crop.

Since fungicide applications select for strains with the highest growth rates, over time they will lead to an increase in the total pathogen population's growth rate. Resistance management will therefore aim at minimising the increase in the total pathogen population's growth rate, $\bar{r}$. We calculate the change in $\bar{r}$ from one year to the next as a measure of selection for fungicide resistance. Denoting the growth rate of the pathogen population in year n by $\bar{r}_n$, the rate of resistance development is measured as $\Delta \bar{r} = \frac{\bar{r}_{n+1} - \bar{r}_n}{\bar{r}_n}$ (1).

Azole fungicides affect pathogen fitness by targeting the CYP51 enzyme, binding to it and inhibiting conversion of lanosterol to ergosterol, reducing the ergosterol production rate, therefore lowering the fungal population growth rate. For the purpose of modelling the application of azole fungicides, we assume that the only process varying between CYP51 haplotypes is the ergosterol production rate. We can therefore calculate a haplotype's population growth rate as affected by azole fungicides at any point in time from Hill's equation (Hill, 1913) as used in enzyme kinetics studies and as a dose response curve in fungicide resistance models (Mikaberidze et al., 2017), generalised here to mixtures of azoles:

$$r_i = \frac{r_0}{1 + \sum_{j=1}^{jmax} B_{ij} D_j} \qquad (2)$$

where r_i is the population growth rate of fungal haplotype i, r_0 is the growth rate of all haplotypes when no fungicide is applied, D_j is the dose of azole j and B_{ij} describes the effect of azole j on the growth rate of haplotype i. The dose D_j follows first-order dissipation kinetics.

The value of B_{ij} was parameterised for each of 116 haplotype-azole combinations (29 haplotypes and 4 azoles: epoxiconazole, prothioconazole, prochloraz and tebuconazole) using *in vitro* EC_{50} dose response measurements (Bart Fraaije, pers. comm.), converted to field-ED_{50} values using the relationships reported in Blake et al. (2018). We estimated foliar half-life as 7.5 days for all azole fungicides, and r_0 as 0.1173 (Hobbelen et al., 2011; te Beest et al., 2009).

The initial frequency of each *Z. tritici* haplotype was estimated from isolates sampled in fields around Rothamsted Research, UK in each of the years 2003 and 2010-2019 (Bart Fraaije, pers. comm.). Simulations were run for a two-year period using the starting haplotype compositions from each year, to represent realistic scenarios. Five azole application scenarios were modelled (Table 6.E.1): solo application, mosaics, mixtures, alternation within a growing season and alternation between years, with multiple combinations of up to four azoles and total azole dose kept constant across all scenarios. Ascospores were assumed to mix fully at the end of the season.

Table 6.E.1: Application scenarios for two-azole programmes. 1.0 j_1 denotes a full label dose of azole 1. Area is split equally between each azole in mosaic programmes.

Application scenario		Spray 1	Spray 2
Mixture		0.5 j_1 + 0.5 j_2	0.5 j_1 + 0.5 j_2
Alternation (within-year)		1.0 j_1	1.0 j_2
Alternation (between years)	Year 1	1.0 j_1	1.0 j_1
	Year 2	1.0 j_2	1.0 j_2
Mosaic	Area 1	1.0 j_1	1.0 j_1
	Area 2	1.0 j_2	1.0 j_2

6.E.3 Results and Discussion

The model showed that within-MoA active substance diversity benefits resistance management for azole fungicides. Mixtures, alternations and mosaics are all useful ways to deploy within-MoA diversity (Figure 6.E.1). The optimal method of deployment of partial cross-resistance varied between years, depending on exact product combinations, pathogen haplotype frequencies and the required level of disease control. Combinations of products with low or negative cross-resistance provided the greatest resistance management benefits. For disease control,

mixtures and within-year alternation were most resilient to declines in fungicide efficacy.
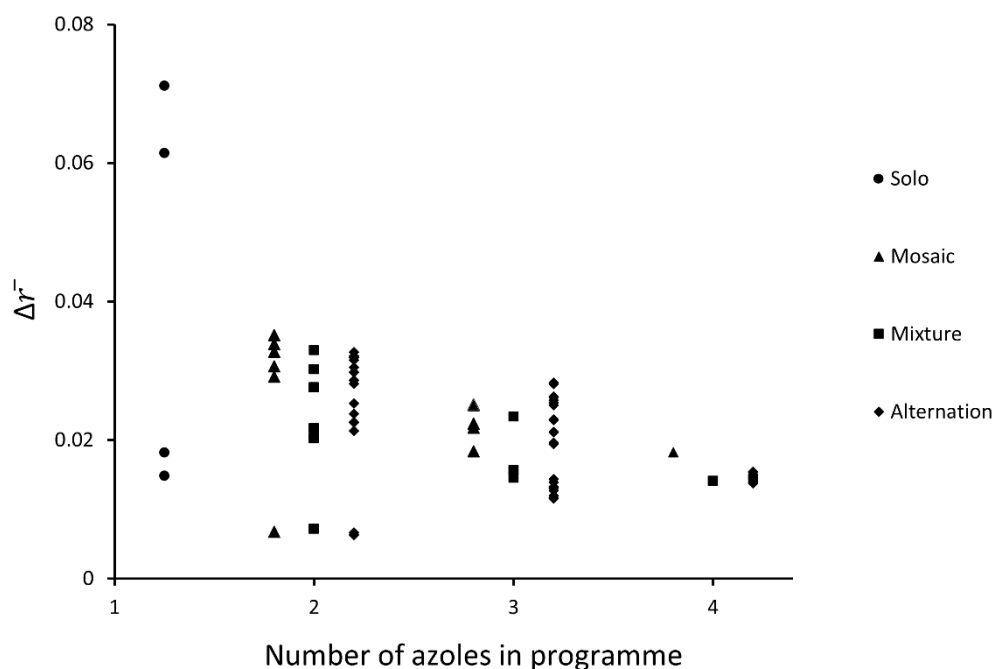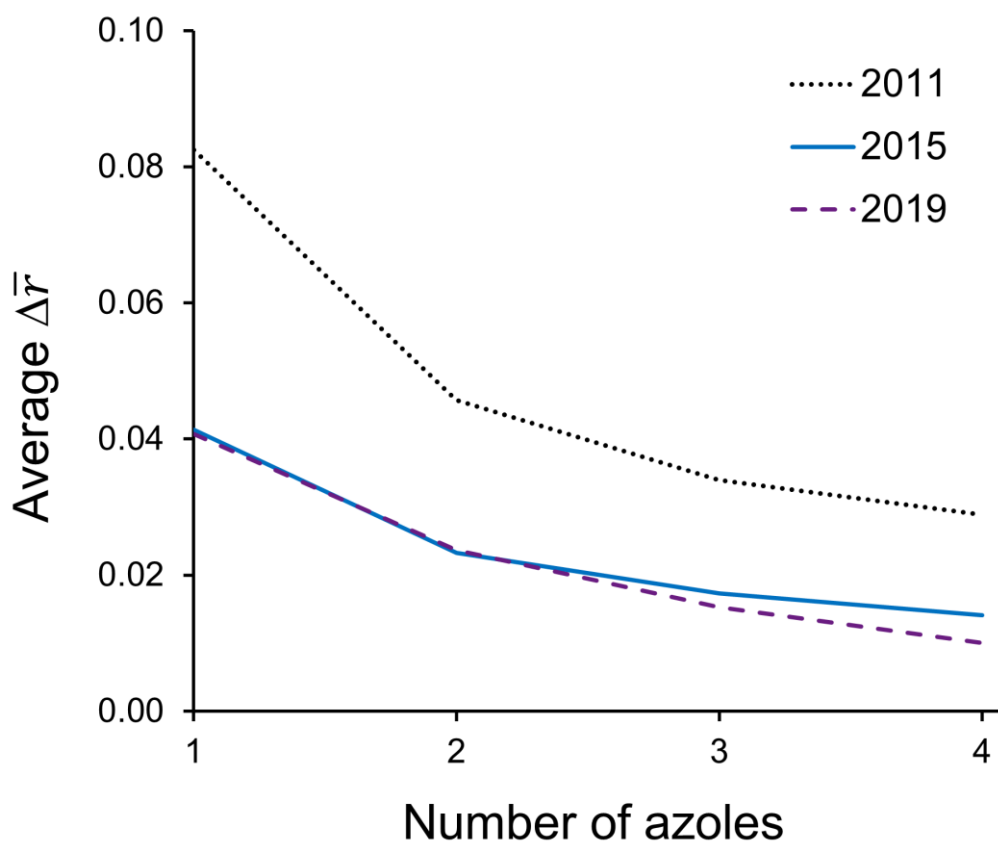

Figure 6.E.1: Rate of selection for resistance ($\Delta \bar{r}$) for solo and 2-, 3- and 4-azole mosaic, mixture and alternation programmes, for 2015 CYP51 haplotype starting frequencies.

On average, across all years and application scenarios, having more azole active substances available enables programmes with lower selection for resistance, although the resistance management benefit varies between years, as illustrated here for mixture programmes (Figure 6.E.2). There are diminishing returns as additional azoles are added to the programme, although it should be noted that our analysis did not include mefentrifluconazole. A well-chosen combination of two azoles can provide the same resistance management benefit as a programme with more azoles, but may be less resilient to changing patterns of cross-resistance as new CYP51 mutations emerge.

In practice, azoles will and should be used in combination with other MoA; this study focused on within-MoA programmes for the purpose of investigating the benefit of azole diversity. Further analysis of the model simulations reported here will focus on how the resistance management benefit varies with the degree of cross-resistance between active substances.

This novel method enables us to model the efficacy of mixtures of active substances within the same MoA with incomplete cross-resistance, and therefore to model evolution of resistance in these cases to inform resistance management strategies. We applied this method to the important example of azole fungicides used to control *Z. tritici*, with scope to extend the approach to other pathosystems and MoA.

Figure 6.E.2: Average rate of selection for resistance ($\Delta\bar{r}$) for solo and 2-, 3- and 4-azole mixture programmes, for starting CYP51 haplotype frequencies as sampled in years 2011, 2015 and 2019.

6.E.4 Acknowledgements

6.E.5 References

Blake, J., Gosling, P., Fraaije, B., Burnett, F., Knight, S., Kildea, S. et al. (2018). Changes in field dose-response curves for DMI and QoI fungicides against *Zymoseptoria tritici. Pest Management Science* 74, 302-313

Cools, H.J., Mullins, J.G., Fraaije, B.A., Parker, J.E., Kelly, D.E., Lucas, J.A. et al (2011). Impact of Recently Emerged Sterol 14α-Demethylase (CYP51) Variants of Mycosphaerella graminicola on Azole Fungicide Sensitivity. *Applied and Environmental Microbiology* 77, 3830-3837.

Cools, H.J., Hawkins, N.J. & Fraaije, B.A. (2013). Constraints on the evolution of azole resistance in plant pathogenic fungi. *Plant Pathology* 62, 36-42.

Corkley, I., Fraaije, B. & Hawkins, N. (2022). Fungicide resistance management: Maximising the effective life of plant protection products. *Plant Pathology* 71, 150-169.

Dooley, H., Shaw, M.W., Spink, J. & Kildea, S. (2015). Effect of azole fungicide mixtures, alternations and dose on azole sensitivity in the wheat pathogen *Zymoseptoria tritici. Plant Pathology* 65: 124-136.

Fraaije, B.A., Cools, H.J., Kim, S.H., Motteram, J., Clark, W.S. & Lucas, J.A. (2007). A novel substitution I381V in the sterol 14α-demethylase (CYP51) of *Mycosphaerella graminicola* is differentially selected by azole fungicides. *Molecular Plant Pathology* 8, 245-254.

Hill, A.V. (1913). The Combinations of Haemoglobin with Oxygen and with Carbon Monoxide. *I Biochemical Journal* 7, 471-480.

Hobbelen, P.H.F., Paveley, N.D. & van den Bosch, F. (2011). Delaying selection for fungicide insensitivity by mixing fungicides at a low and high risk of resistance development: A modeling analysis. *Phytopathology* 101, 1224-1233.

Huf, A., Rehfus, A., Lorenz, K.H., Bryson, R., Voegele, R.T. & Stammler, G. (2018). Proposal for a new nomenclature for CYP51 haplotypes in *Zymoseptoria tritici* and analysis of their distribution in Europe. *Plant Pathology* 67, 1706-1712.

Jørgensen, L.N., Matzen, N., Hansen, J.G., Semaskiene, R., Korbas, M., Danielewicz, J. et al. (2018). Four azoles' profile in the control of Septoria, yellow rust and brown rust in wheat across Europe. *Crop Protection* 105, 16-27.

Leroux, P., Albertini, C., Gautier, A., Gredt, M. & Walker, A.S. (2007). Mutations in the CYP51 gene correlated with changes in sensitivity to sterol 14α-

demethylation inhibitors in field isolates of *Mycospharerella graminicola*. *Pest Management Science* 63, 688-698.

Mikaberidze, A., Paveley, N., Bonhoeffer, S. & van den Bosch, F. (2017). Emergence of resistance to fungicides: the role of fungicide dose. *Phytopathology* 107, 545-560.

Oliver, R. (2016). Fungicide resistance management in practice: mixtures, alternations and cross resistance patterns. *Journal of Plant Pathology* 98, S11.

Stilgenbauer, S., Simões, K., Craig, I.R., Brahm, L., Steiner, U. & Stammler, G. (2023). New CYP51-genotypes in *Phakopsora pachyrhizi* have different effects on DMI sensitivity. *Journal of Plant Diseases and Protection* 130, 973-983.

te Beest, D.E., Shaw, M.W., Pietravalle, S. & van den Bosch, F. (2009). A predictive model for early-warning of septoria leaf blotch on winter wheat. *European Journal of Plant Pathology* 124, 413-425.

van den Bosch, F., Oliver, R., van den Berg, F. & Paveley, N. (2014). Governing principles can guide fungicide-resistance management tactics. *Annual Review of Phytopathology* 52, 175-195.